SOVIET PHYSICS

JETP

A translation of the Journal of Experimental and Theoretical Physics of the USSR.

SOVIET PHYSICS JETP VOL. 35(8), NO. 2, pp. 217-386 FEBRUARY, 1959

ELASTIC SCATTERING OF 300-Mev PIONS BY DEUTERONS

L. S. DUL' KOVA, I. B. SOKOLOVA and M. G. SHAFRANOVA

P. N. Lebedev Physics Institute, Academy of Sciences, U.S.S.R.

Submitted to JETP editor February 8, 1958

J. Exptl. Theoret. Phys. (U.S.S.R.) **35**, 313-315 (August, 1958)

The interactions of 300 ± 15-Mev π^+ mesons and of 295 ± 10-Mev π^- mesons with deuterium were studied in nuclear emulsions impregnated with lithium acetate whose hydrogen was replaced by deuterium. Cross sections and angular distributions of the π^+ and π^- mesons scattered elastically by deuterium were obtained.

IN the present work the elastic scattering of positive and negative π mesons by deuterium was studied with photographic plates. This process has been little studied experimentally. The literature refers to experiments for only two π-meson energies, 85 and 145 Mev.[1,2] Our measurements were made at 300 Mev.

Type R NIKFI nuclear emulsions were used in the work. Deuterium was introduced into the plates in the form of lithium acetate $CH_3COOLi \cdot 2H_2O$, in which 97% of the hydrogen atoms were replaced by deuterium. The method of processing the plates and the properties of the impregnated emulsion were described earlier.[3] The quantity of salt introduced was determined by spectral analysis of the lithium. The number of deuterium nuclei in the impregnated emulsions was roughly equal to the number of hydrogen ones in ordinary plates, 2.2×10^{22} cm^{-3} on the average.

The plates were irradiated by the synchrocyclotron of the Joint Institute for Nuclear Research. The mean energy of the π^+ mesons in the plates was 300 ± 15 Mev, and that of the π^- mesons was 295 ± 10 Mev. The scanning method and the preliminary results were published earlier.[3]

Cases of elastic scattering by deuterium were selected according to the angle of emission and coplanarity of the tracks of the incident meson, scattered meson, and deuteron. In the small-angle scattering (< 30°) the tracks of the deuterons, as a rule, stopped in the emulsions, and the range-angle relationship served as a supplementary selection criterion.

Since the particles are emitted in scattering of π mesons by protons and deuterons at nearly equal angles, a high accuracy of measurement and a strict accounting for the errors are necessary to separate the scattering by deuterons from the scattering by hydrogen of the gelatin. We have selected the cases in which, within the limits of two standard deviations, the tracks were coplanar. Then, if the measurements agreed within two standard deviations with the relation for scattering by deuterons and did not agree with that for scattering by protons, this case was considered to be elastic scattering by deuterons. When the recoil track ended in the emulsion, the separation of H and D cases presented no difficulties.

Some of the cases could not be identified by the means described above; however, 14 of them were separated by the ionization, determined by grain counting. Measurements of grain density were also carried out for all cases of scattering by the deuteron through angles > 0°.

As a result of the analysis, 286 cases of π^+-p scattering, 104 cases of π^+-d scattering, 203 cases of π^--p scattering and 105 cases of π^--d scattering were found. Nine cases involving π^-

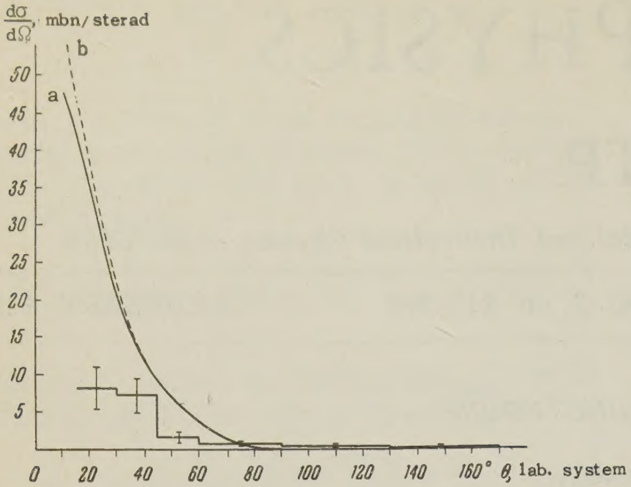

FIG. 1. Angular distribution of π^+ mesons scattered elastically by deuterons: (a) calculated in the impulse approximation neglecting the Coulomb interaction; (b) with account of the Coulomb interaction.

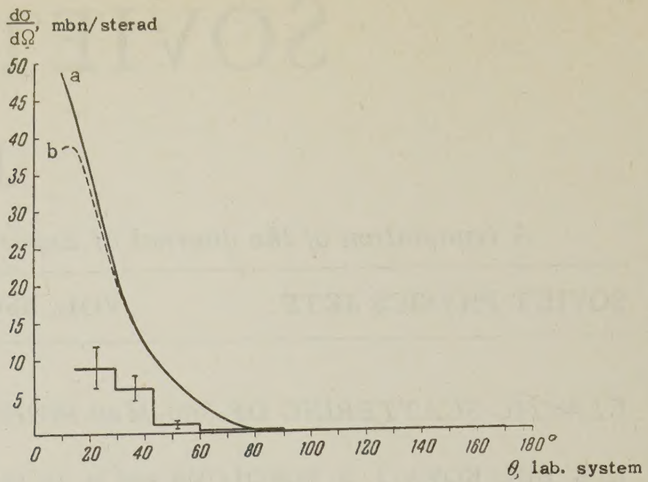

FIG. 2. Angular distribution of π^- mesons scattered elastically by deuterons: (a) calculated in the impulse approximation neglecting the Coulomb interaction; (b) with account of the Coulomb interaction.

mesons, and 26 involving π^+ mesons remained unidentified.

Scanning of control plates which did not contain deuterium showed that the background of two-prong stars, produced in emulsion nuclei and satisfying our criteria for π-d scattering, was small. It was not taken into account in determining the cross section for π-d scattering.

The differential cross sections for scattering of π mesons by hydrogen, and also the results of a phase shift analysis, were published earlier.[4] The increased statistical accuracy here did not change the magnitudes of the cross section and phases, which are in good agreement with the results of other authors.

In the present work we obtained the following integral cross sections for the elastic scattering of π^+ and π^- mesons by deuterium in the angular range 15 – 170° in the laboratory system

$$\sigma(\pi^+ + d \rightarrow \pi^+ + d) = 21 \pm 6\,\text{mbn},$$
$$\sigma(\pi^- + d \rightarrow \pi^- + d) = 14 \pm 4\,\text{mbn}.$$

Corrections were introduced here to take care of cases missed in the scanning, analogously to the way in which this was done for the scattering from hydrogen,[4] and the unidentified cases were taken into account.

The corresponding angular distributions are given in Figs. 1 and 2 in the form of histograms. The solid line was calculated in the impulse approximations,[5] starting from the phases determined by us for π-p scattering.[4] The proportion of elastic scattering was determined here by the factor

$$I(\theta) = \frac{1}{(2\pi)^3}\int \left|\psi_D(r)\right|^2 e^{i|(\mathbf{q}_0 - \mathbf{q})\mathbf{r}|^2} d\mathbf{r},$$

which gives the probability that the deuteron is not broken up in the collision. The dashed line gives the angular distributions, calculated with the inclusion of the Coulomb interaction. The theoretical calculations were made by G. M. Vagradov.

Within the limits of experimental error, the angular distributions of π^--d and π^+-d scattering agree, in contradistinction to results on elastic scattering from helium at the same energy,[6] where the cross sections for π^+ and π^- mesons are different at small angles on account of interference of the Coulomb and nuclear scattering. In the case of scattering from deuterium in the region of small angles (< 30°), the experimental cross sections are significantly below the calculated ones. This divergence cannot be explained by the influence of the Coulomb force. The cause of the difference is not completely clear. The impulse approximation, while satisfactorily describing the results at 85 Mev,[1,7] does not give agreement with our experimental results at 300 Mev. A rigorous calculation of the multiple scattering in the deuteron in the given case is difficult and, apparently, would not lead to a complete agreement with experiment.

It should be noted that cases of backward elastic scattering (~ 7%) are observed for a rather high meson energy. According to the impulse approximation, this process should not be present. In addition, 12 cases of absorption of π^+ mesons in deuterium were found. The cross section for this process turned out to be equal to

$$\sigma(\pi^+ + d \rightarrow p + p) = 2.4 \pm 0.9\,\text{mbn}$$

In conclusion, the authors wish to thank Prof. I. M. Frank and I. Ia. Barit for help in this work, G. M. Vagradov for useful discussion, and also the group of laboratory workers who took part in the scanning of the plates.

---

[1] K. C. Rogers and L. M. Ledermann, Phys. Rev. **105**, 247 (1957).

[2] Arase, Goldhaber, and Goldhaber, Phys. **90**, 160 (1952).

[3] Dul'kova, Romanova, Sokolva, Sukhov, Tolstov, and Shafranova, Dokl. Akad. Nauk SSSR **107**, 43 (1956), Soviet Phys. "Doklady" **1**, 154 (1956).

[4] Dul'kova, Sokolova and Shafranov, Dokl. Akad. Nauk SSSR **111**, 992 (1956), Soviet Phys. "Doklady" **1**, 739 (1956).

[5] Fernbach, Green and Watson, Phys. Rev. **84**, 1084 (1951).

[6] Kozodaev, Suliaev, Filippov, and Shcherbakov, J. Exptl. Theoret. Phys. **33**, 1047 (1957), Soviet Phys. JETP **6**, 806 (1958).

[7] R. M. Rockmore, Phys. Rev. **105**, 256 (1957).

[8] K. A. Brueckner, Phys. Rev. **90**, 715 (1953).

Translated by G. E. Brown
60

SOVIET PHYSICS JETP VOLUME 35(8), NUMBER 2 FEBRUARY, 1959

FISSION OF SILVER BY HIGH-ENERGY PROTONS

V. P. SHAMOV

Radium Institute, Academy of Sciences, U.S.S.R.

Submitted to JETP editor February 18, 1958

J. Exptl. Theoret. Phys. (U.S.S.R.) 35, 316-321 (August, 1958)

Certain parameters for fission of silver induced by protons with energies ranging from 300 to 660 Mev are investigated. An analysis of the experimental data reveals that (1) fission of silver by high-energy protons is characterized by fragments which are predominantly of equal mass; (2) the fission cross section shows no essential change in the region of incident-proton energy which was investigated ($\sigma_f = (3.2 \pm 1) \times 10^{-28}$ cm^2); (3) a large number of charged particles are emitted in fission, indicating a high initial excitation for the fissioning nucleus.

A complete yield curve for the residual nuclei as a function of charge is given along with the differential yield curves for various nuclear interactions: spallation, fission and cascade-evaporation.

EXPERIMENTAL DATA

AT the present time there is available a large body of data concerned with fission in the heavy nuclei (U, Th, Bi) at the end of the periodic table. There is also some information concerning fission of lighter nuclei such as W and Ta. The situation is entirely different with respect to fission of elements at the middle of the periodic table. Aside from the fact that fission does occur in these elements[1] little else is known.

In the present work, using nuclear emulsions, an attempt has been made to obtain certain preliminary information on fission of silver by high-energy protons. A fine-grain nuclear emulsion ("P 9 - sensitive"), sensitive to 45-Mev protons, was irradiated in the intense proton beam from the synchrocyclotron of the Joint Institute for Nuclear Research. The entire area through which the proton beam passed was then scanned with a microscope (all the plates were irradiated with the beam perpendicular to the surface of the emulsion; the same collimator (diameter d = 2 cm) was used in all experiments).

In carrying out the analysis, only those events were selected in which, in addition to the other nuclear disintegration products, (α, p) there were two tracks of highly ionizing fragment-type particles. In order to distinguish the fission events from spallation in heavy elements of the emulsion, we arbitrarily assigned to fission only those events in which the range ratio for the two

TABLE I

l, cm	E'_p, Mev	N	N_p	N_f	N_{AgBr}	σ_f (AgBr)	$\Delta\sigma_f$	$\overline{n}_{\alpha,p}$	$\overline{L},\mu$
0	660	104	$2.14\cdot10^8$	15	$2\cdot10^{20}$	$3.5\cdot10^{-28}$	$1\cdot10^{-28}$	6.5	15
10	500	111	$2.22\cdot10^8$	12	$2\cdot10^{20}$	$2.7\cdot10^{-28}$	$1\cdot10^{-28}$	5.7	16
20	300	118	$2\ \ \cdot10^8$	13	$2\cdot10^{20}$	$3.3\cdot10^{-28}$	$1\cdot10^{-28}$	6.3	15

*l is the thickness of the copper absorber through which the proton beam passes (E_p = 460 Mev); E_p is the proton energy after the absorber; N is the number of pulses counted by the ionization chamber which is calibrated for a proton energy E_p = 660 Mev (one count corresponds to a flux of 2.06×10^6 protons with E_p = 660 Mev); N_p is the number of protons after passage through a collimator 2 cm in diameter; N_f is the number of fissions found in an area $S = 3.14$ cm^2, the area of the collimator; N_{AgBr} is the number of silver nuclei and bromine nuclei in the emulsion of thickness $T = 100\mu$ and area $S = 1$ cm^2; σ_f is the silver-bromine fission cross section obtained under the assumption that σ_f(Ag) = σ_f(Br); $\overline{n}_{\alpha,p}$ is the mean number of charged particles (α, p) found in one fission event; L is the mean range of the fission fragments.

fragments was less than two ($l_l/l_h \leq 2$).* In spallation the range ratio between the multiply charged particle and the recoil nucleus is considerably greater than two. The emulsion contains two kinds of heavy nuclei (Ag and Br) in addition to light nuclei (C, N, O, H). Since it is difficult to distinguish between effects due to these heavy nuclei, in what follows we shall assume that the fission parameters† for Ag and Br are the same in high-energy, proton-induced fission. When this assumption is made, silver fission cross section may be somewhat low, but in preliminary data of this kind this fact is not of great importance.

The result of an analysis of fission events in Ag and Br are given in Table I.

As is indicated by Table I the fission cross section for silver remains essentially constant $\sigma_f = (3.2 \pm 1) \times 10^{-28}$ cm^2 over a wide range of incident-proton energies (E_p = 300 to 660 Mev). Furthermore, fission is generally characterized by the emission of a large number of charged particles; this number is essentially constant in the indicated incident-proton energy range. The average total fission-fragment range is considerably greater than that found in fission of heavier nuclei such as U, Th, Bi and W.

In order to investigate the symmetry characteristics of the fission process an investigation was made of the range ratio for the fission fragments. The results of this analysis are given in Table II.

TABLE II

Range ratio l_l/l_h	Percentage of cases with a given range ratio
1—1.15	42
1.15—1.30	14
1.30—1.45	11
1.45—1.60	9
1.60—1.75	11
1.75—1.90	6.6
1.90—2.05	6.5

Examination of the table shows that the most probable fission process is the one in which two fragments of approximately equal range are produced; thus, in fission of nuclei at the middle of the periodic table, just as in fast proton-induced fission of heavy nuclei, the most probable process is symmetric fission.

An approximate charge distribution for the fission fragments can be obtained by assuming that the fragment range ratio is related to the fragment charge ratio as follows:

$$l_l / l_h \approx (Z_h / Z_l)^{2/3}. \tag{1}$$

The relation given in (1) may be derived on the basis of the following considerations:

1. According to the Bohr formula,[2] for equal velocities $v_\alpha = v_f$ the range ratio for a fragment and an α particle is given by:

$$\frac{R_f}{R_\alpha} \approx 7 \left(\frac{l^2}{\hbar v}\right)^2 \frac{A_f}{Z_f^{2/3}}; \tag{2}$$

2. The dependence of α-particle range on velocity (for velocities $v_\alpha \approx 10^9$ cm/sec) is given by the Geiger relation

$$R_\alpha \approx k_1 v_\alpha^3. \tag{3}$$

Thus, if the velocity of the α particle is equal to the velocity of the fragment, the fragment range is

---

*The subscripts "l" and "h" refer to the light fragment and the heavy fragment respectively.

†By fission parameters we mean the following: fission cross section, mean number of charged particles per fission, distribution over number of charged particles, fragment range ratio (l_π/l_h) etc.

$$R_f \approx \gamma p_f / Z_f^{2/3}, \tag{4}$$

where $\gamma = 7k_1(l^2/\hbar^2)^2$ and $p_f = v_f A_f$ is the fragment momentum.

At fission the momenta of the fission fragments are equal $(P_f)_h = (P_f)_l$; thus, solving Eq. (4) for the ranges of the light fragment and the heavy fragment and taking the range ratio we obtain the expression given in (1)

$$(R_f)_l / (R_f)_h = (Z_f)_h^{2/3} / (Z_f)_l^{2/3}.$$

The validity of (1) can be demonstrated in the case of uranium fission by slow neutrons, where the range ratio and the charge ratio (for the most probable fission case) are well known.

Using (1), we obtain the following expressions for the charge of the light fragment and the heavy fragment:

$$Z_l = \frac{Z_f}{1 + (l_l / l_h)^{3/2}}; \quad Z_h = Z - Z_l; \tag{5}$$

$$Z_f = Z_0 - n_1(\mathrm{H}_1^1) - 2n_2(\mathrm{He}_2^4),$$

where Z_f is the total charge of the light and heavy fragments, Z_0 is the charge of the original nucleus (Ag or Br), n_1 is the number of protons associated with the fission event, and n_2 is the number of α particles associated with the fission event.

The further analysis of the fragment charge distribution is based on the assumption that $Z_0 = Z_{Ag}$, i.e., all fissions are assumed to occur in silver. To obtain the fragment charge distribution for silver fission, we thus determine in each case the number of protons, α particles, and the range ratio l_l/l_h and then, using (1) and (5), the charges Z_l and Z_h.

The results of this analysis are given in Table III.

TABLE III

Charge of the fission fragment Z_l/Z_h	Number of fragments with a given charge	Cross section for the formation of a fragment with a given charge (10^{-9} cm^2)
12	0	
13	2	1.4
14	1	0.7
15	6	4.3
16	8	5.7
17	9	6.4
18	9	6.4
19	13	9.3
20	13	9.3
21	9	6.4
22	8	5.7
23	6	4.3
24	3	2.1
25	2	1.4
26	0	0
27	1	0.7

It is evident from the values given in the table that the most probable fragment charge in silver fission is Z = 19 to 20; the cross section for the formation of these fragments is approximately 0.1 millibarns which, as will be shown below, is approximately two orders of magnitude greater than the cross section for the production of a multiply-charged particle with Z = 19 to 20 in spallation.

YIELD OF RESIDUAL NUCLEI AS A FUNCTION OF CHARGE IN SPALLATION

In certain interactions between fast nucleons with nuclei, the disintegration products include particles with Z ≥ 4 in addition to light charged particles (α, p). The nucleon process that gives rise to these multiply charged particles is usually called spallation. The spallation process in nuclear emulsions has been investigated in considerable detail in a dissertation by Lozhkin.[3] Using the data reported in this work (the total cross section for the formation of spallation products in Ag and Br at an incident proton energy E_p = 460 Mev and the relative yield of spallation products with a given charge (Z_f) we can determine the cross section for the formation of various spallation products from silver nuclei, once again assuming that the spallation process is the same in Ag and Br.

In Fig. 1 (curve B) the circles denote the cross section for the formation of spallation products from Ag with charges Z_f = 4 to 14 at an incident proton energy E_p = 460 Mev. Because this curve is linear over a wide region of Z, it is legitimate to extrapolate to the region of higher charge, making it possible to estimate the cross section for the

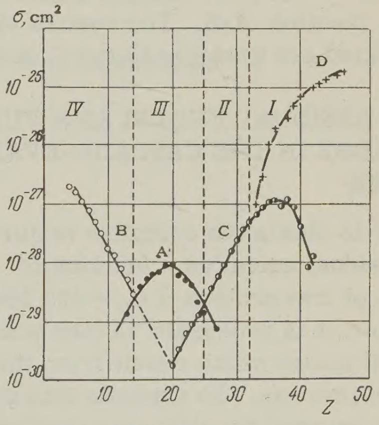

FIG. 1. Production cross sections: (A) fission fragments, (B) light spallation fragments, (C) residual nuclei resulting from spallation, (D) residual nuclei resulting from the cascade-evaporation process. All refer to the interaction of 460-Mev protons with silver.

production of spallation products with charge Z = 19 to 20. It is apparent from the curve that the cross section for the formation of spallation product with charge Z = 20 is of the order of 2×10^{-30} cm^2, that is 50 times smaller than the cross section for the formation of a fission fragment of the same charge in silver fission.

The yield of residual nuclei as a function of charge in spallation can be obtained from the distribution of stars, using the number of light charged particles which appear in spallation. If we select a spallation product of given charge, Z_f = const, the charge of the residual nucleus as a function of Z for the given spallation process is determined by the number of light charged particles which appear:

$$Z_{\text{res. nuc.}} = Z_{\text{Ag}} - Z_f - \Delta Z,$$

where $\Delta Z = n_1 (H_1^1) + 2n_2 (H_2^4)$. If α/p = const (in spallation of Ag and Br, α/p = const = 0.5), then $\Delta Z = 1.33\, n_{\alpha,p}$ and consequently

$$Z_{\text{res. nuc.}} = Z_{\text{Ag}} - Z_f - 1.33\, n_{\alpha p}.$$

Knowing the cross section for a spallation product with a given charge (curve B, Fig. 1) and the probability for the emission of a given number of light charged particles in spallation $W(n_{\alpha,p})_i$, we can estimate the cross section for a residual nucleus with a given charge

$$\sigma_{\text{res. nuc.}} (Z_J) = \sigma_f (Z_f)\, W (n_{\alpha p}).$$

Summing the yields of the residual nuclei with given Z_J resulting from the various processes (Z_f = 4 to 20) we obtain the total yield of residual nuclei as a function of Z. The results of an analysis of this kind are given by Curve C of Fig. 1.

YIELD OF RESIDUAL NUCLEI AS A FUNCTION OF CHARGE IN THE CASCADE-EVAPORATION PROCESS

In order to obtain the complete picture of the yield of residual nuclei as a function of Z in the interaction of fast protons (E_p = 460 Mev) with silver nuclei, it is necessary to take account of the residual nuclei which result from the cascade-evaporation process. To evaluate this part of the yield curve we used the data reported by Ostroumov[4] on the interaction of protons (E_p = 460 Mev) with heavy emulsion nuclei. Knowing the total cross section for the inelastic interaction of fast protons with silver nuclei $\sigma_{\text{inelast.}} \approx 10^{-24}$ cm^2 and the relative yield of stars with a given number of prongs $W(n_{\alpha p})_i$, we can determine the yield of residual nuclei as a function of Z from the following relation:

$$\sigma_{\text{res. nuc.}} (Z_J) = \sigma_{\text{inelast.}} W (n_{\alpha p})_i;$$
$$Z_J = Z_{\text{Ag}} - \Delta Z_{\alpha p};\ \Delta Z_{\alpha p} = \left[\frac{n_{\alpha p}}{1 + (\alpha/p)}\right](2\alpha/p + 1).$$

An analysis of the yield of residual nuclei as a function of Z in cascade-evaporation gives the values shown in Fig. 1 (curve D). Summing all the yields for a given Z we determine the total yield resulting from all three processes: cascade-evaporation, spallation and fission. The total curve showing yield of residual nuclei as function of Z is given in Fig. 2.

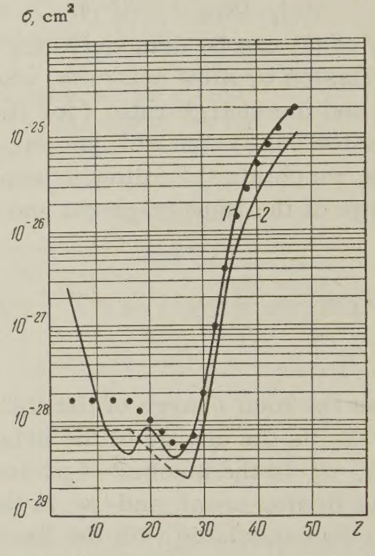

FIG. 2. Total yield curve for various elements produced in the disintegration of silver nuclei by 460-Mev protons. (1) Data of the present work, (2) curve obtained by a radiochemical method.[1] ● – values obtained by normalizing the radiochemical curve to the present curve at the point of highest yield.

DISCUSSION OF RESULTS

In analyzing the total yield for various nuclei produced in the interaction of fast protons with silver nuclei (Figs. 1 and 2) it is convenient to divide the curve into four sections I, II, III, and IV.

(1) Region I: Z ≥ 32. In this region the residual nuclei are formed chiefly in the cascade-evaporation process and are not connected with spallation or fission.

(2) Region II: 25 ≤ Z ≤ 32. The residual nuclei in this region are due chiefly to spallation.

(3) Region III: 15 ≤ Z ≤ 25. In this region of Z the nuclei are formed predominantly as a result of fission.

(4) Region IV: 4 ≤ Z ≤ 15. The multiply charged ions in this region are predominantly spallation products.

Obviously, the boundaries indicated above are arbitrary, since these regions overlap.

The yield curve obtained in the present work, using an emulsion method, is similar to the yield curve obtained by a radiochemical method[1] (curve 2, Fig. 2) in the region $Z > 26$. The numerical values for the yields in this region do not differ from the present values by more than a factor of 2 or 2.5. If curves are normalized at the highest yield (black dots in Fig. 2) the agreement in this region of Z is even more striking.

For silver irradiated by 480-Mev protons the radiochemical work, after summation of all the yields, gives a total inelastic cross section $\sigma = 0.43 \times 10^{-24}$ cm^2 whereas direct measurements[5] of the inelastic cross section for 660-Mev protons with nuclei in the silver region (Sn) give $\sigma = 1.2 \times 10^{-24}$ cm^2. Thus, the total yield curve in the region $Z > 26$ obtained by the radiochemical method is in good agreement with the general shape of the present curve but gives yield values which are too low.

In the region $Z \leq 15$ the data obtained in the present case differ basically from the data obtained by the radiochemical method.[1] In this region the radiochemical method does not give a true picture. There is little doubt that the radiochemical results are more reliable in the region $25 \leq Z \leq 32$ than in the region $Z \leq 15$. Since our yields in this region of Z $(4 \leq Z \leq 15)$ were obtained by calculation, starting from the experimentally obtained yields[3] of multiply charged ions $(4 \leq Z \leq 15)$ and the agreement of the present data with the radiochemical data in the region $25 \leq Z \leq 32$ is rather good, it would seem that the present results on the yield of multiply charged ions $4 \leq Z \leq 15$ are as reliable as the data obtained radiochemically in the region $25 \leq Z \leq 32$.

In the fission-fragment region $15 \leq Z \leq 25$ the present data also differ from the data obtained by radiochemical methods. This discrepancy lies essentially in the fact that the present data lead to a yield curve which exhibits a maximum, indicating symmetric fission for silver, whereas the yield curve obtained radiochemically indicates a predominance of asymmetric fission. However, the statistics used in the present data are still rather inadequate so that the numerical values in this work must be considered as tentative.

In conclusion the author wishes to take this opportunity to thank Professor N. A. Perfilov for a number of valuable comments in discussing the present work. The author is also indebted to O. V. Lozhkin, V. I. Ostroumov and V. F. Darofskii for making certain invaluable data available to the author.

---

[1] B. V. Kurchatov and V. N. Mekhedov, Сессия АН СССР по мирному использованию атомной энергии (Conference of the Academy of Sciences USSR on the Peaceful Use of Atomic Energy), Acad. Sci. Press, p. 178 (1955).

[2] N. Bohr, Kgl. Danske Videnskab. Selskab, Mat-fys. Medd. **18**, 8 (1948).

[3] O. V. Lozhkin, Dissertation, Radium Institute, Leningrad, (1957).

[4] V. I. Ostroumov, J. Exptl. Theoret. Phys. (U.S.S.R.), **32**, 3 (1957), Soviet Phys. **5**, 12 (1957).

[5] V. I. Moskalev and B. V. Gavrilovskii, Dokl. Akad. Nauk SSSR, **110**, 972 (1956), Soviet Phys. "Doklady" **1**, 607 (1956).

Translated by H. Lashinsky
61

INVESTIGATION OF 15 TO 65-Mev PROTONS PRODUCED IN THE PHOTODISINTEGRATION OF ALUMINUM AND NICKEL

E. B. BAZHANOV, Iu. M. VOLKOV, and L. A. KUL' CHITSKII

Leningrad Physico-Technical Institute

Submitted to JETP editor February 27, 1958

J. Exptl. Theoret. Phys. (U.S.S.R.) **35**, 322-327 (August, 1958)

The angular distributions of photoprotons from aluminum and nickel were investigated for a peak bremsstrahlung energy $E_{\gamma\max} = 85$ Mev, and the energy distributions of photoprotons from Al were obtained at angles of 30°, 90° and 130° for $E_{\gamma\max} = 90$ Mev. The results are discussed from the point of view of the interaction of γ rays with nuclei through the quasi-deuteron mechanism.

1. SHORT DESCRIPTION OF THE EXPERIMENT

THE present work is a continuation and development of the work, the results of which were published in an earlier short note.[1] The investigation of the angular and energy distributions of protons was carried out with the 100-Mev synchrotron of the Physico-Technical Institute. The arrangement of the apparatus used in the experiment described below is shown in Fig. 1. Products of photonuclear reactions are registered by two scintillation telescopes, each consisting of two counters. A short description of the telescope arrangement and counting scheme was given in reference 1. The telescopes could be turned in the horizontal plane through the desired angle θ relative to the direction of the γ-rays to an accuracy of better than ± 1°. A target of the desired material was placed in the center of the table. In the study of the proton angular distribution, cylindrical targets were used. These were made of foils of thickness 110 μ for aluminum and 50 μ for nickel.

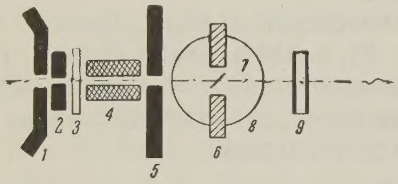

FIG. 1. Arrangement of the apparatus. 1) shielding wall of Pb, 2 and 5) lead collimators, 3) monitor, 4) magnet to clean the beam, 6) telescopes, 7) target, 8) table, 9) standard chamber.

The diameter of the cylindrical targets was 1.6 cm and the diameter of the beam cross section at the point at which the targets were placed was 2.2 cm. In studying the proton energy spectra, flat targets of area more than twice the beam cross section were used. The thickness of the aluminum target was 150 μ. In taking the angular distributions at 60, 75, 90 and 120°, the distance from the center of the target to the crystal of the first counter was 16.7 cm. At angles 25° and 40°, the telescopes were moved outwards to a distance of 23.7 cm. In order to combine data obtained at small and large angles, measurements at 60° were carried out with the telescopes in both positions, and the data were then correspondingly normalized.

In counting heavy charged particles, one must pay special attention to the possibility of counts coming from the sum of pulses from several electrons incident on the telescope within the resolving time of the counting system. The probability of such a count increases with increasing atomic

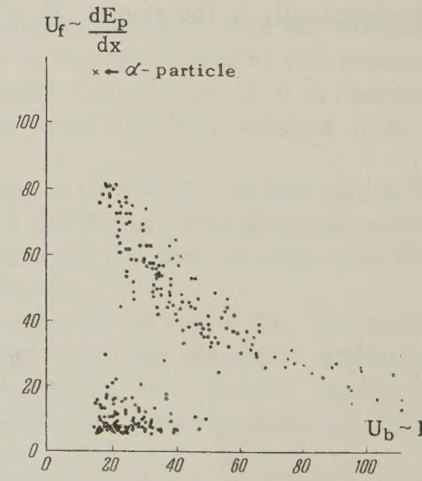

FIG. 2. Illustration of the resolving power of the telescopes: separation of heavy charged particles and electrons in the case of Au at angle 90°; U_f and U_b are the magnitudes of the pulses from the front and back counters, respectively.

number of the element, and also increases in going to small angles relative to the γ-ray beam. The construction chosen for the telescope made it possible to separate the contributions from heavy charged particles and electrons. To determine this, the pulses from both counters were fed after amplification into a double-beam oscilloscope (type OK17M), the horizontal sweep of which was triggered by pulses from the coincidence circuit to which the outputs of both counters of the telescope were connected. Pulses on the screen of the oscilloscope were photographed. Figure 2 illustrates the capabilities of the telescope with respect to the separation of particles emitted from gold at 90°. The abscissa is the amplitude of the pulse (in relative units), proportional to the energy loss of the particle in the crystal of the rear counter. The ordinate is the amplitude of the pulse, proportional to the energy loss of the same particle in traversing the thin crystal of the front counter of the telescope. The lower left group of points corresponds to pulses from electrons; the upper group of points to heavy charged particles. The pulse of an α particle of energy 8.78 Mev from Th C′ is shown by the cross. Using a differential pulse-height analyzer on the rear counter and several integral discriminators on the front counter, it is easy to separate off the electrons, taking here several proton energy intervals.

In this experiment the different types of heavy charged particle were not separated, although a special check, carried out with a telescope of similar construction, but with higher resolving power[2] which made it possible to distinguish between protons and deuterons, showed that the contribution of deuterons in the elements studied was less than 5% for the proton energies counted, and could not change the experimental results essentially. The contribution of tritons and α particles was in general negligible.

2. INTRODUCTION OF CORRECTIONS, ESTIMATES OF ERRORS

In the preliminary processing of results of the measurements of the energy spectra of protons, the data were reduced to 1-Mev proton-energy intervals by dividing the total number of counts in the energy interval of acceptance of a given channel of the pulse-height analyzer by the width of the interval in Mev.

The number obtained could be ascribed to the mean energy of the interval, E_m, defined as the arithmetic mean of the limits E_1 and E_2, only after introduction of several corrections which took into account the decreasing nature of the spectrum with increasing photon energy. The correction factor α_1 can be calculated from

$$\alpha_1 = E_{\mathrm{cp}}^{-\delta}(E_2 - E_1)(1-\delta)/(E_2^{1-\delta} - E_1^{1-\delta}). \tag{1}$$

This formula was obtained under the assumption that the proton spectrum is described by the law $n(E_p) = kE_p^{-\delta}$, which, for the comparatively narrow proton energy intervals used ($\Delta E_p/E_p \approx 20\%$), is a completely satisfactory approximation. In addition to this, it is necessary to correct for the loss in energy of the protons in going through the target. If we count protons with energies in the interval $E_1 - E_2$ ($E_1 < E_2$), defined at the entrance to the telescope, then some protons with energies near to E_1 will be lost because of the finite thickness of the target and, at the same time, some protons with energies slightly larger than E_2 will be included. The correction factor α_2 can be determined by a numerical integration which splits the target into a number of layers, in each of which a power law for the change in proton spectrum with energy is assumed for a small energy interval. The total correction factor for the aluminum target of thickness 150 μ was 13% for a proton energy $E_p = 15.4$ Mev, 1% for $E_p = 36.7$ Mev, and 6% for $E_p = 49.8$ Mev.

The dependence of the total corrections on the magnitude of δ was very weak. Changing δ by a factor of 3 or 4 changed the correction, in absolute value, by less than 20%.

Corrections for multiple scattering and nuclear absorption, estimated for the crystal of the front counter, amounted to only a fraction of a per cent and were not introduced.

The maximum value of $\Delta\theta$, characterizing the angular resolution of the telescope, was ±6.5°. In the practical case, as an estimate showed, about 75% of the protons went within the angular limits ±3.5°.

The background in various experiments was equal to 15% on the average, although at small angles it increased to 25 or 30%, depending on the proton energy.

Both the relative and absolute measurements of the total energy of the γ rays traversing the target were carried out with an apparatus devised by Kruglov.[3] An aluminum ionization chamber with front wall of thickness 4 mm, connected to a stable beam integrator, served as monitor. The stability of operation of the monitor was ~2%. Absolute measurements were carried out using a thick-walled copper standard chamber, calibrated by the calorimetric method.[4] The accuracy of absolute calibration for the maximum bremsstrahlung energy, $E_{\gamma\max} = (90 \pm 5)$ Mev, was 4%.

The energy spectra of protons from Al were given below in units $\mathrm{cm}^2 \times 10^{30}$/sterad-Mev-Q. The relative mean square error, taking into account statistical errors, the mean square error in the number of effective quanta Q, the error in definition of the solid angle, and a series of others, constituted 16% for 30-Mev protons.

3. EXPERIMENTAL RESULTS AND DISCUSSION

(a) Angular Distributions of Protons from Aluminum and Nickel

The angular distributions obtained for several proton energy intervals at maximum bremsstrahlung energy $E_{\gamma\max} = 85 \pm 5$ Mev are given in Figs. 3 and 4. A general characteristic of the distributions is the rise of the anisotropic parts and the increased shift of the maxima of the angular distributions with increasing proton energy.

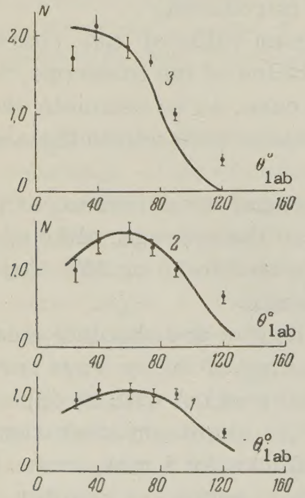

FIG. 3. Angular distributions of photoprotons from Al. The solid curves give the results of calculation. Only statistical errors are shown. 1) E_p = 13.7-17.5; 2) E_p = 17.5-21.5; 3) E_p = 21.5-41.0 Mev.

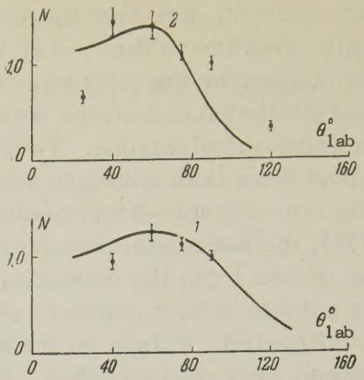

FIG. 4. Angular distributions of photoprotons from Ni. The solid curves give the results of calculation. Only statistical errors are shown. 1) E_p = 13.7-21.5; 2) E_p = 21.5-33.3 Mev.

In order to clarify the role of the quasi-deuteron interaction mechanism of γ rays with Al and Ni nuclei, it is of interest to compare the data obtained with the angular distributions of protons from the photodisintegration of the deuteron. Levinger[5] employed the theoretical cross sections for photodisintegration of the deuteron calculated in references 6 and 7 which, as is well known,[8,9] diverge from the experimental data for γ-ray energies exceeding 50 Mev. We used the experimental curves of the cross section for photodisintegration of the deuteron obtained by Allen[8] and Whalin et al.[10] transposed to the laboratory system. The solid curves in Figs. 3 and 4 were constructed by calculating the integral proportional to the yield of protons $Y(\Delta E_p)$ with energies corresponding to interval $\Delta E_p = E_{p2} - E_{p1}$,

$$Y(\Delta E_p) \sim \int_{E_\alpha}^{E_\beta} N_\gamma(E_\gamma)\,\sigma_d(E_\gamma)\,dE_\gamma. \tag{2}$$

Here $N_\gamma(E_\gamma)$ is the number of γ rays of energy E_γ in the bremsstrahlung spectrum (using the spectrum of Schiff), E_α and E_β are the energies of γ rays corresponding to the production of protons of energies E_{p1} and E_{p2}, respectively. The connection between the γ-ray energy and proton energy is determined by the well-known kinematical relation

$$E_\gamma = 2E'_p/\left(1-\frac{E'_p}{M}+\frac{p}{M}\cos\theta\right), \tag{3}$$

which follows from the conservation laws. Here $E'_p = E_p + E_B$, $\sigma_d(E_\gamma)$ is the cross section for photodisintegration of the deuteron for a γ ray of energy E_γ and a given angle θ_{lab}. The results of the calculation were obtained by numerical integration under the assumption that the residual nucleus is left in the ground state. The curves obtained were normalized so that they coincided with the experimental points at $\theta_{\mathrm{lab}} = 60°$ for all proton-energy intervals.*

In the case of aluminum, the complete agreement of the calculated curves with the experimental points is striking. This serves to indicate the essential contribution of the quasideuteron mechanism for the interaction of γ rays with the Al

---

*In the corresponding graphs presented in the report to the Conference on Nuclear Reactions at Low and Medium Energies (Moscow, November 1957), the comparison was less precise. These curves gave the change in the cross section for deuteron photodisintegration $\sigma_d(E_p)$ with the angle θ_{cm} for protons of energy E_p corresponding to the mean energy of the energy interval chosen.

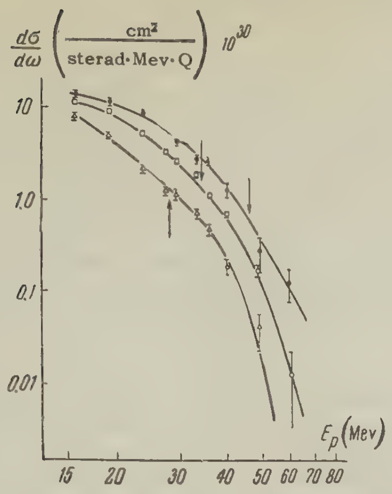

FIG. 5. Energy distributions of photoprotons from Al for various angles, $E_{\gamma\max} = 90$ Mev. Only statistical errors are shown. ● – $\theta = 30°$; ○ – $\theta = 90°$; $\Delta - \theta = 130°$.

nucleus. The deviations of the experimental points from the calculated curves in the interval from 21.5 to 41.0 Mev at small and large angles can be understood if one takes account of the fact that in the production of protons of a given energy E_p, quanta of significantly higher energy are needed in the case of the quasi-deuteron mechanism than in the case of the direct photoeffect, and this difference increases with increasing angle θ. The bremsstrahlung spectrum of the γ rays falls with energy and is limited by $E_{\gamma\max}$. Thus, for comparatively large proton energies, the relative contribution of the direct photoeffect should increase. This effect should first of all show up at large angles. It should be noted that if the angular distribution of protons from the direct photoeffect is described by a law well approximated by $a + b\sin^2\theta\,(1 + c\cos\theta)^2$ and has a maximum shifted to larger angles than in the calculated curves shown in Fig. 3, then a 20 to 30% contribution from the direct photoeffect is sufficient to obtain agreement with experiment for all angles.

For nickel, the agreement with the calculated curves is worse. Especially noticeable is the sharp fall in the points at small angles. It is possible that the contribution from the direct photo effect (or some other mechanism) is larger.

(b) Energy Spectrum of Protons from Aluminum

The energy spectra of protons from Al, taken at angles $\theta_{\text{lab}} = 30$, 90, and 130° for $E_{\gamma\max} = 90 \pm 5$ Mev are given in Fig. 5.

Starting from the idea of the quasi-deuteron mechanism of interaction, one would expect the slope to increase with angle. The determination of the slopes of the spectra in their initial parts is difficult, because the spectra change their slope smoothly and can only approximately be described by the power law $n(E_p) \sim E_p^{-\delta}$. The table lists the approximate values of δ, and for comparison, also values of the slopes for energy spectra of protons from the photodisintegration of deuterium, calculated from the data of references 8 and 9.

θ	δ	
	Al	D
30°	2.1	2.3
90°	2.8	2.6
130°	3.2	2.8

It can be seen from the deuteron data that one should not expect a strong change with θ in the slopes of the energy spectra of protons from aluminum.

The arrows in Fig. 5 indicate the positions of the kinematical cutoffs, determined by Eq. (3), taking the minimum binding energy of the proton in Al to be 8.2 Mev. Sharp changes were not observed in the spectra at energies near the kinematical cutoff. The relatively smooth, but increasing rate of drop (instead of a sharp drop) of the spectra can be caused, on the one hand, by the momentum distribution of protons inside the nucleus, and, on the other hand, by the fact that the direct photoeffect, in this region of energies, can contribute relatively more. The shift in the position of the kinematical cutoff with changing angle shows up possibly only in the fact that the spectra of the higher-energy protons drop off more strongly with the angle than at low energies, and that as the angle increases, this drop begins at lower energies.

In Fig. 6 the experimental spectrum of protons from Al at $\theta = 90°$ is compared with the energy spectrum calculated as done by Levinger.[5]

In the calculations (curve 1) we employed the experimental spectrum of protons in the photodis-

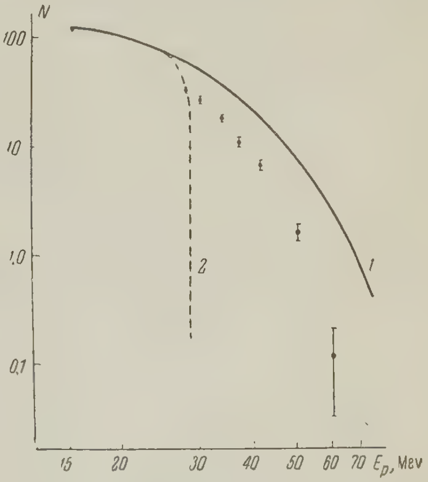

FIG. 6. Comparison of the experimental energy spectrum of photoprotons from Al with the one calculated for $\theta = 90°$.

integration of deuterium, the spectrum of γ rays of Schiff with $E_{\gamma\max} = 90$ Mev, and a Gaussian distribution of nucleon momenta in the nucleus, with parameter $E_0 = 10$ Mev. Curve 2 gives the spectrum with the momentum distribution disregarded.

The experimental curve falls more sharply at high energies than the calculated one.

Taking into account the possibility of the role of the direct photoeffect increasing for high proton energies in our experiments, where the γ-ray spectra was limited by $E_{\gamma\max} = 90$ Mev, we can probably explain the results of the experiment satisfactorily. Choice of a more sharply falling momentum distribution also improves the agreement with experiment.

Thus, the qualitative features of the proton energy spectra, obtained at various angles in Al, and also comparison of the angular distributions of protons for Al and Ni with curves calculated from the quasi-deuteron model, indicate that the quasi-deuteron mechanism of interaction may give a substantial contribution in the case of Al. At the same time it is also very probable that the direct photoeffect also gives an important contribution.

[1] Bazhanov, Volkov, Komar, Kul'chitskii and Chizhov, Dokl. Akad. Nauk SSSR **113**, 65 (1957), Soviet Phys. "Doklady" **2**, 107 (1957).

[2] Bazhanov, Volkov, Komar, Kul'chitskii, Chizhov, and Iavor, Report at the Conference on Nuclear Reactions at Low and Medium Energies, Moscow, November, 1957 (in press).

[3] S. P. Kruglov, J. Exptl. Theoret. Phys. (U.S.S.R.) **33**, 1060 (1957); Soviet Phys. JETP **6**, 817 (1958).

[4] S. P. Kruglov, J. Tech. Phys. (U.S.S.R.) (in press).

[5] J. S. Levinger, Phys. Rev. 84, 43 (1951).

[6] L. I. Schiff, Phys. Rev. **78**, 733 (1950).

[7] J. F. Marschall and E. Guth, Phys. Rev. **78**, 738 (1950).

[8] L. Allen, Phys. Rev. **98**, 705 (1955).

[9] Aleksandrov, Delone, Slovokhotov, Sokol, and Shtarkov, J. Exptl. Theoret. Phys. (U.S.S.R.) **33**, 614 (1957), Soviet Phys. JETP **6**, 472 (1958).

[10] Whalin, Schriever, and Hanson, Phys. Rev. **101**, 377 (1956).

Translated by G. E. Brown
62

SOVIET PHYSICS JETP VOLUME 35(8), NUMBER 2 FEBRUARY, 1959

MAGNETIC PROPERTIES OF METALS AT LOW TEMPERATURES. IV. INFLUENCE OF HOMOGENEOUS COMPRESSION ON THE DE HAAS – VAN ALPHEN EFFECT IN ZINC CRYSTALS

I. M. DMITRENKO, B. I. VERKIN, and B. G. LAZAREV

Physico-Technical Institute, Academy of Sciences, Ukrainian S.S.R.

Submitted to JETP editor March 3, 1958

J. Exptl. Theoret. Phys. (U.S.S.R.) 35, 328-339 (August, 1958)

A method and apparatus have been developed to investigate the influence of homogeneous compression on the anisotropy of the magnetic properties of crystals at low temperatures. The angular dependence of the oscillation periods of the magnetic susceptibility of free zinc crystals due to the two smallest groups of mobile charges has been established. The effect of homogeneous compression at a pressure of 1700 kg/cm^2 on the period and amplitude of the oscillations due to the smallest group of mobile charges has been investigated. A large (40 to 48%) increase in the periods of these oscillations has been found for all values of the angle θ between the field vector and the direction of the principal axis. The homogeneous compression of the crystal is found to cause a strong decrease of the oscillation amplitude and a change in the temperature dependence of the oscillation amplitude. The experimental data are compared with the semi-phenomenological theory of the influence of deformations on oscillation effects in metals at low temperatures.

1. INTRODUCTION

THE homogeneous compression of crystals, or in other words, the homogeneous and large elastic deformation of the lattice, is one of the most direct methods of external action on the periodic electric field within the crystal, meaning also on the electronic properties of metals (conductivity, magnetic and galvanomagnetic phenomena, etc.)

For a long time experimental investigations of the effect of homogeneous lattice compression on the electric properties of metals have been carried out at high temperatures (room temperature and higher), because Bridgman had developed for these experimental conditions a method for the production and measurement of sufficiently high pressures. The development by one of the authors and by Kan[2] of the "ice method" for producing high pressures made it possible, for the first time, to extend experimental investigations of this kind to the more interesting low-temperature region and, in particular, to investigate in detail the effect of homogeneous lattice compression on the superconductivity of a number of metals.[3] The results of these experiments, together with the study of the isotope effect in superconductivity phenomena (e.g. reference 4), gave evidence of the specific interaction of the electrons with the metal lattice, which later on proved so important for the development of a microscopic theory of superconductivity.

In recent years Alekseevskii and his co-workers used the "ice method" to produce high pressures in order to investigate the effect of homogeneous compression on the electromagnetic phenomena in bismuth[5] at low temperatures. Very recently an investigation has been carried out on the effect of homogeneous lattice compression on the temperature variation of the electrical conductivity of a number of metals.[6]

The effect of homogeneous compression on the magnetic properties of crystals was not studied for a long time even at higher temperatures, because the known methods for producing high pressures could not be applied to the measurement of magnetic susceptibility. The systematic investigation of the magnetic properties of unconstrained crystals of feebly magnetic metals at low temperatures led to the discovery of the de Haas — van Alphen effect in a large group of metals[7,8] and to the establishment by Lifshitz et al.[9] of a connection between this phenomenon and the problem of the energy distribution of charge carriers in metals — one of the most important problems of metal physics. It became essential to clarify the effect of the homogeneous compression of the crystal on the de Haas — van Alphen effect, and thus on the energy distribution of charge carriers in metals.

A method and apparatus were developed in the low-temperature laboratory of the Physico-Technical Institute of the Academy of Sciences of the U.S.S.R. to study the effect of homogeneous compression on the anisotropy of the magnetic properties of crystals at low temperatures. Some results of such investigations, made on crystals of bismuth and zinc, have been published previously (references 10 and 11).

This paper is devoted to the description of a method for investigating the effect of homogeneous compression on the anisotropy of the magnetic properties of crystals, to the discussion of the results of investigations concerning the de Haas — van Alphen effect on zinc crystals under homogeneous compression, and also to the comparison of the experimental data with the theory of the phenomenon. Furthermore, some new information is given on the de Haas — van Alphen effect in unconstrained zinc crystals.

2. METHOD AND APPARATUS

The method of investigation consisted of measuring the torque acting on a small anisotropic crystal placed inside a massive but magnetically isotropic high pressure bomb, suspended by means of a thin elastic thread in a homogeneous magnetic field. The homogeneous compression of the crystal was brought about by the "ice method," i.e., by freezing water inside the bomb.[10]

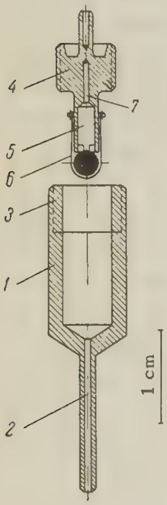

FIG. 1. Pressure bomb for investigation of the magnetic anisotropy of homogeneously compressed crystals.

A diagram of one of the most convenient high-pressure bombs is shown in Fig. 1. The bomb, made of pure beryllium bronze,* consists of the body 1 with capillary 2 and thread 3 into which bronze stopper 4 with crystal holder 5 can be screwed. The crystal holder consists of a thin-walled copper tube (copper tube and stopper are made in one piece) with four perpendicular lugs and with side windows. The cavity 7 in the stopper serves to center the crystal in the crystal holder.

The crystal is initially oriented on the platform of a goniometer and a thin quartz stick is attached to it (in the direction coinciding with the axis of suspension in the apparatus). The sample is then transferred to the crystal holder in such a way that the quartz stick fits into the cavity 7, and wire harness 6 is firmly secured to the lugs. After mounting the crystal, the quartz stick can be detached. The error in the orientation of the crystal axes relative to the axis of suspension of the bomb does not exceed 1°.

The stopper 4 is screwed into the body 1 of the bomb while covered with pure molten indium, which makes the thread gas tight after hardening. This avoids the use of gaskets and enables the bomb and the stopper to be subjected to a sufficiently strong acid etch after the machining is completed, in order to remove ferromagnetic impurities.

After the bomb has been mounted in the apparatus, it is evacuated and filled with water through the capillary 2. The bomb is cooled from the capillary side, and the ice plug which forms in the capillary then securely contains the pressure developing inside the bomb. The ice inside the bomb is thawed from above, from the side of stopper 4; if it were thawed from below, the movement of the ice would upset the suspension of the crystal holder. When the whole suspension system rotates in the magnetic field, a light spot is displaced on a scale; the displacement is measured on a traveling microscope.

The experiments were carried out at pressures of $p \sim 1700$ kg/cm^2 in a magnetic field $H \leq$ 20,000 Oe over the temperature range from 1.6 to 4.2°K.

3. THE SAMPLES

Zinc supplied by the firm Hilger (spectroscopically pure) served as starting material for the preparation of the crystals. Five zinc crystals: Zn-1, Zn-2, Zn-3, Zn-4 and Zn-7, were prepared and investigated; they differed in the method of preparation and the growth rate. Crystals Zn-2, Zn-3, and Zin-4, spherical in shape, were prepared by the method of Obreimov — Shubnikov in quartz tubes at a growth rate of 10, 15 and 50 mm/hr respectively. The crystal Zn-1 was prepared by the same method from Hilger zinc that had been

---

*We wish to take this opportunity to thank I. Bolgov for casting the bronze from copper and beryllium with a high degree of purity.

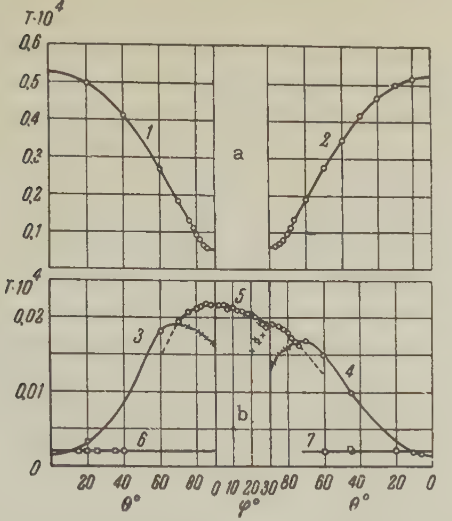

FIG. 2. Angular dependence of the oscillation period of the susceptibility of zinc caused by: a) the smallest group of mobile charges (1 – first, 2 – second orientation of the crystal); b) the group which determines one of the high frequency components (fine structure) of the de Haas – van Alphen effect (curves 3, 4, and 5 refer to the first, second and third orientation of the crystal, respectively), and the group which determines the hyperfine structure of the effect (curves 6 and 7 refer to the first and second orientation of the crystal, respectively). θ = angle between vector H and principal crystal axis; φ = angle between vector H and the diagonal crystal axis in the basal plane. ×, ○ – two fine-structure branches observed on the experimental $\Delta\chi(1/H)$ curves at the large angles θ.

recrystallized seven times. A rather detailed study of Zn-1 was made in one of the preceding papers.[12] The crystal Zn-7, with the hexagonal axis along the geometric axis of the sample, was prepared by Kapitza's method on a plate subjected to a tempera ture gradient at a growth rate of 5 mm/hr. The maximum sample diameter was 4 mm.

A widely-used method for the qualitative estimate of crystal strain is the microscopic investigation of slip along the basal plane.[13] The microscopic investigation of slip in crystals Zn-1, Zn-2, Zn-3, Zn-4, and Zn-7 showed that Zn-7 was the least strained and Zn-4 the most strained.

The crystals were oriented by means of an optical double-arc goniometer.[12] Three orientations of the zinc crystals were investigated: (1) The digonal axis of the crystal was taken parallel to the axis of suspension — the first orientation. (2) The direction perpendicular to the digonal axis and lying in the basal plane was taken parallel to the axis of suspension — the second orientation. (3) The principal axis of the crystal was taken parallel to the axis of suspension — the third orientation.

4. RESULTS OF THE MEASUREMENTS

a. The de Haas — van Alphen Effect in Unconstrained Zinc Crystals

It is known that the experimental curves $\Delta\chi(1/H)$ for Zn crystals represent the superposition of three frequency components of the variation of the susceptibility with the field.[12] Each of these frequency components is caused by a certain group of charge carriers in the metal; the component with the longest period is caused by the smallest group of charge carriers. The high frequency components are usually called the fine and the hyperfine structure of the de Haas — van Alphen effect. Before investigating the effect of homogeneous compression on the de Haas — van

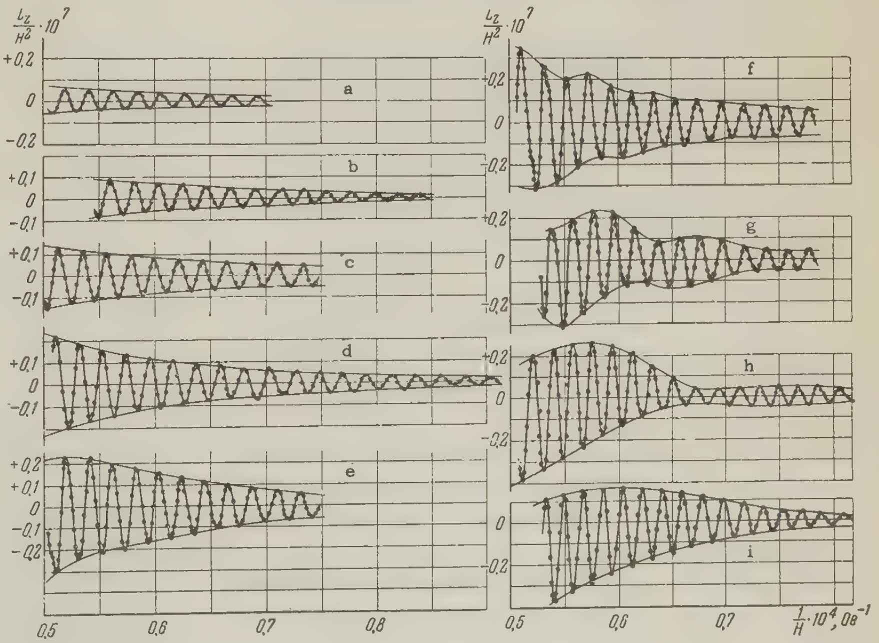

FIG. 3. Variation with 1/H of the torque L_z/H^2, acting on the crystal in its third orientation in the field, at a temperature of T = 4.2°K. Crystal Zn-1: a – φ = 2°; b – φ = 4.5°; c – φ = 7°; d – φ = 9.7°; e – φ = 15°; f – φ = 18°; g – φ = 22°; h – φ = 26°; i – φ = 28°.

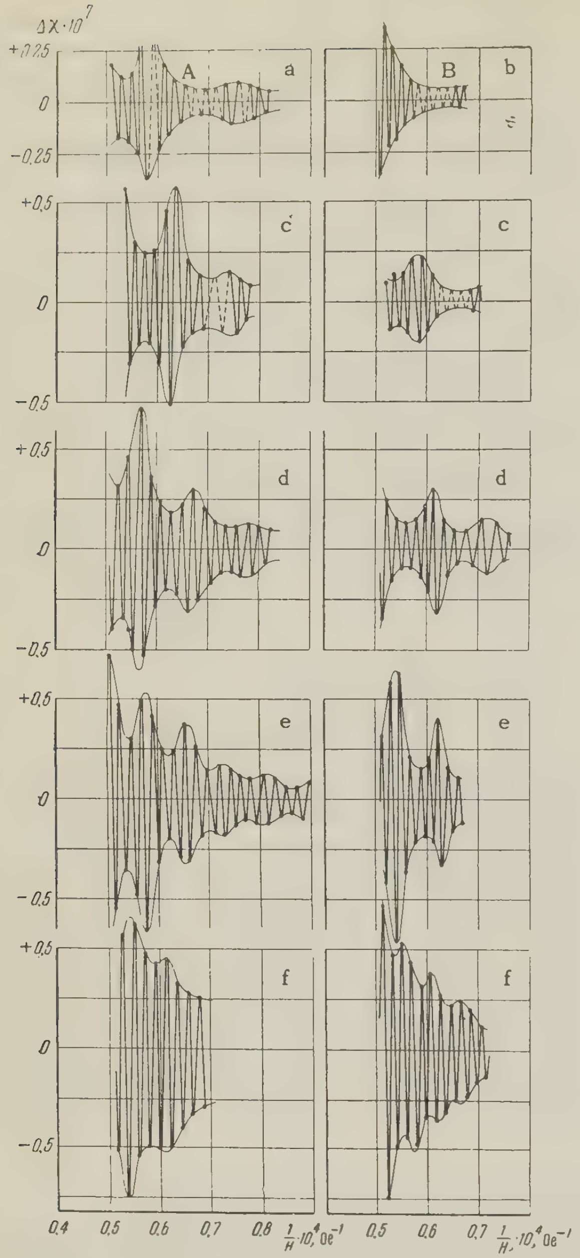

FIG. 4. Resolved oscillations of the high frequency component of the de Haas – van Alphen effect (fine structure): A) in the first, and B) in the second orientation of the crystal Zn-1: a – $\theta = 75°$; b – $\theta = 78°$; c – $\theta = 80°$; d – $\theta = 82°$; e – $\theta = 85°$; f – $\theta = 88°$; T = 4.2°K.

Alphen effect it was necessary to establish more accurately the angular dependence of the periods of susceptibility oscillations, caused by different groups of charge carriers in unconstrained zinc crystals.

The curves of Fig. 2 illustrate the angular dependence of the periods of oscillation of the susceptibility for three orientations of the zinc crystals in the magnetic field.

From the preceding investigations of the crystal Zn-1 it is known[12] that when the sample is oriented in the magnetic field in either the first or second direction, the smallest group of charge carriers produces practically coinciding curves for the angular dependence of the period of oscillation of the susceptibility of zinc. This fact was checked more carefully by an investigation of the crystal Zn-7. The curves of Fig. 2a represent the angular dependence of the periods of oscillation of the susceptibility in this crystal, produced by the smallest group of charge carriers, for the first (1) and the second (2) orientations in the magnetic field respectively. It can be seen that the curves coincide over practically the whole range of values of θ. This smallest group of carriers does not appear at all when investigating the magnetic properties in the basal plane of the zinc crystals. All the above favors the assumption that the Fermi surface for the charges of this group is a surface of revolution elongated along the axis k_z, which approximates an ellipsoid of revolution over a wide range of angles $0 < \theta \le 60°$, and for large θ changes gradually first to a cone, and then to a cylinder.[14]

The anisotropy of the magnetic properties of zinc crystals in the basal plane is due to the same group of charge carriers that is responsible for the fine structure of the effect in the first and second orientations of the zinc crystals in the magnetic field. In fact, an analysis of the magnetic

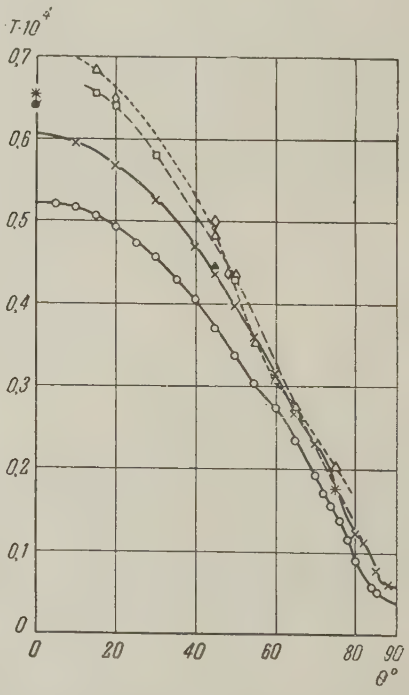

FIG. 5. Angular dependence of the oscillation period of the susceptibility caused by the smallest group of mobile charges in different zinc crystals, obtained from: × – crystal Zn-1, ○ – crystals Zn-2, 3, 4, 7 (this paper); ▲ – Sidoriak and Robinson,[18] Δ – Mackinon,[19] ● – Berlincourt and Steele,[20] □◇ – Donahoe and Mix,[21] * – Dhillon and Shoenberg.[22]

anisotropy in the basal plane of the crystal Zn-1 (the curves of Fig. 3), as well as an analysis of the resolved fine structure of the effect in this crystal (the curves of Fig. 4) made it possible to elucidate the complete angular variation of the periods of oscillation of the susceptibility, caused by the larger group of charge carriers, as shown in Fig. 2b. All the fine-structure $\Delta\chi(1/H)$ curves show modulations, with the modulation period decreasing appreciably as θ increases. An analysis of the curves of Fig. 2 shows that the Fermi surface corresponding to this second larger group of charge carriers has quite a complicated shape far removed from the simple scheme of three ellipsoids, rotated in the plane $k_x k_y$ through an angle of ± 120° relative to each other. It will be the object of further investigations to determine more precisely the shape and the dimensions of the Fermi surface for this group of charge carriers in zinc crystals.

Figure 5 shows the angular dependence of the period of the low-frequency component of the de Haas — van Alphen effect in zinc crystals, studied in this paper and by other authors. It can be seen that for different samples of the same metal the magnitude of the period of oscillations of $\Delta\chi(1/H)$, caused by the smallest group of charge carriers, does not remain constant, with the differences being greatest in the region of small angles θ between the field vector and the principal crystal axis. The periods of oscillation practically coincide in crystals Zn-2, Zn-3, Zn-4 and Zn-7; in the crystal Zn-1 (see also[12]) the periods are appreciably larger.

The facts mentioned above lead to the conclusion that an increase in purity of the samples causes an appreciable increase (up to several tens percent) in the period of oscillation of the susceptibility in the magnetic field, whereas differences in the state of strain of the samples, arising from differences in the method and from thermal conditions during the growth of the crystals, do not have any effect on the magnitude of the period of oscillations. An analysis of the experimental data shows that this conclusion is correct also for the fine structure of the de Haas — van Alphen effect in zinc crystals.

It should be noted that lattice distortions related to the method and conditions of the crystal growth appreciably influence the amplitude of the susceptibility oscillations. The amplitude of the oscillations is largest in the free-grown crystal Zn-7, and is 40 to 50% smaller in crystal Zn-4, obtained under less favorable conditions. On annealing crystal Zn-4, some increase was produced in the amplitude of the susceptibility oscillations.

b. The de Haas — van Alphen Effect in Homogeneously Compressed Zinc Crystals

The crystal Zn-2 was used to investigate the effect of the homogeneous compression of the lattice on the de Haas — van Alphen effect. The second orientation of the crystals has been studied in detail; this is sufficient (see Fig. 2) for a rather complete investigation of the effect of homogeneous compression on the oscillations caused by the smallest group of mobile charges.

Figure 6 shows some $\Delta\chi(1/H)$ curves for the crystal Zn-2 in the second orientation in the field, unconstrained (A) and under homogeneous compression, $p \approx 1700\ \mathrm{kg/cm^2}$ (B). These curves

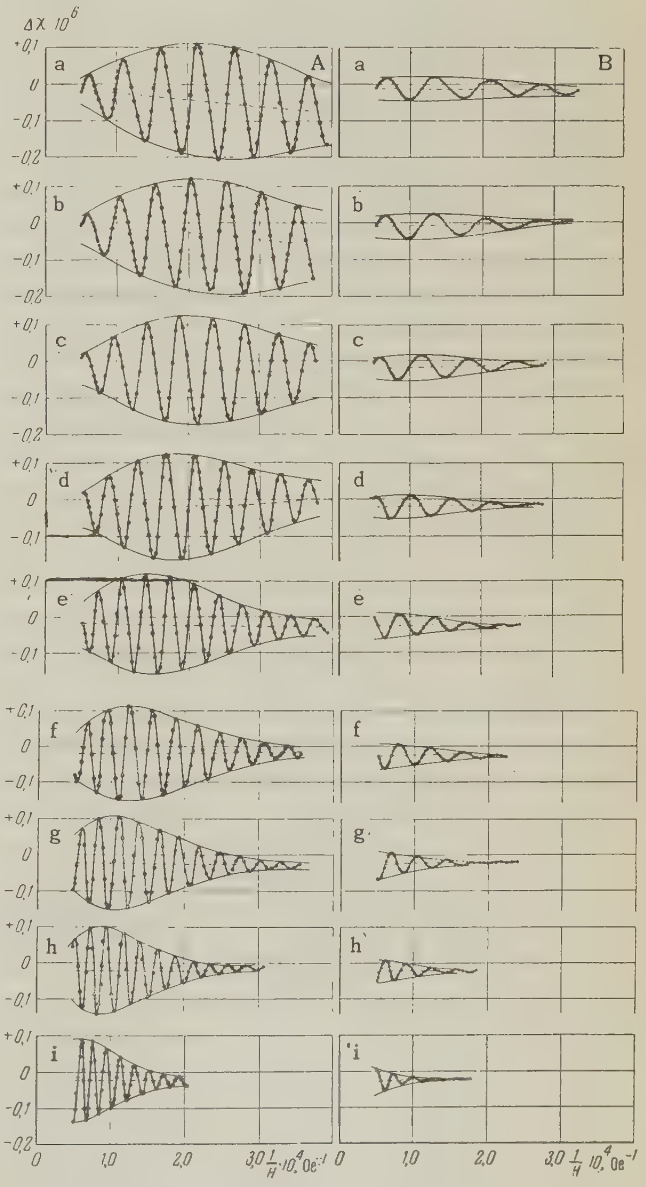

FIG. 6. "Periodic" variation of the susceptibility of the crystal Zn-2 with the magnetic field: A) unconstrained crystal, B) homogeneously compressed crystal at $p = 1700\ \mathrm{kg/cm^2}$; a – $\theta = 10°$; b – $\theta = 20°$; c – $\theta = 30°$; d – $\theta = 40°$; e – $\theta = 50°$; f – $\theta = 55°$; g – $\theta = 60°$; h – $\theta = 65°$; i – $\theta = 70°$; T = 4.2°K.

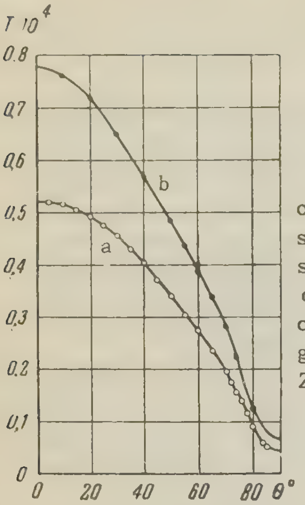

FIG. 7. Angular dependence of the oscillation period of the susceptibility caused by the smallest group of mobile charges: a – for the unconstrained crystal Zn-2 and b – for the homogeneously compressed crystal Zn-2 at p = 1700 kg/cm².

give the low-frequency component of the effect, caused by the smallest group of mobile charges in zinc. It may be seen that the homogeneous compression of the crystals under a pressure of $p \approx 1700\ \mathrm{kg/cm^2}$ changes very markedly all the characteristics of the $\Delta\chi(1/H)$ curves: the period of the oscillations increases noticeably, the amplitude of the oscillations decreases by a large factor (particularly in small fields), and the maximum of the attenuated $\Delta\chi(1/H)$ curves is displaced towards greater field strengths.

The curves of Fig. 7 illustrate the angular dependence of the period of oscillation of the susceptibility without pressure and for a homogeneously-compressed crystal. It can be seen that the period of oscillation has increased in the homogeneously compressed crystal for all values of the angle θ. This increase in the period of oscillation is somewhat larger for small angles, where it reaches 48%, and somewhat less for large angles, where it equals 40 to 43%.

The homogeneous compression of the crystal also changes the period and the amplitude of the oscillations of the fine structure of the de Haas – van Alphen effect. The high-frequency oscillations do not disappear under pressure, but their period increases noticeably; at $\theta = 80°$ the increase in the period of oscillation of the fine structure amounts to 12%. The amplitude of the high-frequency oscillations decreases under pressure.

The numerical values of the periods of oscillation for the low-frequency and high-frequency components of the $\Delta\chi(1/H)$ curves are listed in Table I for Zn-2 crystals, unconstrained and under homogeneous compression. On removing the pressure the values of the periods of oscillation are completely restored.

The homogeneous compression of the crystals leads to a strong decrease in the amplitude of the oscillations. The decrease in the amplitude of the oscillations under pressure is particularly pronounced for large values of θ and for small fields. On removing the pressure the amplitude of the oscillations is not completely restored. The hysteresis is greatest for small fields; it decreases with increasing field strength.

The temperature variation of the amplitude of the oscillations, caused by the smallest group of mobile charges in unconstrained and in homogeneously-compressed crystals, has been investigated at $\theta = 80°$. Numerical values for the ratio of the amplitudes of the oscillations A_2/A_1 are given in Table II for different values of 1/H and for two different experimental temperatures.

5. DISCUSSION OF THE RESULTS

The de Haas – van Alphen effect is a feature common to a group of 15 elements, in which the absolute magnitude of the susceptibility increases with decreasing temperature and which crystallize in anisotropic structures (in many cases in lamellar structures). In crystal chemistry it is usually assumed that complicated mixed types of interaction (partially covalent or van der Waals forces)

TABLE I

	Period of oscillation $T \times 10^4$, $\mathrm{Oe^{-1}}$				
$\theta°$	Low-frequency component $\Delta\chi(1/H)$		$\theta°$	High-frequency component $\Delta\chi(1/H)$	
	p = 0	p ≈ 1700 kg/cm²		p = 0	p ≈ 1700 kg/cm²
10	0.516	0.763	80	0,0138	0.0154
20	0.494	0.724	84	0.0125	0,0145
30	460	650			
40	405	570			
50	340	484			
55	303	435			
60	276	387			
65	237	338			
70	196	283			
74	157	224			
80	93	126			

TABLE II

$p = 0$; $T_1 = 4.2°\mathrm{K}$, $T_2 = 2.0°\mathrm{K}$		$p = 1700\ \mathrm{kg/cm^2}$; $T_1 = 4.2°\mathrm{K}$, $T_2 = 1.6°\mathrm{K}$	
$(1/H)\cdot 10^4$, $\mathrm{Oe^{-1}}$	A_2/A_1	$(1/H)\cdot 10^4$, $\mathrm{Oe^{-1}}$	A_2/A_1
1.2	3,2	0,8	2,2
1.1	2.7	0,75	2.7
1,0	1,9	0.7	2.2
0,9	1,5	0,65	2.0
0.8	1.0	0.6	1,8
0,7	1,05	0,55	1,42
0.6	1,09	0,5	1.23

are playing an important part in the lattices of the above elements along with the metallic type of bond.

The basic experimental data on the de Haas–van Alphen effect (the complicated frequency spectrum, large periods and amplitudes of the susceptibility oscillations), as well as the variation of the susceptibility of these elements with temperature, are explained by the well-known assumption that these elements contain one or more exceptionally small groups of mobile charges besides the large fundamental group. The origin of these exceptionally small groups has not been explained; it is possible that the complicated energy spectrum of the mobile charges is connected with the above-mentioned mixed types of bonds in the lattices of these elements.[14]

The period of oscillation T of the magnetic susceptibility, caused by the small group β of the mobile charges, is determined by the area of the extremal section $S_m^\beta(\zeta_\beta)$ through the Fermi surface for these charges:[9]

$$T = eh / cS_m^\beta(\zeta_\beta), \tag{1}$$

where ζ_β is the chemical potential, measured from the "bottom" of the β-energy zone. The investigation of the temperature variation of the oscillations of the magnetic susceptibility makes it possible to determine still another important characteristic of the energy spectrum of the mobile charges:

$$m_\beta = \frac{1}{2\pi}(dS_m^\beta / d\zeta_\beta). \tag{2}$$

For the general case of an arbitrary dispersion law, m_β is a function of the lattice parameters a_i and of the chemical potential. In the special case of a quadratic dispersion law, m_β coincides with the effective mass of the charge carrier as usually defined. This mass depends only on the lattice parameters and not on the energy.

Very recently Kosevich[15] has treated the effect of an elastic lattice deformation on the electron spectrum in a semi-quantitative manner and has considered the peculiarities of the de Haas–van Alphen effect in a deformed metal. The elastic deformation of the lattice (in particular the homogeneous compression of the lattice) leads to a change in the chemical potential

$$\delta\zeta = \delta S_m^\beta / 2\pi\overline{m}_\beta, \tag{3}$$

where $\overline{m}_\beta = \frac{1}{2}(m_\beta^0 + m_\beta^p)$, and δS_m^β is the variation of the section through the Fermi surface under pressure.* In the case of a homogeneous compression $\delta\zeta = ap$, where

$$a = \delta\zeta / p \tag{4}$$

is of the same order of magnitude as the volume occupied by one particle of the charge-carrier "gas" in the metal.

$\delta\zeta$ may be of the order of ζ_β and then the elastic deformation of the lattice will change little the properties that are determined by the majority group of charges, and will change very strongly those properties which are determined by the minority group of charges. Thus, in spite of the fact that the deformation and consequently the relative changes of the lattice parameters are small, the chemical potential and the oscillation period of the susceptibility will change by a factor comparable to ζ_β and S_m^β, respectively. In the special case of a quadratic dispersion law, m_β depends neither on the energy nor, consequently, on the pressure.

The investigation of the temperature variation of the oscillation period of the susceptibility in the constrained and in the deformed crystal, carried out at $\theta = 80°$, makes it possible to determine m_β^0 and m_β^p in this orientation, without any assumptions concerning the form of the dispersion law for the charge carriers in the small group, and hence to calculate $\delta\zeta$ and a. The results of these calculations are given below.

$$\begin{array}{ll}
T_p/T_0 = 1.355. & m_\beta^p \cdot 10^{29} = 7.5; \\
S_m^p/S_m^0 = 0.740. & \overline{m}_\beta \cdot 10^{29} = 6.3; \\
\delta S_m/S_m^0 = -0.260. & \delta\zeta \cdot 10^{14} = -0.62 \text{ erg}; \\
m_\beta^0 \cdot 10^{29} = 4.9. & a \cdot 10^{23} = 0.36.
\end{array}$$

A comparison of the quantities m_β^0 and m_β^p gives evidence of a considerable dependence of m_β on the pressure, i.e. of a non-quadratic dispersion law for the small group of mobile charges in zinc crystals.

From an analysis of the data quoted it can be seen that the changes of the chemical potential by homogeneous compression of the lattice under a pressure of $p \approx 1700$ kg/cm^2 are of the same order of magnitude as the chemical potential of the charge carriers of the small group.[12,16] The value of the parameter α, calculated on the basis of the experimental data, is also in good agreement with the value estimated for it by Kosevich[15] from general considerations.

Since the theoretical determinations of these quantities are based on the assumption that there exist exceptionally small groups of charge carriers, one may conclude that the experiments on the homogeneous compression of the zinc crystals and the large changes in the oscillation periods and in the chemical potential detected in these experiments support the validity of such an assumption.

---

*In what follows a zero in the superscript indicates a given quantity in the unconstrained crystal, and p in the superscript indicates the same quantity in the deformed crystal.

Further investigations on the pressure variation of the oscillation period of the susceptibility in zinc will make it possible to establish the dispersion law for the small group of charge carriers.[15]

The calculations by Kosevich[15] permit a quantitative determination of the oscillation period of the magnetic susceptibility in a constant magnetic field as a function of the external load. In the case of a homogeneous compression of the crystals the change in pressure Δp, which corresponds to the oscillation period, equals

$$\Delta p = e\hbar H / ca\overline{m}_{\beta}. \qquad (5)$$

This quantity can be determined for the zinc crystals from the experimental data. The results of the calculation are given in Table III ($\theta = 80°$).

TABLE III

H, Oe	Δp, kg/cm^2
1000	75
5000	370
10000	750

It can be seen from the table that it is possible to observe the variation with pressure of the susceptibility oscillations in zinc crystals in a constant field by using the "ice" method for generating high pressures at low temperatures and by varying the pressure in the apparatus.

Two cases have been studied quantitatively and treated theoretically so far, i.e. changes induced in the chemical potential of the charge carriers by some external factor, and the conditions when such changes strongly affect the properties determined by small groups of charge carriers. The discussion here deals with the effect of the temperature on the magnetic properties of those elements which exhibit the de Haas — van Alphen effect,[17] and with the effect of elastic deformations on the oscillations of the magnetic susceptibility caused by small groups of charge carriers.[15]

In Sec. 4 it was noted that small amounts of impurities change the oscillation period of the susceptibility in zinc crystals very strongly. It is probable that the impurities also induce in the chemical potential a change that affects appreciably the filling of the small group of charge carriers, and, correspondingly, the most important characteristic of the de Haas — van Alphen effect, i.e. the oscillation period of the susceptibility.

In conclusion, we wish to express our gratitude to A. M. Kosevich for discussing the experimental results.

---

[1] P. V. Bridgman, The Physics of High Pressures. London, Bell, 1949.

[2] B. G. Lazarev and L. S. Kan, J. Exptl. Theoret. Phys. (U.S.S.R.) **14**, 463 (1944).

[3] B. G. Lazarev and L. S. Kan, J. Exptl. Theoret. Phys. (U.S.S.R.) **14**, 470 (1944); Kan, Lazarev, and Sudovtsov, J. Exptl. Theoret. Phys. (U.S.S.R.) **18**, 825 (1948).

[4] E. Maxwell, Phys. Rev. **78**, 477 (1950); **79**, 173 (1950); Allen, Dawton, Lock, Pippard, and Shoenberg, Nature **166**, 1071 (1950).

[5] Alekseevskii, Brandt, and Kostina, Izv. Akad. Nauk SSSR, Ser. Fiz. **16**, 233 (1952); **21**, 790 (1957); Dokl. Akad. Nauk SSSR **105**, 46 (1955); J. Exptl. Theoret. Phys. (U.S.S.R.) **28**, 379 (1955), Soviet Phys. JETP **1**, 384 (1955).

[6] L. S. Kan and B. G. Lazarev, J. Exptl. Theoret. Phys. (U.S.S.R.) **34**, 258 (1958), Soviet Phys. JETP **7**, 180 (1958).

[7] Verkin, Lazarev, and Rudenko, Dokl. Akad. Nauk SSSR **69**, 773 (1949); J. Exptl. Theoret. Phys. (U.S.S.R.) **20**, 93 (1950); **21**, 658 (1951); Dokl. Akad. Nauk SSSR **73**, 59 (1950); **80**, 45 (1951).

[8] J. A. Marcus, Phys. Rev. **71**, 559 (1947); D. Shoenberg, Nature **164**, 225 (1949); Phil. Trans. Roy. Soc. **245**, 1 (1952); T. Berlincourt, Phys. Rev. **99**, 1716 (1955).

[9] I. M. Lifshitz and A. M. Kosevich, Dokl. Akad. Nauk SSSR **96**, 963 (1954); J. Exptl. Theoret. Phys. (U.S.S.R.) **29**, 730 (1955), Soviet Phys. JETP **2**, 636 (1956); I. M. Lifshitz and A. V. Pogorelov, Dokl. Akad. Nauk SSSR **96**, 1143 (1954).

[10] Verkin, Dmitrenko, and Lazarev, J. Exptl. Theoret. Phys. (U.S.S.R.) **31**, 538 (1956), Soviet Phys. JETP **4**, 432 (1957).

[11] Dmitrenko, Verkin, and Lazarev, J. Exptl. Theoret. Phys. (U.S.S.R.) **33**, 287 (1957), Soviet Phys. JETP **6**, 223 (1958).

[12] B. I. Verkin and I. M. Dmitrenko, Izv. Akad. Nauk SSSR, Ser. Fiz. **19**, 409 (1955), [Columbia Tech. Transl. **19**, 365 (1955)].

[13] B. N. Bushmanov, Физика металлов и металловедение (Physics of Metals and Metal Research) **4**, 310 (1957); H. Schilling, Physics (Amer.) **5**, 1 (1934).

[14] B. I. Verkin, Doctoral Thesis, Khar'kov State University (1956).

[15] A. M. Kosevich, J. Exptl. Theoret. Phys. (U.S.S.R.) **35**, 249 (1958), Soviet Phys. JETP **8**, 171 (1959).

[16] G. E. Zil'berman, J. Exptl. Theoret. Phys. (U.S.S.R.) 21, 1209 (1951).

[17] G. E. Zil'berman and F. I. Itskovich, J. Exptl. Theoret. Phys. (U.S.S.R.) 32, 158 (1957), Soviet Phys. JETP 5, 119 (1957).

[18] S. Sidoriak and J. Robinson, Phys. Rev. 75, 118 (1949).

[19] L. Mackinon. Proc. Phys. Soc. B62, 170 (1949).

[20] T. Berlincourt and M. Steele, Phys. Rev. 95, 1421 (1954).

[21] F. Donahoe and F. Nix, Phys. Rev. 95, 1395 (1954).

[22] J. S. Dillon and D. Shoenberg, Phil. Trans. Roy. Soc. A248, 1 (1955).

Translated by P. F. Schmidt
63

SOVIET PHYSICS JETP VOLUME 35(8), NUMBER 2 FEBRUARY, 1959

ENERGY DEPENDENCE OF $\mu^+ - e^+$ DECAY ASYMMETRY

A. I. MUKHIN, E. B. OZEROV, and B. PONTECORVO

Joint Institute for Nuclear Research

Submitted to JETP editor March 3, 1958

J. Exptl. Theoret. Phys. (U.S.S.R.) 35, 340-347 (August, 1958)

The energy dependence of the asymmetry of electrons originating in the decay of polarized μ mesons was studied with a set of scintillation counters biased against bremsstrahlung. The measurements were carried out for electron energies above 20 Mev. The observations are in a quantitative agreement (within a few percent) with the two-component neutrino theory. The experiments indicate that the degree of polarization of the μ meson beam is 0.81 ± 0.11.

INTRODUCTION

THE hypothesis of parity nonconservation in weak interactions[1] has led[2] to a special variant of the neutrino theory, called the two-component or longitudinal neutrino theory. The attractiveness of such a theory makes it desirable to conduct experiments to decide whether the theory is correct or not.

A study of the spectrum of electrons produced in the decay of polarized μ meson at various angles offers such an opportunity. It is, however, necessary to note that such an investigation can, in principle, only disprove the two-component neutrino theory, but cannot provide a final proof of its validity. In other words, a four-component neutrino theory can, for an appropriate choice of the coupling constants,[3] give a spectrum similar to that predicted by the two-component theory, namely

$$f(E,\theta) = 2E^2\{(3-2E)+\lambda(2E-1)\cos\theta\}. \qquad (1)$$

Here $f(E, \theta)$ denotes the electron energy-distribution function, θ is the angle between the electron momentum and the μ-meson spin, E is the ratio of the electron energy to the maximum energy possible, and λ is a parameter that depends on the coupling constants.

Parity nonconservation in $\pi-\mu-e$ decay was discovered in the classical experiments of Garwin, Lederman, and Weinrich[4] who showed, using electronic methods of particle detection, that μ-meson beams from an internal target of a synchrocyclotron are polarized to a large degree, and that the angular distribution of electrons in $\mu-e$ decay is of the form $1 + a\cos\theta$. It follows from the above that the two-component neutrino theory predicts a definite dependence of the factor a on the electron energy.

The energy dependence of the factor a found in reference 4 is weaker than that given by Eq. (1). The energy of the electrons was estimated in these experiments by determining the penetrating power of electrons passing through a graphite absorber. Taking it into account that the arrangement of counters in reference 4 was such that the bremsstrahlung radiation of the electrons could be recorded,[5] we undertook an experiment in which the detection probability of bremsstrahlung radiation has been markedly lowered by using an appropriate arrangement of counters. It will be shown below that the results of our measurements, in which (apart from strong suppression of the bremsstrahlung) good angular resolution was obtained, made it possible to verify Eq. (1) for electron energies above 20 Mev.

A second publication of the Columbia group[6] appeared after our experiment had been started. The observed energy dependence of electron asymmetry in $\mu - e$ decay reported is close to that predicted by Eq. (1). A qualitative agreement has also been obtained in recently-published experiments using emulsions[7] and a propane bubble chamber.[8] The degree of accuracy of these methods is, however, much lower than that obtained by means of electronic recording.

EXPERIMENTAL ARRANGEMENT

A beam of positive π mesons of ~ 80 Mev, produced on an internal synchrocyclotron target, was used in the experiments. The beam was analyzed and focused after passing through the scattered magnetic field of the accelerator. The beam was analyzed again by a magnetic field before reaching a concrete wall four meters thick, and, passing through a collimator, reached the hall where the experiments were conducted. The intensity of the beam was relatively low (100 mesons/cm^2-sec), and its good monoenergetic qualities permitted it to separate stopping μ mesons from stopping π mesons. It was therefore more convenient for experiments on μ mesons than other, more intense beams available in our laboratory.

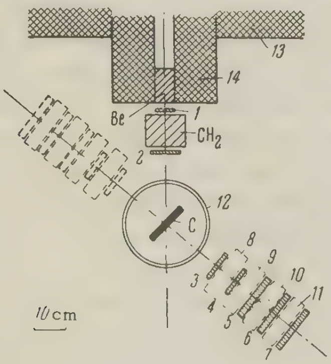

FIG. 1. Diagram of the experimental setup. Be) beryllium absorber, CH$_2$) polyethylene absorber 10 cm thick, C) graphite target, 1, 2, 3, 4, 5, 6, 7) scintillation counters, 8, 9, 10, 11) polyethylene absorbers, 12) magnetic shield, 13) shielding wall, 14) collimator.

The experimental setup is shown in Fig. 1. A beryllium absorber was placed directly in front of the monitoring counters 1 and 2. Its thickness was chosen such as to stop the π mesons in the graphite target. This was necessary for calibration purposes. An additional polyethylene (CH$_2$) absorber 10 cm thick was placed between counters 1 and 2 for asymmetry measurements, when the μ mesons had to be stopped in the graphite.

Two difficulties arise in measurements of the energy dependence of the asymmetry of $\mu - e$ decay electrons by the absorption method: (a) the spectrum of electrons traversing the absorber is distorted by effects of multiple scattering and bremsstrahlung, and (b) electrons with energy lower than that determined by the absorber thickness are detected thanks to the relatively penetrating bremsstrahlung radiation. Point (a) is discussed in the following section. As far as point (b) is concerned, in order to decrease the probability of registration of electrons through their bremsstrahlung radiation, a telescope consisting of a large number of scintillation counters was used for electron detection in our experimental arrangement. The minimum threshold of electron detection in the telescope (3, 4, 5, 6, and 7 in Fig. 1) was therefore relatively high and, including half the thickness of the graphite target, was equivalent to 9.7 g/cm^2 of polyethylene. The electron-detection threshold could be varied by means of polyethylene absorbers, placed between the counters.

The intensity of the vertical magnetic field used to rotate the μ-meson spin was made small in order to improve the angular definition of the recording system as compared with that of reference 4. It was constant throughout the experiment and amounted to 4.4 ± 0.1 oersteds over the total target volume.* A graphite target $2 \times 14 \times 14$ cm was placed in the center of the magnetic shield formed by two iron cylinders placed one above the other with a gap of 11 cm. The shield excluded horizontal components of the magnetic field present in the hall, and ensured at the same time homogeneity of the vertical magnetic field established at the target.

The operation of the electronic apparatus (block diagram shown in Fig. 2) was as follows: a pulse from the monitor coincidence circuit (1, 2) passing through the anticoincidence circuit (1, 2)-3 operated a time discriminator, the channels of which (CF_1, CF_2, CF_3) were gated in turn by triggers T_1, T_2, and T_3. Duration of each gate was equal to 1 μsec. Pulses from the decay electrons detected in a five-fold coincidence were fed into the gated channels of the time discriminator and, in the case when these were open, were recorded by mechanical registers.

---

*The authors are obliged to D. P. Vasilevskaia for the measurements of the topography and of the value of magnetic field inside the magnetic shield.

The rate of $\mu - e$ decay electrons detected in the geometry of Fig. 1 at the minimum threshold setting was 30/min. For the case when only the beryllium absorber remained in the beam, which corresponds to the stopping of π mesons, the rate of $\pi - \mu - e$ decay electrons amounted to 200/min.

The magnetic field applied rotated the angular distribution only by 21° in a microsecond, the μ-meson precession frequency being $f = geH/4\pi m_\mu c$. Two series of measurements were therefore carried out, each at two angles symmetric with respect to the collimator axis (and the target): (1) 52° and 180 + 52°, and (2) 128° and 180 + 128°. The target was placed at 45° to the beam (cf. Fig. 1 for the first case). Taking the rotation of μ-meson spin in constant magnetic field into account, measurements at these four angles (using three time-discrimination channels) made it possible to obtain the angular distribution of electrons with respect to the μ-meson spin between 0 and 360°. After corrections for angular definition and exponential decay within gate duration, these angles were 11, 32, 61, 88, 110, 170, 191, 212, 241, 268, 290, and 350°.

In essence, three pairs of points were in our disposition for determination of the factor a, symmetric with respect to the direction of the μ-meson spin (and shifted by about 21°) at 0° and 180°. Six additional points were available, symmetric in pairs about 90 and 270°. These points, which did not increase appreciably the accuracy of asymmetry determination, served as a check on the geometrical symmetry of the experiment. It follows that a possible difference in gate duration was of no consequence in determination of the factor a since the counting rate at various angles was measured using the same time channels.

A variable delay line (VDL, Fig. 2) made it possible to vary the time of gating from 0 to 5.0 μsec relative to the passage of the meson through the counters (1,2), which was used for determination of the chance coincidence rate. A delay equal to 0.4 μsec was used in the measurements. The background, due mainly to μ mesons stopping in the walls of the magnetic shield and producing decay electrons, depended on the polyethylene absorber thickness practically in the same way as the rate of electrons from μ mesons decaying in the graphite, and amounted to ~ 5 ~ 10%, depending on the number of gates and on the angle of observation.

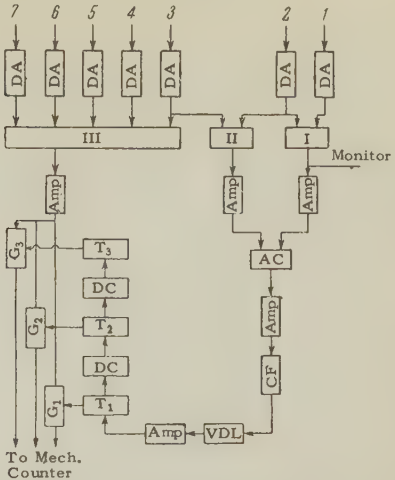

FIG. 2. Block-diagram of the electronic apparatus. DA) distributed amplifiers connected to photomultipliers 1, 2, 3, 4, 5, 6, 7; I, II, III) coincidence circuits ($\tau = 1.5 \times 10^{-8}$ sec.): AC) anticoincidence circuit (1, 2)-3; CF) cathode follower; VDL) variable delay line; DC) differentiating circuits for consecutive operation of trigger circuits. T_1, T_2, T_3; G_1, G_2, G_3) gated channels.

INVESTIGATION OF THE ABSORPTION OF ELECTRONS EMITTED BY UNPOLARIZED μ MESONS

For the interpretation of the absorption curves of polarized μ-meson decay electrons discussed in the following section, it is necessary to know the probability $\varphi(E, R)$ that an electron of a given energy E is detected while traversing the polyethylene absorber of thickness R. In our case R denotes the total thickness of the absorber in the telescope accounting for the thickness of the scintillation counters themselves and of the graphite target.

The passage of electrons through matter is a relatively complicated phenomenon because of multiple scattering and bremsstrahlung. The basic laws of the interaction involving electron deceleration are well known, and the solution of the problem of the passage of electrons through matter is subject to mathematical difficulties only. In practice the problem can be solved experimentally, using a source of monokinetic electrons of different energies, and by the Monte Carlo method. We have made use of the results of Monte Carlo calculations of the probability that an electron traverses different thicknesses of polyethylene, given by Lokanathan and Steinberger.[9]

In order to evaluate the validity of the method used we studied the absorption in polyethylene of electrons possessing a known spectrum, originating in the decay of unpolarized μ mesons. The experimental absorption curve was compared with the theoretical, calculated for the same spectrum according to reference 9.

It is well known that the spectrum of electrons from unpolarized μ mesons is completely described by the Michel parameter ρ. According to experimental data (cf., eg., reference 3), the value of that parameter is close to that predicted by the two-component neutrino theory and we used the value $\rho = 0.75$ in our calculations.*

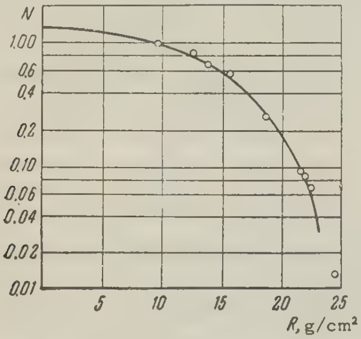

FIG. 3. Absorption curve of electrons from decay of unpolarized μ mesons. Solid curve – calculated dependence of electron intensity on the polyethylene absorber thickness R; o) experimental points. The counting rate of the telescope without additional absorbers (telescope recording threshold equal to 9.7 g/cm²) is taken as unity.

The solid curve in Fig. 3 represents the calculated dependence

$$N(R) = \int_0^1 E^2(3-2E)\varphi(E,R)dE.$$

The curve is normalized so that the counting rate of electrons recorded by the telescope (3, 4, 5, 6, 7) is unity when the telescope threshold is determined by the thickness of scintillation counters only.

In the experimental determination of the curve, no absorber was placed between the counters 1 and 2, and π mesons were stopped in the graphite target. For the detection of electrons the telescope was set at 232° to the direction of the meson beam, in the same geometry as used for the study of $\mu - e$ decay asymmetry. Polyethylene absorbers were placed between the counters. The experimental points are shown in Fig. 1.

It can be seen from the figure that the calculated curve fits well the experimental points. This facts serves as the basis for the method of accounting for the distortion of electron spectrum in passage through polyethylene given in the following section. A marked discrepancy (~ 10%) between the calculated curve and the experimental points can be observed only when the total absorber thickness amounts to more than 21.7 g/cm² of polyethylene. The discrepancy increases with increasing absorber thickness. For an absorber 25.2 g/cm² thick, sufficient for ionization deceleration of 55-Mev electrons, the telescope records 0.4% of the number of electrons detected without additional absorbers. It can be concluded therefore, that the discrepancy is not due to theoretical calculations but to the finite probability of bremsstrahlung radiation detection by the telescope. The fact that this probability is small is due to the large number of counters used for electron detection.

ENERGY DEPENDENCE OF THE ASYMMETRY OF $\mu - e$ DECAY ELECTRONS

Experimental values of the asymmetry factor a, obtained using the least squares method from the angular distribution curves measured for different absorber thickness, are shown in Fig. 4. Statistical errors only are shown in the figure.

It has been shown that, for an absorber 21.7 g/cm² thick (maximum thickness used), about 10% of the counts recorded by the telescope detecting electrons from unpolarized μ mesons were due to the bremsstrahlung. This could cause a decrease of the degree of asymmetry observed using such an absorber. The upper limit of the correction accounting for that effect, is however, much less than the statistical error shown. Nevertheless, it is possible that in references 4 and 6, where the bremsstrahlung detection probability was much higher, this effect could cause a more considerable decrease of asymmetry.

The solid curve in Fig. 4 represents the expected dependence $a(R) = B\alpha(R)$ of the asymmetry factor on the total absorber thickness in the telescope, calculated using the spectrum predicted by the two-component neutrino theory [Eq. (1)]. The value of the constant B (which serves as a scale in the drawing) will be discussed below. Bremsstrahlung and multiple scattering of electrons, as well as the angular definition of the telescope were accounted for. The solid curve represents the relation

$$\alpha(R) = \int_{\Delta\Omega}\int_0^1 E^2(2E-1)\varphi(E,R)\cos\theta\, dE\, d\Omega \Big/ \Delta\Omega\int_0^1 E^2(3-2E)\varphi(E,R)dE,$$

where the finite angular definition of the telescope was accounted for integrating over Ω. The degree of accuracy of the function $\varphi(E, R)$ — the probability that an electron with energy E will be recorded by the telescope for the absorber thickness equal R — was discussed in the preceding section.

---

*Radiative corrections[3] do not introduce any errors important to the problem on hand.

An idea about the good accuracy of the solid curve in Fig. 4 can be obtained by comparing it with the dashed curve

$$\alpha(E) = \int_E^1 E^2(2E-1)dE \Big/ \int_E^1 E^2(3-2E)dE$$

$$= (1 + E + E^2 + 3E^3) \Big/ 3(1 + E + E^2 - E^3),$$

calculated for the idealized case of the absence of any instrumental distortions of the spectrum connected with recording the electrons traversing the absorber. It can be seen from Fig. 4 that the discrepancy between the curves is relatively small, in spite of the fact that the change of spectrum is considerable. This can be explained by the fact that the discrepancy reflects only the varying degree of spectrum distortion at different angles. That fact makes the method used perfectly suitable for the problem under consideration.

It can be seen that the curve calculated on basis of the two-component neutrino theory is, within a few percent, in agreement with experimental points in the investigated energy region above 20 Mev.

The constant $B = 0.70 \pm 0.02$, obtained by comparison of experimental data with the calculated curve, can be expressed as $B = P(1 - W_C)\lambda$, where P is the degree of polarization of the μ-meson beam used, W_C is the probability of depolarization of μ mesons in graphite, and $\lambda = (g_V g_A + g_A^* g_V)/(|g_V|^2 + |g_A|^2)$ is the fundamental constant of $\mu - e$ decay in the two-component neutrino theory [Eq. (1)]. The error given is statistical only. The constant B and its error are based on the results of all four sets of measurements with different absorbers and it has been implicitly assumed that the fit between the theoretical curve and experimental points (Fig. 4) is sufficiently good to confirm the validity of Eq. (1). The integral value of the asymmetry factor a_0 for the whole electron spectrum can be then automatically obtained extrapolating the solid curve to zero absorber thickness. It has been found that $a_0 = B/3 = 0.233 \pm 0.007$. Naturally, this value refers to the μ-meson beam used.

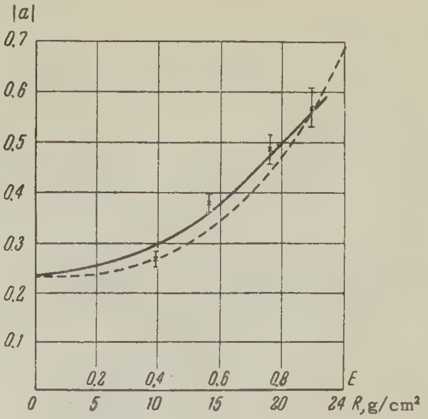

FIG. 4. Dependence of asymmetry coefficient a on electron energy. The solid curve $a(R)$ calculated accounting for the electron detecting efficiency of the experimental arrangement (for total absorber thickness R), the dashed curve $a(E)$ calculated — assuming the absence of any spectrum distortion. X) experimental values of a.

Analyzing the available data on the measurements of the asymmetry of $\pi^+ - \mu^+ - e^+$ decay electrons in emulsions and $\mu^+ - e^+$ decay electrons in emulsions and graphite. Wilkinson came to the conclusion that $(1 - W_C)\lambda = 0.87 \pm 0.12$.[10] Comparing this result with the value of $B = P(1 - W_C)\lambda = 0.70 \pm 0.02$ obtained in the present experiment it may be concluded that the μ-meson beam used had a degree of polarization $P = 0.81 \pm 0.11$, i.e., probably was not totally polarized.

A comparison of the asymmetry factors a_0 obtained for graphite using different μ-meson beams (though extracted from accelerators by analogous methods)[6,11,12] shows that any differences in their value cannot be regarded as essential. It follows that the beams have a similar degree of polarization, independent of the energy of proton beam producing π mesons on the internal synchrocyclotron target.

In conclusion, it should be mentioned that, so far, there is no experimental evidence indicating that λ is less than one, i.e., less than the value required by the Feynmann — Gell-Mann theory.[13]

CONCLUSION

1. The energy dependence of the electron asymmetry in $\mu^+ - e^+$ decay was measured using an electronic method of recording which suppressed strongly the bremsstrahlung recording probability.
2. The asymmetry dependence found for the energy region studied, from 20 Mev to the limit of the electron spectrum, is in quantitative agreement (within a few percent) with the predictions of the two-component neutrino theory.
3. Under the assumption that the dependence remains valid for the non-investigated region of spectrum < 20 Mev, the asymmetry factor a_0 was found for graphite for the total integral spectrum. The value obtained is $a_0 = 0.233 \pm 0.007$.
4. It can be maintained that, most probably, the μ-meson beam used was not totally polarized: its degree of polarization was found to be equal $P = 0.81 \pm 0.11$.

5. μ-meson beams from internal synchrocyclotron targets have an approximately equal degree of polarization, irrespective to the energy of accelerated protons.

---

[1] T. D. Lee and C. N. Yang, Phys. Rev. **104**, 254 (1956).

[2] L. D. Landau, J. Exptl. Theoret. Phys. (U.S.S.R.) **32**, 407 (1957), Soviet Phys. JETP **5**, 337 (1957); T. D. Lee and C. N. Yang, Phys. Rev. **105**, 1671 (1957); A. Salam, Nuovo cimento **5**, 299 (1957).

[3] T. Kinoshita and A. Sirlin, Phys. Rev. **107**, 593 (1957).

[4] Garwin, Lederman, and Weinrich, Phys. Rev. **105**, 1415 (1957).

[5] E. P. Hincks and B. Pontecorvo, Phys. Rev. **75**, 698 (1949).

[6] Berley, Coffin, Garwin, Lederman, and Weinrich, Phys. Rev. **106**, 835 (1957).

[7] A. O. Vaisenberg and V. A. Smirnitskii, J. Exptl. Theoret. Phys. (U.S.S.R.) **32**, 1340 (1957); **33**, 621 (1957); Soviet Phys. JETP **5**, 1093 (1957); **6**, 477 (1958).

[8] Pless, Brenner, Williams, et al., Phys. Rev. **108**, 159 (1957).

[9] S. Lokanathan and J. Steinberger, Nuovo cimento Suppl. 2, Ser. 10, 151 (1955).

[10] D. H. Wilkinson, Nuovo cimento **6**, 516 (1957).

[11] Cassels, O'Keeffe, Rigby, Wetherell, and Wormald, Proc. Phys. Soc. **A70**, 543 (1957).

[12] S. C. Wright et al., Proc. Rochester Conf., April 15-19, 1957.

[13] R. Feynmann and M. Gell-Mann, Phys. Rev. **109**, 173 (1958).

Translated by H. Kasha
64

SOVIET PHYSICS JETP VOLUME 35(8), NUMBER 2 FEBRUARY, 1959

*EFFECT OF FINITE NUCLEAR SIZE ON THE RELATIVE INTERNAL CONVERSION COEFFICIENTS IN L SUBSHELLS**

A. G. SERGEEV, V. D. VOROB' EV, A. S. REMENNYI, T. I. KOL' CHINSKAIA, G. D. LATYSHEV, and Iu. S. EGOROV

Leningrad Institute of Railroad Transport Engineers

Submitted to JETP editor March 6, 1958, resubmitted July 9, 1958

J. Exptl. Theoret. Phys. (U.S.S.R.) **35**, 348-354 (August, 1958)

The relative conversion coefficients in L subshells have been measured for three pure M1 transitions: 46.5 kev in Bi^{210} and 115.1 and 238.6 kev in B^{212}. It is shown that in order to obtain agreement with experimental data the finite nuclear size must be taken into account in theoretical calculations of the L-conversion coefficients. The ratios $L_I : L_{II} : L_{III}$ for the M1 transition of 277.3 kev in Pb^{208} have also been measured.

1. INTRODUCTION

In several experimental papers[1-6] it has been established that the K-conversion coefficients found experimentally for heavy nuclei for M1 transitions turned out to be appreciably lower than the theoretical coefficients calculated by Rose[7] for a point nucleus. This difference agrees approximately with the correction (~30%) for finite nuclear size proposed by Sliv.[8] It has been shown both theoretically[9] and experimentally[1,4,10] that approximately the same correction should be applied also to the L_I-conversion coefficients. At the present time it may be considered as established that it is necessary to take into account the finite nuclear size in making theoretical calculations of internal conversion coefficients for the K and L_I shells in the case of M1 transitions.

---

*This paper has been presented at the eighth annual conference on nuclear spectroscopy held by the Academy of Sciences U.S.S.R. in January 1958 in Leningrad.

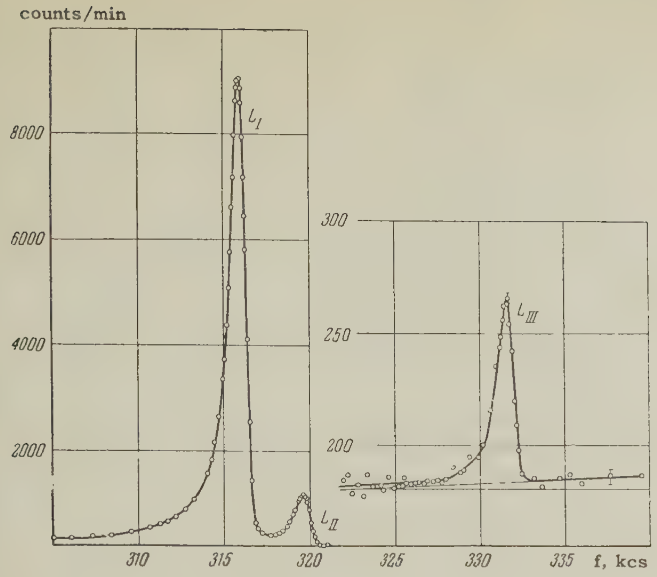

FIG. 1. L_I, L_{II} and L_{III} conversion lines for the 46.5-kev transition in Bi^{210}. In this graph and in subsequent graphs the proton resonance frequency f which is proportional to $H\rho$ has been plotted along the horizontal axis. $\Delta H\rho/H\rho$ is equal to 0.37% for L_I and to 0.35% for L_{III}.

With respect to the effect of the finite nuclear size on the conversion in the L_{II} shell the available experimental data[1,4,10,11] are of a contradictory character, owing to the low accuracy of measurement. Recently Band and Sliv have carried out calculations of conversion coefficients for the L_I, L_{II}, and L_{III} subshells. Preliminary results of these calculations, kindly communicated to us by the authors, show that the effect of finite nuclear size is significantly different for the different L subshells. The correction does not depend strongly on the energy, and for $Z = 83$ amounts to $\sim 33\%$ for the L_I subshell, to 11% for the L_{II} subshell, and is small in the case of the L_{III} subshell. Therefore, the ratios $L_I : L_{II} : L_{III}$ should be sensitive to nuclear size.

The object of the present work consists of the experimental investigation of the effect of finite nuclear size on the relative conversion coefficients in the L subshells for M1 transitions. The following points are significant in such an investigation: (1) the accuracy in the determination of the relative intensities $L_I : L_{II} : L_{III}$ should be not less than 5%; (2) it is necessary to be certain that the lines being studied are pure M1 transitions, for even a small admixture of E2 may strongly affect the ratio $L_I : L_{II} : L_{III}$.

2. EXPERIMENTAL DATA

Internal conversion in L-subshells was studied in the case of the following three M1-transitions: the 46.5-kev transition occurring in the decay RaD $\xrightarrow{\beta}$ RaE ($_{83}Bi^{210}$) and the 115.1 and 238.6-kev transitions occurring in the decay ThB $\xrightarrow{\beta}$ ThC ($_{83}Bi^{212}$). According to Krisiuk et al.,[12] all three transitions take place between levels with spins 0^- and 1^-, and are therefore pure M1 transitions.

The work has been carried out using a magnetic spectrometer of the ketron[13] type. The measurement and the stabilization of the magnetic field was carried out by means of the proton magnetic-resonance method.[14] Electrons were recorded by means of Geiger-Müller counters. The resolving power of the apparatus was varied from 0.05 to 0.36%, and was chosen for each line in such a way as to give a complete resolution of the lines with the maximum possible aperture. Figures 1 and 2 show several sets of measurements of the lines described above. The 115.1-kev transition is a fairly weak one, and therefore the ratio $L_I : L_{II}$ for it was measured with a resolving power of 0.14%, while the ratio $L_I : L_{III}$ was measured with a resolving power of 0.23% (Fig. 2); the L_{III} line for this transition had not been observed previously.

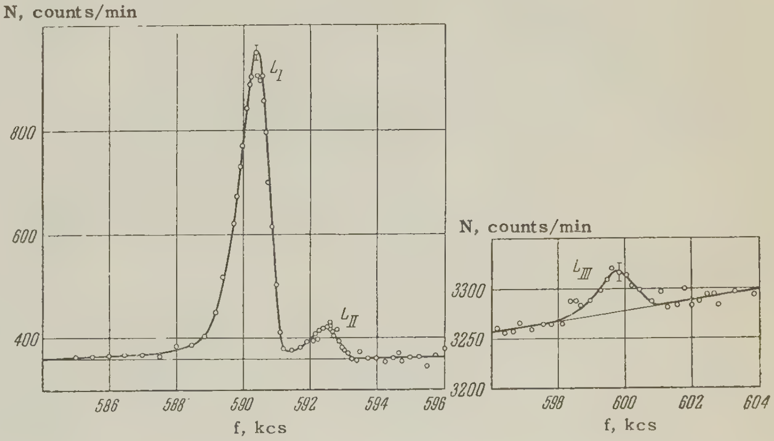

FIG. 2. L_I, L_{II} and L_{III} conversion lines for the 115.1 kev transition in Bi^{212}. The L_{III} line has been measured with a resolution of 0.23%. $\Delta H\rho/H\rho$ = 0.14% for L_I.

TABLE I

Decay	E_γ, kev	$L_I : L_{II} : L_{III}$
RaD → RaE (Bi^{210})	46.5	100 : (10.6 ± 0.2): (0.93 ± 0.05)
ThB → ThC (Bi^{212})	115.1	100 : (10.4 ± 0.3): (0.88 ± 0.10)
ThB → ThC (Bi^{212})	238.6	100 : (10.4 ± 0.2): (0.74 ± 0.05)

TABLE II

Transition	$L_I : L_{II} : L_{III}$	Reference
46.5 kev	100 : (10.2 ± 0.7) : (0.95 ± 0.05) *	
	100 : (10.5 ± 0.4) : (1.0 ± 0.1)	[16]
238.6 kev	100 : (10.8 ± 0.1) : (0.80 ± 0.02)	[17]
	100 : (11.6 ± 0.3) : (0.66 ± 0.04)	[11]
	100 : (10.0 ± 0.7)	[10]

*These results have been obtained by A. A. Bashilov, B. S. Dzhelepov, and L. S. Chervinskaia in 1955 and have been communicated to us privately by the authors.

We determined the ratio $L_I : L_{II} : L_{III}$ directly from the heights of the corresponding lines. In addition to the correction for the decay, the following corrections were introduced during the reduction of the experimental data: (1) a correction for the magnitude of the "tail" of the L_{II} line under the L_I-line, which amounted to 1 or 2%; (2) for the 46.5-kev transition a correction was made, in addition to the above, for the variation in the half-width of the line with variation of H_ρ. Such a dependence of the half-width on H_ρ is explained, in the case of our apparatus, by the distortion of the topography of the field for $H_\rho <$ 1000 Oe-cm, and we have studied it by recording the conversion spectrum of an active radiothorium deposit.[15] The correction amounts to 1.2% for the ratio $L_I : L_{II}$ and to 6.5% for the ratio $L_I : L_{III}$.

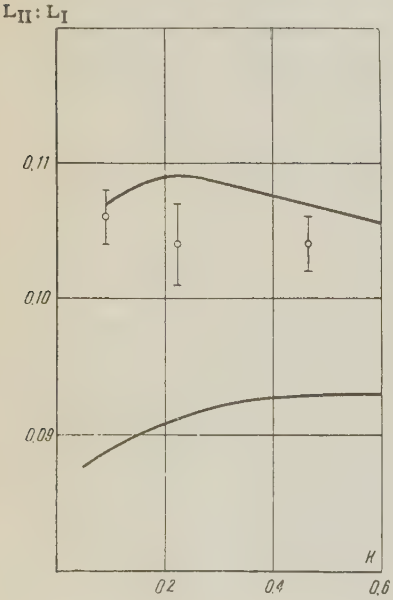

FIG. 3. Comparison of theoretical and experimental values of the ration $L_{II} : L_I$. K is the γ-ray energy in units of m_0c^2.

No corrections were made for absorption in counter windows, and for missed counts; under our conditions they were both small (< 1%).

Four to five sets of measurements were taken for each line. Table I gives averaged results. The errors shown in the table are somewhat larger than statistical, because the possible presence of systematic errors was taken into account.

For comparison with our results, we give in Table II values of relative conversion coefficients in L subshells for the 46.5 and 238.6 kev transitions taken from references 10, 11, 16, and 17, carried out since 1955. The results of earlier work are subject to considerable experimental error and are not given in the table. It can be seen from the table that for both transitions our results agree within experimental error with the results of the other papers, except for the ratio $L_I : L_{II}$ given by Krisiuk et al.[11] which gives a discrepancy of ~ 10%. In this work carried out in our laboratory the errors shown in the table are purely statistical ones, and do not include a systematic error which was discovered by us later. The introduction of an appropriate correction leads to agreement between the results.

It should be noted that in the paper by Bashilov et al.[18] a 31.9-kev line of intensity comparable to the L_{III} line was found between the L_{II} and L_{III} lines in the course of obtaining the conversion spectrum of RaD. As can be seen from Fig. 1, we do not have such a line in this region.

3. COMPARISON WITH THEORY

In order to compare the experimental results with the theoretical ones we have plotted in the graphs of Figs. 3 and 4 the theoretical ratios

$L_{II}:L_I$ and $L_{III}:L_I$ as functions of the energy. We have also given there the corresponding experimental ratios. The lower curves in both graphs have been plotted according to the tables of Dranitsyna[19] who interpolated Rose's results[7] with respect to Z and energy. The upper curves have been plotted according to the tables of Band and Sliv. The accuracy of the theoretical values communicated to us by Band and Sliv amounts to ~2%.

It may be seen from Figs. 3 and 4 that within experimental error the calculations of Band and Sliv, carried out taking finite nuclear size into account, agree well with the experimental results. Rose's calculations for a point nucleus disagree noticeably with the experimental results. Thus from our data it follows that the finite nuclear size makes an appreciable contribution to the relative L-conversion coefficients, and that this contribution has been correctly taken into account in the calculations of Band and Sliv.

In all three cases of γ transitions studied by us, as has been shown by Krisiuk et al.,[12] apparently a transition of one neutron takes place from the $g_{9/2}$ state to the $i_{11/2}$ state, i.e., the transitions are l-forbidden. In all cases when the lifetimes of l-forbidden M1-transitions were measured, a retardation by 2 or 3 orders of magnitude was found. All these transitions take place in odd nuclei. If a similar retardation takes place in the transitions investigated by us in odd-odd nuclei, we can expect to observe the influence of nuclear structure on the relative conversion coefficients for the M1-transitions, which was noted by Church and Weneser.[20] The good agreement between our results and Sliv's calculations indicates that even if nuclear structure does affect the ratio $L_I:L_{II}:L_{III}$ in the M1 transitions studied by us, this effect must be less than 5%.

4. RELATIVE CONVERSION COEFFICIENTS FOR THE 277.3-kev TRANSITION IN Pb^{208}

In addition to the pure M1 transitions discussed above, we have also measured the ratio $L_I:L_{II}:L_{III}$ for the 277.3-kev M1 transition between two excited levels of Pb^{208}, 3474.8 kev (4^-) and 3197.5 kev (5^-). An admixture of E2 radiation is possible in this transition.

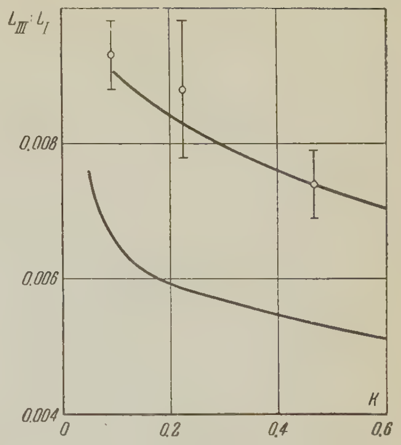

FIG. 4. Comparison of theoretical and experimental values of the ratio $L_{III}:L_I$.

We determined the ratio $L_I:L_{II}$ for this transition with a resolution of 0.05%, and the ratio $L_I:L_{III}$ with a resolution of 0.23%.

The average value of the ratio $L_I:L_{II}:L_{III}$ obtained from 4 or 5 sets of measurements is given in Table III. Moreover, in this table we have also given the value of $K:L_I$ which has been calculated from the ratio $K:(L_I+L_{II})$ found in our laboratory.[21] From the table it may be seen that the value of the ratio $L_I:L_{II}:L_{III}$ for this transition differs appreciably from the corresponding ratios for the pure M1 transitions (cf. Table I). This difference may be easily explained by the existence of a small admixture of E2 radiation in the 277.3-kev transition. In Table III we have shown the values of the admixtures of E2 obtained by using both the new conversion coefficients of Band and Sliv, and also Rose's coefficients.[7] When Sliv's coefficients are used, good agreement is found between the values of admixtures of E2 obtained from the two independent ratios $L_I:L_{II}$ and $L_I:L_{III}$.

The amount of admixture of E2 radiation in the 277.3-kev transition is ~5%. Thus it can be seen that with a sufficient precision of measurement the use of the new conversion coefficients allows us to determine the admixture of E2 radiation even in the case when this admixture amounts to only a few percent of the main radiation. Such small admixtures were previously determined primarily from measurements of angular correlation.

TABLE III

E_γ, kev	$K:L_I$	$L_I:L_{II}:L_{III}$	Admixture of E2, percent			
			$L_I:L_{II}$	$L_I:L_{III}$	$L_I:L_{II}$	$L_I:L_{III}$
			According to Sliv		According to Rose	
277.3	6.15±0.3	100 : (12.5±0.6) : (1.9±0.3)	4.8±1.5	5.2±1.4	11.0±1.5	8.8±1.8

If the probability of γ transitions is assumed to be correctly described by Moszkowski's formula,[22] then the ratio E2 : M1 for the 277.3-kev transition turns out to be equal to $\sim 10^{-4}$. However, the results of our measurements show that this ratio is equal to 0.05. The existence of an appreciable admixture of E2 radiation may be due to a retardation of the M1 transition.

The retardation of the M1 radiation in this case is not explained by the structure of the excited levels of Pb^{208}, proposed by Tauber.[23] According to Tauber the 277.3-kev transition takes place between levels of the same multiplet. The probability of such a transition must agree with the single-particle estimate. This has been confirmed experimentally in the case of the 40-kev M1 transition in Tl^{208}. This transition takes place between the multiplet levels $s_{1/2}\, g_{9/2}$ and direct experimental measurements of the lifetime[24] agree with calculations according to the shell model.[25] Moreover, the ratio $L_I : L_{II} : L_{III}$ for this transition[26] does not allow an admixture of E2 radiation in excess of 0.05%. It is also difficult to expect an appreciable retardation of the M1 transition in the case of transitions between levels of any other multiplet. Therefore the occurrence of an appreciable admixture of E2 radiation in the 277.3-kev transition in Pb^{208} does not agree with Tauber's assumption[23] that the initial and the final levels of this transition belong to the same multiplet.

---

[1] A. H. Wapstra and G. J. Nijgh, Nucl. Phys. **1**, 245 (1956).

[2] Nordling, Siegbahn, Sokolowski and Wapstra, Nucl. Phys. **1**, 326 (1956).

[3] F. K. McGowan and P. H. Stelsen, Phys. Rev. **103**, 1133 (1956).

[4] Michelich, Ward and Jacob, Phys. Rev. **103**, 1285 (1956).

[5] Nielsen, Nielsen and Waggoner, Nucl. Phys. **2**, 476 (1956).

[6] Ewan, Knowles and McKenzie, Phys. Rev. **108**, 1308 (1957).

[7] M. E. Rose (in the book: K. Siegbahn "Beta- and Gamma-Ray Spectroscopy", Amsterdam, 1955, p. 905).

[8] L. A. Sliv, J. Exptl. Theoret. Phys. (U.S.S.R.) **21**, 770 (1951).

[9] L. A. Sliv and M. A. Listengarten, J. Exptl. Theoret. Phys. (U.S.S.R.) **22**, 29 (1952).

[10] Sokolowski, Edwardson, and Siegbahn, Nucl. Phys. **1**, 160 (1956).

[11] Krisiuk, Latyshev, Listengarten, Ostretsov, and Sergeev, Izv. Akad. Nauk S.S.S.R., Ser. Fiz. **20**, 363 (1956) [Columbia Techn. Transl. **20**, 332 (1956)].

[12] Krisyouk, Sergeyev, Latishev, and Vorobyov, Nucl. Phys. **4**, 579 (1957).

[13] Latyshev, Sergeev, Krisiuk, Ostretsov, Egorov, and Shirshov, Izv. Akad. Nauk. S.S.S.R., Ser. Fiz. **20**, 354 (1956) [Columbia Techn. Transl. **20**, 324 (1956)].

[14] Egorov, Latyshev, and Trulev, Приборы и техника эксперимента (Instruments and Meas. Engg.) **5**, 41 (1957).

[15] Zhernovoi, Krisiuk, Latyshev, Remennyi, Sergeev, and Fadeev, J. Exptl. Theoret. Phys. **32**, 682 (1957), Soviet Phys. JETP **5**, 563 (1957).

[16] M. Frilley and M. Valadares, J. phys. et radium **18**, 468 (1957).

[17] Kel'man, Romanov, and Metskhvarashvili, Dokl. Akad. Nauk S.S.S.R. **103**, 577 (1955).

[18] Bashilov, Dzhelepov, and Chervinskaia, Izv. Akad. Nauk S.S.S.R., Ser. Fiz. **17**, 428 (1953).

[19] G. F. Dranitsyna, Коэффициенты внутренней конверсии на L_I, L_{II}, L_{III} подоболочках (Internal Conversion-Coefficients for L_I, L_{II} and L_{III} Subshells) Acad. Sci. Press, 1957.

[20] E. L. Church and J. Weneser, Phys. Rev. **104**, 1382 (1956).

[21] Vorob'ev, Il'in, Kol'chinskaia, Latyshev, Sergeev, Trofimov and Fadeev, Izv. Akad. Nauk. S.S.S.R., Ser. Fiz. **21**, 954 (1957) [Columbia Techn. Transl. **21**, 956 (1957)].

[22] S. A. Moszkowski, (in the book: K. Siegbahn "Beta- and Gamma-Ray Spectroscopy", Amsterdam, 1955, p. 373).

[23] G. E. Tauber, Phys. Rev. **99**, 176 (1955).

[24] J. G. Siekman and H. de Waard, Phys. Rev. **107**, 1731 (1957).

[25] A. de-Shalit, Phys. Rev. **105**, 1531 (1957).

[26] Sergeev, Krisiuk, Latyshev, Vorob'ev, and Kol'chinskaia, Izv. Akad. Nauk S.S.S.R., Ser. Fiz. (in press).

Translated by G. Volkoff
65

SOVIET PHYSICS JETP VOLUME 35(8), NUMBER 2 FEBRUARY, 1959

PHOTOPRODUCTION OF SLOW π^0 MESONS ON COMPLEX NUCLEI

A. S. BELOUSOV, S. V. RUSAKOV, and E. I. TAMM

P. N. Lebedev Physics Institute, Academy of Sciences, U.S.S.R.

Submitted to JETP editor March 13, 1958

J. Exptl. Theoret. Phys. (U.S.S.R.) 35, 355-363 (August, 1958)

Results of measurements of the dependence of the cross section for photoproduction of slow π^0 mesons on the mass number of the target nuclei are presented for nuclei between C and Pb. $\sigma \sim A^{2/3}$ for synchrotron γ-ray beams of maximum energy of 265 and 210 Mev. The dependence of the slow π^0 meson yield on the maximum energy of the γ-ray beam has been measured for carbon and lead. The results agree with the theory of π-meson production on the surface of the nucleus.

1. INTRODUCTION

THE photoproduction of π mesons on nuclei has been studied in a series of papers.[1-5] It was found that in all cases of complex nuclei (heavier than Al) the relationship $\sigma_A \sim A^{2/3}$ holds where σ_A is the cross section for the production by a photon of a meson on a nucleus of mass number A.

There exist two different explanations of the observed dependence of the cross section for the photoproduction of π-mesons on the mass number. The first theory[6] is based on the optical model which takes into account the finite mean free path for the reabsorption of mesons in nuclear matter. According to this theory the cross section for the photoproduction of π mesons on a nucleus of mass number A is given by

$$\sigma_A = \sigma_0 A \eta f_a, \tag{1}$$

where σ_0 is the cross section for the production of mesons on a free nucleon, and η is a factor that takes into account the nuclear binding of the nucleons inside the nucleus. The magnitude of this factor is in the general case less than unity, since the law of conservation of energy and the Pauli exclusion principle impose a restriction on the possible number of final states. However, the value of η must be approximately the same for different nuclei. f_a is the reabsorption coefficient given by

$$f_a = \frac{1}{V}\int e^{-x/\lambda_a}\,d\tau = \frac{3}{4}\frac{\lambda_a}{R}\left[1 - \frac{\lambda_a^2}{2R^2} + \frac{\lambda_a^2}{2R^2}\left(\frac{2R}{\lambda_a} + 1\right)e^{-2R/\lambda_a}\right], \tag{2}$$

where λ_a is the mean free path for absorption, $R_0 = r_0 A^{1/3}$ is the nuclear radius, V is the nuclear volume, and x is the path length traversed by the meson inside the nucleus. From this it may be seen that when $2R/\lambda_a \gg 1$,

$$\sigma_A \approx \sigma_0 \eta\,[3\lambda_a / 4r_0]\,A^{2/3}, \tag{3}$$

i.e., the relationship $\sigma_A \sim A^{2/3}$ is obtained in the case when the mean free path of the meson is considerably smaller than the nuclear dimensions.

The quantity λ_a is found directly from results of experiments on the interaction of π mesons with nuclei.[7] However, in a number of cases the meson mean free path turned out to be too large to explain the dependence $\sigma_A \sim A^{2/3}$ observed in experiments on photoproduction. Therefore a second theory has arisen[8] to explain this dependence, which assumes that the formation of real mesons is possible only on the nuclear surface. Inside a nucleus the absorption of photons is accompanied by photodisintegration which has a greater probability than photoproduction of mesons. According to this theory (the theory of surface production of mesons), the relationship $\sigma_A \sim A^{2/3}$ is obtained automatically in all cases (since the nuclear surface is proportional to $A^{2/3}$). The physical picture of the phenomena occurring when high-energy photons are absorbed inside complex nuclei is given by Wilson.[9] He assumes that the absorption of a photon in the nucleus is accompanied by the production of a virtual meson on one of the nucleons, with a subsequent absorption of it by the system comprising the nucleon that gave rise to the meson and one of its neighbors. Thus the absorption of photons in nuclei leads to the photodisintegration of "quasi-deuterons,"[10] with the latter process having a greater probability than the formation of a real meson.

It has been established experimentally, by recording n-p coincidences, that such a process does in fact occur,[11] and, apparently, is the main source of photoprotons of high energy. A decision between these two theories can be made by measuring the dependence on the mass number of the cross section for the production of mesons on nuclei, for mesons of different energies. As is well known,[7] the mean free path λ_a for a meson in nuclear matter depends strongly on the meson energy, increasing as the energy decreases. Therefore as the energy of the recorded π mesons is reduced, the dependence of σ_A on A must approach a linear one (instead of $A^{2/3}$) if the first theory is valid. However, if the theory of surface production of mesons is valid, then the relationship $\sigma_A \sim A^{2/3}$ must be obtained, independently of the meson energy. These relationships can be obtained in their clearest form in the case of π^0 mesons, which is free of the Coulomb interaction that complicates the interpretation of the results obtained with charged mesons.

Experiments made to study the dependence on A of the photoproduction cross-section for π^0-mesons on complex nuclei,[12-13] carried out by recording π^0 mesons using one of the decay γ quanta, have shown that the relationship $\sigma_A \sim A^{2/3}$ is preserved in the region of complex nuclei at a maximum synchrotron γ-ray beam energy of 265 and 200 Mev. These γ-ray energies correspond to π^0-meson spectra with maxima in the region of 60 and 20 Mev respectively. In the work of Panofsky et al.,[2] the π^0 mesons were recorded using two decay γ quanta. The geometry of the experiment corresponded to recording mesons with energy greater than 100 Mev. However, these experiments can be considered only as preliminary ones, since the results of the work of Panofsky et al.[2] are subject to large error, while the method of recording a π^0 meson by means of only one of its decay γ quanta suffers from certain disadvantages. Firstly, this method does not allow one to determine the energy of the π^0 mesons being recorded. An upper bound on their energy is the maximum energy of the synchrotron γ rays. A reduction of this energy below 200 Mev results in a considerable decrease in the π^0-meson yield, which leads to danger of interference from the background of γ quanta scattered by nuclei, which would be indistinguishable from the effect under observation when such a method of recording mesons is employed. Secondly, the recording of π^0 mesons by means of one of their decay γ quanta requires the knowledge of the angular distribution of mesons produced on nuclei.

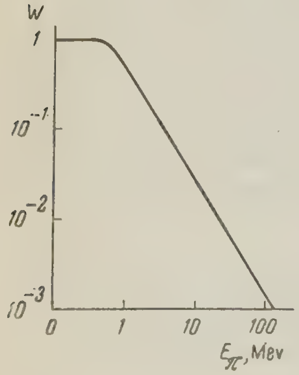

FIG. 1. Energy dependence of the efficiency of recording of π^0 mesons by the measuring equipment.

2. EXPERIMENTAL SETUP

In order to select π^0 mesons of low energy it is necessary to record both the decay γ quanta. In the system of coordinates in which the π^0 meson is at rest the decay γ quanta emerge at an angle of 180° with respect to one another, with the angular distribution of the quanta being isotropic. In the laboratory system the angular distribution of the decay γ quanta from a meson moving with a velocity β is given by

$$P(\alpha)\, d\Omega_\alpha = d\Omega_\alpha / 2\pi\gamma^2 (1 - \beta\cos\alpha)^2, \tag{4}$$

where α is the angle between the direction of motion of the π^0 meson and the direction in which the decay γ quantum is emitted, while $\gamma = 1/\sqrt{1-\beta^2}$. If the angle between the decay γ quanta in the laboratory system is denoted by φ, then

$$\sin(\varphi/2) = (\cos^2\alpha' + \gamma^2 \sin^2\alpha')^{-1/2}. \tag{5}$$

Here α' is the angle of emission of the γ quantum in a system in which the π^0 meson is at rest.

It can be seen thus that corresponding to each value of π^0-meson energy there will exist a minimum angle (critical angle) between the directions of emission of the two decay γ quanta. This angle is determined by the relation

$$\sin(\varphi_k/2) = \gamma^{-1}. \tag{6}$$

Making use of relation (5), we can easily show that the probability that the decay γ quanta are emitted in the laboratory system at an angle φ will be given by

$$p(\varphi)\, d\varphi = \frac{\sin\varphi\, d\varphi}{[(1-\cos\varphi)\gamma^2 - 2]^{1/2}\, \beta\gamma\, (1-\cos\varphi)^{3/2}}. \tag{7}$$

This probability has a sharp maximum near the critical angle φ_k determined by relation (6). Thus, the lower limit on the energy of π^0 mesons recorded by means of two γ quanta will be determined by the angle between the detectors of the decay γ quanta. Let us determine the probability of recording mesons of various energies in the case when the angle between the γ-quanta detectors is 180°. If the angle subtended by the detector at the target is φ_D, the apparatus will record π^0 mesons decaying with emission of γ quanta, the angle between which lies within the limits $\pi - \varphi_D \leq \varphi \leq \pi$. Thus, the probability of recording π^0 mesons will be given by:

$$W = \int_{\pi-\varphi_D}^{\pi} P(\varphi)\,d\varphi \Big/ \int_{\varphi_K}^{\pi} P(\varphi)\,d\varphi = 1 - \frac{1}{\beta\gamma}\left[\gamma^2 - \frac{2}{1-\cos(\pi-\varphi_D)}\right]^{1/2}. \qquad (8)$$

The calculated values of W for $\varphi_D = 9°$ and for different π^0-meson energies are plotted in Fig. 1. It can be seen from the graph that the experimental geometry chosen by us allows us to reduce effectively the recording of high energy mesons, without significantly lowering the efficiency for recording slow π^0 mesons.

There exists still another mechanism which reduces the probability of recording by the apparatus of fast π^0 mesons. It is based on the fact that the efficiency of recording of γ quanta by the telescope depends on the γ-quanta energies. When the γ quanta from the decay of a π^0 meson that moves with a velocity β reach both telescopes, one quantum must be moving in the same direction as the π^0-meson, while the other one moves in the opposite direction. In such a case the energy of the former will be given by $h\nu_{max} = \mu_0 c^2\gamma(1+\beta)/2$, while the energy of the latter will be given by $h\nu_{min} = \mu_0 c^2\gamma(1-\beta)/2$. Thus, there exists an absolute energy threshold for the recording of π^0 mesons by the apparatus, and the magnitude of this threshold is determined by the threshold energy of the telescope at which the efficiency falls to zero, $\epsilon(h\nu_{min}) = 0$.

The next section of this article gives the results of measurements of the efficiency of the telescope, which show that its threshold for γ quanta is equal to 35 Mev (Fig. 2). For π^0 mesons this corresponds to an upper threshold of 40 Mev for the apparatus.

The energy spectrum of the π^0 mesons recorded by the apparatus can be determined if we know the energy dependence of the efficiency of recording and the energy spectrum of the π^0 mesons produced in the target. We know the first of these functions. The energy spectrum of the π^0 mesons originating in the target is determined primarily by the momentum distribution of the nucleons in the nucleus. Baldin has carried out calculations[14] of energy spectra of π^0 mesons formed in nuclei through bremsstrahlung. The results of these calculations are in good agreement with available experimental data. Making use of energy spectra obtained by Baldin,[14] we can easily calculate the energy spectrum of π^0 mesons recorded by the apparatus. The spectrum obtained in this manner has a very flat maximum in the range between 1 to 15 Mev; a rapid decrease takes place above 15 Mev.

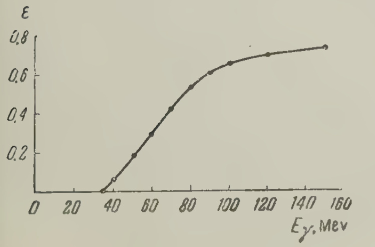

FIG. 2. Efficiency of recording of γ quanta by the telescope.

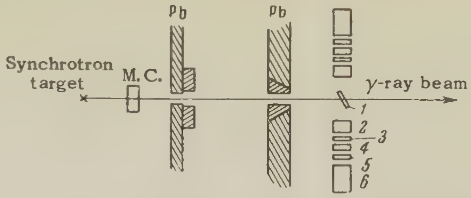

FIG. 3. Experimental geometry. M.C.) monitoring ionization chamber, 1) target, 2) carbon filter, 3) lead converter, 4) scintillator, 5) aluminum absorber, 6) radiator of the Cerenkov counter.

Thus, the recording of π^0 mesons by means of two decay γ quanta first permits us, after making an appropriate choice of geometry, to record mesons of definite energies. Secondly, this method permits us to exclude completely the background of scattered γ quanta. Finally, with the chosen geometry, the apparatus enables us to obtain the total cross section directly without measuring the angular distribution of the mesons, since for slow mesons the probability of emission of decay γ quanta is practically the same in all directions (cf. reference 4).

3. APPARATUS

The measurements were made with the synchrotron of the Physics Institute of the Academy of Sciences, which produces a γ-ray beam with a maximum energy of 265 Mev.

The experimental geometry is shown in Fig. 3. The synchrotron beam passes through a monitor ionization chamber, through two collimators, and falls on the target being investigated. The π^0 mesons formed in the target are recorded by two counter telescopes, each situated at an angle of 90° to the beam on the same straight line passing through the target. The two telescopes are connected for coincidence. Each telescope consists of a carbon filter 6 cm thick, a lead converter 5 mm thick, a scintillation counter, an aluminum absorber 2 cm thick, and a Cerenkov counter. The

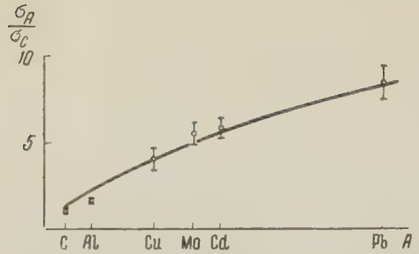

FIG. 4. Results of the measurement of the dependence of the π^0-meson yield on the mass number of the target for maximum energy of the γ-ray beam equal to 265 Mev (circles); the solid curve is $\sigma \sim A^{2/3}$.

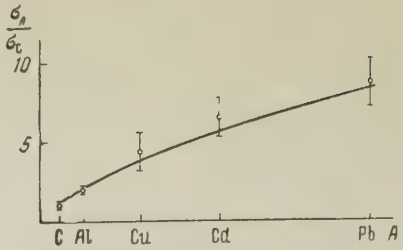

FIG. 5. Results of the measurement of the dependence of the π^0-meson yield on the mass number of the target for maximum energy of the γ-ray beam equal to 210 Mev (circles); the solid curve is $\sigma \sim A^{2/3}$.

carbon filter served to shield the scintillation counter from particles and from the low-energy γ quanta copiously emitted by the target. The scintillator was in the form of a disc 7 cm in diameter and 3 cm thick, and consisted of a solution of terphenyl in toluol (4 g/liter) with addition of a secondary activator. The aluminum absorber served to raise the telescope threshold. The radiator of the Cerenkov counter consisted of a cylindrical vessel 6 cm in diameter and 12 cm long, filled with distilled water. All the counters made use of photomultipliers FEU-33 with improved time characteristics. To reduce the background, the counters were surrounded by lead shields up to 20 cm thick. To decrease the number of accidental coincidences, the duration of the synchrotron pulse was artificially stretched out to 3000 microsec. The intensity of the beam was measured by means of a thin-walled ionization chamber.

When the converters were removed, the counting rate decreased, with the residual counts being determined by the conversion of the γ quanta in the carbon filters and in the scintillators. The targets used in this experiment were situated at an angle of 45° to the γ-ray beam, and were fixed in a device which enabled targets to be changed by remote control. The thickness of each target amounted to 0.1 of a radiation unit. The targets covered the whole beam. To eliminate instabilities, the measurements were carried out using alternately the target investigated and a carbon target, and gave as a result the ratio σ_A/σ_C of the photoproduction cross section for π^0 mesons on the given nucleus to the cross section of production on a carbon nucleus.

The energy dependence of the telescope efficiency was measured by placing the telescope in a beam of monoenergetic electrons. Electrons of a definite energy were selected by means of a magnetic field in which was placed a lead target irradiated by the synchrotron γ-ray beam. Electron-positron pairs were formed in the target.

The range of electron trajectories corresponding to 10% accuracy in determining the electron energy was selected by the current-carrying-filament method. As a measure of efficiency we adopted the ratio of the counting rate of coincidences to the counting rate of pulses of the scintillation counter of a telescope of 100% efficiency. To determine the efficiency of the telescope for γ rays, we measured its efficiency for electrons passing through lead filters of various thicknesses placed in front of the telescope (this corresponds to pair production at various depths within the converter). Using the data received in this manner we calculated the values for the efficiency of the γ telescope. The results are shown in Fig. 2.

4. RESULTS

Measurements of the dependence of the yield of slow π^0 mesons on the mass number were made at maximum γ-ray energies of 265 and 210 Mev. In the case of measurements with $E_\gamma^m = 265$ Mev, we used targets of C, Al, Cu, Mo, Cd, and Pb. The results of these measurements are shown in Fig. 4.

The results of measurements at $E_\gamma^m = 210$ Mev are shown in Fig. 5.

The theoretical curve $\sigma_A \sim A^{2/3}$ in Figs. 4 and 5 was normalized for Pb, with all the experimental points falling on the curve within experimental error in the case of both maximum energies. In the region of light nuclei (C, Al) there is some deviation from the relation $\sigma_A \sim A^{2/3}$, most likely because the number of surface nucleons is not proportional to $A^{2/3}$ in light nuclei.

In order to determine which part of the γ-ray spectrum is responsible for the observed effect, we measured the dependence of the yield of slow mesons on the maximum energy of the γ-ray beam. It can be assumed that the slow π^0 mesons recorded by the apparatus are the result of inelastic scattering of high-energy mesons that originate in the target. If this assumption is correct, the high-energy photons should make an appreciable

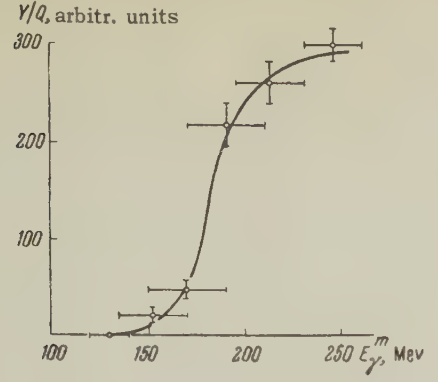

FIG. 6. Dependence of the slow π^0-meson yield in carbon on the maximum energy of the γ-ray beam.

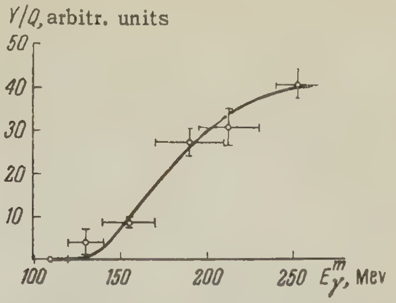

FIG. 7. Dependence of the slow π^0-meson yield in lead on the maximum energy of the γ rays.

contribution to the effect under investigation. Measurements were made for C and Pb targets, and the results are shown in Figs. 6 and 7 respectively. The quantity Y/Q shown in the graphs is the yield of π^0 mesons per "effective" quantum. The number of "effective" quanta Q is defined as the energy flux in a bremsstrahlung beam divided by the maximum energy E_γ^m. The lack of precision in the maximum energy of the beam is determined by the "stretching" of the duration of the accelerator pulse. As can be seen from the graphs, in the region of high γ-ray energies the yield curve has a plateau which indicates that the contribution of high-energy mesons to the effect being investigated is not significant.

From the curves shown in Figs. 6 and 7 it can be seen that the main contribution to the production of slow π^0 mesons on nuclei is made by γ quanta with energies between 160 to 230 Mev. This agrees with the results of Gorzhevskaia and Panova,[15] who showed that production of a photomeson of low energy (up to 6 Mev) on a nucleus is accompanied by emission of a fast ($E \geq 20$ Mev) recoil nucleon which acquires a considerable fraction of the momentum of the incident γ quantum. Because of this, γ quanta with energies even in excess of 200 Mev participate in the formation of slow π^0 mesons.

In addition to the inelastic scattering of high-energy mesons, a definite contribution to the effect recorded may also come from scattering events accompanied by charge exchange of low-energy $\pi^\pm$ mesons. However, available experimental data on scattering of $\pi^\pm$-mesons on nuclei accompanied by charge exchange[16,17] show that the mean free path for scattering accompanied by charge exchange of charged π mesons in nuclear matter amounts to $\sim 100 r_0$ for meson energies from 30 to 50 Mev, and increases rapidly with decreasing meson energy. Thus, in the case of mesons of energy ~ 10 Mev, we can practically neglect scattering accompanied by charge exchange. Moreover, if a significant contribution is made by the scattering accompanied by charge exchange of charged π-mesons, the dependence of the yield of slow π^0 mesons on A must be stronger than $A^{2/3}$, since all the nucleons in the nucleus participate in the scattering.

Thus, experimental results show that the cross-section for the photoproduction of slow π^0 mesons increases in proportion to the $^2/_3$ power of the mass number of the target nuclei, i.e., proportionally to the nuclear surface. The same dependence of the photoproduction cross-section on the mass number was obtained by Popova, Semashko, and Iagudina for low energy π^- mesons.[18]

To be able to draw a final conclusion regarding the mechanism of photoproduction of π mesons on complex nuclei, it is necessary to investigate in greater detail the processes of interaction of mesons with nuclear matter and to make a quantitative estimate of the magnitude of the mean free path λ_a for mesons of definite energies in nuclei. An estimate of the value of the absorption mean free path of slow π mesons in nuclear matter can be made on the basis of the following considerations:

1. The principal process of interaction between a π meson and the nucleus is absorption by a pair of nucleons (two-nucleon absorption).
2. The two-nucleon absorption cross section for a π meson in the nucleus can be related to the absorption cross section for π mesons in deuterium by means of the following formula:

$$\sigma_\pi = \Gamma\sigma(\pi^+ + d \rightarrow p + p). \tag{9}$$

In the reaction $\pi^+ + d \rightarrow p + p$, the absorption of a meson by a pair of nucleons, which acquire in the final state an energy on the order μc^2, takes place when the distance between the latter is reduced to an order of $\hbar/\mu c$. The coefficient Γ in formula (9) represents the ratio of the probabilities that two nucleons are $\hbar/\mu c$ apart in the nucleus and in the deuteron and, consequently, depends on meson energy. However, it is clear that for low π-meson kinetic energies, when $E_\pi \ll \mu_0 c^2$, the quantity Γ must be constant. According to the calculations of Wilson[9] and Levinger,[10] and also from the analysis of experimental data of Byers,[19] Tenney and Tinlot,[20] and Byfield et al.,[21] $\Gamma = 5$ to 6 in the region of small π-meson energies.

3. The quantity $\sigma(\pi^+ + d \to p + p)$ can be obtained from experiments on the absorption of π mesons in deuterium, and also by utilizing the principle of detailed balancing from the cross section of the inverse reaction $p + p \to \pi^+ + d$. It can be easily seen that

$$\sigma(\pi^+ + d \to p + p) = \frac{2}{3}\frac{M}{\mu}\left(\frac{1}{\eta}\right)^2 \sigma(p + p \to \pi^+ + d). \tag{10}$$

Here $\eta = p_\pi/\mu c$ is the momentum of the π meson in units of μc, while M and μ are the masses of the nucleon and the π meson respectively.

The energy dependence of the cross section of the reaction $p + p \to \pi^+ + d$ is derived from semi-empirical considerations. It is shown by Rosenfeld[22] and Gell-Mann and Watson[23] that

$$\sigma(p + p \to \pi^+ + d) = (0.14\eta + 1.0\eta^3)\cdot 10^{-27}\ \text{cm}^2. \tag{11}$$

Frank et al.[24] have made calculations utilizing relations (9) to (11), and they have shown that the mean free path λ_a for the absorption of a π meson in nuclear matter increases as the π-meson energy is decreased right down to 30 Mev. In the energy region from 30 down to 2 Mev, $\lambda_a \approx 10r_0$ and is almost independent of the meson energy. At energies less than 2 Mev, λ_a decreases in proportion to the π-meson momentum. However, these calculations were made for charged π mesons. In the case of π^0 mesons the absorption is due to the reaction $\pi^0 + d \to n + p$. The cross section of this reaction is only half of the cross section of the reaction $\pi^+ + d \to p + p$, since the isotopic spin of the n-p system may be equal to 0 and 1 with equal probability, while the isotopic spin of the p-p system is equal to 1. The transition $I = 0 \to I = 1$ takes place when a meson is absorbed, while the transition $I = 0 \to I = 0$ is forbidden. Thus, only half of the possible final states of the nucleons participate in the π^0-meson absorption reaction, and the value of the mean free path of π^0 mesons in the nucleus will be approximately $20r_0$ in the energy range from 2 to 30 Mev, i.e., practically for all mesons recorded in the present work.

5. CONCLUSION

Present experiments on the study of the dependence of the cross section of photoproduction of slow ($E_\pi \sim 10$ Mev) π^0 mesons on the mass number of the nucleus have shown that the cross section for this process is proportional to $A^{2/3}$. On the other hand, an analysis of the absorption of slow π^0 mesons in nuclei leads to the conclusion that the mean free path for absorption of mesons of this energy in the nucleus amounts to $20r_0$, i.e., all nuclei right up to the heaviest ones must be transparent for such mesons. Consequently the experimentally obtained dependence cannot be explained by the absorption of all mesons formed inside the nucleus, as is done in the description of the process of photoproduction of mesons from the point of view of the optical model.[6] The results obtained support the theory of surface production of π mesons on nuclei,[8,9] according to which real mesons are produced only on the surface of nuclei.

When a γ quantum is absorbed by a nucleon situated inside a nucleus, photodisintegration of this nucleus takes place, whereby the photon energy is transmitted to a pair of nucleons, with the probability of such photodisintegration being greater than the probability of π-meson photoproduction.

The electronic apparatus utilized in the present experiment was constructed and built by engineers P. N. Shareiko and A. A. Rudenko, to whom the authors wish to express their sincere gratitude.

In conclusion we take this opportunity to express our gratitude to Prof. V. I. Veksler and to Prof. P. A. Cerenkov for their interest in our work and for a number of valuable suggestions, to A. D. Makov who participated in the preparation and the performance of the experiment, and also to the members of the accelerator crew for looking after the operation of the synchrotron.

---

[1] R. M. Littauer and D. Walker, Phys. Rev. **86**, 838 (1952).

[2] Panofsky, Steinberger, and Steller, Phys. Rev. **86**, 180 (1952).

[3] Anderson, Kenney, and McDonald, Phys. Rev. **100**, 1798 (1955).

[4] Williams, Crowe, and Friedman, Phys. Rev. **105**, 1840 (1957).

[5] Imhof, Knapp, Easterbey, and Perez-Mendez, Phys. Rev. **108**, 1040 (1957).

[6] Brueckner, Serber, and Watson, Phys. Rev. **84**, 258 (1951).

[7] D. H. Stork, Phys. Rev. **93**, 868 (1954).

[8] S. T. Butler, Phys. Rev. **87**, 1117 (1952).

[9] R. R. Wilson, Phys. Rev. **86**, 125 (1952).

[10] J. S. Levinger, Phys. Rev. **84**, 43 (1951).

[11] Odian, Stein, Wattenberg, et al., Phys. Rev. **102**, 837 (1956).

[12] Belousov, Tamm, and Shitov, Dokl. Akad. Nauk SSSR **112**, 1017 (1957), Soviet Phys. "Doklady" **2**, 90 (1957).

[13] Govorkov, Gol'danskii et al., Dokl. Akad. Nauk SSSR **112**, 37 (1957), Soviet Phys. "Doklady" **2**, 4 (1957).

[14] A. M. Baldin, Thesis, Phys. Inst., Academy of Sciences, U.S.S.R., 1951.

[15] E. G. Gorzhevskaia and N. M. Panova, Dokl. Akad. Nauk SSSR **111**, 1205 (1956), Soviet Phys. "Doklady" **1**, 757 (1956).

[16] W. J. Spry, Phys. Rev. **95**, 1299 (1954).

[17] G. Saphir, Phys. Rev. **104**, 535 (1956).

[18] Belousov, Popova, Semashko, Shitov, Tamm, Veksler, and Jagudina, Proc. CERN Symposium **2**, 288 (1956).

[19] N. Byers, Phys. Rev. **107**, 843 (1957).

[20] F. H. Tenney and J. Tinlot, Phys. Rev. **92**, 974 (1953).

[21] Byfield, Kessler, and Ledermann, Phys. Rev. **86**, 17 (1952).

[22] A. Rosenfeld, Phys. Rev. **96**, 139 (1954).

[23] M. Gell-Mann and K. M. Watson, Ann. Rev. Nucl. Sci. **4**, 219 (1954) [transl. in Usp. Fiz. Nauk **59**, 399 (1954)].

[24] Frank, Gamel, and Watson, Phys. Rev. **101**, 891 (1956).

Translated by G. Volkoff
66

SOVIET PHYSICS JETP VOLUME 35(8), NUMBER 2 FEBRUARY, 1959

INVESTIGATION OF RELAXATION PROCESSES IN A SERIES OF FLUORINE COMPOUNDS OF CARBON

V. S. GRECHISHKIN

Leningrad State University

Submitted to JETP editor March 14, 1958

J. Exptl. Theoret. Phys. (U.S.S.R.) **35**, 364-366 (August, 1958)

A study is made of the influence of anisotropy of the chemical shift tensor on the relaxation time of fluorine nuclei. It is found that the difference in relaxation times of fluorine nuclei and of protons in one and the same molecule depends on the presence of nuclei of another halogen.

FLUORINE is one of the most electronegative elements. The methods of nuclear magnetic resonance are currently applied successfully to the investigation of fluorine compounds. These investigations are devoted chiefly to the fine structure of the fluorine resonances, and also to the study of relaxation processes. Gutowsky and Hoffman[1,2] examined nuclear magnetic screening of hydrogen fluoride and of a large number of other inorganic fluorides. A considerable number of aromatic fluoride compounds have been studied by Borodin and Skripov.[3,4] Gutowsky and Woessner[5] measured relaxation times in a series of fluorocarbons. They found that protons have considerably longer relaxation times than do fluorine nuclei in the same molecule. The maximum value of the ratio $R = T_1(H^1)/T_1(F^{19})$ came to 9.2, in connection with which the authors emphasized the dependence of the given ratio on the strength of the magnetic field. They also express the hypothesis that fluctuations in the screening field, stipulated by the anisotropy of the chemical shift tensor, add a contribution to the relaxation time of the fluorine. On superimposing a constant magnetic field H_0 on the specimen, the molecular electrons undergo a precession, by virtue of which an additional field $-\sigma H_0$ arises, proportional but opposite to the applied field, σ (σ is a constant that characterizes the degree of screening of the nucleus by the electrons). In the general case, σ is represented by some second rank-tensor, since the screening is a function of direction in the molecule. Assuming axial symmetry of the chemical shift tensor (this name is due to the circumstance that a difference in screening leads to a shift of the resonances of nuclei of a given type in various chemical compounds), Gutowsky and Woessner obtained, the approximate formula:

$$R = \frac{T_1(\mathrm{H}^1)}{T_1(\mathrm{F}^{19})} = 1 + \frac{2\gamma_{\mathrm{F}}^2 H_0^2 \left(\sigma_{z'z'} - \sigma_{x'x'}\right)^2 \tau_c T_1(\mathrm{H}^1)}{15(1 + 4\pi^2\nu_0^2\tau_c^2)}, \quad (1)$$

where γ_F is the gyromagnetic ratio of the fluorine nuclei, H_0 is the intensity of the external magnetic field, τ_c is the Debye correlation time, $T_1(H^1)$ the longitudinal relaxation time of the protons, $T_1(F^{19})$ the longitudinal relaxation time of the fluorine nuclei, $(\sigma_{z'z'} - \sigma_{x'x'})$ is the anisotropy of the chemical shift tensor, and ν_0 is the resonance frequency. The authors point out the poor agreement with the experimental data for the compounds which they studied.

The present work was done with the aim of studying the question further. It is necessary to observe that the relaxation mechanism proposed by Gutowsky and Woessner, even in the absence of axial symmetry of the screening field, is not able to explain the great difference in relaxation times of protons and fluorine nuclei in certain compounds.

EXPERIMENTAL PROCEDURE

We measured the relaxation times by Bloch's method of nuclear induction, since in this method the generator and receiver are separated, so that large radio-frequency fields can be used and saturation can be observed in a broad class of substances. The high-frequency generator contained a Hartley oscillator for the 20 to 40 Mcs range. Through a buffer cascade provided with an attenuator, the r-f oscillations were fed to the exciting coil. The Bloch coils were of high mechanical stability; they were encased in polystrene jackets. The exciting coil had 12 turns and the receiving coil 10. Adjustment of the coupling between the coils was accomplished by the use of a little copper flag and the bridge circuit shown in the figure.

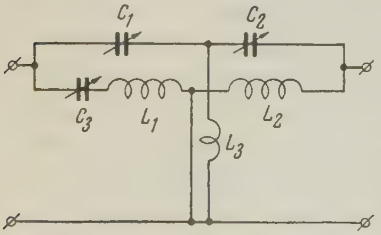

Balanced bridge circuit for observation of nuclear induction signals.

For the circuit given, it is easy to obtain the approximate conditions for complete balance:

$$L_3 = M;\; C_2L_2 + C_2M = MC_1; \qquad \omega^2 = 1/C_2(L_2 + M), \quad (2)$$

where L_1 is the inductance of the exciting coil, L_2 the inductance of the receiving coil, and M the coefficient of mutual inductance of the coils. Capacitors C_3 and C_2 had a maximum rating of 50 $\mu\mu$f, while that of C_1 was 30 $\mu\mu$f. Capacitor C_3 was tuned to precise resonance with L_1. Inductor L_3 consisted of two turns, the distance between which could be varied in the process of tuning the circuit.

Adjustment of the balancing circuit permitted isolation of the dispersion signal or of the absorption signal for observation. After high-frequency amplification, the nuclear-resonance signal was detected and amplified by a broadband low-noise low-frequency amplifier which had two stages with 6Zh4 tubes. The magnet employed gave an effective inhomogeneity of magnetic field on the order of 0.005 Oe/cm^3.

All the measurements were made at 25 Mcs, and the absorption signal was separated out for measurement. The dependence of the amplitude of the nuclear magnetic resonance signals on the intensity of the radiofrequency field was photographed and saturation curves were constructed. The transverse relaxation time was estimated from the half-width of the absorption lines. A multiplet structure of fluorine resonances was observed. Within the limits of error, the components of the multiplets did not show different relaxation times. Distilled water used as a standard, gave a signal of optimum amplitude with a radiofrequency field of the order of 0.01 Oe.

TABLE I*

Substance	T_1 (H^1) sec	T_1 (F^{19}) sec	R
$X\cdot(CF_2-CFCl)_nY$	—	1.21	—
$C_3F_5OH_2COOH$	0.8	0,62	1.29
$C_3F_4OH_3COOH$	0.65	0.47	1.35
$X\cdot(CF_2-CFCl)_nCOOH$	0.21	0.14	1.5
H_2O	2.6	—	—

* $\nu_0 = 25$ Mcs

TABLE II

Substance	R (20 Mcs)
CH_2FCl	3.8
$CHFCl_2$	9.2
CHF_2Cl	3.56
$C_6H_3F_3$	1.56

EXPERIMENTAL RESULTS

Our results are plotted in Table I and those of Gutowsky and Woessner[5] in Table II. Numerical comparison of theory with experiment for $C_3F_5OH_2COOH$ gives

$$(R-1)_{\text{theor}} = 0.147;\ (R-1)_{\text{exptl}} = 0.29.$$

The theoretical calculation made here is very approximate. It is assumed that the value of the anisotropy of the chemical shift tensor of fluorine is of the order of the shift itself, i.e., 7×10^{-4}. The correlation time was estimated from the Debye formula and taken equal to 10^{-10} sec. The difference in results by a factor of two can be regarded as a good approximation of theory to experiment for the estimate given. From Tables I and II it is seen that the value of R decreases with increasing number of fluorine nuclei in a molecule in which the number of nuclei of another halide remains the same. This, apparently, is a consequence of the reduced screening of fluorine. An increase in the number of chlorine nuclei in a molecule leads to an increase in R. The relaxation mechanism in question, connected in all probability with the properties of chlorine atoms, is for the time being still not clear.

Thus, the theory of Gutowsky and Woessner can explain only the not-too-large values of R. Very large values of R are observed, as a rule, in the presence of chlorine atoms in a molecule. Therefore, further development of the theory is required for the detailed explanation of the observed effects. The problem at hand is made difficult at the present time, however, by the fact that no complete theory of screening exists.

In conclusion, I express my thanks to F. I. Skripov and P. M. Borodin for their interest in the work and its evaluation.

---

[1] H. S. Gutowsky and C. J. Hoffman, J. Chem. Phys. 19, 1259 (1951).

[2] H. S. Gutowsky and C. J. Hoffman, Phys. Rev. 80, 110 (1951).

[3] P. M. Borodin and F. I. Skripov, Радиотехника и электроника (Radio Engg. and Electronics) 1, 882 (1956).

[4] P. M. Borodin and F. I. Skripov, Материалы 10 Совещания по спектроскопии (Proceedings of the Tenth Conference on Spectroscopy), Lvov, 1956.

[5] H. S. Gutowsky and D. E. Woessner, Phys. Rev. 104, 843 (1956).

Translated by R. Eisner
67

SOVIET PHYSICS JETP VOLUME 35(8), NUMBER 2 FEBRUARY, 1959

ON THE DISTRIBUTION OF NUCLEON DENSITY IN NUCLEI

F. I. KLIGMAN

Submitted to JETP editor January 12, 1958

J. Exptl. Theoret. Phys. (U.S.S.R.) 35, 367-371 (August, 1958)

The distribution of the orbital moments in nuclei is considered on the basis of the statistical nuclear model using various distribution functions of the nucleon density. It is shown that reasonable nucleon density distribution functions can be found, satisfying the experiments on scattering of fast electrons on nuclei, the saturation properties of nuclear forces, and the fundamental requirements of the shell model.

THE problem of nuclear structure, namely the distribution of nucleons in the nucleus, is being studied at present from different angles of approach.

Experimental and theoretical investigations of the scattering of fast electrons on nuclei[1-4] have shown that the proton density is approximately constant over the main part of the nuclear volume and falls off smoothly at its boundary. The most characteristic feature of the distribution function, found as the result of the above investigations, is the fact that the thickness of the surface layer is constant — independent of the mass number A in a wide range of A — and that the mean (proton) radius of the nucleus varies as $A^{1/3}$,[4] i.e. that there is no affinity of proton distribution in various nuclei. Such a distribution, both for protons and neutrons, is consistent with the saturation properties of nuclear forces[5-7] and with the experiments on the scattering of fast nucleons on nuclei.[8]

The problem of the nucleon distribution is connected with the problem of the distribution of the orbital moments in the nucleus. A series of publications has been devoted to the latter subject[7,9-14] dealing, partly, with the determination of n_l, the number of nucleons with a given l. The results, obtained from statistical considerations, have been compared with those of the shell model. The assumed nucleon distribution is anisotropic, the density falling off according to a Gaussian[7] or exponential[13,14] law for $r \geq R_0$ (where R_0 is the region of constant density).

In the present work, the maximum number of nucleons of one kind (protons or neutrons), with orbital moment $< l$, present in a nucleus has been calculated by means of a statistical method, using various nucleon distribution functions. The different types of distributions are investigated for the correct interpretation of results on the scattering of fast electrons on nuclei, and the values N_l obtained are compared with these predicted by the shell model. Such a comparison is of a special interest, since the empirical values of N_l are given sufficiently accurately by the Mayer scheme, while, at the same time, a statistical (quasi-classical) treatment of the orbital moments can be applied for the calculation of N_l for heavy and even medium nuclei in view of the large values of $l = l_{\text{lim}}$. It is shown that the value of the functional K, which determines the value of N_l according to the statistical theory, and which is calculated on the basis of empirical values of N_l and l taken from the shell model, is approximately constant for all nuclei. At the same time, the value of K obtained by means of the statistical theory depends both on the nucleon distribution function and on the parameter of that function representing the ratio of the thickness of the surface layer to the radius R_0 of the constant-density region (the "mean" nuclear radius). The value of K is constant when the above parameter remains constant, i.e., when there is an "affinity" of the nucleon density distribution in various nuclei. This, however, is not a necessary condition. The possibility is also discussed of selecting a nucleon distribution function leading to a value of K, calculated by the statistical method, constant for all nuclei, adjusting the parameter of the distribution function for agreement with the experimental results of electron scattering on nuclei.

TABLE I

l	N_l	K_{emp}
3	20	0.058
4	40	0.055
5	70	0.053
6	112	0.051

It follows from the Fermi statistics[15] that the number of nucleons of one kind in a nucleus n_l, having the moment of momentum between l and $l + 1$, can be given by the expression

$$n_l = \frac{4}{h}(2l + 1)\int_{r_1}^{r_2}\left\{\left(\frac{3h^3}{8\pi}\rho\right)^{2/3} - \frac{h^2}{4\pi^2}\frac{l(l + 1}{r^2}\right\}^{1/2} dr, \tag{1}$$

where $\rho(r)$ is the density of nucleons of the given kind; the integration is extended over real values of the integrand. For the maximum value of l in the nucleus we have $r_1 = r_2$ and $n_l = 0$ which, according to Eq. (1), corresponds to the maximum of $F(r) = r^3\rho(r)$.

The limiting value of l for particles of a given kind in a nucleus is, therefore, connected with the density distribution function $\rho(r)$ of these particles, by the following relation (for sufficiently large l):

$$[r^3\rho(r)]_{\max} = (2l + 1)^3/24\pi^2. \tag{2}$$

The function $\rho(r)$ must satisfy also the condition

$$4\pi\int_0^\infty \rho(r)\, r^2\, dr = N_l. \tag{3}$$

From Eqs. (2) and (3) we obtain

$$N_l = K(2l + 1)^3, \tag{4}$$

$$K = \frac{1}{6\pi}\int_0^\infty \rho(r)\, r^2\, dr \,/\, [r^3\rho(r)]_{\max}. \tag{5}$$

Equations (4) and (5) are correct for sufficiently heavy spherical or almost spherical nuclei to which can be applied, on the one hand, the statistical method and, on the other, the notion of the orbital momentum of a particle characterized by an individual quantum number l. The second condition, however, is exactly the one necessary for the applicability of the shell model.

The values N and l based on the Mayer level scheme, and the corresponding empirical values of $K_{\text{emp}} = N_l/(2l + 1)^3$, K being defined by Eqs. (4) and (5), are given in Table I. It can be seen that K is almost constant for all nuclei, decreasing slowly for heavier nuclei (larger N_l).

For the calculation of K according to Eq. (5), let us consider the following distribution functions (similar for protons and neutrons):

$$\rho(r) = \rho_0 = \text{const} \text{ for } r \leqslant R_0;$$
$$\rho(r) = \rho_0 f\left(\frac{r - R_0}{a}\right) = \rho_0 f(x) \text{ for } r \geqslant R_0, \tag{6}$$

where f(x) is a decreasing function. We also consider functions of the Fermi type

$$\rho(r) = \rho_0 / [1 + e^{(r-c)/b}], \tag{7}$$

which are similar to (6) for $b/c \ll 1$.

We introduce the following definitions of the thickness of the surface layer d and of the mean nuclear radius R_c:[4]

$$d = r_{0.1} - r_{0.9}; \; r = R_c \text{ for } \rho = \rho_0/2, \tag{8}$$

where $r_{0.1}$ and $r_{0.9}$ are the distances from the center of the nucleus, corresponding to the densities $0.1\rho_0$ and $0.9\rho_0$; ρ_0 is the density in the central region of the nucleus.

According to Eq. (8), d is connected with the parameter b of Eq. (7) by the expression

$$d = b \ln 9 \approx 4.4\, b. \tag{9}$$

The relation between d and the parameter a of Eq. (6) depends on the function f(x) in Eq. (6).

For the case of a Fermi-type distribution [Eq. (7)], we obtain from Eqs. (5) and (8) the following expression for K

$$K = \frac{J}{6\pi x_m^3}(1 + e^{(x_m - 1)/\varepsilon}), \quad \varepsilon = \frac{b}{c},$$
$$J = \int_0^\infty \frac{x^2 dx}{1 + e^{(x-1)/\varepsilon}}, \quad x_m = \frac{r_m}{c}, \tag{10}$$

where r_m is the value of r corresponding to the maximum of the function $r^3\rho(r)$.

From Eqs. (7) and (10) we have

$$x_m = \varepsilon y_m + 1, \tag{11}$$

where y_m is the root of the equation

$$e^{y_m}[y_m + (1/\varepsilon) - 3] = 3. \tag{12}$$

Eq. (12) was solved numerically for various values of ϵ, and the corresponding values of x_m were used to calculate K according to Eq. (10). The value of J, which enters the expression for K, was also determined for various ϵ by means of numerical integration.

Let us introduce a parameter γ, which describes the nucleon distribution. By definition:

$$\gamma = \frac{d}{R_{\text{eff}}}, \quad \frac{4}{3}\pi R_{\text{eff}}^3 \rho_0 = 4\pi \int_0^\infty r^2 \rho(r)\, dr. \tag{13}$$

For the case of the Fermi-type distribution (7) we have

$$R_{\text{eff}} = c(3J)^{1/3}, \quad \gamma = 4.4\varepsilon/(3J)^{1/3}. \tag{14}$$

TABLE II

ε	γ	K	R_{eff}	A
0.088	0.38	0.035	1.02c	197
0.120	0.51	0.038	1.04c	77
0.151	0.62	0.041	1.06c	40

Numerical integration of J yields a number of values of γ according to Eq. (14) and the relation between γ and K, the latter being defined by Eq. (10). The computed values of K for certain values of the parameter $\epsilon = b/c$ of the function (7), and the corresponding values of γ, are given in Table II. The corresponding values of A are also given in the table. The relation between the parameters ϵ, γ, and A is given by Eq. (9) and (14), and the experimental values of d and c have been taken from reference 4, devoted to the scattering of fast electrons on protons:

$$d = (2.4 \pm 0.3)\, 10^{-13} \text{ cm},$$
$$c = (1.07 \pm 0.02\, A^{1/3})\, 10^{-13} \text{ cm}; \tag{15}$$

The relative error of γ and ϵ computed using the experimental values (15) is less than 15%. The values of R_{eff} calculated according to Eq. (14) and (15) are given in the fourth column of Table II. It can be seen that R_{eff} is not very different from $c \approx R_c$, The data in Table II indicate a low sensitivity of the value of K, calculated from the Fermi-type distribution function, with respect to the parameter γ.

The dependence of K on γ has also been calculated using the distribution function (6), for three types of density fall-off at $r \geq R_0$: (a) for a Gaussian fall-off:

$$\rho(r) = \rho_0 \exp\left\{-\left(\frac{r - R_0}{a}\right)^2\right\} \text{ for } r \geqslant R_0; \tag{16}$$

(b) for a linear fall-off

$$\rho(r) = \rho_0 (R_0 + a - r)/a \text{ for } R_0 \leqslant r \leqslant R_0 + a;$$
$$\rho(r) = 0 \text{ for } r \geqslant R_0 + a; \tag{17}$$

(c) for an exponential fall-off:

$$\rho(r) = \rho_0 \exp\{-(r - R_0)/a\} \text{ for } r \geqslant R_0. \tag{18}$$

The functions $K(\gamma)$ obtained for the cases (a), (b), and (c) are represented graphically in the figure (curves A, B, and C, respectively). The function $K(\gamma)$ based upon the Fermi-type distribution is also shown in the figure (curve F). For comparison of the results obtained with those of the shell model, the function $K_{\text{emp}}(\gamma)$ based upon the relations $K_{\text{emp}}(N_l)$ (Table I) and $\gamma(A)$ (Table II) is included. For small N_l (20, 40, 70)

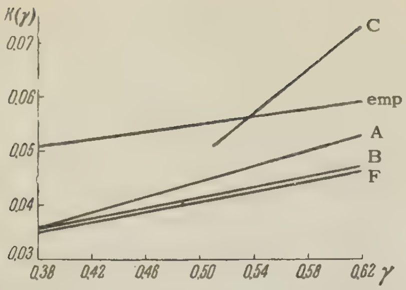

it has been assumed that $A \approx 2Z$ (taking into account that N_l is the number of either the protons or the neutrons, the value of A for real stable nuclei with $N_l = 70$ is in the range from 120 to 176); for $N_l = 112$ it has been assumed that $A = 188$ (the mean of the values 186, 188, and 190 for stable nuclei with 112 neutrons). It should be noted that the spread of the values of A for $N_l = 70$ (120 to 176) corresponds to a variation of γ from 0.40 to 0.45.

It can be seen that in the case (a) and, especially, in the case (b), K is not sensitive to the variation of γ, as in the case of distribution (7): for γ changing form 0.38 to 0.62, the value of K varies between 0.036 and 0.048 in the case (a), between 0.036 and 0.042 in the case (c), and between 0.035 and 0.041 for the Fermi-type distribution. It has been shown, on the basis of Eqs. (6), (16), and (17) that, like in the case of the Fermi-type distribution, R_{eff} is not much different from R_c in the cases (a) and (b). Furthermore, it can be seen that the curves A, B, and F are approximately parallel to $K_{emp}(\gamma)$, although the corresponding theoretical values of K are by $\sim 30\%$ less than those of K_{emp}.

The result for the relation $K(\gamma)$ in the case (c) is different. Curve C rises sharply, in contrast with the empirical curve, and the values $\gamma < 0.51$, which correspond to $\alpha = a/R_0 < 1/3$ according to Eqs. (6), (8), (13), and (18) are not consistent with Eq. (5). At the same time, according to experimental results on electron scattering,[4] the values of $\gamma > 0.51$ correspond to $A < 77$. The statistical determination of N_l using the distribution function with an exponential density fall-off and with parameters determined from electron scattering phenomena is not applicable to heavy nuclei for which, in general, the statistical method is most appropriate. It should be noted also that, independently of the value of the parameters determined from electron scattering experiments, the condition $\alpha \geq 1/3$ for the function with an exponential density fall-off requires, according to Eq. (8), that the minimum value of the ratio of the surface layer thickness d to the radius of the constant density region R_0 were greater than 0.73. For other cases, the above ratio is either unrestricted [case (a)], or sufficiently small [0.23 for the case (b)].

The Fermi-type distribution function and the distribution functions with a Gaussian or linear fall-off at $r \geq R_0$, which describe correctly the scattering of electrons on nuclei,[2,4] lead to a value of K that is almost constant and which varies with γ in an analogy to the empirical dependence $K(\gamma)$ corresponding to the shell model, although the theoretical curves lie somewhat lower than the empirical. It can be seen also that the distribution function with an exponential fall-off leads to a discrepancy with the experiment.

In conclusion we would like to mention that, although neither theoretical nor experimental investigations give at present the exact shape of the distribution function of the nucleons in nuclei, the present work indicates a possibility of application of the statistical method of determining N_l to the selection of a distribution function. The N_l found satisfy both the requirements of the shell model (K independent of A) and the saturation property of nuclear forces, as well as the experiments on scattering of electrons by nuclei (i.e., the requirement that the effective nuclear radius be proportional to $A^{1/3}$ while the thickness of the surface layer be independent of A).

---

[1] Jennie, Ravenhall, and Wilson, Phys. Rev. **95**, 500 (1954).

[2] Hofstadter, Hahn, Knudsen, and McIntyre, Phys. Rev. **95**, 512 (1954).

[3] D. G. Ravenhall and D. R. Jennie, Phys. Rev. **96**, 239 (1954).

[4] Hahn, Ravenhall, and Hofstadter, Phys. Rev. **101**, 1131 (1956).

[5] F. I. Kligman, J. Exptl. Theoret. Phys. (U.S.S.R.) **28**, 297 (1955), Soviet Phys. JETP **1**, 145 (1955).

[6] P. Gombas, Usp. Fiz. Nauk. **49**, 385 (1953).

[7] L. P. Rapoport and V. A. Filimonov, J. Exptl. Theoret. Phys. (U.S.S.R.) **27**, 243 (1954).

[8] P. Williams, Phys. Rev. **98**, 1387 (1955).

[9] D. D. Ivanenko and V. I. Rodichev, Dokl. Akad. Nauk SSSR **70**, 605 (1950).

[10] D. D. Ivanenko and A. A. Sokolov, Dokl. Akad. Nauk SSSR **74**, 33 (1950).

[11] M. Born and L. M. Yang, Nature **166**, 399 (1950).

[12] N. I. Kolesnikov, Dokl. Akad. Nauk SSSR **103**, 1 (1955).

[13] C. I. Larin, J. Exptl. Theoret. Phys. (U.S.S.R.) 30, 587 (1956), Soviet Phys. JETP 3, 615 (1956).

[14] B. K. Kerimov and A. V. Dzhavadov, J. Exptl. Theoret. Phys. (U.S.S.R.) 30, 1065 (1956), Soviet Phys. JETP 3, 878 (1956).

[15] P. Gambos, Die statistische Theorie des Atoms und ihrer Anwendungen, Springer, Wien, 1949, Chap. IV.

Translated by H. Kasha
68

ON THE ELECTRON CAPTURE MECHANISM AND THE CURRENT LIMIT IN BETATRONS

A. N. MATVEEV

Moscow State University

Submitted to JETP editor February 12, 1958

J. Exptl. Theoret. Phys. (U.S.S.R.) 35, 372-380 (August 1959)

Mechanism of electron capture in betatrons is discussed. Its basis is the Coulomb interaction of the electrons in the beam and the losses of electrons to the walls of the doughnut. The problem is treated exactly for a simplified model. It is shown that the considered capture mechanism has a high effectiveness which is in agreement with experiment. An expression for the limiting current, valid also for relativistic energies, is given.

1. INTRODUCTION

No existing theory explains the capture of electrons in betatrons, nor has a satisfactory physical picture of this process been developed. However, several important experiments[1-6] performed during the last years have clarified this problem to a considerable extent. Thev have confirmed that the capture of electrons in betatrons is due to their collective interactions. It is therefore unnecessary to consider one-electron theories of electron capture.[7-8] Their applicability is limited to rather small injection currents.

One can subdivide the capture mechanisms based on collective interactions into three groups: (a) mechanisms connected with the action of self-induction of the non-stationary electron current in the doughnut;[9-10] (b) mechanisms based on the interaction of the electrons with the Coulomb field of the space charge;[10, 11, 13-15] (c) statistical capture mechanisms.[16]

Experimental models have shown that the mechanism based on the self induction of the non-stationary current[4] cannot explain, at the actual strengths of the injection currents, the observed effectiveness of the capture and does not play an important part in the capture process. Its effectiveness is similar to that of the adiabatic contraction of the orbit and of the adiabatic damping of the betatron oscillations. Thus, one can consider it to be sufficently well established at present that the induction-type mechanism does not play an essential part in the overall picture of the electron capture.

As to the statistical capture mechanism, it has been shown earlier[17] that it can work only at sufficiently small injection currents, in the region between the single-electron capture and the collective capture. At such injection currents where the capture process is particularly effective, this mechanism does not play an essential part.

It appears thus that the most likely injection mechanism is that which takes into account the Coulomb interaction of the electrons. The different effects associated with the Coulomb interaction at injection time are discussed in references 10, 11, and 13 to 15. The mechanism treated by Wideroe is based on the energy lost by electrons passing through a space-charge cloud whose charge density decreases in time. This process cannot be decisive since it does not explain the capture on the leading side of the injection pulse. Bardeen has proposed a mechanism based on the use of the azimuthal inhomogeneity of the space charge. This mechanism is in disagreement with the well-known fact that the capture works equally well with injection from the outside (where $n \approx 1$) as from the inside (where $n \approx 0.5$). It also is in disagreement with the fact that if several injectors are used and the first harmonic of the azimuthal inhomogeneity of the space charge disappears the injection does not get worse. Therefore this mechanism also cannot play an important part.

Rodimov[15] has investigated the capture mechanism which is based on the Coulomb interaction between electron beams that have made a different number of revolutions after injection. We believe that this mechanism correctly describes several important elements of the actual capture process. However, he has assumed that the density of the injected electrons roughly equals the final equilibrium density and states that there will be no capture of the electrons if the injection density differs strongly from the equilibrium value. This last deduction does not agree with the experimental results, which show that the capture is highly effective also at injection densities much higher than at equilibrium. The assumption that the injection and equilibrium densities are equal seems to be too restrictive. It is rather obvious that this condition is almost never fulfilled in practice, since it can be obtained for each betatron only with a very special choice of the parameters and of the quantities that characterize the injection conditions. Another important shortcoming of Rodimov's work is his neglect of the loss of electrons to the walls and on the injector. It is well known that a large part of the injected electrons strike either the walls or the injector and only a small fraction survives to be finally accelerated. It appears therefore that the loss of electrons is actually an essential part of the general capture process.

In this paper we investigate a capture process based on consideration of the Coulomb interaction between the electrons and of the role played by the loss of electrons to the walls and the injector.

2. COMMENTS ON THE FORMULATION OF THE PROBLEM

For an accurate formulation and solution of this problem it would be necessary to use the transport equation. However, because of the extreme nonstationarity of the process and the involved boundary conditions, which furthermore depend on the time, this approach does not seem feasible. We shall therefore use a different approach, which, with some simplifying assumptions, makes a treatment possible.

We shall assume first that the duration of the injection pulse equals the period of one revolution of the injected particle. To simplify the calculations, we take the beam to be of infinite extent along the z axis and neglect the axial asymmetry of the problem when considering the acting forces. This is equivalent to neglecting small quantities proportional to the ratio of the radial width of the doughnut to the radius of the equilibrium orbit.

The walls of the doughnut do not exert any forces on the electron beam: no charges will accumulate on the inside wall since there is no electric field present; charges will accumulate on the outside wall but they have no influence on the electron beam.

Thus stated, the problem can be solved exactly. There is no electron capture in the following three cases: (1) when the electrons do not interact, (2) when the electrons interact but there are no walls, and (3) when the density of the injected electrons is less than a certain value even if the electrons interact and the presence of the walls is taken into account. On the other hand, if the electrons interact, the presence of the walls and of the injector is taken into account, and the density of the injected electrons exceeds a certain value, the electrons are effectively captured.

Thus, rigorous calculations with the approximate model show that the capture mechanism is due to the Coulomb interaction of the electrons and to the electron loss on the walls and in the injector. The removal of the simplifying assumptions and the change of the model to a more realistic situation do not change these conclusions.

3. EQUILIBRIUM DENSITY OF THE ELECTRONS

An electron moving in a betatron is acted upon by the Lorenz forces

$$\mathbf{F} = e\left(\mathbf{E} + \frac{1}{c}[\mathbf{v} \times \mathbf{H}]\right). \qquad (1)$$

If a certain volume element is to be in equilibrium, i.e., if it is to move as a whole and if there are to be no forces trying to change the internal arrangement of the particles inside this volume element, then the following condition must be satisfied.

$$\int \mathbf{F} ds = 0, \qquad (2)$$

where the integral is to be taken over any arbitrary closed surface inside the volume element. We thus obtain

$$\operatorname{div}\left(\mathbf{E} + \frac{1}{c}[\mathbf{v}\times\mathbf{H}]\right) = 0. \qquad (3)$$

We consequently obtain for the equilibrium density ρ_e

$$\rho_e = -(1/4\pi c)\,\mathrm{H}\,\mathrm{curl}\,\mathrm{v}\,(\mathcal{E}/m_0c^2)^2, \qquad (4)$$

which becomes at the center of the beam, i.e., on the equilibrium orbit R_0,

$$\rho_e(R_0) = \frac{1}{4\pi}\frac{e\beta^2}{r_0R_0^2}\left(\frac{\mathcal{E}}{m_0c^2}\right)^3, \quad \beta = \frac{v}{c}, \quad r_0 = \frac{e^2}{m_0c^2}. \qquad (5)$$

4. PULSATION OF THE ELECTRON BEAM

Let the electron density upon leaving the injector be ρ_0 and let the width of the injector be l_0. We assume that the density is constant over the width of the injector and that the injected electrons have no radial velocity. The beam will pulsate in a coordinate system tied to its center. Electrons located at a distance x from the center of the beam will be repelled electrostatically from the beam center with a force

$$F_{\mathrm{rep}} = 4\pi e\rho_0 x_0, \qquad (6)$$

where x_0 is the distance of these electrons from the center of the beam at the time of injection. The magnetic focusing forces are given in this coordinate system by

$$F_{\mathrm{att}}(x) = -m_0(v/R_0)^2(1-n)\,x, \qquad (7)$$

where R_0 is the equilibrium orbit radius, n the field index, v the electron velocity ($v << c$), and m_0 the electron mass. No pulsations occur if $|F_{\mathrm{rep}}| = |F_{\mathrm{att}}(x_0)|$. This corresponds to the following electron density at injection

$$\rho_{e1} = \frac{1-n}{4\pi}\frac{e\beta^2}{r_0R_0^2}. \qquad (8)$$

Let us put $\alpha = \rho_0/\rho_{e1}$. Then for $\alpha = 1$ there will be no beam pulsations. For $^1/_2 < \alpha < 1$ the beam will pulsate with a frequency $(v/R_0)\sqrt{1-n}$. The maximum beam width is given by the width at injection, and the electrons do not cross the center of the beam. For $0 < \alpha < {}^1/_2$ the electrons cross the beam center; the maximum beam width is still the width at injection. In both cases the beam density is minimum at injection. For $\alpha > 1$ the frequency of the pulsation is $(v/R_0)\sqrt{1-n}$ and the beam width at the point of largest dimension is given by

$$l = l_0(2\alpha - 1) \qquad (9)$$

and is reached after one-half a pulsation period. The beam width has its minimum at injection. In this case the density is maximum at the instant of injection.

It is easy to see that at each particular time the electron density is constant over the beam cross section.

5. MOTION OF THE ELECTRON BEAM

The center of the beam moves only under the influence of the magnetic focusing forces. When $0 \leq \alpha \leq 1$, no electrons are lost to the walls. In this case the entire motion does not differ essentially from the one-electron case. After the first few revolutions all electrons hit the rear part of the injector and are lost.* We are therefore interested in the case $\alpha > 1$.

We shall characterize the width of the vacuum chamber by the dimensionless parameter $\beta = (L_0/l_0) > 1$ (L_0 is the width of the vacuum chamber.) If $1 < \alpha < \beta$ the beam will start to expand immediately after injection but will not touch the wall on the injector side. In terms of the variable

$$\tau = (v/R_0)\sqrt{1-n}\,t$$

the period of either the pulsations or the oscillations of the center of the beam is 2π. It is convenient to introduce, in lieu the distance y between the center of the beam and the wall of the vacuum chamber, the dimensionless quantity $\xi = y/l_0$. The coordinates of the walls are then given by $\xi = \pm\beta/2$ and the coordinates of the edges of the injector are $\xi_1^{(0)} = -\beta/2$; $\xi_2^{(0)} = -\beta/2 + 1$. In these dimensionless variables the width of the injector equals unity. Let $\tau = 0$ denote the time at which a particular group of electrons is being emitted. Denoting the coordinates of the boundaries of the beam by ξ_1 and ξ_2, we have the following equations of motion

$$\begin{aligned} &\xi_1'' + \xi_1 = -\alpha/2, \qquad \xi_1(0) = -\beta/2, \quad \xi_1'(0) = 0, \\ &\xi_2'' + \xi_2 = \alpha/2, \qquad \xi_2(0) = -\beta/2 + 1, \quad \xi_2'(0) = 0, \end{aligned} \qquad (10)$$

which have the solutions

$$\begin{aligned} \xi_1 &= -\frac{\alpha}{2} + \left(\frac{\alpha-\beta}{2}\right)\cos\tau, \\ \xi_2 &= \frac{\alpha}{2} + \left(1 - \frac{\alpha+\beta}{2}\right)\cos\tau. \end{aligned} \qquad (11)$$

The condition $\alpha < \beta$ insures that the boundary of the beam, ξ_1, does not touch the wall on the injector side right after emission. At the instant τ_0, given by the condition

$$\xi_2(\tau_0) = \beta/2, \qquad (12)$$

the beam will hit the wall opposite of the injector and the loss of electrons will commence. This loss will change the dynamics of the beam, and two competing processes will take place. On the one hand the loss of electrons to the walls eliminates the repulsive forces on the remaining electrons from the side where the electrons hit the wall. This is equivalent to an additional force attracting the remaining electrons to the wall. Thus, for example, the boundary of the beam ξ_1, will be closer to the wall in the presence of electron loss than if there were no loss. On the other hand, the electron loss causes the center of the beam to move away from the wall. This process reduces the amplitude of the oscillations of the center of the beam.

---

*If the injection pulse is longer than the time of one revolution, collective capture occurs also for $0 < \alpha < 1$.

For $\tau > \tau_0$, i.e., after the start electron loss to the walls, the equations of motion for ξ_1 are

$$\xi_1'' + \left(1 - \frac{\alpha}{2f}\right)\xi_1 = -\frac{\alpha\beta}{4f}, \qquad (13)$$

$$f = \alpha(1 - \varepsilon\cos\tau), \quad \varepsilon = \frac{\alpha - 1}{\alpha} < 1, \quad \tau > \tau_0.$$

The initial conditions are given by the values of $\xi_1(\tau_0)$ and $\xi_1'(\tau_0)$ obtained from (11). Utilizing the particular solution of (13),

$$\xi_1 = -\beta/2 + \beta\varepsilon\cos\tau,$$

the problem reduces to solving Hill's equation. The theory of this equation is well developed. However, bearing in mind that the quantity $\alpha/2f$ does not change much during the interval of interest, $\tau > \tau_0$, it is easier to use approximation methods.

If $\xi \ll 1$, we obtain for the maximum excursion $\xi_{1\max}$, at which the electron loss ceases, the following expression:

$$\xi_{1\max} = \frac{\beta}{2} - \alpha + \frac{\alpha^2}{2(\beta - 1)}\varepsilon^2 + O(\varepsilon^3). \qquad (14)$$

The new center of the beam formed of the remaining electrons is located at the time of maximum beam excursion at a distance $\alpha/2$ from the wall. This means that the amplitude of the beam-center oscillations has been reduced. From now on the electrons will no longer hit the walls, but only the back of the injector. However, since the amplitude of the oscillations has decreased, a certain fraction of the electrons will miss the injector and will survive. One can calculate from (14) the number of electrons that will miss the injector and will be accelerated. This way we obtain

$$N_\gamma = N_0(\alpha - 1)^2/(2\alpha - 1) \approx N_0(\alpha - 1)^2, \quad \alpha \approx 1. \qquad (15)$$

Here N_0 is the number of injected electrons and N_γ the number of electrons captured in acceleration.

If α increases, the number of captured electrons increases. If $\alpha > \beta$, Eq. (10) must be replaced from the beginning with equations analogous to (13), to account for the loss of electrons to the wall on the injector side. Proceeding in this manner, one can calculate the number of captured electrons as a function of the number of injected electrons. The curve shown in Fig. 1 indicates the character of this dependence. As the density of the injected electrons increases, the number of captured electrons approaches asymptotically a value which, when spread iniformly over the cross section of the doughnut, would give a density $\rho_{e1}/2$, where ρ_{e1} is given by (8).

FIG. 1

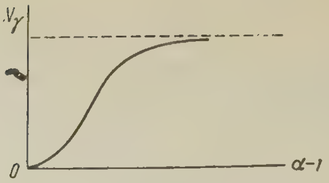

This behavior of the number of captured electrons can be understood from the following considerations, which explain the capture process at high electron dinsities, $\alpha \gg \beta$. Right after emission, the electrons will begin hitting the wall on the side of the injector. After a short time, less than the time of one revolution, the other boundary of the beam will reach the opposite wall. Hereafter the complete cross section of the doughnut will be filled with space charge and electrons will be lost to all walls. The electron density will now steadily decrease. At the instant when the expansion of the beam ceases and the loss of electrons to the wall terminates, the electron density is given by

$$\rho = \rho_{e1}\alpha/(2\alpha - 1) \approx \rho_{e1}/2, \quad \alpha \gg 1, \qquad (16)$$

and the beam fills the entire doughnut cross section. The beam center is located close to the center of the doughnut and continues to oscillate about it with a very small amplitude. Thus almost all electrons distributed with equilibrium density over the full doughnut cross section will be captured to be accelerated.

6. THE CASE OF A ROUND ELECTRON BEAM

The results above are based on a rigorous treatment of a simplified model. The main simplifying assumption, which must be analyzed, is that the beam has a infinite extent along the z axis. If the beam is assumed finite along the z axis, the exact solution becomes rather involved. However, we can estimate the changes that will be introduced into the above picture of the capture process by the finite length of the beam in the z direction.

We assume the focusing magnetic field to be approximately symmetrical. This does not seem to be an overidealization. We can thus assume the

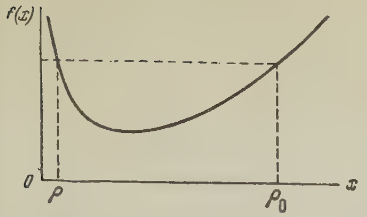

FIG. 2

electron beam to have a round cross section. Then its pulsations will be axially symmetrical with respect to its center. Let r denote the radius of that layer of electrons which had a radius r_0 at injection. We then have the following equation of motion for r

$$r'' + \frac{v^2}{2R_0^2}\, r = \frac{v^2}{2R_0^2}\, q\, \frac{r_0^2}{r}, \quad q = \frac{\rho_0}{\rho_e} > 1, \qquad (17)$$
$$r(0) = r_0, \quad r'(0) = 0,$$

where ρ_0 is the electron density at injection time and ρ_e is the density given by Eq. (5) (in the present nonrelativistic case $\mathscr{E}/m_0c^2 \approx 1$). The solution of (17) is given by the quadrature

$$t = \frac{R_0}{v}\int_1^{r/r_0} d\xi \Big/ \sqrt{q\ln\xi - (\xi^2 - 1)/2}. \qquad (18)$$

The solution has therefore the form

$$r = r_0\varphi(t). \qquad (19)$$

This means that the period of oscillation is the same for all points within the beam. The density thus remains uniform over the beam. The period of oscillation can be obtained from Eq. (18) in an obvious way. One sees immediately from (17) that for small amplitudes this period is smaller than the period of oscillation of the center of the beam about the equilibrium orbit.

The beam radius $r_{\max}$ at the widest point is given by the root of the equation

$$q\ln\frac{r_{\max}}{r_0} - \frac{1}{2}\left[\left(\frac{r_{\max}}{r_0}\right)^2 - 1\right] = 0. \qquad (20)$$

The beam density ρ at maximum beam expansion is evidently

$$\rho = \rho_0 (r_0 / r_{\max})^2. \qquad (21)$$

Transforming (20) algebraically and utilizing (21) we obtain an equation for the density ρ:

$$\rho_0 \exp(\rho_e/\rho_0) = \rho\exp(\rho_e/\rho). \qquad (20a)$$

This equation can easily be solved graphically. After plotting the function $f(x) = x\exp(\rho_e/x)$, we find the connection between ρ_0 and ρ by the construction indicated in Fig. 2.

If we rewrite (20a) in the form

$$\frac{\rho}{\rho_e}\ln\frac{\rho_e}{\rho} - 1 = \frac{\rho}{\rho_e}\ln\frac{\rho_e}{\rho_0} - \frac{\rho}{\rho_0},$$

We can express the solution for the case $\rho_0/\rho_e \gg 1$ as

$$\rho \approx \rho_e / \ln(\rho_0/\rho_e). \qquad (22)$$

It should be noted here that there is an essential difference in the behavior of the electron density at the maximum of the beam expansion compared with the previously-treated case, when this density approached $\rho_{e1}/2$ with increasing density of the injected electrons. In the present case, on the other hand, the density at maximum beam expansion approaches zero asymptotically with increasing density of the injected electrons. As a result, the curve analogous to Fig. 1 has here a different trend: at very large densities of the injected electrons, the number of captured electrons decreases with increasing injection density. At low injection densities the picture is not qualitatively different from Fig. 1. With increasing density the number of captured electrons increases, owing to the increase in the fraction of the doughnut volume filled by the electron beam at the time when the losses to the wall cease. If the beam fills at that time the whole effective doughnut volume, the saturation of the captured beam current has been reached. If the injection density is further increased, the useful doughnut volume does not increase further but the electron density in this cross section continues to decrease and the number of captured electrons, $N\gamma$, starts to decline. The dependence of the number of captured electrons on the injection density is thus represented by a curve of the form shown in Fig. 3.

As can be seen from (22), the curve decreases very slowly in the region past the maximum, since it has only a logarithmic dependence on the injection density. One therefore can utilize Eq. (22) near the maximum. Denoting the area of the injector by S and the effective area of the doughnut by S_{eff}, then if

$$\rho_0/\rho_e \gg S_{\text{eff}}/S > 1 \qquad (23)$$

we obtain for the maximum number of captured electrons, $N\gamma_{\max}$, the equation

$$N_{\gamma\max} = \rho_e V_{\text{eff}} / e\ln(\rho_{0\max}/\rho_e), \qquad (24)$$

where V_{eff} is the effective doughnut volume and

FIG. 3

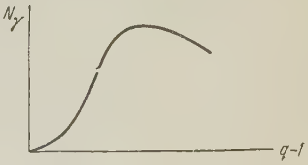

$\rho_{0\,\max}$ is the injection electron density at saturation.

7. CONCLUSIONS

The above calculations and considerations give a clear physical picture of the processes that lead to the capture of electrons at an efficiency that is in agreement with the experiment. This physical picture allows in principle a rigorous mathematical formulation of the problem. However, the solution of this problem is very involved and depends in general on many parameters (form and dimensions of the injector, density distribution of the electrons over the area of the injector, etc.) Evidently it is not worth while to solve this problem in general. The functional dependence and the general character of the dependence of the capture on the different factors can be understood from the general physical picture without a detailed quantitative solution of the problem.

In the present paper we have assumed the injection pulse to have a duration equal to the time of one electron revolution around the betatron orbit. If the injection pulse length exceeds this value one has to take into account the Coulomb interaction between electron beams which have completed a different number of revolutions. The role of this kind of interaction has been investigated by Rodimov[15] for the case $q \approx 1$. For arbitrary values of q this problem becomes considerably more involved. However, the physical picture of the capture process remains essentially unchanged.

In the special case of very high injection electron densities, when conditions (23) are fulfilled and when the duration of the injection pulse exceeds the time of one revolution (these conditions apply in the example of reference 16 on which we have made comments in reference 17, one can make the definite qualitative and quantitative findings which have been given in reference 17. We only add that in this case the main contribution to the electron capture will obviously come from the trailing edge of the injection pulse, which must lie within the acceptance region of the V_{inj} vs. t diagram of the injection voltage.

---

[1] V. S. Melikhov, Dissertation, Tomsk Polytechn. Inst. 1954.

[2] Logunov, Ovchinnikov, and Rusanov, J. Techn. Phys. (U.S.S.R.) 27, 1135 (1957), Soviet Phys. JTP 2, 1032 (1957).

[3] Logunov, Ovchinnikov, Rusanov, and Semenov, J. Techn. Phys. (U.S.S.R.) 27, 1143 (1957), Soviet Phys. JTP 2, 1038 (1957).

[4] Logunov, Ovchinnikov, and Rusanov, Атомная энергия (Atomic Energy) 2, 525 (1957).

[5] Iu. S. Korobochko, J. Techn. Phys. (U.S.S.R.) 27, 745 and 1603 (1957), Soviet Phys. JTP 2, 673 and 1486 (1957).

[6] Iu. N. Lobanov and V. A. Petukhov, Ускорители элементарных частиц (Elementary Particle Accelerators), p. 73 Atomizdat, Moscow (1957).

[7] D. W. Kerst, Phys. Rev. 60, 47 (1941).

[8] D. W. Kerst and R. Serber, Phys. Rev. 60, 53 (1941).

[9] D. W. Kerst, Phys. Rev. 74, 503 (1948).

[10] R. Wideröe, Z. Angew. Physik 5, 187 (1953)

[11] Kerst, Adams, Koch and Robinson, Rev. Sci. Instr. 21, 462 (1950).

[12] P. A. Riasin, Тезисы докладов на Всесоюзной конференции по физике частиц высоких энергий (All Union Conference on High Energy Particle Physics, Abstracts), p. 161 (May, 1956).

[13] R. Wideröe, J. Appl. Phys. 22, 362 (1951).

[14] S. E. Bardeen, Proc. Phys. Soc. 64B, 85 (1951).

[15] B. N. Rodimov, Dissertation, Tomsk Polytechn. Inst. 1954.

[16] V. I. Logunov and S. S. Semenov, J. Exptl. Theoret. Phys. (U.S.S.R.) 33, 1513 (1957), Soviet Phys. JETP 6, 1168 (1958).

[17] A. N. Matveev, J. Exptl. Theor. Phys. (U.S.S.R.) 34, 1331 (1958), Soviet Phys. JETP 7, 918 (1958).

Translated by M. Danos
69

SOVIET PHYSICS JETP VOLUME 35(8), NUMBER 2 FEBRUARY, 1959

SHORT RANGE INTERACTION BETWEEN THE ELECTRON AND OTHER PARTICLES

N. N. KOLESNIKOV and G. A. JACOBI

Moscow State University

Submitted to JETP editor February 13, 1958

J. Exptl. Theoret. Phys. (U.S.S.R.) **35**, 381-391 (August, 1958)

The possibility is discussed of the existence of an electron structure and its description from the viewpoint of the linear theory of extended particles, and also from the viewpoint of nonlinear theory. Both variants of the theory lead to similar results for the interaction of the electron with the proton, the neutron and light nuclei; however, according to the nonlineary theory, the interaction of two electrons at very short ranges must be essentially different from the interaction of the electron with the positron.

RECENTLY, experiments on the scattering of fast electrons on protons[1,3] have revealed a deviation from the usual formula of Mott[3] which is valid for two point particles with strong Coulomb interaction. The character of these deviations point to a failure of the purely Coulomb law of interaction at very short ranges. Hofstadter and others[1,2,4] have shown that to explain the experimental results, it is enough to assume that, in contrast to the electron, the proton is not a point particle, but that its charge and magnetic moment are distributed in space according to some law.[2] However, although contemporary theory does not suggest sufficient arguments in support of the extended electron, still it is not excluded that part of the Hofstadter effect might be connected with the structure of the electron (which a number of authors assume[2,5]). The difficulty of infinite density is avoided in the theory of the extended electron and the so-called classical radius of the electron[6] $r_0 = e^2/mc^2 = 2.8 \times 10^{-13}$ cm takes on a physical significance.

On the other hand, experiments on the scattering of fast electrons on protons could be explained by the hypothesis that there are nonlinear effects of the electromagnetic field at short ranges. We shall consider both possibilities and shall attempt to explain how future experiments could clarify the actual nature of the short-range interactions.

1. LINEAR THEORY OF EXTENDED PARTICLES

The Interaction of the Electron and Proton

We shall consider throughout only the interaction of electrical charges which under the experimental conditions of Hofstadter[3] play an important role at small angles of scattering. Furthermore, we shall consider the charge distribution in the proton $\rho_p(\mathbf{r}_1)$ and in the electron $\rho_e(\mathbf{r}_2)$ to be spherically symmetric ($\mathbf{r}_1$ and $\mathbf{r}_2$ are distances from the center of the proton and electron, respectively).

We can then write the interaction energy of the extended proton with the extended electron, whose centers are separated a distance $\mathbf{r}$, in the form

$$V(r) = -e^2 \iint \frac{\rho_p(r_1)\,\rho_e(r_2)\,dv_1 dv_2}{|\mathbf{r}-\mathbf{r}_1-\mathbf{r}_2|} \tag{1}$$

where $\rho_p(\mathbf{r}_1)$ and $\rho_e(\mathbf{r}_2)$ are normalized to unity.

Integrating over the angles in (1), we get:

$$\begin{aligned} V(r) = {} & -\frac{e^2}{r} + \frac{4\pi e^2}{r}\int_r^\infty \rho_p(r_1)\,r_1(r_1-r)\,dr_1 \\ & + \frac{8\pi^2 e^2}{r}\int_0^\infty \rho_p(r_1)\,r_1 dr_1 \int_{|r-r_1|}^{r+r_1} dr_2 \int_{r_2}^\infty \rho_e(r_2')\,r_2'(r_2'-r_2)\,dr_2'. \end{aligned} \tag{2}$$

For the case of scattering of fast electrons on protons, the relativistic Born approximation[3,4,7]

$$d\sigma = \left(\frac{Ze^2}{2E}\right)^2 \frac{\cos^2(\theta/2)}{\sin^4(\theta/2)}\,|f(\theta)|^2\, 2\pi \sin\theta\, d\theta$$

gives results only slightly different from the values of the effective cross sections given by the exact formula,[4,8] while the dependence on the special features of the interaction at short ranges, i.e., on the structure of the particles, is determined by the form factor[2,7]

$$f(\theta) = -\frac{2m}{\hbar^2}\int_0^\infty \frac{\sin Kr}{Kr}\,V(r)\,r^2\,dr. \tag{3}$$

Substituting (2) in (3) and integrating by parts, we get

$$f(\theta) = \frac{2me^2}{\hbar^2 K^2}\left\{4\pi\int_0^\infty \frac{\sin Kr}{Kr}\,\rho_p(r)\,r^2\,dr\right.$$

$$-8\pi^2K^2\int_0^\infty \frac{\sin Kr}{Kr}\,r\,dr\int_0^\infty \rho_p(r_1)\,r_1 dr_1 \tag{4}$$

$$\left.\times\int_{|r-r_1|}^{r+r_1} dr_2\int_{r_2}^\infty \rho_e(r_2')\,r_2'(r_2'-r_2)\,dr_2'\right\}.$$

We now assume that only the region $Kr \ll 1$ is significant in these integrals, because of the rapid fall-off ρ_p and ρ_e. That is, the momenta $p = \hbar K$ at large distances are not large, which, in any case, is satisfied for energies that are not too large. Then, substituting both terms of the expansion in the first term of (4), we obtain

$$\sin Kr / Kr \approx 1 - K^2r^2/6, \tag{5}$$

In the second term of (4), limiting ourselves to the first term of the expansion, we get

$$f(\theta) = \frac{2a_0}{(a_0K)^2}\left\{1 - \frac{K^2}{6}\left(\langle r_p^2\rangle + \langle r_e^2\rangle\right)\right\}, \tag{6}$$

where $a_0 = \hbar^2/me^2$ is the Bohr radius,

$$\langle r_p^2\rangle \equiv \int \rho_p(r)\,r^2\,dv, \tag{7}$$

$$\langle r_e^2\rangle \equiv \int \rho_e(r)\,r^2 dv = 6\cdot 8\pi^2\int_0^\infty r\,dr\int_0^\infty \rho_p(r_1)\,r_1 dr_1$$

$$\times\int_{|r-r_1|}^{r+r_1} dr_2\int_{r_2}^\infty \rho_e(r_2')\,r_2'(r_2'-r_2)\,dr_2'. \tag{8}$$

The latter equation is obtained by integration of the right side of (7) (by parts) with account of the normalization condition for ρ_p.

The difference between (5) and the corresponding formula that does not take the dimensions of the electron into account lies in the presence of an additional term proportional to $\langle r_e^2\rangle$. Thus, if we assume the non-point character of the electron then the experimental value for the rms radius of the proton[2] ($R_0 = 0.8 \times 10^{-13}$ cm) must be the square root of the sum of the mean squares of the radii of the proton and electron: $R_0 = \sqrt{\langle r_p^2\rangle + \langle r_e^2\rangle}$.

Furthermore, in order to agree with experiment at much higher energies, when the expansion (5) is no longer a good approximation, it is necessary that the extended electron and proton interact exactly the same as, under the assumption of a point nature for the electron, the electron interacts with an extended proton with charge distribution ρ_0 (according to recent data, ρ_0 is best represented by an exponential[2]), i.e., that

$$\int_r^\infty (\rho_0 - \rho_p)\,r_1(r_1 - r)\,dr$$

$$= 2\pi\int_0^\infty \rho_p(r_1)\,r_1\,dr_1\int_{|r-r_1|}^{r+r_1} dr_2\int_{r_2}^\infty \rho_e(r_2')\,r_2'(r_2'-r_2)\,dr_2.$$

Similarly, the effect of structure of the electron would manifest itself in the displacement of the electron levels in the hydrogen atom.[9] The displacement of the electron levels connected with the structure of the proton and electron, in first approximation, without consideration of the deformation of the electronic wave functions and relativistic corrections which are not appreciable in the case under discussion,[10] is equal to

$$\Delta E = -\int |\psi_e(r)|^2\,\{V + e^2/r\}\,dv. \tag{9}$$

Inasmuch as the sum $V + e^2/r$ falls off rapidly at distances much smaller than the radius of the Bohr orbit, we can remove the square of the wave function of the electron for the n-th state of the electron ψ_c from under the integral sign setting it equal to its value at zero. Substituting in (9) the value of V according to (2), and integrating by parts, similarly to what was done previously,[9] we get

$$\Delta E = \frac{\alpha}{3}\,|\psi_e(0)|^2\,\{\langle r_p^2\rangle + \langle r_e^2\rangle\}, \tag{10}$$

where ΔE is expressed in cm^{-1}.

Interaction of the Electron with Other Particles

Employing a method similar to the above, we can show that at relatively low energies the scattering cross section of neutrons on electrons (through electrostatic interaction) depends only on the rms radius of the charge distribution in the neutron, namely:

$$f(\theta) = -2a_0\langle r_n^2\rangle / a_0^2. \tag{11}$$

The elastic scattering cross section of electrons on deuterons at relatively low energies depends not only on $\langle r_p^2\rangle$, $\langle r_e^2\rangle$ and $\langle r_n^2\rangle$, but also on $\langle r_D^2\rangle = \int|\psi_p|^2 r^2\,dv$,[9] where ψ_p is the wave function of the proton in the nucleus of deuterium:

$$f_D(\theta) = \frac{2a_0}{(a_0K)^2}\left\{1 - \frac{K^2}{6}\left(\langle r_D^2\rangle + \langle r_p^2\rangle + \langle r_e^2\rangle - \langle r_n^2\rangle\right)\right\}. \tag{12}$$

The displacement of the electrons of the n-th level in deuterium is determined by the same form factors, namely

$$\Delta E_D = \frac{\alpha}{3}\,|\psi_e(0)|^2\,\{\langle r_D^2\rangle + \langle r_p^2\rangle + \langle r_e^2\rangle - \langle r_n^2\rangle\}. \tag{13}$$

It follows from (13) and (10) that the volume part of the Lamb shift,[11] equal to the energy difference between (13) and (10), does not depend on the dimensions of the electron and the proton:

$$\Delta E_{\mathrm{D}} - \Delta E_n = \frac{\alpha}{3} \, |\psi_e(0)|^2 \{\langle r_{\mathrm{D}}^2\rangle - \langle r_n^2\rangle\}. \tag{14}$$

The difference in the elastic scattering cross section of electrons on deuterons and on protons depends approximately on the same difference $<r_{\mathrm{D}}^2>$ $- <r_{\mathrm{n}}^2>$. If the charge distribution in the positron were the same as for the electron, the effects of structure in its interaction with other particles would be the same as for the electron.

Characteristic Energy and the Dimensions of the Electron

The electrostatic energy $\mathcal{H}$ of the electron with charge distribution ρ_e can be written in the form

$$\mathcal{H} = \frac{1}{8\pi} \int E^2 dv = e^2 / {}_{-1}^{\;1}R_e, \tag{15}$$

where we have used Gauss' theorem and the notation.

$$\frac{1}{{}_{-1}^{\;1}R_e} = \int_0^\infty \frac{\rho_e(r)\, dv}{r} \int_0^r \rho_e(r_1)\, dv_1. \tag{16}$$

Further, assuming that

$$\mathcal{H} = m_0 c^2 \eta, \tag{17}$$

where m_0 is the rest mass of the electron, η is the ratio of the field mass of the electron to its total mass, we have, by (15),

$${}_{-1}^{\;1}R_e = r_0 / \eta,$$

where r_0 is the classical radius of the electron.

We shall show that for any non-alternating $\rho_e(r)$, the rms radius ${}_2R_e = \sqrt{<r_e^2>}$ ought to be larger than ${}_{-1}^{\;1}R_e/2$. Above all it can be established that for fixed values of ${}_{-1}^{+1}R_e$ the rms radius ${}_2R_e$ has a minimum value for uniform charge distribution over the volume.* But the Coulomb energy of the charge, uniformly distributed over the volume of a sphere of radius a, is equal to $3e^2/5a$, and, consequently, ${}_{-1}^{\;1}R_e = 5a/3$, whereas ${}_2R_e = \sqrt{3/5a}$. Consequently, ${}_2R_e \geq (3/5)^{3/2}\, {}_{-1}^{\;1}R_e$, or

$${}_2R_e > {}_{-1}^{\;1}R_e / 2 = r_0 / 2\eta. \tag{18}$$

If neither the charge distribution of the proton ρ_{p} nor the charge distribution of the electron ρ_e are alternating, then the rms radius of the electron ${}_2R_e$ should in every case be not larger than the value of $R_0 = 0.8 \times 10^{-13}$ cm obtained by Hofstadter. But then the inequality (18) can be satisfied for $\eta > 1.75$; η must be > 1 for other considerations also. The extended electron cannot be stable and undeformed in strong external fields in the absence of additional internal forces that are large in magnitude, forces of attraction of a non-electromagnetic character; therefore the non-field mass of the electron must be considerable.

2. NONLINEAR THEORY

General Properties of a Nonlinear Field

In the nonlinear theory there is no need of considering the electron to be an extended particle. If the electromagnetic field has a nonlinear character[6,13-16] that appears at short ranges, then this is equivalent, in a well known sense, to the presence of structured particles. We shall first attempt to make clear in what measure the requirements of the theory and the experimental data limit the choice of the Lagrangian. In order that the Lagrangian of the field L be invariant, it must be a function of the invariants of the electromagnetic field, consisting of the derivatives of the potentials of the electromagnetic field.[6,16] An invariant which consists of the components of the potentials A_μ must not be contained in the Lagrangian; otherwise we would not arrive at equations of the Maxwell type. We shall further consider L to be a function of only a single invariant $I = f_{\mu\nu} f_{\mu\nu}$ consisting of the components of the antisymmetric tensor

$$f_{\mu\nu} = \partial A_\nu / \partial x_\mu - \partial A_\mu / \partial x_\nu. \tag{19}$$

Furthermore, by forming the action integral and varying it with respect to the variable A_ν and $A_{\mu,\nu} = \partial A_\mu / \partial x_\nu$, then equating to zero the variant of the action integral, we obtain Euler's equations:[16]

$$\partial p_{\mu\nu} / \partial x_\mu = 0, \tag{20}$$

where

$$p_{\mu\nu} = \partial L / \partial A_{\mu,\nu} = -\partial L / \partial f_{\mu\nu}. \tag{21}$$

On the other hand, as a consequence of the antisymmetry of the tensor $f_{\mu\nu}$ we get

$$dL = \frac{1}{2} \frac{\partial L}{\partial f_{\mu\nu}}\, df_{\mu\nu} = -\frac{1}{2} p_{\mu\nu} df_{\mu\nu}. \tag{22}$$

---

* For proof, we write on the one hand,

$$\frac{1}{{}_{-1}^{\;1}R} = \frac{\mathcal{H}}{e^2} = \frac{1}{8\pi} \int E^2 dv = \frac{1}{2} \int \left(\frac{d\varphi}{dr}\right)^2 r^2 dr,$$

since $\mathbf{E} = -\operatorname{grad} \varphi$.[12] On the other hand, according to the foregoing [see the derivation of Eq. (10)],

$${}_2R^2 = \langle r^2 \rangle = 6 \int_0^\infty \left(\varphi - \frac{1}{r}\right) r^2 dr.$$

Now, constructing the function ${}_2R^2 - \lambda / {}_{-1}^{\;1}R$ and varying it in φ, we obtain

$$\delta J = \int_0^\infty \left\{6r^2 - \frac{1}{2\lambda} \frac{d}{dr}\left(2r^2 \frac{d\varphi}{dr}\right)\right\} \delta\varphi \, dr.$$

Then, setting the variation equal to zero, we find $\nabla^2 \varphi = 6/\lambda$ $=$ const; this means that the density of charge distribution must be constant.

The invariant properties of the Lagrangian relative to a transformation of the coordinates allows us to write it in a much simpler form. In order to show this, we carry out an infinitely small transformation of the coordinates:[16,17]

$$\bar{x}_\mu = x_\mu + \varepsilon\xi_\mu(\bar{x}_\nu),$$

for which the potentials A_μ and their derivatives are equal to

$$\bar{A}_\mu = A_\mu - \varepsilon\frac{\partial\xi_\nu}{\partial x_\mu}A_\nu,$$

$$\bar{A}_{\mu,\nu} = \frac{\partial\bar{A}_\nu}{\partial\bar{x}_\mu} = \frac{\partial}{\partial x_\sigma}\left(A_\nu - \varepsilon\frac{\partial\xi_\tau}{\partial x_\nu}A_\tau\right)\frac{\partial x_\sigma}{\partial\bar{x}_\mu}$$

We also find that

$$\delta L = \frac{1}{2}p_{\mu\nu}\,\delta A_{\mu\nu} = -\frac{\varepsilon}{2}(p_{\mu\nu}A_{\sigma\nu} + p_{\nu\mu}A_{\nu\sigma})$$

$$\times\frac{\partial\xi_\sigma}{\partial x_\mu} + \frac{1}{2}p_{\sigma\mu}A_\nu\frac{\partial^2\xi_\nu}{\partial x_\sigma\partial x_\mu}$$

and the Jacobian of the transformation is equal to

$$\partial(\bar{x}_1,\ \bar{x}_2,\ \bar{x}_3,\ \bar{x}_4)/\partial(x_1,\ x_2,\ x_3,\ x_4) = 1 + \varepsilon\partial\xi_\mu/\partial x_\mu.$$

From the invariance of the Lagrangian under a coordinate transformation, it follows that

$$\int(L + \delta L)\,dx = \int L\,dx \tag{23}$$

(the integration is carried out over all four variables), whence, taking it into account that $p_{\sigma\mu}A_\nu\partial^2\xi_\nu/\partial x_\sigma\partial x_\mu = 0$ by virtue of the antisymmetry of $p_{\sigma\mu}$, we get (by equating the expressions for $d\xi_\sigma/dx_\mu$):

$$L = \frac{1}{2}(p_{\mu\nu}A_{\mu\nu} + p_{\nu\mu}A_{\nu\mu}) = \frac{1}{2}p_{\mu\nu}f_{\mu\nu}. \tag{24}$$

Furthermore, the energy-momentum tensor of the electromagnetic field can be determined in the usual fashion; it can be shown that in the case of nonlinear electrodynamics the same conservation laws will be satisfied as in the case of the linear theory.[6,16] Moreover, Laue's theorem is valid. The Hamiltonian of the nonlinear field, which is of interest to us, can be written in the following form:

$$H_{44} = {}^1/_2\,p_{\mu\nu}f_{\mu\nu} + p_{\nu4}f_{\nu4}. \tag{25}$$

We now proceed to the usual vector description of electrodynamics, defining the electric field intensity $\mathbf{E}$ and magnetic field intensity $\mathbf{H}$, and the corresponding inductions $\mathbf{D}$ and $\mathbf{B}$, as

$$\mathbf{E} = i\sqrt{4\pi}\{f_{14},\ f_{24},\ f_{34}\},\quad \mathbf{D} = i\sqrt{4\pi}\{p_{14},\ p_{24},\ p_{34}\},$$
$$\mathbf{B} = \sqrt{4\pi}\{f_{23},\ f_{31},\ f_{12}\},\quad \mathbf{H} = \sqrt{4\pi}\{p_{23},\ p_{31},\ p_{12}\}. \tag{26}$$

Then the Euler equations (20) and the integrability conditions

$$\partial f_{\mu\nu}/\partial x_\sigma + \partial f_{\nu\sigma}/\partial x_\mu + \partial f_{\sigma\mu}/\partial x_\nu = 0$$

(which follow from the special choice of the functions $f_{\mu\nu}$) give the Maxwell equations in their usual form.[6,14,16] However, while in the linear theorem, for the case of a vacuum, $\mathbf{E} = \mathbf{D}$, $\mathbf{B} = \mathbf{H}$, these relations are no longer preserved in the nonlinear theory. In fact,

$$p_{\mu\nu} = -\frac{dL}{dI}\frac{\partial I}{\partial f_{\mu\nu}} = \varepsilon(I)\,f_{\mu\nu}$$

or,

$$\mathbf{D} = \varepsilon(I)\,\mathbf{E};\ \ \mathbf{H} = \varepsilon(I)\,\mathbf{B}. \tag{27}$$

In the usual notation, the expressions for I, L and H_{44} take the following form

$$I = -(E^2 - B^2)/8\pi; \tag{28}$$

$$L = (1/8\pi)(-DE + BH); \tag{29}$$

$$H_{44} = (1/8\pi)(DE + BH). \tag{30}$$

The Equivalent Charge Distribution and the Effective Radius of Nonlinearity

We shall show that the Lagrangian of the nonlinear field can also be given with the aid of the density distribution of the equivalent charge of the linear field. For this purpose, we consider a special static case. Let there be a point charge e. The solution of the equation $\operatorname{div}\mathbf{D} = 4\pi e\delta(\mathbf{r})$ is $\mathbf{D} = e\mathbf{r}/r^3$. We now compare the nonlinear field $\mathbf{E} = \mathbf{D}/\epsilon(I)$ with the linear field $\mathbf{E}_{\mathrm{lin}}$ which is equal to it at all points of space. It is obvious that the source of $\mathbf{E}_{\mathrm{lin}}$ could be any distribution ρ_e' of the same charge e (generally speaking, not a point distribution), while, in accord with Gauss' theorem:

$$\mathbf{E}_{\mathrm{lin}} = \frac{e\mathbf{r}}{r^3}\int_0^r\rho_e'dv.$$

But since, by assumption, $\mathbf{E} = \mathbf{E}_{\mathrm{lin}}$ at each point of space, we can write

$$\mathbf{E} = \mathbf{D}\int_0^r\rho_e'dv = \mathbf{D}\int_0^{(e^2/D^2)^{1/4}}\rho_e'dv, \tag{31}$$

since $r = (e^2/D^2)^{1/4}$. But then, by (29),

$$L = \frac{D^2}{8\pi}\int_0^{\sqrt{e/D}}\rho_e'dv \tag{32a}$$

in the static case, and

$$L = I\int_0^{(e^2/8\pi I_1)^{1/4}}\rho_e'dv \tag{32b}$$

in the general case, in which $I_1 = (D^2 - H^2)/8\pi$ and consequently, L is invariant. As is seen from the latter equations, the Lagrangian can actually be written with the aid of functions of the equivalent distribution ρ'_e.[18] Such a form of the solution turns out to be more useful for subsequent analysis. We express the total energy of the field $\mathcal{H} = \int H_{44}\,dv$ as a function of the equivalent distribution of charge ρ'_e, making use of Eqs. (30) and (31), and carrying out the integration by parts. We obtain

$$\mathcal{H} = e^2/2\,{}_{-1}R_e, \quad 1/{}_{-1}R_e = \int\limits_0^\infty \frac{\rho'_e dv}{r}. \tag{33}$$

In the case of the nonlinear theory, it is natural to assume that the mass of the electron has a purely electromagnetic origin i.e., that $\mathcal{H} = m_0c^2$. But it then follows from (33) that

$${}_{-1}R_e = r_0/2. \tag{34}$$

We shall show that for an arbitrary $\rho'_e(r)$ which changes sign nowhere the rms radius of distribution of the effective charge is larger than ${}_{-1}R_e$.[18] For this purpose, we write ${}_2R^2 \equiv \langle r_e^2 \rangle$ in the form

$$\langle r_e^2 \rangle = \int\limits_0^\infty \rho'_e r^4 dr \Big/ \int\limits_0^\infty \rho'_e r^2 dr$$

$$= \frac{1}{{}_{-1}R^2} \int\limits_0^\infty \rho'_e r^4 dr \left[\int\limits_0^\infty \rho'_e r\, dr \right]^2 \left[\int\limits_0^\infty \rho'_e r^2 dr \right]^{-3}$$

and we show that the factor in front of ${}_{-1}R^{-2}$ is not smaller than unity or, otherwise, that

$$F = \int\limits_0^\infty \rho'_e r^4 dr \left[\int\limits_0^\infty \rho'_e r\, dr \right]^2 - \left[\int\limits_0^\infty \rho'_e r^2 dr \right]^3 \geqslant 0.$$

To do this, we introduce the notation $\varphi(r) = \rho'_e r^2$, write F in the form of the limit of the sum

$$F = \lim \left\{ \sum_{i=1}^{\infty} \varphi(r_i)\, r_i^2 \Delta r_i \left[\sum_{j=1}^{\infty} \varphi(r_j) \frac{\Delta r_j}{r_j} \right] - \left[\sum_{i=1}^{\infty} \varphi(r_i)\, \Delta r_i \right]^3 \right\}$$

$$= \lim \sum_{i>j>k} \varphi(r_i)\, \varphi(r_j)\, \varphi(r_k)\, \Delta r_i \Delta r_j \Delta r_k$$

$$\times \left\{ \frac{r_i^2}{r_j r_k} + \frac{r_j^2}{r_k r_i} + \frac{r_k^2}{r_i r_j} - 3 \right\}.$$

But, inasmuch as

$$(r_i^3 + r_j^3 + r_k^3 - 3r_i r_j r_k) = \frac{1}{2}(r_i + r_j + r_k)$$
$$\times [(r_i - r_j)^2 + (r_j - r_k)^2 + (r_k - r_i)^2] \geqslant 0,$$

then $F \geq 0$, and consequently,

$${}_2R_e \geqslant {}_{-1}R_e = r_0/2. \tag{35}$$

The latter equation is similar to Eq. (18) of the linear theory of the extended electron. If the distribution ρ_p is not alternating in sign, then, as can be shown, ${}_2R_e$ should not be larger than the rms radius of Hofstadter, R_0. But this would contradict the inequality (35), since $R_0 < r_0/2$. Thus, either ρ'_e or ρ_p (which is less probable from the viewpoint of meson theory[19,4]) must change sign. This is the essential result of the nonlinear theory.

Particle Interaction in the Nonlinear Theory

The problem of particle interaction in the nonlinear theory is more difficult than in the linear theory. In the nonlinear theory it is difficult to separate the characteristic energy from the energy of interaction. The interaction energy between two (for example, point) particles is no longer equal to the product of the charge of the first particle by the potential created and the charge of the second particle at the location of the first particle (in its absence). In a similar fashion, the usual expression for the Lorentz forces can be shown to be unsatisfactory. For interpretation of the experimental data, it is important to know the law of interaction between the particles. Therefore, we consider the interaction between two charged particles, in the general case of attraction, with the charge distributions ρ_1 and ρ_2. We make use of the fact that in the nonlinear theory the induction vectors add linearly, as before: $\mathbf{D} = \mathbf{D}_1 + \mathbf{D}_2$, which is not valid for the fields. In this case,

$$\mathbf{D}_1 = \frac{e_1 \mathbf{r}_1}{r_1^3} \int\limits_0^{r_1} \rho_1 dv_1, \qquad \mathbf{D}_2 = \frac{e_2 \mathbf{r}_2}{r_2^3} \int\limits_0^{r_2} \rho_2 dv_1. \tag{36}$$

Furthermore, in accord with Eqs. (30) and (31) we can write down the expression for the total field energy in the following form:

$$\mathcal{H} = \int H_{44} dv = \frac{1}{8\pi} \int (D_1^2 + D_2^2 + 2\mathbf{D}_1 \cdot \mathbf{D}_2)\, dv \int\limits_0^{\sqrt{e/D}} \rho' dv',$$

where ρ' is the density of the equivalent charge distribution. Then, computing the energy of the free field (the sum of the characteristic energies of the isolated noninteracting particles)

$$\mathcal{H}_0 = \frac{1}{8\pi} \int D_1^2 dv \int\limits_0^{\sqrt{e/D_1}} \rho' dv' + \frac{1}{8\pi} \int D_2^2 dv \int\limits_0^{\sqrt{e/D_2}} \rho' dv,$$

we get the "pure" interaction energy:

$$W \doteq \mathcal{H} - \mathcal{H}_0 = W_{11} + W_{12} + W_{22}. \tag{37}$$

Here

$$W_{11} = \frac{1}{8\pi} \int D_1^2 dv \int\limits_{r'_1}^{r'_3} \rho' dv', \tag{38}$$

$$W_{12} = \frac{1}{4\pi}\int \mathbf{D}_1 \cdot \mathbf{D}_2 \, dv \int_0^{r_3'} \rho' dv' , \qquad (39)$$

$$W_{22} = \frac{1}{8\pi}\int D_2^2 dv \int_{r_2'}^{r_3'} \rho' dv', \qquad (40)$$

where

$$\left.\begin{aligned} r_1' &= \sqrt{\frac{e}{D_1}} = r_1 \Big/ \left(\int_0^{r_1} \rho_1 \, dv_1\right)^{1/2}; \\ r_2' &= \sqrt{\frac{e}{D_2}} = r_2 \Big/ \left(\int_0^{r_2} \rho_2 dv_1\right)^{1/2}; \end{aligned}\right\} \qquad (41)$$

$$r_3' = \{(r_2')^{-4} + (r_1')^{-4} + 2\,(r_1')^{-2}\,(r_2')^{-2}\cos\chi\}^{-1/4};$$

χ is the angle between the vectors $\mathbf{r}_1$ and $\mathbf{r}_2$.

It is easy to establish the fact that in the transition to ordinary electrodynamics and to point particles, we obtain $W = W_{12} = e_1 e_2 / r_{12}$. We now consider the special case of the interaction of the proton with the electron. We shall assume that the dimensions of the proton (for example, as a consequence of the interaction with the meson field) are much larger than the dimensions of the electron, which we shall consider to be a point (this means that $r_2' = r_2$). Let the nonlinearity appear only in the small region r^0, so that $\int_0^r \rho' dv' \approx 1$ for all $r > r^0$, while r^0 is less than the radius of the proton. We shall show that in this case the expression for the interaction energy of the particles (37) is materially simplified. From the locations of the first particle (the center of the extended proton) and the second particle (the electron) we draw spheres of radius r^0. The following two cases are then possible, depending on the distance between the particles: (a) the spheres do not overlap or (b) they do overlap. We consider the first case, in which $r_0 \leq r/2$ (r = distance between the particles). In the region $r_2 < r^0$, $r_3' \approx r_2$ [see (41)], since $r_2 > r_1'$, inasmuch as r_1' [as follows from its definition, see Eq. (41)] cannot be smaller than the radius of the proton r_p, which in turn is larger (by assumption) than r^0. In the region $r_2 > r_0$, r_3' is not smaller than $1/(r_2^{-1} + r_p^{-1})$, which is in any case larger than r^0, and since $r_2 > r_0$, then, not changing the value of the integral $\int_0^{r_3'} \rho' dv'$, we can substitute the upper limit for r_2.

In similar fashion, we can consider the case (b) and show that for one reason or another we can replace r_3' by r_2. We then have approximately

$$W_{12} \approx \frac{1}{4\pi}\int \mathbf{D}_1 \cdot \mathbf{D}_2 \, dv \int_0^{r_2} \rho \, dv' .$$

Substituting the values for $\mathbf{D}_1$ and $\mathbf{D}_2$ from (36) (and taking it into account that now $\mathbf{D}_2 = e\mathbf{r}_2 / r_2^3$) we have

$$W_{12} \approx \frac{1}{4\pi}\int dv \left\{\frac{e\mathbf{r}_1}{r_1^3}\int_0^{r_1} \rho_p dv_1\right\}\left\{\frac{e\mathbf{r}_2}{r_2^3}\int_0^{r_2} \rho' dv'\right\}. \qquad (42)$$

But this coincides in form with the interaction of two extended particles in the linear theory: the proton with a charge distribution ρ_p and the electron with the distribution ρ'. In other words, Eq. (1) and the consequences obtained in Secs. 1 and 2, for the effective cross section and displacement of the electronic levels in the atoms, remain valid in this case.

An estimate shows that the correction term to (42) is $\frac{1}{2}(r^0/r_p)^2$ times smaller than the principal term; the term W_{11} amounts to less than $\frac{1}{3}(r^0/r_p)^3$ part of W_{12}, while W_{22} is $\frac{1}{4}(r^0/r_p)$ part.

In the case of the interaction of two electrons, the terms W_{11} and W_{22} are still quite substantial at distances of the order of the effective radius of nonlinearity. An important peculiarity of the nonlinear theory is the difference of the scattering cross section of positrons on electrons from the scattering of electrons on electrons, since in the case of the interaction of particles of identical charge sign, W_{12} is added to W_{11} and W_{22}, while for the interaction of differently charged particles, W_{12} is subtracted from the sum $W_{11} + W_{22}$. A similar effect ought to appear in the scattering of positrons on a proton, by comparison with the scattering of electrons. However, if the radius of nonlinearity is smaller than the larger of the radii of the proton and electron, the effect of nonlinearity would show itself to be negligible. On the other hand, inasmuch as from the viewpoint of the nonlinear theory ρ_e' (or ρ_p) must be charge alternating, this would necessarily lead to peculiarities in the angular distribution.

The possible corrections can be deduced with the aid of the dynamic effects, although in principle the interaction of the electric charges under the experimental conditions[1,2] must be distinguished from the two effects.[4] A more precise calculation of the radiative corrections must also be carried out, both for the case of the linear theory of the extended electron and in particular for the nonlinear theory. However, improving the precision of the calculations of the radiative corrections, which are relatively small in magnitude,[20] almost never leads to a serious change in the results obtained.

We take this opportunity to acknowledge our deep gratitude to Prof. Louis de Broglie and D. D. Ivanenko, who maintained constant interest in the research, and also to J. P. Vigier, D. Bohm and T. Takabayashi, who made a number of valuable comments.

---

[1] E. E. Chambers and R. Hofstadter, Phys. Rev. **103**, 1454 (1956).

[2] F. Bumiller and R. Hofstadter, Bull. Am. Phys. Soc., Ser. 2. **2**, 390 (1957); M. R. Yearian and R. Hofstadter, Bull. Am. Phys. Soc. Ser. 2, **2**, 389 (1957).

[3] N. F. Mott, Proc. Roy. Soc. (London) **A124**, 425 (1929).

[4] R. Hofstadter, Revs. Modern Phys. **28**, 214 (1956); Yennil, Levy and Ravenhall, Revs. Modern Phys. **29**, 144 (1957).

[5] V. A. Petukhov, J. Exptl. Theoret. Phys. (U.S.S.R.) **32**, 379 (1957); Soviet Phys. JETP **5**, 317 (1957).

[6] D. D. Ivanenko and A. A. Sokolov, Классическая теория поля (Classical Theory of Fields), GITTL, 1951.

[7] H. Mott and G. Massey, Theory of Atomic Collisions (Oxford, 1933).

[8] H. Feshbach, Phys. Rev. **84**, 1206 (1951). A. Bodmer, Proc. Phys. Soc. (London) **66**, 1041 (1953).

[9] N. N. Kolesnikov, J. Exptl. Theoret. Phys. (U.S.S.R.) **33**, 819 (1957); Soviet Phys. JETP **6**, 631 (1958).

[10] D. D. Ivanenko and N. N. Kolesnikov, Dokl. Akad. Nauk SSSR **91**, 47 (1953).

[11] Lamb, Triebwasser, and Dayhoff, Phys. Rev. **89**, 98 (1953).

[12] L. Cooper and E. Henley, Phys. Rev. **92**, 801 (1953).

[13] D. I. Blokhintsev, Usp. Fiz. Nauk **61**, 137 (1957).

[14] M. Born, Proc. Roy. Soc. (London) **A143**, 410 (1934).

[15] M. Born and L. Infeld, Proc. Roy. Soc. **A144**, 425 (1934); L. Infeld, Proc. Camb. Phil. Soc. **32**, 127 (1936); **33**, 70 (1937).

[16] M. Born, Annales de l'institut Henri Poincaré, v. 7, Paris, 1937.

[17] W. Pauli, Relativitatstheorie, Encylcop. d. Math. Wiss. v. 19.

[18] G. Jacobi and N. Kolesnikov, Comp. rend. **245**, 285 (1957).

[19] I. E. Tamm, J. Exptl. Theoret. Phys. (U.S.S.R.) **32**, 178 (1957); Soviet Phys. JETP **5**, 154 (1957).

[20] J. Schwinger, Phys. Rev. **75**, 898 (1949); H. Suura, Phys. Rev. **99**, 1020 (1955).

Translated by R. T. Beyer
70

SOVIET PHYSICS JETP VOLUME 35(8), NUMBER 2 FEBRUARY, 1959

THE TEMPERATURE OF PLASMA ELECTRONS IN A VARIABLE ELECTRIC FIELD

A. V. GUREVICH

P. N. Lebedev Physics Institute, Academy of Sciences, U.S.S.R.

Submitted to JETP editor April 22, 1958

J. Exptl. Theoret. Phys. (U.S.S.R.) **35**, 392-400 (August, 1958)

The heating of electrons in a plasma in a variable electric field is considered. It is shown that the electron gas can exist in two stable states with different temperatures; the transition from one state to the other takes place at certain critical values of the field and is accompanied by an appreciable change in the electron temperature. A peculiar type of hysteresis takes place in the dependence of the electron temperature on the field amplitude and frequency. The influence of a constant magnetic field on this effect is also taken into account. An expression is obtained for the complex conductivity of the plasma in variable electric and constant magnetic fields (with account of interelectronic collisions).

1. We consider an unbounded plasma placed in a spatially homogeneous electric field. We assume that the plasma is sufficiently strongly ionized that the principal influence on the distribution of the electrons is that due to collisions between electrons and between electrons and ions; we shall con-

sider these to be elastic.

In this case, as is shown in the Appendix, if the condition

$$dT_e / dt \ll \nu_{\text{eff}} T_e, \tag{1}$$

is satisfied, the symmetric part of the electron distribution function is Maxwellian; the electron temperature T_2 is defined by the equation

$$\frac{dT_e}{dt} + \delta\nu_{\text{eff}\,i}(T_e)(T_e - T) = \frac{2e\mathrm{E}}{3kN}\,\mathrm{j}(T_e). \tag{2}$$

Here, as usual, k is Boltzmann's constant, T the ion temperature, e the electronic charge, N the density of the electrons, and E the electric field intensity. Furthermore, $\delta = 2m/M$ is the average fraction of the energy given by an electron to an ion in a single collision (m is the electron mass and M the ion mass), and ν_{eff} is a parameter which it is reasonable to call the effective collision frequency of electrons with ions:*

$$\nu_{\text{eff}\,i} = \frac{4}{3}\sqrt{2\pi}\,\frac{e^4 N_i}{\sqrt{m}\,(kT_e)^{3/2}} \ln\left(\frac{kT_e}{e^2}\,p_{\max}\right), \tag{3}$$

where $p_{\max}$ is the maximum of the impact parameter, which must be taken as equal to the Debye radius [but sometimes another, somewhat different quantity is used (see reference 2, Sec. 82; also reference 4)]. We note that the quantity appearing in (3) under the logarithm sign is always much larger than unity. As a consequence, even for large changes in the electron temperature, the logarithm does not change appreciably, and it can be taken approximately that

$$\nu_{\text{eff}\,i} = \nu_0 (T_e / T)^{-3/2}, \tag{3'}$$

where ν_0 is the effective collision frequency of electrons with ions in a weak field (when $T_e = T$).

x	K_σ	K_ε
0	1.950	4.595
0.05	1.921	4.512
0.1	1.859	4.340
0.2	1.652	3.792
0.5	1.075	2.297
1.0	0.721	1.405
2.0	0.623	1.048
4.0	0.727	0.972
6.0	0.824	0.976
10.0	0.917	0.987
35.0	0.992	0.997

Finally, j is the electron current density

$$\mathrm{j} = \left(\sigma + i\omega\frac{\varepsilon - 1}{4\pi}\right)\mathrm{E} \tag{4}$$

$$= \frac{e^2 N}{m}\left\{\frac{\nu_{\text{eff}\,i}}{\omega^2 + \nu^2_{\text{eff}\,i}} K_\sigma\left(\frac{\omega}{\nu_{\text{eff}\,i}}\right) - i\,\frac{\omega}{\omega^2 + \nu^2_{\text{eff}\,i}} K_\varepsilon\left(\frac{\omega}{\nu_{\text{eff}\,i}}\right)\right\}\mathrm{E}.$$

Here ν_{eff_i} is the effective collision frequency of the electrons, defined by (3), (3′), while $K_\sigma(x)$ and $K_\epsilon(x)$ are certain functions the computed values of which are given in the table.*

It is seen from the table that the functions K_σ and K_ϵ do not change very markedly; therefore, for qualitative estimates, we can set them equal to unity, i.e., we can use the simple ("elementary") formulas† for σ and ϵ.

2. We now turn to the analysis of the solution of Eq. (2). In this case we assume that the temperature of the heavy particles in the plasma is constant (this case, which was considered in Sec. 3, is of interest in a methodological way, since it allows us to clarify some peculiarities of the heating of an electron gas in a plasma).

We first assume that the electric field $\mathrm{E} = \mathrm{E}_0 \cos \omega t$ changes rapidly ($\omega \gg \delta\nu_0$). In this case the field changes more rapidly with time than the electron temperature can be changed. Therefore, this temperature must be established at some mean value of T_{e0} that is time independent; deviations from this value are small. Actually, the solution of Eq. (2) in the case under consideration has the following form:

---

*We note that the effective collision frequency of the electron thus introduced coincides with that considered in reference 1. In reference 2 (see Secs. 61 ff) some other quantity is used as $\nu_{\text{eff}\,i}$ (its use leads to a series of difficulties which are pointed out in references 1 and 3).

*If we neglect the coefficients K_σ and K_ε in Eq. (4), then it coincides with the well known "elementary" expression which is obtained in the hydrodynamic approximation (see, e.g., reference 2, Sec. 57). As is well known,[3] the latter is strictly valid for electrons in a plasma for any frequency of the electric field, only if the condition is satisfied that the frequency of collision of the electron with heavy particles is independent of their velocity. In the case of collision with ions, this condition is naturally not satisfied ($\nu \sim v^{-3}$). Therefore, the kinetic consideration given in the Appendix is also necessary. It leads to the appearance of corrected coefficients K_σ and K_ε which reflect the dispersion of the electron collision frequency. For $\omega \gg \nu_{\text{eff}\,i}$, the coefficients K_σ and K_ε tend to unity, which is in accord with reference 5. In the case of a constant electric field ($\omega = 0$), the conductivity computed by Eq. (4) [see also Eq. (10)] coincides with that obtained in reference 6, as it must.

†It should be noted that the values of the functions K_σ and K_ε given in the table were computed for the case in which the electron density in the plasma is equal to the ion density. The functions K_σ and K_ε in the case in which the ion density is much greater than that of electrons (i.e., when there are more negative ions in the plasma and, therefore, collisions between the electrons are not important) were obtained in reference 1 (Fig. 7). The same functions K_σ and K_ε are also valid for multiply ionized plasma, when $Z \gg 1$ (it must be kept in mind that the effective collision frequency of the electron is increased Z-fold in this case). The functions K_σ and K_ε for doubly, triply, . . . , ionized plasma lie between the limiting functions for $Z = 1$ (the table) and for $Z \gg 1$; it is easy to compute them by making use of the results of Landshoff[6] (comparing the results of reference 6 with Eq. (10) for the case $\omega = 0$).

$$T_e = T_{e0} + \frac{\delta\nu_0}{2\omega}\frac{T_{e0} - T}{(T_{e0}/T)^{3/2}}\sin 2\omega t + O\left[\left(\frac{\delta\nu_0}{\omega}\right)^2\right], \tag{5}$$

where the temperature T_{e0} is determined from the transcendental equation

$$\frac{T_{e0}}{T} - 1 = \frac{e^2E_0^2}{3kTm\delta\nu_0^2}\frac{K_\sigma\left[(\omega/\nu_0)(T_{e0}/T)^{3/2}\right]}{(\omega/\nu_0)^2 + (T_{e0}/T)^{-3}}\,. \tag{6}$$

The condition (1) for establishing the solution (5) is always satisfied.

Analysis of the solution of the latter equation shows that at high frequencies $(\omega > \nu_0)$ there corresponds to each value of the field a particular value of the temperature T_{e0} as, generally speaking, ought to be the case. However, at low frequencies $(\omega \ll \nu_0)$, an interesting peculiarity arises: to a definite value of the field (in the region $E_k^{II} < E_0 < E_k^{I}$) there corresponds not one but three values of the temperature T_{e0} (see Fig. 1).* The reason for this is that the electron gas in the plasma is not a closed system: in the particular model it absorbs energy from the electric field and transfers it to the heavy particles of the plasma; its stationary temperature is determined, naturally, by the condition of energy balance between that absorbed from the field and that given to the heavy particles [Eq. (6)]. In this case it is shown that for low frequencies the amount of energy absorbed and transmitted by the electron gas is linearly independent of its temperature and, thanks to this fact, Eq. (6) can be satisfied simultaneously for several different values of the electron temperature. However, only two of them, which correspond to the upper and lower curve (the solid line plotted in Fig. 1), are stable; the state corresponding to the middle curve (the dotted line in Fig. 1) is not stable. Moreover, the solution corresponding to the upper and lower curves becomes unstable at points where they join to the middle curve, i.e., at $E_0 = E_k^{I}$ for the lower curve and for $E_0 = E_k^{II}$ for the upper curve.*

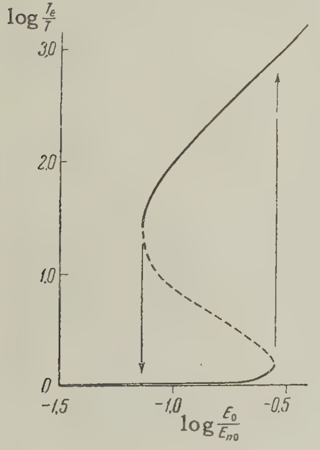

FIG. 1. Dependence of T_e/T on E_0/E_{n0} for $\omega = 0.01\nu_0$.

In the following, we restrict ourselves to the state corresponding to the lower curve, called state I, and to the upper, state II. The value of the electron temperature in state I at $\omega \ll \nu_0$ is given approximately by the following expression:

$$T_{e0}^{I} = T\left(1 + \frac{K_\sigma(0)\,(E_0/E_{n0})^2}{1 - 4.5K_\sigma(0)\,(E_0/E_{n0})^2}\right),$$

and in state II by

$$T_{e0}^{II} = T\left(\frac{E_0}{E_{n0}}\right)^2\left(\frac{\nu_0}{\omega}\right)^2\left[1 + \left(\frac{\omega}{\nu_0}\right)^4\Big/\left(\frac{E_0}{E_{n0}}\right)^6\right]^{-1}. \tag{7}$$

Here E_{n0} is the characteristic field for the plasma:[3]

$$E_{n0} = \sqrt{3kTm\delta\nu_0^2}/e \approx 2\cdot 10^{-8}\frac{N_i}{T}\sqrt{\delta}\ \text{V/cm}. \tag{8}$$

The first critical value of the field $E_k^{I} \approx 0.28\,E_{n0}$; the corresponding temperature is $T_k^{I} = 1.5\,T$ in state I and T_k^{II}; $0.076(\nu_0/\omega)^2T$ in state II. For a sufficiently low frequency ω, the temperature T_k^{II} is many times larger than T_k^{I} (for example, in the case shown in Fig. 1 $(\omega = 0.01\nu_0)$, $T_k^{I} \approx 1.5\,T$, and $T_k^{II} \approx 760\,T$). The second critical value for the field is $E_k^{II} \approx 1.7(\omega/\nu_0)^{2/3}E_{n0}$; the corresponding value of the temperature in state I is $T_k^{I} \approx T$, and in state II, $T_k^{II} \approx 1.2(\nu_0/\omega)^{2/3}T$.

We now consider how the heating of the electron gas in the plasma will take place at slow changes in the amplitude of the intensity of the variable electric field. At small values of E_0 the electron gas is located in state I and the temperature of the electrons differs slightly from the ion temperature (see Fig. 1). However, when the field E_0 reaches its own first critical value E_k^{I}, state I becomes unstable (since the electrons can no longer transfer all their absorbed energy to the heavy particles). Therefore the electron gas at $E_0 = E_k^{I}$ is heated,

---

*In constructing the dependence of T_{e0}/T on E_0/E_{n0}, it is particularly useful to inverse the problem and construct the graph of the dependence of E_0/E_{n0} on T_{e0}/T.

*For analysis of the stability of a stationary value of T_{e0}, it is necessary to investigate the behavior of the derivative dT_e/dt close to T_{e0}. This can be done both analytically (by considering the change in time of a small perturbation ΔT_e) and graphically [by constructing the dependence of dT_e/dt on T_e, with the help of Eq. (2)].

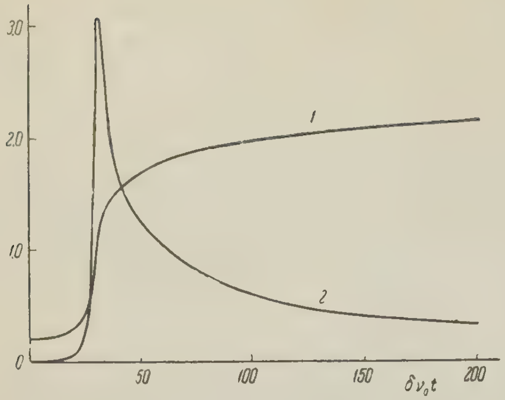

FIG. 2. Time dependence of the electron temperature and its derivative for the transition I→ II (for $\omega = 0.01\nu_0$); curve 1 – for log (T_e/T), 2 – for $(1/T\delta\nu_0)dT_e/dt$.

and its temperature rises to the corresponding value in state II (this transition is shown by the dashed curve in Fig. 1).

If the field E_0 now begins to fall below the value E_k^I, then T_{e0} takes on still higher values, corresponding to state II. However, when the field decreases to its second critical value E_k^{II}, state II becomes unstable (the electrons transfer more energy to the heavy particles than the field gives to them). Therefore, at $E_0 = E_k^{II}$, the electron gas is cooled and its temperature drops to the value corresponding to state I, i.e., to T (this transition is also shown by the dashed curve in Fig. 1). Thus, in the case under consideration, an unusual hysteresis takes place in the dependence of the electron temperature on the amplitude of the intensity of the variable electric field.

The process of transition from state I to state II, and vice versa, is described by Eq. (2).* The corresponding solution for the transition (for $\omega = 0.01\,\nu_0$) is shown in Fig. 2. It is seen from the figure that the rate of increase of the electron temperature increases rapidly at first, reaches a maximum, and then falls off slowly; its maximum value is rather high:

$$(dT_e/dt)_{\max} \approx 0.03\,(\nu_0/\omega)\,\delta\nu_0 T. \tag{9}$$

The change in the electron temperature for the transitions is naturally accompanied by corresponding changes in the effective collision frequency of the electrons (3) and, consequently, of the kinetic coefficients, too.

The dependence of the temperature T_{e0} on the frequency ω is completely analogous to the dependence of T_{e0} on E_0. For large values of E_0, only one stationary value of electron temperature corresponds to each value of the frequency; for small E_0, two values of T_{e0} can correspond to a single value of ω (see Fig. 3). In this case, however, transitions from state I (lower curve) to state II (upper curve) are possible only for E_0 larger than E_k^I; therefore state I at $E_0 < E_k^I$ is stable for arbitrary values of the frequency ω.

The critical frequency ω_k and the critical field E_k (above which only a single stationary state exists) are determined from the conditions

$$dT_{e0}/d\,[(E_0/E_{n0})^2] \to \infty,\quad d^2T_{e0}/d^2\,[(E_0/E_{n0})^2] \to \infty,$$

from which it follows that $\omega_k \approx 0.2\,\nu_0$; $E_k \approx 0.4\,E_{n0}$. Hysteresis of the dependence of T_{e0} on E_0 is possible only for $\omega < \omega_k$, while hysteresis of the dependence of T_{e0} on ω is possible for $E_k^I < E_0 < E_k$.

The external electric field is assumed to be rapidly changing ($\omega \gg \delta\nu_0$). Quite analogous effects take place also in the opposite case, when $\omega \lesssim \delta\nu_0$. Their analysis is, generally speaking, more complicated. However, we can note that if the amplitude of E_0 is larger than $E_k^I/\sqrt{2}$, the electron temperature executes a complete hysteresis cycle during each period, similar to that described above.* In this case the temperature corresponding to state II increases with decrease in ω as $1/\omega^2$ (this is seen, for example, from Eq. (7); see also Fig. 3). For a constant field ($\omega = 0$) no stationary state II exists in general: in this case, if only the field E_0 is larger than $E_k^I/\sqrt{2}$, the energy of the electrons increase continuously with time. Condition (1) is violated here; the electron velocity distribution function takes on a sharply directional character.†

3. It is not difficult to generalize these results to the case where a constant magnetic field **H** is present in the plasma. Equation (2) for the electron temperature and Eq. (3) for the effective collision frequency are preserved in this case; only the expression for the electron current is changed: the conductivity and the dielectric constant of the plasma become tensors.

The tensor components of σ and ϵ are expressed by means of the functions K_σ and K_ϵ, developed above. For the components of the tensors σ and ϵ in the direction parallel to the magnetic field, the same expressions (4) are still valid; in a plane perpendicular to H (the plane xy), we have:

---

*Although dT_e/dt increases appreciably in the transition, the condition (1) is seen to be satisfied as previously (for arbitrary $\omega > \delta\nu$).

*It should be noted, however, that condition (1) in this case is not always satisfied; the electron velocity distribution function in this case is definitely not Maxwellian.

†It should be emphasized that, as is seen from the results of this section, the stationary low frequency state ($\omega \ll \nu$) can exist only in the case of a weak electric field ($E_0 \ll E_{n0}$). Therefore the expressions for the complex conductivity and thermoelectric coefficient, obtained in reference 6 (see also references 4 and 7), are also valid in the present case.

$$\sigma_{xx}=\sigma_{yy}=\frac{e^2N}{m}\frac{\nu_{\text{eff}\,i}}{2}\left\{\frac{K_\sigma[|\omega-\omega_H|/\nu_{\text{eff}\,i}]}{(\omega-\omega_H)^2+\nu_{\text{eff}\,i}^2}+\frac{K_\sigma[(\omega+\omega_H)/\nu_{\text{eff}\,i}]}{(\omega+\omega_H)^2+\nu_{\text{eff}\,i}^2}\right\},$$

$$\sigma_{xy}=-\sigma_{yx}=-i\frac{e^2N}{m}\frac{\nu_{\text{eff}\,i}}{2}\left\{\frac{K_\sigma[|\omega-\omega_H|/\nu_{\text{eff}\,i}]}{(\omega-\omega_H^2)+\nu_{\text{eff}\,i}^2}-\frac{K_\sigma[(\omega+\omega_H)/\nu_{\text{eff}\,i}]}{(\omega+\omega_H)^2+\nu_{\text{eff}\,i}^2}\right\}, \tag{10}$$

$$\varepsilon_{xx}=\varepsilon_{yy}=1-\frac{4\pi e^2N}{m}\frac{1}{2\omega}\left\{\frac{(\omega-\omega_H)K_\varepsilon[|\omega-\omega_H|/\nu_{\text{eff}\,i}]}{(\omega-\omega_H)^2+\nu_{\text{eff}\,i}^2}+\frac{(\omega+\omega_H)K_\varepsilon[(\omega+\omega_H)/\nu_{\text{eff}\,i}]}{(\omega+\omega_H)^2+\nu_{\text{eff}\,i}^2}\right\},$$

$$\varepsilon_{xy}=-\varepsilon_{yx}=i\frac{4\pi e^2N}{m}\frac{1}{2\omega}\left\{\frac{(\omega-\omega_H)K_\varepsilon[|\omega-\omega_H|/\nu_{\text{eff}\,i}]}{(\omega-\omega_H)^2+\nu_{\text{eff}\,i}^2}-\frac{(\omega+\omega_H)K_\varepsilon[(\omega+\omega_H)/\nu_{\text{eff}\,i}]}{(\omega+\omega_H)^2+\nu_{\text{eff}\,i}^2}\right\}.$$

Here $\omega_H = eH/mc$ is the gyromagnetic frequency.

Now, substituting the expression for the electron current in (2), we get an equation through which the temperature of the electrons is also determined. In a rapidly varying field, it is stationary and is equal to T_{e0}; the latter satisfies the following transcendental equation (see reference 1):

$$\frac{T_{e0}}{T}-1=\left(\frac{E_0}{E_{n0}}\right)^2\left\{\frac{\cos^2\beta K_\sigma[(\omega/\nu_0)(T_{e0}/T)^{3/2}]}{(\omega/\nu_0)^2+(T_{e0}/T)^{-3}}+\frac{\sin^2\beta K_\sigma[(|\omega-\omega_H|/\nu_0)(T_{e0}/T)^{3/2}]}{2[(\omega-\omega_H)^2/\nu_0^2+(T_{e0}/T)^{-3}]}+\frac{\sin^2\beta K_\sigma[((\omega+\omega_H)/\nu_0)(T_{e0}/T)^{3/2}]}{2[(\omega+\omega_H)^2/\nu_0^2+(T_{e0}/T)^{-3}]}\right\}. \tag{11}$$

Here β is the angle between **E** and **H**. For $H = 0$ (and also if $\beta = 0$) Eq. (11) coincides with (6), as it should.

Analysis of the dependence of the temperature T_{e0} on the amplitude of the field intensity E_0 is not difficult to carry out, in the same fashion as was done above in the case $H = 0$. For a high frequency ω_H ($\omega_H \gg \nu_0$), effects similar to those considered above (two stationary states with different electron temperatures) take place in the gyro-resonance frequency region, when $|\omega - \omega_H| \ll \nu_0$, $\sin\beta \neq 0$. It is interesting to observe that in this case, for small values of the amplitude of the field ($E_0 < \sqrt{2}\,E_k^I/\sin\beta$) there is no sort of resonance increase in the electron temperature in the vicinity of the gyro-frequency (state I, for $E_0 < \sqrt{2}\,E_k^I/\sin\beta$, is stable for an arbitrary frequency ω). On the other hand, in the case in which $E_0 \geq \sqrt{2}\,E_k^I/\sin\beta$, a strong resonance effect appears close to the gyro-frequency.

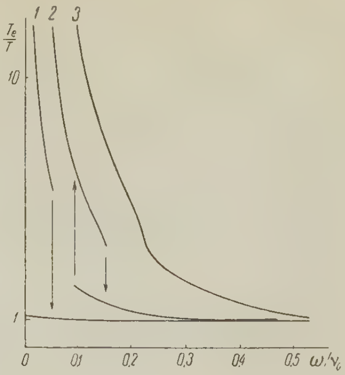

FIG. 3. Dependence of T_e/T on ω/ν_0 for various values of E_0: curve 1 – $E_0 < E_k^I$; curve 2 – $E_k^I < E_0 < E_k$; curve 3 – $E_k < E_0$.

4. The heating of the plasmas by the heavy particles was not considered above. However, it is entirely understood that in the adiabatic, isolated plasma, under conditions for which the gas is heated more slowly by the heavy particles, than the electron gas,* the consideration carried out is valid; it suffices only to assume that the temperature of the plasma T increases slowly with time. This leads to a situation in which the relative magnitude of the variable electric field E_0/E_{n0} increases with time (i.e., the point describing the state of the system on Fig. 1 is shifted to the right). When the ratio E_0/E_{n0} is equal to E_0/E_k^I, a transition takes place from state I to state II. It is essential that the temperature of the electrons in this transition changes rather sharply [see Eq. (9)]; therefore, even in the case in which the heating of the heavy particles, generally speaking, cannot be regarded as slow (for example, in a completely ionized gas, when $\alpha \approx 1$, see footnote below), the process of the transition of the electron gas from state I to state II at sufficiently low frequency is expressed explicitly, as before.

In this connection it should also be noted that the entire argument above was based on the assumption that the electric field is homogeneous in space. In a real system the field is usually in-homogeneous. Therefore, the critical value E_k^I is achieved initially only in a certain region of the plasma (and not throughout its volume); in this region the transition of the electron gas also begins from state I to state II.* A sharp electron temperature rise (and, consequently, in the pressure) in this region of the plasma during the transition ought to lead to the excitation of essentially nonstationary effects.

---

*The heavy particles in the plasma are heated through the work of the ion current and the energy transferred to it by electrons in collisions. The ion current in the cases of interest to us is always much weaker than the electron current; therefore, the condition of quasi-stationarity for the plasma heating due to the work of the ion current is always satisfied. The heating of the heavy particles due to collisions with electrons can be regarded as slow (quasi-stationary) for the case that $\alpha = N/(N_i + N_m) \ll 1$ (here N, N_i, N_m are the densities of electrons, ions, and molecules, respectively). This condition is well satisfied, for example, in the upper ionosphere.

The author expresses his thanks to V. L. Ginzburg for interest in the research.

APPENDIX

ELECTRON-VELOCITY DISTRIBUTION FUNCTION IN A STRONGLY-IONIZED PLASMA IN A VARIABLE ELECTRIC FIELD†

As is well known,[8] we can write the electron velocity distribution function for the plasma in the form

$$f(\mathbf{v}, t) = f_0(v, t) + \frac{\mathbf{v}}{v}\mathbf{f}_1(v, t). \tag{A.1}$$

The Boltzmann equation reduces in this case to the following system of equations for the functions f_0 and $\mathbf{f}_1$:

$$\frac{\partial f_0}{\partial t} + \frac{e}{3mv^2}\frac{\partial}{\partial v}(v^2\mathbf{E}\cdot\mathbf{f}_1) - \frac{1}{v^2}\frac{\partial}{\partial v}\left\{\nu v^2\frac{kT}{M}\frac{\partial f_0}{\partial v} + \nu\frac{m}{M}v^3 f_0\right\}$$
$$= -\int \sigma_{ee}(w, \theta')\, w\, \{f_0(v,t) f_0(v_1, t) \tag{A.2}$$
$$- f_0(v', t) f_0(v_1', t)\}\, d\mathbf{v}_1 d\Omega';$$

$$\frac{\partial \mathbf{f}_1}{\partial t} + \frac{e}{mc}[\mathbf{H}\times\mathbf{f}_1] + \frac{e\mathbf{E}}{m}\frac{\partial f_0}{\partial v} + \nu\mathbf{f}_1$$
$$= -\frac{3}{4\pi}\int \sigma_{ee}(w, \theta')\, w \left\{\frac{\mathbf{v}\cdot\mathbf{f}_1(v, t)}{v} f_0(v_1, t)\right. \tag{A.3}$$
$$+ \frac{\mathbf{v}_1\cdot\mathbf{f}_1(v_1, t)}{v_1} f_0(v, t) - \frac{\mathbf{v}'\cdot\mathbf{f}_1(v', t)}{v'} f_0(v_1', t)$$
$$\left. - \frac{\mathbf{v}_1'\cdot\mathbf{f}_1(v_1', t)}{v_1'} f_0(v_1, t)\right\} d\mathbf{v}_1 d\Omega' d\Omega.$$

These equations differ from those obtained by Davydov[8] by the fact that interelectronic collisions are considered in them. These collisions are described by the integral terms on the right-hand side. Here $\mathbf{v}, \mathbf{v}_1$ and $\mathbf{v}', \mathbf{v}_1'$ are, respectively, the velocities of the two electrons before and after their collisions; $\mathbf{w} = \mathbf{v} - \mathbf{v}_1$, θ' is the angle between $\mathbf{w}$ and $\mathbf{w}'$, $d\Omega' = \sin\theta'\, d\theta'\, d\varphi'$ and $\sigma_{ee}(w, \theta')$ is the effective differential scattering cross section for collisions between electrons; $\nu = \nu(v)$, as usual, is the collision frequency of the electron with heavy particles (see, for example, reference 2).

The expansion (A.1), and consequently Eqs. (A.2) and (A.3), are valid under the conditions*

$$\delta = 2m/M \ll 1, \quad \partial f_0/\partial t \ll \nu_{\text{eff}} f_0. \tag{A.4}$$

Here ν_{eff} is the effective collision frequency of the electrons with the heavy particles.

We shall seek a solution of Eqs. (A.2) and (A.3) by the method of successive approximations $f_0 = f_{00} + f_{01} + \ldots$, $\mathbf{f}_1 = \mathbf{f}_{10} + \mathbf{f}_{11} + \ldots$. We assume that the form of the symmetric part of the distribution function (f_{00}) in the zeroth approximation is determined by the integral term (i.e., that interelectronic collisions play a dominant role†). The solution of Eq. (A.2) in this approximation is, of course, the Maxwell distribution function. However, the latter is determined only with accuracy up to some arbitrary function of time $T_e(t)$ (the electron temperature) which must be found from the equation for the subsequent approximation (see below).

In order to find the zero approximation for the directional part of the distribution function $\mathbf{f}_{10}$, it is necessary to solve the integro-differential equation (A.3). This problem is generally very complicated. It was solved by Landshoff[8] for the case of a constant electric field (see also reference 7). The results of this work can be generalized to the case of a variable electric field.‡ In fact, if use is made of the condition (A.4), it is not difficult to show (similarly to what was done in reference 9) that the dependence of the function f_{00} on time does not have to be taken into account in the integration of Eq. (A.3). In this approximation, Eq. (A.3) is a linear integro-differential equation with time independent coefficients; obviously, the time variation in such an equation is easily separated, after which the equation becomes quite analogous to the one considered by Landshoff. The solution of this equation was found in reference 6 in the form of a series of Laguerre polynomials of order $^3/_2$. The same expression for the function $\mathfrak{f}_{10}$ is valid even in the case of a variable electric field. It is only necessary to replace the gyrofrequency ω_H by $\omega \pm \omega_H$). Making use of this, it is not difficult to obtain expressions for the conductivity and dielectric constant of the plasma [which were obtained above, Eqs. (4) and (10)], and also for the other coefficients of transfer in a variable electric field.

---

*Heat exchange with the other parts of the plasma can be reduced by eliminating the magnetic field. This also leads to a weakening of the effect of boundaries which, generally speaking, is very important (especially under conditions where the characteristic dimensions of the plasma are less than or comparable with $l\sqrt{\delta}$, where l is the electron mean free path).

†The corresponding calculation was carried out by Landshoff[6] (see also references 4 and 7) only for the case of a quasistationary ($\omega \ll \nu$) electric field. The case of a variable field of arbitrary frequency was considered for a weakly-ionized plasma, in which one could neglect collisions between electrons (see references 1 and 10 to 12).

*We note that the condition $\partial f_0/\partial t \ll \nu_{\text{eff}} f_0$ was not noted by Davydov.

†The opposite extreme, in which the integral term is not important, was considered in references 1 and 8 to 12.

‡The possibility of such a generalization is based on the physically evident equivalence of the motion of the electrons in the direction of a weak electric field in the variable field case and in a constant field perpendicular to the magnetic (if only $\omega_H = \omega$).

Now substituting f_{00} and $\mathfrak{f}_{10}$ in (A.2), we obtain the following equation for the first approximation (f_{01}):

$$\begin{aligned}&\int \sigma_{ee}\cdot w\,\{f_{01}(v,\ t)\,f_{00}(v_1,\ t)+f_{01}(v_1,\ t)\,f_{00}(v,\ t)\\&-f_{01}(v',\ t)\,f_{00}(v_1',\ t)-f_{01}(v_1',\ t)\,f_{00}(v',\ t)\}\,d\mathbf{v}_1\,d\Omega'\\&=-\frac{1}{v^2}\frac{\partial}{\partial v}\left\{\frac{v^3}{2T_e}f_{00}(v,\ t)\left[\frac{dT_e}{dt}-\delta\nu\,(T_e-T)\right]\right.\\&\left.-v^2\frac{e\mathbf{E}}{3m}\mathfrak{f}_{10}(v,\ t)\right\}.\end{aligned}\tag{A.5}$$

This integral equation is degenerate: if we multiply it by v^4 and integrate over dv, the integral term vanishes identically. It is natural that the right hand side of the equation must also vanish in this case [in the opposite case Eq. (A.5) has no solution]. This condition reduces to Eq. (2), (as can easily be seen) which also determines the temperature of the electrons $T_e(t)$.

If we estimate the value of terms of the second approximation and compare them with the zero approximation, we find that we can neglect them if the conditions

$$\delta\nu_{\text{eff}}/\nu_e \ll 1, \quad dT_e/dt \ll \nu_e T_e, \tag{A.6}$$

are satisfied, where ν_e is the mean collision frequency between electrons.

In a strongly ionized plasma ν_e and ν_{eff} are of the same order. Consequently, conditions (A.6) and (A.4) are identical in this case. This means that in the case of a strongly ionized plasma, the solution of Eqs. (A.2) and (A.3), obtained above as a zeroth approximation, is the complete solution; it is valid with the same degree of accuracy with which Eqs. (A.2) and (A.3) are themselves valid.

---

[1] A. V. Gurevich, J. Exptl. Theoret. Phys. (U.S.S.R.) **30**, 1112 (1956), Soviet Phys. JETP **3**, 895 (1957).

[2] Al'pert, Ginzburg, and Feinberg, **Распространение радиоволн** (Radiowave Propagation) (GITTL, Moscow-Leningrad, 1953).

[3] A. V. Gurevich, Dissertation, Physics Inst., Academy of Sciences, U.S.S.R.

[4] S. I. Braginskii, J. Exptl. Theoret. Phys. (U.S.S.R.) **33**, 459 (1957), Soviet Phys. JETP **3**, 358 (1958).

[5] V. L. Ginzburg, J. Exptl. Theoret. Phys. (U.S.S.R.) **21**, 788 (1951).

[6] R. Landshoff, Phys. Rev. **76**, 964 (1949).

[7] L. Spitzer, Jr. and R. Härm, Phys. Rev. **89**, 977 (1953).

[8] B. I. Davydov, J. Exptl. Theoret. Phys. (U.S.S.R.) **7**, 1069 (1937).

[9] A. V. Gurevich, J. Exptl. Theoret. Phys. (U.S.S.R.) **32**, 1237 (1957), Soviet Phys. JETP **5**, 1006 (1957).

[10] H. Margenau, Phys. Rev. **69**, 508 (1946).

[11] R. Jancel and T. Kahan, Compt. rend. **238**, 995 (1954).

[12] V. M. Fain, J. Exptl. Theoret. Phys. (U.S.S.R.) **28**, 422 (1955); Soviet Phys. JETP **1**, 205 (1955).

Translated by R. T. Beyer
71

SOVIET PHYSICS JETP VOLUME 35(8), NUMBER 2 FEBRUARY, 1959

PRODUCTION OF TWO π MESONS IN COLLISIONS BETWEEN π MESONS OR γ QUANTA WITH NUCLEONS OR DEUTERONS

N. V. DUSHIN

Leningrad Polytechnic Institute

Submitted to JETP editor March 3, 1958

J. Exptl. Theoret. Phys. (U.S.S.R.) **35**, 401-407 (August, 1958)

The production of two π mesons in collisions between π mesons or γ quanta with nucleons or deuterons is studied by a phenomenological method for small angles of emission of the π mesons produced.

1. Let us consider the reaction $\pi^+ + p \rightarrow n + \pi^+ + \pi^+$ and let us denote the amplitude of that process for the pseudopotential given in references 1 and 2 by A. We have

$$V = A\delta(\mathbf{r}_n - \mathbf{r})\tau_n. \qquad (1)$$

where τ_n is an operator acting on the isotopic variable of the nucleon.

The π mesons are pseudoscalar particles. The amplitude A, corresponding to the transformation of one π meson into two π mesons in collision with nucleons, should therefore be a pseudoscalar. In the following, we shall limit ourselves to reactions in which the produced π mesons are emitted at small angles. The expression $\mathbf{A}\sigma$, where $\mathbf{A} = a\mathbf{k}_1 + b\mathbf{k}_2 + c\mathbf{k}_0$, represents then the only pseudoscalar which can be constructed from the given $\mathbf{k}_0$, $\mathbf{k}_1$, $\mathbf{k}_2$ (wave vectors of the incident and the produced mesons, respectively) and nucleon spin vector $\boldsymbol{\sigma}$. In consequence, the amplitude should be of the form

$$A = \mathbf{A}\sigma = (a\mathbf{k}_1 + b\mathbf{k}_2 + c\mathbf{k}_0)\sigma, \qquad (2)$$

where a, b, c are invariant functions of the vectors $\mathbf{k}_0$, $\mathbf{k}_1$, $\mathbf{k}_2$. The differential cross-section for the reaction $\pi^+ + p \rightarrow n + \pi^+ + \pi^+$ can be expressed in terms of the amplitude **A** of the reaction:

$$d\sigma = \frac{2\pi}{k_0 / E_0} |\mathbf{A}_p|^2 \delta(E_0 - E_f) \frac{d\mathbf{k}_1}{(2\pi)^3} \frac{d\mathbf{k}_2}{(2\pi)^3}. \qquad (3)$$

where E_0 is the energy of the incident meson. The vector **A** in Eq. (3) has an index p indicating that the reaction goes on a proton.

2. Let us consider the transformation reaction of one π meson into two in collisions with deuterons. The interaction between the incident π meson and a deuteron can be described by a pseudopotential which is a sum of pseudopotentials (1):

$$V = V(1) + V(2). \qquad (4)$$

where 1 and 2 denote the coordinates of the first and second nucleons in the deuteron.

The reaction $\pi^- + d \rightarrow n + n + \pi^- + \pi^+$. The pseudopotential is then

$$V = \mathbf{A}_p\sigma_1\delta(\mathbf{r}_1 - \mathbf{r})\tau_1^+ + \mathbf{A}_p\sigma_2\delta(\mathbf{r}_2 - \mathbf{r})\tau_2^+. \qquad (5)$$

For the differential cross-section of the reaction $\pi^- + d \rightarrow n + n + \pi^- + \pi^+$ we obtain (after some intermediate calculations):

$$d\sigma(\mathbf{k}_1\mathbf{k}_2\mathbf{q}) = \frac{2\pi}{k_0 / E_0}\frac{2}{3}|\mathbf{A}_p|^2\{2|I^-|^2 + |I^+|^2\} \times \delta(E_0 - E_f)\frac{d\mathbf{k}_1}{(2\pi)^3}\frac{d\mathbf{k}_2}{(2\pi)^3}\frac{d\mathbf{q}}{(2\pi)^3}. \qquad (6)$$

Here **q** is the momentum of the relative motion of produced nucleons and where

$$I^{\pm} = \int \varphi_{\mathbf{q}}^{\pm}(\mathbf{r}) e^{i\boldsymbol{\varkappa}\cdot\mathbf{r}} \varphi_0(r)\, d\mathbf{r}. \qquad (7)$$

In the above integrals $\varphi_0(\mathbf{r})$ denotes the coordinate part of the deuteron wave function (we assume that the ground state of the deuteron is a S state), $\varphi_{\mathbf{q}}^{\pm}(\mathbf{r})$ are the symmetric and antisymmetric coordinate parts, respectively, of the wave function of the relative motion of two nucleons with relative momentum **q**. We have, furthermore,

$$\varkappa = {}^1/_2(\mathbf{k}_0 - \mathbf{k}_1 - \mathbf{k}_2),$$

$$E_0 - E_f = \sqrt{m^2 + k_0^2} - \sqrt{m^2 + k_1^2} - \sqrt{m^2 + k_2^2} - \frac{\varkappa^2}{M} - \frac{q^2}{M} + \varepsilon = 0; \qquad (8)$$

where κ^2/M and q^2/M are, respectively, the energy of motion of the center of mass of two nucleons and the energy of the relative motion of the nucleons, and ε is the deuteron binding energy. In Eq. (8) the difference between the mass of charged and neutral π mesons and between the mass of protons and neutrons h has been neglected.

The reaction $\pi^- + d \rightarrow p + n + \pi^- + \pi^0$. For the pseudopotential we have:

$$V = \frac{1}{2}\{\mathbf{A}_p\sigma_1(1+\tau_3^{(1)}) + \mathbf{A}_n\sigma_1(1-\tau_3^{(1)})\}\,\delta(\mathbf{r}_1 - \mathbf{r})$$
$$+\frac{1}{2}\{\mathbf{A}_p\sigma_2(1+\tau_3^{(2)}) + \mathbf{A}_n\sigma_2(1-\tau_3^{(2)})\}\,\delta(\mathbf{r}_2 - \mathbf{r}). \tag{9}$$

For the differential cross section of the reaction $\pi^- + d \rightarrow p + n + \pi^- + \pi^0$ we obtain:

$$d\sigma(\mathbf{k}_1\mathbf{k}_2\mathbf{q}) = \frac{2\pi}{k_0/E_0}\frac{1}{3}\{|I^-|^2(2|\mathbf{A}_p - \mathbf{A}_n|^2 + |\mathbf{A}_p + \mathbf{A}_n|^2)$$
$$+|I^+|^2(2|\mathbf{A}_p + \mathbf{A}_n|^2 + |\mathbf{A}_p - \mathbf{A}_n|^2) \tag{10}$$
$$+(I^{+*}I^-[2(\mathbf{A}_p+\mathbf{A}_n)^*(\mathbf{A}_p-\mathbf{A}_n) + (\mathbf{A}_p-\mathbf{A}_n)^*(\mathbf{A}_p+\mathbf{A}_n)]$$
$$+\text{compl. conj.})\}\,\delta(E_0 - E_f)\frac{d\mathbf{k}_1}{(2\pi)^3}\frac{d\mathbf{k}_2}{(2\pi)^3}\frac{d\mathbf{q}}{(2\pi)^3}.$$

The integrals $I^{\pm}$ of Eq. (10) are given by Eq. (7).

In the case when the reaction goes without deuteron disintegration, i.e., $\pi^- + d \rightarrow d + \pi^- + \pi^0$, the differential cross section is given by the expression

$$d\sigma(\mathbf{k}_1\mathbf{k}_2) = \frac{2\pi}{k_0/E_0}\frac{2}{3}|\mathbf{A}_p + \mathbf{A}_n|^2|I_0|^2$$
$$\delta(E_0 - E_f),\frac{d\mathbf{k}_1}{(2\pi)^3}\frac{d\mathbf{k}_2}{(2\pi)^3}. \tag{11}$$

where

$$I_0 = \int\varphi_0^2(r)\,e^{i\varkappa\mathbf{r}}\,d\mathbf{r}, \tag{12}$$

$$E_0 - E_f = \sqrt{m^2 + k_0^2} - \sqrt{m^2 + k_1^2}$$
$$-\sqrt{m^2 + k_2^2} - \varkappa^2/M. \tag{13}$$

3. Let us determine the differential cross section $d\sigma(\mathbf{k}_1\mathbf{n}_2)$, corresponding to a given momentum of one meson $\mathbf{k}_1$ and to a given angle of emission of the other $\mathbf{n}_2 = \mathbf{k}_2/k_2$ independently from the state of the nucleons produced. For that purpose we shall integrate Eq. (6) and (10) over all possible values of $\mathbf{q}$. The values of $\mathbf{q}$ are determined by the law of conservation of energy [Eq. (8)]. The integration over $d\mathbf{q}$ can be carried out easily taking into account that the integrals of $I^{\pm}$ are markedly different from zero only for a small region of the values of q permitted by the conservation law (8).[1,2]

Taking into account that the functions $\varphi_{\mathbf{q}}^{\pm}(\mathbf{r})$ form a complete system, we obtain, approximately,

$$\int|I^{\pm}|^2\frac{d\mathbf{q}}{(2\pi)^3} = \frac{1}{2}\left(1 \pm \frac{\alpha}{\varkappa}\tan^{-1}\frac{\varkappa}{\alpha}\right). \tag{14}$$

For the differential cross-section $d\sigma(\mathbf{k}_1\mathbf{n}_2)$ for the reaction $\pi + d \rightarrow n + n + \pi' + \pi''$ (two neutrons in the final state) we find

$$d\sigma(\mathbf{k}_1\mathbf{n}_2) = \frac{2\pi}{k_0/E_0}|\mathbf{A}_p|^2\left(1 - \frac{\alpha}{3\varkappa}\tan^{-1}\frac{\varkappa}{\alpha}\right)$$
$$\times(E_0 - E_1)\sqrt{(E_0 - E_1)^2 - m^2}\,\frac{d\mathbf{k}_1}{(2\pi)^3}\frac{d\Omega_2}{(2\pi)^3}. \tag{15}$$

For the reaction $\pi + d \rightarrow p + n + \pi' + \pi''$ (a neutron and a proton are present in the final state) we have:

$$d\sigma(\mathbf{k}_1\mathbf{n}_2) = \frac{2\pi}{k_0/E_0}\Big\{|\mathbf{A}_p|^2 + |\mathbf{A}_n|^2$$
$$+\frac{\alpha}{6\varkappa}\tan^{-1}\frac{\varkappa}{\alpha}(|\mathbf{A}_p + \mathbf{A}_n|^2 - |\mathbf{A}_p - \mathbf{A}_n|^2)\Big\} \tag{16}$$
$$\times(E_0 - E_1)\sqrt{(E_0 - E_1)^2 - m^2}\,\frac{d\mathbf{k}_1}{(2\pi)^3}\frac{d\Omega_2}{(2\pi)^3}.$$

A correction to the differential cross sections (15) and (16) for the existence of deuterons in the D state contributes about 10% to $d\sigma(\mathbf{k}_1\mathbf{n}_2)$ (the correction is less for $\kappa \ll \alpha$ and for large κ).

4. It is easy to show on the basis of the isotopic-invariance hypothesis that the amplitudes A_p and A_n are equal and have opposite signs near the thresholds of the reactions $\pi^- + p \rightarrow p + \pi^- + \pi^0$ and $\pi^- + n \rightarrow n + \pi^- + \pi^0$, as well as in the production of π mesons with equal momentum $\mathbf{k}_1 = \mathbf{k}_2$.

In fact, the initial state is a superposition of states with total isotopic spin T equal to ½ and 3/2. The system of two π mesons can be found in states with total isotopic spin t equal to 0, 1, and 2.

Let us introduce amplitudes A_t^T corresponding to a given value of the isotopic spin of the whole system T and a given value of the isotopic spin of the produced mesons t. For the amplitude of the process of transmutation of one π meson into two π mesons $A(m_1m_2s'; sm)$ we have the following expression

$$A(m_1m_2s';\ sm) = \sum_{T,t}A_t^T C^{Tm+s}_{1m\,{}^1\!/_2 s}\ C^{tm_1+m_2}_{1m_11m_2}C^{Tm+s}_{tm_1+m_2\,{}^1\!/_2 s'}. \tag{17}$$

where $C^{jm}_{j_1m_1j_2m_2}$ are the Clebsch-Gordan coefficients; m, m_1, and m_2 are the projections of the isotopic spin of the incident and of the produced π mesons, and s and s′ are the projections of the isotopic spin of the nucleon in the initial and final state.

The amplitudes $A(m_1m_2s'; sm)$ satisfy the following symmetry relations:

$$A(m_1m_2s';\ sm) = -A(-m_1 - m_2 - s';\ -s - m),$$
$$A(m_1m_2s';\ s0) = -A(m_2m_1 - s';\ -s0). \tag{18}$$

Near the reaction threshold, the π mesons are produced in the s state. Since the wave function of the π meson system would be symmetric with respect to a permutation of the mesons, production of two π mesons with t = 1 is forbidden near the threshold of the reaction $\pi + n \rightarrow n' + \pi' + \pi''$.[3] It follows then from Eq. (17) that

$$A(m_1m_2s,\ sm) = -A(m_1m_2 - s;\ -sm). \tag{19}$$

A similar symmetry relation holds, apart from the reaction threshold, when the two π mesons are produced in course of the considered reactions with identical momentum, $\mathbf{k}_1 = \mathbf{k}_2$.

Taking the above into account we find that the differential cross-section for the reaction $\pi + \mathrm{d} \rightarrow \mathrm{p} + \mathrm{n} + \pi' + \pi''$ for small angles of emission of π ·mesons and equal momenta $\mathbf{k}_1 = \mathbf{k}_2$ can be written in the form

$$d\sigma(\mathbf{k}_1\mathbf{k}_2\mathbf{q}) = \frac{2\pi}{k_0/E_0}\frac{4}{3}|\mathrm{A}_p|^2\{2|I^-|^2 + |I^+|^2\} \times \delta(E_0 - E_f)\frac{d\mathbf{k}_1}{(2\pi)^3}\frac{d\mathbf{k}_2}{(2\pi)^3}\frac{d\mathbf{q}}{(2\pi)^3}. \tag{20}$$

For the same conditions the transmutation reaction of one π meson into two without deuteron disintegration $\pi + \mathrm{d} \rightarrow \mathrm{d} + \pi' + \pi''$ is forbidden.

5. The reactions of photoproduction of π mesons can be treated by an analogous method, using a pseudopotential.[2]

The amplitude of photoproduction of two π mesons should be a scalar. Limiting ourselves to the reactions in which the produced π mesons are emitted at small angles, we shall construct the following scalar expression containing $\mathbf{k}_1$, $\mathbf{k}_2$, σ, and the polarization vector ϵ of the γ quantum:

$$[(a_1\mathbf{k}_1 + a_2\mathbf{k}_2) \times \varepsilon]\sigma, \tag{21}$$

where a_1 and a_2 are invariant functions of the vectors $\mathbf{k}_0$, $\mathbf{k}_1$, and $\mathbf{k}_2$. The expression (21) represents the most general scalar containing $\mathbf{k}_1$, $\mathbf{k}_2$, and σ, and linear with respect to ϵ.

The pseudopotential of photoproduction of two π mesons on a nucleon is given by the expression

$$V = [(a_1\mathbf{k}_1 + a_2\mathbf{k}_2) \times \varepsilon]\sigma\delta(\mathbf{r}_n - \mathbf{r})\tau_n. \tag{22}$$

Since Eq. (22) is analogous to Eq. (1), the formulae for differential cross sections of photoproduction can be obtained directly from the analogous expressions, (3) to (16).

For small angles of emission of π mesons, the momentum of these mesons is approximately perpendicular to the polarization vector ϵ. The cross sections of the studied processes for unpolarized nucleons and deuterons are, therefore, independent of the direction of polarization of the γ quanta.

6. We shall determine now the momentum and angle distributions of nucleons in the deuteron reactions under consideration.

In formulae (6) and (10) for the differential cross sections we eliminated momentum of the center of mass of the system consisting of two nucleons by using the law of conservation of momentum. It is convenient to make use of this law for the elimination of other variables.

We shall determine the momentum distribution function of the nucleons separately for three different specifications of the π-meson variable in the final state.

(a) Let the meson momenta $\mathbf{k}_1$ and $\mathbf{k}_2$ be given. Out of six other variables $\mathbf{p}_1$, and $\mathbf{p}_2$, the three variables of the vector $\mathbf{p}_2$ are eliminated by the momentum-conservation law. The energy-conservation law yields:

$$\sqrt{m^2 + k_0^2} - \sqrt{m^2 + k_1^2} - \sqrt{m^2 + k_2^2} - p_1^2/M - 2\varkappa^2/M + 2\varkappa\mathbf{p}_1/M + \varepsilon = 0. \tag{23}$$

Since $\kappa = (\mathbf{k}_0 - \mathbf{k}_1 - \mathbf{k}_2)/2 = \mathrm{const}$, we shall choose the z axis as the direction of the vector κ and integrate, in the differential cross section, over the angle variables of the vector $\mathbf{p}_1$.

The integration over the azimuth $d\varphi_1$ is carried out from 0 to 2π. The integration over the polar angle $d\vartheta_1$ can be carried out easily thanks to the existence of the energy δ-function.

We finally obtain for the momentum distribution function $W(\mathbf{p}_1, \mathbf{k}_1, \mathbf{k}_2)$ of the nucleons in the reaction $\pi + \mathrm{d} \rightarrow \mathrm{n} + \mathrm{n} + \pi' + \pi''$

$$W(p_1, \mathbf{k}_1\mathbf{k}_2)\,dp_1\,d\mathbf{k}_1\,d\mathbf{k}_2 = \frac{|\mathrm{A}_p|^2}{3k_0/E_0}\frac{M}{(2\pi)^7\varkappa}\{2|I^-|^2 + |I^+|^2\}\,p_1\,dp_1\,d\mathbf{k}_1\,d\mathbf{k}_2. \tag{24}$$

where the integrals $I^{\pm}$ are given by the expressions:

$$I^- = -\sqrt{4\pi\alpha}\left(\frac{1}{\alpha^2 + p_1^2} - \frac{1}{\alpha^2 + 2M\Delta - p_1^2}\right), \tag{25}$$

$$I^+ = \sqrt{4\pi\alpha}\left(\frac{1}{\alpha^2 + p_1^2} + \frac{1}{\alpha^2 + 2M\Delta - p_1^2} + \frac{1 - e^{2i\delta_0}}{2\varkappa\sqrt{M\Delta - \varkappa^2}}\left[\frac{1}{2}\ln\frac{\alpha^2 + (\sqrt{M\Delta - \varkappa^2} - \varkappa)^2}{\alpha^2 + (\sqrt{M\Delta - \varkappa^2} + \varkappa)^2} + i\tan^{-1}\frac{\sqrt{M\Delta - \varkappa^2} + \varkappa}{\alpha} - i\tan^{-1}\frac{\sqrt{M\Delta - \varkappa^2} - \varkappa}{\alpha}\right]\right), \tag{26}$$

$$\Delta = \sqrt{m^2 + k_0^2} - \sqrt{m^2 + k_1^2} - \sqrt{m^2 + k_2^2}. \tag{27}$$

(b) The momentum of one meson $\mathbf{k}_1$ and the direction of emission of the other, $\mathbf{n}_2 = \mathbf{k}_2/\mathrm{k}_2$, are given. The momentum-conservation law yields:

$$\mathbf{k}_0 - \mathbf{k}_1 - \mathbf{n}_2\left[\left(E_0 - E_1 - \frac{p_1^2 + p_2^2}{2M} + \varepsilon\right)^2 - m^2\right]^{1/2} - \mathbf{p}_1 - \mathbf{p}_2 = 0. \tag{28}$$

Integrating over the angle variables ϑ_1, φ_1, ϑ_2, and φ_2 of the vectors $\mathbf{p}_1$ and $\mathbf{p}_2$ we obtain the following expression for the distribution function $W(\mathbf{p}_1\mathbf{p}_2, \mathbf{k}_1\mathbf{n}_2)$:

$$W(p_1 p_2, \mathbf{k}_1 \mathbf{n}_2)\, dp_1\, dp_2\, d\mathbf{k}_1\, d\Omega_{2k} = \frac{|A_p|^2}{3k_0/E_0} \frac{\Delta \sqrt{\Delta^2 - m^2}}{(2\pi)^7 \varkappa}$$
$$\times \{2|I^-|^2 + |I^+|^2\} p_1 p_2\, dp_1\, dp_2\, d\mathbf{k}_1\, d\Omega_{2k}. \qquad (29)$$

where I^- and I^+ are expressed in terms of the variables $\mathbf{p}_1$ and $\mathbf{p}_2$:

$$I^- = -\sqrt{4\pi\alpha}\left(\frac{1}{\alpha^2 + p_1^2} - \frac{1}{\alpha^2 + p_2^2}\right), \qquad (30)$$

$$I^+ = \sqrt{4\pi\alpha}\left(\frac{1}{\alpha^2 + p_1^2} + \frac{1}{\alpha^2 + p_2^2}\right.$$
$$+ \frac{1 - e^{2i\delta_0}}{2q\varkappa}\left[\frac{1}{2} \ln \frac{\alpha^2 + (q - \varkappa)^2}{\alpha^2 + (q + \varkappa)^2}\right.$$
$$\left.\left. + i \tan^{-1}\frac{q + \varkappa}{\alpha} - i \tan^{-1}\frac{q - \varkappa}{\alpha}\right]\right), \qquad (31)$$

where

$$q^2 + \varkappa^2 = {}^1/_2 (p_1^2 + p_2^2), \quad \varkappa = {}^1/_2 |\mathbf{k}_0 - \mathbf{k}_1 - \mathbf{n}_2 \sqrt{\Delta^2 - m^2}|,$$

$$\Delta = E_0 - E_1 - (p_1^2 + p_2^2)/2M + \varepsilon \approx E_0 - E_1.$$

(c) Let the momentum $\mathbf{k}_1$ of one meson be given. It follows from the energy-conversation law that

$$\sqrt{m^2 + k_0^2} - \sqrt{m^2 + k_1^2} - \sqrt{m^2 + (\mathbf{k}_0 - \mathbf{k}_1 - \mathbf{p}_1 - \mathbf{p}_2)^2}$$
$$- (p_1^2 + p_2^2)/2M + \varepsilon = 0. \qquad (32)$$

Taking into account that we deal with reactions in which fast mesons are emitted at small angles, we have, approximately

$$\sqrt{m^2 + k_0^2} - \sqrt{m^2 + k_1^2}$$
$$- \sqrt{m^2 + (\mathbf{k}_0 - \mathbf{k}_1)^2 - 2(\mathbf{k}_0 - \mathbf{k}_1)(\mathbf{p}_1 + \mathbf{p}_2)} = 0. \qquad (33)$$

The integration over the angular variables of the vector $\mathbf{p}_1$ can be carried out easily thanks to the existence of the energy δ-function. Integrating over the angular variables of the vector $\mathbf{p}_2$ we take it into account that the integrals $I^\pm$ depend on these variables through the variables q and κ. Since we have

$$q^2 + \varkappa^2 = {}^1/_2 (p_1^2 + p_2^2),$$

$$\varkappa = (\mathbf{k}_0 - \mathbf{k}_1)(\mathbf{p}_1 + \mathbf{p}_2)/2|\mathbf{k}_0 - \mathbf{k}_1| + O(p^2/k^2),$$

then the integrals $I^\pm$ contain the variables ϑ_1 and ϑ_2 in the form $p_1 \cos\vartheta_1 + p_2 \cos\vartheta_2$ only.

The result of integration of the differential cross-section over $d\vartheta_1$ depends therefore only on p_1 and p_2. The limits of integration over $d\vartheta_2$ are determined by the energy conservation law (33).

Finally, we obtain for the distribution function $W(p_1 p_2, \mathbf{k}_1)$:

$$W(p_1 p_2, \mathbf{k}_1)\, dp_1\, dp_2\, d\mathbf{k}_1 = \frac{2|A_p|^2}{3k_0/E_0} \frac{E_0 - E_1}{(2\pi)^6 |\mathbf{k}_0 - \mathbf{k}_1|}$$
$$\times \{2|I^-|^2 + |I^+|^2\}(p_1 + p_2 - 2\varkappa) p_1 p_2\, dp_1\, dp_2\, d\mathbf{k}_1. \qquad (34)$$

In Eq. (34), $I^\pm$ have their previous meanings [cf. Eqs. (30) and (31)] and

$$\varkappa = \frac{1}{4}\left(|\mathbf{k}_0 - \mathbf{k}_1| - \frac{(E_0 - E_1)^2 - m^2}{|\mathbf{k}_0 - \mathbf{k}_1|}\right).$$

We consider now the angular distribution of nucleons in two cases. In the first we assume that $\mathbf{k}_1$ and $\mathbf{k}_2$ are given, and denote the corresponding distribution function by $W(\vartheta_1, \mathbf{k}_1, \mathbf{k}_2)$. In the second, we assume that $\mathbf{k}_1$ and $\mathbf{n}_2$ are given, and denote the corresponding distribution function by $W(\vartheta_1 \vartheta_2, \mathbf{k}_1 \mathbf{n}_2)$.

(a) Given $\mathbf{k}_1$ and $\mathbf{k}_2$, we express Eq. (6) in terms of $\mathbf{k}_1$, $\mathbf{k}_2$, and p_1. Integrating over dp_1 and $d\varphi_1$, we obtain the distribution function:

$$W(\vartheta_1, \mathbf{k}_1 \mathbf{k}_2) \sin\vartheta_1\, d\vartheta_1\, d\mathbf{k}_1\, d\mathbf{k}_2$$
$$= \frac{|A_p|^2}{3k_0/E_0} \frac{M p_1^2}{(2\pi)^7 (\varkappa^2 \cos^2\vartheta_1 - 2\varkappa^2 + M\Delta)^{1/2}} \qquad (35)$$
$$\times \{2|I^-|^2 + |I^+|^2\} \sin\vartheta_1\, d\vartheta_1\, d\mathbf{k}_1\, d\mathbf{k}_2.$$

where $I^\pm$ are given, as before, by Eqs. (25) and (26), and are expressed in terms of ϑ_1. It follows from Eq. (23) that

$$p_1 = \varkappa \cos\vartheta_1 + \sqrt{\varkappa^2 \cos^2\vartheta_1 - 2\varkappa^2 + M\Delta}. \qquad (36)$$

(c) Given $\mathbf{k}_1$ and $\mathbf{n}_2$, we choose the z axis in direction of the vector $\mathbf{n}_2$. Expressing p_1, p_2, and the azimuth φ_2 of the vector $\mathbf{p}_2$ through the variables k_2, ϑ_1, ϑ_2, φ_1 (using the momentum-conservation law) and integrating over dk_2 we find:

$$W(\vartheta_1 \vartheta_2 \varphi_1, \mathbf{k}_1 \mathbf{n}_2) \sin\vartheta_1 \sin\vartheta_2\, d\vartheta_1\, d\vartheta_2\, d\varphi_1\, d\mathbf{k}_1\, d\Omega_{2k}$$
$$= \frac{2|A_p|^2}{3k_0/E_0} \frac{(E_0 - E_1)\sqrt{(E_0 - E_1)^2 - m^2}}{(2\pi)^8}$$
$$\times \frac{p_1^4 \sin\varphi_1 \sin\vartheta_1 / \sin\varphi_2 \sin^3\vartheta_2}{|[\mathbf{n}_2 \times (\mathbf{k}_0 - \mathbf{k}_1)]| \cos\varphi_2 \cot\vartheta_2 - \mathbf{n}_2(\mathbf{k}_0 - \mathbf{k}_1)} \qquad (37)$$
$$\times \{2|I^-|^2 + |I^+|^2\} \sin\vartheta_1 \sin\vartheta_2\, d\vartheta_1\, d\vartheta_2\, d\varphi_1\, d\mathbf{k}_1\, d\Omega_{2k}.$$

where $I^\pm$ are given by Eqs. (30) and (31) and are expressed in terms of ϑ_1, ϑ_2, and φ_1:

$$p_2 = -p_1 \sin\vartheta_1 \sin\varphi_1 / \sin\vartheta_2 \sin\varphi_2, \qquad (38)$$

$$\mathbf{n}_2(\mathbf{k}_0 - \mathbf{k}_1) - p_1 \cos\vartheta_1$$
$$+ p_1 \sin\vartheta_1 \sin\varphi_1 \cos\vartheta_2 / \sin\vartheta_2 \sin\varphi_2 = 0. \qquad (39)$$

The angle φ_2 is determined by the equation

$$\cot\varphi_2 = \cot\varphi_1 - |[\mathbf{n}_2 \times (\mathbf{k}_0 - \mathbf{k}_1)]| / p_1 \sin\vartheta_1 \sin\varphi_1. \qquad (40)$$

For $[\mathbf{n}_2 \times (\mathbf{k}_0 - \mathbf{k}_1)] = 0$, we have $\varphi_2 = \varphi_1 \pm \pi$. For this condition we find the following distribution function:

$$W(\vartheta_1\vartheta_2, \mathbf{k}_1\mathbf{n}_2)\sin\vartheta_1\sin\vartheta_2\,d\vartheta_1\,d\vartheta_2\,d\mathbf{k}_1\,d\Omega_{2k} = \frac{2\,|\mathbf{A}_p|^2}{3k_0/E_0}\,\frac{(E_0-E_1)\,|\mathbf{k}_0-\mathbf{k}_1|^3\sqrt{(E_0-E_1)^2-m^2}}{(2\pi)^7}\,\{2\,|I^-|^2+|I^+|^2\}$$

$$\times\frac{\sin\vartheta_1\sin\vartheta_2}{(\cos\vartheta_1+\cos\vartheta_2)^4}\sin\vartheta_1\sin\vartheta_2\,d\vartheta_1\,d\vartheta_2\,d\mathbf{k}_1\,d\Omega_{2k}, \qquad (41)$$

$$p_{1,2} = |\mathbf{k}_0-\mathbf{k}_1|\sin\vartheta_{2,1}/(\cos\vartheta_1+\cos\vartheta_2). \qquad (42)$$

The author would like to thank I. M. Shmushkevich for suggesting the present work and for advice in the course of its execution.

---

[1] I. Ia. Pomeranchuk, J. Exptl. Theoret. Phys. (U.S.S.R.) **21**, 1113 (1951); **23**, 129 (1952); V. B. Berestetskii and I. Ia. Pomeranchuk, Dokl. Akad. Nauk SSSR **81**, 1019 (1951).

[2] B. L. Ioffe and I. M. Shmushkevich, Dokl. Akad. Nauk SSSR **82**, 869 (1952).

[3] N. V. Dushin, Dokl. Akad. Nauk SSSR **106**, 977 (1956), Soviet Phys. "Doklady" **1**, 128 (1956).

Translated by H. Kasha
72

SOVIET PHYSICS JETP VOLUME 35(8), NUMBER 2 FEBRUARY, 1959

PHENOMENOLOGICAL THEORY OF SUPERFLUIDITY NEAR THE λ POINT

L. P. PITAEVSKII

Institute for Physical Problems, Academy of Sciences, U.S.S.R.

Submitted to JETP editor, March 12, 1958

J. Exptl. Theoret. Phys. (U.S.S.R.) 35, 408-415 (August, 1958)

A complete set of phenomenological equations is derived to describe the behavior of superfluid helium near the λ point. The normal part of the liquid is described in the usual way, while the superfluid part is described by an "effective" wave function.

In the present work, equations obtained earlier by V. L. Ginzburg and the author to describe the behavior of helium II in the immediate vicinity of the λ point[1] are extended to include the nonstationary case. In contrast with the ordinary hydrodynamics of helium II, in the scheme considered here the density of the superfluid part ρ_s is not assumed a given function of p and T, but is determined from the equations; these equations characterize the approach of ρ_s to its equilibrium value. As in reference 1, the superfluid part of the liquid is described by a complex function $\psi(x, y, z, t) = \eta e^{i\varphi}$ which is so defined that

$$\rho_s = m\,|\psi|^2, \quad \mathbf{v}_s = \frac{\hbar}{m}\nabla\varphi \qquad (1)$$

(m is the mass of the helium atom). This function is introduced to take account of the quantum nature of the effect; its role in this scheme is the same as that of the expansion parameter in the usual theory of second-order phase changes.[2] The helium state is characterized by the density of the liquid ρ, the velocity of the normal part $\mathbf{v}_n$, and the entropy per unit volume S in addition to ψ.

1. BASIC EQUATIONS

In reference 1 an equation was obtained to determine the equilibrium values of ψ for $\mathbf{v}_n = 0$. Here, we first examine the equilibrium condition for the case $\mathbf{v}_n \neq 0$. At low values of the velocities $\mathbf{v}_n$ and $\mathbf{v}_s$, the energy per unit volume of the liquid can be written in the form

$$E = (\rho - m\,|\psi|^2)\frac{\mathbf{v}_n^2}{2} + \frac{\hbar^2}{2m}|\nabla\psi|^2 + \varepsilon(\rho, S, |\psi|^2). \qquad (1.1)$$

This expression is the first term in the energy expansion in terms of the velocity $\mathbf{v}_n$ and the gradient of ψ. Expressing ψ in terms of ρ_s and $\mathbf{v}_s$ we rewrite Eq. (1.1) in the form

$$E = \rho_n \frac{\mathbf{v}_n^2}{2} + \rho_s \frac{\mathbf{v}_s^2}{2} + \varepsilon + \frac{\hbar^2}{8m^2} \frac{(\nabla \rho_s)^2}{\rho_s}; \qquad (1.1a)$$
$$\rho_n = \rho - m|\psi|^2.$$

The first three terms in (1.1a) are the usual energy density, while the last term is a specific quantum energy which can be attributed to the uncertainty principle. The equilibrium condition can be obtained by minimizing (1.1) with respect to ψ^* or ψ. However, this procedure must be carried out for the total momentum $\mathbf{j}$ per unit volume of the liquid; if this procedure were not followed we would also be minimizing the kinetic energy of the liquid as a whole, a quantity which bears no relation to the thermodynamic properties. Thus $\mathbf{v}_n$ is a function of ψ and $\mathbf{j}$. The expression for $\mathbf{j}$ follows immediately from the definition of ψ [Eq. (1)]:

$$\mathbf{j} = (\rho - m|\psi|^2)\mathbf{v}_n + \rho_s \mathbf{v}_s$$
$$= (\rho - m|\psi|^2)\mathbf{v}_n + \frac{i\hbar}{2}(\psi\nabla\psi^* - \psi^*\nabla\psi). \qquad (1.2)$$

We use the Lagrangian-multiplier method to express $\mathbf{v}_n$ in terms of $\mathbf{j}$ and ψ from Eq. (1.2). Multiplying (1.2) by an undetermined multiplier μ and adding the result to (1.1) we obtain the expression

$$(\rho - m|\psi|^2)\frac{\mathbf{v}_n^2}{2} + \frac{\hbar^2}{2m}|\nabla\psi|^2 + \varepsilon$$
$$+ \mu\left\{\mathbf{j} - (\rho - m|\psi|^2)\mathbf{v}_n - \frac{i\hbar}{2}(\psi\nabla\psi^* - \psi^*\nabla\psi)\right\}. \qquad (1.3)$$

Varying (1.3) independently with respect to ψ^* and $\mathbf{v}_n$ (with fixed values of ρ, $\mathbf{j}$, S and ψ), and eliminating μ we obtain the required condition

$$\frac{1}{2}\left(-\frac{i\hbar}{m}\nabla - \mathbf{v}_n\right)^2\psi + \left(\frac{\partial\varepsilon}{\partial\rho_s}\right)_{\rho,\,S}\psi = 0, \qquad (1.4)$$

this expression takes the place of the basic equation in reference 1.

We turn now to the immediate problem, that of deriving a complete system of equations for ψ, $\mathbf{v}_n$, S, and ρ. As is well known,[3,4] in ordinary two-velocity hydrodynamics the equations are determined uniquely by the conservation laws. There is an analogous situation in the present case. In order to simplify the analysis we shall formulate the equations using heuristic reasoning and then demonstrate that these equations do in fact satisfy the conservation laws.

The scheme being developed here is based on the assumption that the state of the system at any instant of time is completely determined by ψ, $\mathbf{v}_n$, ρ, and S. In particular, the derivative $\partial\psi/\partial t$ must also be determined by these quantities at a given time. If the above assumptions are valid the change of ψ with time must be described by a first-order equation which, by analogy with quantum mechanics, can be written in the form

$$i\hbar\,\partial\psi/\partial t = \hat{L}\psi, \qquad (1.5)$$

where $\hat{L}$ is a nonlinear operator which acts on ψ. It will be apparent that the operator $\hat{L}$ cannot be Hermitian. If $\hat{L}$ were Hermitian, it would follow from Eq. (1.5), in the usual way, that

$$\frac{d}{dt}\int|\psi|^2\,dV = \frac{d}{dt}\frac{1}{m}\int\rho_s dV = 0, \qquad (1.6)$$

and we would obtain the usual conservation relation for ρ_s. But Eq. (1.6) cannot hold if we consider relaxation, i.e., the fact that ρ_s is "converted" into ρ_n up to the point at which equilibrium is reached. Thus, the anti-Hermitian part of $\hat{L}$ is associated with the process by which thermodynamic equilibrium is approached; it becomes larger the more rapidly the system relaxes.

As in (1.1) we limit ourselves to the first term in the expansion in the gradient of ψ, writing the Hermitian part of $\hat{L}$ in a form similar to the right-hand side of the Schrödinger equation

$$-(\hbar^2/2m)\,\Delta\psi + U\psi, \qquad (1.7)$$

where the function U will be determined below. At the outset it is convenient to write U in the form

$$U = (\partial\varepsilon/\partial|\psi|^2)_{\rho_n,\,S} - gm$$
$$= (\partial\varepsilon/\partial\rho)_{\rho_s S}\,m + (\partial\varepsilon/\partial\rho_s)_{\rho,S}\,m - gm. \qquad (1.8)$$

Separation of the term containing the derivative $(\partial\epsilon/\partial|\psi|^2)$ corresponds to the physical meaning of this quantity as the "potential energy" of the superfluid part. The quantity g is to be determined from the conservation relation.

As we have already indicated, the anti-Hermitian part of $\hat{L}$ characterizes the approach to equilibrium and must vanish at equilibrium, i.e., when the left-hand side of Eq. (1.4) is zero. Hence, if the deviation from equilibrium is small, the anti-Hermitian part of $\hat{L}$ can be written in the form

$$-i\Lambda\left\{\left(-\frac{i\hbar}{m}\nabla - \mathbf{v}_n\right)^2 m\psi + (\partial\varepsilon/\partial\rho_s)_{\rho,\,S}\,m\psi\right\}. \qquad (1.9)$$

Here Λ is a dimensionless factor which is inversely proportional to the relaxation time.

Finally we obtain the equation for ψ:

$$i\hbar\frac{\partial\psi}{\partial t}=-\frac{\hbar^2}{2m}\Delta\psi+\left\{\left(\frac{\partial\varepsilon}{\partial\rho}\right)_{\rho_s,S}+\left(\frac{\partial\varepsilon}{\partial\rho_s}\right)_{\rho,S}-g\right\}m\psi$$
$$-i\Lambda\left\{\frac{1}{2}\left(-\frac{i\hbar}{m}\nabla-\mathbf{v}_n\right)^2+\left(\frac{\partial\varepsilon}{\partial\rho_s}\right)_{\rho,S}\right\}m\psi. \qquad (1.10)$$

It does not follow from the above reasoning that Λ must be pure real. We assume to begin with that Λ is complex: $\Lambda = \Lambda_1 + i\Lambda_2$. Then, multiplying (1.10) by ψ^* and subtracting the complex conjugate equation, we easily verify that with $\Lambda_2 \neq 0$ part of the superfluid mass is carried with the normal velocity rather than with the superfluid velocity; obviously this contradicts the physical meaning of these quantities. On this basis, which admittedly is not a rigorous one, we take $\Lambda_2 = 0$, i.e., we assume that Λ is real.

In carrying out the calculations it is sometimes useful to write Eq. (1.10) in symbolic form

$$i\hbar\,\partial\psi/\partial t=\hat{A}\psi-i\Lambda\hat{B}\psi \qquad (1.10a)$$

using the properties of $\hat{A}$ and $\hat{B}$:

$$\begin{aligned}\psi^*\hat{A}\psi-\psi\hat{A}^*\psi^*&=-(i\hbar/m)\operatorname{div}\rho_s\mathbf{v}_s,\\ \psi^*\hat{B}\psi-\psi\hat{B}^*\psi^*&=-(i\hbar/m)\operatorname{div}(\mathbf{j}-\rho\mathbf{v}_n).\end{aligned} \qquad (1.11)$$

The present theory must satisfy the conservation laws in addition to Eq. (1.10). The conservation-of-mass relation is of the obvious form

$$\partial\rho/\partial t+\operatorname{div}\mathbf{j}=0, \qquad (1.12)$$

where $\mathbf{j}$ is determined by Eq. (1.2).

In the momentum flux Π_{ik}, which satisfies the conservation law

$$\partial j_i/\partial t+\partial\Pi_{ik}/\partial x_k=0, \qquad (1.13)$$

we can immediately separate the terms

$$\Pi_{ik}=\frac{\hbar^2}{4m^2}\left\{\frac{\partial\psi}{\partial x_i}\frac{\partial\psi^*}{\partial x_k}-\psi\frac{\partial^2\psi^*}{\partial x_i\,\partial x_k}+\text{c.c.}\right\}$$
$$+\rho_n v_{ni}v_{nk}+p\delta_{ik}-\tau_{ik} \qquad (1.14)$$

(p is the pressure and c.c. denotes the complex conjugate of a given expression). The separation of the first term is due to the fact that Eq. (1.10) is analogous to the Schrödinger equation and this term acts as the expression for momentum flux which follows from the usual Schrödinger equation. Here τ_{ik} is a symmetric tensor which is to be determined; it can be given in the form

$$\tau_{ik}=\tau\delta_{ik}+\mu_{ik}, \qquad (1.15)$$

where μ_{ik} is a tensor whose trace is zero ($\mu_{ii}=0$).

We write the entropy equation in the form

$$\partial S/\partial t+\operatorname{div}\{S\mathbf{v}_n-\mathbf{q}\}=R/T. \qquad (1.16)$$

In writing Eq. (1.16) we have used the fact that the entropy is carried with the normal part of the liquid. In Eq. (1.16) $\mathbf{q}$ is the entropy flux, as yet unknown, and R is the dissipation function for the liquid, i.e., the energy dissipation per unit time per unit volume. The problem now is essentially that of choosing the quantities g, τ_{ik}, $\mathbf{q}$ and R in such a way as to satisfy energy conservation. This requirement turns out to be a sufficient condition for the unique determination of all these quantities.

2. EQUATION OF ENERGY CONTINUITY

In view of Eqs. (1.10), (1.12), (1.13), and (1.16), energy conservation requires that the following relations be satisfied identically:

$$\partial E/\partial t+\operatorname{div}\mathbf{Q}=0 \qquad (2.1)$$

($\mathbf{Q}$ is the energy loss vector). Now we differentiate the right-hand side of Eq. (1.1) with respect to time, expressing $\dot{\psi}$, $\dot{\mathbf{v}}_n$, $\dot{\rho}$, and $\dot{S}$ from Eqs. (1.10), (1.12), (1.13), and (1.16) and choosing g, τ_{ik}, $\mathbf{q}$ and R in such a way as to cancel terms which cannot be written in the form of a divergence. Expressing $\mathbf{v}_n$ in Eq. (1.1) in terms of ρ, $\mathbf{j}$, and ψ, and differentiating and collecting terms with derivatives of the same order we have:

$$\frac{\partial E}{\partial t}=\mathbf{v}_n\frac{\partial\mathbf{j}}{\partial t}+\left[\left(\frac{\partial\varepsilon}{\partial\rho}\right)_{S,\psi}-\frac{v_n^2}{2}\right]\frac{\partial\rho}{\partial t}+\left(\frac{\partial\varepsilon}{\partial S}\right)_{\rho_s,\rho}\frac{\partial S}{\partial t}+\left\{\frac{\partial\psi}{\partial t}\left[\left(\frac{\partial\varepsilon}{\partial\rho_s}\right)_{\rho,S}+\frac{v_n^2}{2}-\frac{i\hbar}{2m}\mathbf{v}_n\nabla\right]m\psi^*+\left(\frac{\hbar^2}{2m}\nabla\psi^*+\frac{i\hbar}{2}\psi^*\mathbf{v}_n\right)\frac{\partial\nabla\psi}{\partial t}+\text{c.c.}\right\}. \qquad (2.2)$$

Assuming that $\partial\epsilon/\partial S = T$ and substituting the time derivatives of the equations, and after some lengthy calculations which are carried out most conveniently in symbolic form (1.10a), we finally obtain from (1.11):

$$\frac{\partial E}{\partial t}+\operatorname{div}\mathbf{Q}=\mathbf{v}_n\left(S\nabla T+\rho\nabla\frac{\partial\varepsilon}{\partial\rho}+\rho_s\nabla\frac{\partial\varepsilon}{\partial\rho_s}-\nabla p\right)+R-\frac{2\Lambda}{\hbar}|\hat{B}\psi|^2-\tau\operatorname{div}\mathbf{v}_n-g\operatorname{div}(\mathbf{j}-\rho\mathbf{v}_n)-\mathbf{q}\nabla T$$
$$-\frac{1}{2}\mu_{ik}\left(\frac{\partial v_{ni}}{\partial x_k}+\frac{\partial v_{nk}}{\partial x_i}-\frac{2}{3}\delta_{ik}\operatorname{div}\mathbf{v}_n\right), \qquad (2.3)$$

where

$$Q_i = \left(\frac{i\hbar}{2m}\frac{\partial\psi^*}{\partial x_i}\hat{A}\psi + \frac{\Lambda\hbar}{2m}\frac{\partial\psi^*}{\partial x_i}\hat{B}\psi + \text{c.c.}\right) + \left[TS + \frac{1}{2}\rho_n v_n^2 + \left(\frac{\partial\varepsilon}{\partial\rho}\right)_{S,\psi}\rho_n - \tau + \rho_s g + \frac{\hbar\Lambda}{2m}\operatorname{div}(\mathbf{j} - \rho\mathbf{v}_n)\right] v_{ni} - Tq_i - v_{nk}\mu_{ik}. \tag{2.4}$$

In order to satisfy energy conservation, the right-hand side of Eq. (2.3) must vanish. Then Q is the energy loss vector. Setting the right-hand side of Eq. (2.3) equal to zero, we first obtain an expression for the pressure in terms of the variables ρ, S and ρ_s (it is assumed that the pressure can be determined in terms of the thermodynamic variables without their coordinate derivatives).

$$\nabla p = \rho\nabla\left(\frac{\partial\varepsilon}{\partial\rho}\right)_{\rho_s,S} + S\nabla T + \rho_s\nabla\left(\frac{\partial\varepsilon}{\partial\rho_s}\right)_{\rho,S} = \nabla\left[\rho\left(\frac{\partial\varepsilon}{\partial\rho}\right)_{\rho_s,S} + \rho_s\left(\frac{\partial\varepsilon}{\partial\rho_s}\right)_{\rho,S} + TS - \varepsilon\right]. \tag{2.5}$$

Thus

$$p = -\varepsilon + TS + \rho\left(\frac{\partial\varepsilon}{\partial\rho}\right)_{\rho_s,S} + \rho_s\left(\frac{\partial\varepsilon}{\partial\rho_s}\right)_{\rho,S}. \tag{2.6}$$

Further, for R we find:

$$\begin{aligned} R &= \frac{2\Lambda}{\hbar}|\hat{B}\psi|^2 + \mathbf{q}\nabla T + \frac{1}{2}\mu_{ik}\left(\frac{\partial v_{ni}}{\partial x_k} + \frac{\partial v_{nk}}{\partial x_i} - \frac{2}{3}\delta_{ik}\operatorname{div}\mathbf{v}_n\right) + \tau\operatorname{div}\mathbf{v}_n + g\operatorname{div}(\mathbf{j} - \rho\mathbf{v}_n) \\ &= \frac{\Lambda}{2\hbar|\psi|^2}(\psi^*\hat{B}\psi + \psi\hat{B}^*\psi^*)^2 + \mathbf{q}\nabla T + \frac{1}{2}\mu_{ik}\left(\frac{\partial v_{ni}}{\partial x_k} + \frac{\partial v_{nk}}{\partial x_i} - \frac{2}{3}\delta_{ik}\operatorname{div}\mathbf{v}_n\right) + \tau\operatorname{div}\mathbf{v}_n + \left[\frac{\Lambda\hbar}{2m^2|\psi|^2}\operatorname{div}(\mathbf{j} - \rho\mathbf{v}_n) + g\right]\operatorname{div}(\mathbf{j} - \rho\mathbf{v}_n). \end{aligned} \tag{2.7}$$

Reasoning as in reference 5, we see that in small deviations from the equilibrium state the following equality must be satisfied when R is quadratic in the velocity derivatives and thermodynamic variables:

$$\mathbf{q} = \frac{\varkappa}{T}\nabla T, \quad \mu_{ik} = \eta\left(\frac{\partial v_{ni}}{\partial x_k} + \frac{\partial v_{nk}}{\partial x_i} - \frac{2}{3}\delta_{ik}\operatorname{div}\mathbf{v}_n\right). \tag{2.8}$$

It is apparent from Eq. (2.7) that τ and g contain those terms with the second viscosities of helium which are not related to the relaxation ρ_s. However, close to the λ point the relaxation of ρ_s makes the chief contribution in the second viscosities. Hence, terms with τ and g are set equal to zero.

It is obvious that κ is the thermal conductivity and η is the first viscosity of the normal part.

We now have the final system of equations (the extremely complicated expression for Q is not of general interest and is not given here):

$$i\hbar\frac{\partial\psi}{\partial t} = -\frac{\hbar^2}{2m}\Delta\psi + \left[\left(\frac{\partial\varepsilon}{\partial\rho}\right)_{\rho_s,S} + \left(\frac{\partial\varepsilon}{\partial\rho_s}\right)_{\rho,S}\right]m\psi - i\Lambda\left[\frac{1}{2}\left(-\frac{i\hbar}{m}\nabla - \mathbf{v}_n\right)^2 + \left(\frac{\partial\varepsilon}{\partial\rho_s}\right)_{\rho,S}\right]m\psi; \tag{2.9}$$

$$\frac{\partial\rho}{\partial t} + \operatorname{div}(\rho - m|\psi|^2)\mathbf{v}_n + \frac{i\hbar}{2}(\psi\Delta\psi^* - \psi^*\Delta\psi) = 0; \tag{2.10}$$

$$\begin{aligned} \frac{\partial}{\partial t}\left\{(\rho - m|\psi|^2)v_{ni} + \frac{i\hbar}{2}\left(\psi\frac{\partial\psi^*}{\partial x_i} - \psi^*\frac{\partial\psi}{\partial x_i}\right)\right\} = -\frac{\partial}{\partial x_k}\Big\{(\rho - m|\psi|^2 v_{ni}v_{nk} + \frac{\hbar^2}{2m}\left(\frac{\partial\psi}{\partial x_i}\frac{\partial\psi^*}{\partial x_k} - \psi\frac{\partial^2\psi^*}{\partial x_i\partial x_k} + \text{c.c.}\right) \\ + p\delta_{ik} - \eta\left(\frac{\partial v_{ni}}{\partial x_k} + \frac{\partial v_{nk}}{\partial x_i} - \frac{2}{3}\delta_{ik}\operatorname{div}\mathbf{v}_n\right)\Big\}; \end{aligned} \tag{2.11}$$

$$\frac{\partial S}{\partial t} + \operatorname{div}(S\mathbf{v}_n) = \frac{1}{T}\operatorname{div}(\varkappa\nabla T) + \frac{1}{T}\left\{\frac{2\Lambda}{\hbar}\left|\left[\frac{1}{2}\left(-\frac{i\hbar}{m}\nabla - \mathbf{v}_n\right)^2 + \left(\frac{\partial\varepsilon}{\partial\rho_s}\right)_{\rho,S}\right]m\psi\right|^2 + \frac{1}{2}\eta\left(\frac{\partial v_{ni}}{\partial x_k} + \frac{\partial v_{nk}}{\partial x_i} - \frac{2}{3}\delta_{ik}\operatorname{div}\mathbf{v}_n\right)^2\right\}. \tag{2.12}$$

Making use of Eq. (2.9) we can write Eq. (2.11) in another somewhat more convenient form:

$$\frac{\partial\rho_n v_{ni}}{\partial t} + i\Lambda\left\{\frac{\partial\psi}{\partial x_i}\hat{B}^*\psi^* - \text{c.c.}\right\} + v_{ni}\operatorname{div}(\rho_n\mathbf{v}_n) + \rho_n(\mathbf{v}_n\nabla)v_{ni} + \frac{\partial}{\partial x_k}\left\{p\delta_{ik} - \eta\left(\frac{\partial v_{ni}}{\partial x_k} + \frac{\partial v_{nk}}{\partial x_i} - \frac{2}{3}\delta_{ik}\operatorname{div}\mathbf{v}_n\right)\right\}. \tag{2.11a}$$

3. CASES IN WHICH THE GRADIENT OF ρ_S IS SMALL

We now consider the equations in the limit of a small gradient for ρ_S, in which case the quantum energy terms in Eq. (1.1a) are small. Again we replace the operators $-(i\hbar/m)\nabla$ (which act on ψ in $\hat{L}\psi$), Π_{ik} and j by $\mathbf{v}_S$. Making this substitution and applying the gradient operator to (2.9), from we have Eqs. (2.9) to (2.12)

$$\mathbf{v}_s + \nabla\left\{\frac{v_s^2}{2} + \left(\frac{\partial\varepsilon}{\partial\rho}\right)_{\rho_s,\,S} + \left(\frac{\partial\varepsilon}{\partial\rho_s}\right)_{\rho,S} - \frac{\hbar\Lambda}{2m\rho_s}\operatorname{div}\rho_s(\mathbf{v}_s-\mathbf{v}_n)\right\} = 0; \tag{3.1}$$

$$\partial\rho/\partial t + \operatorname{div}(\rho_s\mathbf{v}_s + \rho_n\mathbf{v}_n) = 0; \tag{3.2}$$

$$\frac{\partial}{\partial t}(\rho_n v_{ni} + \rho_s v_{si}) + \frac{\partial}{\partial x_k}\left\{\rho_n v_{ni} v_{nk} + \rho_s v_{si} v_{sk} + p\delta_{ik} - \eta\left(\frac{\partial v_{ni}}{\partial x_k} + \frac{\partial v_{nk}}{\partial x_i} - \frac{2}{3}\delta_{ik}\operatorname{div}\mathbf{v}_n\right)\right\} = 0; \tag{3.3}$$

$$\begin{aligned}\frac{\partial S}{\partial t} + \operatorname{div}(S\mathbf{v}_n) &= \frac{1}{T}\operatorname{div}(\varkappa\nabla T) + \frac{1}{T}\left\{\frac{\hbar\Lambda}{2m\rho_s}[\operatorname{div}\rho_s(\mathbf{v}_s-\mathbf{v}_n)]^2\right.\\ &\left.+ \frac{2\Lambda m}{\hbar}\left[\frac{1}{2}(\mathbf{v}_s-\mathbf{v}_n)^2 + \left(\frac{\partial\varepsilon}{\partial\rho_s}\right)_{\rho,\,S}\right]^2\rho_s + \frac{\eta}{2}\left(\frac{\partial v_{ni}}{\partial x_k} + \frac{\partial v_{nk}}{\partial x_i} - \frac{2}{3}\delta_{ik}\operatorname{div}\mathbf{v}_n\right)^2\right\};\end{aligned} \tag{3.4}$$

$$\frac{\partial\rho_s}{\partial t} + \operatorname{div}\rho_s\mathbf{v}_s = -\frac{\Lambda m}{2\hbar}\left\{\frac{(\mathbf{v}_n-\mathbf{v}_s)^2}{2} + \left(\frac{\partial\varepsilon}{\partial\rho_s}\right)_{\rho,\,S}\right\}\rho_s. \tag{3.5}$$

Formally Eqs. (3.1) to (3.4) are similar to the usual equations for the hydrodynamics of the superfluid liquid, in which the role of the chemical potential is played by the quantity

$$(\partial\varepsilon/\partial\rho)_{\rho_s,\,S} + (\partial\varepsilon/\partial\rho_s)_{\rho,S},$$

with this difference, that the density ρ_s is not given in these equations. This density is taken as an unknown quantity whose approach to its equilibrium value is described by the auxiliary equation (3.5).

In order to find the parameter Λ we make a brief analysis of the propagation of sound in helium II near the λ point. (The absorption of first sound near the λ point has been computed by Landau and Khalatnikov.[6]) Linearizing Eqs. (3.1) to (3.5) and eliminating ρ_s from the first three equations, we arrive at the usual equation for the propagation of sound in a superfluid. In this case the second viscosities, which are responsible for the absorption of sound, are expressed in terms of Λ (the definition of the coefficients ζ are those used by Khalatnikov[7]):

$$\zeta_1 = \zeta_4 = \frac{2\hbar}{\Lambda m}\frac{\rho}{\rho_s}\frac{\left(\frac{1}{\rho}\frac{\partial\rho}{\partial T}\right)_p\left(\frac{1}{\rho}\frac{\partial\rho_s}{\partial T}\right)_p - \left(\frac{\partial\rho_s}{\partial p}\right)_T\frac{c_p}{T}}{\left(\frac{\partial\rho}{\partial p}\right)_T\frac{c_p}{T} - \left(\frac{1}{\rho}\frac{\partial\rho}{\partial T}\right)_p^2}\left\{1 + \frac{\left(\frac{1}{\rho}\frac{\partial\rho_s}{\partial T}\right)_p\left(\frac{1}{\rho}\frac{\partial\rho}{\partial T}\right)_p - \frac{c_p}{T}\left(\frac{\partial\rho_s}{\partial p}\right)_T + \sigma\left(\frac{1}{\rho}\frac{\partial\rho_s}{\partial T}\right)_p\left(\frac{\partial\rho}{\partial p}\right)_T - \sigma\left(\frac{1}{\rho}\frac{\partial\rho}{\partial T}\right)_p\left(\frac{\partial\rho_s}{\partial p}\right)_T}{\left(\frac{\partial\rho}{\partial p}\right)_T\frac{c_p}{T} - \frac{1}{\rho^2}\left(\frac{\partial\rho}{\partial T}\right)_p^2}\right\}; \tag{3.6}$$

$$\zeta_2 = \frac{2\hbar}{\Lambda m\rho_s}\rho^2\left[\frac{\frac{1}{\rho}\left(\frac{\partial\rho}{\partial T}\right)_p\frac{1}{\rho}\left(\frac{\partial\rho_s}{\partial T}\right)_p - \left(\frac{\partial\rho_s}{\partial p}\right)_T\frac{c_p}{T}}{\left(\frac{\partial\rho}{\partial p}\right)_T\frac{c_p}{T} - \frac{1}{\rho^2}\left(\frac{\partial\rho}{\partial T}\right)_p^2}\right]^2; \tag{3.7}$$

$$\zeta_3 = \frac{\hbar\Lambda}{2m\rho_s}\left\{1 + \frac{4}{\Lambda^2}\right.\left[\frac{\frac{1}{\rho}\left(\frac{\partial\rho_s}{\partial T}\right)_p\frac{1}{\rho}\left(\frac{\partial\rho}{\partial T}\right)_p - \frac{c_p}{T}\left(\frac{\partial\rho_s}{\partial p}\right)_T + \sigma\frac{1}{\rho}\left(\frac{\partial\rho_s}{\partial T}\right)_p\left(\frac{\partial\rho}{\partial p}\right)_T - \sigma\frac{1}{\rho}\left(\frac{\partial\rho}{\partial T}\right)_p\left(\frac{\partial\rho_s}{\partial p}\right)_T}{\left(\frac{\partial\rho}{\partial p}\right)_T\frac{c_p}{T} - \frac{1}{\rho^2}\left(\frac{\partial\rho}{\partial T}\right)_p^2} + 1\right]^2. \tag{3.8}$$

(In these expressions $\sigma = S/\rho$.)

For simplicity we limit ourselves to the low-frequency case, which is of practical interest; at low frequencies the dispersion properties of the coefficients ζ can be neglected.

The absorption coefficients for first sound and second sound are expressed in terms of ζ_1, ζ_2 and ζ_3, the first viscosity and thermal conductivity. In the absorption coefficient for first sound, only the term containing ζ_2 increases without limit as the λ point is approached. In the absorption coefficients for second sound, however, the terms containing ζ_1, ζ_2, ζ_3 and κ all increase.

Comparing the computed value of the absorption coefficient for first sound

$$\alpha = (\omega^2/2\rho u_1^3)\zeta_2 \tag{3.9}$$

(u_1 is the velocity of first sound) with the measured value,[8] it is possible to determine Λ. The derivative $(\partial\rho_s/\partial p)_T$ which appears in Eq. (3.7) can be found from the pressure dependence of the temperature of the λ point. Differentiating ρ_s along the λ line, we have

$$(\partial\rho_s/\partial p)_T = -(\partial\rho_s/dT)_p dT_\lambda/dp. \tag{3.10}$$

The calculations yield a value of approximately 15 for Λ.

In order to carry out the analysis, the function $\epsilon(\rho, S, \rho_s)$ must be known. It is determined from the experimental data on the specific heat of helium and the density of the superfluid component as functions of temperature and pressure in the vicinity of the λ point.

The equations which have been obtained apply only for temperatures such that $T_\lambda - T \ll T_\lambda$, exactly as is the case for the equations obtained in reference 1.

The most interesting application of the system being described appears in processes which take place in the presence of vortices in which high gradients of ρ_s exist. Under these conditions the quantum terms in the equations turn out to be important. The equations which have been derived make it possible to compute the coefficients B and B^1 of Hall and Vinen[9] because of friction between the superfluid part and the normal part in the presence of a vortex; it is proposed to carry out this calculation in a subsequent paper.

In conclusion the authors wish to express their gratitude to L. D. Landau and V. L. Ginzburg for help and advice in the course of this work.

---

[1] V. L. Ginzburg and L. P. Pitaevskii, J. Exptl. Theoret. Phys. (U.S.S.R.) **34**, 1240 (1958), Soviet Phys. JETP **7**, 858 (1958).

[2] L. D. Landau and E. M. Lifshitz, Статистическая физика (Statistical Physics) Gostekhizdat (1951) Chapter XIV.

[3] L. D. Landau and E. M. Lifshitz, Механика сплошных сред (Mechanics of Continuous Media) 2nd edition, Gostekhizdat (1954) Chapter XVI.

[4] I. M. Khalatnikov, Usp. Fiz. Nau, **60**, 69 (1956).

[5] I. M. Khalatnikov, J. Exptl. Theoret. Phys. (U.S.S.R.) **23**, 265 (1952).

[6] L. D. Landau and I. M. Khalatnikov, Dokl. Akad. Nauk SSSR, **96**, 469 (1954).

[7] I. M. Khalatnikov, J. Exptl. Theoret. Phys. (U.S.S.R.) **23**, 8 (1952).

[8] C. E. Chase, Proc. Roy. Soc. (London) **220A**, 116 (1953).

[9] H. E. Hall and W. F. Vinen, Proc. Roy. Soc. (London) **238A**, 204 (1956).

Translated by H. Lashinsky
73

SOVIET PHYSICS JETP VOLUME 35(8), NUMBER 2 FEBRUARY, 1959

THE SPECTRAL REPRESENTATION OF THE TWO-MESON GREEN'S FUNCTION

V. N. GRIBOV

Leningrad Physico-Technical Institute, Academy of Sciences, U.S.S.R.

Submitted to JETP editor March 13, 1958

J. Exptl. Theoret. Phys. (U.S.S.R.) **35**, 416-427 (August, 1958)

A spectral representation has been found for the two-meson Green's function which is analogous to that found earlier[1-3] for the vertex part. The analytic properties of this function are examined. It follows from the representations that dispersion relations exist for the scattering amplitude for a fixed scattering angle in the center-of-mass system. These relations are obtained and discussed.

1. INTRODUCTION

IN a previous paper by the writer[3] the causality conditions were used to obtain the spectral representation of the vacuum expectation value of the T-product of three Heisenberg operators. In the present paper this same method is used to obtain the spectral representation of the vacuum expectation value of the T-product of four operators, i.e., for the two-particle Green's function. In order not to encumber the discussion with elaborate computations associated with the spinor character of the meson-nucleon Green's function and its possession of poles, we shall confine ourselves in this paper to the derivation of the spectral representation for the two-meson Green's function and the study of the analytical properties of the meson-meson scattering amplitude.

From the spectral representation it follows that the scattering amplitude is an analytic function in the upper half-plane and has no essential singularity at infinity, not only for a fixed preassigned momentum, but also for a fixed scattering angle in the center-of-mass system. Owing to this, it is possible to write dispersion relations for a fixed value of the scattering angle. These relations are written out, but they contain the scattering amplitude in the region of imaginary angles. Analytic continuation into this region by means of expansion in Legendre polynomials is evidently impossible.

2. THE SPECTRAL REPRESENTATION FOR $<| Tj_i(x_1) j_j(x_2) j_k(x_3) j_l(x_4) | >$

Let us consider the symmetrical pseudoscalar meson theory. In this theory one ordinarily takes the two-meson Green's function to mean the expression

$$\langle | T\varphi_i(x_1)\varphi_j(x_2)\varphi_k(x_3)\varphi_l(x_4)|\rangle,$$

with terms corresponding to unconnected diagrams removed. The ψ_i are meson field operators, which can be taken to be Hermitian. This quantity, however, does not occur directly in the scattering amplitude, and it contains singularities not related to the interaction of the mesons. A more interesting quantity, with its Fourier components proportional to the matrix elements of the S matrix is (cf. reference 4)

$$K_1 K_2 K_3 K_4 \langle | T\varphi_i(x_1)\varphi_j(x_2)\varphi_k(x_3)\varphi_l(x_4)|\rangle = \tau_{ijkl}(x_1, x_2, x_3, x_4), \qquad K_1 = \Box_1 - \mu^2. \tag{1}$$

The differentiations in this expression are easily performed if we use the formula

$$\begin{aligned} K_1 \langle | T\varphi_i(x_1) A(x_2) B(x_3) C(x_4)|\rangle &= \langle | Tj_i(x_1) A(x_2) B(x_3) C(x_4)|\rangle \\ + \delta(t_1 - t_2)\langle | T[\varphi_i(x_1) A(x_2)] B(x_3) C(x_4)\rangle &+ (2 \to 3) + (2 \to 4), \qquad j_i(x_1) = K_1\varphi_i(x_1), \end{aligned} \tag{2}$$

for which the proof is simple if we use the fact that the operators commute on a space-like surface. Here A, B, C are arbitrary operators.

Using Eq. (2) and dropping terms that are of the form $f_1(x_1 - x_2) \cdot f_2(x_3 - x_4)$ (these correspond to unconnected diagrams and make no contribution to the scattering amplitude), we get after simple calculations:

$$K_1 K_2 K_3 K_4 \langle | T\varphi_i(x_1)\varphi_j(x_2)\varphi_k(x_3)\varphi_l(x_4)|\rangle = \langle | Tj_i(x_1) j_j(x_2) j_k(x_3) j_l(x_4)|\rangle + \ldots . \tag{3}$$

The terms not written out here are given in detail in Appendix I and correspond to diagrams in which two, three, or four external meson lines emerge from a single point. All these terms can be expressed in terms of vacuum expectation values of two or three operators for which the spectral representations are known. We note that they are all equal to zero if there is no contact interaction of the mesons described by a term $\lambda\varphi_i\varphi_k\varphi_k$ in the current j_i.

We assume that terms corresponding to the mass renormalization and a term $\lambda\varphi^4$ are introduced into the Hamiltonian, but the multiplicative renormalization is carried out only in the final result.

We note that the essential part of all the following does not depend on the explicit form of the interaction.

To establish the spectral representation for $<| Tj_i(x_1) j_j(x_2) \cdot j_k(x_3) j_l(x_4) | >$ we first consider, as in reference 3, the simple product:

$$\begin{aligned} \langle | j_k(x_1) j_j(x_2) j_k(x_3) j_l(x_4)|\rangle &= \int d^4p_1\, d^4p_4\, d^4p \exp\{ip_1(x_1 - x_2) + ip(x_2 - x_3) \\ &+ ip_4(x_3 - x_4)\}\, \vartheta(p_{10})\,\vartheta(p_{40})\,\vartheta(p_0) \sum (j_i)_{0p_1}(j_j)_{p_1p}(j_k)_{pp_4}(j_l)_{p_40}, \qquad (j_j)_{p_1p} = \langle p_1 | j_j(0) | p\rangle. \end{aligned} \tag{4}$$

The summation is taken over all states with given p_1, p, p_4. In virtue of the properties of the operators $j_i(x)$ the smallest possible values of $-p_1^2$ and $-p_4^2$ correspond to three-meson states, and the four-dimensional momentum p can correspond either to the vacuum state or to states beginning with the two meson states. To the vacuum state there corresponds the term in Eq. (4)

$$\delta(p)\left[\sum (j_i)_{0p_1}(j_j)_{p_10}\right]\left[\sum (j_k)_{0p_4}(j_l)_{p_40}\right].$$

For what follows it is convenient to split off this term and consider it separately. Individually, however, this term does not satisfy the causality condition (that the operators commute on a space-like surface). Therefore we also separate from Eq. (4) a number of further terms, which will satisfy the causality condition together with the above term. If we imagine the operators $j_i(x_1)$, $j_j(x_2)$, $j_k(x_3)$, and $j_l(x_4)$ expanded in terms of creation and annihilation operators, then the term that has been written out corresponds to those terms of Eq. (4) in which the creation and annihilation operators of $j_i(x_1)$ are contracted completely with corresponding operators of $j_j(x_2)$ and are not contracted with any others. There also exist other terms in which the operators of $j_i(x_1)$ are contracted only with operators of $j_k(x_3)$, or only with those of $j_l(x_4)$. They contain the respective factors $\delta(p - p_1 - p_4)$ and $\delta(p_1 - p_4)$. Separating out these terms also, we can write:

$$\sum (j_i)_{0p_1} (j_j)_{p_1p} (j_k)_{pp_4} (j_l)_{p_40} = \frac{\delta(p)}{(2\pi)^6} \rho_{ij}(-p_1^2) \rho_{kl}(-p_4^2) + \frac{\delta(p - p_1 - p_4)}{(2\pi)^6} \rho_{ik}(-p_1^2) \rho_{jl}(-p_4^2) + \frac{\delta(p_1 - p_4)}{(2\pi)^6} \rho_{il}(-p_1^2) \rho_{jk}(-p^2)$$
$$+ \frac{1}{(2\pi)^{18}} \rho_{ijlk}(p_1^2, p^2, p_4^2, (p_1 - p)^2, (p_1 - p_4)^2, (p -- p_4)^2); \qquad \rho_{ij}(-k^2) = (2\pi)^{-3} \sum (j_i)_{0k} (j_j)_{k0}. \tag{5}$$

After the vacuum state has been separated out, the smallest value of $-p^2$ belongs to a two-meson state, and consequently

$$\rho_{ijlk}(p_1^2, p^2, p_4^2, (p - p_1)^2, (p_1 - p_4)^2, (p - p_4)^2) = 0,$$

if one of the inequalities

$$-p_1^2 < 9\mu^2, \qquad -p_4^2 < 9\mu^2, \qquad -p^2 < 4\mu^2. \tag{6}$$

is satisfied. Substituting Eq. (5) into Eq. (4), and Eq. (4) into the causality condition, written in the form (for example for $x_{12}^2 > 0$)

$$\langle | j_i(x_1) j_j(x_2) j_k(x_3) j_l(x_4) | \rangle = \langle | j_j(x_2) j_i(x_1) j_k(x_3) j_l(x_4) | \rangle, \tag{7}$$

one can easily show that the terms that have been separated out satisfy this condition automatically. In addition they make no contribution to the scattering amplitude (they correspond to unconnected diagrams), and therefore they can be omitted from the further treatment.

In order to satisfy the causality condition, in analogy with reference 3 we shall write $\rho_{ijlk}(p_1^2, p^2, p_4^2, (p_1 - p)^2, (p_1 - p_4)^2, (p - p_4)^2)$ in the form:

$$\rho_{ijlk}(p_1, p, p_4) = \int \vartheta(k_{12}) \vartheta(k_{13}) \vartheta(k_{14}) \vartheta(k_{23}) \vartheta(k_{24}) \vartheta(k_{34}) \; f_{ijlk}(-k_{12}^2, -k_{13}^2, \ldots -k_{34}^2) \delta(p_1 - k_{12} - k_{13} - k_{14})$$
$$\times \delta(p - k_{13} - k_{14} - k_{23} - k_{24}) \delta(p_4 - k_{14} - k_{24} - k_{34}) (dk); \qquad \vartheta(k) = \begin{cases} 1 & k_0 > 0 \\ 0 & k_0 < 0, \end{cases} \tag{8}$$

regarding this relation as an equation with respect to $f_{ijlk}(-k_{12}^2, -k_{13}^2, \ldots, -k_{34}^2)$. From the invariance of ρ_{ijlk} it follows that $f_{ijlk} = 0$ if any one of its arguments is smaller than zero (if $k_{12}^2 > 0$, then $\vartheta(k_{12})$ is a noninvariant quantity).

We shall not carry out a detailed analysis of the equation (8), as was done at the corresponding point in the argument of reference 3, but we shall assume that it has a solution. We remark only that if we write Eq. (8) in the form

$$\rho_{ijlk}(p_1, p, p_4) = \int_0^\infty \cdots \int_0^\infty d\varkappa_{12}^2 \ldots d\varkappa_{34}^2 K(p_1, p, p_4; \varkappa_{12}^2 \ldots \varkappa_{34}^2) f_{ijlk}(\varkappa_{12}^2, \varkappa_{13}^2 \ldots \varkappa_{34}^2);$$
$$K(p_1, p, p_4; \varkappa_{12}^2, \varkappa_{13}^2 \ldots \varkappa_{34}^2) = \int \vartheta(k_{12}) \delta(k_{12}^2 + \varkappa_{12}^2) \vartheta(k_{13}) \delta(k_{13}^2 + \varkappa_{13}^2) \ldots \tag{9}$$
$$\ldots \vartheta(k_{34}) \delta(k_{34}^2 + \varkappa_{34}^2) \delta(p_1 - k_{12} - k_{13} - k_{14}) \delta(p - k_{13} - k_{14} - k_{23} - k_{24}) \delta(p_4 - k_{14} - k_{24} - k_{34}) (dk),$$

then it is easy to see that $K(p_1, p, p_4, \kappa_{12}^2 \ldots \kappa_{34}^2) \neq 0$ only if

$$-p_1^2 \geqslant (\varkappa_{12} + \varkappa_{13} + \varkappa_{14})^2; \; -p_4^2 \geqslant (\varkappa_{14} + \varkappa_{24} + \varkappa_{34})^2, \qquad -p_1^2 \geqslant (\varkappa_{13} + \varkappa_{14} + \varkappa_{23} + \varkappa_{24})^2. \tag{10}$$

In order that the function $\rho_{ijlk}(p_1, p, p_4)$ automatically satisfy the conditions (6), we set, as in reference 3,

$$f_{ijlk}(\varkappa_{12}^2, \varkappa_{13}^2, \ldots \varkappa_{34}^2) = 0,$$

whenever even a single one of the conditions

$$\varkappa_{12} + \varkappa_{13} + \varkappa_{14} \geqslant 3\mu; \; \varkappa_{13} + \varkappa_{14} + \varkappa_{23} + \varkappa_{24} \geqslant 2\mu; \; \varkappa_{14} + \varkappa_{24} + \varkappa_{34} \geqslant 3\mu; \tag{11}$$

is not satisfied.

Substituting Eq. (9) into Eq. (5) and then into Eq. (4), we get:

$$\langle | j_i(x_1) j_j(x_2) j_l(x_3) j_k(x_4) | \rangle = \int_0^\infty \cdots \int_0^\infty d\varkappa_{12}^2 \ldots d\varkappa_{34}^2 \Delta^+(x_{12}, \varkappa_{12}) \ldots \Delta^+(x_{34}, \varkappa_{34}) \; f_{ijlk}(\varkappa_{12}^2, \varkappa_{13}^2 \ldots \varkappa_{34}^2);$$
$$\Delta^+(x_{12}, \varkappa_{12}) = (2\pi)^{-3} \int d^4k e^{ikx_{12}} \delta(k^2 + \varkappa_{12}^2) \vartheta(k). \tag{12}$$

Substituting Eq. (12) into the causality condition (7) and using the fact that $\Delta^+(x, \kappa) = \Delta^+(-x, \kappa)$ for $x^2 > 0$, we get

$$\int_0^\infty \cdot\cdot \int_0^\infty d\varkappa_{12}^2 \ldots d\varkappa_{34}^2 \Delta^+(x_{12}, \varkappa_{12}) \ldots \Delta^+(x_{34}, \varkappa_{34}) \, f_{ijlk}(\varkappa_{12}^2, \varkappa_{13}^2, \varkappa_{14}^2, \varkappa_{23}^2, \varkappa_{24}^2, \varkappa_{34}^2) - f_{jilk}(\varkappa_{12}^2, \varkappa_{23}^2, \varkappa_{24}^2, \varkappa_{13}^2, \varkappa_{14}^2, \varkappa_{34}^2)] = 0 \tag{13}$$

and other analogous conditions from which if follows that $f_{ijlk}(\kappa_{12}^2, \kappa_{13}^2, \ldots k_{34}^2)$ is a symmetric function with respect to simultaneous interchange of any two of the indices $ijlk$ and the corresponding indices on the κ_{ik}.

From the symmetry of $f_{ijlk}(\kappa_{12}^2, \ldots \kappa_{34}^2)$ and the conditions (11) it follows that $f_{ijlk}(\kappa_{12}^2, \kappa_{13}^2, \ldots \kappa_{34}^2) = 0$ if any one of the conditions

$$\begin{gathered} \varkappa_{12} + \varkappa_{13} + \varkappa_{14} \geqslant 3\mu, \quad \varkappa_{12} + \varkappa_{23} + \varkappa_{24} \geqslant 3\mu, \quad \varkappa_{13} + \varkappa_{23} + \varkappa_{34} \geqslant 3\mu, \quad \varkappa_{14} + \varkappa_{24} + \varkappa_{34} \geqslant 3\mu, \\ \varkappa_{13} + \varkappa_{14} + \varkappa_{23} + \varkappa_{24} \geqslant 2\mu, \quad \varkappa_{12} + \varkappa_{13} + \varkappa_{24} + \varkappa_{34} \geqslant 2\mu, \quad \varkappa_{23} + \varkappa_{34} + \varkappa_{12} + \varkappa_{14} \geqslant 2\mu. \end{gathered} \tag{14}$$

is not satisfied.

We obtain further information about $f_{ijlk}(\kappa_{12}^2, \kappa_{13}^2, \ldots \kappa_{34}^2)$ if we use the fact that the operators $\varphi_i(x)$, and consequently also $j_i(x)$, can be chosen to be Hermitian. With such a choice it follows from Eqs. (4) and (5) that

$$\rho_{ijlk}(p_1, p, p_4) = \rho^*_{klji}(p_4, p, p_1), \tag{15}$$

but from symmetry of $f_{ijlk}(\kappa_{11}^2, \ldots \kappa_{34}^2)$ it follows that

$$\rho_{ijlk}(p_1, p, p_4) = \rho_{klji}(p_4, p, p_1). \tag{16}$$

Consequently the $\rho_{ijlk}(p_1, p, p_4)$ are real, and therefore the $f_{ijlk}(\kappa_{12}^2 \ldots \kappa_{34}^2)$ can also be taken to be real.

Using the symmetry of the function $f_{ijlk}(\kappa_{12}^2, \kappa_{13}^2, \ldots \kappa_{34}^2)$, we can go over to the representation of the vacuum expectation value of the T-product of the operators $j_i(x)$. To do this we have only to replace the functions $\Delta^+(x, \kappa)$ in Eq. (12) by functions

$$\Delta_F(x) = \vartheta(x)\Delta^+(x) + \vartheta(-x)\Delta^+(-x). \tag{17}$$

Making this replacement, we obtain the desired spectral representation in the coordinate space

$$\begin{gathered} \langle | T j_i(x_1) j_j(x_2) j_k(x_3) j_l(x_4) | \rangle = \int_0^\infty \cdot\cdot \int_0^\infty d\varkappa_{12}^2 \ldots d\varkappa_{34}^2 f_{ijlk}(\varkappa_{12}^2, \varkappa_{13}^2 \ldots \varkappa_{34}^2) \\ \times \Delta_F(x_{12}, \varkappa_{12}) \Delta_F(x_{13}, \varkappa_{13}) \Delta_F(x_{14}, \varkappa_{14}) \Delta_F(x_{23}, \varkappa_{23}) \Delta_F(x_{24}, \varkappa_{24}) \Delta_F(x_{34}, \varkappa_{34}). \end{gathered} \tag{18}$$

Equation (18) follows directly from Eqs. (12), (17) and the definition of the T-product when account is taken of the symmetry properties of $f_{ijlk}(\kappa_{12}^2, \ldots \kappa_{34}^2)$.

To obtain the spectral representation in the momentum space it is necessary to calculate the following integral

$$(2\pi)^{-12} \int dk_{12} \ldots dk_{34} \quad \frac{\delta(l_1 - k_{12} - k_{13} - k_{14})\,\delta(l_2 + k_{12} - k_{13} - k_{14})\,\delta(l_3 + k_{13} + k_{23} - k_{34})\,\delta(l_4 + k_{14} + k_{24} + k_{34})}{(k_{12}^2 + \varkappa_{12}^2)(k_{13}^2 + \varkappa_{13}^2)(k_{14}^2 + \varkappa_{14}^2)(k_{23}^2 + \varkappa_{23}^2)(k_{24}^2 + \varkappa_{24}^2)(k_{34}^2 + \varkappa_{34}^2)} \tag{19}$$

which diverges logarithmically. Since, however, we assume that the meson-meson scattering amplitude exists, this divergence must not appear in the result. If to remove the divergence we introduce a cut-off radius Λ, then the term that goes to infinity for $\Lambda \to \infty$ will be proportional to $\ln \Lambda$ and will not depend on κ_{ik}. When substituted into the integral with respect to κ_{ik}^2 it gives a contribution proportional to

$$\ln\Lambda \int d\varkappa_{12}^2 \, d\varkappa_{13}^2 \ldots d\varkappa_{34}^2 f_{ijkl}(\varkappa_{12}^2, \varkappa_{13}^2, \ldots \varkappa_{34}^2).$$

In order for this term to make no contribution to the scattering amplitude, it must either be equal to zero or else cancel with the infinite terms written out in Appendix 1.

As is shown in Appendix 2, the integral (19) can be brought into a simpler form. We thus get the following spectral representation in momentum space:

$$\tau_{ijkl}(l_1, l_2, l_3, l_4) = \frac{-i}{3(4\pi)^6}\int_0^\infty\cdots\int_0^\infty d\varkappa_{12}^2\ldots d\varkappa_{34}^2 f_{ijkl}(\varkappa_{12}^2\varkappa_{13}^2\ldots\varkappa_{34}^2)$$
$$\times\int_0^1\cdots\int_0^\infty d\alpha_{12}\ldots d\alpha_{34}\delta(\alpha_{12}+\alpha_{13}+\ldots+\alpha_{34}-1)\varphi^{-2}\ln(\Box-i\varepsilon)\delta(l_1+l_2+l_3+l_4). \tag{20}$$

(The factor $\delta(l_1 + l_2 + l_3 + l_4)$ will be omitted hereafter). Here

$$\varphi(\alpha) = \alpha_{12}\alpha_{13}\alpha_{23} + \alpha_{12}\alpha_{13}\alpha_{24} + \alpha_{12}\alpha_{13}\alpha_{34} + \alpha_{12}\alpha_{14}\alpha_{23} + \alpha_{12}\alpha_{14}\alpha_{23} + \alpha_{12}\alpha_{14}\alpha_{34} + \alpha_{12}\alpha_{23}\alpha_{34} + \alpha_{12}\alpha_{24}\alpha_{34}$$
$$+ \alpha_{13}\alpha_{14}\alpha_{23} + \alpha_{13}\alpha_{14}\alpha_{24} + \alpha_{13}\alpha_{14}\alpha_{34} + \alpha_{13}\alpha_{23}\alpha_{24} + \alpha_{13}\alpha_{24}\alpha_{34} + \alpha_{14}\alpha_{23}\alpha_{24} + \alpha_{14}\alpha_{23}\alpha_{34} + \alpha_{23}\alpha_{24}\alpha_{34} \tag{21}$$

(the sum of all products of three different variables α_{ik} under the condition that no index can occur more than twice in a given term);

$$\Box = l_1^2\alpha_{12}\alpha_{13}\alpha_{14}(\alpha_{23} + \alpha_{24} + \alpha_{34}) + l_2^2\alpha_{12}\alpha_{23}\alpha_{24}(\alpha_{13} + \alpha_{14} + \alpha_{34}) + l_3^2\alpha_{13}\alpha_{23}\alpha_{34}(\alpha_{12} + \alpha_{14} + \alpha_{24}) + l_4^2\alpha_{14}\alpha_{24}\alpha_{34}(\alpha_{12} + \alpha_{13} + \alpha_{23})$$
$$+ \alpha_{13}\alpha_{14}\alpha_{23}\alpha_{24}(l_1 + l_2)^2 + \alpha_{12}\alpha_{14}\alpha_{23}\alpha_{34}(l_1 + l_3)^2 + \alpha_{12}\alpha_{13}\alpha_{24}\alpha_{34}(l_2 + l_3)^2 + \varphi(\alpha)\varkappa^2; \quad \varkappa^2 = \varkappa_{12}^2\alpha_{12} + \varkappa_{13}^2\alpha_{13} + \ldots + \varkappa_{34}^2\alpha_{34}. \tag{22}$$

Formulas (20) to (22) provide a convenient means for studying the analytical properties of $\tau(l_1, l_2, l_3, l_4)$ as affected by the variation of any one of the independent invariants. Since, however, we shall be interested in the scattering amplitude, we set $l_1^2 = l_2^2 = l_3^2 = l_4^2 = -\mu^2$ and consider τ as a function of $(l_1 + l_2)^2$, $(l_1 + l_3)^2$, and $(l_2 + l_3)^2$, regarding them at first as independent.

The behavior of $\tau((l_1 + l_2)^2, (l_1 + l_3)^2, (l_2 + l_3)^2)$ depends essentially on whether, for given values of $(l_1 + l_2)^2$, $(l_1 + l_3)^2$, and $(l_2 + l_3)^2$, the quantity $\Box$ can vanish for any particular values of the variables α_{ik} and κ_{ik}^2 We shall show that $\Box > 0$ if

$$-(l_1 + l_2)^2 < 4\mu^2; \; -(l_1 + l_3)^2 < 4\mu^2; \; -(l_2 + l_3)^2 < 4\mu^2. \tag{23}$$

The proof reduces to a matter of regrouping the terms in Eq. (22) and using the conditions (14).

Let us first consider those terms $\varphi(\alpha)$ which, when multiplied by κ^2, can give terms containing $\alpha_{13}\alpha_{14}\alpha_{23}\alpha_{24}$. These are the following terms:

$$\alpha_{13}\alpha_{14}\alpha_{23} + \alpha_{13}\alpha_{14}\alpha_{24} + \alpha_{13}\alpha_{23}\alpha_{24} + \alpha_{14}\alpha_{23}\alpha_{24}.$$

Multiplying them by κ^2 and adding and subtracting terms containing the products $\kappa_{13}\kappa_{14}$, $\kappa_{13}\kappa_{23}$, and so on, we get

$$\alpha_{13}\alpha_{14}\alpha_{23}\alpha_{24}(\varkappa_{13} + \varkappa_{14} + \varkappa_{23} + \varkappa_{24})^2 + \alpha_{13}\alpha_{14}(\varkappa_{23}\alpha_{23} - \varkappa_{24}\alpha_{24})^2 + \alpha_{13}\alpha_{23}(\varkappa_{14}\alpha_{14} - \varkappa_{24}\alpha_{24}) + \alpha_{13}\alpha_{24}(\varkappa_{14}\alpha_{14} - \varkappa_{23}\alpha_{23})^2$$
$$+ \alpha_{14}\alpha_{23}(\varkappa_{13}\alpha_{13} - \varkappa_{24}\alpha_{24})^2 + \alpha_{14}\alpha_{24}(\varkappa_{13}\alpha_{13} - \varkappa_{23}\alpha_{23})^2 + \alpha_{23}\alpha_{24}(\varkappa_{13}\alpha_{13} - \varkappa_{14}\alpha_{14})^2 + \varkappa_{12}^2(\alpha_{12}\alpha_{13}\alpha_{14}(\alpha_{23} + \alpha_{24})$$
$$+ \alpha_{13}\alpha_{23}\alpha_{24}(\alpha_{13} + \alpha_{14})] + \varkappa_{34}^2[\alpha_{13}\alpha_{23}\alpha_{34}(\alpha_{14} + \alpha_{24}) + \alpha_{14}\alpha_{24}\alpha_{34}(\alpha_{13} + \alpha_{23})].$$

Selecting in the same way the terms of $\varphi(\alpha)$ which when multiplied by κ^2 will contain $\alpha_{12}\alpha_{14}\alpha_{23}\alpha_{34}$ and $\alpha_{12}\alpha_{13}\alpha_{24}\alpha_{34}$, and grouping the remaining terms not containing squares of differences, we get

$$\Box = \alpha_{13}\alpha_{14}\alpha_{23}\alpha_{24}[(l_1 + l_2)^2 + (\varkappa_{13} + \varkappa_{14} + \varkappa_{23} + \varkappa_{24})^2] + \alpha_{12}\alpha_{14}\alpha_{23}\alpha_{24}[(l_1 + l_2)^2 + (\varkappa_{12} + \varkappa_{14} + \varkappa_{23} + \varkappa_{24})^2] + \alpha_{12}\alpha_{13}\alpha_{24}\alpha_{34}[(l_2 + l_3)^2$$
$$+ (\varkappa_{12} + \varkappa_{13} + \varkappa_{24} + \varkappa_{34})^2] + \alpha_{12}\alpha_{13}\alpha_{14}(\alpha_{23} + \alpha_{24} + \alpha_{34})(l_1^2 + \varkappa_{12}^2 + \varkappa_{13}^2 + \varkappa_{14}^2) + (1 \to 2) + (1 \to 3) + (1 \to 4)$$
$$+ \sum_{ikl}(\alpha_{ik}\varkappa_{ik})^2\alpha_{il}\alpha_{kl} + \sum_{\substack{i \neq m \\ k \neq l}}\alpha_{ik}\alpha_{il}(\varkappa_{mk}\alpha_{mk} - \varkappa_{ml}\alpha_{ml})^2. \tag{24}$$

From the condition $\kappa_{12} + \kappa_{13} + \kappa_{14} \geq 3\mu$ it follows that $\kappa_{12}^2 + \kappa_{13}^2 + \kappa_{14}^2 \geq 3\mu^2$. Since $l_1^2 = -\mu^2$, all the terms in Eq. (24) except the first three are always positive. The condition that the first three terms be positive, together with the second group of conditions (14), reduces to Eq. (23).

If we regard τ as a function of one of the variables [for example $(l_1 + l_2)^2$] for fixed values of the others, then starting from Eq. (20) we can easily show (for example, by means of Titchmarsh's theorem) that on the hypothesis of uniform convergence of the integrals with respect to κ_{ik}^2 for real $(l_1 + l_2)^2$ this formula defines a function analytic in the entire plane with the exception of those points of the real axis for which $\Box$ can be equal to zero.

If these singularities are removed by the introduction of a term $-i\epsilon$, then at the corresponding points $\operatorname{Re}\tau \neq 0$. It is easy to show, by using the results of reference 3, that terms depending on a contact interaction $\lambda\varphi^4$ do not change this result.

In concluding this section we point out the following important fact. The expression (20) has a direct meaning provided that

$$\int \ln(\varkappa^2\varphi)\, f(\varkappa_{12}^2 \ldots \varkappa_{34}^2)\, d\varkappa_{12}^2 \ldots d\varkappa_{34}^2 < \infty.$$

In cases in which $f(\kappa_{12}^2, \ldots \kappa_{34}^2)$ does not decrease rapidly enough, the integral must be regularized, and its divergent terms must be cancelled with the infinite terms written out in Appendix 1. The degree of divergence of the integral is closely connected with the behavior of τ_{ijkl} at large energies. Therefore in obtaining spectral representations, just as in the derivation of dispersion relations, it is necessary to make an assumption about the behavior of the quantity in question at large energies.

3. THE DISPERSION RELATIONS FOR THE SCATTERING AMPLITUDE FOR CONSTANT SCATTERING ANGLE IN THE CENTER-OF-MASS SYSTEM

In order to go over directly to the relations for the scattering amplitude, we take l_1 and l_2 as the four-momenta of the mesons in the initial state. Then

$$\begin{aligned}(l_1+l_2)^2 &= -4\omega^2;\\ (l_1+l_3)^2 &= 2p^2(1-\cos\vartheta) = 2(\omega^2-\mu^2)(1-\cos\vartheta); \quad (25)\\ (l_2+l_3)^2 &= 2p^2(1+\cos\vartheta) = 2(\omega^2-\mu^2)(1+\cos\vartheta);\end{aligned}$$

ω is the energy of one of the mesons in the center-of-mass system, and ϑ is the scattering angle. The scattering amplitude is

$$T_{kl,\,ij}(\omega, \cos\vartheta) = \frac{-i}{4\pi\omega}\tau_{ijkl}[(l_1+l_2)^2, (l_1+l_3)^2, (l_2+l_3)^2]. \quad (26)$$

From the formulas of the preceding section it follows that the function $\tau((l_1+l_2)^2, (l_1+l_3)^2, (l_2+l_3)^2)$ is analytic not only as a function of one of the invariants for fixed values of the others, but also as a function of ω^2 for fixed $\cos\vartheta$, if we draw the cuts along the real axis from $\omega^2 = \mu^2$ to $\omega^2 = \infty$ and, depending on whether $\vartheta < \pi/2$ or $\vartheta > \pi/2$, from $\omega^2 = -\mu^2\tan^2\vartheta/2$ or $\omega^2 = -\mu^2 \times \cot^2\vartheta/2$ to $-\infty$. The position of the cuts is determined by means of the conditions (23) and the formulas (25).

Using these analytic properties or, with a procedure like that of Goldberger,[5] changing the order of integration in Eq. (20), we can write the following dispersion relations for $\tau_{ijkl}(\omega, \cos\vartheta)$ for $\vartheta < \pi/2$:

$$\begin{aligned}&-\frac{\operatorname{Im}\tau_{ijkl}(\omega, \cos\vartheta)}{(\omega^2-\omega_{10}^2)(\omega^2-\omega_{20}^2)} + \frac{\operatorname{Im}\tau_{ijkl}(\omega_{10}, \cos\vartheta)}{(\omega^2-\omega_{10}^2)(\omega_{10}^2-\omega_{20}^2)}\\ &+\frac{\operatorname{Im}\tau_{ijkl}(\omega_{20}, \cos\vartheta)}{(\omega^2-\omega_{20})^2(\omega_{20}^2-\omega_{10}^2)} = \frac{P}{\pi}\int\limits_{\mu^2}^{\infty}\frac{\operatorname{Re}\tau_{ijkl}(\omega', \cos\vartheta)\,d\omega'^2}{(\omega'^2-\omega^2)(\omega'^2-\omega_{10}^2)(\omega'^2-\omega_{20}^2)}\\ &-\frac{P}{\pi}\int\limits_{-\infty}^{-\mu^2\tan^2(\vartheta/2)}\frac{\operatorname{Re}\tau_{ijkl}(\omega', \cos\vartheta)\,d\omega'^2}{(\omega'^2-\omega^2)(\omega'^2-\omega_{10}^2)(\omega'^2-\omega_{20}^2)}.\end{aligned} \quad (27)$$

In obtaining this formula we have made the same assumption about the behavior of τ for large ω^2 as is made (cf. reference 5) for the scattering amplitude of π mesons on nucleons. ω_{10}^2, ω_{20}^2 are so far arbitrary.

The second term of the right member appears with a minus sign, since in the derivation of the dispersion relations we integrate along the top edge of the cut, whereas for $(l_1+l_3)^2 < -4\mu^2$ or $(l_2+l_3)^2 < -4\mu^2$ the function $\tau((l_1+l_2)^2, (l_1+l_3)^2, (l_2+l_3)^2)$ is defined by Eq. (20) as the value on the bottom side of the cut.

The first integral in the right member contains the scattering amplitude in the physical region. The second contains the scattering amplitude for imaginary energies. Using the symmetry of the function $\tau_{ijkl}(l_1, l_2, l_3, l_4)$, we transform it into an integral over real energies, but containing the scattering angle for an imaginary angle. For this purpose we change the variable in the second integral of Eq. (27) in the following way:

$$2(\omega'^2-\mu^2)(1+\cos\vartheta) = -4\omega_1^2, \quad (28)$$

and define a quantity $\cos\vartheta_1$ by the relation:

$$-4\omega'^2 = 2(\omega_1^2-\mu^2)(1+\cos\vartheta_1). \quad (29)$$

In the new variables

$$\begin{aligned}(l_1+l_2)^2 &= 2(\omega_1^2-\mu^2)(1+\cos\vartheta_1), \quad (l_1+l_3)^2\\ &= 2(\omega_1-\mu^2)(1-\cos\vartheta_1); \quad (30)\\ (l_2+l_3)^2 &= -4\omega_1^2.\end{aligned}$$

Since

$$\begin{aligned}&\tau_{ijkl}[(l_1+l_2)^2, (l_1+l_3)^2, (l_2+l_3)^2]\\ &= \tau_{kjil}[(l_2+l_3)^2, (l_1+l_3)^2, (l_1+l_2)^2],\end{aligned} \quad (31)$$

we get

$$\tau_{ijkl}(\omega', \cos\vartheta) = \tau_{kjil}(\omega_1, \cos\vartheta_1). \quad (32)$$

In particular

$$\tau_{ijkl}\left(-\mu\tan\frac{\vartheta}{2}, \cos\vartheta\right) = \tau_{kjil}(\mu, \infty), \quad (33)$$

where use has been made of the fact that

$$\cos\vartheta_1 = 1 + \frac{2\omega_1^2}{\omega_1^2-\mu^2}\tan^2\frac{\vartheta}{2}. \quad (34)$$

Since, however, the scattering amplitude at zero energy does not depend on the angle, we have

$$\tau_{ijkl}(\mu,\ \infty) = \tau_{ijkl}(\mu,\ 0) \equiv \tau(\mu). \tag{35}$$

Using these equations, we take $\omega_{10}^2 = \mu^2$, $\omega_{20}^2 = -\mu^2 \tan^2 \vartheta/2$. Then, using also Eq. (26), we can write instead of Eq. (27)

$$\begin{aligned} &\frac{\omega \operatorname{Re} T_{kl,ij}(\omega,\ \cos\vartheta)}{(\omega^2-\mu^2)(\omega^2+\mu^2\tan^2(\vartheta/2))} \\ &\quad - \frac{\cos^2(\vartheta/2)}{\mu}\left[\frac{\operatorname{Re} T_{kl,ij}(\mu)}{\omega^2-\mu^2} - \frac{\operatorname{Re} T_{il,kj}(\mu)}{\omega^2+\mu^2\tan^2(\vartheta/2)}\right] \\ &= \frac{2}{\pi} P \int_\mu^\infty \frac{\omega'^2 d\omega' \operatorname{Im} T_{kl,ij}(\omega',\ \cos\vartheta)}{(\omega'^2-\omega^2)(\omega'^2-\mu^2)(\omega'^2+\mu^2\tan^2(\vartheta/2))} \\ &\quad - \frac{2}{\pi}\cos^4\frac{\vartheta}{2}\int_\mu^\infty \frac{\operatorname{Im} T_{il,kj}(\omega_1,\ \cos\vartheta_1)\, d\omega_1}{(\omega^2+\omega_1^2-\mu^2\cos^2(\vartheta/2))(\omega_1^2-\mu^2)}. \end{aligned} \tag{36}$$

For $\pi/2 < \vartheta < \pi$ one gets analogous relations differing only in the replacement of ϑ by $\pi - \vartheta$.

By taking advantage of isotopic invariance, we can express the amplitudes $T_{kl,ij}$ in terms of the scattering amplitudes in the states with total isotopic spins T_0, T_1, and T_2 and reduce the system of equations (36) to three equations for T_0, T_1, and T_2. It is easy to show that

$$\begin{aligned} T_{kl,ij} &= \frac{2}{3} T_0 \delta_{ij}\delta_{kl} + T_1(\delta_{ik}\delta_{jl} - \delta_{il}\delta_{jk}) \\ &\quad + T_2\left\{\delta_{ik}\delta_{jl} + \delta_{il}\delta_{jk} - \frac{2}{3}\delta_{ij}\delta_{kl}\right\}. \end{aligned} \tag{37}$$

Substituting this expression into Eq. (36), we get the following system of equations:

$$\begin{aligned} &\frac{\omega \operatorname{Re} T_i(\omega,\ \cos\vartheta)}{(\omega^2-\mu^2)\left(\omega^2+\mu^2\tan^2\frac{\vartheta}{2}\right)} \\ &\quad - \frac{\cos^2(\vartheta/2)}{\mu}\left[\frac{\operatorname{Re} T_i(\mu)}{\omega^2-\mu^2} - \frac{\sum\limits_k A_{ik} \operatorname{Re} T_k(\mu)}{\omega^2+\mu^2\tan^2\frac{\vartheta}{2}}\right] \\ &= \frac{2}{\pi} P \int_\mu^\infty \frac{\omega'^2 d\omega' \operatorname{Im} T_i(\omega',\ \cos\vartheta)}{(\omega'^2-\omega^2)(\omega'^2-\mu^2)(\omega'^2+\mu^2\tan^2(\vartheta/2))} \\ &\quad - \frac{2}{\pi}\cos^4\frac{\vartheta}{2}\sum_k A_{ik}\int_\mu^\infty \frac{\operatorname{Im} T_k(\omega,\ \cos\vartheta_1)\, d\omega_1}{(\omega^2+\omega_1^2-\mu^2\cos^3(\vartheta/2))(\omega_1^2-\mu^2)}; \end{aligned} \tag{38}$$

$$(A_{ik}) = \begin{pmatrix} 2/3 & -1/2 & 5/6 \\ -2/3 & 1 & 5/3 \\ 2/3 & 1 & 1/3 \end{pmatrix}.$$

The equations that have been obtained would be of considerably greater interest if one could indicate a simple method for analytic continuation of the scattering amplitude into the region of imaginary angles. It seems natural to use for this purpose an expansion of the scattering amplitude in series of Legendre polynomials

$$T_i(\omega,\ \cos\vartheta) = \sum_l T_i^l(\omega) P_l(\cos\vartheta). \tag{39}$$

Such an expansion is especially attractive because the conditions for the S matrix to be unitary have a simple form for the quantities T_i^l. Such an expansion, however, can scarcely allow us to continue the scattering amplitude into a region of values of $\cos\vartheta$ that are much larger than 1. Namely, it follows from Eqs. (23) and (24) that the scattering amplitude has singularities of the type of branch points for those values of the variables at which one of the invariants $(l_1 + l_2)^2$, $(l_1 + l_3)^2$, $(l_2 + l_3)^2$ becomes equal to $-4\mu^2$. According to Eq. (25) this means that as a function of $\cos\vartheta$ the scattering amplitude has singularities at

$$\cos\vartheta = \pm(\omega^2+\mu^2)/(\omega^2-\mu^2). \tag{40}$$

Therefore the radius of convergence of the series (39) cannot exceed this value. This means that we can use the expansion (39) in the last integral in the right member of Eq. (38) in the region of values of ω_1 for which

$$\cos\vartheta_1 < (\omega_1^2+\mu^2)/(\omega_1^2-\mu^2).$$

Recalling the expression (34) for $\cos\vartheta_1$, we get the condition

$$\omega_1^2 < \mu^2\cot^2\frac{\vartheta}{2}, \tag{41}$$

which shows that the expansion can be used only for the forward scattering amplitude, since the contribution to the integral in question from the region $\omega_1 > \mu\cot(\vartheta/2)$ is of the order

$$\left(\mu\cot\frac{\vartheta}{2}\right)^{-2} \approx \mu^{-2}(1-\cos\vartheta),$$

i.e., of the order of the first term of the expansion of $T_i(\omega,\ \cos\theta)$ in powers of $1 - \cos\vartheta$. Therefore in order to give meaning to the dispersion relations for the scattering amplitude one must find some other method of analytic continuation.

APPENDIX 1

Let us write out the formula (3) in detail using the fact that when we introduce a contact interaction

$$[\dot{\varphi}_i(x),\ j_k(x')]\,|_{t=t'} = \lambda\delta(\mathbf{r}-\mathbf{r}')\,\{\varphi_\lambda^2\delta_{ik} + 2\varphi_i\varphi_k\};$$

this gives

$$K_1K_2K_3K_4\langle| T\varphi_i(x_1)\varphi_j(x_2)\varphi_k(x_3)\varphi_l(x_4)|\rangle = \langle| Tj_i(x_1)j_j(x_2)j_k(x_3)j_l(x_4)|\rangle$$
$$+\lambda\{\delta(x_1-x_2)\langle| T\{\varphi_\lambda^2(x_1)\delta_{ij}+2\varphi_i(x_1)\varphi_j(x_1)\}j_k(x_3)j_l(x_4)|\rangle+\ldots\}_{\mathrm{sym}}$$
$$+2\lambda\{\delta(x_1-x_2)\,\delta(x_2-x_3)[\delta_{kj}\langle| T\varphi_i(x_1)\,j_l(x_4)|\rangle+\delta_{ik}\langle| T\varphi_j(x_2)\,j_l(x_4)|\rangle$$
$$+\delta_{ij}\langle| T\varphi_k(x_3)j_l(x_4)|\rangle]+\ldots\}_{\mathrm{sym}}+\lambda^2\{\delta(x_1-x_2)\,\delta(x_3-x_4)\langle| T\{\varphi_\lambda^2(x_1)\delta_{ij}+2\varphi_i(x_1)\varphi_j(x_1)\}\{\varphi_\nu^2(x_3)\delta_{kl}$$
$$+2\varphi_k(x_3)\varphi_l(x_3)\}|\rangle+\ldots\}_{\mathrm{sym}}+2\lambda\delta(x_1-x_2)\,\delta(x_2-x_3)\,\delta(x_3-x_4)\,[\delta_{ij}\delta_{kl}+\delta_{ik}\delta_{jl}+\delta_{kj}\delta_{il}].$$

Here $\{\ \}_{\mathrm{sym}}$ means that we are to take the sum of terms corresponding to all permutations of x_1, x_2, x_3, x_4 together with the associated isotopic indices.

APPENDIX 2

The integral (19) can be easily reduced to integrations over parameters if we use the formula

$$\frac{1}{a_1a_2\ldots a_n}=(n-1)!\int_0^1\!\!\int_0^1 dz_1dz_2\ldots dz_n\,\frac{\delta(z_1+z_2+z_3+\ldots+z_{n-1})}{(a_1z_1+a_2z_2+\ldots+a_nz_n)^n}. \tag{A.1}$$

Denoting the integral (19) by I and dropping the factor $\delta(l_1+l_2+l_3+l_4)$, we can write

$$I=-\frac{5!}{(2\pi)^{12}}\int d\alpha_{12}d\alpha_{12}\ldots d\alpha_{34}\int\frac{dk_{12}dk_{13}dk_{23}\delta(\alpha_{12}+\alpha_{13}+\ldots+\alpha_{34}-1)}{[k_{12}^2\alpha_{12}+\ldots+k_{34}^2\alpha_{34}+\varkappa_{12}^2\alpha_{12}+\ldots+\varkappa_{34}^2\alpha_{34}]^6}, \tag{A.2}$$
$$k_{14}=l_1-k_{12}-k_{13},\ k_{24}=l_2+k_{12}-k_{23};\ k_{34}=l_3+k_{13}+k_{23}.$$

Instead of the variables $z_1, z_2, \ldots, z_6$ we have here introduced the variables α_{12}, α_{13}, α_{14}, α_{23}, α_{24}, α_{34}.

If in the denominator of the expression (A.2) we insert instead of k_{14}, k_{24}, and k_{34} their expressions in terms of l_1, l_2, l_3 and k_{12}, k_{13}, k_{23}, then besides quadratic terms the denominator will contain linear terms in k_{12}, k_{13}, and k_{23}. To get rid of these terms we make the change of variables

$$k_{12}=q_{12}+\Delta_{12};\ k_{13}=q_{13}+\Delta_{13};\ k_{23}=q_{23}+\Delta_{23}. \tag{A.3}$$

The conditions for the determination of Δ_{ik} have the form:

$$\Delta_{12}(\alpha_{12}+\alpha_{14}+\alpha_{24})+\alpha_{14}\Delta_{13}-\alpha_{24}\Delta_{23}+l_2\alpha_{24}-l_1\alpha_{14}=0;\quad \alpha_{14}\Delta_{12}+(\alpha_{13}+\alpha_{14}+\alpha_{34})\Delta_{13}+\alpha_{34}\Delta_{23}+l_3\alpha_{34}-l_1\alpha_{14}=0;$$
$$-\alpha_{24}\Delta_{12}+\alpha_{34}\Delta_{13}+(\alpha_{23}+\alpha_{24}+\alpha_{34})\Delta_{23}+l_3\alpha_{34}-l_2\alpha_{24}=0. \tag{A.4}$$

The determinant $\varphi(\alpha)$ of this system is the sum (21). Then

$$\Delta_{12}=\{l_1\alpha_{14}\varphi_{24}^1-l_2\alpha_{24}\varphi_{14}^2+l_3\alpha_{34}(\alpha_{23}\alpha_{14}-\alpha_{13}-\alpha_{24})\}/\varphi;\qquad \Delta_{13}=\{l_1\alpha_{14}\varphi_{34}^1-l_3\alpha_{34}\varphi_{14}^3+l_2\alpha_{24}(\alpha_{14}\alpha_{23}-\alpha_{12}\alpha_{34})\}/\varphi; \tag{A.5}$$

$$\Delta_{23}=\{l_2\alpha_{24}\varphi_{34}^2-l_3\alpha_{34}\varphi_{24}^3+l_1\alpha_{14}(\alpha_{13}\alpha_{24}-\alpha_{12}\alpha_{34})\}/\varphi;\qquad \varphi_{24}^1=\alpha_{13}\alpha_{23}+\alpha_{13}\alpha_{24}+\alpha_{13}\alpha_{34}+\alpha_{23}\alpha_{34}. \tag{A.6}$$

φ_{24}^1 consists of the products by pairs of all the variables except α_{12} and α_{14}, taken so that the indices 2 and 4 do not occur twice in any product. Substituting Eqs. (A.5) and (A.6) into the denominator of (A.2), we get for the latter the expression

$$(\alpha_{12}+\alpha_{14}+\alpha_{24})q_{12}^2+(\alpha_{13}+\alpha_{14}+\alpha_{34})q_{13}^2+(\alpha_{23}+\alpha_{24}+\alpha_{34})q_{23}^2+2\alpha_{14}q_{12}q_{13}+2\alpha_{13}q_{13}q_{23}-2\alpha_{24}q_{12}q_{23}+\Box/\varphi;$$

$$\Box=\varphi\Delta_{12}(l_2\alpha_{24}-l_1\alpha_{14})+\varphi\Delta_{13}(-l_1\alpha_{14}+l_3\alpha_{34})+\varphi\Delta_{23}(l_3\alpha_{34}-l_2\alpha_{24})$$
$$+\varphi(\alpha_{14}l_1^2+\alpha_{24}l_2^2+\alpha_{34}l_3^2)+\varphi\varkappa^2=l_1^2\alpha_{14}\varphi_{14}+l_2^2\alpha_{24}\varphi_{24}+l_3^2\alpha_{34}\varphi_{34}+2l_1l_2\alpha_{14}\alpha_{24}\varphi_{12}^4+2l_1l_3\alpha_{14}\alpha_{34}\varphi_{13}^4+2l_2l_3\alpha_{24}\alpha_{34}\varphi_{23}^4+\varphi\varkappa^2; \tag{A.7}$$

φ_{14} is the sum of those terms of φ which do not contain α_{14}; and

$$\varkappa^2=\varkappa_{12}^2\alpha_{12}+\varkappa_{13}^2\alpha_{13}+\varkappa_{14}^2\alpha_{14}+\varkappa_{23}^2\alpha_{23}+\varkappa_{24}^2\alpha_{24}+\varkappa_{34}^2\alpha_{34}.$$

[If in Eq. (A.7) we express l_1l_2, l_1l_3 and l_2l_3 in terms of $(l_1+l_2)^2$, $(l_1+l_3)^2$, and $(l_2+l_3)^2$ and note that

$$(l_1+l_2)^2+(l_1+l_3)^2+(l_2+l_3)^2=l_1^2+l_2^2+l_3^2+l_4^2,$$

then we can easily get for $\Box$ the expression (22) given in the text.]

It is now easy to carry out the integrations with respect to q_{12}, q_{13}, q_{23} by introducing new variables q'_{12}, q'_{13}, q'_{23} in such a way that the quadratic terms reduce to a sum of squares. We thus get

$$\int\frac{d^4q'_{12}d^4q'_{13}d^4q'_{23}}{[\lambda_{12}q'^2_{12}+\lambda_{13}q'^2_{13}+\lambda_{23}q'^2_{23}+\Box/\varphi]^6}=\frac{(i\pi^2)}{5!\lambda_3^2\lambda_{23}^2}\int d^4q'_{12}\frac{1}{[\lambda_{12}q'^2_{12}+\Box/\varphi]^2}.$$

To perform the last integration we introduce the cut-off parameter Λ, and then

$$I = \frac{i}{(4\pi)^6}\frac{i}{\lambda_{12}^2\lambda_{13}^2\lambda_{23}^2}[\ln\varphi\Lambda + 1 - \ln(\Box - i\varepsilon)]. \tag{A.8}$$

Noting that $\lambda_{12}\lambda_{13}\lambda_{23} = -\varphi$ and that the terms that do not depend on κ_{ik} make no contribution, we get the result (20) given in the text.

---

[1] J. Schwinger, Proceedings of the Seventh Rochester Conference.

[2] Y. Nambu, Nuovo cimento **6**, 1064 (1957).

[3] V. N. Gribov, J. Exptl. Theoret. Phys. (U.S.S.R.) **34**, 1310 (1958), Soviet Phys. JETP **7**, 903 (1958).

[4] Lehmann, Symanzik, and Zimmermann, Nuovo cimento **1**, 205 (1955).

[5] M. Goldberger, Phys. Rev. **99**, 979 (1955).

Translated by W. H. Furry
74

SOVIET PHYSICS JETP VOLUME 35(8), NUMBER 2 FEBRUARY, 1959

PROPAGATION OF A NON-SELF-SIMILAR THERMAL WAVE

E. I. ANDRIANKIN

Institute of Chemical Physics, Academy of Sciences U.S.S.R.

Submitted to JETP editor March 15, 1958

J. Exptl. Theoret. Phys. (U.S.S.R.) **35**, 428-432 (August, 1958)

The propagation of a thermal wave from an instantaneous point source in a gas is investigated with account of the temperature dependence of the internal energy of the gas. The case when the internal energy is associated not only with the matter but also with radiation is considered. The range of the radiation is assumed to depend on the temperature in accordance with a power law. An approximate method can also be used in the case of an arbitrary dependence of the internal energy and of the heat flux on the temperature.

LET a quantity of heat Q_0 be liberated at a given initial instant of time within a small volume (at a point). Then, if the density of the medium is constant, and the thermal conductivity and the specific heat are each proportional to the temperature raised to a certain power, the problem is a self-similar one and its solution can be obtained in closed form. Such a problem was investigated by Zel'dovich and Kompaneets.[1]

If a thermal wave propagates in a gas then, because of the high temperature, the molecules of the gas break up into atoms and the latter are ionized, and this leads to a temperature dependence of the internal energy of the gas. Calculations[2,3] show that the internal energy of a gas may be approximated over a wide range of temperatures by a power of the temperature ($\sim aT^{\lambda}$). However, at very high temperatures (on the order of several millions of degrees for air of normal density) it is necessary to take into account, in addition to the energy of the matter, also the radiation energy, which is proportional to the fourth power of the temperature $\sim bT^4$. Such a problem is no longer self-similar even if the radiation range is expressed by a power of the temperature. Another non-self-similar problem will be one in which the internal energy is given by a power of the temperature, but the range of radiation is given not by a single power, but involves two or more terms.

We shall discuss the problem of the propagation of a non-self-similar thermal wave by considering a special case when the internal energy is expressed by the following two term formula

$$E = aT^{\lambda} + bT^4 \tag{1}$$

(here $b = 4\sigma/c$, c is the velocity of light, $\sigma =$

5.67×10^{-5} ergs/cm^2 sec deg^4 is the Stefan-Boltzmann constant, and a and λ are arbitrary), while the mean free path of the radiation depends on the temperature in accordance with the power law $l = l_0 T^n$. The heat balance equation can be written in the form:

$$\frac{\partial E(T)}{\partial t} = \frac{c_0}{r^2}\frac{\partial}{\partial r} r^2 \frac{\partial T^k}{\partial r}, \qquad (2)$$
$$k = n + 4, \quad c_0 = 16\sigma l_0 / 3k.$$

We present an approximate method of solving Eq. (2), based on a number of physical considerations. Since the thermal conductivity depends strongly on the temperature ($\kappa \sim T^{k-1}$), then in the course of propagation of the thermal wave the temperature tends to a uniform distribution more rapidly in regions which have undergone greater heating, thus forming a "plateau." A sharp variation in the temperature occurs only in the narrow zone near the front, which in the first approximation need not be taken into account in the energy balance if the temperature of the "plateau" is expressed in terms of the radius of the wave front as follows:

$$Q_0 = 4\pi \int_0^{r_f} (aT_*^\lambda + bT_*^4) r^2 dr. \qquad (3)$$

In order to determine $r_f(t)$, we shall make use of the integral relationship between the moments, which was investigated by Barenblatt.[4] If we multiply Eq. (2) by r^m ($m = 2, 3, 4 \ldots$) and integrate with respect to r between the limits from 0 to r_f, taking into account the conditions that the heat flux vanishes at the center and at the wave front:

$$r^2 \frac{\partial T^k}{\partial r}\bigg|_0 = r^2 \frac{\partial T^k}{\partial r}\bigg|_{r_f} = T(r_f, t) = 0, \qquad (4)$$

we obtain an infinite number of relations which, taken together, are equivalent to Eq. (2). The first of these relations ($m = 2$) gives us the law of conservation of energy [Eq. (3)], the second ($m = 3$) leads to the additional condition

$$\frac{d}{dt}\int_0^{r_f} (aT_*^\lambda + bT_*^4) r^3 dr = 2c_0 \int_0^{r_f} rT_*^k dr. \qquad (5)$$

In spite of the fact that the remaining equations remain unsatisfied, we can hope that there will be reasonably good agreement between the approximate and the exact solutions, since the temperature behind the wave front varies smoothly and monotonically.

Our problem is characterized by the following parameters, whose dimensions are expressed in terms of length [L], time [t], temperature [T] and quantity of heat [Q] as follows:

$$[a] = [Q]/[L]^3[T]^\lambda, \quad [b] = [Q]/[L]^3[T]^4, \qquad (6)$$
$$[c_0] = [Q]/[L][T]^k[t], \quad [Q_0] = [Q].$$

It is not possible to form a dimensionless constant from these quantities. The solution has therefore the important property of similarity. It can be recalculated independently for arbitrary values of the parameters a, b, c_0, and Q_0. If we eliminate T from (3) and (5) and introduce dimensionless variables, we obtain the law of motion of the wave front:

$$x^3\left[\left(\frac{1}{x^2}\frac{dx}{d\tau}\right)^{\lambda/k} + \left(\frac{1}{x^2}\frac{dx}{d\tau}\right)^{4/k}\right] = 1, \qquad (7)$$
$$x = \left[\frac{4\pi}{3}\frac{a}{Q_0}\left(\frac{a}{b}\right)^{\lambda/(4-\lambda)}\right]^{1/3} r, \quad \tau = \left[\frac{16\pi^2}{9aQ_0^2}\left(\frac{a}{b}\right)^{(3k-\lambda)/(4-\lambda)}\right]^{1/3} 4c_0 t.$$

By denoting $x^{-2}dx/d\tau = p$ we can easily write down the solutions of Eq. (7) in parametric form:

$$\tau = \int_p^\infty \frac{x^2(\lambda p^{\lambda/k} + 4p^{4/k})\,dp}{3kp^2}, \quad x = (p^{\lambda/k} + p^{4/k})^{-1/3}. \qquad (8)$$

In those cases when any one of the combinations

$$(\lambda - 3k)/\beta, \ (3\lambda - k - 8)/\beta,$$

(where $\beta = 12 - 3\lambda$) and one of the two ratios $(12 - 3k - 2\lambda)/\beta$ and $(4 - 3k)/\beta$ are integers simultaneously, the integral (8) can be expressed in terms of elementary functions. Figure 1 shows the dependence of the dimensionless coordinate of the wave front x on the time τ obtained from the solution (8) for $\lambda = 1$ and $k = 4$ and 6. From an analysis of (7) it follows that the solution of our problem $x(\tau)$ approaches, for small values of τ, the limiting self-similar solution $x_1 = \left(\frac{(3k-4)}{4}\tau\right)^{4/(3k-4)}$ while for large τ it tends to $x_2 = \left(\frac{3k-\lambda}{\lambda}\tau\right)^{\lambda/(3k-\lambda)}$

For all values of τ, the curve $x(\tau)$ lies lower than in both self-similar cases (dotted curve in Fig. 2). However, the solution $x(\tau)$ practically turns out to be close to $x_1(\tau)$ as long as the value of the quantity $x^{(12-3\lambda)/4} = \mu$ is small compared to unity. If, for example, we consider $\mu = 0.03$ as small, then our solution coincides with the curve $x_1(\tau)$, so long as $x < x_{10}$, $x_{10} = (0.03)^{4/(12-3\lambda)}$ (if $\lambda = 1$, $x_{10} = 0.210$). In the case $x > x_{20}$, when we can neglect the quantity $x_2^{(3\lambda-12)/\lambda} = \nu$ compared to unity, our solution approaches the other self-similar solution $x_2(\tau)$ (if we set $\nu = 0.03$ then $x_{20} = 1.475$ for $\lambda = 1$). In spite of the fact that in terms of dimensionless coordinates the zone of the non-self-similar solution is important only within the narrow interval $x_{10} < x < x_{20}$, it turns out in practice to be the most interesting one, since outside this interval the solution (8) loses its meaning in a number of cases, owing to

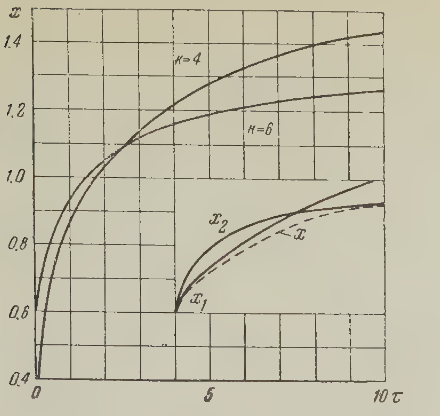

FIG. 1

the fact that the gas begins moving. The large pressure gradients at the wave front, correspond-to the temperature gradients, lead to the formation of a shock wave. After this has occurred the energy is transferred by a gas-dynamic mechanism, whereby the law of motion of a strong discontinuity differs from the law of propagation of a thermal wave, and our solution becomes unjustified.

A strong discontinuity can exist only if small perturbations propagated with the speed of sound $c_*(T)$ can catch up to the wave front. Since the thermal wave is slowed down very sharply, the limits of validity of the solution may be found, following a remark of A. S. Kompaneets, from the physical requirement $c_*(T_*) = \dot{r}_f$. In this connection it turns out that, for example, for air of normal density, $x_* < x_{20}$.

It is interesting to compare the solution of a self-similar problem obtained by the method just described with the exact solution, which in the case $\lambda = b = 0$ is given by the following formulas:

$$r_a = \left(t\,\frac{c_0}{a}\right)^{1/(3k-1)} \left[\frac{Q_0}{2\pi a\gamma(k)}\right]^{(k-1)/(3k-1)};$$

$$T = \left[\frac{a}{c_0}\,\frac{k-1}{k}\,r_f\dot{r}_f\right]^{1/(k-1)} [\eta - 0.5\,\eta^2]^{1/(k-1)}, \quad \eta = 1 - r/r_f; \tag{9}$$

$$\gamma(k) = \left[\frac{k-1}{2k(3k-1)}\right]^{1/(k-1)} \Gamma\left(\frac{3}{2}\right)\Gamma\left(\frac{k}{k-1}\right)\left[\Gamma\left(\frac{3}{2}+\frac{k}{k-1}\right)\right]^{-1};$$

where Γ is the gamma-function.

For the approximate solution we obtain:

$$r_0 = \left[t\,\frac{c_0}{a}\,(12k-4)\right]^{1/(3k-1)} \left[\frac{3Q_0}{4\pi a}\right]^{(k-1)/(3k-1)},$$

$$T_*(t) = \frac{3Q_0}{4\pi a r_0^3}. \tag{10}$$

Figure 2 gives the temperature distribution for $\lambda = b = 0$ and $k = 6$, obtained by means of the exact solution (9) (solid line) and by the approximate method, on the assumption that there is a temperature "plateau" behind the wave front (curve 1). The temperature distribution is given in dimensionless form in terms of its value $T_a = T(0, t)$, at the center of the self-similar wave,

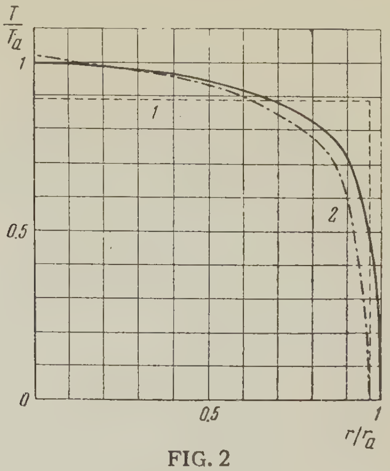

FIG. 2

and is shown as a function of the ratio of the coordinate r to the radius of the front of the self-similar wave $r_a(t)$. If we compare (9) and (10) we find that the approximate solution agrees well with the exact one. For $k = 6$ we have

$$r_0 / r_a = 0.962, \quad T_* / T(0, t) = 0.889.$$

If we know the law of wave propagation (10) we can also find the temperature distribution near the front by expanding the solution in powers of η:

$$T = T_1(\eta, t) + T_2(\eta, t) + \cdots \tag{11}$$

We write Eq. (2) in terms of the variables t and $\eta(r, t)$:

$$\frac{\partial(aT^\lambda + bT^4)}{\partial t} + \frac{\dot{r}_f}{r_f}(1-\eta)\frac{\partial(aT^\lambda + bT^4)}{\partial\eta} = \frac{2c_0}{r_f^2(\eta-1)}\,\frac{\partial T^k}{\partial\eta} + \frac{c_0}{r_f^2}\,\frac{\partial^2 T^k}{\partial\eta^2}. \tag{12}$$

Near the front of the wave $(\eta \to 0)$ the temperature tends to zero, and therefore the main terms of Eq. (12) must cancel one another:

$$\dot{r}_f r_f \partial T_1^\lambda / \partial\eta = c_0 \partial^2 T_1^k / \partial\eta^2.$$

This leads to the well known law for the variation of temperature near the wave front:

$$T_1 = \left[\frac{a}{c_0}\,\eta\,\frac{k-\lambda}{k}\,r_f\dot{r}_f\right]^{1/(k-\lambda)} = A_1\eta^{1/(k-\lambda)}. \tag{13}$$

For the second term we obtain:

$$T_2 = A_2\eta^{(5-\lambda)/(k-\lambda)}, \quad A_2 = bA_1^{5-\lambda} / a(4+k-2\lambda). \tag{14}$$

The series expansion gives the solution as a function of one arbitrary function $r_f(t)$, which can be approximately determined by the method described earlier. We note that the method of solving the problem for small values of η is analogous to the method of "short" waves proposed by Khristianovich[5] for treating a number of gas-dynamic problems that are physically characterized by the fact that an appreciable variation in the parameters of the gas occurs only in a narrow zone close to the front.

In the case of a self-similar problem, the first two terms of the expansion (11) give good agreement with the exact solution over the whole range $0 \leq \eta \leq 1$. The solution obtained by means of such an expansion in the case $\lambda = b = 0$, $k = 6$, is given by curve 2 of Fig. 2. Therefore the function $r_f(t)$ may be determined for such problems directly from the condition of heat balance:

$$Q_0 = 4\pi a A_1(t) r_f^3 \int_0^1 (1-\eta)^2 \left[\eta^{1/(k-1)} + \eta^{k/(k-1)} \frac{A_2}{A_1} + \cdots \right] d\eta. \tag{15}$$

It follows hence that γ_0 is given by formulas (9), in which one should set $\gamma \approx \gamma_0$:

$$\gamma_0 = 2\left[\frac{k-1}{k(3k-1)}\right]^{1/(k-1)} \left[\frac{4k^2-5k+2}{k(3k-2)} - \frac{8k^2-11k+4}{(2k-1)(4k-3)}\right]. \tag{16}$$

This value of γ_0 agrees well with the exact one. Thus, for example, for $k = 6$ we get $\gamma = 0.251$ and $\gamma_0 = 0.252$.

The approximate method just described may be made more precise if, for example, we replace T_* of Eqs. (3) and (5) with an expression for T which takes into account the variation of temperature in the zone near the wave front.

By the method described above we can also investigate the problem arising when both the internal energy and the range of radiation are expressed by formulas that contain several terms.

The author expresses his sincere gratitude to A. S. Kompaneets for valuable remarks.

---

[1] Ia. B. Zel'dovich and A. S. Kompaneets, Сб., посвященный 70-летию А. Ф. Иоффе (Collection dedicated to A. F. Ioffe on his Seventieth Birthday), Acad. of Sci. Press, 1950.

[2] Ia. B. Zel'dovich and Iu. P. Raiser, Usp. Fiz. Nauk **63**, 613 (1957).

[3] V. V. Selivanov and I. Ia. Shliapintokh, J. Phys. Chem. **32**, 670 (1958).

[4] G. I. Barenblatt, Прикладная математика и механика (Appl. Math. and Mech.) **18**, 351 (1954).

[5] S. A. Khristianovich, Прикладная математика и механика (Appl. Math. and Mech.) **20**, 599 (1956).

Translated by G. Volkoff
75

SOVIET PHYSICS JETP VOLUME 35(8), NUMBER 2 FEBRUARY, 1959

DISPERSION RELATIONS IN NON-RELATIVISTIC SCATTERING THEORY

L. D. FADDEEV

Leningrad State University

Submitted to JETP editor March 16, 1958

J. Exptl. Theoret. Phys. (U.S.S.R.) **35**, 433-439 (August, 1958)

It is proposed that the dispersion relations for the scattering amplitude for potential scattering be deduced by studying the Green's function of the total Hamiltonian. The method is illustrated for the case of a three-dimensional non-relativistic equation for scattering from a fixed center. The relations previously obtained by Wong and Khuri are derived rigorously. The existence of dispersion relations is related to the problem of a complete description of the S matrix for various potential scattering equations.

SEVERAL recent papers appeared again to direct attention to the properties of the S matrix elements for complex energies in the non-relativistic theory.[1,2] It seems that, contrary to the previous work of van Kampen,[3] it is not necessary to require the validity of any special principle of causality. The locality of the potential in position space guarantees all properties necessary for a derivation of the dispersion relations.

The dispersion relations are derived in the paper of Wong[1] under the assumption that the perturbation expansion converges. This is too much of a restriction. The derivation of Khuri is based on the Fredholm theory for the integral equation of the scattering theory developed by Jost and Pais.[4] This involves a rather unwieldy mathematical apparatus; furthermore, the paper of Jost and Pais contains an incorrect proof of the assertions used by Khuri.

We propose a comparatively simple derivation of the dispersion relations based on the properties of the Green's function of the total Hamiltonian. The derivation is general and applies to an arbitrary potential scattering equation if the behavior of the corresponding Green's function is known. Our discussion uses the example of scattering from a three-dimensional center. The corresponding Green's function was investigated by Povzner.[5,6] The asymptotic behavior of this function for high energies was investigated by the author.[7,8]

The second part of the paper contains some considerations of mathematical character, which may be useful in discussing the possibilities for applying the dispersion relations.

1. DERIVATION OF THE DISPERSION RELATIONS FOR THE SCATTERING FROM A THREE-DIMENSIONAL CENTER

As is known, for the existence of a dispersion relation of the non-relativistic type

$$\mathrm{Re}\, f(E) = \frac{1}{\pi}\, \mathrm{P} \int_0^\infty \frac{\mathrm{Im}\, f(E')}{E'-E}\, dE' + \sum_j \frac{d_j}{E-E_j}, \qquad (1)$$

$$0 \leqslant E < \infty,$$

for the amplitude $f(E)$, the following properties of $f(E)$ are sufficient:

(a) $f(E)$ is the limiting value on the positive real axis of a function which is analytic in the plane of the complex variable E with a cut along the positive real axis, except for a finite number of points E_j on the negative real axis, where the function may have simple poles with real residues d_j;

(b) $f(E + i0) = f^*(E - i0)$;

(c) for large $|E|$, $f(E) \to 0$.

We consider the matrix element of the T matrix

$$T_{ab} = \langle \Phi_a | V | \Psi_b^{(+)} | \rangle, \quad E_a = E_b. \qquad (2)$$

Here Φ_a is an eigenfunction of the free Hamiltonian H_0, and $\Psi_a^{(+)}$ is a solution of the integral equation of the scattering theory

$$\Psi_a^{(+)} = \Phi_a - G_0(E_a + i0)\, V \Psi_a^{(+)}. \qquad (3)$$

Here $G_0(E)$ is the Green's function of the free Hamiltonian.

Instead of Eq. (3) we shall use the representation of the function $\Psi_a^{(+)}$ in terms of the Green's function of the total Hamiltonian $H = H_0 + V$:

$$\Psi_a^{(+)} = \Phi_a - \lim_{\varepsilon\to 0} G(E_a + i\varepsilon) V \Phi_a. \qquad (4)$$

For complex energies, $G(E)$ is the solution of the equation

$$G(E) = G_0(E) - G_0(E) V G(E). \qquad (5)$$

This expression we now use in writing down the elements of the T matrix:

$$T_{ab} = \langle \Phi_a | V | \Phi_b | - \lim_{\varepsilon\to 0} \langle \Phi_a | V G(E_a + i\varepsilon) V | \Phi_b \rangle. \qquad (6)$$

For scattering from a three-dimensional center, where

$$H_0 = -\nabla^2, \quad V = \delta^3(\mathrm{x} - \mathrm{x}') V(\mathrm{x}),$$

we have:

$$\Phi_a = \frac{E_a^{1/4}}{\sqrt{2}} \left(\frac{1}{2\pi}\right)^{3/2} \exp\{i\sqrt{E_a}(\mathrm{x}, \alpha)\},$$
$$(\alpha, \alpha) = 1; \; G_0(E) = \frac{\exp\{i\sqrt{E}\,|\mathrm{x} - \mathrm{x}'|\}}{4\pi\,|\mathrm{x} - \mathrm{x}'|} \qquad (7)$$

The functions $\Psi_a^{(+)}$ depend on the same parameters as Φ_a, i.e.,

$$\Psi_a^{(+)} = \Psi(\mathrm{x};\; E_a, \alpha). \qquad (8)$$

We consider the resolvent $G(E) = G(\mathbf{x}, \mathbf{x}', E)$. In the following we shall assume that the potential satisfies the condition

$$|V(\mathrm{x})| \leqslant C / |\mathrm{x}|^{3+\varepsilon}, \; \varepsilon > 0. \qquad (9)$$

Povzner, investigating the integral equation (5), obtained the following properties* of the function $G(\mathbf{x}, \mathbf{x}', E)$:

(1) The function $G(\mathbf{x}, \mathbf{x}', E)$ is analytic in the complex plane of E with a cut along the positive real axis, except for a finite number of points E_j on the negative real axis and, possibly at the origin, where it has simple poles. The points E_j correspond to discrete eigenvalues and

$$\operatorname{Res} G(\mathrm{x}, \mathrm{x}', E)|_{E=E_j} = \sum_k \psi_k(\mathrm{x}) \psi_k(\mathrm{x}'), \qquad (10)$$

where $\psi_k(\mathbf{x})$ are orthonormal eigenfunctions corresponding to the eigenvalue E_j.

(2) The limit

$$\lim_{\varepsilon\to 0} G(\mathrm{x}, \mathrm{x}', E + i\varepsilon), \quad \varepsilon > 0$$

exists for all $E > 0$, with the exclusion, perhaps, of a finite number of points $E_i > 0$, for which the homogeneous equation

$$u = G_0(E_i + i0) V u \qquad (11)$$

has a non-trivial solution. At these points $G(\mathbf{x}, \mathbf{x}', E)$ has a singularity of type

$$G(\mathrm{x}, \mathrm{x}', E) \sim \sum u_k(\mathrm{x}) u_k(\mathrm{x}') / (E - E_i),$$

where $u_k(\mathbf{x})$ are linearly independent solutions of equation (11). These solutions satisfy the requirement

$$\int \exp\{i\sqrt{E_i}(\mathrm{x}, \alpha)\} V(\mathrm{x}) u(\mathrm{x})\, d\mathrm{x} = 0 \qquad (12)$$

for arbitrary α, $(\alpha, \alpha) = 1$.

We note here that the values $E > 0$ for which equation (11) has non-trivial solutions correspond to a positive discrete spectrum, the absence of which has so far not been rigorously proven for a potential satisfying only condition (9). It is precisely this point which has been treated incorrectly in the paper of Jost and Pais. From their considerations it follows only that the solutions of Eq. (11) satisfy condition (12), but it does not follow that $u = 0$.

(3) The following condition is satisfied:

$$G(\mathrm{x}, \mathrm{x}', E + i0) = G^*(\mathrm{x}, \mathrm{x}', E - i0). \qquad (13)$$

The behavior of $G(\mathbf{x}, \mathbf{x}', E)$ for large $|E|$ was investigated by the author.

(4) From the results of references 7 and 8 it follows that

$$\left| G(\mathrm{x}, \mathrm{x}', E) - \frac{1}{4\pi} \frac{\exp\{i\sqrt{E}\,|\mathrm{x} - \mathrm{x}'|\}}{|\mathrm{x} - \mathrm{x}'|} \right| \leqslant C_E$$
$$\times \exp\{-\operatorname{Im}\sqrt{E}\,|\mathrm{x} - \mathrm{x}'|\}, \qquad (14)$$

where $C_E \to 0$ for $|E| \to \infty$.

The properties (1) to (4) are sufficient for the derivation of the dispersion relations. We consider the forward scattering amplitude:

$$T_{aa} = \left(\frac{1}{2\pi}\right)^3 \frac{\sqrt{E}}{2} \int V(\mathrm{x})\, d\mathrm{x} - \frac{\sqrt{E}}{2} \left(\frac{1}{2\pi}\right)^3 \frac{1}{4\pi}$$
$$\int e^{i\sqrt{E}(\mathrm{x}, \alpha)} V(\mathrm{x}) G(\mathrm{x}, \mathrm{x}', E) V(\mathrm{x}') e^{-i\sqrt{E}(\mathrm{x}', \alpha)} d\mathrm{x}\, d\mathrm{x}'. \qquad (15)$$

Using the obvious estimate

$$|\exp\{i\sqrt{E}(\mathrm{x} - \mathrm{x}', \alpha)\}| \leqslant \exp\{\operatorname{Im}\sqrt{E}\,|\mathrm{x} - \mathrm{x}'|\}$$

and relation (14), we obtain the result that the integral on the right hand side of (15) is absolutely convergent for all E of the complex plane. Due to the analyticity of the function under the integral, the integral itself is analytic in the whole plane, excluding the cut and the points of singularity of the function $G(E)$. At these points we have simple poles with the residues

---

*These results remain valid when the potential has singularities of type $\alpha/|r|^{2-\varepsilon}$ at a finite distance. The integral condition of Khuri is equivalent to this requirement.

$$\gamma_j = \frac{i\sqrt{|E_j|}}{2}\, d_j = -\frac{i\sqrt{|E_j|}}{4}\left(\frac{1}{2\pi}\right)^4$$

$$\times \sum_k \int \exp\{\sqrt{|E_j|}\ (\mathbf{x},\ \alpha)\}\, V(x)\, \psi_k(\mathbf{x})\, d\mathbf{x}$$

$$\times \int \exp\{-\sqrt{|E_j|}(\mathbf{x}', \alpha)\}\, V(\mathbf{x}')\, \psi_k(\mathbf{x}')\, d\mathbf{x}'.$$

Since the eigenfunctions can be chosen to be real, the d_j are real.

There are no singularities on the cut due to property (12).

Thus, the function

$$f(E) = \frac{2}{\sqrt{E}}\left[T_{aa} - \frac{\sqrt{E}}{2}\left(\frac{1}{2\pi}\right)^3 \int V(\mathbf{x})\, d\mathbf{x}\right] \tag{16}$$

has been shown to have the property (a). Furthermore, property (b) for $f(E)$ follows from property (13) for $G(\mathbf{x}, \mathbf{x}', E)$. Finally, one can show with the help of (14) that $f(E)$ also has the property (c). From this there follows a dispersion relation of type (1) for the function $f(E)$, which can also be written in terms of the forward scattering amplitude.

Similar considerations apply for the scattering amplitude with fixed transferred momentum τ. In this case condition (9) is not sufficient, and we must require that

$$|V(\mathbf{x})| \leqslant C|x|^{-3-\varepsilon} \exp(-\tau|\mathbf{x}|/2), \quad \varepsilon > 0$$

(cf. reference 2 on this point).

2. DISCUSSION OF THE DISPERSION RELATIONS

In the above derivation it was evident that we did not require any special causality conditions, except for the locality of the potential in position space, for the existence of dispersion relations in the case of scattering from a three-dimensional center. The locality of the potential apparently plays the same role in the non-relativistic theory as the requirement of microscopic causality in field theory.

We add a number of formal considerations, which may be useful for an analysis of the reasons for the existence of dispersion relations, and of the possibilities for applying them.

In non-relativistic scattering problems in which dispersion relations appear, the situation is such that the complete S matrix of the system is a function of a greater number of variables than the potential. The general requirements which the S matrix has to fulfil, such as unitarity and symmetry, do not sufficiently lower the number of variables. For example, for scattering from a three-dimensional center, the S matrix is a complex function of the energy E, $0 \leq E < \infty$, and of two unit vectors defining the directions of the incident and the scattered particles, while the potential is a real point function in three-dimensional space, i.e., a function of the radius r, $0 \leq r < \infty$, and of one unit vector.

The requirements of symmetry and unitarity lead to the possibility of expressing the S matrix elements through a real and symmetric function of the energy and two unit vectors. For example, one can use the representation of the S matrix in terms of the K matrix:

$$S = (1 + iK)(1 - iK)^{-1}. \tag{17}$$

But this function still depends on a greater number of parameters than the potential. An analogous situation obtains even for the scattering from a one-dimensional potential barrier. In this case the S matrix is a 2×2 unitary and symmetric matrix

$$S(E) = \begin{pmatrix} a(E) & b(E) \\ b(E) & c(E) \end{pmatrix}, \tag{18}$$

consisting of the coefficients for reflection to the right and to the left, $a(E)$ and $c(E)$, and the transmission coefficient, $b(E)$. The requirements of symmetry and unitarity lead to the possibility of expressing all S matrix elements by three real functions of E, $0 \leq E < \infty$, for example, by $a(E)$ and the argument of the function $b(E)$, while the potential is a real function of the variable x, $-\infty < x < \infty$, which may be regarded as two real functions of a variable going from 0 to ∞.

Since the potential determines the S matrix uniquely, it is natural to expect that in these cases there exist additional relations between the S matrix elements, which lower the number of variables on which these elements depend. The dispersion relations are examples for such connections. This is particularly clear in the example of scattering from a one-dimensional barrier. In this case an analysis similar to that of part 1 shows that the transmission coefficient $b(E)$ is the limiting value of a function which is analytic in the cut plane of E and has simple poles at points corresponding to a discrete spectrum. For large $|E|$

$$b(E) = 1 + O(|E|^{-1/2}), \qquad b(E + i0) = b^*(E - i0).$$

Thus, conditions (a), (b), and (c) are satisfied for the function $f(E) = b(E) - 1$, and thus there exists a relation of type (1). It is more convenient to consider the function $g(E) = \ln b(E)$. We obtain a relation for it which in terms of $b(E)$ has the form:

$$\arg b(E) = \frac{1}{\pi} P \int \frac{\ln|b(E')|}{E'-E} dE' + 2\sum_j \arctan\left(\frac{|E_j|}{E}\right)^{1/2}. \qquad (19)$$

Relation (19) allows us to construct the whole S matrix from the reflection coefficient $a(E)$. Indeed, from the unitarity requirement we have

$$|b(E)| = (1-|a(E)|^2)^{1/2}; \qquad c^*(E) = -a(E)\, b^*(E)/b(E). \qquad (20)$$

We determine $\arg b(E)$ from formula (19), and we obtain $b(E)$ and $c(E)$.

In the three-dimensional case the relation introduced for T_{aa} does not sufficiently reduce the number of parameters. There must exist a whole series of additional relations, possibly of a completely different type. Here it is interesting to note a result of Wong and Toll.[9] For a spherically symmetric potential they obtain the result that, together with the forward scattering amplitude

$$f_0 = \sum_{l=0}^{\infty} (2l+1)[S_l(E)-1] \qquad (21)$$

the expressions

$$f_n(E) = \left(\frac{1}{E}\right)^n \sum_{l=n}^{\infty} (2l+1)\frac{(l+n)!}{(l-n)!}[S_l(E)-1] \qquad (22)$$

have properties of types (a), (b), and (c). Hence there exists an infinite system of relations connecting all $S_l(E)$. Here it appears that only one function among all the $S_l(E)$ can be taken independently. Under the assumption that the perturbation theory converges, all $S_l(E)$ can then be expressed through $S_0(E)$.

The above examples show that if the potential depends on less parameters than the S matrix, then there exist a whole series of relations between its elements, which reduce the number of variables on which the S matrix depends. On the other hand, in the one-dimensional case, where the S matrix is a simple function with modulus one $[S(E) = \exp\{2i\delta(E)\}$, where $\delta(E)$ is a real function of $E]$ and where the potential also depends on one variable going from 0 to ∞, relations of this type do not exist. Indeed, it follows from the theory of the reverse problem adapted to this case by Krein and Marchenko,[10, 11] that for every function $S(E)$ such that $|S(E)| = 1$, $S(0) = \pm 1$, and $S(E) - 1 \to 0$ for $E \to \infty$ sufficiently fast, one can find a potential, which is local in position space, and for which $S(E)$ is the S function. Thus the S function corresponding to a potential which is not subject to any requirements except that of locality (and, of course, to the requirements which guarantee the existence of the S function, e.g., the decrease like $1/r^{2+\epsilon}$ for $r \to \infty$) cannot satisfy any relations of the dispersion type. We note here that our assertions do not contradict the results of van Kampen,[3] since the causality principle, which is the basis for his derivation of the dispersion relations, is equivalent to the assumption that the potential vanishes outside a finite interaction range. As is known, $\tilde{S}(E) = S(E)\exp(2iE^{1/2}a)$ satisfies the dispersion relation if $V(r) = 0$ for $r > a$.

Analogous considerations lead to the result that, in the case of scattering from a one-dimensional barrier, the relation (19) is the only relation, except for the requirements of symmetry and unitarity, to which the elements of the S matrix may be subject. Indeed, an investigation of the reverse problem, conducted for this case by Moses[12] and the author,[13] shows that for every function $a(E)$ such that $|a(E)| < 1$, except at $E = 0$, where possibly $a(0) = -1$, and such that $a(E) \to 0$ for $E \to \infty$, one can find a potential for which the matrix constructed from $a(E)$ with the help of formulas (19) and (20) is the S matrix.

Finally, the relations of Toll and Wong for the case of a three-dimensional spherically symmetric potential also are a complete system of relations in the sense that, if there exists a system of functions $S_l(E)$ subject to the conditions resulting from the analyticity properties (22), then it is possible to construct a spherically symmetric potential for which this system is a system of eigenvalues of the S matrix.

This last result shows that any relations between the S matrix elements which may later be introduced are consequences of the relations of Toll and Wong, although they may be different in form. This does not mean that the relations of Toll and Wong are the most convenient system. This system has a whole series of deficiencies. Firstly, one must require the fast decrease of the potential for $r \to \infty$ to guarantee the convergence of the series of type (22). Thus, for the convergence of the series determining f_n it is necessary that the integral $\int_0^\infty r^{2n+1}|V(r)|dr$ converge; thus, for f_n to have a meaning, the potential has to decrease faster than r^{-m} for arbitrary m. Interpreting the summation in (22) in some general sense, we can justify the relation of the Toll-Wong type also for an arbitrary potential (which decreases faster than $1/r^2$), but this has not yet been done. Secondly, it is not clear what the analogous relations in the spherically non-symmetric case look like. Therefore, one wishes to find possibly a new system of relations, which is valid also in the general case. In this connection it is interesting to note a paper by Moses,[14] in which a formal procedure is developed for the construction of a potential from the known backward scattering amplitude for all energies and all directions of the incident particles over a hemisphere. Moses points out the analogy between these data and the reflection coefficient in the case of a uni-dimensional barrier. It is of interest to note that these data consist of two real functions of the parameter E and a unit vector describing a hemisphere, while the potential depends on the parameter r and on a unit vector describing a full sphere.

---

[1] D. J. Wong, Phys. Rev. **107**, 302 (1957).
[2] N. N. Khuri, Phys. Rev. **107**, 1148 (1957).
[3] N. G. van Kampen, Phys. Rev. **91**, 1267 (1953).
[4] R. Jost and A. Pais, Phys. Rev. **82**, 840 (1951).
[5] A. Ia. Povzner, Матем. сб. (Math. Collection) **32** (74), 1 (1953).
[6] A. Ia. Povzner, Dokl. Akad. Nauk SSSR **104**, 360 (1955).
[7] L. D. Faddeev, Вестник ЛГУ (Bulletin Leningrad State University) **7**, 126 (1956).
[8] L. D. Faddeev, Вестник ЛГУ (Bulletin Leningrad State University) **7**, 166 (1957).
[9] D. J. Wong and J. S. Toll, Annals of Phys. **1**, 91 (1957).
[10] M. G. Krein, Dokl. Akad. Nauk SSSR **105**, 433 (1955).
[11] V. A. Marchenko, Dokl. Akad. Nauk SSSR **104**, 695 (1955).
[12] I. Kay and H. E. Moses, Nuovo cimento **3**, 276 (1956).
[13] L. D. Faddeev, Dokl. Akad. Nauk SSSR (in press).
[14] H. E. Moses, Phys. Rev. **102**, 559 (1956).

Translated by R. Lipperheide
76

SOVIET PHYSICS JETP VOLUME 35(8), NUMBER 2 FEBRUARY, 1959

ROTATIONAL STATES OF NONAXIAL NUCLEI

A. S. DAVYDOV and G. F. FILIPPOV

Moscow State University

Submitted to JETP editor March 17, 1958

J. Exptl. Theoret. Phys. (U.S.S.R.) **35**, 440-447 (August, 1958)

A theory is developed for the energy states of nuclei which have no axial symmetry, and for the electromagnetic transitions between these states. It is shown that the breakdown of axial symmetry, though it does not appreciably change the rotational states from those for axial nuclei, leads to the appearance of new energy states. Comparison of theory with experiment shows that the so-called γ-vibrational levels of even-even nuclei should be regarded as rotational levels. The levels of some nuclei with the spin sequence 0, 2, 2, 3 should be assigned to this same type.

INTRODUCTION

ON the basis of the uniform nuclear model of A. Bohr and Mottelson,[5,6] the present authors have investigated[1-4] the energy levels of nonspherical nuclei corresponding to collective excitations in which there is no breakdown of the axial symmetry of the nucleus. It was shown that the rotation-vibration energy of the collective excited states of the nucleus is a function of only two parameters — the frequency of the surface oscillations of the nucleus and the ratio of the equilibrium deformation to the amplitude of the zero-point vibrations. The question naturally arises as to the extent to which these results remain valid when one takes account of possible breakdown of axial symmetry of the nucleus.

The question of the breakdown of axial symmetry of the nucleus has already been discussed qualitatively in some papers.[5,7,8] Recently it has even become customary (cf. for example references 9 and 10) to assign certain excited nuclear states to the so-called γ-vibrations. Such an assignment is usually based on the values of the spins of the levels and the occurrence of a high probability for electromagnetic transitions, which confirms the collective nature of the levels. No quantitative theory of γ vibrations exists.

In the present paper we investigate the energy levels corresponding to rotation of the nucleus without change of its internal state. It will be shown that, with the breakdown of axial symmetry of even-even nuclei, the rotational spectrum corresponding to the axial nucleus is changed comparatively little but that new rotational states with total angular momentum $J = 2, 3, 4 \ldots$ appear. For small deviations from axial symmetry these levels lie very high and are not excited, but with increasing deviation from axial symmetry some of the additional levels are lowered appreciably. So, for example, the ratio of the second excited level with spin 2 to the first level, which is also present in an axial nucleus, changes from infinity to two. The probabilities of electromagnetic transitions between rotational states of nonaxial nuclei are calculated in Sec. 2. From a comparison of the theory with experimental data (Sec. 3) one can conclude that the properties of the experimentally observed energy states of even-even nuclei are satisfactorily explained if one assumes that these nuclei do not have axial symmetry.

1. ROTATIONAL LEVELS OF NONSPHERICAL EVEN-EVEN NUCLEI

On the basis of the uniform model, let us consider the nuclear levels corresponding to rotation of the nucleus as a whole without change of its internal state. The operator for the rotational energy of the nucleus has the form

$$H = \frac{A}{2}\sum_{\lambda=1}^{3}\frac{\hat{J}_\lambda^2}{\sin^2(\gamma - 2\pi\lambda/3)}, \qquad (1.1)$$

where $A = \hbar^2/4B\beta^2$ is a quantity having the dimensions of an energy; γ varies between 0 and $\pi/3$ and determines the deviation of the shape of the nucleus from axial symmetry; the $\hat{J}_\lambda$ are the operators for the projections of the angular momentum of the nucleus on the axes of a coordinate system fixed in the nucleus. The commutation rules for these operators differ from those for the corresponding operators relative to a fixed coordinate system by a change in sign of their right-hand side.

According to (1.1), for $\gamma \neq 0$ or $\pi/3$ the nucleus should be treated as an asymmetric top. In the stationary states of the asymmetric top, none of the projections of the total angular momentum on the axes 1, 2, 3 of the coordinate system fixed in the nucleus can have definite values, so that the energy levels cannot be classified by means of the value of $K = J_3$. In the asymmetric top there are $2J + 1$ different energy levels for each value of the total angular momentum. These levels can be classified in terms of the irreducible representations of the group D_2 (with symmetry elements C_2^1, C_2^2, C_2^3, corresponding to rotation through π around each of the coordinate axes 1, 2, 3), since the operator (1.1) and the commutation relations of the $\hat{J}_\lambda$ are invariant under this group of transformations. Thus the energy levels of the asymmetric top split into four types, corresponding to the four irreducible representations of the group D_2 (cf. reference 11, § 101, and reference 12).

In the case of even-even nuclei, of the $2J + 1$ different energy levels with given J, only those can occur which correspond to the completely symmetric representation of D_2. For $J = 1$, there are no rotational levels of the required symmetry. For $J = 2$ there are two such states, there is one for $J = 3$, three for $J = 4$, two for $J = 5$, four for $J = 6$, etc.

If we express the energy in units of A, the energies of the two states that have the required symmetry for $J = 2$ are given by

$$\varepsilon_1(2) = \frac{9\left(1 - \sqrt{1 - {}^8/_9 \sin^2 3\gamma}\right)}{\sin^2 3\gamma}, \qquad \varepsilon_2(2) = \frac{9\left(1 + \sqrt{1 - {}^8/_9 \sin^2 3\gamma}\right)}{\sin^2 3\gamma} \qquad (1.2)$$

The energy levels with angular momentum $J = 3$ are given by the formula

$$\varepsilon(3) = \sum_{\lambda=1}^{3} 2/\sin^2\left(\gamma - \frac{2\pi}{3}\lambda\right) = 18/\sin^2 3\gamma. \qquad (1.3)$$

The three energy levels with spin 4 are determined by the roots of the cubic equation

$$\varepsilon^3 - \frac{90}{\sin^2 3\gamma}\varepsilon^2 + \frac{48}{\sin^4 3\gamma}[27 + 26\sin^2 3\gamma]\,\varepsilon - \frac{640}{\sin^4 3\gamma}[27 + 7\sin^2 3\gamma] = 0.$$

The two energy levels with spin 5 are given by

$$\varepsilon_\tau(5) = [45 \pm 9\sqrt{9 - 8\sin^2 3\gamma}]/\sin^2 3\gamma. \qquad (1.4)$$

In (1.4), $\tau = 1$ for the minus sign on the square root and $\tau = 2$ for the plus sign. The energy of the rotational states with angular momentum equal to six is determined from the solution of a quartic equation which we shall not give here.

From (1.2) and (1.3) we get the simple relation

$$\varepsilon_1(2) + \varepsilon_2(2) = \varepsilon(3), \qquad (1.5)$$

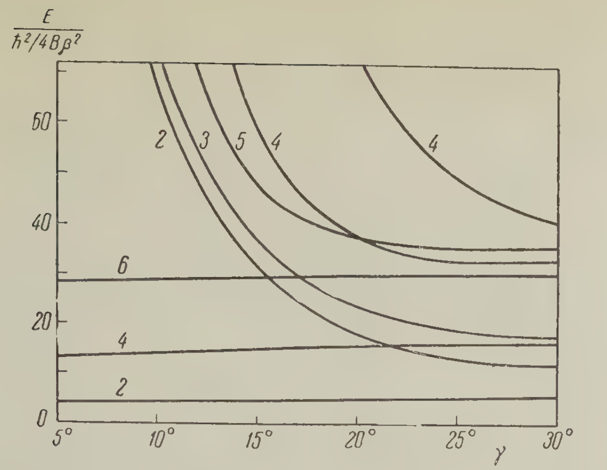

which relates the energies of the levels with spins 2 and 3.

The energy levels of even-even nuclei, calculated on the basis of these formulas, are shown in the figure as functions of the parameter γ. For $\gamma = 0$, the energy spectrum coincides with that for an axially symmetric nucleus. For fixed β, the breakdown of the axial symmetry leads to an increase in energy of the levels which occur in the axial nucleus. This increase in energy corresponds to a reduction of the effective nuclear momentum of inertia or the effective deformation parameter β_{eff}. For the first excited state with spin 2, the effective deformation parameter can be defined by the formula

$$\beta_{\text{eff}} = \beta\left(\frac{4\sin^2 3\gamma}{9 - \sqrt{81 - 72\sin^2 3\gamma}}\right)^{1/2}$$

In addition to the comparatively small change in energy of those levels which occur in axially symmetric nuclei, the breakdown of axial symmetry results in the appearance of new energy levels $\epsilon_2(2)$, $\epsilon(3)$, $\epsilon_2(4), \ldots$. By using the dependence of $\epsilon_2(2)/\epsilon_1(2)$ on γ, one can from the experimental value of this ratio determine the appropriate value of γ.

Then we can use the figure to determine the sequence of spins and energies of the other collective levels of the nucleus. Comparison of the theory with experimental data will be made in Sec. 3.

2. ELECTROMAGNETIC TRANSITIONS BETWEEN ROTATIONAL STATES OF NUCLEI

It is well known that measurements of probabilities of transitions between nuclear states enables one to obtain valuable information concerning the nature of the excited states. In particular, to clarify the nature of the second excited 2^+ state in even-even nuclei, one can study the relative probability of transitions from this level directly to the ground state (0^+) and to the first excited 2^+ state. It has been assumed in various papers that the first two experimentally observed levels with spin 2 correspond to one-phonon and two-phonon oscillation of the nuclear surface. Then the transition from the second spin 2 level to the ground state can occur only because of breakdown of the oscillator approximation. However no one has as yet succeeded in giving a quantitative estimate of this effect.

Starting from the assumption that both of the spin-2 levels are to be assigned as rotational levels, we shall calculate the ratio of the reduced probabilities for the transitions $\epsilon_2(2) \rightarrow \epsilon_1(2)$ and $\epsilon_2(2) \rightarrow \epsilon(0)$ as a function of the parameter γ and, consequently, as a function of the ratio $\epsilon_2(2)/\epsilon_1(2)$, since the latter depends on γ.

To calculate the probability of E2 transitions between rotational states we must express the nuclear quadrupole moment operator

$$\hat{Q}_{2\mu} = 2e\sqrt{4\pi/5}\sum_{i=1}^{Z} r_i^2\, Y_{2\mu}(\vartheta_i\varphi_i)$$

in terms of the Euler angles which determine the orientation of the nucleus and the collective coordinates measured relative to axes fixed in the nucleus. Making use of the transformation

$$Y_{2\mu}(\vartheta\varphi) = \sum_{\nu} D^2_{\mu\nu}(\theta)\, Y_{2\nu}(\vartheta'\varphi')$$

of the spherical functions when we go to a coordinate system fixed in the nucleus, and expressing the proton coordinates r, ϑ_i, φ_i in this system (assuming that they are uniformly distributed inside the nucleus) in terms of collective coordinates a_ν, where

$$a_0 = \beta\cos\gamma,\ a_1 = a_{-1} = 0,\ a_2 = a_{-2} = \frac{\beta}{\sqrt{2}}\sin\gamma,$$

we can use the formula

$$a_\nu = \frac{4\pi}{Z}\sum_{i=1}^{Z}\left(\frac{r_i}{R}\right)^2 Y_{2\nu}(\vartheta_i'\varphi_i'),$$

to obtain the following expression for the μ-th component of the electric quadrupole-moment operator:

$$\hat{Q}_{2\mu} = eQ_0\left(D^2_{\mu 0}\cos\gamma + \frac{1}{\sqrt{2}}(D^2_{\mu 2} + D^2_{\mu,-2})\sin\gamma\right), \quad (2.1)$$

where

$$Q_0 = 3ZR^2\beta/\sqrt{5\pi} \quad (2.2)$$

is the intrinsic quadrupole moment of an axial nucleus with deformation parameter β; $D^2_{\mu\nu}$ are generalized spherical functions, dependent on the Euler angles, determine the unitary transformation from the coordinate system fixed in space to the coordinate system fixed in the nucleus.

The wave functions of the rotational states of the nonaxial nucleus which we want can be written in the form

$$\begin{aligned}\psi_{001} &= (1/8\pi^2)^{1/2}\varphi(\beta\gamma),\\ \psi_{2m1} &= (5/8\pi^2)^{1/2}\varphi(\beta\gamma)\left[a_1D^2_{m0}+\frac{b_1}{\sqrt{2}}(D^2_{m2}+D^2_{m,-2})\right],\\ \psi_{2M2} &= (5/8\pi^2)^{1/2}\varphi(\beta\gamma)\left[a_2D^2_{M0}+\frac{b_2}{\sqrt{2}}(D^2_{M2}+D^2_{M,-2})\right],\end{aligned} \tag{2.3}$$

where $\varphi(\beta\gamma)$ is a function describing the internal state of the nucleus, which is assumed to be the same in all three rotational states;

$$\begin{aligned}a_1N_1 &= -[\sqrt{9-8\sin^2 3\gamma}+\sin\gamma\sin 3\gamma+3\cos\gamma\cos 3\gamma],\\ b_1N_1 &= 3\sin\gamma\cos 3\gamma-\cos\gamma\sin 3\gamma,\\ N_1^2 &= 2\sqrt{9-8\sin^2 3\gamma}\,[\sqrt{9-8\sin^2 3\gamma}\\ &\quad+\sin\gamma\sin 3\gamma+3\cos\gamma\cos 3\gamma],\\ a_2N_2 &= \sqrt{9-8\sin^2 3\gamma}-\sin\gamma\sin 3\gamma-3\cos\gamma\cos 3\gamma,\\ b_2N_2 &= 3\sin\gamma\cos 3\gamma-\cos\gamma\sin 3\gamma,\\ N_2^2 &= 2\sqrt{9-8\sin^2 3\gamma}\,[\sqrt{9-8\sin^2 3\gamma}\\ &\quad-\sin\gamma\sin 3\gamma-3\cos\gamma\cos 3\gamma].\end{aligned} \tag{2.4}$$

As already mentioned, γ varies between the limits 0 and $\pi/3$ and determines the deviation of the nucleus from axial symmetry. The axes of the ellipsoid by means of which the shape of the nucleus is approximated are expressed in terms of γ by means of the formulas

$$R_\lambda = R\,[1+\beta\sqrt{5/4\pi}\cos(\gamma-2\pi\lambda/3)],\quad \lambda=1,2,3.$$

For $\gamma = 0$, the nucleus is a prolate ellipsoid of rotation with symmetry axis along 3. For $\gamma = \pi/3$, the nucleus is an oblate ellipsoid with symmetry axis along 2. The rotational states as determined by the operator (1.1), and the probabilities of electromagnetic transitions between them are the same for values of γ equal to γ_1 and $\pi/3 - \gamma_1$. We therefore give all quantities only in the interval $0 \leq \gamma \leq \pi/6$.

In connection with the above, it should be remarked that the measurement of energies of rotational states and of electromagnetic transitions between them cannot give any indication as to whether the nucleus is a prolate or an oblate ellipsoid. The answer to this question could be obtained by measurement of average values of electric quadrupole moments in stationary states $(J;\ M = J)$. In even-even nuclei, the average values of electric quadrupole moments in the ground state $(J = 0)$ are zero. In the first excited state with spin 2 the average value of the quadrupole moment is

$$Q_1 = -Q_0\,6\cos 3\gamma/7\sqrt{9-8\sin^2 3\gamma},$$

where Q_0 is defined in (2.2). The average electric quadrupole moment of the second excited state with spin 2 has the opposite sign: $Q_2 = -Q_1$.

The reduced probability for an electric quadrupole transition $(J\tau) \rightarrow (J'\tau')$, averaged over initial states of polarization of the nucleus, is

$$B(E2;\,J\tau\rightarrow J'\tau') = \frac{5}{16\pi(2J+1)}\sum_{M,m,\mu}|(J'm\tau'|\,\hat{Q}_{2\mu}\,|JM\tau)|^2. \tag{2.5}$$

Since we are assuming that there is no change in the internal state of the nucleus in the transition, the reduced transition probability can be expressed in terms of average values of β and γ in the state $\varphi(\beta, \gamma)$. Substituting (2.3) in (2.5) and using (2.4), we find the following values for the reduced probabilities of electric quadrupole transitions, expressed in units of $e^2Q_0^2/16\pi$ which is the reduced probability for electric quadrupole transition in an axially symmetric nucleus between rotational states with spins 2 and 0:

$$b(E2;\,21\rightarrow 0) = \frac{B(E2;\,21\rightarrow 0)}{(e^2Q_0^2/16\pi)} = \frac{1}{2}\left[1+\frac{3-2\sin^2 3\gamma}{\sqrt{9-8\sin^2 3\gamma}}\right]; \tag{2.6}$$

$$b(2E;\,22\rightarrow 0) = \frac{1}{2}\left[1-\frac{3-2\sin^2 3\gamma}{\sqrt{9-8\sin^2 3\gamma}}\right]; \tag{2.7}$$

$$b(E2;\,22\rightarrow 21) = \frac{10}{7}\,\frac{\sin^2 3\gamma}{9-8\sin^2 3\gamma}. \tag{2.8}$$

In Table I we give, for several values of γ, the ratio $\epsilon_2(2)/\epsilon_1(2)$, the values of the reduced probabilities of the transitions (2.6) to (2.8) and the ratio of the reduced probabilities of the electric quadrupole transitions $b(E2;\,22\rightarrow 21)/b(E2;\,22\rightarrow 0)$. From the data of Table I it follows that with the breakdown of axial symmetry of the nucleus, the reduced probability of the transition from the first excited level to the ground state changes little. The reduced probability (2.7) of the transition from the second excited level with spin 2 directly to the ground state is equal to zero for $\gamma = 0$ and 30°, and for $\gamma = 15 - 24°$ amounts to approximately 5 to 7% of the probability of the corresponding transition between the first excited state and the ground state. The reduced probability of the E2 transition from the second excited state with spin 2 to the first excited level is very small for $\gamma \approx 0$, but it then increases rapidly and in the region of $\gamma \sim 20°$ it amounts to approximately 40%, in the region $\gamma \sim 30°$ to approximately 140% of the reduced probability of the ground state

TABLE I

$\gamma°$	$\frac{\varepsilon_2(2)}{\varepsilon_1(2)}$	$b(E2;\ 21 \to 0)$	$b(E2;\ 22 \to 0)$	$b(E2;\ 22 \to 21)$	$\frac{b(E2;\ 22 \to 21)}{b(E2,\ 22 \to 0)}$
0	∞	1.000	0	0	1.43
5	64.2	0.993	0.0074	0.011	1.49
10	15.9	0.972	0.028	0.051	1.70
15	6.85	0.947	0.053	0.143	2.70
20	3.73	0.933	0.067	0.357	5.35
22.5	2.93	0.937	0.0625	0.563	9.02
24	2.59	0.948	0.052	0.782	15.1
25	2.41	0.955	0.0425	0.865	20.6
26	2.26	0.968	0.0324	1.01	31.2
28	2.07	0.99	0.010	1.28	126
29	2.01	0.996	0.004	1.41	363
30	2.00	1.000	0.000	1.43	∞

transition in the axial nucleus.

Especially interesting is the ratio of the reduced probabilities $b(E2;\ 22 \to 21)/b(E2;\ 22 \to 0)$, since this quantity is independent of the occupation of the level $\epsilon_2(2)$ and can be measured directly.

Using the explicit form of the wave function for the level with energy $\epsilon(3)$,

$$\psi_{3m1} = \sqrt{7/16\,\pi^2}\,\varphi(\beta\gamma)\,[D^3_{m2} - D^3_{m,-2}],$$

we can calculate the reduced probabilities (in our units) of the electric quadrupole transitions

$$b(2E; 3 \to 22) = \frac{25}{28}\left(1 + \frac{3 - 2\sin^2 3\gamma}{\sqrt{9 - 8\sin^2 3\gamma}}\right),$$

$$b(2E; 3 \to 21) = \frac{25}{28}\left(1 - \frac{3 - 2\sin^2 3\gamma}{\sqrt{9 - 8\sin^2 3\gamma}}\right).$$

The values of these probabilities and their ratio are given in Table II.

TABLE II

$\gamma°$	$b(E2:\ 3 \to 21)$	$b(E2;\ 3 \to 22)$	$\frac{b(E2;\ 3 \to 21)}{b(E2;\ 3 \to 22)}$
10	0,0132	1,77	0,0075
15	0,095	1,69	0,056
20	0,12	1,67	0,072
25	0,079	1,70	0,044
29	0,0696	1,72	0,039
30	0	1.78	0

3. COMPARISON WITH EXPERIMENT

The results obtained in the preceding sections are based on the assumption that the internal state of the nucleus is not changed during its rotation. This assumption can be satisfied only approximately, the better the farther the rotational levels are from those levels (with the same J, parity, etc) corresponding to excitation of the internal state of the nucleus.

In Table III we give experimental data on the ratio of the energy of the second level with spin 2 to the first. This ratio enables us to calculate the value of the parameter γ using formulas (1.2). Using this value of γ, we can calculate the ratio $N = b(E2;\ 22 \to 21)/b(E2;\ 22 \to 0)$ from (2.7) and (2.8). Comparison of these ratios with the experimentally observed values (column 7) shows that the theory gives a good description of the experimentally-observed marked change in the ratio of reduced probabilities when we go from one nucleus to another. Comparison of the experimental values of the sum of the energies of the two 2^+ levels with the energy of the 3^+ level, as we see from comparison of columns 4 and 5 of Table III, confirms the identity (1.5) which is demanded by the theory to within 1% for all elements except Cd^{114}, where a deviation of 5% is observed. In

TABLE III

Nucleus	$\frac{\varepsilon_2(2)}{\varepsilon_1(2)}$	$\gamma°$	Exper. (kev)		N		Reference
			$\varepsilon_2(2) + \varepsilon_1(2)$	$\varepsilon(3)$	Theoret.	Exptl.	
Pt^{192}	1,94	30	929	920,9	∞	163	[13]
Xe^{128}	2.0	30	1445	—	∞	197	[14]
Cd^{114}	2,17	26,75	1771	1860	78	77,9	[15]
Se^{76}	2,2	26.6	1760	—	68	23.5	[16]
Te^{122}	2,25	26,5	1760	—	66	78,2	[17]
Gd^{154}	8.21	13,7	1133	1140	2,0	—	[18]
W^{186}	8,08	13.9	1000	1000	2.0	—	[19]
Sm^{152}	8.9	13,48	1206	1226	1,9	1.7	[18, 22]
Dy^{160}	11	12.2	1051	1047	1,9	2,38	[10]
W^{182}	12,1	11,6	1322	1331	1.6	1,59	[20]
Pu^{238}	23,4	8,13	1074	1076	1,2	1,3—1,5	[19, 23]
Pu^{240}	23.7	8,0	1063	1060	1,2	—	[19]

the case of Cd^{114}, in the region of the second excited 2^+ level there are still three nearby levels 4^+, 0^+, 2^+, which may have an effect. From the figure we see that for $\gamma < 21.5°$, the second excited spin-2 level should lie above the 4^+ level, while it lies below for $\gamma > 21.5°$. The spin-3 level should always lie higher than the 4^+ level. These rules are satisfied for all those nuclei of Table III for which the positions of the levels with spins 2^+, 4^+, and 3^+ are known.

It is interesting to note that for $\gamma = 30°$ the theory leads to equal separations between the levels $\epsilon_1(2)$, $\epsilon_2(2)$, $\epsilon(3)$. Such an arrangement of levels also follows from the oscillator approximation for the energy of the surface oscillations. It is true that in the latter case the levels $\epsilon_2(2)$ and $\epsilon(3)$ should be degenerate with spin values 0, 2, 4, and 0, 2, 3, 4, 6, respectively.

Unfortunately there is little experimental information from which one could determine the ratio $b(E2; 3\rightarrow 21)/b(E2; 3\rightarrow 22)$. This ratio is known only for Kr^{82} and is equal to 0.016[21], which corresponds to a value of γ a little greater than 29°. The value $\gamma \sim 30°$ is in agreement with the observed value of $\epsilon_2(2)/\epsilon_1(2) = 1.9$ if we assume that the adiabatic conditions are broken down in this nucleus.

Thus a comparison of the results of the theory with the known experimental data confirm the assumption that certain even-even nuclei do not possess axial symmetry.

It should be noted that Gursky[24] in 1955, using a three-dimensional harmonic oscillator model, showed that the minimum energy of the nucleons corresponds to a nonaxial shape of the nucleus. In Fig. 6 of reference 7 the data of Gursky for the energy of the nucleons in the nucleus with $Z = 55$ and $N = 91$ are shown as a function of β and γ. From the figure we see that the minimum energy corresponds to $\gamma = 7.5°$.

---

[1] G. F. Filippov, Dokl. Akad. Nauk SSSR 115, 696 (1958), Soviet Phys. "Doklady" **2**, 378 (1958).

[2] A. S. Davydov and G. F. Filippov, J. Exptl. Theoret. Phys. (U.S.S.R.) **33**, 723 (1957); Soviet Phys. JETP **6**, 555 (1958).

[3] A. S. Davydov and A. A. Chaban, J. Exptl. Theoret. Phys. (U.S.S.R.) **33**, 547 (1957); Soviet Phys. JETP **6**, 428 (1958).

[4] A. S. Davydov and B. M. Murashkin, J. Exptl. Theoret. Phys. (U.S.S.R.) **34**, 1619 (1958), Soviet Phys. JETP **7**, 1113 (1958).

[5] A. Bohr, Kgl. Danske Videnskab. Selskab Mat. fys. Medd. **26**, No. 14 (1952).

[6] A. Bohr and B. Mottelson, Kgl. Danske Videnskab. Selskab Mat. fys. Medd. **27**, No. 16 (1953).

[7] L. Wilets and M. Jean, Phys. Rev. **102**, 788 (1956).

[8] C. Marty, Nucl. Phys. **1**, 85 (1956); **3**, 193 (1957).

[9] Alder, Bohr, Huus, Mottelson, and Winter Revs. Modern Phys. **28**, 432 (1956).

[10] O. Nathan, Nucl. Phys. **4**, 125 (1957).

[11] L. D. Landau and E. M. Lifshitz, **Квантовая механика** (Quantum Mechanics), GITTL, 1948; English translation, Pergamon Press, 1958.

[12] D. Dennison, Revs. Modern Phys. **3**, 280 (1931).

[13] Baggerly, Marmier, Boehm, and DuMond, Phys. Rev. **100**, 1364 (1955).

[14] Benczer, Farrelly, Koerts, and Wu, Phys. Rev. **101**, 1027 (1955).

[15] H. Motz, Phys. Rev. **104**, 1353 (1956).

[16] Kurbatov, Murray, and Sakai, Phys. Rev. **98**, 674 (1955).

[17] M. J. Glaubman, Phys. Rev. **98**, 645 (1955).

[18] O. Nathan and M. Waggoner, Nucl. Phys. **2**, 548 (1956/57).

[19] L. Peker, **Доклады на 8 совещании по ядерной спектроскопии** (Reports of the 8'th conference on nuclear spectroscopy) Leningrad, 1958.

[20] Boehm, Marmier, and DuMond, Phys. Rev. **95**, 864 (1954).

[21] R. Waddell and E. Jensen, Phys. Rev. **102**, 816 (1956).

[22] Bhattcherjee, Nainan, Raman, and Sahai, Nuovo cimento **7**, 501 (1958).

[23] T. Lindqvist and I. Marklund, Nucl. Phys. **4**, 189 (1957).

[24] M. Gursky, Phys. Rev. **98**, 1205 (1955).

Translated by M. Hamermesh
77

SOVIET PHYSICS JETP VOLUME 35(8), NUMBER 2 FEBRUARY, 1959

GENERALIZED SELF-CONSISTENT FIELD EQUATIONS

P. S. ZYRIANOV

Ural' Polytechnic Institute

Submitted to JETP editor March 19, 1958; resubmitted April 24, 1958

J. Exptl. Theoret. Phys. (U.S.S.R.) **35**, 448-451 (August, 1958)

The Hartree equations generalized to the case of nonstationary states are modified to incorporate processes of scattering of particles at small distances as a sort of momentum interaction. The relation of these equations to the theories of Landau and Silin is shown. On the basis of the generalized equations, dispersion relations are found for Fermi and Bose systems of interacting particles.

In systems of interacting particles, the density fluctuations can be divided conditionally into "coarse-grained" and "fine-grained" fluctuations.[1] This separation is related to the approximate methods of description of the sole actually occurring fluctuations. In condensed systems, the "coarse-grained" fluctuations describe density changes over regions of space with linear dimensions which are appreciably greater than the distance between particles, while the changes in number density of particles over space regions of dimensions comparable with or smaller than the average distance between particles are described by the "fine-grained" fluctuations. The "coarse-grained" fluctuations, in which the properties of the system manifest themselves as if it were a continuous medium, can be described by means of the Hartree self-consistent field. This field contains the effect of long range force correlations in the system.

The self-consistent field is too poor an approximation to describe the "fine-grained" fluctuations. This is due primarily to the large fluctuations of the actual (but not of the average) field at small distances, even for the case of a spatially uniform density. Processes of interaction of particles at small distances have rather the character of collisions, and they are to be described preferably in terms of a scattering problem. Here the fundamental quantity is the scattering amplitude, which depends on the potential of the interaction between the particles and on their momenta. If we neglect the effect of the self-consistent Hartree field on the scattering processes at small distances, the scattering amplitude will be independent of the spatial coordinates. This statement is equivalent to neglecting the interaction between the "coarse-grained" and "fine-grained" fluctuations.

The interaction energy of the particles at small distances can then be assumed to be some function of the scattering amplitude. In the simplest case of small scattering amplitudes, this function can be expanded in series and one can limit oneself to the linear approximation; the interaction energy will then be proportional to the scattering amplitude. In general the interaction at small distances can be regarded as a sort of momentum interaction, and the scattering amplitude or some function of it as the operator of this interaction.

As will be clear from the sequel, such interactions describe the force correlations over small distances. The momentum interactions described above can be included in the Hartree equations generalized to the case of nonstationary states,[2] and can be expressed in the following form:

$$i\hbar\dot{\psi}_j = \left\{-\frac{\hbar^2}{2m}\frac{\partial^2}{\partial \mathbf{q}^2} + \int G(|\mathbf{q}-\mathbf{x}'|)\sum_i |\psi_i(\mathbf{x}')|^2 dx'\right\}\psi_j(\mathbf{q}) + \sum_i \int \psi_i(\mathbf{x}')\Phi(\hat{\mathbf{p}}, \hat{\mathbf{p}}'^*; \mathbf{q}, \mathbf{x}')\psi_i^*(\mathbf{x}')\,dx'\psi_j(\mathbf{q}), \tag{1}$$

where

$$\Phi(\hat{\mathbf{p}}, \hat{\mathbf{p}}'^*; \mathbf{q}, \mathbf{x}') = {}^1/_2\,[\delta(\mathbf{x}'-\mathbf{q})F(\ \hat{\mathbf{p}}-\hat{\mathbf{p}}'^*|) + F(|\hat{\mathbf{p}}-\hat{\mathbf{p}}'^*|)\delta(\mathbf{x}'-\mathbf{q})],$$

$$\hat{\mathbf{p}} = -i\hbar\partial/\partial\mathbf{q}, \quad \hat{\mathbf{p}}'^* = i\hbar\partial/\partial\mathbf{x}',$$

$F(|\hat{\mathbf{p}}|)$ is some function of the scattering amplitude.

One can establish the relation of these equations to the Landau equation for a Fermi liquid[3] and with the equation for a degenerate electron fluid which was obtained by Silin[1] as a generalization of the work of Landau, as well as with the Hartree-Fock equations.

A more complete and consistent description of fluctuations, not assuming a separation of the fluctuations into "coarse and fine grained", should start from a single interaction kernel depending on coordinates as well as momenta of the interacting particles. In Eq. (1) the interaction kernel is a sum of coordinate and momentum interactions. This is the cause of the formal division of the fluctuations into two types.

1. To establish the connection of (1) with the Landau and Silin equations, which arise from (1) as a quasi-classical approximation in the limit $\hbar \rightarrow 0$, we introduce the density matrix

$$\rho(\mathbf{q}, \mathbf{q}') = \sum_i \psi_i(\mathbf{q})\, \psi_i^*(\mathbf{q}'). \tag{2}$$

For the case of particles with spin, the spin coordinates may be assumed to be contained in $\mathbf{q}$.

Using (1), we can find the equation of motion for $\rho(\mathbf{q}, \mathbf{q}')$. This equation has the following form:

$$\begin{aligned} i\hbar\rho'(\mathbf{q}, \mathbf{q}') = \Big\{ & -(\hbar^2/2m)(\partial^2/\partial\mathbf{q}^2 - \partial^2/\partial\mathbf{q}'^2) \\ & + \int dx' \,[G(|\mathbf{q}-\mathbf{x}'|) \\ & - G(|\mathbf{q}'-\mathbf{x}'|)]\,\rho(\mathbf{x}', \mathbf{x}') \\ & + \int dx''\, dx' \,\delta(\mathbf{x}'-\mathbf{x}'')\,\Phi(\mathbf{q}, \mathbf{x}';\ \hat{\mathbf{p}}, \hat{\mathbf{p}}'^*)\,\rho(\mathbf{x}'', \mathbf{x}') \\ & - \int dx''\, dx'\,\delta(\mathbf{x}''-\mathbf{x}')\,\Phi(\mathbf{q}', \mathbf{x}';\ \hat{\mathbf{p}}, \hat{\mathbf{p}}'^*)\,\rho(\mathbf{x}', \mathbf{x}'')\Big\}\,\rho(\mathbf{q}, \mathbf{q}'). \end{aligned} \tag{3}$$

We can go over from this equation to the equation of motion for the quantum distribution function $f(\mathbf{p}, \mathbf{q})$, which is related to $\rho(\mathbf{q}, \mathbf{q}')$ by the well known relation[5]

$$f_{s,s'}(\mathbf{p}, \mathbf{q}) = \frac{1}{(2\pi)^3}\int \rho(\mathbf{q} - \hbar\tau/2;\ \mathbf{q} + \hbar\tau/2)\, e^{-i\tau\mathbf{p}}\, d\tau, \tag{4}$$

where s and s' are spin indices. We can introduce a distribution function $f(\mathbf{p}, \mathbf{q})$ which is independent of the spin indices:

$$f(\mathbf{p}, \mathbf{q}) = \sum_s f_{ss}(\mathbf{p}, \mathbf{q}). \tag{5}$$

If we assume that the magnetization of the system is equal to zero and neglect fluctuations of the spin density in phase space, we can obtain the following quantum-kinetic equation for $f(\mathbf{p}, \mathbf{q})$ by using Eq. (3):

$$\begin{aligned} & \frac{\partial f}{\partial t} + \frac{\mathbf{p}}{m}\frac{\partial f}{\partial \mathbf{q}} - \frac{i}{(2\pi)^3\hbar}\int dx'\, dp'\, dp''\, d\tau\,[G(|\mathbf{x}' - \mathbf{q} + \hbar\tau/2|) \\ & - G(|\mathbf{x}' - \mathbf{q} - \hbar\tau/2|)]\, f(\mathbf{p}', \mathbf{x}')\, f(\mathbf{p}'', \mathbf{q}) \exp\{i\tau(\mathbf{p}'' - \mathbf{p})\} \\ & - \frac{i}{(2\pi)^3\hbar}\int d\varkappa\, d\tau\, dp'\, dp''\, F(|\varkappa|)\{f(\mathbf{p}', \mathbf{q} + (\hbar\tau/2) - \hbar\varkappa/2) \\ & \times f(\mathbf{p}'', \mathbf{q} - \hbar\varkappa/2) - f(\mathbf{p}', \mathbf{q} - (\hbar\tau/2) + h\varkappa/2) \\ & \times f(\mathbf{p}'', \mathbf{q} + \hbar\varkappa/2)\}\exp\{i\varkappa(\mathbf{p}'' - \mathbf{p}') + i\tau(\mathbf{p}'' - \mathbf{p})\}. \end{aligned} \tag{6}$$

Making the limiting transition $\hbar \rightarrow 0$ in (6), we obtain the quasi-classical kinetic equation in the following form:

$$\frac{\partial f}{\partial t} + \frac{\partial}{\partial \mathbf{q}}(\mathbf{v}, f) + \frac{\partial}{\partial p}(\mathbf{P}, f) = 0, \tag{7}$$

$$\mathbf{v} = \partial\varepsilon/\partial\mathbf{p}, \quad \mathbf{P} = -\partial\varepsilon/\partial\mathbf{q};$$

$$\begin{aligned} \varepsilon(\mathbf{p}, \mathbf{q}) = \frac{p^2}{2m} & + \int F(|\mathbf{p} - \mathbf{p}'|)\frac{\partial f(\mathbf{p}'\mathbf{q})}{\partial \mathbf{p}'}\, dp' \\ & + \int G(|\mathbf{q} - \mathbf{x}'|)\, f(\mathbf{p}', \mathbf{x}')\, dx'\, dp'. \end{aligned} \tag{8}$$

If we neglect the last term in (8), which describes the energy of interaction of the particle with the Hartree field, we get a kinetic equation analogous to the corresponding equation in reference 3.

The function $\epsilon(\mathbf{p}, \mathbf{q})$ is the energy of the particle in the self-consistent Hartree field, including scattering processes at small distances which describe force correlations of small range; $\mathbf{v}$ and $\mathbf{P}$ can be treated as the velocity and the self-consistent force, respectively.

We note that Eq. (7), though it is a quasi-classical approximation, contains exchange effects or, in other words, takes account of the symmetry of the wave function of the initial system. Actually the initial equations (1), from which (7) was obtained, go over into the Hartree-Fock equations if we set

$$F(|\mathbf{p}|) = \int G(|\mathbf{r}|)\, e^{i\mathbf{r}\cdot\mathbf{p}/\hbar}\, dr, \tag{8a}$$

where $G(|\mathbf{r}|)$ is the interaction potential between the particles in vacuum.

2. To find the energy spectrum of low excited states of a system of interacting particles, it is preferable to use Eq. (1) rather than (7). The point is that (1) contains quantum effects which are essential for Bose systems near the ground state (at absolute zero), while the equations of (7) no longer contain them since they are obtained in the limit $\hbar \rightarrow 0$.

A procedure for finding dispersion equations for the states of a system which are close to a homogeneous, isotropic distribution of particles in coordinate space and chaotic in the velocities was given briefly in reference 2. We shall follow this procedure.

Let us represent the function $\psi_j(\mathbf{x})$ as

$$\psi_j(\mathbf{x}, t) = \rho_j^{1/2}(\mathbf{x}, t)\exp\{(i/\hbar)\, S_j(\mathbf{x}, t)\}. \tag{9}$$

Substituting (9) in (1), we get a system of equations for the functions ρ_j, S_j. Since the state of the system with constant density, $\rho_j = \text{const}$, is an exact solution, the nonlinear system of equations for the functions ρ_j and S_j can be linearized in the neighborhood of this exact solution with $\rho_j = \text{const}$.

If we look for a solution of the linear equations for ρ_j and S_j in the form of a superposition of plane traveling waves with frequency ω and wave vector $\mathbf{k}$, we find the following dispersion equation for Bose systems:

$$\omega^2 = (k^2/m^*)\langle N_0 G^*(k) + \hbar^2 k^2/4m^*\rangle; \qquad (10)$$

Here $G^*(k) = G(k) + \frac{1}{2}[F(\hbar k) + F(0)]$, $G(k)$ is the Fourier component of the interaction kernel, $F(x)$ is the kernel of the momentum interaction, and m^* is the effective mass which is defined by the expression:

$$(m^*)^{-1} = (1/m)\langle 1 + (3m/\hbar^2 k^2)[F(\hbar k) - F(0)]\rangle.$$

The structure of the energy spectrum (10) of the weakly excited states of a Bose system coincides in form with the results which were first obtained by Bogoliubov,[6] but differs in that the mass of the original particles is replaced by their effective mass, and that the function $\frac{1}{2}[F(\hbar k) + F(0)]$, which takes account of correlations over small distances, is added to the Fourier component of the kernel of the interaction between particles. If we define $F(x)$ from (8a), Eq. (10) coincides with the corresponding result from the Hartree-Fock equation.

In the case of perfectly elastic spheres of diameter a, the interaction kernel can be taken in the form

$$G(|\mathbf{q} - \mathbf{x}'|) = (\hbar^2/ma^2)\,\delta(|\mathbf{q} - \mathbf{x}'|a). \qquad (11)$$

Then Eq. (10) gives results which are analogous to those of Brueckner and Sawada[7] (cf. also reference 8), and in the limit $k \to 0$ with those of Lee and Yang.

In the case of systems of Fermi particles, to find the spectrum of collective oscillations we get the dispersion equation

$$1 = \sum_j (k^2/m_j^*)\,G_j^*(k)\langle[\omega - \mathbf{k}\mathbf{v}_j^*]^2 - \hbar^2 k^4/4m_j^*\rangle^{-1}, \qquad (12)$$

where

$$G_j^*(k) = G(k) + {}^1\!/_4 \sum_i [F(|\mathbf{p}_i - \mathbf{p}_j + \hbar\mathbf{k}|) - F(|\mathbf{p}_i - \mathbf{p}_j - \hbar\mathbf{k}|) + 2F(|\mathbf{p}_i - \mathbf{p}_j|)],$$

$$(m_j^*)^{-1} = (1/m) + (1/\hbar^2 k^2)\sum_i [F(|\mathbf{p}_i - \mathbf{p}_j + \hbar\mathbf{k}|) + F(|\mathbf{p}_i - \mathbf{p}_j - \hbar\mathbf{k}|) - 2F(|\mathbf{p}_j - \mathbf{p}_i|)],$$

$$\mathbf{k}\mathbf{v}_j^* = (\mathbf{k}\mathbf{p}_j/m) + (1/2\hbar)\sum_i [F(|\mathbf{p}_i - \mathbf{p}_j + \hbar\mathbf{k}|) - F(|\mathbf{p}_i - \mathbf{p}_j - \hbar\mathbf{k}|)],$$

and $\mathbf{p}_j$ is the momentum of the j-th particle in the state with constant density.

In the case of Coulomb forces, as $k \to 0$ we get the following expression for the limiting frequency of plasma oscillations:

$$\omega_0^2 = \frac{4\pi N_0 e^2}{m^*}; \quad \frac{1}{m^*} = \frac{1}{m} + \sum_{ij} \frac{2}{N_0} \frac{\partial^2 F(|\mathbf{p}_i - \mathbf{p}_j|)}{\partial \mathbf{p}_i^2}.$$

If we define $F(|\mathbf{p}|)$ by Eq. (8a), the dispersion equation (12) coincides with the corresponding equation obtained from the Hartree-Fock equations.

---

[1] P. S. Zyrianov, J. Exptl. Theoret. Phys. (U.S.S.R.) **29**, 344 (1955); Soviet Phys. JETP **2**, 236 (1956).

[2] P. S. Zyrianov and V. M. Eleonskii, J. Exptl. Theoret. Phys. (U.S.S.R.) **30**, 592 (1956); Soviet Phys. JETP **3**, 620 (1956).

[3] L. D. Landau, J. Exptl. Theoret. Phys. (U.S.S.R.) **30**, 1058 (1956); Soviet Phys. JETP **2**, 920 (1956).

[4] V. P. Silin, J. Exptl. Theoret. Phys. (U.S.S.R.) **33**, 495 (1957); Soviet Phys. JETP **6**, 387 (1958).

[5] V. P. Silin, Физика металлов и металловедение (Phys. of Metals and Met. Research) **3**, 193 (1956).

[6] N. N. Bogoliubov, Jour. of Phys. (U.S.S.R.) **11**, 23 (1947).

[7] K. A. Brueckner and K. Sawada, Phys. Rev. **106**, 1128 (1957).

[8] V. M. Eleonskii and P. S. Zyrianov, J. Exptl. Theoret. Phys. (U.S.S.R.) **34**, 770 (1958), Soviet Phys. JETP **7**, 530 (1958).

[9] Lee, Huang and Yang, Phys. Rev. **106**, 1135 (1957).

Translated by M. Hamermesh
78

SOVIET PHYSICS JETP VOLUME 35(8), NUMBER 2 FEBRUARY, 1959

AN INVESTIGATION OF PARTICLE-LIKE SOLUTIONS OF A NONLINEAR SCALAR FIELD EQUATION

V. B. GLASKO, F. LERIUST, Ia. P. TERLETSKII, and S. F. SHUSHURIN

Moscow State University

Submitted to JETP editor March 22, 1958

J. Exptl. Theoret. Phys. (U.S.S.R.) **35**, 452-457 (August, 1958)

We investigate how the field energy of the particle-like solutions of a nonlinear complex scalar field equation is related to the parameters of the equation and the frequency of oscillations. For the case of the simplest cubic nonlinear term, the first three particle-like solutions are derived and the relevant mass spectrum is analyzed by numerical integration. Under some natural physical assumptions, the spectrum is found to be bounded.

1. It is of interest, in order to clarify the potentialities of a nonlinear field theory of elementary particles,[1-9] to investigate the particle-like solutions* of the simplest nonlinear complex scalar field equation. This equation can be used as an example to investigate qualitative questions such as the existence and nature of a mass spectrum. It is of course clear that an attempt to construct a quantitative theory giving the relation between mass, charge, spin, coupling constants, radii, and other structural elements of particles can be undertaken only after all possible fields and interactions have been investigated.

2. Consider a complex scalar field whose Lagrangian is

$$L = -\nabla\psi^*\nabla\psi + \frac{\partial\psi^*}{\partial x_0}\frac{\partial\psi}{\partial x_0} - m^2[\psi^*\psi + F(\psi^*\psi)], \tag{1}$$

where $x_0 = ct$, the function $F(v)$ is nonlinear, and m is a parameter whose units are the reciprocal of length (we are using units in which $\hbar = c = 1$, so that on going to ordinary units m must be replaced by $mc/\hbar$).

According to (1), the field equations are

$$\begin{gathered}\nabla^2\psi - \partial^2\psi/\partial x_0^2 - m^2[1 + F'(\psi^*\psi)]\psi = 0,\\ \nabla^2\psi^* - \partial^2\psi^*/\partial x_0^2 - m^2[1 + F'(\psi^*\psi)]\psi^* = 0,\end{gathered} \tag{2}$$

where $F'(v) = dF(v)/dv$.

If T_{ik} is the energy-momentum tensor and J_k is a vector, which we shall provisionally call the current vector, then according to (1) the field energy $E = \int_V T_{00}\,dV$ and the quantity $Q = \int_V J_0\,dV$, which we shall also provisionally call the charge, are given by

$$E = \frac{1}{2}\int_V\left\{\frac{d\psi^*}{dx_0}\frac{d\psi}{dx_0} + \nabla\psi^*\nabla\psi + m^2[\psi^*\psi + F(\psi^*\psi)]\right\}dV, \tag{3}$$

$$Q = \frac{i}{2}\int_V\left(\psi^*\frac{d\psi}{dx_0} - \psi\frac{d\psi^*}{dx_0}\right)dV. \tag{4}$$

For the case of spherical symmetry, the particle-like solution ψ decays exponentially as $r \to \infty$.[6,10] Using this fact and Eq. (2) in the integration indicated in (3), we obtain

$$E = \frac{1}{2}\int_V\left\{\frac{\partial\psi^*}{\partial x_0}\frac{\partial\psi}{\partial x_0} - \psi^*\frac{\partial^2\psi}{\partial x_0^2} + m^2[F(\psi^*\psi) - \psi^*\psi F'(\psi^*\psi)]\right\}dV. \tag{5}$$

3. As did Rosen and Rosenstock,[6] let us restruct our considerations to the simplest form of nonlinear function, namely $F(v) = -\lambda v^2/2$, and let us attempt to find a spherically symmetric particle-like solution of Eq. (2) in the form

$$\psi = u(r)e^{-i\varepsilon x_0}, \quad \psi^* = u(r)e^{i\varepsilon x_0}, \tag{6}$$

where ϵ is a parameter proportional to the frequency. Then the equation for $u(r)$ and the expressions for E and Q become

$$\frac{1}{r}\frac{d^2}{dr^2}(ru) + [\varepsilon^2 - m^2 + \lambda u^2]u = 0, \tag{7}$$

$$E = \varepsilon^2\int_0^\infty u^2 4\pi r^2 dr + \frac{\lambda m^2}{4}\int_0^\infty u^4 4\pi r^2 dr, \tag{8}$$

$$Q = \varepsilon\int_0^\infty u^2 4\pi r^2 dr. \tag{9}$$

If we assume that $\epsilon < m$, we can introduce the dimensionless quantity $\rho = r\sqrt{m^2 - \epsilon^2}$ and the dimensionless function $\eta = \sqrt{\lambda}\,mru$ to transform

---

*We call a solution particle-like if it decreases monotonically as $r \to \infty$ and has no singularity at the origin.

(7), (8), and (9) to the form*

$$d^2\eta / d\rho^2 = [1 - \eta^2/\rho^2]\,\eta, \tag{10}$$

$$E = \frac{4\pi}{\lambda m^2}\left[\frac{\varepsilon^2}{\sqrt{m^2-\varepsilon^2}} I_1 + \frac{\sqrt{m^2-\varepsilon^2}}{4} I_2\right], \tag{11}$$

$$Q = \frac{4\pi}{\lambda m^2}\,\frac{\varepsilon}{\sqrt{m^2-\varepsilon^2}}\, I_1, \tag{12}$$

$$I_1 = \int_0^\infty \eta^2 d\rho, \quad I_2 = \int_0^\infty \frac{\eta^4}{\rho^2}\, d\rho. \tag{13}$$

(According to (10) it is obvious for particle-like solutions that $I_2 = I_1 + \int_0^\infty \dot{\eta}^2\, d\rho$, so that the relation $I_2 > I_1$ holds in all cases.)

Eliminating λ from (11) and (12), we obtain the relation between E, Q, and ϵ, namely

$$\frac{E}{m} = Q\left\{\frac{\varepsilon}{m} + \frac{1-(\varepsilon/m)^2}{4\,\varepsilon/m}\,\frac{I_2}{I_1}\right\}. \tag{14}$$

4. It is easily seen that particle-like solutions (i.e., solutions which satisfy the condition $\eta(0) = 0$ and which approach zero monotonically as $r \to \infty$) exist only for Eq. (10); no such solutions can be found for Eqs. (10a) or (10b). This means that (7) has particle-like solutions only if $\epsilon < m$. To see this, consider the equation

$$\eta'' = [\beta - \eta^2/\rho^2]\,\eta, \tag{10c}$$

which is a unified statement of (10), (10a), and (10b) with $\beta = 1$ for $\epsilon < m$, $\beta = -1$ for $\epsilon > m$, and $\beta = 0$ for $\epsilon = m$.

It is evident that in the two last cases ($\beta = -1$ and $\beta = 0$) the sign of η'' is the opposite of the sign of η. Therefore any integral curve is convex upward for $\eta > 0$ and convex downward for $\eta < 0$ for all values of ρ. This means that all solutions of (10a) and (10b), except those with $\eta \equiv 0$, oscillate about the ρ axis as $\rho \to +\infty$.

Let us now consider the following Cauchy problem for Eq. (10):

$$\frac{d^2\eta}{d\rho^2} = \left(1 - \frac{\eta^2}{\rho^2}\right)\eta, \quad \eta(0) = 0, \quad \frac{d\eta}{d\rho}(0) = \alpha, \tag{15}$$

where α is a parameter.

This problem is easily solved in the neighborhood of $\rho = 0$, giving the power series

$$\eta = \alpha\left(\rho + \frac{1-\alpha^2}{6}\rho^3 + \ldots\right). \tag{16}$$

As $\rho \to +\infty$, any solution of (15) which approaches zero is a monotonic function of ρ, since in this case the sign of η'' is the same as that of η.

We shall show that there exist values of α such that (15) has a solution which approaches zero as $\rho \to +\infty$ and has, for instance, a single node (at $\rho = 0$). We shall call this solution the first eigensolution, and the corresponding value of α the first eigenvalue.

Figure 1 shows the regions in which the sign of η'' is constant. Consider the line $\eta = \rho/\sqrt{3}$. Numerical integration shows that there exists an $\alpha = \alpha_1^{(0)} > 1$, such that the corresponding integral curve $\eta = \eta_1^{(0)}(\rho)$ enters into the region $0 < \eta < \rho/\sqrt{3}$ for some value of $\rho = \bar{\rho}$ and has a single zero at $\rho = 0$. There also exists an $\alpha = \alpha_2^{(0)} > \alpha_1^{(0)}$ whose integral curve $\eta = \eta_2^{(0)}(\rho)$ has a second zero at some value $\rho = \rho_1^{(0)} > \bar{\rho}$. If α^* and α^{**} satisfy the condition

$$\alpha_1^{(0)} < \alpha^* < \alpha^{**} < \alpha_2^{(0)},$$

then the corresponding $\eta^*(\bar{\rho})$ and $\eta^{**}(\bar{\rho})$ satisfy the condition

$$\eta_1^{(0)}(\bar{\rho}) > \eta^*(\bar{\rho}) > \eta^{**}(\bar{\rho}) > \eta_2^{(0)}(\bar{\rho}). \tag{17}$$

We shall now prove that under these conditions there exists a first eigensolution.

We note that in the region $0 < \eta < \rho/\sqrt{3}$, any two solutions η_1 and η_2 have the property that

$$\operatorname{sign}(\eta_1'' - \eta_2'') = \operatorname{sign}\left[(\eta_1 - \eta_2)\left(1 - \frac{\eta_1^2 + \eta_1\eta_2 + \eta_2^2}{\rho^2}\right)\right] = \operatorname{sign}(\eta_1 - \eta_2).$$

Therefore segments of the integral curves corresponding to α values from the interval $\alpha_1^{(0)} < \alpha < \alpha_2^{(0)}$ starting from points whose abcissas are $\rho = \bar{\rho}$ do not intersect before leaving the region $0 < \eta < \rho/\sqrt{3}$.

Let $\bar{\eta}(\rho)$ be a solution of the Cauchy problem $\bar{\eta}'' = \bar{\eta}$, $\bar{\eta}(\bar{\rho}) = k$ [with $k > \eta_1^{(0)}(\rho)$], which ap-

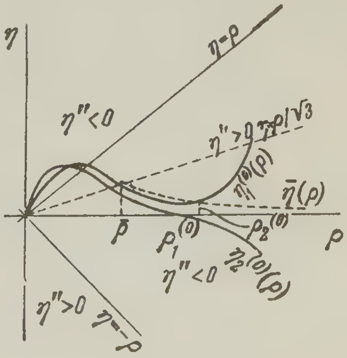

FIG. 1

---

*If $\varepsilon > m$, we can set $\rho = r\sqrt{\varepsilon^2 - m^2}$, in which case (10) is replaced by

$$d^2\eta / d\rho^2 = -[1 + \eta^2/\rho^2]\,\eta. \tag{10a}$$

If, finally, $\varepsilon = m$, we set $\eta = \sqrt{\lambda}\, ru$, and (7) can be written

$$d^2\eta / dr^2 = -(\eta^2/r^2)\,\eta. \tag{10b}$$

proaches zero as $\rho \to +\infty$. There obviously exists an interval $\bar{\rho} < \rho < \rho_2^{(0)}$ on which $0 < \eta_1^{(0)}(\rho) < \bar{\eta}(\rho)$ (Fig. 1).

Let us choose $\alpha = (\alpha_1^{(0)} + \alpha_2^{(0)})/2$. To this α corresponds either $\eta_1^{(1)}(\rho)$ which crosses $\bar{\eta}(\rho)$ at $\rho = \rho_2^{(1)}$, or $\eta_2^{(1)}(\rho)$, which crosses the ρ axis at $\rho_1^{(1)}$. Since the integral curves do not intersect in the region of interest, $\rho_2^{(1)} > \rho_2^{(0)}$, and $\rho_1^{(1)} > \rho_1^{(0)}$. In the first case we set $\alpha_1^{(1)} = (\alpha_1^{(0)} + \alpha_2^{(0)})/2$ and $\alpha_1^{(1)} = \alpha_2^{(0)}$, and in the second case we set $\alpha_1^{(1)} = \alpha_1^{(0)}$ and $\alpha_2^{(1)} = (\alpha_1^{(0)} + \alpha_2^{(0)})/2$, which gives a new pair of values of α (namely $\alpha_1^{(1)}$ and $\alpha_2^{(1)}$) to which correspond the integral curves $\eta_1^{(1)}(\rho)$ and $\eta_2^{(1)}(\rho)$, which are located in the region $0 < \eta < \bar{\eta}(\rho)$ on the segment $\bar{\rho} \le \rho \le \min(\rho_1^{(1)}, \rho_2^{(1)})$.

Continuing this process ad infinitum, in the limit we obtain $\alpha = \bar{\alpha} = \lim\limits_{i\to+\infty} \alpha_1^{(i)} = \lim\limits_{i\to+\infty} \alpha_2^{(i)}$. Since at least one of the two sequences $\{\rho_1^{(i)}\}$ or $\{\rho_2^{(i)}\}$ is unbounded, to the value of $\bar{\alpha}$ corresponds an integral curve which lies entirely within the region $0 < \eta < \bar{\eta}(\rho)$ for $\rho > \bar{\rho}$ and is thus an eigensolution.

In a similar way we can prove the existence of successive eigensolutions whose indices are determined by the number of intersections with the ρ axis.

5. The eigensolutions of (10) and their corresponding eigenvalues were found by numerical integration of (15) for different α.

Since the equation is singular at $\rho = 0$, the initial conditions were given for $\rho = \rho_0 > 0$ using the series of (16). The integration was performed for $\rho_0 = 10^{-3}$ and $\rho_0 = 10^{-6}$, and the results were found to agree within the required accuracy.

The calculations were performed on the high-speed electronic computer "Strela" (Arrow) of the computing center at the Moscow State University.

The region in which the eigenvalues $[\alpha_1^0, \alpha_2^0]$ are situated and the eigenvalues α_2 were found to a predetermined accuracy automatically, by programming the calculation described above.

In the interval $3 \le \alpha \le 90$, we obtained five first eigenvalues with a relative accuracy of 5×10^{-5}. These were $\alpha_1 = 4.33$, $\alpha_2 = 14.10$, $\alpha_3 = 29.13$, $\alpha_4 = 49.36$, and $\alpha_5 = 74.77$ (all the figures are significant). Figure 2 shows the behavior of the first three integral curves for α somewhat larger and smaller than the corresponding value of α_2.

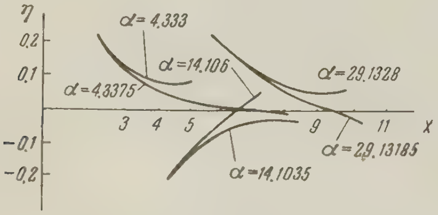

FIG. 2

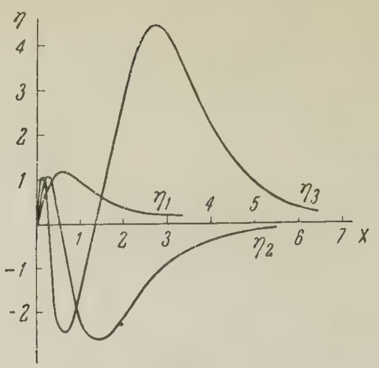

FIG. 3

The eigensolutions, the first three of which are shown in Fig. 3, were tabulated with a relative error $\epsilon = 10^{-4}$, and then checked with an accuracy for which $\epsilon = 10^{-5}$ in steps for intervals $\rho_0 \le \rho \le \bar{\rho}_i$ such that when $\rho = \bar{\rho}_i$ the solutions approach their asymptotic curves with an accuracy of no less than 1%. With this accuracy, the following asymptotic expressions are obtained for $\rho > \bar{\rho}_i$:

$$\eta_1 = 2.70\, e^{-\rho}\ (\bar{\rho}_1 = 3.45);\quad \eta_2 = -17{,}0\, e^{-\rho}\ (\bar{\rho}_2 = 5.07);$$
$$\eta_3 = 83\, e^{-\rho}\ (\bar{\rho}_3 = 6);\ \eta_4 = -375\, e^{-\rho}(\bar{\rho}_4 = 6.85);$$
$$\eta_5 = 1611\, e^{-\rho}(\bar{\rho}_5 = 8.1).$$

The integrals

$$I_1^{(i)} = \int_0^\infty \eta_i^2\, d\rho,\quad I_2^{(i)} = \int_0^\infty \frac{\eta_i^4}{\rho^2}\, d\rho$$

were obtained graphically with an accuracy of 1 or 2%. Their values were $I_1^{(1)} = 1.53$, $I_1^{(2)} = 9.4$, $I_1^{(3)} = 27.7$, $I_1^{(4)} = 63.6$, $I_1^{(5)} = 212.8$, $I_2^{(1)} = 5.5$, $I_2^{(2)} = 39.4$, $I_2^{(3)} = 123$, $I_2^{(4)} = 255$, and $I_2^{(5)} = 476$.

6. Equations (11), (12), and (14) can be used to obtain further results only if we make additional assumptions on the relation between E, ϵ, and Q, and their physical meaning.

If, as in de Broglie's concept of the double solution,[10] we consider a particle-like solution of a nonlinear equation to be a "singularity moving in the proper way,* we must require that

$$\varepsilon = E = M, \tag{18}$$

---

*According to the hypothesis of a double solution,[10] Eq. (6) is a solution of the nonlinear equation (2) such that there is at least some region in which the phase is the same as that of the usual quantum mechanical wave (cons e^{iMx_0}).

where M is the true mass of the particle. Then according to (11), the quantity

$$X = M / \sqrt{m^2 - M^2} \tag{19}$$

should be given by

$$X^2 - \frac{\lambda m^2}{4\pi I_1} X + \frac{I_2}{4I_1} = 0, \tag{20}$$

whose solution is of the form

$$X = (\lambda m^2 / 8\pi I_1)\,[1 \pm (1 - 16\pi^2 I_1 I_2 / \lambda^2 m^4)^{1/2}]. \tag{21}$$

According to (21), for every eigensolution of (10) there exist two values of X, and therefore also two of M. These two values, however, also give different values of Q, so that according to (12) and (19)

$$Q = (4\pi / \lambda m^2)\, I_1 X = {}^1\!/_2\,[1 \pm (1 - 16\pi^2 I_1 I_2 / \lambda^2 m^4)^{1/2}]. \tag{22}$$

In order that there actually exist values of M and X, it is necessary that there exist I_1 and I_2 satisfying the inequality $16\pi^2 I_1 I_2 < \lambda^2 m^4$. From the values of I_1 and I_2 obtained, as well as from the graphs of the η functions, it is seen that $I_1 I_2$ increases with the index N of the eigensolution. It is quite probable that this is true for all eigensolutions, since their maxima move toward larger ρ as N increases, while the solutions themselves oscillate about the lines $\eta = \pm x$ before they begin to approach their asymptotic forms. In any case, if it is true that $I_1 I_2$ increases with N, it is possible to find values of N such that the roots of (21) are complex, and are therefore physically meaningless. In this case the mass spectrum of M values is cut off, which means that it contains a finite number of terms.

The mass spectrum may be even further restricted if Q, like an electric charge, can take on only integral values. Such an assumption does not follow, however, from a theory which includes only a scalar field with no electromagnetic field, so that it must be introduced artificially.

Thus for certain definite values of λm^2 the simplest equation for a scalar complex field can have a bounded number of particle-like eigensolutions, which means that the mass spectrum of M values is bounded.*

[1] N. Rosen, Phys. Rev. **55**, 94 (1949).

[2] A. C. Menius and N. Rosen, Phys. Rev. **62**, 436 (1942).

[3] R. J. Finkelstein, Phys. Rev. **75**, 1079 (1949).

[4] S. Drell, Phys. Rev. **79**, 220 (1950).

[5] Finkelstein, Le Levier, and Ruderman, Phys. Rev. **83**, 326 (1951).

[6] N. Rosen and H. B. Rosenstock, Phys. Rev. **85**, 257 (1952).

[7] N. Mitskevich, J. Exptl. Theoret. Phys. (U.S.S.R.) **29**, 354 (1955), Soviet Phys. JETP **2**, 197 (1956).

[8] Finkelstein, Fronsdal, and Kaus, Phys. Rev. **103**, 1571 (1956).

[9] S. F. Shushurin, Научные доклады Высшей школы, серия физ.-мат. наук (Scient. Reports of the Higher Inst. of Learning, Phys.-Math. Series), No. 3, (1959).

[10] L. de Broglie, J. phys. et radium **8**, 225 (1927).

Translated by E. J. Saletan
79

---

*Thus, for instance, if we set $\lambda m^2 = 242$ ($4\pi\sqrt{I_1 I_2} = 242$ for the second eigensolution), then only the first and second eigensolutions are possible according to (21). For the first of these we obtain two masses, and for the second only one. These three masses are related as 1:10:14. As λm^2 is increased, the mass of the second eigensolution splits into two terms, and as it is further increased, the mass of a third eigensolution appears, etc. For very large values of λm^2 the number of possible masses becomes very large; the five lowest masses will be related as 0.14 : 1 : 3.1 : 6.4 : 12 : . . . , and the largest masses will concentrate about the value m, which forms their upper limit.

SOVIET PHYSICS JETP VOLUME 35(8), NUMBER 2 FEBRUARY, 1959

HYPERON BETA DECAY

V. M. SHEKHTER

Leningrad Physico-Technical Institute

Submitted to JETP editor March 26, 1958

J. Exptl. Theoret. Phys. (U.S.S.R.) **35**, 458-466 (August, 1958)

The probability for hyperon decay into nucleons (hyperons) and leptons is computed. The energy distribution, correlations, polarization, and asymmetry of emission of the particles are determined. Numerical calculations are given for the case of a universal V-A interaction.[1] The probabilities for the leptonic decay modes of Σ^- and Λ^0 are found to exceed considerably the corresponding experimental upper limits.

1. INTRODUCTION

RECENTLY Feynman and Gell-Mann,[1] as well as Marshak and Sudershan,[2] proposed the V-A covariants as a universal four-fermion interaction and listed a number of points in favor of this proposal. As was shown in reference 1 the general character of the interaction was such that the following β decays of hyperons, thus far not observed, should be possible

$$\begin{array}{ll} \Lambda^0 \rightarrow p + e^- + \tilde{\nu}, & \Lambda^0 \rightarrow p + \mu^- + \tilde{\nu}. \\ \Sigma^- \rightarrow n + e^- + \tilde{\nu}, & \Sigma^- \rightarrow n + \mu^- + \tilde{\nu}, \\ \Sigma^- \rightarrow \Lambda^0 + e^- + \tilde{\nu}, & \Sigma^+ \rightarrow \Lambda^0 + e^+ + \nu, \\ \Xi^- \rightarrow \Lambda^0 + e^- - \tilde{\nu}, & \Xi^- \rightarrow \Lambda^0 + \mu^- + \tilde{\nu}, \\ \Xi^- \rightarrow \Sigma^0 + e^- + \tilde{\nu}, & \Xi^- \rightarrow \Sigma^0 \rightarrow \mu^- + \tilde{\nu}. \end{array} \qquad (1)$$

The probabilities of the electron decay modes of Λ^0 and Σ^- were computed in reference 1. In this work we compute, in addition to total probabilities, the energy distribution, correlation, polarization, and asymmetry of emission of particles formed in the decay of a polarized hyperon. Since the coupling constant of the axial-vector interaction may be renormalized by strong interactions in a manner different from the vector constant, one must take in general $C_A \neq -C_V$. In the computation of polarization and asymmetry it was found convenient to calculate traces and integrate over unobserved variables in a coordinate system in which the momentum of the particle under study was equal to the momentum of the decaying hyperon, and only afterwards to transform to the rest system of the hyperon.[3] The assumption of nonzero rest mass for all four fermions participating in the decay process does not complicate the calculations and permits application to processes involving neutral currents such as $\Lambda^0 \rightarrow n + e^- + \mu^+$, if it should turn out that these exist. The total decay probability is given in terms of an integral which is given explicitly when the mass of one of the decay products equals zero.

Numerical values for the probability of hyperon β decay and emission asymmetry are obtained for the V-A universal interaction without renormalization effects ($C_A = -C_V$). In Appendix B we discuss possible types of universal parity-nonconserving interactions, and outline simple methods for deriving the S + P − T interaction results from the V-A (and vice versa) for processes involving free particles as well as for the usual β-decay process.

2. ENERGY CORRELATIONS

The various processes given by Eq. (1) can be written in a unified form as

$$Y \rightarrow \left\{ \begin{matrix} N \\ Y' \end{matrix} \right\} + \left\{ \begin{matrix} e^- \\ \mu^- \end{matrix} \right\} + \tilde{\nu} \qquad (2)$$

where Y stands for a hyperon and N for a nucleon. The universal four-fermion interaction responsible for these processes can be written as follows (we consider the V and A covariants only):

$$H_{\text{int}} = (\bar{\psi}_N \gamma_\mu (C_V - C_A \gamma_5) \psi_Y)(\bar{\psi}_e \gamma_\mu (1 - \gamma_5) \psi_\nu). \qquad (3)$$

(From now on we shall write all formulas for the decay of a hyperon into a nucleon and electron only. The corresponding expressions for the hyperonic or μ-mesonic modes of decay are obtained by replacing the index N by Y′ or e by μ.)

The transition probability [calculated using the Hamiltonian (3)] for the decay of a hyperon Y at rest with polarization ζ_Y accompanied by the emission of an electron of energy E_e into the solid angle element $d\Omega_e$ and a nucleon into the solid angle element determined by its energy E_N and the azimuth angle φ_N about the axis $\mathbf{p}_e$ (measured from the $\zeta_Y \mathbf{p}_e$ plane) is given by (E_i, m_i, $\mathbf{p}_i$, ζ_i stand for the energy, mass, momentum, and polarization respectively of the i-th particle in its rest frame):

$$dW(\zeta_Y;\ E_e, E_N, \Omega_e, \varphi_N) = \frac{1}{2\pi^3}\frac{d\Omega_e}{4\pi}\frac{d\varphi_N}{2\pi}\,dE_e dE_N\,\{\eta^2[(m_Y - E_N - E_e) - \zeta_Y(\mathbf{p}_N + \mathbf{p}_e)][E_N E_e - s_{Ne}]$$
$$+ \xi^2[E_e - (\zeta_Y\cdot\mathbf{p}_e)][E_N(m_Y - E_e) - m_N^2 + s_{Ne}] + \eta\xi m_N[E_e(m_Y - E_N) - m_e^2 + s_{Ne} - (m_Y - E_N)(\zeta_Y\cdot\mathbf{p}_e) + E_e(\zeta_Y\cdot\mathbf{p}_N)]\}. \qquad (4)$$

Here

$$\eta = C_V - C_A, \quad \xi \equiv C_V + C_A; \qquad (5)$$

$$s_{Ne} \equiv (\mathbf{p}_N\cdot\mathbf{p}_e) = {}^1\!/_2[m_Y^2 + m_N^2 + m_e^2 - m_\nu^2 - 2m_Y(E_N + E_e) + 2E_N E_e], \qquad (6)$$

so that the direction of the vector $\mathbf{p}_N$ in $\zeta_Y\cdot\mathbf{p}_N$ is free to vary only in the angle φ_N. Integration over this angle yields

$$(\zeta_Y\cdot\mathbf{p}_N) \to (\zeta_Y\cdot\mathbf{p}_e)\, s_{Ne}/(E_e^2 - m_e^2). \qquad (7)$$

The electron-antineutrino correlation is given by a more symmetric expression (we continue to write simply ν instead of $\widetilde{\nu}$):

$$dW(\zeta_Y;\ E_e, E_\nu, \Omega_e, \varphi_\nu) = \frac{1}{2\pi^3}\frac{d\Omega_e}{4\pi}\frac{d\varphi_\nu}{2\pi}\,dE_e dE_\nu\,\{\eta^2[E_\nu + (\zeta_Y\cdot\mathbf{p}_\nu)][E_e(m_Y - E_\nu) - m_e^2 + s_{e\nu}]$$
$$+ \xi^2[E_e - (\zeta_Y\cdot\mathbf{p}_e)][E_\nu(m_Y - E_e) - m_\nu^2 + s_{e\nu}] + \eta\xi m_N[E_e(\zeta_Y\cdot\mathbf{p}_\nu) - E_\nu(\zeta_Y\cdot\mathbf{p}_e)]\}, \qquad (8)$$

where, as in Eq. (6)

$$s_{e\nu} \equiv (\mathbf{p}_e\cdot\mathbf{p}_\nu) = {}^1\!/_2[m_Y^2 - m_N^2 + m_e^2 + m_\nu^2 - 2m_Y(E_e + E_\nu) + 2E_e E_\nu]. \qquad (9)$$

The nucleon-antineutrino correlation can be obtained from Eqs. (4) to (7) by interchanging the indices e and ν and by using the substitution

$$\eta \rightleftarrows \xi \ \ (\text{i.e., } C_A \to -C_A), \quad \zeta_Y \to -\zeta_Y. \qquad (10)$$

3. ENERGY DISTRIBUTION, POLARIZATION, AND EMISSION ASYMMETRY OF PARTICLES PRODUCED IN THE DECAY OF A POLARIZED HYPERON

In order to obtain the probability for the emission of a nucleon in the direction $\mathbf{n}_N \equiv \mathbf{p}_N/|\mathbf{p}_N|$ and with the polarization ζ_N, we must integrate the expression for the decay probability over the electron and neutrino variables, subject to conservation laws. Some of the details of the calculation are given in Appendix A. The result is

$$dW(\zeta_Y;\ E_N, \mathbf{n}_N, \zeta_N) = \frac{\sqrt{E_N^2 - m_N^2}\,dE_N}{2(2\pi)^3}\frac{d\Omega_N}{4\pi}\frac{\sqrt{[R_N - (m_e + m_\nu)^2][R_N - (m_e - m_\nu)^2]}}{R_N^3}\,T^N, \qquad (11)$$

where

$$R_N = m_Y^2 + m_N^2 - 2m_Y E_N, \qquad (12)$$

$$T^N = T_1^N + T_2^N(\zeta_Y\cdot\mathbf{n}_N) + T_3^N(\zeta_N\cdot\mathbf{n}_N) + T_4^N(\zeta_Y\cdot\mathbf{n}_N)(\zeta_N\cdot\mathbf{n}_N) + T_5^N[(\zeta_Y\cdot\zeta_N) - (\zeta_Y\cdot\mathbf{n}_N)(\zeta_N\cdot\mathbf{n}_N)]. \qquad (13)$$

In (13) T_1^N describes the nucleon-energy distribution, T_2^N the emission asymmetry, T_3^N and T_4^N the longitudinal polarization, and T_5^N the transverse polarization. The T_j^N are given by

$$T_1^N = (\xi^2 + \eta^2)\{(m_Y - E_N)(m_Y E_N - m_N^2)\Gamma_1^N - {}^1\!/_3 m_Y(E_N^2 - m_N^2)\Gamma_2^N\} - \xi\eta m_N R_N[\Gamma_1^N + \Gamma_2^N];$$
$$T_2^N = (\xi^2 - \eta^2)\sqrt{E_N^2 - m_N^2}\{(m_Y E_N - m_N^2)\Gamma_1^N - {}^1\!/_3 m_Y(m_Y - E_N)\Gamma_2^N\};$$
$$T_3^N = (\xi^2 - \eta^2)\sqrt{E_N^2 - m_N^2}\{m_Y(m_Y - E_N)\Gamma_1^N - {}^1\!/_3(m_Y E_N - m_N^2)\Gamma_2^N\}; \qquad (14)$$
$$T_4^N = (\xi^2 + \eta^2)\{m_Y(E_N^2 - m_N^2)\Gamma_1^N - {}^1\!/_3(m_Y - E_N)(m_Y E_N - m_N^2)\Gamma_2^N\} + \xi\eta m_N R_N[\Gamma_1^N - \Gamma_2^N];$$
$$T_5^N = -{}^1\!/_3(\xi^2 + \eta^2)m_N R_N\Gamma_2^N + \xi\eta[E_N(m_Y^2 + m_N^2) - 2m_Y m_N^2][\Gamma_1^N - \Gamma_2^N];$$
$$\Gamma_1^N \equiv [R_N + m_e^2 - m_\nu^2][R_N - m_e^2 + m_\nu^2]; \quad \Gamma_2^N \equiv [R_N - (m_e + m_\nu)^2][R_N - (m_e + m_\nu)^2].$$

If we set $m_e = m_\nu = 0$ in Eqs. (11) to (14), we obtain the formulas of the V-A theory for the polarization and emission asymmetry of the electrons in the decay of a μ meson (the index Y would refer to the μ meson and N to the electron). Such formulas have been given before.[3,4]

In analogy with Eq. (11), we have for the electron

$$dW(\zeta_Y; E_e, \mathbf{n}_e, \zeta_e) = \frac{\sqrt{E_e^2 - m_e^2}}{2(2\pi)^3} \frac{d\Omega_e}{4\pi} \frac{\sqrt{[R_e - (m_N + m_\nu)^2][R_e - (m_N - m_\nu)^2]}}{R_e^3} T^e, \tag{15}$$

where

$$R_e = m_Y^2 + m_e^2 - 2m_Y E_e; \tag{16}$$

$$T^e = T_1^e + T_2^e(\zeta_Y \cdot \mathbf{n}_e) + T_3^e(\zeta_e \cdot \mathbf{n}_e) + T_4^e(\zeta_Y \cdot \mathbf{n}_e)(\zeta_e \cdot \mathbf{n}_e) + T_5^e[(\zeta_Y \cdot \zeta_e) - (\zeta_Y \cdot \mathbf{n}_e)(\zeta_e \cdot \mathbf{n}_e)]; \tag{17}$$

$$\begin{gathered}
T_1^e = \eta^2\{(m_Y E_e - m_e^2)(m_Y - E_e)\Gamma_1^e - {}^1\!/_3\, m_Y(E_e^2 - m_e^2)\Gamma_2^e\} + \xi^2 E_e R_e[\Gamma_1^e + \Gamma_2^e] - 2\xi\eta m_N(m_Y E_e - m_e^2) R_e[R_e - m_N^2 + m_\nu^2];\\
T_2^e = -\sqrt{E_e^2 - m_e^2}\,\{\eta^2[(m_Y E_e - m_e^2)\Gamma_1^e - {}^1\!/_3\, m_Y(m_Y - E_e)\Gamma_2^e] + \xi^2 R_e[\Gamma_1^e + \Gamma_2^e] + 2\xi\eta m_Y m_N R_e[R_e - m_N^2 + m_\nu^2]\};\\
T_3^e = -\sqrt{E_e^2 - m_e^2}\,\{\eta^2[m_Y(m_Y - E_e)\Gamma_1^e - {}^1\!/_3\,(m_Y E_e - m_e^2)\Gamma_2^e] + \xi^2 R_e[\Gamma_1^e + \Gamma_2^e] - 2\xi\eta m_Y m_N R_e[R_e - m_N^2 + m_\nu^2]\};\\
T_4^e = \eta^2\{m_Y(E_e^2 - m_e^2)\Gamma_1^e - {}^1\!/_3\,(m_Y - E_e)(m_Y E_e - m_e^2)\Gamma_2^e\} + \xi^2 m_e R_e[\Gamma_1^e + \Gamma_2^e] + 2\xi\eta m_Y m_N(m_Y - E_e) R_e[R_e - m_N^2 + m_\nu^2];\\
T_5^e = -{}^1\!/_3\,\eta^2 m_e R_e \Gamma_2^e + \xi^2 E_e R_e[\Gamma_1^e + \Gamma_2^e] + 2\xi\eta m_N(m_Y E_e - m_e^2) R_e[R_e - m_N^2 + m_\nu^2];\\
\Gamma_1^e \equiv [R_e + m_N^2 - m_\nu^2][R_e - m_N^2 + m_\nu^2]; \quad \Gamma_2^e \equiv [R_e - (m_N + m_\nu)^2][R_e - (m_N - m_\nu)^2].
\end{gathered} \tag{18}$$

The formulas for polarization, emission asymmetry, and energy distribution of the antineutrino can be obtained from Eqs. (15) to (18) by interchanging the e and ν indices and applying the substitution (10).

4. DISCUSSION OF RESULTS

The total decay probability and integrated emission asymmetry are obtained from Eq. (15) by summing over the directions of ζ_e and integrating over E_e between the limits m_e and $[m_Y^2 + m_e^2 - (m_N + m_\nu)^2]/2m_Y$.

An analogous procedure should be applied to Eq. (11). The results may be written as

$$dW(\zeta_Y, \mathbf{n}_i) = W_0[1 - \alpha_0^i(\zeta_Y \cdot \mathbf{n}_i)]\, d\Omega_i/4\pi, \quad i = N, e. \tag{19}$$

The energy integral entering into the expression for W_0 must be evaluated numerically if none of the masses vanish. For $m_\nu = 0$ the integral can be performed analytically and we find

$$W_0 = \frac{m_Y^5}{2(2\pi)^3}[(\xi^2 + \eta^2)A_1 + \xi\eta A_2], \tag{20}$$

where

$$\begin{gathered}
A_1 = \left(\frac{m_N}{m_Y}\right)^4\left[1 - \left(\frac{m_e}{m_Y}\right)^4\right]\ln y_1 + \left(\frac{m_e}{m_Y}\right)^4\left[1 - \left(\frac{m_N}{m_Y}\right)^4\right]\ln y_2 + \frac{z}{24}\left\{1 + \left(\frac{m_N}{m_Y}\right)^6 + \left(\frac{m_e}{m_Y}\right)^6 + 12\left(\frac{m_N}{m_Y}\right)^2\left(\frac{m_e}{m_Y}\right)^2\right.\\
\left. - 7\left[\left(\frac{m_N}{m_Y}\right)^2 + \left(\frac{m_e}{m_Y}\right)^2 + \left(\frac{m_N}{m_Y}\right)^4 + \left(\frac{m_e}{m_Y}\right)^4 + \left(\frac{m_N}{m_Y}\right)^2\left(\frac{m_e}{m_Y}\right)^4 + \left(\frac{m_N}{m_Y}\right)^4\left(\frac{m_e}{m_Y}\right)^2\right]\right\};\\
A_2 = \frac{m_N}{m_Y}\left\{\left[\left[1 - \left(\frac{m_e}{m_Y}\right)^2\right]^2 + \left(\frac{m_N}{m_Y}\right)^2\right]\ln y_1 - \left(\frac{m_e}{m_Y}\right)^4\left[1 - \left(\frac{m_N}{m_Y}\right)^2\right]\ln y_2 - \frac{z}{24}\left[1 + \left(\frac{m_N}{m_Y}\right)^4 - 2\left(\frac{m_e}{m_Y}\right)^4 + 10\left(\frac{m_N}{m_Y}\right)^2\right.\right.\\
\left.\left. - 5\left(\frac{m_e}{m_Y}\right)^2 - 5\left(\frac{m_N}{m_Y}\right)^2\left(\frac{m_e}{m_Y}\right)^2\right]\right\};\\
z = \left\{\left(1 + \frac{m_N}{m_Y} + \frac{m_e}{m_Y}\right)\left(1 + \frac{m_N}{m_Y} - \frac{m_e}{m_Y}\right)\left(1 - \frac{m_N}{m_Y} - \frac{m_e}{m_Y}\right)\left(1 - \frac{m_N}{m_Y} + \frac{m_e}{m_Y}\right)\right\}^{1/2};\\
y_1 = \frac{m_Y}{2m_N}\left[1 + z + \left(\frac{m_N}{m_Y}\right)^2 - \left(\frac{m_e}{m_Y}\right)^2\right], \quad y_2 = \frac{m_Y}{2m_e}\left[1 + z - \left(\frac{m_N}{m_Y}\right)^2 + \left(\frac{m_e}{m_Y}\right)^2\right]
\end{gathered} \tag{21}$$

The coefficients α_0^i of Eq. (19) can also be given in analytic form, but the resultant expressions are unwieldy. It is simpler to calculate them for each specific case by a numerical integration of T_2^N and T_2^e over the energy. We give above a table of values of W_0 and α_0 for the decays enumerated in (1). Since at this time only the order of magnitude of these quantities is of interest, we make use of the simplifying assumptions $\xi = 0$, $\eta = \sqrt{2}\,G = 2 \times 10^{-49}$ erg-cm (i.e., $C_V = -C_A = G/\sqrt{2}$, where G is the constant of Feynman and Gell-Mann[1]). This means that no renormalization is taken into account for either the vector or axial-vector coupling con-

Probabilities for Leptonic Decays of Hyperons and Emission Asymmetries of the Produced Particles

Decay mode	W_0 (sec^{-1})	$\tau\times10^{10}$ (sec)	$W_0\tau$ (%)	α_0^N or $\alpha_0^{Y'}$	α_0^e or α_0^μ
$\Lambda^0\to p+e^-+\tilde{\nu}$	$7.4\cdot10^7$	2.8	2,1	0.6	0.05
$\Lambda^0\to p+\mu^-+\tilde{\nu}$	$1.2\cdot10^7$	2.8	0,33	0,4	0.06
$\Sigma^-\to n+e^-+\tilde{\nu}$	$5.4\cdot10^8$	1,8	9,6	0,55	0.175
$\Sigma^-\to n+\mu^-+\tilde{\nu}$	$2.4\cdot10^8$	1.8	4.3	0.5	0.09
$\Sigma^-\to\Lambda^0+e^-+\tilde{\nu}$	$2.1\cdot10^6$	1.8	0.037	0.65	
$\Sigma^+\to\Lambda^0+e^++\nu$	$1.4\cdot10^6$	0.9	0.013	0,5	
$\Xi^-\to\Lambda^0+e^-+\tilde{\nu}$	$1.6\cdot10^8$	1	1,6	0,6	
$\Xi^-\to\Lambda^0+\mu^-+\tilde{\nu}$	$4.3\cdot10^7$	1	0.4	0.5	

stants. The table also lists values of τ, the experimental hyperon lifetime, and of $W_0\tau$ which is the ratio of hyperon β decays to total number of decays.

It follows from the above that approximately $1/7$ of the total number of decays of the Σ^- hyperon and $1/20$ of the decays of the Λ^0 hyperon should proceed through the leptonic modes.* Therefore a contradiction with the universal V-A interaction would arise should the absence of these decay modes be confirmed. On the other hand, taking into account renormalization and the energy form factor of the interaction may decrease the value of W_0.

As can also be seen from the table the integrated emission asymmetry of the electrons and μ mesons is small. This smallness is a consequence of the assumption $C_A=-C_V$. It follows that a measurement of lepton-emission asymmetry would provide a sensitive test of this assumption.

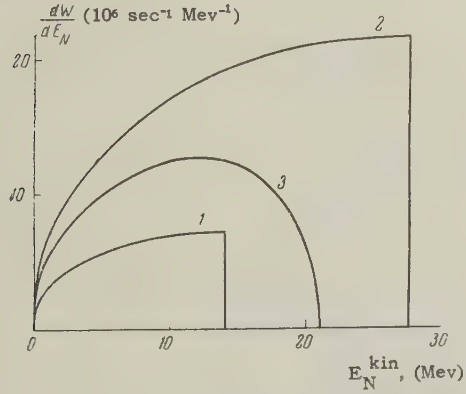

FIG. 1. Dependence of the hyperon decay probability on the energy of the produced nucleon.

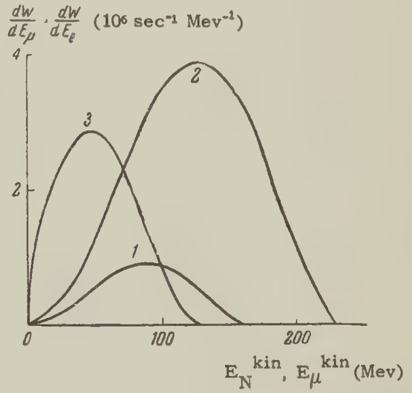

FIG. 2. Dependence of the hyperon decay probability on the electron or on the μ-meson energy.

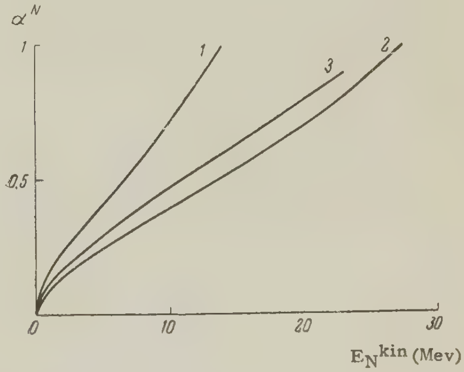

FIG. 3. Energy dependence of the nucleon emission asymmetry.

Figure 1 gives the dependence of the hyperon decay probability on the kinetic energy of the nucleon $E_N^{kin}\equiv E_N-m_N$. Figure 2 gives the dependence on the energy of the electron, E_e^{kin}, or of the μ meson E_μ^{kin}. The energy dependences of the asymmetry coefficients of the nucleon $[\alpha^N(E_N)\equiv-T_2^N/T_1^N]$ and of the electron and μ meson $[\alpha^e(E_e)\equiv-T_2^e/T_1^e$ and $\alpha^\mu(E_\mu)\equiv-T_2^\mu/T_1^\mu]$ are shown in Figs. 3 and 4 respectively.

---

*The values for the decay probabilities for $\Lambda^0\to p+e^-+\tilde{\nu}$ and $\Sigma^-\to n+e^-+\tilde{\nu}$ quoted by Feynman and Gell-Mann are somewhat smaller than those given in the table. This discrepancy disappears if it is assumed that the quantity C(x) introduced in reference 1 has been set approximately equal to unity by the authors in their calculations.

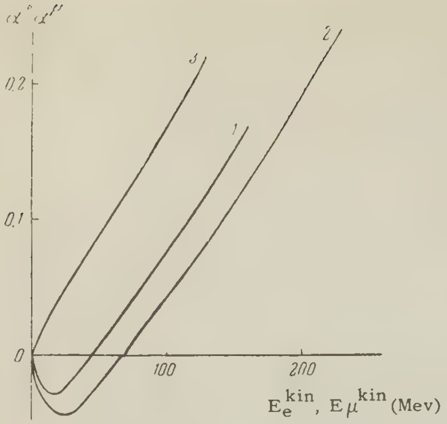

FIG. 4. Energy dependence of the electron or μ-meson emission asymmetry.

In all figures the curves labelled 1 refers to the decay $\Lambda^0 \rightarrow p + e^- + \tilde{\nu}$, those labelled 2 to $\Sigma^- \rightarrow n + e^- + \tilde{\nu}$, and those labelled 3 to $\Sigma^- \rightarrow n + \mu^- + \tilde{\nu}$. The remaining decays in (1) are characterized by analogous curves.

APPENDIX A

Calculation of Decay Probability

If the interaction Hamiltonian is of the form (3), the decay probability of type (2) is given by

$$dW = 2\pi \frac{d^3p_N}{(2\pi)^3} \frac{d^3p_e}{(2\pi)^3} d^3p_\nu \delta(p_Y - p_N - p_e - p_\nu) \,|M|^2, \quad (A.1)$$

where

$$|M|^2 = 4\mathrm{Sp}\,\{\eta^2 R_1^N \gamma_\mu R_1^Y \gamma_\nu + \xi^2 R_2^N \gamma_\mu R_2^Y \gamma_\nu + \eta\xi [R_3^N \gamma_\mu R_4^Y \gamma_\nu + R_4^N \gamma_\mu R_3^Y \gamma_\nu]\}\mathrm{Sp}\,\{R_1^e \gamma_\mu R_1^\nu \gamma_\nu\}. \quad (A.2)$$

Here

$$\left.\begin{array}{l} R_1^i = a\rho^i \bar{a}, \; R_2^i = \bar{a}\rho^i a, \\ R_3^i = a\rho^i a, \; R_4^i = \bar{a}\rho^i \bar{a} \end{array}\right\} i = Y, N, e, \nu, \quad (A.3)$$

$$a \equiv (1 + \gamma_5)/2, \quad \bar{a} \equiv (1 - \gamma_5)/2, \quad (A.4)$$

and ρ^i is the usual density matrix for the i-th particle.[5]

It is easy to show that $(\hat{A} \equiv \gamma_\mu A_\mu)$:

$$R_1^i = -ia\hat{t}_i/4E_i, \; R_2^i = -i\bar{a}\hat{t}'_i/4E_i, \\ R_3^i = a(m_i + \hat{\zeta}'_i\hat{p}_i)/4E_i, \; R_4^i = \bar{a}(m_i - \hat{\zeta}'_i\hat{p}_i)/4E_i, \quad (A.5)$$

where

$$t_i \equiv p_i - m_i\zeta'_i, \quad t'_i \equiv p_i + m_i\zeta'_i, \quad (A.6)$$

where

$$\zeta'_i = \zeta_i + (\zeta_i \cdot \mathbf{p}_i)\mathbf{p}_i/m_i(E_i + m_i), \quad \zeta'_{i0} = (\zeta_i \cdot \mathbf{p}_i)/m_i. \quad (A.7)$$

ζ'_i differs from ζ_i by having the component along the p_i direction increased E_i/m_i times, and ζ'_{i0} is defined by the equation

$$(\zeta'_i p_i) \equiv \zeta_{i\mu} p_{i\mu} = 0. \quad (A.8)$$

When Eq. (A.5) is introduced into Eq. (A.2) the result is

$$|M|^2 = (1/4\, E_Y E_N E_e E_\nu)\,\{\eta^2 (t_Y t_\nu)(t_N t_e) + \xi^2 (t'_Y t_e)(t'_N t_\nu) \\ + \eta\xi\, [m_Y m_N (t_e t_\nu) - m_Y \{(\zeta'_N t_e)(p_N t_\nu) - (\zeta'_N t_\nu)(p_N t_e)\} \\ + m_N \{(\zeta'_Y t_e)(p_Y t_\nu) - (\zeta'_Y t_\nu)(p_Y t_e)\} \quad (A.9) \\ - \frac{1}{8}\mathrm{Sp}\,(\hat{\zeta}'_N \hat{p}_N \gamma_\mu \hat{\zeta}'_Y \hat{p}_Y \gamma_\nu) \\ \times (-(t_e)_\mu (t_\nu)_\nu - (t_e)_\nu (t_\nu)_\mu + (t_e)_\alpha (t'_\nu)_\beta\, \varepsilon_{\alpha\beta\mu\nu})]\}$$

($\epsilon_{\alpha\beta\mu\nu}$ is the totally antisymmetric tensor with components 0, ±1).

The last trace in Eq. (A.9) is easy to calculate; subsequent substitution into Eq. (A.1) yields all possible distributions and correlations in the decay of a hyperon. However, for our purposes, it is not necessary to write out the general expression since $\zeta_N = 0$ and the last trace vanishes in all cases, except Eqs. (11) to (14). In the case when $\zeta_N \neq 0$ the calculation is carried out in the coordinate system in which $\mathbf{p}_Y = \mathbf{p}_N$, i.e., $\mathbf{p}_e = -\mathbf{p}_\nu$. In that case the last term of Eq. (A.9) after integration over the directions of $\mathbf{p}_e$ reduces to

$$^1/_4 \sum_\mu \mathrm{Sp}\,(\hat{\zeta}'_N \hat{p}_N \gamma_\mu \hat{\zeta}'_Y \hat{p}_Y \gamma_\mu)\;(p_e)_\mu (p_\nu)_\mu. \quad (A.10)$$

It is easy to see that (no summation over μ)

$$(p_e)_\mu (p_\nu)_\mu = -{}^1/_3\, \mathbf{p}_e^2 - \delta_{\mu 4}(E_e E_\nu - {}^1/_3\, \mathbf{p}_e^2). \quad (A.11)$$

Introducing Eqs. (A.11) and (A.8) into Eq. (A.10) gives

$$(E_e E_\nu - {}^1/_3\, \mathbf{p}_e^2)\,[(\zeta'_N \zeta'^*_Y)(p_N p^*_Y) - (\zeta'_N p^*_Y)(p_N \zeta'^*_Y)], \quad (A.12)$$

where * indicates that the purely imaginary fourth component of the given vector should be taken with the opposite sign.

The averaging over the directions of $\mathbf{p}_e$ in the remaining terms of Eq. (A.9), as well as the analogous integration over the directions of $\mathbf{p}_N$ in the case when electron polarization is studied, is elementary; after this Eq. (A.9) is expressed in terms of $\mathbf{p}_i$, E_i and the unchanged vectors ζ_i. The resultant expression is substituted into Eq. (A.1) and the expressions (11) to (18) are obtained after a Lorentz transformation to the frame $\mathbf{p}_Y = 0$ is performed.

We note that rule (10) for the interchange of electron and neutrino follows directly from Eqs. (A.9) and (A.6). In the most general case, when $\zeta_N \neq 0$, rule (10) should be amplified to include the condition $\zeta_N \rightarrow -\zeta_N$.

APPENDIX B

Universal Four-Fermion Interactions with Parity Nonconservation

As is well known,[6] five types of parity conserving interactions exist, universal in a narrower sense than that used in reference 1. The universality is defined by the condition that in going from the ordering

$$H_{\text{int}}=\sum_j g_j(\bar{\psi}_2 O_j \psi_1)(\bar{\psi}_3 O_j \psi_4) \tag{A.13}$$

to the ordering

$$H_{\text{int}}=\sum_j f_j(\bar{\psi}_2 O_j \psi_4)(\bar{\psi}_3 O_j \psi_1) \tag{A.14}$$

one should have $f_j = pg_j$ for all j (with the same $p = \pm 1$). The indices 1, 2, 3, 4 refer to the particles participating in the reaction, which need not be the decay of the particle labeled 1. One has $p = +1$ for the covariants V-A, S + P − T and 2(S − P) − (A + V), whereas $p = -1$ for 2(S − P) + (A + V) and 3(S + P) + T. It is easy to show, by the method of reference 7, that these interactions are also universal for the covariants with the primed constants, however then 2(S − P) − (A + V) has $p = -1$ and 2(S − P) + (A + V) has $p = +1$. Consequently, when both C_j and C'_j are nonzero, the last two combinations of covariants are no longer universal. Of the remaining three, 3(S + P) + T corresponds to $p = -1$ and, apparently, contradicts experimental data. For example, the Michel parameter determining the energy spectrum in μ-decay comes out equal to 0.25 whereas the experiment gives 0.68 ± 0.02.

The V-A and S + P − T covariants both have $p = 1$. They give similar results in the calculation of various processes and one may give a simple rule for going over from one to the other.

It is shown in reference 1 that the interaction corresponding in the notation of Lee and Yang[8] to

$$\begin{aligned} C_V = C'_V = -C_A = -C'_A \equiv G/\sqrt{2}, \\ C_S = C'_S = C_P = C'_P = C_T = C'_T = 0, \end{aligned} \tag{A.15}$$

may be brought into the form

$$H_{\text{int}} = 4\sqrt{8}\,G\,[(\varphi_2^*\varphi_1)(\varphi_3^*\varphi_4) - (\varphi_2^*\sigma\varphi_1)(\varphi_3^*\sigma\varphi_4)], \tag{A.16}$$

where

$$\varphi_i = {}^1\!/_2\,(v_i + w_i), \quad \psi_i = \begin{pmatrix} v_i \\ w_i \end{pmatrix}. \tag{A.17}$$

In turn, the interaction

$$\begin{aligned} C_S = -C'_S = C_P = -C'_P = -C_T = C'_T \equiv G/\sqrt{2}, \\ C_V = C'_V = C_A = C'_A = 0 \end{aligned} \tag{A.18}$$

(the relative sign of C and C′ is here different than in the V-A covariant to give electron polarization correctly in normal β decay) leads to

$$H_{\text{int}} = 4\sqrt{8}\,G\,[(\varphi_2^*\varphi'_1)(\varphi_3^*\varphi'_4) - (\varphi_2^*\sigma\varphi'_1)(\varphi_3^*\sigma\varphi'_4)], \tag{A.19}$$

where

$$\varphi'_1 = {}^1\!/_2\,(v_i - w_i). \tag{A.20}$$

Consequently the transition from V − A to S + P − T requires the replacement of φ_1 and φ_4 by φ'_1 and φ'_4 i.e. a change in sign of w_1 and w_4. Since $w_i = \sigma\cdot p_i v_i/(E_i + m_i)$ this implies changing of the sign of p_1 and p_4 in the matrix element. On the other hand, the sign of the momentum does not change in the conservation laws for free particles or in the $\exp\{i(p_e + p_\nu)\cdot r\}$ in forbidden transitions for the β decay. However, as can be seen from Eq. (A.9) for free particles, when $\xi = 0$ and $\eta = \sqrt{2}\,G$, the square of the matrix element contains the variables of the first and fourth particle only in the combination $(t_1 t_4)$, for which the sign change of p_1 and p_4 is equivalent to a sign change of ζ_1 and ζ_4 with unchanged p_1 and p_4. Consequently, for free particles, the transition from Eq. (A.15) to (A.18) is accomplished by

$$\zeta_1 \to -\zeta_1, \quad \zeta_4 \to -\zeta_4. \tag{A.21}$$

Precisely such a sign change for ζ_1 was noted in reference 4 in the discussion of μ-meson decay.

In the case of β decay, particles 1 and 4 are the neutron (n) and antineutrino (ν). The change in sign of p_1 is equivalent to the introduction of the additional matrix $\beta = \gamma_4$ into the nuclear matrix element. For the neutrino we have $w_\nu = \sigma\cdot n_\nu v_\nu$ $(n_\nu = p_\nu/|p_\nu|)$, and strictly speaking it is n_ν and not p_ν that changes sign. The quantity that enters into $\exp\{i(p_e + p_\nu)\cdot r\}$ is $p_\nu = |p_\nu|\,n_\nu$. In order that p_ν remain unchanged we must require that $|p_\nu|$ change sign along with n_ν. Consequently the transition from Eq. (A.15) to (A.18) is accomplished, in the case of β decay, by

$$\int O \to \int O\beta, \quad n_\nu \to -n_\nu, \quad |p_\nu| \to -|p_\nu|. \tag{A.22}$$

This leads to a different sign in the β-ν correlation in allowed transitions and to a change in the energy spectrum in forbidden transitions. Both these phenomena are well known (see, e.g., reference 9).

---

[1] R. P. Feynman and M. Gell-Mann, Phys. Rev. **109**, 193 (1958).

[2] E. C. G. Sudarshan and R. E. Marshak, Phys. Rev. **109**, 1860 (1958).

[3] R. T. Sharp and G. Bach, Canad. J. Phys. **35**, 1199 (1957).

[4] L. B. Okun' and V. M. Shekhter, J. Exptl. Theoret. Phys. (U.S.S.R.) **34**, 1250 (1958), Soviet Phys. JETP **7**, 864 (1958).

[5] H. A. Tolhoek, Rev. Mod. Phys. **28**, 277 (1956).

[6] D. C. Peaslee, Phys. Rev. **91**, 1447 (1953).

[7] M. Fierz, Z. Phys. **104**, 553 (1937).

[8] T. D. Lee and C. N. Yang, Phys. Rev. **104**, 254 (1956).

[9] A. Z. Dolginov, Nucl. Phys. **5**, 512 (1958).

Translated by A. Bincer
80

SOVIET PHYSICS JETP VOLUME 35(8), NUMBER 2 FEBRUARY, 1959

SPLITTING OF ATOMIC TERMS WITH INTEGER TOTAL ANGULAR MOMENTUM IN A MAGNETIC CRYSTAL

B. A. TAVGER

Moscow State Pedagogical Institute

Submitted to JETP editor March 27, 1958

J. Exptl. Theoret. Phys. (U.S.S.R.) **35**, 467-473 (August, 1958)

A method is proposed for finding the degeneracy caused by magnetic symmetry. The method is used to examine the nature of the splitting of atomic terms in a magnetic crystal for all cases of magnetic symmetry, under the assumption that the total angular momentum of the atom is integral. The results are compared with the splitting of atomic terms in a nonmagnetic crystal. It is found that the magnetic interaction in the crystal does not always remove the degeneracy of the atomic energy levels completely. It is shown that the results obtained are applicable to finding the splitting of terms of an atom in a nonmagnetic crystal which is placed in a magnetic field.

1. The field due to the other atoms of the crystal acts on an atom located in a crystal. This field has a definite symmetry which depends on both the crystal symmetry and on the position of the atom under consideration. The symmetry of the crystal field is a subgroup of the symmetry class of the crystal. The crystalline field can be treated as a perturbation which splits the energy levels of the unperturbed atom. This splitting is completely dependent on the symmetry of the crystal field at the point where the atom is located.

The question of splitting of atomic terms under the action of the crystalline field was treated by Bethe.[1] If we assume that the perturbation due to the crystal field is so small that the spin-orbit coupling in the atom is not broken down, we can start from a state of the free atom which is given by its total angular momentum J and its parity. Under the influence of the crystal field, the symmetry of the atom is reduced, which leads to partial or complete lifting of the degeneracy of the atomic state. To find this splitting we must expand the irreducible representation of the symmetry group of the free atom in irreducible representations of the symmetry group of the crystal field. The irreducible representation of the symmetry group of the free atom (spherical symmetry) gives the term of the unperturbed atom, while the irreducible representations of the symmetry group of the crystal field which are found in the expansion give the components in the splitting of the term.

We must however make one important reservation. The free atom is symmetric under time inversion. If the crystal field is purely electric, it is also symmetric under the time inversion R. Then the perturbed atom must also possess this symmetry. One might think that the symmetry with respect to R could be taken into account in the usual scheme of expansion in irreducible representations by assuming that the symmetry group of the crystal field also includes the time inversion. However this approach is incorrect. The point is that time inversion results in the replacement of the wave functions by their complex conjugates (when the spin is omitted). Complex conjugation is not a linear operation and, consequently, the symmetry group including the time inversion can have nonlinear representations in the basis of the wave functions. For this reason the effect of the time inversion on the splitting of atomic terms is treated outside the usual scheme:[2] one first treats the term splitting omitting the symmetry under the time inversion R, and then counts the two nonequivalent complex conjugate irreducible representations not as two different states, but as a single state with a degeneracy twice as great as the dimensionality of the representations.*

2. In the present paper the treatment of the splitting of atomic terms by a crystal field is extended to the case of magnetic crystals (ferromagnetics and antiferromagnetics). In this case an atom in the crystal is acted on not only by an electric field but also by the magnetic field due to the other atoms in the crystal. Thus the symmetry group of the crystal field is not one of the 32 crystallographic classes, but is a magnetic symmetry group (magnetic class).[3,4] Since the symmetry of the free atom contains all the elements of the magnetic classes, the symmetry of the perturbed atom will coincide with the symmetry of the field of the magnetic crystal.

The magnetic classes are of two types.[3] The first consists of those magnetic classes which coincide with the 32 crystallographic classes. The term splitting in a field with such a symmetry can be found as in reference 1. The results will be different, however, in that the components in the split term, which correspond to nonequivalent complex conjugate irreducible representations, should be counted as different, and not as coincident, as is the case when there is symmetry with respect to R.

The remaining 58 magnetic classes contain symmetry elements which are products of "rotations"† A with the time inversion R, but do not contain R itself. It is easily understood that, because of the time inversion, an operation like RA transforms the wave functions nonlinearly. The usual procedure for finding the splitting of atomic terms is therefore not applicable in this case.

The splitting of atomic terms when the crystal field has the symmetry of one of the 58 magnetic classes will differ essentially from the splitting in the case of the crystallographic classes.

3. We now formulate the problem. A state of the free atom constitutes an irreducible representation of the symmetry group of the sphere, with definite total angular momentum J and definite parity. The state is (2J + 1)-fold degenerate. Now we introduce the atom into a field having the symmetry of one of the 58 magnetic classes, and try to find the resulting term splitting.*

The symmetry group G of a magnetic class can be divided into two parts (cf. reference 3). The first part consists of all the "rotations" in the group G and does not include transformations involving the time inversion. These "rotations" form a subgroup H of index 2 in the group G, i.e., H contains half the elements of G. The symmetry elements of G which are not contained in H are products of "rotations" and the time inversion.

To find the term splitting we proceed as follows. First we consider the term splitting which would occur if H were the symmetry group of the perturbing field. This splitting is found in the usual fashion by expanding the irreducible representation corresponding to the free atom state in irreducible representations of H. In doing this, it is necessary to count nonequivalent complex-conjugate irreducible representations as belonging to different components in the split term. The resulting splitting will be more complete than the actual splitting since the symmetry of H is lower than the actual symmetry of the perturbed atom. Actually the presence in G of symmetry elements which are not contained in H can lead to indistinguishability of components corresponding to different irreducible representations of H. Consequently to find the actual splitting of atomic terms under the influence of a perturbation with the symmetry G we must establish how the irreducible representations of H change under the action on the basis of the representation of those symmetry elements in G which are not in H. The initial and the resultant representations are to be counted as belonging to the same component.

It is obviously sufficient to take only those ele-

---

*This is correct if the wave functions satisfy a Schrödinger equation, i.e., if the spin is not included. When the spin is included, the same result is found if the angular momentum of the atom is integral.[1]

†By "rotations" we always understand both true rotations and rotation-reflections which are a product of a true rotation and the space inversion.

*We are interested only in the number and degeneracy of the components in the splitting of the term. Naturally, the magnitude of the splitting, i.e., the distance between components, cannot be found on the basis of symmetry alone.

TABLE I. Tabulation of the 35 magnetic classes G whose "rotation" subgroup H has only real irreducible representations

G	H	G	H	G	H
$\underline{\bar{1}}$	1	$\underline{4}$	2	$\underline{\bar{3}}m$	$3m$
$\underline{2}$	1	$\underline{4}2$	222	$\underline{\bar{6}}\underline{2}m$	$3m$
$\underline{m}$	1	$\underline{4}/m$	$2/m$	$\underline{6}2$	32
$2/\underline{m}$	2	$\underline{4}m\underline{m}$	$2mm$	$\underline{\bar{6}}2m$	32
$\underline{2}/m$	m	$4/\underline{m}\underline{m}\underline{m}$	42	$\underline{6}m\underline{m}$	$3m$
$\underline{2}/\underline{m}$	$\bar{1}$	$4/\underline{m}mm$	$4mm$	$\underline{6}/m\underline{m}m$	$\bar{6}2m$
$2\underline{2}\underline{2}$	2	$\underline{4}/mmm$	mmm	$\underline{6}/\underline{m}\underline{m}m$	$\bar{3}m$
$2\underline{m}m$	2	$\underline{4}/\underline{m}\underline{m}m$	$\bar{4}2m$	$6/\underline{m}\underline{m}\underline{m}$	62
$2\underline{m}\underline{m}$	m	$\underline{\bar{4}}$	2	$6/\underline{m}mm$	$6mm$
$\underline{m}\underline{m}\underline{m}$	222	$\bar{4}2m$	222	$\underline{m}3\underline{m}$	43
$mm\underline{m}$	$2mm$	$\underline{\bar{4}}\underline{2}m$	$2mm$	$\underline{m}3m$	$\bar{4}3m$
$\underline{m}\underline{m}m$	$2/m$	$\underline{\bar{3}}\underline{m}$	32		

ments which when adjoined to H generate the whole group G.

Since the subgroup H has index 2, it is sufficient to adjoin to it any element of G-H in order to get G. We denote this element by RB, where R is the time inversion and B is some "rotation."

4. Let us consider any irreducible representation of the group, with the basis $\psi_1(x)$, $\psi_2(x)$, ... $\psi_n(x)$, where x is the set of arguments of the wave functions. The action of RB on the basis functions can be divided into the action of the "rotation" B and the action of the time inversion. In the present paper we limit ourselves to the case of integral J. In this case the results of including symmetry under time inversion are the same as when the spin is omitted entirely.[2] Thus we may assume that the wave functions satisfy the Schrödinger equation and are consequently transformed into their complex conjugates by the time inversion.

The 58 magnetic classes which do not reduce to the 32 crystallographic classes can be divided into two categories. Those magnetic classes whose groups have only real irreducible representations, (where by a real representation we mean one whose characters are real numbers), belong to the first category, while the remaining magnetic classes belong to the second.

Let us consider the change in the irreducible representations of the first category of groups when the element B acts on the basis. We choose a basis consisting of real functions.* In this case the "rotation" B transforms the old basis into a new one which again consists of real functions. Then the subsequent action on the basis by the element R produces no change. Thus the action of RB on the basis reduces to that of the "rotation" B alone. The splitting of the term will be the same as it would be if the time inversion R were replaced by the unit element E in the symmetry group of the perturbing field. Thus for those magnetic classes for which the representations are real, we can obtain the splitting of the atomic term by the standard procedure, as in reference 1, by choosing as the symmetry group the crystallographic class G′ which is obtained from the magnetic class G by replacing R by E.

By using the table of characters of irreducible representations of the groups of the crystallographic classes (cf. for example reference 5), it is easy to find all the magnetic classes belonging to the first category. There are 35 such classes (Table I).

We now go over to those magnetic classes for which the subgroup H has complex representations. For these magnetic classes, the action of elements RB on the basis of the irreducible representations of H does not reduce to the action of a "rotation" alone.

Under the action of B, the basis ψ_i changes to $\psi_i' = B_{ik}\psi_k$, and the representation $T(h)$, where h is an element of H, changes into $BT(h)B^{-1}$. The additional action of R on the basis changes the basis functions and the representations to their complex conjugates. The net result is that RB changes the representation $T(h)$ to $(BT(h)B^{-1})^*$. We must now demand

TABLE II. Characters of irreducible representations of the group 4

Irreducible representations	Group elements			
	E	L_4	L_2	L_4^{-1}
A	1	1	1	1
B	1	—1	1	—1
E_1	1	i	—1	—i
E_2	1	—i	—1	i

that the representations $T(h)$ and $(BT(h)B^{-1})^*$ belong to the same component in the split term. We note that $BT(h)B^{-1} = T(BhB^{-1})$. The rotations B and h form the group G′, which is obtained from G if the element RB is replaced by B. The group H will be a subgroup of index 2 in G as well as in G. We know that every subgroup of index 2 is a normal divisor (invariant subgroup). Therefore the element BhB^{-1} belongs to the subgroup H. Consequently the change of the representation under transformations of the type RB is found by using the table of irreducible representations. Actually the matter is further simplified by the fact that the irreducible representations are given by their characters.

We shall first apply these considerations to two examples. Suppose the atom is in a field of symmetry[*] $4/\underline{m}$: E, L_4, L_2, L_4^{-1}, $R\sigma_h$, RS_4, Ri, RS_4^{-1}. Here the subgroup H will be the group $4(C_4)$: E, L_4, L_2, L_4^{-1}. The group 4 has the irreducible representations A, B, E_1, E_2 (cf. Table II). It is most convenient to choose Ri as the element RB. The elements BhB^{-1} are $ihi^{-1} = h$, i.e., the matrix $T(h)$ and consequently the character $\chi(h)$ are not changed by the "rotation" i. The time inversion changes $\chi(h)$ to $\chi^*(h)$. This means that the irreducible representations A and B are not changed, while the irreducible representations E_1 and E_2 are transformed into one another. Consequently the representations E_1 and E_2 are indistinguishable in our problem. Thus in this example the splitting occurs as for a perturbation with symmetry 4, but the complex conjugate irreducible representations E_1 and E_2 belong to the same doubly degenerate subterm.

Let us treat another example. Suppose that the atom is in a field with the symmetry $4\underline{mm}$: E, L_4, L_2, L_4^{-1}, $4R\sigma_V$. The subgroup H is again the group 4. As the element RB it is convenient to choose $R\sigma_x$. The elements BhB^{-1} will be L_4^{-1} for L_4, L_4 for L_4^{-1}, and L_2 itself for L_2. From this we see that the irreducible representations A and B are transformed into themselves by the "rotation" σ_x, while the complex conjugate representations E_1 and E_2 transform into one another. Application of R again does not change A and B, while the complex conjugate representations E_1 and E_2 once again change places. Thus as a result of applying $R\sigma_x$ each irreducible representation of 4 goes over into itself. Consequently the splitting when the symmetry of the perturbation is $4\underline{mm}$ will be the same as when the symmetry is 4, and the complex conjugate irreducible representations must be counted as belonging to two different nondegenerate subterms.

TABLE III. Summary of the 12 magnetic classes for which inclusion of magnetic symmetry leads to no additional degeneracy

G	H
$4\underline{2}$	4
$4\underline{m}\underline{m}$	4
$4/m\underline{m}\underline{m}$	$4/m$
$\bar{4}\underline{2}\underline{m}$	$\bar{4}$
$3\underline{2}$	3
$3\underline{m}$	3
$\bar{3}\underline{m}$	$\bar{3}$
$\bar{6}\underline{2}\underline{m}$	$\bar{6}$
$6\underline{2}$	6
$6\underline{m}\underline{m}$	6
$6/m\underline{m}\underline{m}$	$6/m$
$\underline{\bar{4}}3\underline{m}$	23

All 23 magnetic classes for which the "rotation" subgroup H has complex irreducible representations are treated analogously to the examples presented above. One finds the result that the splitting is the same as when one includes only the symmetries in the subgroup H instead of the whole symmetry of the magnetic class, with the one important proviso that in 12 cases the complex conjugate irreducible representations of the subgroup H correspond to different nondegenerate subterms (Table III), while in the other 11 cases the complex conjugate irreducible representations of the subgroup H must be counted as belonging to the same doubly-degenerate component in the splitting of the term of the unperturbed atom (Table IV).

---

[*] We use the "international" notation for designating the symmetry classes, where the dash below a symbol means that instead of the underlined element we should take its product with the time inversion.

TABLE IV. Summary of the 11 magnetic classes for which inclusion of magnetic symmetry leads to additional degeneracy

G	H
$4/\underline{m}$	4
$\underline{4}/\underline{m}$	$\bar{4}$
$\underline{\bar{3}}$	3
$\underline{\bar{6}}$	3
$\underline{6}$	3
$\underline{6}/m$	$3/m$
$6/\underline{m}$	6
$\underline{6}/\underline{m}$	$\bar{3}$
$\underline{m}3$	23
$\underline{4}3$	23
$m3\underline{m}$	$m3$

From the group-theoretical point of view these cases differ in that in the first case the classes of conjugate elements of the group H do not coincide with the classes of conjugage elements of H when it is regarded as a subgroup of G, whereas in the second case the classes of conjugate elements are the same whether H is regarded as a subgroup of G or as a group by itself.

5. Let us discuss the results and explain the effect of inclusion of magnetic symmetry on the splitting of terms compared to the splitting when only the crystallographic symmetry is taken into account.

Disregard of the magnetic symmetry, i.e., omission of elements like RA, means that instead of the actual symmetry G of the perturbed atom we are taking the subgroup H of G which contains only "rotations." However, when this is done it is not assumed that there is no magnetic interaction.

In the case of magnetic symmetry, when the magnetic class coincides with one of the 32 crystallographic classes, elements like RA do not occur in the symmetry group, and the magnetic symmetry of the crystal field coincides with the crystallographic symmetry. Because of the presence of the magnetic interaction, the crystal field is not invariant with respect to R, so that the nonequivalent complex conjugate irreducible representations correspond to different components in the splitting of the term.

The other case of magnetic symmetry is that in which the magnetic class contains elements of the type RA, while the subgroup H containing all the "rotations" has only real irreducible representations (Table I). In this case the consideration of the magnetic symmetry, i.e., the inclusion of elements of the type RA, is essential. The removal of the degeneracy will in general be less complete than when only the crystallographic symmetry (i.e., the subgroup H) is considered. Despite the presence of the magnetic interaction, the removal of the degeneracy may be incomplete.

In the third case (Table III), taking account of the magnetic symmetry does not lead to new results. The presence of magnetic interaction results in the perturbed atom being nonsymmetric with respect to R.

In the fourth case (Table IV), the magnetic symmetry elements make those components in the splitting indistinguishable which belong to complex conjugate irreducible representations of the crystallographic symmetry group.

6. The treatment given above refers not only to the splitting of atomic terms in a magnetic crystal, but can also be applied without any restriction to the splitting of atomic terms in a nonmagnetic crystal which is in an external magnetic field. In this case the symmetry of the perturbed atom will contain the symmetry elements which are common to the crystal symmetry and to the symmetry of the external magnetic field for the given orientation of the crystal in the field; by the symmetry of the crystal we here mean its crystallographic class multiplied by R. If the orientation of the crystal in the field is arbitrary, the removal of the degeneracy will be complete, since there is no symmetry. But for certain positions of the crystal relative to the field it may happen that the degeneracy is not completely removed, in which case the consideration of magnetic symmetry is essential.

We also note that an atom in a uniform magnetic field has the symmetry $\infty/\underline{mm}$, and belongs to case 3 (Table III), for which consideration of the magnetic symmetry does not change the term splitting. This is in accord with the fact that the Zeeman effect is obtained correctly from symmetry considerations without taking magnetic symmetry into account.

In conclusion I express my thanks to Academician L. D. Landau and Prof. B. T. Geilikman for discussions.

---

[1] H. A. Bethe, Ann. d. Phys. 3, 133 (1929).

[2] E. P. Wigner, Gött. Nachr. 546 (1932).

[3] B. A. Tavger and V. M. Zaitsev, J. Exptl. Theoret. Phys. (U.S.S.R.) 30, 564 (1956); Soviet Phys. JETP 3, 430 (1956).

[4] L. D. Landau and E. M. Lifshitz, Электродинамика сплошных сред (Electrodynamics of Continuous Media), Gostekhizdat, 1957.

[5] L. D. Landau and E. M. Lifshitz, Квантовая механика (Quantum Mechanics), Gostekhizdat, 1948; English translation, Pergamon Press, 1958.

Translated by M. Hamermesh
81

SOVIET PHYSICS JETP VOLUME 35 (8), NUMBER 2 FEBRUARY, 1959

EFFECT OF THERMOELECTRIC FORCES ON THE SKIN EFFECT IN A METAL

M. I. KAGANOV and V. M. TSUKERNIK

Physico-Technical Institute, Academy of Sciences, Ukrainian S.S.R.

Submitted to JETP editor March 26, 1958

J. Exptl. Theoret. Phys. (U.S.S.R.) **35**, 474-478 (August, 1958)

The surface impedance of a metal is calculated with thermoelectric forces taken into account.

1. In the calculation of the surface resistance (impedance) of metals, one usually starts with Ohm's law,

$$j_i = \sigma_{ik} E_k,$$

where σ_{ik} is the conductivity tensor, and **E** and **J** are the vector electric field intensity and current density.* One thereby neglects the effect of heat waves that are produced in the metal by passage of an electromagnetic wave through it. As will be evident later, this is correct only in isotropic metals in the absence of a magnetic field, and in anisotropic metals when the surface of the metal coincides with a principal plane of the resistivity tensor.

The complete system of equations describing the propagation of waves in a metal, with heat flow taken into account, has the form

$$\mathrm{curl}\,\mathbf{H} = \frac{4\pi}{c}\mathbf{j}; \mathrm{curl}\,\mathbf{E} = -\frac{1}{c}\frac{\partial \mathbf{H}}{\partial t}; \quad C\frac{\partial \Theta}{\partial t} + \mathrm{div}\,\mathbf{q} = 0;$$
$$E_i = \rho_{ik} j_k + \alpha_{ik}\partial\Theta/\partial x_k; \quad q_i = T\alpha_k\, j_k - \varkappa_{ik}\partial\Theta/\partial x_k. \qquad (1)$$

Here Θ is the high-frequency addition to the mean temperature T of the specimen; C is the heat capacity of unit volume of the metal; **q** is the heat current; ρ_{ik} is the resistivity tensor; κ_{ik} is the heat conductivity tensor; and α_{ik} is the tensor of thermoelectric coefficients.

The tensor α_{ik}, in general, is not symmetric. However, all metals possess lattice symmetry that excludes an antisymmetric part of the tensor α_{ik}. Therefore we shall hereafter suppose, in the absence of a magnetic field, that $\alpha_{ik} = \alpha_{ki}$.

Besides the usual boundary conditions of continuity of the tangential components of the vectors **E** and **H**, we must add to the system of equations (1) boundary conditions for the temperature. We shall consider two limiting cases:

(a) Heat current equal to zero at the surface:

$$\mathbf{q}\cdot\mathbf{n} = 0 \qquad (2a)$$

(**n** = unit vector normal to the surface).

(b) Surface temperature maintained constant and equal to T:

$$\Theta = 0. \qquad (2b)$$

2. We consider normal incidence of a plane monochromatic electromagnetic wave, of frequency ω, on the surface of a uniaxial metal, whose principal axis (1 in the figure) makes an angle φ with the normal to the surface of the metal; we choose for the z axis the direction of the normal. Then all quantities (**E**, **H**, Θ) depend on the coordinate z alone. With the x and y axes chosen as shown in the figure, it is easy to show that $\rho_{xy} = \rho_{yx} = \rho_{xz} = 0$ and $\alpha_{xy} = \alpha_{yx} = \alpha_{zx} = 0$. It follows furthermore from Maxwell's equations, in this case, that $j_z = 0$

---

*We are interested here in the range of frequencies and temperatures in which there is a normal skin effect.

and $H_z = 0$. Therefore the complete system of equations takes the form

$$-\frac{\partial H_y}{\partial z} = \frac{4\pi}{c} j_x, \quad \frac{\partial E_x}{\partial z} = \frac{i\omega}{c} H_y, \; E_x = \rho_{xx} j_x, \tag{3}$$

$$\frac{\partial H_x}{\partial z} = \frac{4\pi}{c} j_y, \quad -\frac{\partial E_y}{\partial z} = \frac{i\omega}{c} H_x,$$

$$E_y = \rho_{yy} j_y + \alpha_{yz} \frac{\partial \Theta}{\partial z}, \quad -i\omega C\Theta + \frac{\partial q_z}{\partial z} = 0, \tag{4}$$

$$q_z = T\alpha_{yz} j_y - \varkappa_{zz} \frac{\partial \Theta}{\partial z}$$

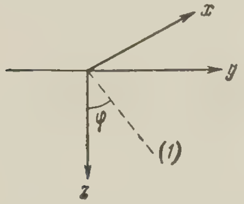

As is evident from (3) and (4), the complete system of equations separates into two independent systems. If the incident electromagnetic wave is so polarized that the vector E is parallel to the x axis, the field in the metal is described by the system (3). In this case no heat flow occurs, and the surface impedance is determined by the usual formula*

$$\zeta_x = \zeta_{0x} = \sqrt{\omega\rho_{xx} / 4\pi i} = \sqrt{\omega\rho_\perp / 4\pi i}, \tag{5}$$

where $\rho_\perp$ is one of the principal values of the tensor ρ_{ik} (the principal values of the tensor ρ_{ik} are equal to $\rho_{22} = \rho_{33} = \rho_\perp$ and $\rho_{11} = \rho_\parallel$).

Now let the electric field of the incident wave be directed along the y axis. On eliminating the magnetic field from the system (4) and representing $-\alpha_{yz}\partial\Theta/\partial z$ by E_T, we get

$$\left(k_\rho^2 + \frac{d^2}{dz^2}\right) E_y + k_\rho^2 E_T = 0,$$

$$-k_\rho^2 \frac{a}{1+a} E_y + \left(\frac{d^2}{dz^2} + k_\rho^2 \frac{b-a}{1+a}\right) E_T = 0, \tag{6}$$

$$a = T\alpha_{yz}^2 / \rho_{yy}\varkappa_{zz}, \quad b = c^2 C\rho_{yy} / 4\pi\varkappa_{zz}.$$

Here $k_\rho = (4\pi i\omega/c^2\rho_{yy})^{1/2}$ is the complex wave vector of the electromagnetic wave in the metal without allowance for thermoelectric forces (with $\alpha_{yz} = 0$).

From the system (6) we get for the half-space ($z > 0$) occupied by the metal

$$E_y = Ae^{ik_1 z} + Be^{ik_2 z}, \tag{7}$$

$$E_T = -(1 - k_1^2 / k_\rho^2)\, Ae^{ik_1 z} - (1 - k_2^2 / k_\rho^2)\, Be^{ik_2 z},$$

where

$$k_{1,2} = k_\rho \left[\frac{1 + b \pm \sqrt{(1-b)^2 - 4ab}}{2(1+a)}\right]^{1/2}, \tag{8}$$

and where A and B are constants, a relation between which is determined by the boundary conditions for the temperature. The sign of the root in formula (8) must be so chosen that the imaginary parts of the wave vectors k_1 and k_2 are positive.

According to the definition of the impendance we have

$$\zeta_y = (\omega / c)(A + B) / (k_1 A + k_2 B). \tag{9}$$

In the case in which the heat current vanishes on the surface (2a),

$$B = -\frac{(a+1)(k_1 / k_\rho)^2 - 1}{(a+1)(k_2 / k_\rho)^2 - 1} A, \tag{10}$$

$$\zeta_y^{\text{ad}} = \zeta_{0y} \sqrt{\frac{1+a}{2}} \tag{11a}$$

$$\times \frac{\left(1 + a + \sqrt{(1-b)^2 - 4ab}\right)^{1/2} + \left(1 + a - \sqrt{(1-b)^2 - 4ab}\right)^{1/2}}{1 + \sqrt{(a+1)\, b}},$$

where $\zeta_{0y} = \sqrt{\omega\rho_{yy}/4\pi i}$

Under the condition (2b) (isothermal surface), we obtain similarly

$$\zeta_y^{\text{is}} = \zeta_{0y} \sqrt{2}$$

$$\times \frac{\sqrt{b} + \sqrt{1+a}}{\left(1 + b + \sqrt{(1-b)^2 - 4ab}\right)^{1/2} + \left(1 + b - \sqrt{(1-b)^2 - 4ab}\right)^{1/2}}. \tag{11b}$$

For $a \ll 1$, formulas (11a) and (11b) simplify considerably:

$$\zeta_y^{\text{ad}} \approx \zeta_{0y} \left\{1 + \frac{a}{2} \frac{1 + 2\sqrt{b}}{(1 + \sqrt{b})^2}\right\}; \tag{12a}$$

$$\zeta_y^{\text{is}} \approx \zeta_{0y} \left\{1 + \frac{a}{2} \frac{1}{(1 + \sqrt{b})^2}\right\}. \tag{12b}$$

We remark that the dependence of the impedance ζ_y on the angle between the normal to the metal surface and the crystal axis, in contrast to ζ_{0y}, is determined not solely by the quantity

$$\rho_{yy} = \rho_\perp \cos^2\varphi + \rho_\parallel \sin^2\varphi, \tag{13}$$

but also by the parameters a and b, which vary with the angle as follows:

$$a = \frac{T(\alpha_\perp - \alpha_\parallel)^2 \sin^2\varphi \cos^2\varphi}{(\rho_\perp \cos^2\varphi + \rho_\parallel \sin^2\varphi)(\varkappa_\perp \sin^2\varphi + \varkappa_\parallel \cos^2\varphi)};$$

$$b = \frac{c^2 C(\rho_\perp \cos^2\varphi + \rho_\parallel \sin^2\varphi)}{4\pi(\varkappa_\perp \sin^2\varphi + \varkappa_\parallel \cos^2\varphi)}. \tag{14}$$

From the first formula (14) it is clear that a vanishes when $\varphi = 0$ or $\pi/2$. Then heat current is absent, and the expression for the surface impedance ζ_y coincides with the ordinary ζ_{0y}. We

---

*We define the impedance as follows:

$$\zeta_x = E_x(0) / H_y(0); \quad \zeta_y = -E_y(0) / H_x(0).$$

write an expression for the impedance near these values of the angle. For $\varphi \ll 1$,

$$\zeta_y^{\mathrm{ad}} \approx \sqrt{\frac{\rho_\perp \omega}{4\pi i}}\Bigg\{1 + \frac{\varphi^2}{2}\Bigg[\frac{\rho_\parallel}{\rho_\perp} - 1 + \frac{T(\alpha_\parallel - \alpha_\perp)^2}{\rho_\perp \varkappa_\parallel}\,\frac{1 + \sqrt{c^2 C\rho_\perp / \pi\varkappa_\parallel}}{(1 + \sqrt{c^2 C\rho_\perp / 4\pi\varkappa_\parallel})^2}\Bigg]\Bigg\}; \tag{15a}$$

$$\zeta_Y^{\mathrm{is}} \approx \sqrt{\frac{\rho_\perp \omega}{4\pi i}}\Bigg\{1 + \frac{\varphi^2}{2}\Bigg[\frac{\rho_\parallel}{\rho_\perp} - 1 + \frac{T(\alpha_\parallel - \alpha_\perp)^2}{\rho_\perp \varkappa_\parallel}(1 + \sqrt{c^2 C\rho_\perp / 4\pi\varkappa_\parallel})^{-2}\Bigg]\Bigg\} \tag{15b}$$

For $\psi \ll 1$ $(\psi = \pi/2 - \varphi)$,

$$\zeta_y^{\mathrm{ad}} \approx \sqrt{\frac{\omega\rho_\parallel}{4\pi i}}\Bigg\{1 + \frac{1}{2}\psi^2\Bigg[\frac{\rho_\perp}{\rho_\parallel} - 1 + \frac{T(\alpha_\perp - \alpha_\parallel)^2}{\rho_\parallel \varkappa_\perp}\,\frac{1 + \sqrt{c^2 C\rho_\parallel / \pi\varkappa_\perp}}{(1 + \sqrt{c^2 C\rho_\parallel / 4\pi\varkappa_\perp})^2}\Bigg]\Bigg\}; \tag{16a}$$

$$\zeta_y^{\mathrm{is}} \approx \sqrt{\frac{\omega\rho_\parallel}{4\pi i}}\Bigg\{1 + \frac{1}{2}\psi^2\Bigg[\frac{\rho_\perp}{\rho_\parallel} - 1 + \frac{T(\alpha_\perp - \alpha_\parallel)^2}{\rho_\parallel \varkappa_\perp}\left(1 + \sqrt{\frac{c^2 C\rho_\parallel}{4\pi\varkappa_\perp}}\right)^{-2}\Bigg]\Bigg\}. \tag{16b}$$

3. The effect under consideration can be observed even in anisotropic metal (polycrystal) if the latter is placed in a constant magnetic field. In this case the most general possible linear relation between the electric field and heat current, on the one hand, and the electric current and temperature gradient, on the other, has the form

$$\begin{aligned} \mathbf{E} &= \rho\mathbf{j} + R[\mathbf{H}_0 \times \mathbf{j}] + \beta\mathbf{H}_0(\mathbf{H}_0 \cdot \mathbf{j}) \\ &\quad + \alpha\nabla T + N[\mathbf{H}_0\nabla T] + \gamma\mathbf{H}_0(\mathbf{H}_0\nabla T), \\ \mathbf{q} &= T\alpha\mathbf{j} - \varkappa\nabla T + NT[\mathbf{H}_0 \times \mathbf{j}] \\ &\quad + L[\mathbf{H}_0\nabla T] + T\gamma\mathbf{H}_0(\mathbf{H}_0 \cdot \mathbf{j}) - \delta\mathbf{H}_0(\mathbf{H}_0\nabla T). \end{aligned}$$

The phenomenological constants introduced (ρ, R, α, β, etc.) may, in general, depend on the magnitude of the magnetic field.

The greatest change of surface resistance resulting from the effect of the heat wave will occur in a magnetic field parallel to the metal surface. After a calculation similar to that carried out above, we get

$$\zeta_x^{\mathrm{ad}} = \zeta_0 \sqrt{\frac{1 - a'}{2}} \tag{17a}$$

$$\times \frac{(1 + b' + \sqrt{(1 - b')^2 + 4a'b'})^{1/2} + (1 + b' - \sqrt{(1 - b')^2 + 4a'b'})^{1/2}}{1 + \sqrt{(1 - a')b'}};$$

$$\zeta_x^{\mathrm{is}} = \zeta_0 \sqrt{2} \tag{17b}$$

$$\times \frac{\sqrt{b'} + \sqrt{1 - a'}}{(1 + b' + \sqrt{(1 - b')^2 + 4a'b'})^{1/2} + (1 + b' - \sqrt{(1 - b')^2 + 4a'b'})^{1/2}}$$

$$\zeta_y^{\mathrm{ad}} = \zeta_y^{\mathrm{is}} = \zeta_0 = \sqrt{\omega\rho / 4\pi i}.$$

Here

$$a' = (NH_0)^2 T / \rho\varkappa; \quad b' = c^2 C\rho / 4\pi\varkappa.$$

It is interesting to note that for $a' = 1$, $\zeta_x^{\mathrm{ad}} = 0$; i.e., the metal behaves in this case like an ideal conductor. The vanishing of the impedance (ζ_x^{ad}) is essentially connected with the rigorous vanishing of the heat current on the surface. Actually, when account is taken of heat radiation, q_z always differs from zero. Therefore even for $a' = 0$, $\zeta_x \neq 0$; but it has a minimum there.

4. As is clear from the formulas presented, the magnitude of the expected effect (the dependence of the surface resistance on the heat emission conditions) is determined by the value of the constant

$$a = T\alpha_{yz}^2 / \rho_{yy}\varkappa_{zz}.$$

The parameter a can be estimated only in order of magnitude, since there are no direct measurements of the components of the tensor α_{ik}. If we suppose that the quantities α_{ik} have the same order of magnitude as the Thomson coefficient and that $\rho\kappa/T$ has the order of magnitude of the constant in the Wiedemann-Franz law, then a has a value of order 10^{-2} for ordinary metals (Pt, Pd, W). For metals such as Bi, the Thomson coefficient is anomalously large ($\sim 10^3$),[2] and a may be of order unity (or even greater).

In the case of small a, observation of the described effect by reflection is difficult. However, if the length of the heat wave in the metal is much larger than the skin depth (for $a \ll 1$, this corresponds to a small value of the parameter b), then there can be a peculiar "pulling" of the electromagnetic wave by the heat wave. For films whose thickness d satisfies the condition

$$\delta_{\mathrm{sk}} \ll d \ll \delta_T$$

($\delta_{\mathrm{sk}} = \sqrt{c^2\rho_{yy}/2\pi\omega}$ is the thickness of the skin layer, $\delta_T = \sqrt{2\kappa_{zz}/\omega C}$ is the depth of penetration of the heat wave), the amplitude of the transmitted wave is expressed in terms of the amplitude of the incident wave by the equation

$$E_{\mathrm{tr}} / E_{\mathrm{inc}} = -(c^2 C\alpha_{yz}^2 T / 2\pi\varkappa_{zz}^2)\,\zeta_{0y}. \tag{18}$$

The last formula was obtained on the assumption that the heat current vanishes on both sides of the film. We have neglected terms of order

$\exp(-d/\delta_{sk})$.

5. We further consider oblique incidence of an electromagnetic wave on an isotropic conductor. In metals the surface impedance is independent of the angle of incidence φ and of the polarization of the wave because of the fact that $4\pi\sigma/\omega \gg 1$. Therefore the following consideration relates to semiconductors, for which the dependence on angle of incidence is appreciable. On representing by $\epsilon = \epsilon' + i\epsilon''$ the complex dielectric constant ($\epsilon'' = 4\pi\sigma/\omega$), we get the known value for the impedance in the case in which the electric field **E** of the incident wave is perpendicular to the plane of incidence:

$$\zeta = 1/\sqrt{\varepsilon - \sin^2\varphi}.$$

In the case in which **E** lies in the plane of incidence, consideration of thermoelectric forces naturally changes the value of the impedance:

$$\zeta^{\mathrm{ad}} = \frac{1}{\varepsilon}\left\{\sqrt{\varepsilon - \sin^2\varphi} - \frac{T\sigma\alpha^2}{\varkappa}\,\frac{i\varepsilon''\sin^2\varphi}{\varepsilon + T\sigma\alpha^2\varepsilon'/\varkappa}\left[\frac{ic^2C}{\omega\varkappa}\,\frac{1}{1 + T\alpha^2\sigma\varepsilon'/\varkappa\varepsilon} - \sin^2\varphi\right]^{-1/2}\right\}.$$

This expression corresponds to absence of heat current at the surface. Under isothermal conditions at the surface, no heat wave is produced, and therefore

$$\zeta^{\mathrm{is}} = \sqrt{\varepsilon - \sin^2\varphi}/\varepsilon.$$

In closing, the authors express their gratitude to L. D. Landau for helpful discussions.

---

[1] L. D. Landau and E. M. Lifshitz, Электродинамика сплошных сред (Electrodynamics of Continuous Media), Gostekhizdat, M. 1957, Sect. 25.

[2] Сборник физических констант (Collection of Physical Constants), ONTI, L.-M. 1937.

Translated by W. F. Brown, Jr.
82

SOVIET PHYSICS JETP VOLUME 35(8), NUMBER 2 FEBRUARY, 1959

KINETICS OF DIFFUSIVE DECOMPOSITION OF SUPERSATURATED SOLID SOLUTIONS

I. M. LIFSHITZ and V. V. SLEZOV

Physico-Technical Institute, Academy of Sciences, Ukrainian S.S.R. and Khar'kov State University

Submitted to JETP editor March 24, 1958

J. Exptl. Theoret. Phys. (U.S.S.R.) **35**, 479-492 (August, 1958)

The kinetics of the diffusive process of formation of grains of a new phase in a supersaturated solid solution is studied at a late stage of the process (coalescence of the grains). The exact asymptotic solution of the problem is obtained and investigated. The asymptotic distribution function is derived, the asymptotic number and average size of the grains are determined and the process of establishment of the asymptotic laws is analyzed. As an example of application of the theory, the mechanism of sintering is considered.

1. INTRODUCTION. STATEMENT OF THE PROBLEM

DURING the decomposition of a supersaturated solid solution, two stages must be distinguished in the diffusive process of formation of grains of a new phase. In the first stage there occur the fluctuating formation of nucleation centers of the new phase and their growth directly out of the supersaturated solution. In the second stage, when the grains are fairly large and the degree of supersaturation becomes extremely small, the principal process is coalescence: large grains "devour" small grains (the larger grains grow by the dissolution of smaller grains). In this second stage new nuclei would have to be of macroscopic size; thus their formation is practically excluded.

In the present paper we consider the kinetics of grain growth (coalescence) in the later stage. Other writers$^{1-4}$ have considered a problem of this type without arriving at a correct solution. Todes^4 has made the most thorough study of the question and has stated correctly that the asymptotic process for long times is independent of the initial conditions (the initial grain size distribution). He also correctly determined the order of magnitude of the rate of decrease of the number of grains with time. However, his quantitative solutions contain logarithmic divergences without physical meaning, which show that his reasoning is incorrect and also throw doubt on those of his qualitative results which are actually correct. The extremely peculiar behavior of the exact solution and the entire analysis which will be given below permit us to understand the origin of Todes' erroneous solution.

In stating the problem we shall, for simplicity, neglect anisotropy and assume the grains to be spherical. Allowance for nonspherical shapes would only change some numerical constants in the equations which follow. The equilibrium concentration C_R at the surface of a grain has the following usual relation to its radius R:

$$C_R = C_\infty + \alpha / R, \tag{1}$$

where C_∞ is the concentration of a saturated solution and α is associated with the interphase surface tension, with $\alpha = (\sigma/kT)VC_\infty$ (V is the volume of an atom of the solute).

Assuming the degree of supersaturation $\Delta = C - C_\infty$ to be small, i.e., $\Delta \ll 1$, and neglecting the "interaction" between grains (which is permissible because the grain diameter is small compared with the intergranular separation), we obtain for the diffusion flux of the dissolved substance per unit of grain surface the expression*

$$j = D\left.\frac{\partial C}{\partial R}\right|_{r=R} = \frac{D}{R}(C - C_R) = \frac{D}{R}\left(\Delta - \frac{\alpha}{R}\right)$$

and thus for the change of grain radius with time†

$$\frac{dR}{dt} = \frac{D}{R}\left(\Delta - \frac{\alpha}{R}\right). \tag{2}$$

Thus for each value of the supersaturation Δ there exists a critical radius $R_{cr} = \alpha\Delta$ at which the grain is in equilibrium with the solution; when $R > R_{cr}$ the grain grows while when $R < R_{cr}$ it dissolves. This is the evident cause of the "devouring" of small grains by large grains. Δ and R_{cr} vary with time.

---

*The expression given for the flux corresponds to a stationary value of the gradient $\partial C/\partial r$ on the grain boundary. It is easily seen that this is permissible when the initial supersaturation is amall, $\Delta_0 \ll 1$.

†We note that if the grains are nonspherical but preserve similarity of their shapes while growing during the later stage (a similarity associated with the anisotropy α), Eq. (2) and all subsequent quantitative results remain valid. Then R signifies $(3V/4\pi)^{1/3}$, V being the grain volume, and α and D differ from their previous values by only a numerical factor which takes the grain shape into account.

We shall hereafter use the dimensionless quantities $\rho = R/R_{cr}$, $t' = t/T$, ($R_{cr0} = \alpha/\Delta_0$, $T = R_{cr0}^3/\alpha\Delta$, Δ_0 is the initial supersaturation, R_{cr0} is the initial critical radius). Omitting the prime in t', we obtain

$$d\rho^3/dt = 3(\rho/x - 1), \tag{3}$$

where $x(t)$ is the dimensionless critical radius and $x(0) = 1$.

Introducing a grain-size distribution function $f(\rho, t)$ and regarding $v_\rho = d\rho/dt$ as the rate of grain travel in the space of grain sizes, we can write down the equations for the unknown functions $f(\rho, t)$ and $x(t)$. The first of these is the continuity equation in grain-size space:

$$\frac{\partial f}{\partial t} + \frac{\partial}{\partial \rho}(f v_\rho) = 0, \tag{4}$$

while the second equation is the law of conservation of matter:

$$Q_0 = \Delta_0 + q_0 = \Delta + q, \quad q = \frac{4\pi}{3} R_{cr0}^3 \int_0^\infty f\rho^3\, d\rho$$

or, with $x = \Delta_0/\Delta$,

$$1 = \frac{\Delta_0}{Q_0 x} + \varkappa \int_0^\infty f\rho^3\, d\rho, \quad \varkappa = 4\pi R_{cr0}^3/3Q_0. \tag{5}$$

In this equation Q_0 is the total initial supersaturation, including the initial volume of matter q_0 in the grains. In (5) f is normalized to unit volume: $n = \int_0^\infty f\, d\rho$ is the number of grains per unit volume.

Our problem thus becomes the asymptotic solution of (4) and (5) for a given initial condition $f(\rho, 0) = f_0(\rho)$.

2. ASYMPTOTIC VARIATION OF CRITICAL SIZES

To solve our problem we must first determine the asymptotic variation of critical sizes $x(t)$ [or of the supersaturation $\Delta(t) = \Delta_0/x(t)$, which amounts to the same thing]. The motion of the point ρ which represents a grain radius on the axis of sizes, as determined by the equation of motion (3), presents the following picture: The points located to the left of $x(t)$ are accelerated toward the left and disappear upon reaching the coordinate origin (complete dissolution of the grain). The points which are originally to the right of $x(t)$ move to the right (the grains grow), but as the supersaturation diminishes the critical size $x(t)$ increases and successively "overtakes" points moving to the right, after which these points begin to move in the opposite direction and also "disappear" at the origin. This movement is always orderly; the original order of position of the points is preserved.

Both the form of Eq. (3) and the physical meaning of $x(t)$ suggest that for the independent variable in Eqs. (3), (4), and (5) we take instead of the grain radius ρ the relative radius (with respect to the critical radius)

$$u = \rho/x(t). \tag{6}$$

Since for $t \to \infty$ the supersaturation $\Delta \to 0$, we have $x(t) \to \infty$. Thus $x(t)$ can be used to compute time.* The "equation of motion" (3) acquires a canonical form when "time" is represented by the quantity

$$\tau = \ln x^3. \tag{7}$$

Insertion of (6) and (7) into (3) gives

$$du^3/d\tau = \gamma(u - 1) - u^3, \tag{8}$$

$$\gamma = \gamma(\tau) = 3dt/dx^3. \tag{9}$$

If $u(v, \tau)$ denotes the solution of (8) for the initial condition $u|_{\tau=0} = v$ and we consider that $\rho(v, \tau) = xu(v, \tau)$, $x(0) = 1$, and $\tau|_{t=0} = 0$, the total quantity q of matter in the grains can be expressed through the initial distribution function $f_0(\rho)$ as follows:

$$q = \varkappa Q_0 \int_{v_0(\tau)}^\infty f_0(v)\, x^3(\tau)\, u^3(v, \tau)\, dv. \tag{10}$$

Here $v_0(\tau)$, the solution of the equation $u(v_0(\tau), \tau) = 0$, is the lower limit of the original sizes of grains which had not dissolved up to the time τ. Noting that $x^3 = e^\tau$, we can write (5) as

$$1 - e^{-\tau/3} = \varkappa e^\tau \int_{v_0(\tau)}^\infty f_0(v)\, u^3(v, \tau)\, dv. \tag{11}$$

Equations (8) and (11) form a complete system. These equations can be used to determine the unknown function $\gamma(\tau) = 3dt/dx^3$ and thus ultimately $x(t)$.

Three possibilities exist for the asymptotic behavior of $\gamma(\tau)$ as $\tau \to \infty$: (1) $\gamma(\tau) \to \infty$; (2) $\gamma(\tau) \to$ const; (3) $\gamma(\tau) \to 0$. We shall begin

---

*A formal exception is the case in which the initial distribution is a δ function [$f_0 = A\delta(\rho - \rho_0)$] or a sum of δ functions. In this case $x(t) \to$ const and the common size ρ assumes an equilibrium value. But the case is also unstable since even an extremely small spread of the initial distribution leads to $x(t) \to \infty$.

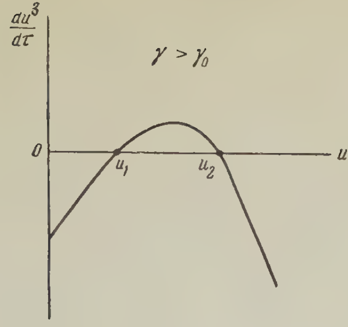

FIG. 1

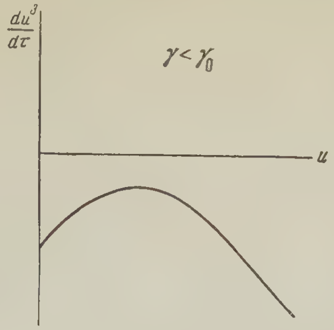

FIG. 2

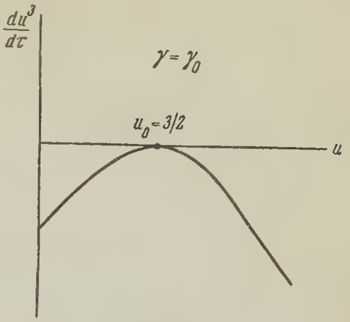

FIG. 3

our analysis with the case $\gamma = \text{const}$. Depending on the value of γ, the curve of the velocity $du^3/d\tau$ as a function of u can be tangent to the horizontal axis (for $\gamma = \gamma_0 = 27/4$), lie below this axis (for $\gamma < \gamma_0$), or have a positive section (for $\gamma > \gamma_0$) (Figs. 1, 2, 3).

(a) When $\gamma > \gamma_0$ all points that lie to the left of u_1 move toward the left and disappear when they reach the coordinate origin. All points that lie to the right of u_1 move to the point u_2, approaching it asymptotically from either the left or right. Therefore for $\tau \to \infty$ the integral in the right member of (11) approaches the constant value

$$I_0 = u_2^3 \int_{u_1}^{\infty} f_0(v)\, dv,$$

and the combined volume q of the grains, which is also in the right member, increases as e^{τ},

$$q = \varkappa I_0 e^{\tau} \to \infty, \tag{12}$$

so that Eq. (11) is not satisfied. When we take into account the fact that a constant value $\gamma > \gamma_0$ is reached only asymptotically, the foregoing description remains unchanged: we need only shift the time origin and let $f_0(v)$ refer to the time when $\gamma(\tau)$ is close to its asymptotic value.

(b) When $\gamma < \gamma_0$ all points move to the left and reach the origin in a finite time. It follows from (8) that at the time τ all grains have been dissolved whose original sizes were smaller than $v_0(\tau)$. These sizes are determined from the equation

$$\int_0^{v_0(\tau)} \frac{3u^2\, du}{u^3 - \gamma(u-1)} = \tau.$$

When $\tau \gg 1$ we have $v_0(\tau) = e^{\tau/3}$. Therefore the combined volume of the grains will be determined from the "tail" of the original distribution $f_0(v)$:

$$q(\tau) = \varkappa e^{\tau} \int_{e^{\tau/3}}^{\infty} f_0(v)\, u^3(v, \tau)\, dv \sim \varkappa \int_{e^{\tau/3}}^{\infty} f_0(v)\, v^3\, dv \to 0 \tag{13}$$

[since $u(v, \tau) \sim ve^{\tau/3}$].* Thus in this case $q(\tau)$ approaches zero and Eq. (11) again lacks a solution.

When $\gamma \to \infty$ and $\gamma \to 0$ the reasoning for $\gamma > \gamma_0$ and $\gamma < \gamma_0$ is even more fully justified. Thus we need only investigate the case $\gamma(\tau) \to \gamma_0 = 27/4$. We note first that for the exact equality $\gamma = \gamma_0$ all points that lie to the right of the point of tangency $u_0 = 3/2$ move to the left but cannot pass through u_0 and "stick" at this point. Therefore, just as for $\gamma > \gamma_0$, Eq. (11) cannot be satisfied [$q(\tau) \sim e^{\tau} \to \infty$ for $\tau \to \infty$]. This means that $\gamma(\tau)$ must approach γ_0 from below; thus

$$\gamma(\tau) = \gamma_0 (1 - \varepsilon^2(\tau)). \tag{14}$$

The points that arrive at u_0 from the right "filter" more and more slowly through the "blocking" point $u_0 = 3/2$ at a rate that depends on the value of $\epsilon(\tau)$, which like $\gamma(\tau)$ must be obtained from (11) and the equation of motion (8):

$$\frac{du^3}{d\tau} = -\left(u - \frac{3}{2}\right)^2 (u + 3) - \frac{1}{2}\gamma_0 \varepsilon^2(\tau), \tag{15}$$

where $\epsilon(\tau) \to 0$ for $\tau \to \infty$. Near $u_0 = 3/2$ this equation becomes

$$\frac{du}{d\tau} = -\frac{2}{3}\left(u - \frac{3}{2}\right)^2 - \frac{1}{2}\varepsilon^2(\tau). \tag{16}$$

With the introduction of the new function $z = (u - 3/2)/\epsilon$ it can be written as

$$\frac{3}{2}\frac{dz}{\varepsilon d\tau} = -z^2 - \frac{3}{4} + \frac{3}{2} z \frac{d(1/\varepsilon)}{d\tau}.$$

---

*The exact value of $u(v, \tau)$ is the solution of

$$R(u) = R(v)\, e^{-\tau/3}, \quad R(u) = \exp\left[\int_0^u \frac{u^2\, du}{u^3 - \gamma(u-1)}\right],$$

$R(0) = 1$, $R(v) = v$ for $v \gg 1$; therefore for $v \gg 1$ we have $v = R(u)e^{\tau/3}$ and the correct asymptotic expression for q is

$$q(\tau) \sim \varkappa x^4 \int_1^{\infty} f_0(xR)\, u^3(R)\, dR; \quad x = e^{\tau/3}.$$

For $u \gg 1$, $R \approx u$ and we obtain (13).

A similar study shows that asymptotically

$$\frac{d(1/\varepsilon)}{d\tau} \to \frac{2}{\sqrt{3}}, \qquad \varepsilon^2 \to \frac{3}{4\tau^2}. \tag{17}$$

At the same time we have

$$\frac{3}{2}\frac{dz}{d\ln\tau} \to -\left(z - \frac{\sqrt{3}}{2}\right)^2,$$

which means that the velocity $dz/d\ln\tau$ vanishes asymptotically at the "blocking" point $z_0 = \sqrt{3/2}$.

Thus for sufficiently large τ the improved value of $\gamma(\tau)$ will be

$$\gamma(\tau) = \gamma_0(1 - 3/4\,\tau^2), \tag{18}$$

and the more precise location of the "blocking" point on the axis will be

$$u = 3/2 + z_0\varepsilon(\tau) = 3/2 + 3/4\,\tau. \tag{19}$$

Continuing the same line of reasoning, we obtain an asymptotic expansion for $\gamma(\tau)$:*

$$3\frac{dt}{dx^3} = \gamma(\tau) = \gamma_0\left[1 - \frac{3}{4\tau^2}\left(1 + \frac{1}{(\ln\tau)^2}(1+\ldots)\right)\right], \tag{20}$$

and accordingly

$$x^3 = \frac{4}{9}t\left(1 + \frac{3}{4(\ln t)^2}(1+\ldots)\right). \tag{21}$$

This expansion can be terminated at any term that is followed by a relatively small term. Thus the basic approximation $\gamma(\tau) = \gamma_0$, and accordingly $x^3 = 4/9\,t$, is valid if $\tau^2 = (\ln t)^2 \gg 1$.

An interesting property of the expansions (20) and (21) is the fact that although the corrections to γ_0 decrease rapidly in magnitude as τ increases and the first approximation (21) becomes increasingly accurate the behavior of the solution near the blocking point is determined by these corrections.

In the entire region outside the vicinity of $u_0 = 3/2$ the velocity $du/d\tau$ is given by

$$\frac{du}{d\tau} = -g(u); \qquad g(u) = \left(u - \frac{3}{2}\right)^2 (u+3)/3u^2. \tag{22}$$

3. ASYMPTOTIC DISTRIBUTION FUNCTION

In accordance with the preceding section, the distribution function will also be obtained in terms of the new variables u and τ. When expressed in terms of the relative size $u = \rho/x$ the distribution function $\varphi(u, \tau)$ has the following obvious relation to $f(\rho, t)$:

$$\varphi(u, \tau)\,du = f(\rho, t)\,d\rho = xf(\rho, t)\,du,$$

whence

$$f = \varphi(u, \tau)/x.$$

Except in the vicinity of u_0, when $\tau \gg 1$ the continuity equation for $\varphi(u, \tau)$ is given by

$$\frac{\partial\varphi}{\partial\tau} - \frac{\partial\varphi g(u)}{\partial u} = 0. \tag{23}$$

The solution of this equation to the left of u_0 is

$$\varphi = \chi(\tau + \psi)/g(u),$$

where

$$\psi = \int_0^u \frac{du}{g(u)} = \frac{4}{3}\ln(u+3) + \frac{5}{3}\ln\left(\frac{3}{2} - u\right) + \frac{1}{1 - 2u/3} - \ln\frac{3^3 e}{2^{5/3}},$$

and χ is an arbitrary function still to be determined.

It follows from the analysis (given in the previous section) of the equation of motion (8) or (15) and thus of the characteristics of Eq. (23) that the vicinity of the point u_0 is to be regarded as a sink for all points $u > u_0$ and a source for the region $u < u_0$; for $u < u_0$ the sink is the coordinate origin $u = 0$. Moving from right to left all points pass through the vicinity of u_0 and remain there longer the later they arrive.

The distribution function to the right of u_0 for $\tau \to \infty$ is given by an infinitely distant portion of the "tail" of the original distribution, and its integral contribution to both the absolute and relative expressions rapidly approaches zero (Appendix, Sec. 1). It will be shown below that the relative contribution from the vicinity of u_0 also approaches zero as $\tau \to \infty$ (Appendix, Sec. 2). Thus the predominant contribution to matter conservation comes from grains with $u < u_0$. It follows that this conservation law can be used as an integral equation to determine the asymptotic behavior of the distribution function in zero approximation for $u < u_0$. (For $u > u_0$ the distribution function vanishes in this approximation.) From the foregoing considerations, by inserting the solution of (23) into the law of mass conservation we obtain an asymptotic equation for χ:

$$1 = \varkappa e^{\tau}\int_0^{3/2} \chi(\tau + \psi)\frac{u^3}{g(u)}\,du. \tag{24}$$

From this equation it is easy to determine $\chi(\tau + \psi)$ and thus $\varphi(u, \tau)$:

---

*$\gamma(\tau)$ can be written formally as $\gamma(\tau) = \gamma_0(1 - 3/4\,w(\tau))$, where $w(\tau)$ satisfies the functional equation $w(z) = z^{-2} + (1 + w(\ln z))$ when $z > 1$.

$$\chi(\tau+\psi) = Ae^{-\tau-\psi}, \tag{25}$$

$$\varphi(u,\tau) = Ae^{-\tau-\psi}\frac{1}{g(u)} = \frac{3^4 e}{2^{5/3}}Ae^{-\tau}\frac{u^2\exp[-1/(1-2u/3)]}{(u+3)^{7/3}(3/2-u)^{11/3}},$$

where

$$A = \left[\varkappa\int_0^{3/2} e^{-\psi}\frac{u^3}{g(u)}\,du\right]^{-1} = \frac{3Q_0}{4\pi R^3_{\mathbf{cr0}}1.11} \approx 0.22\frac{Q_0}{R^3_{\mathbf{cr0}}}. \tag{26}$$

We thus see that the asymptotic behavior of the distribution function for $u < u_0$ is independent of the form of the original distribution function.*

According to (25) the number of particles per unit volume is given by

$$n(\tau) = \int_0^{3/2}\varphi(u,\tau)\,du = Ae^{-\tau} = \left(\frac{3}{2}\right)^{3/2}\frac{A}{t}. \tag{27}$$

Let $P(u)\,du$ be the probability that the size of a particle is between u and $u + du$. Then

$$\varphi(u,\tau) = n(\tau)P(u), \tag{28}$$

where

$$P(u) = \begin{cases} \dfrac{3^4 e}{2^{5/3}}\dfrac{u^2\exp[-1/(1-2u/3)]}{(u+3)^{7/3}(3/2-u)^{11/3}}, & u < u_0 = 3/2; \\ 0 & u > u_0 = 3/2. \end{cases} \tag{29}$$

This probability can be expressed conveniently with a different relative variable obtained by introducing the maximum size:

$$\rho_m = 3x/2, \quad v = \rho/\rho_m = u/u_m = 2u/3.$$

Then

$$P(u)\,du = P_1(v)\,dv, \quad P(u) = 2P_1(v)/3;$$

$$P_1(v) = \begin{cases} 2^{7/3}ev^2\exp[-1/(1-v)]/(v+2)^{7/3}(1-v)^{11/3}, & v<1; \\ 0 & , v>1. \end{cases}$$

Thus these formulas completely determine the asymptotic size and time distributions of the particles.† $P(u)$ is plotted in Fig. 4.

We now note that

$$\int_0^{3/2} e^{-\psi}\frac{u-1}{g(u)}\,du = \int_0^{\infty} e^{-\psi}(u(\psi)-1)\,d\psi = e^{-\psi}u^3(\psi)\Big|_0^{\infty} = 0. \tag{30}$$

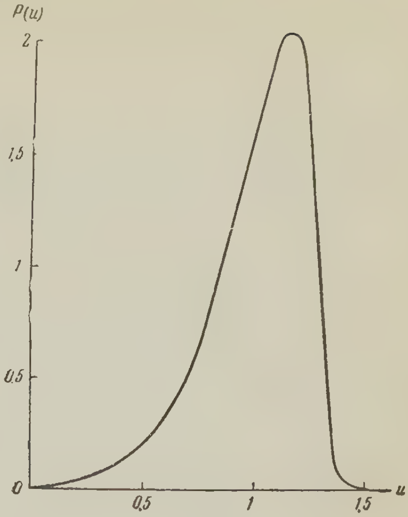

FIG. 4

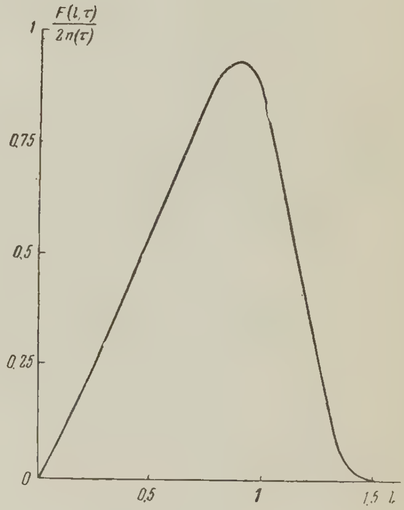

FIG. 5

We have used here the relation

$$du^3/d\psi = u^3 - 4(u-1)/27. \tag{31}$$

This indicates that $\bar{u} = 1$; it thus follows that

$$\bar{\rho} = \bar{u}x = x(\tau). \tag{32}$$

In order to obtain the distribution over absolute values of the radius ρ we need only replace u by ρ/x in (25) and divide by x, for which

$$x^3 = 4t/9. \tag{33}$$

Considering that, according to (32), $u = R/\bar{R}$ and returning to the original dimensional quantities, we obtain

$$\begin{gathered} f(R,t) = n(t)P(R/\bar{R})/\bar{R}, \\ n(t) = \beta Q_0/\bar{R}^3 = B/t, \quad \beta \approx 0.22, \quad B \approx 1/2D\alpha, \\ \bar{R}^3 = 4D\alpha t/9, \end{gathered} \tag{34}$$

where $P(u)$ is given by (28). The supersaturation at a given time is given by

---

*It should be noted that the distribution given by Todes corresponds in form to the case $\gamma < \gamma_0$ of the present scheme. Our discussion makes it clear that such a distribution can never arise and that the case $\gamma < \gamma_0$ is meaningless. This accounts for the divergence of the integrals in Todes' equations.

†For measurements performed by means of a grain-size classifier it is easily shown that the distribution $\Phi(r,\tau)$ over the sizes r of the openings is given by

$$F(l,\tau)\,dl = \Phi(r,\tau)\,dr, \quad \Phi(r,\tau) = x^{-1}F(r/x(\tau)\ \tau),$$

$$F(l,\tau) = 2x(\tau)\int_l^{3/2}\frac{\varphi(u,\tau)\,du}{\sqrt{(u/l)^2-1}}, \quad l = \frac{r}{x(\tau)}, \quad r = \frac{R}{R_{\mathbf{cr0}}}$$

$$\Delta(t) = \frac{\Delta_0}{x(t)} = \left(\frac{3}{2}\right)^{2/3} \Delta_0 \left(\frac{T}{t}\right)^{1/3} = \lambda t^{-1/3}, \quad \lambda = \left(\frac{3}{2}\right)^{2/3} \left(\frac{\alpha^2}{D}\right)^{1/3} \tag{35}$$

Finally, we shall discuss the limits of applicability of the formulas which have been derived. The preceding analysis shows that the asymptotic expressions are valid subject to the condition

$$\tau^2 = (3 \ln x)^2 = 9\left(\ln \frac{\overline{R}}{R_{\mathrm{cr}0}}\right)^2 \gg 1; \quad \overline{R} \gg R_{\mathrm{cr}0}.$$

Here $R_{\mathrm{cr}0} = \alpha/\Delta_0$ is the initial critical radius for the coalescence process (Δ_0 is the initial degree of supersaturation). We must also take it into account that if the initial average grain size is of the order of the critical size ($\overline{R}_0 \sim R_{\mathrm{cr}0}$), this size will enter into the calculation performed above. But if $\overline{R}_0 \gg R_{\mathrm{cr}0}$ the grains will grow directly from the solution in the first stage. This process will continue until the degree of saturation drops to the point where the average size is of the order of the critical size $\overline{R}_1 \sim R_{\mathrm{cr}1}$), after which coalescence will generally begin. This size must then be used as the initial size, with its magnitude determined essentially by both the initial degree of supersaturation and the initial number of nuclei (if the latter can be regarded as fixed).

Thus with initial supersaturation Δ_0 and initial number n_0 of grains, and with $\overline{R}_0 \gg R_{\mathrm{cr}0} = \alpha/\Delta_0$, growth from the solution will continue up to the size

$$\tfrac{4}{3}\pi \overline{R}_1^3 \approx \Delta_0 / n_0,$$

and in the initial stage

$$\frac{d\overline{R}^2}{dt} = 2D\left(\Delta_0 - \frac{4\pi}{3}\overline{R}^3 n_0\right) = 2D\Delta_0\left(1 - (\overline{R}/R_{\mathrm{cr}1})^3\right). \tag{36}$$

$t_1 \sim \overline{R}_1^2/D\Delta_0$ is the duration of the first stage.

The characteristic time of the first portion of the second stage (coalescence) is

$$t_0 \sim \overline{R}_1^3 / D\alpha \sim t_1 \overline{R}_1 / R_{\mathrm{cr}0};$$

in our case $\overline{R}_1 \gg R_{\mathrm{cr}0}$, that is, $t_0 \gg t_1$. The dependence of the average size on time in this case is plotted in Fig. 6.

4. PRESENCE OF A BOUNDARY. THEORY OF SINTERING

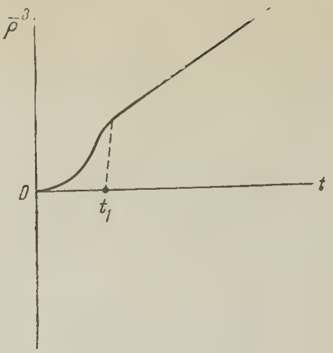

FIG. 6

In the preceding sections we have investigated coalescence in infinite space. Thus the problem did not involve macroscopic diffusive flow of the solute. The situation changes when spatial uniformity is absent, the most important case being the presence of a boundary between the solution and a different phase. When this second phase is the pure solute (or, more generally, the phase for which we are investigating the grain growth), we get on this boundary $\Delta_{z=0} = 0$, which produces macroscopic diffusive flow to the boundary.

An important special case occurs when the part of solute atoms is played by vacancies and the part of the grains is played by pores which result from the coagulation of vacancies in a crystal that is "supersaturated with vacancies." When a free surface exists in such a crystal, two competing processes will occur: far from the boundary — the growth of pores (vacuum crystals) and their coalescence according to the scheme developed previously; near the boundary — the dissolution of pores and the diffusion of vacancies to the boundary (which can be regarded as a pore of infinitely large radius). Sintering is associated with this process of pore expulsion.

We shall discuss henceforth this specific process although all results will, of course, also apply to the more general case of a supersaturated solution.

For a half-space, Eq. (3) for grain growth and Eq. (4) for the distribution function [or the equivalent Eqs. (8) and (10)] will be retained. But instead of the conservation law $Q_0 = \Delta + q$, which corresponds to (5) [or (11) respectively], we must write a diffusion equation. Then each point z is a source (or sink) of strength dq/dt, $q = q(z, t)$ resulting from dissolution of the pores. Thus the exact system of equations will be

$$\frac{\partial(\Delta + q)}{\partial t} = D\frac{\partial^2 \Delta}{\partial z^2}, \quad \Delta|_{z=0} = 0; \tag{37}$$

$$q = \varkappa x^3 \int_{v(\tau)}^{\infty} f_0(v)\, u^3(v, \tau)\, dv, \quad x = \Delta_0/\Delta(z, t), \tag{38}$$

where $u(v, \tau)$ satisfies (8) and is itself determined by the function $\Delta(z, t)$.

The analysis in Sec. 2 has shown the peculiar "stability" of the asymptotic law found for the variation of supersaturation (35),

$$\Delta = \lambda t^{-1/3},$$

which means that the slightest retardation of the asymptotic reduction of supersaturation results in the infinite growth of grains $(q \to \infty)$ and is thus impossible. On the other hand, even a slight acceleration of the asymptotic reduction of supersaturation leads relatively rapidly to complete dissolution of the grains $(q \to 0)$. Therefore the asymptotic process of sintering must be the following. Three sharply separated regions are present:

(a) The region most distant from the boundary $(z_2 < z < \infty)$, which is not affected by the boundary and where, as in the case of infinite space, supersaturation is given by Eq. (35).

(b) The region $z_1 < z < z_2$, where dissolution of pores (grains) occurs.

(c) The region $0 < z < z_1$, where pores are already completely absent and purely diffusive expulsion of vacancies occurs. The boundaries of these regions $z_1(t)$ and $z_2(t)$ move deeper into the specimen so that the "crust," which is free of pores, is continuously thickening. Strictly speaking, Eqs. (37) and (38) may be solved only for the intermediate region $z_1 < z < z_2$. But, as will be shown below, $(z_2 - z_1)/z_2 \ll 1$. Therefore in first approximation we set $(z_1 + z_2)/2 = \xi$, and replacing this region by the corresponding boundary condition, we determine the position of the boundary $\xi(t)$ and the variation of the concentration in the surface layer $0 < z < \xi$ (in the crust). Thus

$$\frac{\partial\Delta}{\partial t} = D\frac{\partial^2\Delta}{\partial z^2}; \tag{39}$$

$$\Delta\Big|_{z=0} = 0; \qquad \Delta\Big|_{z=\zeta} = \lambda t^{-1/3}; \quad D\frac{\partial\Delta}{\partial z}\Big|_{z=\zeta} = Q_0\frac{d\zeta}{dt}. \tag{40}$$

The last condition replaces the transition region and expresses the fact that the boundary $\xi(t)$ is a source of strength $Q_0 d\xi/dt$ (since to the right practically all excess vacancies are within pores). The solution of (38) together with the boundary condition $(\Delta|_{z=0} = 0)$ will be obtained in the form $\Delta = \sum_{n=1}^{\infty} \alpha_n(t) z^n$; we then obtain from (39)

$$\Delta = \sum_{n=0}^{\infty} \frac{\hat{p}^n \alpha_1(t)}{(2n+1)!} z^{2n+1}, \qquad \hat{p} = \frac{1}{D}\frac{d}{dt}.$$

Before satisfying the other two boundary conditions, we note that $\alpha_1(t)$ is an asymptotically decreasing function of time (since it represents flow on the boundary $z = 0$, $\alpha_1(t) = D\partial\Delta/\partial z|_{z=0}$).

We shall therefore obtain α_1 asymptotically in the form $\alpha_1 = B/t^s$, $s > 0$. Then we have from (39)

$$\Delta = B\frac{z}{t^s}\sum_{n=0}^{\infty}(-1)^n\left(\frac{z^2}{Dt}\right)^n\frac{s(s+1)\ldots(s+n)}{(2n+1)!} \tag{41}$$

As will be shown below, $\xi^2(t)$ varies asymptotically more slowly than t $(\xi^2(t)/t \to 0$ for $t \to \infty)$. Thus the main term of the asymptotic expression is that with $n = 0$:

$$\Delta = Bz/t^s \equiv \alpha_1 z. \tag{42}$$

Inserting (41) into (39), we have

$$\alpha_1\zeta = \lambda t^{-1/3}, \qquad \alpha_1 = \frac{Q_0}{D}\frac{d\zeta}{dt}.$$

As a result we obtain

$$\zeta = \sqrt{3}\,(3/2)^{2/3}\,\bar{R}/Q_0^{1/2} = m\,(D\alpha t)^{1/3}/Q_0^{1/2}; \; m = (3/2)^{1/3}\sqrt{3} \approx 2;$$

$$\Delta = \lambda t^{-1/3} z/\zeta = \frac{m}{3}\,Q_0^{1/2}\,\frac{\alpha^{1/3} z}{(Dt)^{2/3}}. \tag{43}$$

The relative width of the intermediate region now remains to be determined. According to (43)

$$\delta\zeta/\zeta = \delta t/3t = T_d(t)/3t, \tag{44}$$

where T_d is the time of dissolution of the largest grains present at the boundary at time t, $R_{max} = 3R_{cr}/2$. In region I the critical radius as a function of time is

$$R_{cr}^3 \sim t^2.$$

A simple calculation shows that in the equation of motion (8) $\gamma = 3dt/dx^3 \le 27/8 < \gamma_0$. From this equation we obtain the time of dissolution of the largest grains $(u_0 = 3/2)$, $T_d(t) \approx t/3$. This gives for the relative width

$$\delta\zeta/\zeta \approx 1/9.$$

We note that

$$\delta\zeta/\bar{R} = 1/3\,Q_0^{1/2} \gg 1. \tag{45}$$

Moreover,

$$\delta\zeta/l \approx Q_0^{1/3}/3Q_0^{1/2} = 1/3\,Q_0^{1/6} \gg 1, \tag{46}$$

where l is the average distance between grains. The inequalities (45) and (46) denote that $d\xi \gg l \gg \bar{R}$, which means that the width of the intermediate region is considerably larger than the average separation of the pores and the average size of the pores (grains), while at the same time it is considerably smaller than the first region (the crust). This also justifies all assumptions which we made in order to obtain the asymptotic expressions.

The periods of time for which the asymptotic formula (43) can be used are the same as for the asymptotic expression for coalescence in infinite space.

A special situation occurs when we take into account the finite size of a specimen instead of only a single boundary. For example, for a plate of thickness a there exist three characteristic times: the time for diffusive escape of vacancies at the surface of the plate ($T_0 \sim a^2/D$), the time for growth of pores from the solution ($T_1 \sim \bar{R}_1^2/D\Delta_0$, see page 336), and the characteristic time for coalescence ($T_{co} \sim \bar{R}^3/D\alpha$)

In order to make the foregoing "crust-forming" sintering mechanism possible, the diffusive escape time T_0 must be considerably longer than T_{co}, that is, $a^2 \gg \bar{R}_1^3/\alpha$, and the average size of the pores which enter into this inequality must be in accord with the development of the coalescence process, $\bar{R} \gg R_1$. In the other limiting case $T_0 \ll T_1$ the vacancies escape without forming pores. In the intermediate case $a^2 \sim R_1^3/\alpha$ the kinetics of the process is determined by factors associated with the initial distribution and is not of a general character.

The method which has been proposed here can be applied to a number of similar problems, which will be investigated separately.

APPENDIX

Determination of the Distribution Function for $u > u_0$ in the Vicinity of the Point u_0

1. We shall determine the distribution function for $u > u_0$. Introducing $\psi = \int du/g(u)$ we note that $g(u) \rightarrow u/3$, $u \rightarrow e^{\psi/3}$ for $u \rightarrow \infty$, that is,

$$ux^{1/3} \rightarrow \exp[(\tau + \psi)/3]. \qquad (A.1)$$

In addition, the solution on the right for $u \rightarrow \infty$ must be determined by the initial distribution function:

$$\chi(\tau + \psi) \rightarrow f_0(ux^{1/3})\, x^{1/3} g(u), \qquad (A.2)$$

where f_0 is the initial distribution over ρ. From this condition we determine the distribution for $u > u_0$:

$$\chi(\tau + \psi) = f_0(z)\, z/3, \quad z = e^{(\tau+\psi)/3} \qquad (A.3)$$

or

$$\varphi(u, \tau) = f_0(z)\, z/3\, g(u). \qquad (A.4)$$

$f_0(z)$ varies at least more rapidly than z^{-4} (which is necessary for the existence of $\int\limits_0^\infty f_0(z)\, z^3\, dz$), and usually is an exponential function of z. Hence the probability density for $u > u_0$ in zero approximation vanishes:

$$P(u, \tau) = \varphi(u, \tau)/n(\tau)$$
$$= \frac{1}{3A} f_0(z)\, z^4 \frac{e^{-\psi}}{g(u)} \rightarrow 0 \text{ for } z \rightarrow \infty. \qquad (A.5)$$

The probability density for $u < u_0$ is known to be finite.

2. We shall show that the integral contribution from the vicinity of the point is negligibly small for $\tau \rightarrow \infty$. The amount of matter in this vicinity is given by

$$q_\delta = x^3 \int\limits_{u_0-\delta}^{u_0+\delta} \varphi u^3 du = u_0^3 e^\tau n_\delta(\tau), \qquad (A.6)$$

$$n_\delta(\tau) = \int\limits_{u_0-\delta}^{u_0+\delta} \varphi\, du, \quad 1 \gg \delta \gg \varepsilon(\tau). \qquad (A.7)$$

From the equation of continuity we obtain

$$\frac{dn_\delta}{d\tau} = \varphi g(u) \Big|_{u_0-\delta}^{u_0+\delta} = Ae^{-\tau} e^{-\psi(u_0-\delta)} = Ae^{-\tau} \exp(-3/2\,\delta)$$
$$(A.8)$$

(the flow to the right is determined for $\tau \rightarrow \infty$ by the infinitely distant tail of the distribution and can thus be neglected),

$$n_\delta = Ae^{-\tau} \exp(-3/2\delta) + B;$$
$$q_\delta = A \exp(-3/2\,\delta) + Be^\tau. \qquad (A.9)$$

It is evident that $B = 0$, since matter must be conserved. We finally obtain the quantity of matter in the vicinity of u_0 for $\tau \rightarrow \infty$:

$$q_\delta = A \exp(-3/2\,\delta) \rightarrow 0, \ \delta \rightarrow 0. \qquad (A.10)$$

3. We shall show how a more accurate expression for the distribution function is obtained in the vicinity of the point $u_0 = 3/2$. The continuity equation in the vicinity of this point is

$$\frac{\partial \varphi}{\partial \tau} + \frac{\partial}{\partial u} \varphi g(u) = 0, \quad g(u)$$
$$= -\frac{2}{3}\left[\left(u - \frac{3}{2}\right)^2 + \varepsilon^2(\tau)\right], \quad \varepsilon(\tau) = 3/4\,\tau. \qquad (A.11)$$

Introducing the notation

$$z = \frac{2}{3}\left(u - \frac{3}{2}\right)\tau, \quad f(z, \tau)\, dz = \varphi(u, \tau)\, du. \qquad (A.12)$$

we obtain

$$\frac{\partial f}{\partial \ln \tau} - \frac{\partial}{\partial z} f g(z) = 0, \quad g(z) = \left(z - \frac{1}{2}\right)^2. \qquad (A.13)$$

The solution of this equation is

$$f = f\left(\ln\left[\tau \exp \int \frac{dz}{g(z)}\right]\right). \qquad (A.14)$$

We now note that

$$\tau + \int_0^u \frac{du}{g(u)} \rightarrow \tau \exp \int \frac{dz}{g(z)}, \quad \frac{1}{g(z)} \rightarrow \frac{2}{3} \frac{\tau^2}{g(z)} \exp \int \frac{dz}{g(z)},$$
$$1 \gg \left| u - \frac{3}{2} \right| \gg \varepsilon(\tau). \qquad \text{(A.15)}$$

In actuality

$$\tau + \int_0^u \frac{du}{g(u)} = \tau\left(1 - 1 \Big/ \frac{2}{3}\left(u - \frac{3}{2}\right)\tau\right) = \tau\left(1 - \frac{1}{z}\right)$$
$$= \tau \exp \int \frac{dz}{g(z)}; \; z \gg 1. \qquad \text{(A.16)}$$

Also, for such values of u we must obtain the previous distribution function in zero approximation:

$$f \frac{dz}{du} \rightarrow \frac{A}{{}^2/_3 \, (u - {}^3/_2)^2} \exp\left\{-\left(\tau - \frac{1}{{}^2/_3 \, (u - {}^3/_2)}\right)\right\}, \; z \gg 1. \qquad \text{(A.17)}$$

Hence we obtain immediately

$$f = A \frac{\tau}{g(z)} \exp\left[\int \frac{dz}{g(z)} - \tau \exp \int \frac{dz}{g(z)}\right]. \qquad \text{(A.18)}$$

---

[1] O. M. Todes, J. Phys. Chem. (U.S.S.R.) **20**, 630 (1946).

[2] O. M. Todes and V. V. Khrushchev, J. Phys. Chem. (U.S.S.R.) **21**, 302 (1947).

[3] N. N. Sirota, Dokl. Akad. Nauk SSSR **40**, 265 (1943).

[4] I. V. Salli and V. I. Psarv, Физика металлов и металловедение (Physics of Metals and Metal Research) **5**, 268 (1957).

Translated by I. Emin
83

SOVIET PHYSICS JETP VOLUME 35(8), NUMBER 2 FEBRUARY, 1959

PROJECTION OPERATORS IN THE THEORY OF ELEMENTARY PARTICLES

F. I. FEDOROV

Institute of Physics and Mathematics, Academy of Sciences, Belorussian S.S.R.

Submitted to JETP editor March 26, 1958

J. Exptl. Theoret. Phys. (U.S.S.R.) **35**, 493-500 (August, 1958)

Minimal polynomials in the matrices occurring in relativistic wave equations and the spin matrices are used to construct projection matrices, which are dyads describing arbitrary possible states of a free particle of arbitrary spin. The fundamental physical quantities (energy and momentum, charge and current, transition probabilities) are expressed directly in terms of these projection operators in an invariant way (independent of the choice of basis for the representation). Thus the calculation of various effects for particles of any spin is reduced to the computation of the traces of certain combinations of matrices. As examples of the application of the method we obtain the general conditions for definiteness of the energy and charge for particles with a single mass and give a simple derivation of the general commutation relations for particles of arbitrary spin.

IN various calculations relating to particles with spin one needs to find the free-field wave functions, which are solutions of the first order equations

$$(\gamma_k \nabla_k + \varkappa)\psi = 0,$$

where $x_4 = it$, $c = h = 1$, and the γ_k are square matrices. For plane waves $\psi \sim e^{ipx}$, corresponding to the four-momentum $p = (p_k)$, these equations take the form

$$(ip_k\gamma_k + \varkappa)\psi = 0. \qquad (1)$$

We use the notation $\hat{p} = ip_k\gamma_k$. As has been shown in reference 1, the minimal equation for the matrix p in the general case has the form

$$P(\hat{p}) = \hat{p}^n (\hat{p}^2 + \lambda_1^2 p^2)(\hat{p}^2 + \lambda_2^2 p^2) \ldots (\hat{p}^2 + \lambda_q^2 p^2) = 0, \quad (2)$$

where λ_l $(l = 1, 2, \ldots q)$ are distinct nonvanishing eigenvalues of the matrix γ_4. To each value $\pm\lambda_l$ there corresponds a set of states of the particle.

Since $p^2 = -m^2$ and $\lambda_l = \kappa/m_l$, where $m_l^2 = -p^{(l)2}$, we can write instead of Eq. (2)

$$P(\hat{p}) = \hat{p}^n\left(\hat{p}^2 - \varkappa^2\frac{m^2}{m_1^2}\right)\left(\hat{p}^2 - \varkappa^2\frac{m^2}{m_2^2}\right)\cdots\left(\hat{p}^2 - \varkappa^2\frac{m^2}{m_q^2}\right) = 0. \quad (3)$$

Let us introduce the operator

$$\sigma = \frac{i}{2|\mathbf{p}|}\delta_{abc}\,p_a\,J^{bc}; \quad a, b, c = 1, 2, 3, \quad (4)$$

where J^{bc} are the infinitesimal matrix operators of the representation of the Lorentz group in the space of the functions ψ which correspond to space rotations, and $\mathbf{p}$ is the three-dimensional momentum vector. Using the condition for invariance of Eq. (1)

$$[\gamma_k J^{lm}] = \delta_{kl}\gamma_m - \delta_{km}\gamma_l, \quad (5)$$

it is not hard to verify that the operators $\hat{p}$ and σ commute with each other. Therefore when $p^{(l)}$ and λ_l are prescribed the states of the particle can be characterized also by the different eigenvalues of the operator σ, which is the operator for the component of the spin along the momentum of the particle. Here in the general case we have corresponding to each "mass" state $\pm\lambda_l$ its own maximum value $s^{(l)}$ of the component of the spin along the momentum, i.e., its own value of the spin. Thus for prescribed $p^{(l)}$ and λ_l the particle can still be in $2s^{(l)} + 1$ different spin states. As is well known, the spins for the states of a particle described by the nonseparable equation (1) must be either all integral or all half-integral. Let s be the maximum value of the spin component for all possible states of the particle. Then in the case of half-integral spin the minimal equation for the operator σ must have the form [$s = (2n + 1)/2$, n an integer]

$$Q(\sigma) = \left(\sigma^2 - \left(\frac{1}{2}\right)^2\right)\left(\sigma^2 - \left(\frac{3}{2}\right)^2\right)\cdots\left(\sigma^2 - \left(\frac{2n+1}{2}\right)^2\right) = 0 \quad (6)$$

and in the case of integral spin ($s = n$) it is

$$Q(\sigma) = \sigma(\sigma^2 - 1)(\sigma^2 - 2^2)\cdots(\sigma^2 - n^2) = 0. \quad (7)$$

In the solution of various problems about spinning particles and their interactions it is necessary to know the wave functions characterizing a particle that has given energy and momentum and is in a prescribed mass and spin state. Usually these wave functions are found in explicit form by the solution of Eq. (1) with a definite choice of the basis for the representation in the space of the functions ψ. For the classification into the various spin states one has further to solve the equations for the characteristic values of the operator σ. Not only are these calculations very cumbersome, especially in the case of higher spins, but also this method is in principle an unsatisfactory one. The point is that for a single type of particle with prescribed physical properties the equations (1) can be written in an indefinite number of forms that differ from each other in the choice of basis. This is due to the fact that every representation of the Lorentz group (or of any group) is defined only to within the choice of an arbitrary nonsingular basis. It is obvious that all results having physical significance cannot depend on the specific choice of the basis of the representation, i.e., they must be invariant with respect to changes in this choice. Therefore in principle there must exist the possibility of solving problems relating to particles with various spins altogether without reference to any choice of the basis of the representation, i.e., in a consistently invariant way. On the other hand the usual methods of calculation, based on the use of a concrete basis, introduce into the treatment accidental features that have no relation to the essential problem.

As is shown below, the use of the minimal polynomials (3), (6), and (7), which are usually known, make it possible in the general case to reduce the calculation of the main physical quantities to the computation of the traces of certain combinations of matrices, which in many cases can be done in an invariant way.

Let us define the diminished minimal polynomial $P_{\pm l}(\hat{p}^{(l)})$ of the matrix $\hat{p}^{(l)}$, corresponding to the mass state $\pm\lambda_l = \pm\kappa/m_l$, by the following relation [cf. Eq. (3) for $m = m_l$]:

$$(\hat{p}^{(l)} \mp \varkappa)\,P_{\pm l}(\hat{p}^{(l)}) = P(\hat{p}^{(l)}) = 0. \quad (8)$$

As has been shown in reference 1, the columns of the matrix $P_{\pm l}$ contain all the linearly independent eigenvectors of the matrix $\hat{p}^{(l)}$ that correspond to the eigenvalue $\pm\lambda_l m_l = \pm\kappa$. Let us further introduce a matrix $\alpha_{\pm l}$ differing from $P_{\pm l}$ by a numerical factor

$$\alpha_{\pm l} = P_{\pm l}(\hat{p}^{(l)})\,/\,P_{\pm l}(\pm\varkappa). \quad (9)$$

Since by the results of reference 1 all nonvanishing eigenvalues of the matrix $\hat{p}$ must be single, $P_{\pm l}(\pm\kappa) \neq 0$, and the matrix $\alpha_{\pm l}$ always exists. Since, by Eq. (8), $\hat{p}^{(l)}P_{\pm l} = \pm\kappa P$, multiplication of the matrix $P_{\pm l}(\hat{p}^{(l)})$ by an arbitrary polynomial $R(\hat{p}^{(l)})$ is equivalent to multiplying it by $R(\pm\kappa)$. From this it follows that

$$[\alpha_{\pm l}(\hat{p}^{(l)})]^2 = \alpha_{\pm l}(\hat{p}^{(l)}). \quad (10)$$

Thus the operator $\alpha_{\pm l}$ is a projection operator. This means that by multiplying any state vector ψ by $\alpha_{\pm l}$ we extract from it the part that corresponds to states with the mass m_l.

In just the same way, by using the minimal polynomial $Q(\sigma)$ of the spin operator [cf. Eqs. (6) and (7)], we can construct a projection operator

$$\beta_k = Q_k(\sigma)/Q_k(s_k), \quad (\sigma - s_k)\, Q_k(\sigma) = Q(\sigma) = 0, \tag{11}$$

which extracts from any state the part it contains corresponding to the value s_k for the spin component along the momentum.

Let us consider an arbitrary polynomial $f(x)$ of degree n which has all its roots x_k distinct. Defining $f_k(x) = f(x)/(x - x_k)$, we construct a new polynomial of degree $n - 1$:

$$\Phi(x) = 1 - \sum_{k=1}^{n} f_k(x)/f_k(x_k).$$

Since $f_k(x_l) \neq 0$ for $k \neq l$, we have $\Phi(x_k) = 0$ for $k = 1, 2, \ldots n$. Therefore the polynomial $\Phi(x)$ of degree $n - 1$ has n distinct roots, which is possible only when it is identically equal to zero. Consequently, $\Sigma f_k(x)/f_k(x_k) \equiv 1$. Since the minimal polynomial of the operator σ has no multiple roots, the identity that has been obtained can be applied to it and we get

$$\sum_k \beta_k \equiv I, \tag{12}$$

where I denotes the unit matrix, and the sum is taken over all values of the spin component. Therefore for an arbitrary state ψ we can write

$$\psi = \sum_k \psi_k, \quad \psi_k = \beta_k \psi, \quad \sigma\psi_k = s_k \psi_k. \tag{13}$$

This relation gives the resolution of an arbitrary state into states corresponding to all the possible values s_k of the spin component. If the state ψ contains no component corresponding to some values s_k of the spin component, then for these k's we have $\beta_k \psi = 0$.

In the general case an analogous resolution into the mass states cannot be carried out, because for this one would have to take into account all the eigenvalues of $\hat{p}$. The zero eigenvalues of $\hat{p}$ operators, however, do not correspond to real states, and furthermore these zero eigenvalues can be multiple (cf. reference 1).

Knowing the minimal polynomials $P(\hat{p})$ and $Q(\sigma)$, we can obtain without any calculations any eigenstate vector $\psi_{lk}(\hat{p}^{(l)})$, corresponding to prescribed energy and momentum $p^{(l)}$, mass m_l, and spin component s_k. For this purpose we have only to multiply together the corresponding projection operators (9) and (11):

$$\tau_{lk} = \alpha_l \beta_k. \tag{14}$$

Since all the α_l and β_k commute with each other, the product (14) is also a projection operator. The matrix τ_{lk} has the property that each of its columns is an eigenvector of the operators $\hat{p}^{(l)}$ and σ for the eigenvalues $\lambda_l m_l = \kappa$ and s_k, respectively. Since such a state is unique, all the columns of the matrix τ_{lk} are proportional to each other. Therefore the matrix τ_{lk} is a simple dyad. By a dyad we mean a matrix in which each element is the product of the corresponding components of two vectors. Thus if A is a dyad formed from the vectors ψ and φ

$$A_{ik} = \psi_i \varphi_k. \tag{15}$$

We shall write the expression for a dyad as a whole in terms of the components of its vectors in the form

$$A = \psi \cdot \varphi. \tag{16}$$

Obviously

$$\widetilde{A} = \varphi \cdot \psi, \quad A^{+} = \varphi^{*} \cdot \psi^{*}, \tag{17}$$

where ~ is the sign of transposition, + is that of the Hermitian adjoint, and * that of the complex conjugate.

Thus we can write

$$\tau_{lk}(\hat{p}^{(l)}) = \alpha_l \beta_k = \psi_{lk} \cdot \varphi. \tag{18}$$

Here the antecedent vector of the dyad ψ_{lk} is the vector for the state in question. We as yet do not know the consequent φ, but it is not hard to determine it. For this it is enough to note that the matrix $\hat{p}$ and the matrix of the invariant bilinear form η satisfy the relation[2]

$$\hat{p}\eta = \eta \hat{p}^{+}. \tag{19}$$

At the same time the Hermitian spin-component operator σ of Eq. (4) commutes with η[3]:

$$\eta\sigma = \sigma\eta. \tag{20}$$

Therefore the matrix τ_{lk} satisfies the same relation (19) as $\hat{p}$: $\tau_{lk}\eta = \eta\tau_{lk}^{+}$. Substituting in this the right member of Eq. (18) we get

$$\psi \cdot \varphi\eta = \eta\varphi^{*} \cdot \psi^{*}. \tag{21}$$

Multiplying this relation on the left by an arbitrary vector χ and on the right by η, and using the properties

$$\eta = \eta^{*} = \widetilde{\eta} = \eta^{+} = \eta^{-1}, \tag{22}$$

we get

$$\varphi = \frac{\chi\eta\varphi^{*}}{\chi\varphi} \cdot \psi^{*}\eta = C\psi^{*}\eta. \tag{23}$$

From this we find for τ_{lk}

$$\tau_{lk} = C_{lk}\psi_{lk} \cdot \bar{\psi}_{lk}, \quad \bar{\psi}_{lk} = \psi^{*}_{lk}\eta. \tag{24}$$

Since the matrix τ_{lk} is a projection operator $(\tau_{lk}^2 = \tau_{lk})$,

$$C_{lk}\bar{\psi}_{lk}\psi_{lk} = (\tau_{lk})_c = 1. \tag{25}$$

Here $(\tau_{lk})_c$ denotes the trace of the matrix τ_{lk}. Since η is a Hermitian matrix, $\bar{\psi}\psi = \psi^*\eta\psi$ is a real number, and therefore C_{lk} is also always real. Replacing ψ_{lk} by $C'\psi_{lk}$, we can normalize C_{lk} to $+1$ for $\bar{\psi}_{lk}\psi_{lk} > 0$ and to -1 for $\bar{\psi}_{lk}\psi_{lk} < 0$. Consequently

$$\tau_{lk} = \alpha_l\beta_k = \pm\psi_{lk}\cdot\bar{\psi}_{lk},$$

and the normalization conditions are, respectively,

$$\bar{\psi}_{lk}\psi_{lk} = \psi_{lk}^*\eta\psi_{lk} = \pm 1. \tag{27}$$

Instead of the invariant normalization (27) the charge normalization by

$$\bar{\psi}\gamma_4\psi = \pm 1. \tag{28}$$

is frequently used. The change from one normalization to the other is accomplished very simply, if we use the fact that, by Eq. (1),

$$\bar{\psi}^{(l)}\hat{p}^{(l)}\psi^{(l)} = -\varkappa\bar{\psi}^{(l)}\psi^{(l)}, \quad (\psi^{(l)} = \psi(p^{(l)})). \tag{29}$$

On the other hand, $\bar{\psi}^{(l)}\hat{p}^{(l)}\psi^{(l)} = ip_k^{(l)}\bar{\psi}^{(l)}\gamma_k\psi^{(l)}$. Since the last expression is an invariant, we must have

$$\bar{\psi}^{(l)}\gamma_k\psi^{(l)} = Cp_k^{(l)}. \tag{30}$$

Multiplying Eq. (30) by $ip_k^{(l)}$ and comparing with Eq. (29), we get

$$iCp^{(l)^2} = -iCm_l^2 = -\varkappa\bar{\psi}^{(l)}\psi^{(l)} = -\lambda_l m_l\bar{\psi}^{(l)}\psi^{(l)}$$

Consequently, $C = (\lambda_l/im_l)\bar{\psi}^{(l)}\psi^{(l)}$ and, by Eq. (30),

$$\bar{\psi}^{(l)}\gamma_4\psi^{(l)} = \frac{\lambda_l p_4^{(l)}}{im_l}\bar{\psi}^{(l)}\psi^{(l)} = \frac{\lambda_l p_0^{(l)}}{m_l}\bar{\psi}^{(l)}\psi^{(l)}, \quad (p_4 = ip_0). \tag{31}$$

Thus with the normalization (27)

$$\bar{\psi}^{(l)}\gamma_4\psi^{(l)} = \pm(\lambda_l/m_l)\,p_0^{(l)} = \pm\lambda_l^2 p_0^{(l)}/\varkappa. \tag{32}$$

If, on the other hand, we take the normalization (28), then

$$\bar{\psi}^{(l)}\psi^{(l)} = \pm\varkappa/\lambda_l^2 p_0^{(l)}. \tag{33}$$

Corresponding to this normalization we get instead of Eq. (26)

$$\psi_{lk}\cdot\bar{\psi}_{lk} = \pm(\varkappa/\lambda_l^2 p_0^{(l)})\,\alpha_l\beta_k. \tag{34}$$

Thus a knowledge of the minimal polynomials of the operators $\hat{p}$ and σ is enough to enable us to get in invariant form the solution of Eq. (1) for any state of the free field, normalized by the condition (27) or (28). The signs in the relations (27) and (28) relate to the definiteness of the energy and the charge, respectively. As is well known (cf., e.g., reference 3), the energy is definite if $\bar{\psi}_0^{(l)}\psi_0^{(l)} > 0$ for all $\psi_0^{(l)}$ that correspond to a particle at rest. Analogously, for definiteness of the charge we must have $\bar{\psi}_0^{(l)}\gamma_4\psi_0^{(l)} > 0$ for all these $\psi_0^{(l)}$. According to Eq. (26) $(\tau_{lk}\eta)_c = \pm\psi_{lk}\psi_{lk}^*$, with the sign here corresponding to that in the relation (26) or (27). Since $\psi_{lk}\psi_{lk}^* > 0$, the sign of the expression $(\tau_{lk}\eta)_c$ will be the sign of the energy. Since for the state at rest all the values of the spin component are on an equal footing (cf. reference 1) and the sign of the energy can change only when there is a change of the mass state, instead of $\tau_{lk} = \alpha_l\beta_k$ we can take $\alpha_l = \sum_k \tau_{lk}$. Consequently, for positive definiteness of the energy it is necessary and sufficient that for all l

$$(\alpha_{\pm l}^0\eta)_c > 0, \tag{35}$$

where $\alpha_{\pm l}^0$ denotes the operator $\alpha_{\pm l}(\hat{p}^{(l)})$ for $p^{(l)} = (0, im_l)$. Similarly, the requirement of definiteness of the charge reduces to the condition

$$(\gamma_4\alpha_{\pm l}^0\eta)_c > 0. \tag{36}$$

Let us examine the application of these general criteria to the case of a particle with a single rest mass. For such a particle the minimal polynomial of the matrix γ_4 can always be written in the form

$$\gamma_4^n(\gamma_4^2 - 1) = 0. \tag{37}$$

From this we get for $\alpha_\pm^0$, according to Eq. (9),

$$\alpha_\pm^0 = \frac{\gamma_4^n(\gamma_4 \pm 1)}{(\pm 1)^n(\pm 2)} = \frac{1}{2}(\pm 1)^{n+1}(\gamma_4^{n+1} \pm \gamma_4^n). \tag{38}$$

According to Eq. (35) a necessary and sufficient condition for definiteness of the energy is that the expressions

$$2(\alpha_+^0\eta)_c = (\gamma_4^{n+1}\eta)_c + (\gamma_4^n\eta)_c,$$

$$2(\alpha_-^0\eta)_c = (-1)^{n+1}[(\gamma_4^{n+1}\eta)_c - (\gamma_4^n\eta)_c]$$

have the same sign, i.e., that their product be positive:

$$(-1)^{n+1}[((\gamma_4^{n+1}\eta)_c)^2 - ((\gamma_4^n\eta)_c)^2] > 0. \tag{39}$$

Since $\gamma_4\alpha_\pm^0 = \pm\alpha_\pm^0$, the analogous condition for the definiteness of charge (36) becomes

$$(-1)^n[((\gamma_4^{n+1}\eta)_c)^2 - ((\gamma_4^n\eta)_c)^2] > 0. \tag{40}$$

Taking n to be even or odd, we can conclude from this that in both cases a necessary and sufficient condition for definiteness of the energy (charge) is that the larger of the two expressions $|(\gamma_4^{n+1}\eta)_c|$

and $|(\gamma_4^n\eta)_c|$ be the one in which the exponent of γ_4 is even (or odd).

It is not hard to verify that for spin $1/2$ and spin $3/2$ (reference 3) that one of the traces $(\gamma_4^{n+1}\eta)_c$ and $(\gamma_4^n\eta)_c$ in which γ_4 has an even exponent vanishes, and that for the spins 0, 1, and 2 (references 4 and 5) the trace with the odd power of γ_4 vanishes. This is in full agreement with the facts of the definiteness of the energy (charge) of particles with integral (half-integral) spin.

We see that although the projection matrix τ_{lk} gives not the wave function ψ_{lk} itself, but the dyad (26), nevertheless such fundamental quantities as the charge and energy of the field are expressed directly in terms of τ_{lk}. This fact is of general significance, and all the basic bilinear expressions in ψ that have direct physical meaning, and the calculation of which is the main problem of the theory, can be expressed directly in terms of τ_{lk}.

In particular, let us consider the transition probability for a certain particle to go from the state ψ_1 to the state ψ_2 as the result of an interaction. As is well known, the general expression for this probability w is proportional to the square of the absolute value of the corresponding matrix element for the transition:

$$w = C\,|\psi_2 R\psi_1|^2 = C\,(\psi_2 R\psi_1)^*\bar{\psi}_2 R\psi_1, \tag{41}$$

where R is an operator of a form determined by the nature of the interaction. Since

$$(\bar{\psi}_2 R\psi_1)^* = \bar{\psi}_2^* R^* \psi_1^* = \psi_1^* R^+ \eta\psi_2 = \bar{\psi}_1 \eta R^+ \eta\psi_2,$$

Eq. (41) can be written in the form

$$w = C\bar{\psi}_1\eta R^+\eta\,(\psi_2\cdot\bar{\psi}_2)\,R\psi_1 = C\,[\bar{R}\,(\psi_2\cdot\bar{\psi}_2)R\,(\psi_1\cdot\bar{\psi}_1)]_c, \tag{42}$$

where $\bar{R} = \eta R^+\eta$. According to Eqs. (18) and (26) the dyads $\psi_1\cdot\bar{\psi}_1$ and $\psi_2\cdot\bar{\psi}_2$ can be represented in the form

$$\begin{aligned} \psi_1\cdot\bar{\psi}_1 &= \alpha(\hat{p}_1)\,\beta(\sigma_1) = \alpha_1\beta_1, \\ \psi_2\cdot\bar{\psi}_2 &= \alpha(\hat{p}_2)\,\beta(\sigma_2) = \alpha_2\beta_2, \end{aligned} \tag{43}$$

where $\hat{p}_1$, $\hat{p}_2$, σ_1, σ_2 are the operators for the states ψ_1 and ψ_2 respectively. Thus in the general case the calculation of transition probabilities or effective cross-sections for various processes reduces to the computation of traces of products of operators:

$$w = C\,[\bar{R}\alpha_1\beta_1 R\alpha_2\beta_2]_c. \tag{44}$$

Since computations of traces can be carried out in an invariant way, the expression (44) can be obtained without the use of the explicit form of the matrices γ_k in any particular basis.

In many calculations of various interaction effects it is required to find the corresponding probabilities summed over the spins in the final states and averaged over the spins in the initial states. In the expression (44) the summation over the spins is obtained remarkably simply. Since according to Eq. (12) $\sum_k \beta_k \equiv 1$, for a particle with the spin s the expression (44), averaged over the spin of the initial state and summed over the spin of the final state, will have the form

$$\frac{1}{2s_1+1}\sum_{s_1,s_2} w = \frac{C}{2s_1+1}\,(\bar{R}\alpha_1 R\alpha_2)_c. \tag{45}$$

Here it is assumed that the operator R does not depend on the spin of the particle.

Expressions of the type (45) are used for the calculation of various effects in quantum electrodynamics.[6] It follows from the above developments, however, that such expressions have an extremely general significance and are valid for the calculation of all sorts of interaction effects for particles of arbitrary spin. It must be noted that in all its generality the method used here to derive these basic relations is considerably simpler than those used in the standard literature[6,7] to obtain results that relate to just the special case of the interaction of electrons with the electromagnetic field.

By means of these same relations, (26) and (34), we can work out in a very simple way the general commutation relations for particles with arbitrary spin. As is well known (cf., e.g., reference 8):

$$\begin{aligned} &[\psi_\alpha(x'), \bar{\psi}_\beta(x'')]_\pm \\ &= \sum_{l,k}\frac{1}{(2\pi)^3}\int d\mathbf{p}\,\{\psi_\alpha(p^{(l)}, \lambda_l, s_k)\,\bar{\psi}_\beta(p^{(l)}, \lambda_l, s_k)\,e^{ip^{(l)}x} \\ &\pm\psi_\alpha(p^{(l)}, -\lambda_l, s_k)\,\bar{\psi}_\beta(p^{(l)}, -\lambda_l, s_k)\,e^{-ip^{(l)}x}\}. \end{aligned} \tag{46}$$

Here $x = x' - x''$; the expressions $\psi_\alpha\bar{\psi}_\beta$ form the dyad $(\psi\cdot\bar{\psi})_{\alpha\beta}$ [cf. Eq. (15)]. We use the normalization (28). Then in the case of integral spin, on account of the definiteness of the energy, by Eq. (27) we must take the positive sign for both the states $\psi_{\pm lk}$ in Eq. (34), that is,

$$\psi_{\pm lk}\cdot\bar{\psi}_{\pm lk} = \tau_{\pm lk} = (\varkappa/\lambda_l^2 p_0^{(l)})\,\alpha_{\pm l}\beta_k. \tag{47}$$

For half-integral spin (indefinite energy), on the other hand, we get

$$\psi_{\pm lk}\cdot\bar{\psi}_{\pm lk} = \pm\tau_{\pm lk} = \pm(\varkappa/\lambda_l^2 p_0^{(l)})\,\alpha_{\pm l}\beta_k. \tag{48}$$

According to Eq. (12) the summation over the spins k in Eq. (46) reduces simply to striking out β_k, and we obtain for the two cases of integral and half-integral spins

$$[\psi(x')\cdot\overline{\psi}(x'')]_{\pm}=\sum_{l}(2\pi)^{-3}\frac{\varkappa}{\lambda_l^2}\int\frac{d\mathrm{p}}{p_0^{(l)}}\left(\alpha_{+l}(\hat{p}^{(l)})\,e^{ip^{(l)}x}-\alpha_{-l}(\hat{p}^{(l)})\,e^{-ip^{(l)}x}\right)\tag{49}$$

$$=\sum_{l}\frac{1}{(2\pi)^3}\,\frac{\varkappa}{\lambda_l^2}\int\frac{d\mathrm{p}}{p_0^{(l)}}\left(\alpha_{+l}(\nabla)\,e^{ip^{(l)}x}-\alpha_{-l}(-\nabla)\,e^{-ip^{(l)}x}\right).$$

By means of Eqs. (3), (8), (9), setting $\mathrm{m}=\pm\mathrm{m}_l=\pm\kappa/\lambda_l$, we get

$$\alpha_{\pm l}(\hat{p}^{(l)})=\frac{(\hat{p}^{(l)}\pm\varkappa)(\hat{p}^{(l)})^n}{\pm 2\varkappa(\pm\varkappa)^n}\prod_{\substack{l'=1\\ l'\neq l}}^{q}\frac{(\hat{p}^{(l)})^2-\lambda_{l'}^2m_l^2}{\varkappa^2-\lambda_{l'}^2m_l^2}.\tag{50}$$

Therefore $\alpha_{-l}(\hat{\mathrm{p}}^{(l)})=\alpha_{+l}(-\hat{\mathrm{p}}^{(l)})$, since change of the sign of κ in Eq. (50) gives the same result as change of the sign of $\mathrm{p}^{(l)}$. Consequently, $\alpha_{+l}(\nabla)=\alpha_{-l}(-\nabla)$, and it follows from Eq. (49) that

$$[\psi(x')\cdot\overline{\psi}(x'')]_{\pm}=2i\varkappa\sum_{l=1}^{q}\frac{1}{\lambda_l^2}\,\alpha_l(\nabla)\,D_l(x),$$

$$D_l(x)=(2\pi)^{-3}\int\frac{d\mathrm{p}}{p_0^{(l)}}\,e^{i\mathrm{px}}\sin p_0^{(l)}x_0.\tag{51}$$

It has here taken only a few lines to derive this result, which was obtained in the paper of Karpman[9] by rather lengthy arguments. The example that has been given can serve as an illustration of the effectiveness of the method expounded above. Obviously the relations (26) and (34) can find application in all sorts of other calculations relating to spinning particles.

[1] F. Fedorov, Dokl. Akad. Nauk SSSR **79**, 787 (1951).

[2] E. Corson, *Introduction to Tensors, Spinors, and Relativistic Wave Equations*. New York, 1953.

[3] I. Gel'fand and A. Iaglom, J. Exptl. Theoret. Phys. (U.S.S.R.) **18**, 703 (1948).

[4] W. Pauli, *Relativistic Theory of Elementary Particles* (Russ. Trans.), IL 1947.

[5] F. Fedorov, **Уч. зап. Белорусск. гос. ун-та им. Ленина, серия физ.-мат.** (Scient. Notes, Beloruss. State Univ., Math.-Phys. Series) **12**, 156 (1951).

[6] A. I. Akhiezer and V. B. Berestetskii, **Квантовая электродинамика** (*Quantum Electrodynamics*), GITTL 1953. [Engl. Transl. publ. by U. S. Dept. of Commerce].

[7] W. Heitler, *Quantum Theory of Radiation*, Oxford, 1953.

[8] N. N. Bogoliubov and D. V. Shirkov, **Введение в теорию квантованных полей** (*Introduction to the Theory of Quantized Fields*), GITTL 1957.

[9] V. Karpman, J. Exptl. Theoret. Phys. (U.S.S.R.) **21**, 1337 (1951).

Translated by W. H. Furry
84

SOVIET PHYSICS JETP VOLUME 35(8), NUMBER 2 FEBRUARY, 1959

DIFFRACTION SCATTERING OF 6.15-Bev PROTONS BY PROTONS

V. G GRISHIN

Joint Institute for Nuclear Research

Submitted to JETP editor March 28, 1958

J. Exptl. Theoret. Phys. (U.S.S.R.) **35**, 501-504 (August, 1958)

A phase shift analysis is carried out for the diffraction scattering of 6.15-Bev protons by protons. The spatial distribution of the absorbing field is deduced from results of an analysis using the semiclassical approximation. The value 0.79×10^{-13} cm is obtained for the mean-square proton-proton nuclear interaction radius.

1. SCATTERING OF IDENTICAL PARTICLES AT HIGH ENERGIES

We consider the interaction of identical particles, which is taken to be independent of their spins (s). The differential cross section for elastic scattering is described by the well-known formula* (see, for example, reference 1):

$$\frac{d\sigma}{d\omega} = \Big\{ |f(\vartheta)|^2 + |f(\pi-\vartheta)|^2 \pm \frac{1}{2s+1}\left[f(\vartheta) f(\pi-\vartheta)^* + f(\vartheta)^* f(\pi-\vartheta)\right]\Big\}. \tag{1}$$

Here, $f(\vartheta)$ is the scattering amplitude and ϑ is the scattering angle. The upper sign refers to integral s, the lower, to half-integral s. The experimental data[2] indicate that elastic p-p scattering at high energies goes mainly through small angles. In this case, if $f(\vartheta)$ has significant values only for small ϑ, then in this region of angles it can be seen from Eq. (1) that

$$d\sigma / d\omega = |f(\vartheta)|^2. \tag{2}$$

Here

$$f(\vartheta) = \frac{i\lambda\!\!\!^{-}}{2} \sum_{l=0}^{\infty} (2l+1)(1-\beta_l) P_l(\cos\vartheta). \tag{3}$$

In Eq. (3) the notation is as usual; in particular, $\beta_l = \exp\{2i\eta_l\}$, where $\eta_l = \alpha_l + i\zeta_l$ and η_l is the scattering phase.

We assume that all of the elastic scattering at high energies is diffraction (by "diffraction" we mean here that approximation in which all $\alpha_l = 0$). Then the scattering amplitude will be imaginary, which substantially simplifies the phase shift analysis. In fact, because of the orthogonality of the Legendre polynomials in Eq. (3) it is easy to obtain

$$i\lambda\!\!\!^{-}(1-\beta_l) = \int_{-1}^{+1} P_l(x) f(x)\, dx. \tag{4}$$

($x = \cos\vartheta$). From Eq. (2) we find

$$f(x) = e^{i\gamma} \sqrt{d\sigma / d\omega}. \tag{5}$$

Substituting Eq. (5) into Eq. (4) we obtain

$$i\lambda\!\!\!^{-}(1-\beta_l) = \int_{-1}^{+1} P_l(x) e^{i\gamma} \sqrt{\frac{d\sigma}{d\omega}}\, dx. \tag{6}$$

Since the scattering amplitude is imaginary in the case considered, γ can take on only the values $\pi/2$ and $3\pi/2$. From Eq. (3) it can be seen that $\gamma = \pi/2$ at zero angle. The differential scattering cross section changes monotonically with ϑ at high energies and is never zero in the measured range of angles. Taking this latter fact into account, and also the fact that $f(\vartheta)$ is a continuous function of ϑ, we make the simplest assumption, that $\gamma = \pi/2$ at all angles. Then Eq. (6) has the form

$$\lambda\!\!\!^{-}(1-\beta_l) = \int_{-1}^{+1} P_l(x) \sqrt{\frac{d\sigma}{d\omega}}\, dx. \tag{7}$$

Some theoretical basis for the assumptions made has been given by Belenkii.[3] The phenomenological analysis of elastic π-p and p-p scattering showed that for $E_\pi \gtrsim 1$ Bev and $E_p \gtrsim 5$ Bev all of the elastic scattering can be considered diffractional.[4,5] We give below a phase-shift analysis of elastic p-p scattering at 6.15 Bev within the framework of these assumptions.

2. ANALYSIS OF p-p SCATTERING AT 6.15 Bev

The experimental data are described by empirical formulae of the form

$$d\sigma / d\omega = a^2 / (b - \cos\vartheta)^2, \tag{I}$$

$$d\sigma / d\omega = c \exp(-k\vartheta^2). \tag{II}$$

---

*All considerations in this article are in the center-of-mass system of the colliding particles.

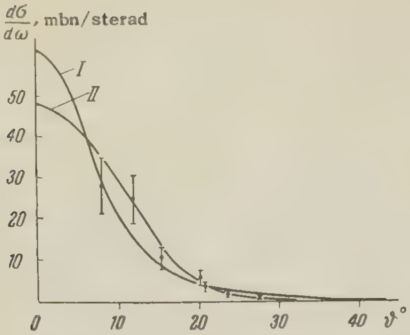

FIG. 1. Differential cross section for the elastic p – p interaction at $E_p = 6.15$ Bev. The experimental values are taken from Ref. 2, with account of a systematic error of ± 15%. The solid curves give the approximating functions $d\sigma, d\omega = 0.0244/(1.02\text{-}\cos\vartheta)^2$ mbn/sterad (I) and $d\sigma/d\omega = 48.0 \exp\{-19.2\,\vartheta^2\}$ mbn/sterad (II).

Curves of type (I), with suitable choice of a and b, go up sharply at small angles and give values for the cross section in excess of the experimental ones at large angles. Curves of type (II) go up more slowly towards zero angle, within the limits of experimental error, and drop sharply at larger angles (see Fig. 1).

Calculations were carried out for various choices of the constants a, b, c, and k, satisfying the experimental data. In the future, only the results of a phase shift analysis for the empirical curves in Fig. 1 will be given. Various other possible choices of the constants give analogous results.

For curve (I), β_l was calculated from Eq. (7) using the Legendre function of the second type.[4] For the Gaussian curve (II) it was assumed that[6]

$$1 - \beta_l = \alpha_0 \exp\{-0.026\, l^2\}.$$

The value of α_0 was determined from β_0, calculated from Eq. (7).

Ambiguity in the choice of approximation at large angles leads to a large indeterminacy in values of β_0 and β_1 for curve (I); we therefore omit them from our consideration.

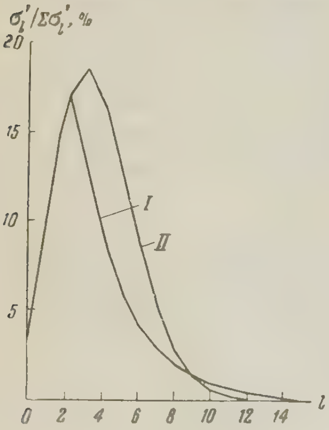

FIG. 2. Values of the partial contributions to the total cross section for elastic scattering in percentages for curves (I) and (II).

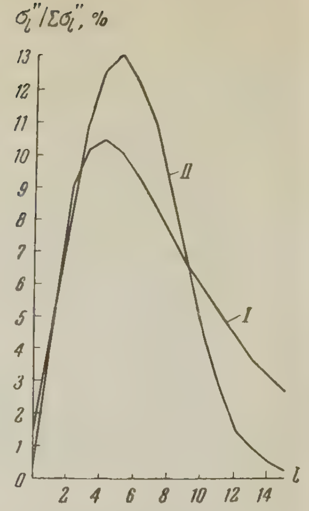

FIG. 3. Values of the partial contributions to the total inelastic cross section in percentages for curves (I) and (II).

According to general scattering theory, the partial contributions to the cross section for elastic and inelastic scattering are respectively equal to

$$\sigma'_l = \pi\bar{\lambda}^2 (2l+1)(1-\beta_l)^2, \tag{8}$$

$$\sigma''_l = \pi\bar{\lambda}^2 (2l+1)(1-\beta_l^2). \tag{9}$$

Using the values of β_l obtained earlier, σ'_l and σ''_l were calculated. In Figs. 2 and 3 the values of partial contributions σ'_l and σ''_l are given in percentages of the corresponding (elastic or inelastic) cross sections as a function of l.

It can be seen from Fig. 2 that the main contributions to the elastic scattering come from the partial waves with $l = 0$ to 8. The main contributions to the inelastic scattering come from waves with $l = 1$ to 12 (Fig. 3).

In order to check the possibility of neglecting contributions from waves with $l > 15$ for the approximations chosen, the total interaction cross section σ_t was calculated from the well-known formula

$$4\pi\bar{\lambda}\,\mathrm{Im}\, f(0°) = \sigma_t. \tag{10}$$

Substituting f(0°) from our empirical formulae (I) and (II) we find σ_t equal to 36.0 mbn and 32.2 mbn respectively. On the other hand, $\sigma_t^{15} = \sum_{l=0}^{15} (\sigma'_l + \sigma''_l)$ is equal to 32.3 mbn and 31.7 mbn, respectively, which agree well with values of σ_t calculated from Eq. (10). The values $\sigma' = \sum_{l=0}^{15} \sigma'_l = 7.6$ to 7.8 mbn agree well with the experimental value[2] of 8 mbn for the cross section for elastic scattering.

We consider the results obtained using the quasiclassical approximation. The assumption that all elastic scattering is diffractional means that the scattering system is purely absorptive.

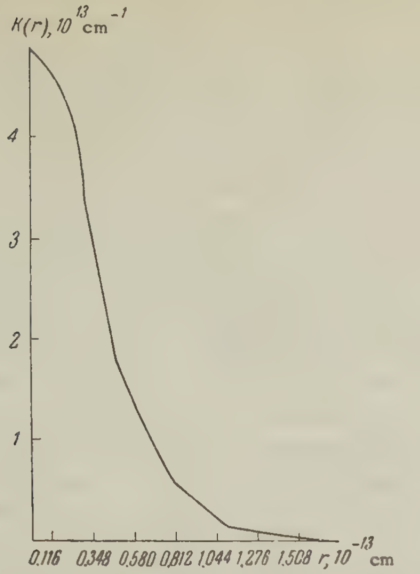

FIG. 4. Absorption coefficient for the nucleon-nucleon system of a function of distance between the centers of the nucleons.

In order to find the absorption coefficient K(r), results of the phase shift analysis for the curve (II) were used; these describe the experimental data well even if the systematic error of ±15% is not taken into account. K(r) was calculated by the method considered in reference 7. In our case r can be considered as the distance between "centers" of the nucleons. The results of calculation are given in Fig. 4.

From the formula

$$\overline{\rho^2} = \int_0^R r^4 K(r)\, dr \Big/ \int_0^R r^2 K(r)\, dr \qquad (11)$$

the value of the mean square radius of nuclear proton-proton interaction was found to be equal to 0.79×10^{-13} cm. This value agrees well with the electromagnetic radius of the proton, equal to 0.78×10^{-13} cm.[8]

The author is grateful to R. A. Asanov, V. S. Barashenkov, D. I. Blokhintsev, P. V. Vavilov, and V. I. Ogievetskii for helpful discussion, and also to L. A. Shustrova for carrying out numerical calculations for the present work.

---

[1] L. Landau and E. Lifshitz, Квантовая механика (Quantum Mechanics), GTTI, M. 1948. [Engl. Transl., Pergamon, 1958].

[2] Cork, Wenzel and Causey, Phys. Rev. **107**, 859 (1957).

[3] S. Z. Belenkii, J. Exptl. Theoret. Phys. (U.S.S.R.) **33**, 1248 (1957); Soviet Phys. JETP **6**, 960 (1958).

[4] D. Ito and S. Minami, Progr. Theor. Phys. **14**, 198 (1955).

[5] Grishin, Saitov and Chuvilo, J. Exptl. Theoret. Phys. (U.S.S.R.) **34**, 1221 (1958), Soviet Phys. JETP **7**, 844 (1958).

[6] V. G. Grishin and I. S. Saitov, J. Exptl. Theoret. Phys. (U.S.S.R.) **33**, 1051 (1957); Soviet Phys. JETP **6**, 809 (1958).

[7] Blokhintsev, Barashenkov and Grishin, Nuovo cimento **9**, 249 (1958); J. Exptl. Theoret. Phys. (U.S.S.R.) **35**, 311 (1958), Soviet Phys. JETP **8**, 215 (1959).

[8] E. E. Chambers and R. Hofstadter, Phys. Rev. **103**, 1454 (1956).

Translated by G. E. Brown
85

Letters to the Editor

CROSS SECTIONS OF POSSIBLE NONRADIATIVE RECOMBINATION IN SEMICONDUCTORS

Iu. M. POPOV

P. N. Lebedev Physics Institute, Academy of Sciences, U.S.S.R.

Submitted to JETP editor April 22, 1958

J. Exptl. Theoret. Phys. (U.S.S.R.) **35**, 505-506 (August, 1958)

ONE process that can occur in a semiconductor is nonradiative recombination, the inverse of the ionization of trap electrons by conduction electrons (or holes). Using the wave functions and ideas proposed by Bess[1] for the character of this interaction, we performed the calculations (in a manner somewhat different than in reference 1) for the collision between a thermal hole and a slow conduction electron near a filled trap with subsequent recombination of the trap electron with a hole (the trap electron is considered as a free level for the hole) and transfer of the liberated energy to the conduction electron. We used the following wave functions,

$$u_{\mathrm{I}}(r_1r_2) = u_n(r_1)\,u_h(r_2) \quad \text{(initial state)},$$

$$u_{\mathrm{II}}(r_1r_2) = u_f(r_1)\,u_{bh}(r_2) \quad \text{(final state)}.$$

Here $u_{bh}(r_2)$ is the wave function of the hole localized on the impurity, and the remaining symbols are those used in reference 1. In this case the electron and the hole are different particles and the wave functions need not be symmetric.

Considering that $p \gg p_0$, we obtain:

$$\sigma_{2e}(p_0) = 4\pi^2\left(\frac{16\hbar^2c^2m^*}{p^2a_H m\varepsilon_0}\right)^2\left(\frac{p}{p_0}\right)(a_t^3N_e)\,F^4\left(\frac{pa_t}{\hbar c}\right),$$

$$\sigma_{2h}(p_0) = \sigma_{1e}(p_0) = \sigma_{2e}(p_0)\,N_h/N_e, \quad \sigma_{1h}(p_0) = \sigma_{2e}(p_0),$$

where

$$a_t = \sqrt{\frac{\mathscr{E}_r}{\Delta}}\,a_H, \quad F(x) = \frac{1}{1+x^2}.$$

$\mathscr{E}_r$ is the Rydberg energy, Δ the depth of the level from the bottom of the conduction band (for holes — the height from the valence band); m and m* are the ordinary and effective masses of the electrons (or holes), a_H the radius of the Bohr orbit, ϵ_0 the dielectric constant, N_e and N_h the concentrations of the conduction electrons and holes in the valence band respectively, σ_{2e} the cross section for the collision of two conduction electrons with subsequent transition of one electron to the free impurity level, σ_{2h} the cross section for the collision of two holes with transition of one hole to the impurity level occupied by the electrons, σ_{1e} the cross section for the collision between a conduction electron and a hole with transition of the electron to the free impurity level, and σ_{1h} the cross section for the collision between a hole and a conduction electron with transition of the hole to impurity level occupied by the electron.

If the carrier concentration N_e or N_h is $\sim 3 \times 10^{13}\ \mathrm{cm}^{-3}$, then σ_{1e} and σ_{2e} are of the same order ($3 \times 10^{-21}\ \mathrm{cm}^2$), and are even one order of magnitude less than the cross sections obtained by Bess for radiative recombination (σ_{re} and σ_{rh}). The above mechanism of nonradiative recombination cannot therefore explain the experimentally-observed short lifetime of the carriers in germanium (at a carrier concentration $\sim 3 \times 10^{13}\ \mathrm{cm}^{-3}$), and will come into play only when this concentration is substantially increased.

It must be said that Bess' cross sections σ_{1h} and σ_{1e} include recombinations between a conduction electron and a thermal hole, which is considered a free level for the electron. But in this case he merely assumed, for the electron in the valence band, the wave function of the free hole without the Bloch factor. Since the wave functions $u_n(r_1)$ and $u_h(r_1)$, taken for this case in reference 1, describe an electron with the same momentum p_0 in the conduction and the valence bands respectively, they should be orthogonal to each other, a fact not taken into account by Bess. It is therefore natural that in this very case the matrix element (3) of reference 1 (and consequently the cross sections σ_{1h} and σ_{1e}), calculated without orthogonal functions, is many orders of magnitude greater than that calculated by us.

---

[1] L. Bess, Phys. Rev. **105**, 1469 (1957).

Translated by J. G. Adashko
86

SPIN-SPIN PARAMAGNETIC RELAXATION TIME IN THE ABSENCE OF A STATIC MAGNETIC FIELD FOR $Co(NH_4)_2(SO_4)_2 \cdot 6H_2O$ AT HELIUM TEMPERATURES

U. Kh. KOPVILLEM

Kazan' State University

Submitted to JETP editor April 4, 1958

J. Exptl. Theoret. Phys. (U.S.S.R.) 35, 506-507 (August, 1958)

UNTIL now, the spin-spin paramagnetic relaxation time τ_{ss} in magnetically anisotropic monocrystals has been calculated theoretically only for some substances which contain magnetically equivalent ions.[1] In single crystals with magnetic ions situated in diverse intracrystalline electric fields E, the relaxation process has a more complex character. The time τ_{ss}, generally speaking, does not have extrema along the principal axes K_1, K_2 and K_3 (reference 2) of the static magnetic susceptibility tensor χ_0, and in case of strong anisotropy of the g factors, the value of τ_{ss} can vary within wide limits. Calculations were carried out by us under the following assumptions: (1) The spin-system consists of an equal number of ions of two sorts. (2) In the absence of the static magnetic field H_0, the ground state of all the ions has twofold Kramers degeneracy. (3) The spin temperature T is so low that only the principal doublet is occupied, i.e., the effective spin is $S = \frac{1}{2}$ for all the ions. (4) The interactions in the paramagnets can be described by means of the two-particle $P^{ik}_{\gamma\delta}\sigma^i_\gamma\sigma^k_\delta$ and one-particle $\frac{1}{2}A^k_{\gamma\delta}\sigma^k_\gamma I_\delta$ tensor operators, where σ^i_γ is a Pauli matrix, I_δ is a matrix spin-vector, and k and δ are indices which label the particles and the coordinate axes respectively. In the calculations it was supposed that the principal axes of the tensors P and A do not coincide with one another, and that the g tensors pertaining to different type ions have different forms. (5) The aperiodic curve $f(\nu)$ (where ν is the frequency of the applied magnetic field H_t)[3] of paramagnetic absorption has a gaussian shape at $H_0 = 0$.

Taking into account conditions 1 to 4, we obtained a formula for the tabulated second moment[3] $\langle\nu^2\rangle$ of the curve $f(\nu)$ for arbitrary direction of the field H_t relative to the principal axes of the tensor χ_0. The theoretical value for $\langle\nu^2\rangle$ can be directly compared with the experimental data. If condition 5 is satisfied, $\langle\nu^2\rangle$ can be used for the calculation of τ_{ss} according to Broer's formula:[3] $\tau_{ss} = [\pi/2\langle\nu^2\rangle]^{1/2}$. The components of the tensors P and A, which determine the quantity $\langle\nu^2\rangle$, also enter into the formulas for χ_0, the magnetic specific heat C_0 (reference 2), and the paramagnetic resonance line breadth $\Delta H_{1/2}$.[1] Our formulae thus establish a connection between $\langle\nu^2\rangle$, τ_{ss}, χ_0, C_0 and $\Delta H_{1/2}$.

Specific calculations have been carried out for $Co(NH_4)_2(SO_4)_2 \cdot 6H_2O$ at helium temperatures. In this case, P characterizes the dipole-dipole ($\mathcal{H}_d$) and exchange ($\mathcal{H}_{ex}$) interactions; A characterizes the hyperfine spin interaction $\mathcal{H}_{hfs}$ between the nucleus and the unpaired electrons within one and the same paramagnetic ion. The numerical values of the components of the tensor A along the principal axes were taken by us from reference 4 and pertain to Co^{59}. In the calculation of the components $P^{ik}_{\gamma\delta}$ we used the values of the g factors and the true eigenfunctions of the fundamental Kramers doublet given in references 4 and 5 respectively. The lattice sums, which enter in $\langle\nu^2\rangle$, were evaluated by means of the tables compiled in references 2 and 6. We evaluated the exchange integrals J_1 and J_2, between the nearest and next nearest neighbors of a paramagnetic ion respectively, by means of formulae from reference 6. Upon correction of one arithmetical error in the derivation of these formulae, we obtained $J_1/k = 0.017°$ and $J_2/k = -0.0104°$, where k is Boltzman's constant.

The table lists the results of calculations of $\langle\nu^2\rangle \times 10^{-18}$ sec^{-2} and of τ_{ss} sec for the directions K_1, K_2, K_3, and ϵ, where ϵ is the axis of symmetry of the field E for one of the nonequivalent ions and $\langle\nu^2\rangle_d$, $\langle\nu^2\rangle_{ex}$, $\langle\nu^2\rangle_{hfs}$ and $\langle\nu^2\rangle_{d\text{-}ex}$ are additive contributions due to

	$\langle\nu^2\rangle_d$	$\langle\nu^2\rangle_{ex}$	$\langle\nu^2\rangle_{d\text{-}ex}$	$\langle\nu^2\rangle_{hfs}$	τ_{ss}
$H_t \parallel K_1$	334	33	—110	30	$7.4 \cdot 10^{-10}$
$H_t \parallel K_2$	616	217	70	283	$3.75 \cdot 10^{-10}$
$H_t \parallel K_3$	527	—99	237	12	$4.81 \cdot 10^{-10}$
$H_t \parallel \varepsilon$	256	33	—93	25	$8.43 \cdot 10^{-10}$

$\mathcal{H}_d$, $\mathcal{H}_{ex}$, $\mathcal{H}_{hfs}$ and the dipole-exchange interactions, respectively.

In conclusion, the author expresses his thanks to Prof. S. A. Al'tshuler for suggesting the topic and for his interest in the work.

---

[1] U. Kh. Kopvillem, J. Exptl. Theoret. Phys. (U.S.S.R.) **34**, 1040 (1958), Soviet Phys. JETP **7**, 719 (1958).

[2] J. M. Daniels, Proc. Phys. Soc. **A66**, 673 (1953).

[3] A. Wright, Phys. Rev. **76**, 1826 (1949).

[4] B. Bleaney and D. J. E. Ingram, Proc. Roy. Soc. **A208**, 143 (1951).

[5] A. Abragam and M. H. L. Pryce, Proc. Roy. Soc. **A206**, 173 (1951).

[6] T. Nakamura and N. Uryu, J. Phys. Soc. Japan, **11**, 760 (1956).

Translated by R. Eisner
87

ON THE THEORY OF COMPOSITE π^0 MESONS

M. E. PEREL' MAN

Institute of Physics, Academy of Sciences, Georgian S.S.R.

Submitted to JETP editor April 4, 1958

J. Exptl. Theoret. Phys. (U.S.S.R.) **35**, 508-509 (August, 1958)

IT is generally acknowledged today that the π mesons spend part of their time in the form of a baryon-antibaryon pair, i.e., the π mesons are represented at least part of the time (and in the model of Fermi and Yang,[1] all the time) as a tightly bound nucleon-antinucleon pair. If we require the π mesons to form an isotopic triplet, we obtain

$$\pi^+ = p\bar{n},\ \pi^0 = (p\bar{p} + n\bar{n})/\sqrt{2} = (\pi_1 + \pi_2)/\sqrt{2},\quad \pi^- = n\bar{p}. \tag{1}$$

Recently, the possibility also of the existence of an isotopic singlet was noted.[2,3] In the theory of composite particles this is represented as

$$\rho^0 = (p\bar{p} - n\bar{n})/\sqrt{2} = (\pi_1 - \pi_2)/\sqrt{2}. \tag{2}$$

Obviously, the Coulomb interaction in the $\pi_1 = p\bar{p}$ compound will result in different properties for the π_1 and π_2 mesons.

Following Zel' dovich,[4] it is easy to show that the masses of the π_1 and π_2 compounds are different:

$$\Delta M = m_{\pi_2} - m_{\pi_1} = c^{-2}\langle W_{\text{el-mag}}\rangle_{\text{av}} = (e/c)^2\langle -r^{-1}\rangle_{\text{av}} = 12.7\, m_e, \tag{3}$$

where m_e is the electron mass. The averaging is over the wave function found by Fermi and Yang.[1] It is clear that the life times of these compounds will also be different. Thus, according to the calculations of Romankevich, which use lowest-order perturbation theory,[5]

$$\tau(\pi_1)/\tau(\pi_2) = (3/\pi^2)(g^2/\hbar c)^2$$

($g^2/\hbar c$ is the dimensionless coupling constant for the coupling of the π meson field with the nucleons). Therefore, if initially the beam contains only π^0 mesons and if the corresponding wave function has the form $\Psi(0) = (\pi_1 + \pi_2)/\sqrt{2}$, then the amplitudes for the states π_1 and π_2 at time t will not be equal, and

$$\Psi(t) = \{\pi_1 \exp[-t/2\tau(\pi_1) + i\omega_1 t] + \pi_2 \exp[-t/2\tau(\pi_2) + i\omega_2 t]\}/\sqrt{2}, \tag{4}$$

where $\hbar\omega_i = c\sqrt{p^2 + m_i^2c^2}$.

Thus it is possible that the relative phase of the states π_1 and π_2 changes, i.e., we have the possibility of the transition of the π^0 meson into a ρ^0 meson in real or, at least, virtual (when the mass of ρ^0 is greater than the mass of π^0) processes.

In the calculation of the probability for finding the π^0 or the ρ^0 mesons we can neglect the strongly oscillating term containing $\cos(c^2\Delta Mt/\hbar)$, since, according to (3), $c^2\Delta M/\hbar \sim 10^{-21}$ sec^{-1}. Normalized for one particle, the probability for finding either meson has the form:

$$P(\pi^0 t) = P(\rho^0 t) = \tfrac{1}{4}\{\exp[-t/\tau(\pi_1)] + \exp[-t/\tau(\pi_2)]\},$$

i.e., our calculations lead to a decay scheme for the π^0 meson which is characterized by the sum of two exponentials.

Thus, according to the proposed scheme, π^0 and ρ^0 mesons participate in strong interactions, where the total isotopic spin is conserved, and π_1 and π_2 mesons participate in electromagnetic and weak interactions.

We do not exclude the possibility that the difference in the life times of the mesons emitted in different processes is connected with precisely this circumstance. For π^0 mesons produced in nucleon-nucleon collisions (strong interaction) $\tau \sim 5 \times 10^{-15}$ sec (reference 6), and for π^0 mesons arising in the K-meson decay (weak interaction), $\tau \lesssim 5 \times 10^{-16}$ sec (reference 7). According to our scheme, π^0 or ρ^0 mesons are emitted in the first case, and π_1 or π_2 mesons in the second case.

Obviously, this situation is entirely similar to that arising for neutral K mesons.[8]

In conclusion the author expresses his deep gratitude to V. V. Chavchanidze for his guidance.

Note added in proof (June 15, 1958): If we take, for example, $m_{\pi^+} \sim (\pi^+)^* Q\pi^+$, where Q is some "mass" operator, one can roughly estimate the mass of ρ^0 as ~139 Mev, using formulas (1) to (3). Hence, the investigation of π^0 production processes appears to be the most convenient way to discover the ρ^0 meson (cf. Fliagin, Dzhelepov, Kiselev, and Oganesian, Preprint R-188 Joint Inst. for Nucl. Prob.).

---

[1] E. Fermi and C. N. Yang, Phys. Rev. **76**, 1739 (1949).

[2] D'Espagnat, Prentki, and Salam, Nucl. Phys. **3**, 446 (1957).

[3] L. B. Okun', J. Exptl. Theoret. Phys. (U.S.S.R.) **34**, 469 (1958), Soviet Phys. JETP **7**, 322 (1958).

[4] Ia. B. Zel'dovich, Dokl. Akad. Nauk SSSR **97**, 225 (1954).

[5] A. V. Romankevich, J. Exptl. Theoret. Phys. (U.S.S.R.) **32**, 615 (1957); Soviet Phys. JETP **5**, 509 (1957).

[6] B. M. Anand, Proc. Royal Soc. **A220**, 183 (1953).

[7] Harris, Orear, and Taylor, Phys. Rev. **106**, 327 (1957).

[8] M. Gell-Mann and A. Pais, Phys. Rev. **97**, 1387 (1955). A. Pais and Piccioni, Phys. Rev. **100**, 1487 (1955).

Translated by R. Lipperheide
88

SIMPLE MAGNETOACOUSTIC WAVES

G. Ia. LIUBARSKII and P. V. Polovin

Physico-technical Institute, Academy of Sciences, Ukrainian S.S.R.

Submitted to JETP editor April 4, 1958

J. Exptl. Theoret. Phys. (U.S.S.R.) **35**, 509 (August, 1958)

IN ordinary hydrodynamics, it is shown[1] that points of high density in a simple wave move more rapidly than points with low density, if the inequality

$$\left(\frac{\partial^2}{\partial p^2}\frac{1}{\rho}\right) > 0 \qquad (1)$$

is satisfied.

In magnetic hydrodynamics, three types of simple waves are present:[2] fast and slow magnetoacoustic, and Alfven (magnetohydrodynamic) waves. The latter wave type is characterized by a constant density and constant velocity. As regards the first two types of waves, it can be shown that points of high density in them are displaced with higher velocity if condition (1) is satisfied.

It follows from this, in particular, that self-similar waves are always waves of discontinuity. The dependence of the phase velocity on the density leads, just as in ordinary hydrodynamics, to the result that in regions of compression the liquid continues to be compressed as long as a shock wave is not formed.

The authors thank A. I. Akhiezer and A. S. Kompaneits for valuable advice.

---

[1] L. D. Landau and E. M. Lifshitz, **Механика сплошных сред** (Mechanics of Continuous Media) (GITTL, Moscow, 1953).

[2] Akhiezer, Luibarskii and Polovin, (Ukr. Phys. J.) (in press).

Translated by R. T. Beyer
89

IMPOSSIBILITY OF RAREFACTION SHOCK WAVES IN MAGNETOHYDRODYNAMICS

R. V. POLOVIN and G. Ia. LIUBARSKII

Physico-Technical Institute, Academy of Sciences, Ukrainian S.S.R.

Submitted to JETP editor April 4, 1958

J. Exptl. Theoret. Phys. (U.S.S.R.) **35**, 510 (August, 1958)

AS is known,[1] according to Zemplen's theorem in hydrodynamics, rarefaction shock waves are impossible if

$$\left(\frac{\partial^2}{\partial p^2}\frac{1}{\rho}\right)_s > 0 \qquad (1)$$

Landau and Lifshitz[2] have shown that in magnetohydrodynamic low-amplitude shock waves are compression waves if conditions (1) are satisfied.

Hoffmann and Teller[3] have shown that in an ideal gas the compressed shock wave is thermodynamically unstable if the magnetic field is parallel to the plane of explosion. They left open the problem of thermodynamic instability of rarefaction shock waves.

It turns out, however, that Zemplen's theorem is correct also in magnetohydrodynamics for an arbitrary explosion intensity and for an arbitrary magnetic-field direction, provided condition (1) is augmented by the condition

$$(\partial p / \partial T)_{\rho} > 0. \qquad (2)$$

The increase in shock-wave pressure leads to an increase in density.

To explain how the tangential magnetic field $H_{\perp}$ changes upon passage of a shock wave, it is enough to use the formula

$$H_{\perp} = H_{0\perp}\rho (v_{0x}^2 - V_{0x}^2) / (\rho_0 v_{0x}^2 - \rho V_{0x}^2), \qquad (3)$$

which follows from the conditions on the surface of the explosion (the subscript 0 refers to the region ahead of the shock wave, and V_x is the normal projection of the Alfven velocity). Small magnetic fields $[H_x^2 < 2\pi v_{0x}^2 (\rho_0/\rho)(\rho + \rho_0)]$ become reinforced by passage of a shock wave, while large magnetic fields $[H_x^2 > 2\pi v_{0x}^2 (\rho_0/\rho)(\rho + \rho_0)]$ are attenuated. This indicates that shock waves play a certain equalizing role.

The reinforcement of weak magnetic field by passage of shock waves was noted by Helfer.[4] In his opinion this is one of the mechanisms of formation of strong interstellar magnetic fields.

The authors are grateful to A. I. Akhiezer and A. S. Kompaneets for valuable advice.

---

[1] L. D. Landau and E. M. Lifshitz, Механика сплошных сред (Mechanics of Continuous Media), GITTL, M., 1953.

[2] L. D. Landau and E. M. Lifshitz, Электродинамика сплошных сред (Electrodynamics of Continuous Media), GITTL, M., 1958.

[3] F. Hoffmann and E. Teller, Phys. Rev. **80**, 692 (1950).

[4] H. L. Helfer, Astrophys. J. **117**, 177 (1953).

Translated by J. G. Adashko
90

ON THE PROBLEM OF TWO-NUCLEON INTERACTION IN THE TAMM-DANCOFF METHOD

A. A. RUKHADZE

Submitted to JETP editor April 7, 1958

J. Exptl. Theoret. Phys. (U.S.S.R.) 35, 511-512 (August, 1958)

In the field theory of nucleon interactions, the effective potential is usually calculated with the help of the so-called "adiabatic" approximation (i.e., neglecting the motion of the nucleons during the meson exchange).[1-8] Here the potential obtained in the adiabatic approximation is attractive already in the second order term in the coupling constant (g^2), and contains a singularity of type r^{-3}. In higher approximations with respect to the coupling constant, the singularity of the potential increases.

In the investigation of a system of two nucleons with the help of such mesonic potentials one usually introduces into the theory a second arbitrary constant,[6,7] the cut-off constant for the interaction r_c. This is a great deficiency of the theory. However, the author has shown[9] that this arbitrariness of the theory can be excluded in the non-adiabatic treatment of the nucleons, and that a theory can be constructed with a single arbitrary constant, the coupling constant. In the paper[9] it was shown that the Tamm-Dancoff method[1-2] for the two-nucleon system may be applied in its two-meson approximation only. It appeared that the terms of order g^4 in the nucleon interaction are significant only in the nonrelativistic energy region of the interacting particles, while the interaction in the relativistic energy region is completely determined by the terms of order g^2. This result permits one to replace the exact equations for the state amplitude of the two-nucleon system by approximate equations in which the terms of order g^4 are treated only adiabatically (with $p, p' \leq P < M$), while the terms of order g^2 are treated exactly. This greatly simplifies the solution of the equations.

Recently these equations were integrated numerically on the "Strela" electronic computer of the U.S.S.R. Academy of Sciences. For the state $^3S_1 + {}^3D_1$ of the two-nucleon system, we found the lowest eigenvalue of the coupling constant for which the system is in the bound state with binding energy $\mathscr{E} = 2.227$ Mev. The scattering problem was solved for the $^1S_0$ state with a given value for g^2.

TABLE I

	$P=0$, $g^2/4\pi=7.60$	$P=3$, $g^2/4\pi=7.40$	$P=5$, $g^2/4\pi=7.55$	**Experiment**
P_d	10%	8%	10%	$2\% \leqslant P_d \leqslant 6\%$
$^3r_1$	$1.8\cdot10^{-13}$ cm	$1.7\cdot10^{-13}$cm	$1.9\cdot10^{-13}$ cm	$(1.704\pm0.03)\cdot10^{-13}$ cm
Q	$4.0\cdot10^{-27}$ cm^2	$3.8\cdot10^{-27}$ cm^2	$4.0\cdot10^{-27}$ cm^2	$(2.738\pm0.016)\cdot10^{-27}$ cm^2
$\left.\frac{u}{r}\right\|_{r=0}$	0.7	0.6	0.65	—

TABLE II

T, Mev	$P=0$ $g^2/4\pi=10;\ 12;\ 15$	$P=3$ $g^2/4\pi=10;\ 12;\ 15$	$P=5$ $g^2/4\pi=10;\ 12;\ 15$	Potentials G. T.[8] and S. M.[11]
0.7	8°, 11°, 16°	12°, 17°, 27°	12°, 17°, 27°	28°, 28°
5	12°, 17°, 26°	22°, 31°, 45°	22°, 30°, 44°	54°, 55°
15	0°, 0°, 7.5°	10°, 18°, 37°	11°, 18°, 37°	51°, 52°
50	—6°, —6°, —6.5°	—4°, —3° —2°	—4°, —3°, —3°	35°, 39°

From the solutions for the amplitudes u(p) and w(p) of the two-nucleon system in the $^3S_1$ and $^3D_1$ states, obtained by numerical integration, we can find the wave functions for the $^3S_1$ and $^3D_1$ states of the deuteron in coordinate space:

$$u(r)=\frac{2}{(2\pi)^2}\int_0^\infty p\,dp\sqrt{\frac{2M}{M+E_p}}\,u(p)\sin pr,$$

$$w(r)=\frac{2}{(2\pi)^2}\int_0^\infty p\,dp\sqrt{\frac{2M}{M+E_p}}\,w(p)\times\left\{\sin pr+\frac{3\cos pr}{pr}-\frac{3\sin pr}{(pr)^2}\right\}, \tag{1}$$

where M is the mass of the nucleon, and $E_p = \sqrt{p^2+M^2}$ is the energy of the nucleon with momentum p. With the help of known formulas[6] we can use the functions u(r) and w(r) to determine the interaction parameters of the nucleons in the state $^3S_1 + {}^3D_1$ for low energies, viz.: $^3r_1$, P_d, and Q.

From the numerical results of the scattering problem for two nucleons in the $^1S_0$ state, we can determine the scattering phase for this state. In agreement with Dalitz and Dyson[10] we have

$$\tan\delta(^1S_0)=-\pi u_0(p_0), \tag{2}$$

where p_0 is the relative momentum of the nucleons in the center-of-mass system; it is connected with the kinetic energy T of the incident nucleon in the laboratory system by the relation $p_0 = \sqrt{MT/2}$.

Table I shows the results of the numerical calculations for the deuteron and gives a comparison of theoretical and experimental values. In Table II the results of the calculation of the phase $\delta(^1S_0)$ are compared with the results obtained with the use of various phenomenological potentials,[8,11] which agree well with experiment up to energies of 50 Mev. It is seen that the contribution of the terms of order g^4 to the interaction in the bound state problem of the deuteron is small. But in the scattering problem of nucleons in the $^1S_0$ state the terms of order g^4 give a significant contribution. The comparison of experimental and theoretical values shows that the theory is qualitatively right in the description of the interaction of the nucleons at low energies (T < 20 Mev). For T = 50 Mev the calculated phase $\delta(^1S_0)$ is significantly smaller than the experimental phase, which indicates the breakdown of the two-meson approximation used here for relatively high energies.

In conclusion I express my deep gratitude to Academician I. E. Tamm for suggesting the topic and for numerous discussions and advice. I also express my gratitude to N. N. Strelkova, who did nearly all the calculational part of this work on the "Strela" electronic computer. I am very grateful to N. E. Nikulkina, who performed much of the numerical work.

---

[1] I. E. Tamm, Journ. of Phys. **9**, 449 (1945).

[2] S. Dancoff, Phys. Rev. **78**, 382 (1950).

[3] K. Brueckner and K. Watson, Phys. Rev. **90**, 699; and **92**, 1023 (1953).

[4] J. Greene, Dissertation, University of Rochester, N. Y., 1956.

[5] J. Iwadare, Otsuki, Tamagaki, and Watari, Progr. Theor. Phys. **16**, 455, 472, 604, and 658 (1956).

[6] M. M. Lévy, Phys. Rev. **88**, 72 and 725 (1952).

[7] A. Klein, Phys. Rev. **89**, 1158; and **90**, 1101 (1953).

[8] J. Gammel and R. Thaler, Phys. Rev. **107**, 291 (1957).

[9] A. A. Rukhadze, Тр. Тбилисск. политехн. ин-та (Trans. Tiflis Polytechn. Inst.) **4**, 185 (1957).

[10] K. Dalitz and F. Dyson, Phys. Rev. **99**, 301 (1955).

[11] R. Signell and R. Marshak, Phys. Rev. **106**, 832 (1957).

Translated by R. Lipperheide
91

DEPOLARIZATION OF ELECTRONS DUE TO RADIATION IN A MAGNETIC FIELD

Iu. F. ORLOV and S. A. KHEIFETS

Physical Institute, Academy of Sciences, Armenian S.S.R.

Submitted to JETP editor April 10, 1958

J. Exptl. Theoret. Phys. (U.S.S.R.) **35**, 513-514 (August, 1958)

THE change in electron polarization (from initial longitudinal polarization) under rotation in a magnetic field may be utilized for the purpose of measuring the electron anomalous magnetic moment.[1] It is useful here to obtain the magnitude of depolarization due to the side effects of radiation in a magnetic field.

It is convenient, for the purpose of calculating the probability of radiation with spin flip in a uniform magnetic field H, to express the wave functions in the coordinates z, φ and $y = eHr^2/2$:[2]

$$\psi^{(k)} = D_k (2\varepsilon s!\, n!\, 2\pi v^{1/s})^{-1/2} L_s^p\, y^{p/2} \exp(-y/2 + il\varphi + ip_z z);$$
$$k = 1,\ 2,\ 3,\ 4;$$
$$p = l + 1/2 + (-1)^k/2; \quad D_1 = A\sqrt{n(\varepsilon + m)};$$
$$D_2 = iB\sqrt{\varepsilon + m},$$
$$D_3 = \sqrt{n}(\sqrt{2eHn}\,B + P_z A)/\sqrt{\varepsilon + m};$$
$$D_4 = i(\sqrt{2eHn}\,A - P_z B)/\sqrt{\varepsilon + m};$$
$$\varepsilon = \sqrt{m^2 + P_z^2 + 2eHn}.$$

Here ϵ stands for the total electron energy ($\hbar = c = 1$), $s = n - l - 1$; v is the normalization volume and $L_s^p(y)$ is the associated Laguerre polynomial as defined in reference 3. The constants A and B specify the spin state, $|A|^2 + |B|^2 = 1$.

For the intensity of the transition from n, s = 0, A = 1, 0 to $n' = n - \nu$, $s' = 0$, $A' = 0, 1$ we find ($P_z = 0$ in the initial state):

$$dI_{10}^{\nu} = \frac{1}{2\pi}\left(\frac{\beta^2\nu^2 e^2 H}{4n\varepsilon}\right)^2 \left\{\left(\frac{\varepsilon\beta\sin\theta}{\varepsilon + m} J_\nu - J_{\nu-1}\right)^2 + \cos^2\theta J_{\nu-1}^2\right\}; \quad (1)$$

$$dI_{01}^{\nu} = \frac{1}{2\pi}\left(\frac{\beta^2\nu^2 e^2 H}{4n\varepsilon}\right)^2 \left\{\left(\frac{\varepsilon\beta\sin\theta}{\varepsilon + m} J_\nu - J_{\nu+1}\right)^2 + \cos^2\theta J_{\nu+1}^2\right\}, \quad (2)$$

where $J_n = J_n(n\beta\sin\theta)$ is a Bessel function, $\beta = v/c$, and θ is the angle between the z axis and the direction of the wave vector of the emitted photon. Transitions in which the quantum number s changes do not contribute significantly to the total transition probability for the process n, A = 1, 0 → $n' = n - \nu$, $A' = 0, 1$. For $\overline{\nu}^2/n \ll 1$ [i.e., up to energies ~100 Mev since $\overline{\nu}^2/n \sim R^{-1}(\hbar/mc) \times (\epsilon/mc^2)^5$ where R is the radius of curvature], Eqs. (1) and (2) describe the intensity of emission of photons with frequency $\omega_0\nu = eH\nu/\epsilon$ in the direction θ when the electron spin is flipped. Comparison of these expressions with the classical Schott formula

$$dI^{\nu} = \frac{1}{2\pi}\left(\frac{\nu e^2 H}{\varepsilon}\right)^2 (\cot^2\theta J_\nu^2 + \beta^2 J_\nu'^2)\, do,$$

which describes the intensity of radiation without spin flip, gives

$$dI_{10}^{\nu}/do \sim (\beta\nu/n)^2\, dI^{\nu}/do \ll dI^{\nu}/do,$$

and $dI_{01}^{\nu} \sim \beta^2 dI_{10}^{\nu}$. Consequently, radiation accompanied by spin flip is of order $(\beta\nu/n)^2$ relative to the total radiation. The quantum corrections of order ν/n, calculated by Sokolov and Ternov,[2] refer to radiation without spin flip.

We conclude that electron depolarization due to radiation is exceptionally small. For an electron of energy ϵ the radiation maximum occurs in the region $\overline{\nu} \sim (\epsilon/m)^3$. Making use of the relations $eHR = \beta\epsilon$, $2ec\hbar Hn = \epsilon^2\beta^2$ we find that the emission probability with spin flip during one rotation in the magnetic field is of the order of magnitude

$$dw_{10}/dN \sim \beta^2 (e^2/\hbar c) R^{-2} (\hbar/mc)^2 (\varepsilon/mc^2)^5, \quad (3)$$

where R = radius of curvature, N = number of rotations. N must equal 10^4 to 10^5 for the magnetic moment of the electron to be measured with an accuracy sufficient to include the second correction[4] $\Delta\mu^{(2)}/\mu_0 \approx -0.3(e^2/\hbar c)^2$. Clearly, in such an experiment depolarization due to emission of photons is unimportant.

---

[1] H. Mendlowitz and K. M. Case, Phys. Rev. **97**, 33 (1955).

[2] A. A. Sokolov and I. M. Ternov, Dokl. Akad. Nauk SSSR **92**, 3 (1953).

[3] I. M. Ryzhik and I. S. Gradshtein, Таблицы интегралов, сумм, рядов и произведений (Tables of Integrals, Sums, Series and Products), Gostekhizdat, M. 1951, p. 414.

[4] R. Karplus and N. Kroll, Phys. Rev. **77**, 536 (1950).

Translated by A. Bincer
92

PRODUCTION OF TWO TEMPERATURES IN AN IONIZED GAS IN A MAGNETIC FIELD

E. LARISH and I. SHEKHTMAN

Institute for Applied Mechanics, Bucharest;
Institute for Atomic Physics, Bucharest-Magurele

Submitted to JETP editor April 12, 1958

J. Exptl. Theoret. Phys. (U.S.S.R.) **35**, 514-515 (August, 1958)

WE consider an ionized gas in which the ionic temperature is assumed given. The energy radiated by the electrons per unit time by virtue of cyclotron radiation is:

$$(dE_e/dt)_c = -\frac{E_{e\perp}}{t_c} = -(4e^4H^2/3c^5m_e^3)\,E_{e\perp}. \qquad (1)$$

Here e is the charge of the electron, H is the magnetic field, m_e is the mass of the electron and $E_{e\perp}$ is the electron energy due to motion in the transverse magnetic field. In order-of-magnitude terms, the energy radiated in a time t_c is equal to the energy of the electrons. The frequency of the cyclotron motion is $\nu \sim eH/m_e$; in what follows it will be assumed that the gas is transparent in this frequency region. This condition is rather stringent; given characteristic dimensions, we assume either a highly rarified gas or high values of the magnetic field and ionic temperature.

If the electrons radiate a significant part of their energy in a time short compared to the relaxation time t_{eq} of the electronic and ionic components of the gas, i.e., if $t_{eq} > t_c$, it can be shown that the electronic temperature will differ considerably from the ionic temperature.

The relaxation time for the electronic component is[1]

$$t_r = m_e^{1/2}(3kT_e)^{3/2}/8\cdot 0.714\,\pi n_e e^4 \ln\Lambda. \qquad (2)$$

Here T_e is the kinetic temperature of the electrons, n_e the number of electrons per unit volume and $\ln\Lambda$ is the Coulomb logarithm. It will be assumed that $t_c \gg t_r$ so that the electron gas is characterized by a Maxwellian distribution. Thus, the Spitzer formula[1] can be used in analyzing the exchange of energy between the electron gas and the ion gas:

$$\left[\frac{dE_e}{dt}\right]_i = \frac{E_i - E_e}{\alpha t_{eq}}$$
$$= (E_i - E_e)\Big[\Big(\frac{3\alpha m_e m_i k^{3/2}}{8\pi^{3/2} n_i Z^2 e^4 \ln\Lambda}\Big(\frac{T_e}{m_e} + \frac{T_i}{m_i}\Big)^{3/2}\Big]^{-1} \qquad (3)$$

Here m_i is the ion mass, Z is the charge of the ion and n_i is the number of ions per unit volume.

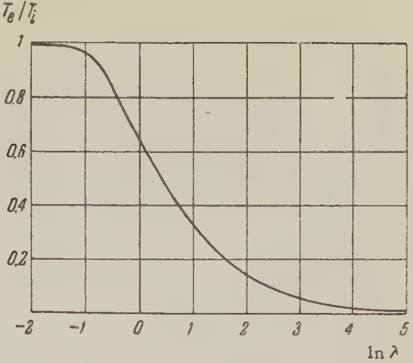

The factor α takes account of the retardation of the relaxation process because of the magnetic field, α ~ 3.

In the quasi-stationary state we can equate (1) and (3). Whence the following expression is obtained for the ratio $T_e/T_i = \theta$:

$$\lambda^2 = \frac{(1/\theta - 1)}{\theta^3(1 + m_e/m_i\theta)}, \quad \lambda = \frac{\alpha k^{2/3} m_i}{3(2\pi)^{1/2} c^5 m_e^{7/2} Z^2 \ln\Lambda}\,\frac{T_i^{2/3} H^2}{n_i} \qquad (4)$$

The condition $t_c \gg t_r$ is equivalent to the inequality $\lambda \ll 10^6$ in which case $m_e/\theta m_i \ll 1$, so that Eq. (4) can be simplified: $\lambda = \theta^{-5/2}(1-\theta)$. The function $\theta = \theta(\lambda)$ is given in the figure. At large values of λ it is apparent that $\theta = \lambda^{-2/5}$. Thus, the difference in temperatures for the ionic component and the electronic component can become very large.

---

[1] Spitzer. Physics of Fully Ionized Gases, Interscience, New York (1955).

Translated by H. Lashinsky
93

INVESTIGATION OF K_{e3}-DECAY WITH THE EMISSION OF A GAMMA PHOTON

I. M. DREMIN

Moscow Engineering-Physics Institute

Submitted to JETP editor April 17, 1958

J. Exptl. Theoret. Phys. (U.S.S.R.) **35**, 515-517 (August, 1958)

THE spectra of π mesons and electrons produced in K_{e3} decay have been investigated by a number of authors.[1-3] An important contribution to these spectra is due to the K_{e3} decay with the emission of a hard γ photon. Hence we investigate this process in this paper:

$$K^0 \rightarrow \pi^\pm + e^\pm + \nu + \gamma. \tag{1}$$

If it is assumed that the π meson, electron, and neutrino are created at one point on the Feynman diagram for the process and that the spin of K^0 meson is zero, the most general form of the interaction Lagrangian for the K_{e3} decay in the x representation is:

$$\begin{aligned} L_{e3} = \Big\{ & g'_S (\bar{\psi}_e (1 + \alpha'_S \gamma_5) \psi_\nu) \varphi^*_\pi \varphi_K \\ & + \frac{g''_S}{M^2} (\bar{\psi}_e (1 + \alpha''_S \gamma_\nu) \psi_\nu) \frac{\partial \varphi^*_\pi}{\partial x_\mu} \frac{\partial \varphi_K}{\partial x_\mu} \\ & + \frac{g'_V}{M} (\bar{\psi}_e (1 + \alpha'_V \gamma_5) \gamma_\mu \psi_\nu) \varphi^*_\pi \frac{\partial \varphi_K}{\partial x_\mu} \\ & + \frac{g'_T}{M^2} (\bar{\psi}_e (1 + \alpha'_T \gamma_5) \gamma_{\mu\rho} \psi_\nu) \frac{\partial \varphi^*_\pi}{\partial x_\mu} \frac{\partial \varphi_K}{\partial x_\rho} \Big\} \frac{1}{M}, \end{aligned} \tag{2}$$

$$\gamma_{\mu\rho} = {}^1/_2 (\gamma_\mu \gamma_\rho - \gamma_\rho \gamma_\mu); \; \gamma^+_\mu = \gamma_\mu; \; \hbar = c = 1.$$

Here ψ_e, ψ_ν, φ_π, and φ_K are the wave functions for the electron, neutrino, π meson and K meson respectively while M is the mass of the K meson. The mass of the electron is neglected in comparison with the momenta which are of importance in this decay.

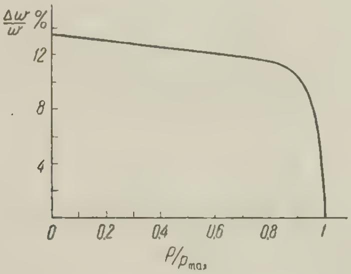

In considering the process in (1), it is necessary to replace $\partial\varphi^*_\pi/\partial x_\mu$ in (2) by $\partial_\mu \varphi^*_\pi = (\partial/\partial x_\mu - ieA_\mu)\varphi^*_\pi$. In this case we already have $\psi_e(\partial/\partial x_\mu + ieA_\mu)\gamma_\mu = 0$.

The complete matrix element for the decay (1) in the rest system of the K^0 meson is of the form (in Heaviside units):

$$\begin{aligned} M_{i\rightarrow f} = e & \frac{(2\pi)^4}{(2M)^{3/2} (E\omega)^{1/2}} \bar{\psi}_e \\ \times & \sum_{i=S,V,T} g_i (1 + \alpha_i \gamma_5) \Phi_i \psi_\nu \delta (P - p - p_e - k - k_\nu). \end{aligned} \tag{3}$$

We use the notation:

$$\Phi_S = \frac{\hat{\varepsilon} \hat{k}}{2(kp_e)} + \delta_0; \; \Phi_V = \left(\frac{\hat{\varepsilon} \hat{k}}{2(kp_e)} + \delta_0\right) \gamma_4;$$

$$\Phi_T = \frac{i}{M} \left[\left(\frac{\hat{\varepsilon} \hat{k}}{2(kp_e)} + \delta_0 \right) \gamma_4 \boldsymbol{\gamma} \mathbf{p} + \gamma_4 \left(\hat{\varepsilon} - \frac{(\varepsilon p)}{(kp)} \boldsymbol{\gamma} \mathbf{k} \right) \right];$$

$$\delta_0 = \frac{(\varepsilon p_e)}{(kp_e)} - \frac{(\varepsilon p)}{(kp)}; \; \hat{a} = \gamma_\mu a_\mu = \boldsymbol{\gamma} \mathbf{a} + \gamma_4 a_4;$$

$$(ab) = \sum_{\mu=1}^{1} a_\mu b_\mu, \; a^*_4 = - a_1.$$

P is the four-momentum of the K meson and ϵ is the polarization vector of the photon. **p**, E; $\mathbf{p}_e$, $\epsilon_0 \approx |\mathbf{p}_e|$; **k**, ω; $\mathbf{k}_\nu$, k_ν are respectively the momenta and energies of the π meson, the electron, the γ photon and the neutrino.

In the limiting case (emission of soft protons) we have:

$$M_{i\rightarrow f} = (e/\sqrt{2\omega}) \delta_0 M^{(0)}_{i\rightarrow f}, \tag{4}$$

where $M^{(0)}_{i\rightarrow f}$ is the matrix element for the K_{e3} decay. This means that in the present case the ratio $\Delta w/w$ the probability of the decay in (1) to the probability for K_{e3} decay is a quantity which is independent of the particular interaction.

If the emission of the π meson is neglected, we have for a scalar interaction:

$$\Delta w / w = (e^2 / 2 (2\pi)^2) A_S, \tag{5}$$

where

$$\begin{aligned} A_S = & \left(z \ln \frac{z+1}{z-1} - 2 \right) \left(\ln \frac{2}{\delta} + 4 \right) \\ & + 2 \left(\ln \frac{2}{\delta} - 2 \right) \left(\ln \frac{p(z+1)}{2\omega_{\min}} - \frac{1}{2} \ln \frac{z+1}{z-1} - 1 \right) \\ & - \ln^2 \frac{z+1}{z-1} + \frac{1}{2} \left(\ln \frac{2}{\delta} - z \ln \frac{z+1}{z-1} + \frac{5}{2} \right) + \frac{\pi^2}{3} + 2. \end{aligned} \tag{6}$$

Here $z = (M - E)/p \leq 1$ while $\omega_{\min}$ is the minimum frequency of the photon. In the integration over electron emission angles we take account of the electron mass, writing $1/v_e = 1 + \delta$; if this is not done, an expression which diverges logarithmically is obtained. Assuming that on the average the energy going to the electron, photon, and neutrino is distributed uniformly between these, we find $\delta = {}^9/_2 (m/pz)^2$. It is easy to show that an error in the estimate of δ cannot change these results by more than 10%. Equation (6) applies when $z - 1 \gg \delta$. Assuming $\omega_{\min} = m \approx 0.5$ Mev, we obtain the dependence of $\Delta w/w$ on π-meson energy shown in the figure.

Because of the relations in (4) and (6), the value of $\Delta w/w$ in vector or tensor interactions does not differ greatly from this value in the scalar case.

The nonconservation of parity in K_{e3} decay appears in the polarization of the electrons and protons. Using the electron spin-projection operator,[4] it is easy to show that the electrons will be longitudinally polarized and that the degree of polarization for each of the "pure" interactions is given by the expression

$$P_i = (\alpha_i + \alpha^*_i) / (1 + |\alpha_i|^2) \; (i = S, V, T). \tag{7}$$

If the two-component neutrino theory is valid, $\alpha_S = \alpha_T = 1$ and $\alpha_V = -1$, that is to say, the polarization can be incomplete only if there is a mixture of vector interaction with scalar or tensor. In this case the direction of polarization can yield information as to the predominance of one or the other of the interactions.

In the case of nonconservation of parity, the photons are circularly polarized. The dependence of the circular polarization on the frequency of the photon for a given π-meson energy and emission angle for the π meson and photon is given by:

$$P_{\gamma}^{i} = \frac{\Delta\omega_R - \Delta\omega_L}{\Delta\omega_R + \Delta\omega_L} = \frac{2x(1-x)}{1+(1-x)^2}\,\frac{\alpha_i + \alpha_i^*}{1+|\alpha_i|^2},$$
$$x = \omega/\omega_m, \quad \omega_m = p(z^2-1)/2(z+\cos\theta). \tag{8}$$

Here Δw_R and Δw_L are the differential probabilities for decay with the emission of right-polarized or left-polarized radiation respectively; ω_m is the maximum photon frequency for a given π-meson energy and angle of emission. The maximum value of the polarization $P_{\gamma m}^{i} = 0.41$, for $\alpha = 1$, is achieved with $x = 0.6$.

There is no circular polarization for charge invariance ($\alpha = -\alpha^*$) or if parity is conserved ($\alpha = 0$). It is easy to show that in these cases the radiation will consist of a superposition of unpolarized light and linearly polarized light.

In conclusion we wish to express our gratitude to Professor I. Ia. Pomeranchuk for suggesting this problem and for guiding its execution and to A. F. Grashin for a discussion of the results.

---

[1] Furuichi, Kodama, Sugahara, Wakasa and Yonezawa, Progr. Theor. Phys. **16**, 64 (1956); **17**, 89 (1957).

[2] A. Pais and S. B. Treiman, Phys. Rev. **105**, 1616 (1957).

[3] L. B. Okun', J. Exptl. Theoret. Phys. (U.S.S.R.) **33**, 525 (1957), Soviet Phys. JETP **6**, 409 (1958).

[4] L. Michel and A. S. Wightman, Phys. Rev. **93**, 354 (1954).

Translated by H. Lashinsky
94

ON THE HALL EFFECT AT THE CURIE POINT

N. S. AKULOV and A. V. CHEREMUSHKINA

Moscow Institute for Geological Prospecting

Submitted to JETP editor April 18, 1958

J. Exptl. Theoret. Phys. (U.S.S.R.) **35**, 518-519 (August, 1958)

THE magnetization of ferromagnets in the low-temperature region[1] is determined, roughly speaking, by an inversion process (the spontaneous-magnetization vector switches from one direction of easy magnetization to another) and a rotation process (the spontaneous-magnetization vector of the domain shifts away from the direction of easy magnetization). Sufficiently far above the Curie point Θ the magnetization is caused by the change in the number of parallel and antiparallel spins when short-range order is absent. We shall call such a process true magnetization, in contradistinction to paraprocesses when short-range order is present and microdomains are formed. A paraprocess causes magnetization by the rotation of microdomains.

Measurements performed by us show that for each of these four processes of magnetization there is a corresponding Hall parameter. As far as the inversion and rotation is concerned, we have obtained the following results. When investigating the Hall effect in iron-aluminum alloys we have observed that the Hall voltage depends in a nonlinear fashion on the magnetization I in the region of technical saturation. However, for an alloy with a zero value of the anisotropy constant (12% Al),[2] we obtained a strictly linear dependence, while the slopes of the straight lines are the same in the regions of inversion and rotation. For alloys with a non-vanishing anisotropy constant we have observed a bending of the curve in the transition region from inversion to rotation. Since this bending is not substantial or very pronounced, it is desirable to perform a direct measurement of the Hall effect on single crystals to bring out the role

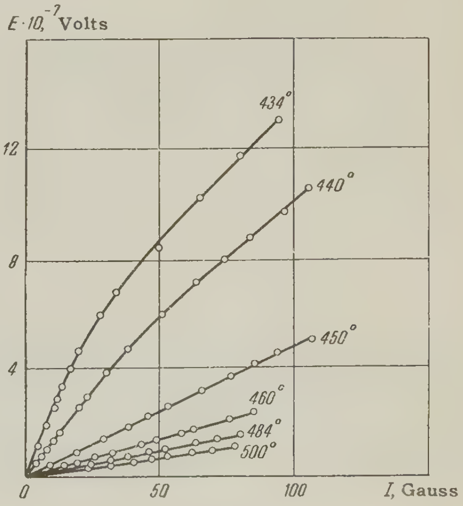

FIG. 1

played by anisotropy.

We further observed a sharp difference in the Hall parameters for the paraprocess and the true magnetization. It was established that the ferromagnetic Hall constant is practically equal to zero for true magnetization. This follows from the curves giving the dependence of the Hall emf E on the magnetization I above the Curie point (Fe-Ni, 46% Ni). As can be seen from Fig. 1, the tangent of the angle of inclination sharply decreases above the Curie point to zero (within the limits of experimental accuracy). This indicates that the spin distribution does not lead to a Hall effect, when there is no short-range order, even if $I \neq 0$ (for $H \neq 0$). When the Curie point is approached, short-range order sets in, as characterized by the formation of microdomains (complexes of electrons with a parallel spin alignment). The larger the number of such microdomains, the higher will be the value of the ferromagnetic Hall constant R. If we neglect the dependence of the Hall effect on the magnitude of the microdomains, we can thus consider such a curve R(T) above the Curie point (Fig. 2) as the characteristic probability for the formation of microdomains at different temperatures.

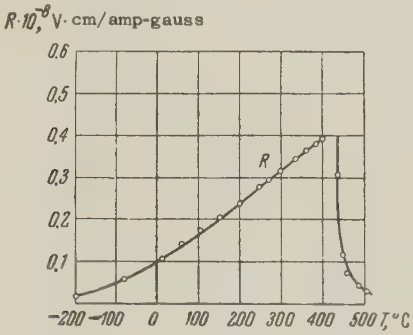

FIG. 2

Below the Curie point the microdomains agglomerate in the well-known way, forming larger complexes — the domains. The dependence of the Hall constant on the temperature becomes of the kind depicted in Fig. 2.

This dependence below the Curie point was shown by us[3,4] to be characterized by the relation

$$e = [a(\rho - \rho_0) + b(\rho - \rho_0)^2]\, I, \tag{1}$$

where e is the Hall emf per unit current density and unit distance between the Hall electrodes, ρ the specific electrical resistivity, ρ_0 the residual resistivity, while a and b are temperature-independent constants. From (1) it follows that there are two effects, one proportional to ρ, and the other to ρ^2.

A number of authors[5] have found a relation different from Goldhammer's (i.e., a linear dependence of e on I), namely,

$$e = (c - f I_s^2)\, I_s, \tag{2}$$

where c and f are constants.

An analysis performed by us showed that (2) is a consequence of the general relation (1). To see this, one must take into account (for instance, using Gerlach's equation[6]) that the ohmic resistivity is itself a function of the spontaneous magnetization, i.e.,

$$\rho = \rho_0 - \alpha T + \beta (I_0^2 - I_s^2), \tag{3}$$

where I_s and I_0 are the values of the spontaneous magnetization at the given temperature and at absolute zero, and α and β are constants. After substituting (3) into (1) we get a relation of the kind (2), because the term βI_s^4 is relatively small and the term αT can for relatively small changes in T be considered to be a constant quantity. Combining (1) to (3) we have thus

$$dR / dI_s^2 = a\, d\rho / dI_s^2 \quad \text{or} \quad f = a\beta. \tag{4}$$

This condition agrees well with experiments in the region of the Curie temperature. The relation (2), found by Komar and Volkenshtein, is thus a consequence of the general law (1) which is shown to be correct in a number of cases where (2) does not agree with experiments (e.g., for the alloy Fe_3Al).

---

[1] N. S. Akulov, Ферромагнетизм (Ferromagnetism), ONTI, 1939.

[2] J. Snoek, New Developments in Ferromagnetic Materials, New York, 1947.

[3] N. S. Akulov and A. V. Cheremushkina, Dokl. Akad. Nauk SSSR **98**, 35 (1954).

[4] N. S. Akulov and A. V. Cheremushkina, J. Exptl. Theoret. Phys. (U.S.S.R.) **31**, 152 (1956), Soviet Phys. JETP **4**, 150 (1957).

[5] A. P. Komar and N. V. Volkenshtein, Dokl. Akad. Nauk SSSR **60**, 785 (1948).

[6] W. Gerlach, Ann. Physik. **12**, 849 (1932).

Translated by D. ter Haar
95

SHOCK WAVES IN A CONDUCTING ULTRARELATIVISTIC GAS

K. P. STANIUKOVICH

Bauman Higher Technical School

Submitted to JETP editor April 19, 1958

J. Exptl. Theoret. Phys. (U.S.S.R.) 35, 520-521 (August, 1958)

WHEN a stream of conducting gas passes through the front of a normal shock wave the following quantities are conserved:[1,2]

$$\frac{1}{\theta^2}\left[p+\rho a^2+\frac{\mu H^2}{8\pi}\left(1+\frac{a^2}{c^2}\right)\right]=J; \qquad (1)$$

$$\frac{1}{\theta}\left[pV+\rho Vc^2+\frac{\mu H^2 V}{4\pi}\right]=\frac{w^*}{\theta}=w_0^*; \qquad (2)$$

$$a/V\theta=m. \qquad (3)$$

At the same time the following condition is also satisfied.

$$HV=b=\text{const}. \qquad (4)$$

Here p is the pressure, ρ the density, V the specific volume, a the velocity, $\theta=\sqrt{1-a^2/c^2}$, and H the intensity of the magnetic field ($H\perp a$).

On eliminating the quantity H from Eqs. (1) and (2) with the aid of (4), we arrive at the following equations:

$$\left[\frac{1}{\theta^2}\left(p+\rho a^2+\frac{b_0c^2}{2V^2}\right)\right]=0; \qquad (5)$$

$$\left[\frac{1}{\theta}\left(pV+\rho Vc^2+\frac{b_0c^2}{V}\right)\right]=0, \qquad (6)$$

where

$$b_0=\mu b^2/4\pi c^2.$$

For an ultrarelativistic gas we have

$$p=(k-1)\rho c^2; \quad \rho V^k=\sigma^k, \qquad (7)$$

where σ is the entropy function.

On eliminating from Eq. (6) the pressure and the specific volume we shall find that

$$\left[\frac{2\rho}{\theta^2}\left(k-1+\frac{a^2}{c^2}\right)+\frac{b_0m^2}{a^2}\right]=0;$$

$$\left[a\left(\frac{k\rho}{\theta^2}+\frac{b^0m^2}{a^2}\right)\right]=0. \qquad (8)$$

Denoting the parameters of the gas ahead of the front by the subscript 1 and behind the front of the shock wave by the subscript 2, we obtain, on the basis of (8), the following equations:

$$2\frac{\rho_1}{\theta_1^2}\left(k-1+\frac{a_1^2}{c^2}\right)+\frac{b_0m^2}{a_1^2}=2\frac{\rho_2}{\theta_2^2}\left(k-1+\frac{a_2^2}{c^2}\right)+\frac{b_0m^2}{a_2^2};$$

$$k\rho_1a_1/\theta_1^2+b_0m^2/a_1=k\rho_2a_2/\theta_2^2+b_0m^2/a_2. \qquad (9)$$

If we eliminate ρ_2 from the system (9) we obtain a cubic equation for a_2. This equation has, first, the trivial solution $a_1=a_2=c$ which has a meaning in the case of a photon gas whose equation of state is the same as for the case of the ultrarelativistic gas. As is well known, no shock wave arises in this case.

The resulting equations lead to the solution

$$\beta_2=\frac{1}{4\beta_1}\{k-1+\alpha^2+((k-1+\alpha^2)^2 \qquad (10)$$

$$+8\beta_1^2[\alpha^2-(k-1)])^{1/2}\},$$

where

$$\beta_1=\frac{a_1}{c}; \quad \beta_2=\frac{a_2}{c};$$

$$\alpha=\frac{\omega^*}{c}=\left(\frac{k-1+b_0/k\rho_1V_1^2}{1+b_0/k\rho_1V_1^2}\right)^{1/2}.$$

(Evidently the only meaningful solution is one with a plus sign in front of the square root). Analysis of this solution shows that if $\beta_1=\alpha$, then also $\beta_2=\alpha$.

Further, it is evident that the condition $\beta_2<\beta_1$ yields the result: $\beta_1>\alpha$; $\beta_2<\alpha$. For $\beta_1<\alpha$, no shock wave is formed.

If the gas pressure is negligibly small in comparison with the field pressure (there is no gas), then $\alpha=1$, and since the condition $1\geq\beta_1\geq\alpha$ must be satisfied, $\beta_1=\beta_2=1$ and, consequently, the shock wave can not be formed.

If there is no field ($H=0$; $b=0$), $\alpha=(k-1)^{1/2}$ and (10) leads to

$$\beta_1\beta_2=k-1. \qquad (11)$$

If $\beta_1=(k-1)^{1/2}$, then $\beta_2=(k-1)^{1/2}$ and there is no shock wave. As β_1 increases, the amplitude of the shock wave also increases.

In the system of reference in which the gas ahead of the wave front is at rest, and the speed of the wave front is $D=a_1$, the velocity of the gas behind the front of the shock wave will be given by

$$a_H=\frac{a_1-a_2}{1-a_1a_2/c^2}=c\,\frac{\beta_1^2-(k-1)}{\beta_1(2-k)}. \qquad (12)$$

When $\beta_1=1$, then $\beta_2=k-1$, but $a_H/c=1$.

It is evident that a shock wave is impossible when the speed of gas flow behind its front is equal to the velocity of light for particles with a rest mass different from zero, because such a speed is not attainable.

It may turn out that for a given $a_H = a_H^*$ the amplitude of the shock wave will be a maximum. In the case of a further increase in the speed a_H, a part of the energy of the particles will be converted into energy of radiation, pairs will begin to be created in the photon gas, and the amplitude of the shock wave will be reduced.

---

[1] F. Hoffman and E. Teller, Phys. Rev. **80**, 692 (1950).

[2] K. P. Staniukovich, Неустановившиеся движения сплошной среды (Unsteady Motion of Continuous Media), Gostekhizdat, 1955, Ch. 15, § 87.

Translated by G. Volkoff
96

THE ENERGY OF EXCITONS FOR VERY SMALL QUASI-MOMENTA

S. I. PEKAR

Institute of Physics, Academy of Sciences, Ukrainian S.S.R.

Submitted to JETP editor April 30, 1958

J. Exptl. Theoret. Phys. (U.S.S.R.) **35**, 522-523 (August, 1958)

LET us divide the crystal into cubic regions, let the edge of the cube L contain a large number of lattice constants, and let the exciton quasi-momentum **k** have an absolute magnitude much less than 1/L. We construct the wave function of the crystal in the form of a linear combination of antisymmetrized products of wave functions of the separate regions:

$$\Psi_{\mathbf{k}} = A \sum_{\mathbf{m} l \lambda} e^{i\mathbf{k}\cdot\mathbf{m}} (-1)^{\lambda} \prod_{\substack{\mathbf{n}=1 \\ \mathbf{n}\neq\mathbf{m}}}^{N} \psi_{\mathbf{n}}(\lambda)\, c_l \varphi_{\mathbf{m}}\ (\lambda). \tag{1}$$

Here **n** (or **m**) is a vector determining the position of the center of the cube and at the same time an index, numbering the cube. $\psi_{\mathbf{n}}$ is the (antisymmetrized) ground state of the separate cube, $\varphi_{\mathbf{m}l}$ an excited state of the cube, l numbers the degenerate excited states of the cube, and λ is the number giving the distribution of the electrons over the cube. The distribution is numbered arbitrarily but in such a way that each subsequent distribution is obtained from the previous one by the interchange of two electrons belonging to different cubes.

The exciton energy is evaluated from the wave function (1) in the same way as in the Heitler-London-Heisenberg method (see reference 1, § 2, case b). The only difference is that the Heitler-London-Heisenberg method involves the wave functions of the elementary cells of the crystal, while here we have instead the wave functions of the above-mentioned cubes. We can neglect the exchange interaction energy for electrons belonging to different cubes. The energy is then equal to

$$\mathscr{E}(\mathbf{k}) = \mathscr{E}_0 + u(\mathbf{k}), \quad u(\mathbf{k}) = \sum_{\mathbf{m}} L^{(\mathbf{m})} e^{i\mathbf{k}\mathbf{m}}, \tag{2}$$

where $\mathscr{E}_0$ is a constant that does not depend on the quasi-momentum **k**, and

$$L^{(\mathbf{m})} = \sum_{ll'} c_l^* c_{l'} \int \varphi_{0l}^*(r_0)\, \psi_{\mathbf{m}}^*(r_{\mathbf{m}})\, V_{\mathbf{m}0}(r_{\mathbf{m}} r_0)\, \varphi_{\mathbf{m}l'}(r_{\mathbf{m}})\, \psi_0(r_0)\, dr_0 dr_{\mathbf{m}}. \tag{3}$$

$V_{\mathbf{m}0}$ is the potential energy of the Coulomb interaction between charged particles belonging to cubes at the points **m** and 0; $r_{\mathbf{m}}$ and r_0 indicate the totality of the coordinates of these particles (for an arbitrary distribution λ). Since the cubes are electrically neutral, $V_{\mathbf{m}0}$ can be reduced to their dipole-dipole interaction. Let $\mathbf{P}(\mathbf{m})$ and $\mathbf{P}(0)$ be the dipole moments of the cube. We introduce the notation

$$\mathbf{P}_l = \int \varphi_{0l}^*(r_0)\, \mathbf{P}(0)\, \psi_0(r_0)\, dr_0, \quad \mathbf{P} = \sum_l c_l^* \mathbf{P}_l. \tag{4}$$

One can then easily show by expressing $V_{\mathbf{m}0}$ explicitly in terms of $\mathbf{P}(\mathbf{m})$ and $\mathbf{P}(0)$, substituting the result into (3) and using the notation (4) that the quantity $u(\mathbf{k})$ can be interpreted in the following way: u is equal to the electrostatic energy of the interaction of the dipole **P** at the origin with all dipoles $\mathbf{P}^* e^{i(\mathbf{k}\cdot\mathbf{m})}$ at the centers of all the cubes. Since $kL \ll 1$ one can replace the collection of dipoles placed at the centers of the cubes by a polarized continuum with a specific dipole moment $L^{-3}\mathbf{P}^* e^{i(\mathbf{k}\cdot\mathbf{r})}$. The latter produces, as is well-known, a fictitious dielectric polarization field which is equal to

$$\mathbf{E}'(\mathbf{r}) = -4\pi L^{-3} \mathbf{s}\, (\mathbf{P}^*, \mathbf{s})\, e^{i\mathbf{k}\mathbf{r}}, \quad \mathbf{s} = \mathbf{k}/k. \tag{5}$$

In this way u can be evaluated as the energy of the interaction between the dipole **P** and the field $\mathbf{E}'(0)$:

$$u = -\mathbf{P}\cdot\mathbf{E}'(0) = 4\pi L^{-3} |\mathbf{P}\cdot\mathbf{s}|^2 = 4\pi L^{-3} |\mathbf{P}|^2 \cos^2\alpha, \tag{6}$$

where α is the angle between **P** and **s**. We can show that the quantity (6) does not depend on L, since **P** is proportional to $L^{3/2}$. We can thus, for the sake of convenience, put $L = 1$ or put L^3 equal to the volume of the elementary crystal cell. The meaning of $\mathbf{P}_l$ is then that it is the matrix element of the dipole moment per unit volume, or, respectively, of the elementary cell. Below we shall consider only excited states for which $\mathbf{P} \neq 0$.

The coefficients of the linear combination of the degenerate functions c_l are determined from the condition that $\mathscr{E}(\mathbf{k})$ or the quantity $|(\mathbf{P}\cdot\mathbf{s})|$ is extremum under the supplementary condition $\Sigma|c_l|^2 = 1$.

If the excited state of the cube (cell) is nondegenerate, the single coefficient c is equal to 1. This occurs for all excited states of a rhombic crystal and also, for instance, for those states of a tetragonal crystal for which $\mathbf{P}_l$ is directed along the tetragonal axis. Then α is the angle between the uniquely determined direction in the crystal $\mathbf{P} = \mathbf{p}_l$ and the direction $\mathbf{s}$. Depending on the direction of $\mathbf{s}$, $\cos^2\alpha$ takes on all values from 0 to 1.

Apart from the just mentioned states there are in a tetragonal crystal still two-fold degenerate excitations of the cube for which $\mathbf{P}$ lies in the plane perpendicular to the tetragonal axis, z. There are thus two sets of extremal values c_1 and c_2 and correspondingly two exciton states for a given direction of $\mathbf{s}$:

(1) $\mathbf{P}\perp\mathbf{s}$, $u = 0$; (2) $\mathbf{P}$ coplanar with $\mathbf{s}$ and $\mathbf{z}$,

$$u = 4\pi L^{-3}|\mathbf{P}|^2\sin^2(\mathrm{s},z). \tag{7}$$

In both cases $|\mathbf{P}|$ is unique and is independent of the direction of $\mathbf{s}$.

In cubic crystals there are two kinds of exciton for any given direction of $\mathbf{s}$:

(1) $\mathbf{P}\perp\mathbf{s}$ and otherwise arbitrary in direction; $u = 0$,

$$(2)\quad \mathbf{P}\parallel \mathrm{s} \quad\text{and}\quad u = 4\pi L^{-3}|\mathbf{P}|^2. \tag{8}$$

In both cases $|\mathbf{P}|$ is unique and is independent of the direction of $\mathbf{s}$.

The dependence of $u(\mathbf{k})$ on the direction of $\mathbf{k}$ as $|\mathbf{k}|\to 0$, just proven, means that the function $\mathscr{E}(\mathbf{k})$ has a discontinuity at $\mathbf{k} = 0$. One must thus introduce the corresponding corrections in many earlier papers in which $\mathscr{E}(\mathbf{k})$ was expanded in a power series in k_x, k_y, k_z, in particular in reference 2. However, for each given direction $\mathscr{E}(\mathbf{k})$ can be considered to be an analytical function of the absolute magnitude k and can be expanded in a power series in it. In this way one obtains all basic results of reference 2, including Eqs. (39) to (44). One must only consider the parameter $\mathscr{E}(0)$ to be a constant for a given direction of $\mathbf{s}$, and generally speaking, a quantity depending on the angle between the direction of $\mathbf{s}$ and $\mathbf{P}_{0\mathbf{k}}(0)$.

The discontinuous dependence of the exciton energy on k of the above discussed type was earlier obtained for particular models for the exciton: for a Frenkel exciton in molecular crystals (naphthalene and anthracene)[3] and for a plasmon in an anisotropic medium.[4]

---

[1] S. I. Pekar, J. Exptl. Theoret. Phys. (U.S.S.R.) **18**, 525 (1948).

[2] S. I. Pekar, J. Exptl. Theoret. Phys. (U.S.S.R.) **33**, 1022 (1957), Soviet Phys. JETP **6**, 785 (1958).

[3] D. Fox and S. Yatsiv, Phys. Rev. **108**, 938 (1957).

[4] V. L. Bonch-Bruevich, **Физика металлов и металловедение** (Physics of Metals and Metal Research) **4**, 546 (1957), The Physics of Metals and Metallography, **4**, No. 3, p. 133 (1957).

Translated by D. ter Haar
97

ON THE STABILITY OF A FERMI LIQUID

I. Ia. POMERANCHUK

Submitted to JETP editor May 7, 1958

J. Exptl. Theoret. Phys. (U.S.S.R.) 35, 524-525 (August, 1958)

IN the theory of the Fermi liquid proposed by Landau[1,2] the energy of the system is a functional of the distribution of the excitations among the quantum states (in particular, among values of the momentum). When the distribution function of the excitations has only small deviations δn from the equilibrium distribution corresponding to the filling up of all states with $p < p_0$ (all the notations are the same as in reference 1), the energy functional E has the form

$$E = \sum_{\sigma}\int \varepsilon(p)\,\delta n(\mathbf{p})\,\frac{d^3p}{(2\pi\hbar)^3} + \frac{1}{2}\sum_{\sigma}\sum_{\sigma'}\iint f(\mathbf{pp}')\,\delta n(\mathbf{p})\,\delta n(\mathbf{p}')\,\frac{d^3p\,d^3p'}{(2\pi\hbar)^6} \tag{1}$$

(σ is the excitation spin).

Stability will exist for small δn if $E > 0$ for arbitrary δn. The values of p actually involved in the integrals of Eq. (1) are those close to p_0 (the temperature is zero). Therefore $\epsilon(p) = (d\epsilon/dp)_{p_0}(p - p_0) = v_0(p - p_0)$. The variations δn appearing in Eq. (1) are due to deformations of the Fermi surface, and we shall find the criterion for stability with respect to such deformations (see diagram).

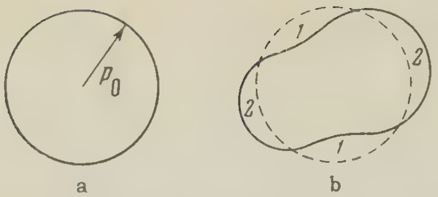

(a) unperturbed distribution (all states inside occupied). (b) perturbed distribution; in regions 1, $\delta n = -1$, in regions 2, $\delta n = 1$; inside the solid line all states are occupied.

Let us expand the momentum p corresponding to the solid line of diagram b in a series of spherical surface harmonics:

$$p = p_0 + \sum_{lm} \Phi_{lm} Y_{lm}(\theta,\varphi), \quad Y_{l0}(0) = 1. \tag{2}$$

The first term in Eq. (1) takes the following form:

$$\frac{2v_0 p_0^2}{(2\pi\hbar)^3}\int do \int\limits_0^{p-p_0} (p' - p_0)dp' = \frac{p_0^2 v_0}{(2\pi\hbar)^3} \sum_{lm} \Phi_{lm}^2 \frac{4\pi}{2l+1}\frac{(l+m)!}{(l-m)!} \tag{3}$$

The potential energy reduces to the expression

$$2p_0^4/(2\pi\hbar)^{-6}\iint [p(\theta_1,\varphi_1) - p_0][p(\theta_2,\varphi_2) - p_0]\, do_1 do_2 f(\theta_{12}), \tag{4}$$

$$\cos\theta_{12} = \cos\theta_1\cos\theta_2 + \sin\theta_1\sin\theta_2\cos(\varphi_1 - \varphi_2).$$

We now expand $f(\theta_{12})$ in a series of surface harmonics:

$$f(\theta_{12}) = \sum_l f_l P_l(\cos\theta_{12})$$

$$= \sum_l \sum_{m'}^{l} Y_{lm'}(\theta_1,\varphi_1) Y_{lm'}(\theta_2,\varphi_2) \frac{(l-m')!}{(l+m')!} f_l, \tag{5}$$

$$f_l = \frac{2l+1}{4\pi}\int f(\theta) P_l(\cos\theta)\, do.$$

Substituting Eq. (5) into (4) and combining with Eq. (3), we get the total energy functional

$$E = \frac{p_0^2 v_0}{(2\pi\hbar)^3}\sum \Phi_{lm}^2 \frac{4\pi}{2l+1}\frac{(l+m)!}{(l-m)!}$$
$$+ \frac{2p_0^4}{(2\pi\hbar)^6}\sum_{lm}\Phi_{lm}^2\left(\frac{4\pi}{2l+1}\right)^2 f_l \frac{(l+m)!}{(l-m)!}. \tag{6}$$

The conditions for stability are written separately for each l, m:

$$1 + \frac{8\pi}{2l+1}\frac{p_0^2 f_l}{v_0(2\pi\hbar)^3} > 0, \quad 1 + \frac{2p_0^2}{v_0(2\pi\hbar)^3}\int f P_l(\cos\theta)\, do > 0. \tag{7}$$

For $l = 0$ and $l = 1$ these conditions agree with the conditions (11) and (18) of reference 1, where they characterized the positiveness of the square of the speed of sound and of the effective mass.

So far we have supposed that $f(\mathbf{p}, \mathbf{p}')$ does not depend on the mutual orientation of the spins of the excitations. If we take into account this dependence, then instead of f we have the function

$$f(\mathbf{pp}') + (\sigma_1\sigma_2)\, g(\mathbf{p}_1\mathbf{p}_2). \tag{8}$$

The perturbation of the Fermi surface is now expressed by the formula

$$p = p_0 + \sum_{lm}\sigma\Phi_{lm}Y_{lm}(\theta,\varphi). \tag{9}$$

instead of Eq. (2). Since E involves the trace with respect to σ and σ', we get instead of Eq. (6):

$$E = \frac{p_0^2 v_0}{2(2\pi\hbar)^3}\sum_{lm}\Phi_{lm}^2\frac{4\pi}{2l+1}\frac{(l+m)!}{(l-m)!}$$
$$+ \frac{p_0^4}{2(2\pi\hbar)^6}\sum_{lm}\Phi_{lm}^2\left(\frac{4\pi}{2l+1}\right)^2\frac{(l+m)!}{(l-m)!} g_l, \tag{10}$$

where g_l are the expansion coefficients of the function $g(\mathbf{p}_1\mathbf{p}_2) = g(\cos\theta_{12})$ (all taken from the Fermi surface) in a series of Legendre polynomials:

$$g(\cos\theta_{12}) = \sum_l g_l P_l(\cos\theta_{12}). \tag{11}$$

The stability conditions following from Eq. (10) have the form

$$1 + \frac{p_0^2}{v_0(2\pi\hbar)^3}\int g(\cos\theta) P_l(\cos\theta)\, do > 0. \tag{12}$$

For $l = 0$ this condition means the absence of ferromagnetism and is contained in the condition $\chi > 0$ (Eq. (26) of reference 1).

In conclusion I express my gratitude to L. D. Landau for a discussion of this note.

---

[1] L. D. Landau, J. Exptl. Theoret. Phys. 30, 1058 (1956), Soviet Phys. JETP 3, 920 (1956).

[2] L. D. Landau, J. Exptl. Theoret. Phys. 32, 59 (1957), Soviet Phys. JETP 5, 101 (1957).

Translated by W. H. Furry
98

ON THE MECHANISM OF THE DAMPING OF FREE OSCILLATIONS IN A CYCLIC ACCELERATOR

Iu. F. ORLOV

Physics Institute, Academy of Sciences, U.S.S.R.

Submitted to JETP editor May 8, 1958

J. Exptl. Theoret. Phys. (U.S.S.R.) 35, 525-527 (August, 1958)

REFERENCES 1 and 2 contained a statement about the absence of damping of betatron oscillations, which is connected with the emission of radiation in an electron accelerator. We show here that, in actual fact, both the normal adiabatic damping and the damping connected with emission of radiation occur when the beam is straightened when passing through the accelerating gaps.

Let an arbitrary number of accelerating gaps be distributed along the length of the accelerator ring. When a particle passes through a section with a uniform electric field directed along the ideal unperturbed equilibrium trajectory, the components of its momentum on the transverse axes $p_z = Ec^{-2}dz/dt$ and $p_r = Ec^{-2}dr/dt$ remain constant, where E is the total energy of the particle. Therefore $\dot{z}$ and $\dot{r}$ experience a jump $\Delta\dot{z} = -e\dot{z}U/E$, $\Delta\dot{r} = -e\dot{r}U/E$, where U is the potential difference passed through by the particle, $eU/E \ll 1$. Assuming the accelerating sections to be sufficiently short, one may assume $\Delta z = \Delta r = 0$. This consideration is not essential, but it corresponds to the usual condition of acceleration in a synchroton. The action of the gap is thus described by the matrix

$$\Pi = \begin{pmatrix}1 & 0\\ 0 & 1-eU/E\end{pmatrix}, \quad z_1 = \Pi z_0, \quad z = \begin{pmatrix} z\\ dz/dt\end{pmatrix} \qquad (1)$$

with the determinant $|\Pi_{ik}| = 1 - eU/E$. Outside the accelerating gaps the transition from the point $x_1 = vt_1$ to the point $x_2 = vt_2$ is described for free oscillations by a matrix M with determinant $|M_{ik}| = 1$. If in a time Δt the particle passes n times through an accelerating gap, then

$$z(t+\Delta t) = M_n\Pi_n \ldots M_2\Pi_2M_1\Pi_1 z(t).$$

The determinant of the product of matrices is

$$|M_n\Pi_n \ldots M_1\Pi_1| = \left(1-\frac{eU_1}{E_1}\right)\left(1-\frac{eU_2}{E_2}\right)\ldots\left(1-\frac{eU_n}{E_n}\right) \approx 1-\frac{edU/dt}{E(t)}\Delta t, \quad \frac{eU_k}{E} \ll 1, \qquad (2)$$

where dU/dt is the potential difference passed through by the particle in unit time. It is well known that the determinant of the matrix of the transition from t to $t+\Delta t$ is equal to the ratio of the phase volumes. From expression (2) it is clear that the phase volume for the variables $z, \dot{z}$ or $r, \dot{r}$ is decreased for each passage through an accelerating gap. From (2) it follows that the free transverse oscillations are damped according to the relation

$$z \sim \exp\left\{-\frac{1}{2}\int_0^t \frac{edU/dt}{E(t)}dt\right\}. \qquad (3)$$

In an electron accelerator we have $e\,dU/dt = \dot{\overline{E}} + \overline{P}_\gamma$, where $\dot{\overline{E}}$ is the average energy increment of the particle, $\overline{P}_\gamma$ the average power spent in compensating for the radiation losses. In a proton accelerator $\overline{P}_\gamma = 0$ and Eq. (3) gives (taking the change of frequency into account) for the oscillation amplitude $A(t)/A(0) = (p(0)/p(t))^{1/2}$.

The clearcut considerations given here confirm the correctness of the equations for the vertical and radial oscillations for an electron accelerator obtained by Kolomenskii.[3]

The damping mechanism just described does not pertain to forced radial-phase oscillations. The mechanism of damping of synchrotron oscillations is essentially different. In particular, radiation leads directly to the damping of phase oscillations, thanks to the fact that the radiation intensity is proportional to E^2. If the particle energy is increased by an amount δE, the average radiation power is also increased by an amount $2\overline{P}_\gamma\delta E/E$ so that the phase oscillations are damped according to the rule

$$\varphi \sim \exp\left\{-\int_0^t \frac{\overline{P}_\gamma}{E}dt\right\},$$

in agreement with the equations obtained in references 3 and 4.

The presence of a connection between radial and phase oscillations which shows up on the one hand in the fact that $\overline{P}_\gamma$ is proportional to H^2, $H = H(r)$, and on the other hand in the appearance of a term $\delta p/p \sim d\varphi/dt$ in the equation for the radial oscillations, leads to a redistribution of the damping decrements while their sum remains equal to its original value.[3-5] In the usual accelerator with fixed focusing, the radial-phase connection leads to unstable radial oscillations.[3] The most convenient method to damp the radial oscillations is, apparently, the variation of the magnetic field along the orbit.[5]

The fact that the energy loss by radiation does not directly influence the velocity of damping of the free transverse oscillations (as follows, in particular, from reference 6) is connected with the fact that the radiation is directed on the average along the motion of the particle so that the particle receives at the moment of emission a transverse recoil momentum proportional to dz/dx: $c\Delta p_2 = -\epsilon dz/dx$, where ϵ is the energy of the quantum. Hence $\Delta(Edz/dx) = -\epsilon dz/dx$, $x = ct$, which gives $(\Delta dz/dx)_{\mathrm{rad}} = 0$, while at the same time we have for the passage through an accelerating gap $\Delta dz/dx = -(eU/E)dz/dx$.

---

[1] A. A. Sokolov and I. M. Ternov, Dokl. Akad. Nauk SSR 117, 967 (1957), Soviet Phys. "Doklady" 2, 573 (1957).

[2] A. N. Matveev, Nuovo cimento 6, 1296 (1957).

[3] A. A. Kolomenskii, J. Exptl. Theoret. Phys.

(U.S.S.R.) **30**, 207 (1956), Soviet Phys. JETP **3**, 132 (1956); Thesis, Phys. Inst. Acad. Sc. (U.S.S.R.) 1957.

[4] M. Sands, Phys. Rev. **97**, 470 (1955).

[5] Iu. F. Orlov and E. K. Tarasov, J. Exptl. Theoret. Phys. (U.S.S.R.) **34**, 651 (1958), Soviet Phys. JETP **7**, 449 (1958).

[6] A. A. Sokolov and I. M. Ternov, J. Exptl. Theoret. Phys. (U.S.S.R.) **28**, 431 (1955), Soviet Phys. JETP **1**, 227 (1955).

Translated by D. ter Haar
99

PHENOMENOLOGICAL EQUATIONS OF STATISTICAL DYNAMICS OF AN INCOMPRESSIBLE TURBULENT LIQUID

B. I. DAVYDOV

Institute of Earth Physics, Academy of Sciences, U.S.S.R.

Submitted to JETP editor May 16, 1958

J. Exptl. Theoret. Phys. (U.S.S.R.) **35**, 527-529 (August, 1958)

A closed system of differential equations, which describe statistically the turbulent flow of a liquid, can be obtained only by limiting the number of variables that characterize the motion of the liquid. The appropriate variables to take here are the mean velocity $U_i = \overline{u_i}$ at a given point, and the mean pressure $P = \overline{p}$, and also the (one-sided) second moments of the fluctuating velocity $R_{ij} = v_i v_j$, and the turbulent viscosity N.

The equations for U_i are obtained from the usual averaging of the equations of hydrodynamics:

$$\frac{dU_i}{dt} + \frac{\partial R_{ik}}{\partial x_k} + \frac{\partial P}{\partial x} = 0, \qquad \frac{\partial U_k}{\partial x_k} = 0. \tag{1}$$

In the averaging of the equation for $v_i v_j$, obtained from the Navier-Stokes equation, there appear third moments of the fluctuating velocity $v_i v_j v_k$, and also moments that contain derivatives with respect to the coordinates. All these moments can be expressed phenomenologically, in first approximation, in terms of the variables enumerated above and their derivatives. The requirements of dimensionality, tensor invariance, and parity must be satisfied here. If tensor combinations are chosen and known experimental data[1] are followed, then a quasi-diffusion equation is obtained for R_{ij}:

$$\begin{aligned}&\frac{dR_{ij}}{dt} - \frac{\partial}{\partial x_k}\Big[\frac{1}{3} N\Big(\delta_{ij}\frac{\partial R}{\partial x_k} + \delta_{jk}\frac{\partial R}{\partial x_i} + \delta_{ki}\frac{\partial R}{\partial x_j}\Big) \\ &\qquad - \alpha R\Big(\delta_{ij}\frac{\partial N}{\partial x_k} + \delta_{jk}\frac{\partial N}{\partial x_i} + \delta_{ki}\frac{\partial N}{\partial x_j}\Big)\Big] \qquad (2)\\ &+ \frac{\partial}{\partial x_i}\Big(\frac{1}{3} N\frac{\partial R}{\partial x_j} - \frac{5\alpha}{2} R\frac{\partial N}{\partial x_j}\Big) + \frac{\partial}{\partial x_j}\Big(\frac{1}{3} N\frac{\partial R}{\partial x_i} - \frac{5\alpha}{2} R\frac{\partial N}{\partial x_i}\Big) \\ &+ R_{ik}\frac{\partial U_j}{\partial x_k} + R_{jk}\frac{\partial U_i}{\partial x_k} + \frac{\beta}{N}\Big(R_{ik}R_{jk} - \frac{\delta_{ij}}{3}R_{kl}^2\Big) + \frac{\delta_{ij}}{3}\frac{\gamma R^2}{N} = 0\end{aligned}$$

Here $R = R_{kk}$. The physical meaning of the separate terms is as follows: the second term is connected with the transfer of turbulence energy ($v_i v_j v_k$ is contained in the square brackets); this transfer is directed, as is well known, from the walls to the middle of the flow. The maximum of R on the boundary between the turbulent boundary layer and the laminar underlayer serves as the source. The third and fourth terms take into account the transfer of energy by the fluctuating pressure; it proceeds in the opposite direction and partially cancels the second term. In summation, all these terms give:

$$-\frac{\delta_{ij}}{3}\frac{\partial}{\partial x_k}\Big(N\frac{\partial R}{\partial x_k}\Big) + \alpha\delta_{ij}\frac{\partial}{\partial x_k}\Big(R\frac{\partial N}{\partial x_k}\Big) - \frac{3\alpha}{2}\Big[\frac{\partial}{\partial x_i}\Big(R\frac{\partial N}{\partial x_j}\Big) + \frac{\partial}{\partial x_j}\Big(R\frac{\partial N}{\partial x_i}\Big)\Big].$$

Further, the increase of the turbulent energy derives from the gradient of the mean velocity; it is obtained directly from the Navier-Stokes equation. The next-to-last term of the equation describes the shift of the anisotropy of the turbulence due to the scattering of the fluctuating velocity on the fluctuating pressure; finally, the last term represents the viscous dissipation of energy in fine-grained turbulence. The dimensional universal constants α, β, and γ must be determined by experiment.

With regard to the turbulent viscosity, in first approximation, for each given flow, we must set N = const everywhere, with the exception of the boundary layer. In the turbulent boundary layer, N falls off with approach to the wall. In this case, however, there is an added condition: the divergence of the total flow of turbulent energy is practically equal to zero:

$$\frac{\partial}{\partial x_k}\Big(N\frac{\partial R}{\partial x_k}\Big) = 0. \tag{3}$$

This also gives the lacking equation for the determination of the value of N in the boundary layer.

As a condition for joining the solution of the equation for the two regions [the middle part of the flow (N = const) and the boundary layer — condition (3)] we use the requirement of continuity of all functions and their first derivatives. On the walls, then, $U_i = 0$ and $N = 0$, and also $NR_{ij} = 0$.

Equations (1) to (3) are found to be in satisfactory quantitative agreement with experiment.[1] In this case the following approximate values are obtained for the constants: $\alpha = 5$; $\beta = 0.16$; $\gamma = 0.022$.

The approximate solution for the boundary layer can be obtained in the form of an expansion in powers of R_{yy}/R (x is directed along the current and y along the normal to the wall). The first approximation gives the following dependencies:

$$\begin{gathered} R_{xy}\frac{dU_x}{dy} \sim \frac{1}{y}, \quad R^3 \sim \log\frac{l}{y}, \ N \sim y\left(\log\frac{l}{y}\right)^{2/3}, \\ R_{xy} \sim a - y, \quad R_{yy} \sim R_{xy}^2/R, \quad R_{zz} \sim R. \end{gathered} \tag{4}$$

For flow in the tube, $2l = a$, where a is the radius of the tube.

These dependencies are confirmed by experiment. In particular, the logarithmic dependence for R^3 is confirmed.

---

[1] J. Laufer, NACA Report 1174, 1954. A. A. Townsend, The Structure of Turbulent Shear Flow (Cambridge, 1956).

Translated by R. T. Beyer
100

ON THE DEVIATION OF THE EQUILIBRIUM SHAPE OF ATOMIC NUCLEI FROM AXIAL SYMMETRY

D. A. ZAIKIN

P. N. Lebedev Physics Institute, Academy of Sciences, U.S.S.R.

Submitted to JETP editor May 9, 1958

J. Exptl. Theoret. Phys. (U.S.S.R.) 35, 529-530 (August, 1958)

An analysis of the experimental data on the levels of atomic nuclei indicates that a number of nuclei do not have an axis of symmetry.[1] Therefore it appears advisable to investigate the behavior of nucleons in a potential field without axial symmetry. As an example of such a field we consider an infinitely deep potential well with vertical walls which has the shape of an ellipsoid with semi-axes a_xR_0, a_yR_0, and a_zR_0, where R_0 is the radius of a sphere of equal volume. The problem of determining the nucleon states in such a potential well is reduced to the solution of the equation

$$(2M)^{-1}(\hat{p}_x^2 + \hat{p}_y^2 + \hat{p}_z^2)\psi_i(\mathbf{r}) = E_i\psi_i(\mathbf{r}) \tag{1}$$

inside the ellipsoid with zero boundary conditions. By considering the deviations from spherical shape as being small we set

$$a_x^{-1} = 1 + \lambda, \ a_y^{-1} = 1 + \nu, \ a_z^{-1} = 1 + \varkappa,$$

where κ is related to λ and ν by the condition that the volume remains the same. By going over in (1) to the variables

$$x' = xa_x^{-1}, \quad y' = ya_y^{-1}, \quad z' = za_z^{-1}$$

and by restricting ourselves to quantities of the second order of smallness, we obtain

$$\begin{gathered} [(2M)^{-1}\hat{p}^2 + V(\mathbf{r}')]\,\psi_i(\mathbf{r}') = E_i\psi(\mathbf{r}'), \\ \psi(\mathbf{r}') = 0 \quad \text{for } r' = R_0, \\ V(\mathbf{r}') = (2M)^{-1}[(\alpha^2 + {}^1/_3\delta^2)\,\hat{p}^2 \\ + (\alpha - {}^3/_4\alpha^2 - {}^1/_{12}\delta^2)(\hat{p}^2 - 3\hat{p}_{z'}^2) + \delta(1 + {}^1/_2\alpha)(\hat{p}_{x'}^2 - \hat{p}_{y'}^2)], \\ \alpha = \lambda + \nu, \quad \delta = \lambda - \nu. \end{gathered}$$

We regard $V(\mathbf{r}')$ as a perturbation. The wave functions of the unperturbed problem (up to the normalization factor) and the corresponding eigenvalues are equal to

$$\begin{gathered} \psi_i(\mathbf{r}') \equiv \psi_{nlm}(\mathbf{r}') = r'^{-1/2} j_{l+1/2}(\mu_{nl+1/2} r'/R_0) Y_{lm}(\theta'\varphi'), \\ E_i^0 \equiv E_{nl}^0 = \hbar^2\mu_{nl+1/2}^2/2MR_0^2, \end{gathered}$$

where $\mu_{nl+\frac{1}{2}}$ is the n-th root of the Bessel function $j_{l+\frac{1}{2}}(z)$, and Y_{lm} is a spherical harmonic.

Already in the first order of perturbation theory the degeneracy with respect to m is completely removed. Calculations carried out up to second-order perturbation theory inclusive lead to quite awkward expressions for the energies, which in the case $\delta = 0$ (axial symmetry) reduce to the corresponding expressions given by Moszkowski[2] (when $\delta = 0$, his parameter d is related to the parameter α by the expression $d = \alpha + \alpha^2/4$). Qualitatively the behavior of the nucleon levels can be studied as with the s and p shells as examples. In the case of s nucleons we obtain

$$E_{n0} = E_{n0}^0\left\{1 + \left[1 - \frac{144}{5}s_2(\mu_{n^1/_2})\right]\left(\alpha^2 + \frac{1}{3}\delta^2\right)\right\}. \tag{2}$$

and the p level splits up into three:

$$\begin{gathered} (E_{n1})_1 = E_{n1}^0\left\{1 - \frac{4}{5}\alpha + \alpha^2\left[\frac{8}{5} - \frac{432}{7}s_3(\mu_{n^3/_2})\right] \right. \\ \left. + \delta^2\left[\frac{2}{5} - \frac{80}{7}s_3(\mu_{n^3/_2})\right]\right\}, \\ (E_{n1})_2 = E_{n1}^0\left\{1 + \frac{2}{5}\alpha - \frac{2}{5}\delta + \alpha^2\left[\frac{7}{10} - \frac{288}{7}s_3(\mu_{n^3/_2})\right] \right. \\ \left. + \delta^2\left[\frac{3}{10} - \frac{128}{7}s_3(\mu_{n^3/_2})\right] - \alpha\delta\left[\frac{1}{5} - \frac{96}{7}s_3(\mu_{n^3/_2})\right]\right\}, \\ (E_{n1})_3 = E_{n1}^0\left\{1 + \frac{2}{5}\alpha + \frac{2}{5}\delta + \alpha^2\left[\frac{7}{10} - \frac{288}{7}s_3(\mu_{n^3/_2})\right] \right. \\ \left. + \delta^2\left[\frac{3}{10} - \frac{128}{7}s_3(\mu_{n^3/_2})\right] + \alpha\delta\left[\frac{1}{5} - \frac{96}{7}s_3(\mu_{n^3/_2})\right]\right\}, \end{gathered}$$

$$s_{l+2}\,(\mu_{nl+{}^1/_2}) = \sum_{n'} \mu^2_{n'l+{}^5/_2} / (\mu^2_{n'l+{}^5/_2} - \mu^2_{nl+{}^1/_2})^3 = \frac{2l+7}{16\,(2l+3)^2} - \frac{\mu^2_{nl+{}^1/_2}}{8\,(2l+3)^3}. \tag{3}$$

The wave-functions corresponding to these states are given in zeroth approximation (up to the normalization factor) by

$$(\psi_{n1})_1 = \psi_{n10},\ (\psi_{n1})_2 = \psi_{n11} + \psi_{n1-1},\ (\psi_{n1})_3 = \psi_{n11} - \psi_{n1-1}.$$

From (2) and (3) it may be easily seen that for a filled shell the spherical shape is energetically the most favorable one. As the p shell is gradually filled the equilibrium shape, starting with the third nucleon, will deviate not only from the spherical one but also from the axially-symmetric one. For example, for the $(1s)^2(1p)^4$ configuration, in which the levels E_{10}, $(E_{11})_1$ and $(E_{11})_2$ are filled, the minimum total energy is at $\alpha \approx 0.015$ and $\delta \approx 0.3$.

A detailed analysis of the deviations of the equilibrium shape of actual nuclei from axial symmetry will be published later.

Similar calculations for the oscillator potential have been made by Garskii (cf. Wilets and Jean[3]) and Geilikman[4].

The author expresses his thanks to A. S. Davydov for discussing the results of this work.

---

[1] A. S. Davydov and G. V. Filippov, J. Exptl. Theoret. Phys. (U.S.S.R.) **35**, 440 (1958), Soviet Phys. JETP **8**, 303 (this issue).

[2] S. A. Moszkowski, Phys. Rev. **99**, 803 (1955).

[3] L. Wilets and M. Jean, Phys. Rev. **102**, 788 (1956).

[4] B. T. Geilikman, J. Exptl. Theoret. Phys. (U.S.S.R.) **35**, 989 (1958), Soviet Phys. JETP **8**, (in press).

Translated by G. Volkoff
101

SECOND RELAXATION IN A SPIN SYSTEM IN CERTAIN COMPOUNDS OF ELEMENTS OF THE IRON GROUP

N. S. GARIF' IANOV

Physico-Technical Institute, Kazan' Branch, Academy of Sciences, U.S.S.R.

Submitted to JETP editor May 10, 1958

J. Exptl. Theoret. Phys. (U.S.S.R.) **35**, 530-532 (August, 1958)

SPIN-SPIN absorption in parallel fields, $\chi''(H_{||})$, decreases monotonically with increase of the constant magnetic field $H_{||}$.[1-5] The experimental curves of $\chi''(H_{||})$ that have been obtained are described by the theory of Shaposhnikov.[6]

In a number of cases,[7-9] the spin-spin absorption curves of hydrated salts of elements of the iron group have a maximum in $\chi''(H_{||})$, dependent both on the frequency of the alternating field H_ν and on the intensity of $H_{||}$. Gorter and de Vrijer[7] suggested that the maximum in the spin-spin absorption curve in chromium-potassium alums at 20°K is due to relaxation between two spin systems (second relaxation in the spin system).

Conditions for production of second relaxation are created also as a result of nonuniform heating (or ventilation) of certain hydrated salts of Mn^{++} Fe^{+++}, and Cu^{++}. In such slightly hydrous salts, the ions in different elementary cells have different environments, and this leads to production of second relaxation in the spin system. Similar conditions should be present likewise in substances with residual antiferromagnetism.

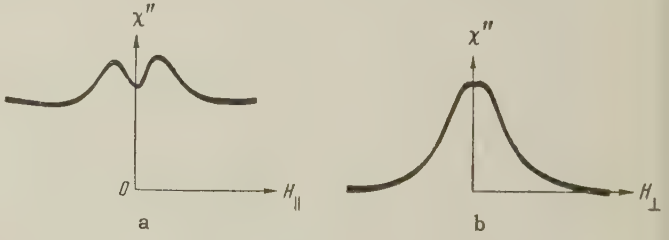

Double absorption curves χ'' (arbitrary units) in $FeNH_4(SO_4)_2 \cdot H_2O$; ν = 296 Mc/sec, T = 300°K. a – absorption in parallel fields; b – absorption in perpendicular fields.

Actually, in $Mn(COCH_3)_2$, $FeNH_4(SO_4)_2 \cdot H_2O$, $Fe_2(SO_4)_3 \cdot 3H_2O$, and $CuCl_2$, in the frequency range 600 to 150 megacycle/sec, by the method described earlier,[10] we have succeeded in obtaining curves of the absorption in parallel fields with a maximum in $\chi''(H_{||})$. In these substances the position of the maximum is independent of temperature* (in the range 300 to 90°K); on decrease of the frequency ν, it moves toward lower magnetic fields $H_{||}$ (cf. table).

In the magnetically concentrated salts listed

Substance	$\nu = 542$	$\nu = 296$	$\nu = 146$
$FeNH_4(SO_4)_2 \cdot H_2O$	450 Oe	220 Oe	Not resolved
$Fe_2(SO_4)_3 \cdot 3H_2O$	300 „	160 „	„ „
$Mn\,(CO_2CH_3)_2$	320 „	200 „	„ „
$CuCl_2$	400 „	200 „	90 Oe

above, quite narrow resonance curves of $\chi''(H_\perp)$ are observed at 542 Mcs in perpendicular fields. This indicates the presence of incomplete exchange interaction between the ions. In such substances the spin-spin absorption depends very little on the field intensity $H_{\parallel}$; therefore the absorption observed by us, at sufficiently low values of $H_{\parallel}$, is due only to second relaxation in the spin system.

In the frequency range 600 to 150 Mcs in Cr_2O_3, CuO, and Nd_2O_3,[1] we have succeeded in detecting absorption at T = 90°K and 295°K both in perpendicular and in parallel fields. In these oxides, the absorption decreases monotonically with increase of the field $H_{\parallel}$. The half-widths $\Delta H_{\parallel}$ and $\Delta H_\perp$ become narrower with decrease of frequency and with rise of temperature.

Apparently the absorption observed by us in oxides and anhydrous salts is due to relaxation between two antiferromagnetic sublattices, which are partly preserved even above the Curie temperature in these substances. At frequency 10,000 Mcs in Cr_2O_3 and CuO, no paramagnetic resonance absorption below the Curie point has been observed.[11] Furthermore, second relaxation is also observed upon partial dilution of hydrated paramagnetic salts with diamagnetic ones. No second relaxation was detected in the interval 90 to 300°K in substances with strong exchange ($CuCl_2 \cdot 2H_2O$, $Fe_2(SO_4)_3$, $Mn(SO_4)_2$, in free radicals, and in alkaline metals), in liquid solutions of paramagnetics, and in vitreous systems. Apparently, in all these substances there is a single spin system.

---

*In $CuCl_2$ at T = 90°K, there is a phase transition; consequently the absorption both in parallel and in perpendicular fields changes.

---

[1] N. S. Garif'ianov, Dissertation, Kazan' State University, 1953.

[2] N. S. Garif'ianov, J. Exptl. Theoret. Phys. (U.S.S.R.) **25**, 359 (1953).

[3] K. P. Sitnikov, Dissertation, Kazan State University, 1954.

[4] A. I. Kurushin, Izv. Akad. Nauk SSSR, Ser. Fiz., **20**, 1232 (1956) [Columbia Tech. Transl. **20**, 1122 (1956)].

[5] T. I. Volokhova, J. Exptl. Theoret. Phys. (U.S.S.R.) **31**, 889 (1956), Soviet Phys. JETP **4**, 918 (1957).

[6] I. G. Shaposhnikov, J. Exptl. Theoret. Phys. (U.S.S.R.) **18**, 533 (1948).

[7] F. W. de Vrijer and C. J. Gorter, Physica **18**, 549 (1952).

[8] Smits, Derksen, Verstelle, and Gorter, Physica **22**, 773 (1956).

[9] P. G. Tishkov, J. Exptl. Theoret. Phys. (U.S.S.R.) **32**, 620 (1957), Soviet Phys. JETP **5**, 514 (1957).

[10] N. S. Garif'ianov and B. M. Kozyrev, J. Exptl. Theoret. Phys. (U.S.S.R.) **30**, 272 (1956), Soviet Phys. JETP **3**, 255 (1956).

[11] L. R. Maxwell and T. R. McGuire, Revs. Modern Phys. **25**, 279 (1953).

Translated by W. F. Brown, Jr.
102

FISSION CROSS SECTION OF Pu^{240} *BY FAST NEUTRONS*

V. G. NESTEROV and G. N. SMIRENKIN

Submitted to JETP editor May 10, 1958

J. Exptl. Theoret. Phys. (U.S.S.R.) 35, 532-533 (August, 1958)

ALL that is known from published data on the cross section for the fission of Pu^{240} by fast neutrons is that its plateau amounts to 1.4 to 1.6 barns[1,2] and that the threshold of the (n, f) reaction is in the neutron-energy interval from 250 to 900 kev.[1]

In the present work we measured the fission cross section of Pu^{240} relative to the fission cross section of Pu^{239}, using a double ionization chamber. Layers of Pu^{240} (2.5 mg) and Pu^{239} (4 mg), 5 centimeters in diameter, were deposited on a common high-voltage electrode and were consequently located in an identical neutron flux. The collecting electrodes were hemispheres of 14 cm diameter. Electrodes of this shape, along with the use of a working gas mixture of 90% Ar + 10% CO_2 at a pressure of 35 mm Hg, made it possible to separate reliably the fission fragments from the α particles.

The Pu^{239} layer contained Pu^{240} impurities amounting to 1.80 ± 0.05%, while the concentration of Pu^{239} in the Pu^{240} specimen amounted to 7.7 ± 0.5%. The Pu^{241} content was negligibly small in the first layer and less than 0.2% in the second one. The source of fast neutrons of energy < 2 Mev was the T(p, n)He^3 reaction, those from 2 to 4 Mev were obtained from the D(d, n)He^3 reaction, and those with energies of 15 Mev from the T(d, n)He^4 reaction. The first reaction was produced in a van de Graaf generator, and the remaining two in a cascade generator. The fissions were counted in the two halves of the chamber both by fast and by thermal neutrons. Measurements with thermal neutrons are essential to determine the ratio of the effective amounts of fissionable matter in the chambers. Thermal neutrons were obtained by moderating fast neutrons in a paraffin block. The cadmium-difference method was used to exclude the influence of resonant neutrons and of fast neutrons passing through the paraffin. An experimental check disclosed practically no screening of one layer by the other.

To determine the absolute value of the Pu^{240} fission cross section, we used the energy dependence of the Pu^{239} fission cross section, obtained by averaging the data of our latest investigations. The energy dependence of the Pu^{240} fission cross section is shown in the diagram.

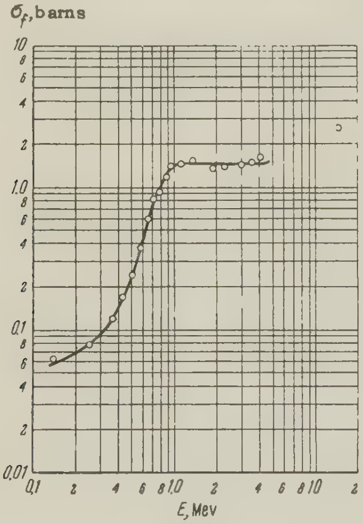

The Pu^{240} fission cross section is 1.50 ± 0.15 barns at the plateau and agrees with the results obtained by Dorofeev and Dobrynin[1] by measurements with neutrons from a Ra-Be source (1.40 ± 0.15 barns). The fission cross section obtained for 15-Mev neutrons was 2.6 ± 0.2 barns.

The authors express their deep gratitude to Prof. A. I. Leipunskii and I. I. Bondarenko for attention to this work and for valuable comments.

---

[1] G. A. Dorofeev and Iu. P. Dobrymin; Атомная энергия (Atomic Energy), No. 2, 10 (1957).

[2] Iu. S. Zamiatin, Приложение к журн. Атомная энергия (Atomic Energy Supplement) No. 1, 27 (1957).

Translated by J. G. Adashko
103

DIAMAGNETISM AND INTERATOMIC BONDS IN MOLECULES AND NON-METALLIC CRYSTALS

Ia. G. DORFMAN

Submitted to JETP editor May 15, 1958

J. Exptl. Theoret. Phys. (U.S.S.R.) 35, 533-535 (August, 1958)

THE majority of magnetic investigations of diamagnetic substances has remained up to now practically useless for a study of the nature of interatomic binding forces. The method suggested by us to treat diamagnetism[1] enables one to approach this problem anew. In the present note we intend to show some possibilities and perpectives of this method in an application to diamagnetic molecules and non-metallic crystals.

It is known that the diamagnetic susceptibility χ of molecules and non-metallic bodies, which is experimentally measured, can theoretically be written in the form[2]

$$\chi = \chi_d + \chi_p = -(Ne^2/6mc^2)\sum \overline{r_i^2} + 2N\sum |(n|\mu_z|0)|^2/(E_n - E_0). \quad (1)$$

Although the terms χ_d and χ_p are individually not invariant with respect to a transformation of the origin of coordinates, only their sum being invariant, they take on a unique physical meaning, if we take for each electron the center of gravity of the corresponding electron shell as the origin. The Langevin component χ_d depends only on the dimensions of the electron shells. The Van Vleck component χ_p, on the other hand, depends on the symmetry type of these shells and on their deformability; for atoms and spherically-symmetric shells $\chi_p = 0$. In this way χ_p can be used as a source of interesting information about the structure of the electron shells.

Since there is no method to split χ experimentally into χ_d and χ_p an estimate of χ_p can only be performed by means of comparing χ_d with χ, if there is a reliable method to determine χ_d independently for each given substance. Kirkwood[3] has given by an approximate variational method an expression for the polarizability of atoms,

$$\alpha = (4/9ka_0) \left| \sum \overline{r_i^2} \right|^2, \qquad (2)$$

which enables us, by using (1), to connect χ_d with the experimentally measured α, i.e.,

$$\chi_d = -(Ne^2 a_0^{1/2}/4mc^2)\sqrt{k\alpha}. \qquad (3)$$

In spite of the fact that expressions (2) and (3) were only derived for atoms, we see easily that this derivation can be extended to any polyatomic system built up out of more or less symmetrical electron shells, if in the summation over the different electrons we take for the coordinate origin for each electron the center of gravity of the corresponding shell and if we understand by α, χ, χ_d, and χ_p the averaged (over-all directions) values of these quantities. We have shown recently[1] that actually the relation (3) can be successfully applied both to ionic crystals and to complex organic molecules. It has been shown then that for those substances of this group for which the electronic shells can be assumed a priori to be sufficiently symmetric, i.e., for which $\chi_p \approx 0$, the values of χ_d evaluated from (3) agree with the experimentally measured χ.

If we now turn to polar crystals with ions known to be deformed such as, for instance, KCl, KBr, and KI, we see that $\chi_p \times 10^6$ is equal to +1, +5.2, +8.8, respectively.

From dispersion theory it is known that α is inversely proportional to $(E_n - E_0)$, like χ_p in (1), so that in a number of closely similar substances χ_p must change approximately parallel to α. Indeed, for KCl, KBr, and KI, α is equal to 4.33, 5.57, and 8.1×10^{-24}, respectively. In the above-mentioned paper[1] we have shown that χ_p is appreciable in atomic groups (C=O, O=N=O, C=C, C≡C, and so on) in which the interatomic binding occurs through π electrons. A further study of this problem shows that the evaluated values of χ_p for the groups N=O and O=N=O are practically coincident and agree with χ_p for the NO_3^- ion in crystals. The values of χ_p for the carbonyl group >C=O and the carbonate ion CO_3^{--} also coincide exactly. In other words at each given moment only one of the equivalent bonds is actually a multiple one in the CO_3^{--} and NO_3^- ions, and also in the O=N=O group. This can be considered to be a direct confirmation of Pauling's hypothesis[4] that the bonds C–O and N–O in the CO_3^{--} and NO_3^- ions are only ⅓ of the time in a state of a double π bond and in the nitro-group only half of the time.

	$\chi_p \cdot 10^6$	ΔE (ev)		$\chi_p \cdot 10^6$	ΔE (ev)
Si	19.35	1.12	InP	24.6	1.25
Ge	29	0.75	InAs	31.78	0.33
GaP	27.54	2.28	InSb	48	0.18
GaAs	38.14	1.35	ZnS	25.3	
GaSb	56.6	0.67			

A large value of χ_p is observed in the semiconductor crystals given in the table which is explained by the strong spreading out of the valence electron shells. Following Krumhansl and Brooks[5] one can assume that $(E_n - E_0)$ in semiconductors corresponds to the width of the forbidden band ΔE. This apparently explains the fact that in a number of similar substances an increase in χ_p goes parallel with an increase in α.

The anomalously large polarization paramagnetism is apparently characteristic also for purely molecular semiconductors, of which the aromatic compounds are typical representatives. $\chi_p \times 10^6$ is, for instance, equal to +15.4 for naphthalene, +20.8 for anthracene, +19.0 for phenantrene, and +27 for naphthacine. One can therefore assume that also metal-organic compounds belong to the group of semi-conductors since for many of them one finds a very large value of χ_p. For instance, $\chi_p \cdot 10^6$ is equal to +20 for $Hg(CH_3)_2$, +37.8 for $Hg(C_4H_9)_2$, and +43.5 for $Pb(C_2H_5)_4$.

The examples given can serve to illustrate the magnetochemical study of interatomic binding forces in very diverse diamagnetic substances.

In conclusion I express my deep gratitude to a number of friends for critical remarks and especially to A. G. Samoilovich and L. L. Korenblit for valuable advice.

---

[1] Ia. G. Dorfman, Dokl. Akad. Nauk SSSR, **119**, 305 (1958), Soviet Phys. "Doklady" (in press); J. Phys. Chem. (U.S.S.R.) (in press).

[2] J. H. Van Vleck, The Theory of Electric and Magnetic Susceptibilities, Oxford University Press, 1932.

[3] J. G. Kirkwood, Physik. Z. 33, 57 (1932).

[4] L. Pauling, The Nature of the Chemical Bond, Ithaca, 1945.

[5] J. A. Krumhansl and H. Brooks, Bull. Am. Phys. Soc. **1**, 117 (1956).

Translated by D. ter Haar
104

AVERAGE NUMBER OF NEUTRONS EMITTED IN THE FISSION OF Th^{229} *BY THERMAL NEUTRONS*

V. I. LEBEDEV and V. I. KALASHNIKOVA

Submitted to JETP editor May 10, 1958

J. Exptl. Theoret. Phys. (U.S.S.R.) **35**, 535-537 (August, 1958)

IN order to measure the mean number ν of neutrons emitted by Th^{229} fissioned by thermal neutrons, we used a thorium sample weighing 1.5 mg and containing approximately 10% of Th^{229}. The sample was a spot 20 mm in diameter and 0.5 mg/cm^2 thick on a thin platinum foil. The foil carrying the sample was placed in a flat ionization chamber on the axis of the slow neutron beam from the RFT reactor. Both the fission fragments from Th^{229} and the fast neutrons emitted by the excited fragments at the instant of fission were detected. BF_3 counters were used to detect the neutrons. Any multiplicative correction factors which should be applied to the experimental result were eliminated by making similar measurements on a sample of U^{235} and obtaining the ratio of $\nu(Th^{229})$ to $\nu(U^{235})$, the latter being known with good accuracy.[1] Details of the method are given in reference 2.

Since the cross section for the fission of Th^{229} by thermal neutrons is small (45 ± 11 barns[3]), and since we had only 150 micrograms of Th^{229} at our disposal, we used a current of 2 to 4×10^5 neutrons/cm^2 sec to obtain a noticeable effect in the ionization chamber. Since the spot had a fairly large diameter (20 mm), we used a neutron beam with a cross section of 3 cm^2. Under these conditions, the detector counted a considerable number of scattered neutrons, not arising from fission in our sample. The neutron current was so chosen, that when there were several counts per second in the ionization chamber, the background of accidental coincidences between pulses from the fission fragments and pulses from scattered neutrons did not exceed the number of true coincidences between fission fragments and fast fission neutrons. There were several tens of the latter per second (the detector efficiency was about 5%).

Since our thorium sample was extracted from a considerable amount of U^{233}, the sample was carefully cleaned by chromatographic methods to rid it of uranium traces. Special control experiments showed that the uranium contamination in the sample was no more than a few hundredths of a percent. Thus the presence of U^{233} could not have contributed to the observed effect by more than 1%, while the error in $\nu(Th^{229})$ due to the different values of $\nu(Th^{229})$ and $\nu(U^{233})$ is a few tenths of a percent.

Several series of measurements yielded the following ratio of the average number of neutrons emitted in one fission of Th^{229} induced by thermal neutrons to the same number for U^{235}:

$$\nu(Th^{229}) / \nu(U^{235}) = 0.864 \pm 0.008.$$

Taking $\nu(U^{235})$ to be 2.47 ± 0.03 (reference 1), we obtain

$$\nu(Th^{229}) = 2.13 \pm 0.03.$$

It is interesting to note that slow neutrons with an energy of 0.5 ev to several tens of electron volts have a larger effect on Th^{229} than they do on U^{235}. If the incident neutron beam is filtered through 1 mm of cadmium, the rate of fission in the chamber with Th^{229} goes down by a factor of 10, while in a chamber with U^{235} the rate goes down by a factor of 200. The fission rate with the cadmium filter is thus about 20 times bigger in Th^{229} than it is in U^{235}. Filtering the neutron beam through 2.2 g/cm^2 of boron carbide decreases the fission rate in Th^{229} by a factor of 300 to 400, while the rate in U^{235} goes down by a factor of 2000. The boron carbide filter is 5 times more effective in reducing fission rate for U^{235} than it is in Th^{229}. One can suppose that the cross section for the fission of Th^{229} by neutrons having an energy equal to several electron volts is at least no smaller than the cross section for fission by thermal neutrons. This should have no effect on the value of $\nu(Th^{229})$ quoted above, since the measurements on which this value is based were carried out with an unfiltered beam. Even if the Th^{229} were to have some resonances in the cross section for fission by neutrons of a few electron volts, the value of ν near the resonances should not differ markedly from its value for thermal neutrons, as shown by several authors.[4-6]

In conclusion, the authors consider it their pleasant duty to thank G. N. Iakovlev and S. V. Pirozhkov for preparing the clean thorium samples.

---

[1] D. J. Hughes and R. B. Schwartz, Neutron Cross Sections, BNL-325, Suppl. 1, 1957.

[2] Kalashnikova, Zakharova, Krasnushkin, Lebedev, and Pevzner, Сессия АН СССР по мирному использованию атомной энергии (Academy of Sciences U.S.S.R. Session on the Peaceful Uses of Atomic Energy), July 1-5, 1955, (Section on physics and mathematics), Acad. Sci. Press, 1955, page 161. (Translation in Atomic

Energy Commission document AEC-tr-2435).

[3] D. J. Hughes and J. A. Harvey, Neutron Cross Sections, BNL-325, 1955.

[4] Leonard, Seppi, and Friesen, Bull. Am. Phys. Soc. 1, 8 (1956).

[5] Anclair, Landon, and Jacob, Compt. rend. **241**, 1935 (1955).

[6] Kalashnikova, Lebedev, Mikaelian, and Pevzner, Атомная энергия (Atomic Energy) **3**, 11 (1956).

Translated by R. Krotkov
105

NUCLEAR ORIENTATION IN RADIATIVE K CAPTURE

V. B. BERESTETSKII

Submitted to JETP editor May 19, 1958

J. Exptl. Theoret. Phys. (U.S.S.R.) **35**, 537-538 (August, 1958)

As is well known, the nucleus becomes oriented as a consequence of parity nonconservation in beta decay. For the case of an allowed beta-transition of a nonoriented nucleus, the average value $\langle \mathbf{J} \rangle$ of the angular momentum of the daughter nucleus is given by

$$\langle \mathbf{J} \rangle = {}^{1}\!/_{3}\,(j+1)\,\zeta \mathbf{v}, \tag{1}$$

where j is the angular momentum of the daughter nucleus, $c\mathbf{v}$ is the velocity of the β electron (the neutrino direction is not observed), and ζ is the coefficient in the formula

$$w = 1 + \zeta \mathbf{v} \cdot \langle \mathbf{J} \rangle / j,$$

which describes the electron angular distribution for decays of oriented nuclei.[1-3] This orientation is responsible for effects in the electromagnetic transitions of the daughter nucleus such as the circular polarization of photons,[3] and the polarization of conversion electrons.[4]

An analogous orientation of the nucleus also takes place in radiative orbital electron capture $e + p \rightarrow n + \nu + \gamma$ (see reference 5). The nuclear orientation is given in this case by Eq. (1), in which $c\mathbf{v}$ is the photon velocity and ζ is the coefficient that appears in positron emission.

To prove this premise, let us consider the matrix element $V_{m_1 m}$ for radiative K capture with the nucleus going from the state $j_1 m_1$ into jm. Accurate to within an overall multiplicative factor, we have

$$V_{m_1 m} = (jm \,|\, O_i \,|\, j_1 m_1)\,(\bar{u}_\nu(q)\, O_i\, (\hat{p} - \hat{k} + im)\, \hat{e} u_e(p)),$$

where $(jm \,|\, O_i \,|\, j_1 m_1)$ is the nuclear matrix element, $u_\nu(q)$ is the amplitude of a neutrino with four-momentum q, $u_e(p)$ is the electron amplitude, e is the polarization vector of the photon, and k is its four-momentum. The polarization density matrix of the daughter nucleus is of the following form (accurate up to an overall multiplicative factor):

$$\rho_{mm'} = \sum_{m_1} (jm \,|\, O_i \,|\, j_1 m_1)\,(jm' \,|\, O_j \,|\, j_1 m_1)^*\, \mathrm{Sp}\, Q, \tag{2}$$

$$\mathrm{Sp}\, Q = \mathrm{Sp}\, \{(\hat{p} + im)\, \hat{e}\, (\hat{p} - \hat{k} + im)\, O_j \hat{q} O_i\, (\hat{p} - \hat{k} + im)\, \hat{e}\},$$

where $\bar{O}_j = \gamma_4 O_j^{+} \gamma_4$. Since for K capture $\hat{p} = \gamma_4 p_4$, hence

$$\mathrm{Sp}\, Q = \mathrm{Sp}\, \hat{k} \bar{O}_j \hat{q} O_i. \tag{3}$$

In the case of positron emission $\rho_{mm'}$ is also of the form (2) and

$$\mathrm{Sp}\, Q = (\hat{p}_+ + im) \bar{O}_j \hat{q} O_i, \tag{4}$$

where p_+ is the positron four-momentum. For an extremely relativistic positron ($m = 0$, $p_+^2 = k^2 = 0$) Eq. (4) goes over into (3), thus proving Eq. (1) with $\mathbf{v}$ equal to the photon velocity. (We have here the same relationship as in the formulas for photon polarization.[6])

At first sight it may seem peculiar that the pseudovector $\langle \mathbf{J} \rangle$ is proportional to the vector representing the photon momentum since photon emission proceeds through a parity conserving mechanism. In actuality, the nucleus becomes polarized because the virtual electron can be absorbed by the nucleus only in a state with a definite polarization, namely in the direction of its momentum, which in turn is opposite to the direction of the momentum of the emitted photon.

I express gratitude to A. I. Alikhanov, V. A. Liubimov, and L. B. Okun' for discussions.

---

[1] T. D. Lee and C. N. Yang, Phys. Rev. **104**, 254 (1956).

[2] Berestetskii, Ioffe, Rudik, and Ter-Martirosian, Nucl. Phys. **5**, 464 (1958); Phys. Rev. **111**, 522 (1958). B. T. Feld, Phys. Rev. **107**, 797 (1957). I. M. Shmushkevitch, J. Exptl. Theoret. Phys. (U.S.S.R.) **33**, 1477 (1957), Soviet Phys. JETP **6**, 1139 (1958).

[3] Alder, Stech and Winther, Phys. Rev. **107**, 728 (1957).

[4] V. B. Berestetskii and A. P. Rudik, J. Exptl. Theoret. Phys. (U.S.S.R.) (in press).

[5] Koh, Miyatake, and Watanabe, Progr. Theor. Phys. **18**, 663 (1957).

[6] R. E. Cutkosky, Phys. Rev. **107**, 330 (1957).

Translated by A. Bincer
106

RECOIL RANGE OF Na^{24} *AND THE MECHANISM OF* Al^{27} *(p, 3pn),* Si^{28} *(p, 4pn) AND* P^{31} *(p, 5p3n) FOR 660-Mev PROTONS*

L. V. VOLKOVA and F. P. DENISOV

P. N. Lebedev Physics Institute, Academy of Sciences, U.S.S.R.

Submitted to JETP editor May 21, 1958

J. Exptl. Theoret. Phys. (U.S.S.R.) **35**, 538-539 (August, 1958)

ACCORDING to the Serber model of high-energy nuclear reactions, which has been widely discussed in the literature, the products of deep nuclear disintegration result from two successive processes, a nucleonic cascade and evaporation.[1,2] As a test of this model we have measured the recoil range of Na^{24} nuclei produced when Al, Si and P were bombarded with 660-Mev protons. This experiment was performed in the external proton beam of the synchrocyclotron of the Joint Nuclear Research Institute. The experimental method and the treatment of the data have been described in detail in reference 3.

The table contains the mean ranges of Na^{24} in terms of the effective specimen thickness t (reference 3). The range-energy relation for Na^{24} must be known for an interpretation of the results.

Effective thicknesses for recoil Na^{24} emitted from specimens placed parallel to the proton beam (t_p), and from specimens placed perpendicular to the beam, forward (t_f) and backward (t_b)

Reaction	t_f ($\mu g/cm^2$), experimental	t_b ($\mu g/cm^2$), experimental	t_p ($\mu g/cm^2$)	
			Experimental	Serber model
Al^{27} (p, 3pn)	180 ± 2	46 ± 1	112 ± 2	170 ± 30
Si^{28} (p, 4pn)	158 ± 3	25 ± 2	63 ± 2	200 ± 40
P^{31} (p, 5p3n)	134 ± 2	29 ± 1	127 ± 4	200 ± 40

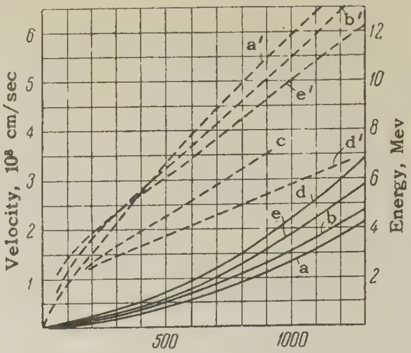

Experimental range-energy relations (solid lines) and range-velocity relations (dashed lines) for the following ions: a and a′ – F_9^{19} (reference 4), b and b′ – Ne_{10}^{20} (reference 5), c – Ar_{20}^{40} (reference 6), d and d′ – light fission fragments (reference 7), and the corresponding interpolated relations e and e′ for Na_{11}^{24}. The information in the review article by Allison and Warshaw[10] was used to relate the experimental ranges in the various substances to the range in Al.

In the present work the range-velocity relation for Na^{24} was obtained by comparing the experimental range-velocity relations for a large number of ions, from light nuclei to fission fragments.[4-7] The figure shows the experimental range-velocity and range-energy curves in Al for several nuclides and the corresponding interpolated curves for Na^{24}. The table gives the experimental thicknesses t and the effective thicknesses for recoil nuclides ejected from a sample positioned parallel to the proton beam (t_p); these were calculated by means of the Serber model, using the range-energy relation for Na^{24} (which is shown in the figure) and the results obtained by Turkevich et al.[8] in a detailed calculation of the nucleonic cascade. It can be seen that the calculated values of t_p are considerably larger than the experimental values. This discrepancy can be removed by assuming that the incident high-energy proton beam interacts with a group of nucleons in the nucleus whose momenta are correlated so that the combined momenta of all these nucleons does not exceed 5 $Mev^{1/2}$ for reactions in Al, 3.2 $Mev^{1/2}$ for reactions in Si and 5.5 $Mev^{1/2}$ for reactions in P (the momenta being expressed in terms of the unit $\sqrt{ME_k/m}$, where E_k is the kinetic energy of the particle in Mev, M is its mass and m is the nucleon mass).

It is still not clear whether the incident nucleon interacts with each nucleon of the group separately or essentially with the group as a whole. An answer to this question would be of considerable interest in connection with interactions between high-energy nucleons and nuclear fragments which are being discussed in the literature.[9]

In conclusion the authors wish to thank Professor P. A. Cerenkov for his interest, Professor V. P. Dzhelepov for placing the synchrocyclotron of the Joint Nuclear Research Institute at our disposal, and G. A. Leksin for valuable discussions.

---

[1] P. Serber, Phys. Rev. 72, 1114 (1947).

[2] Bernardini, Booth, and Lindenbaum, Phys. Rev. 85, 826 (1952).

[3] F. P. Denisov and P. A. Cerenkov, J. Exptl. Theoret. Phys. (U.S.S.R.) **35**, 544 (1958), Soviet

Phys. JETP 8, 376 (this issue).

[4] N. Feather, Proc. Roy. Soc. (London) **A141**, 194 (1933).

[5] J. T. McCarty, Phys. Rev. **53**, 30 (1938); W. W. Eaton, Phys. Rev. **48**, 921 (1935).

[6] P. Blackett and D. Lees, Proc. Roy. Soc. (London) **A134**, 658 (1932).

[7] Bohr, Boeggild, Brostroem, and Lauritsen, Phys. Rev. **58**, 839 (1940).

[8] Turkevich, Miller, Friedlander, et al., Preprint, 1957.

[9] O. V. Lozhkin and N. A. Perfilov, J. Exptl. Theoret. Phys. (U.S.S.R.) **31**, 913 (1956), Soviet Phys. JETP **4**, 790 (1957).

[10] S. K. Allison and S. D. Warshaw, Revs. Modern Phys. **25**, 779 (1953).

Translated by I. Emin
107

ABSORPTION OF SLOW π^- MESONS BY NUCLEI

A. T. VARFOLOMEEV

P. N. Lebedev Physics Institute, Academy of Sciences, U.S.S.R.

Submitted to JETP editor May 21, 1958

J. Exptl. Theoret. Phys. (U.S.S.R.) **35**, 540-541 (August, 1958)

EXPERIMENTS on nuclear disintegrations induced by slow π^- mesons[1-6] so far do not permit drawing final conclusions with respect to the primary distribution of the rest energy of the π^- meson. In particular, the assumption that the meson rest energy is distributed primarily among a small group (2 to 4) of nucleons cannot be regarded as experimentally proven.

We have tried to explain the possible influence of collective interactions between nucleons in the nucleus on the above process. We have investigated nuclear disintegrations induced by the absorption of slow π^- mesons by light emulsion nuclei. The data are being reduced and the results will be published in a forthcoming article.

At present we shall limit ourselves to one specific example of a disintegration in which collective interactions are displayed especially prominently. The reaction in question is of the type

$$A+\pi^-\rightarrow B+n, \tag{1}$$

in which the absorption of a slow π^- meson by the nucleus A is accompanied by the production of a fast neutron and a residual nucleus in ground state (or a slightly excited state, leading to the release of a low-energy gamma ray). The attempt of finding a reaction of the above type was undertaken after a detailed study of disintegrations of a wider class. It was found that the absorption of a slow π^- meson by a nucleus leads often to a reaction of the type

$$A+\pi^-\rightarrow B^*+n, \tag{2}$$

in which the momentum of a fast (~80 to 100 Mev) neutron is compensated by an excited residual nucleus which disintegrates emitting several secondary particles. Reaction (1) can be evidently considered as a particular case of a more general reaction (2). After finding a considerable contribution due to disintegrations corresponding to reactions (2) we tried, therefore, to find also disintegrations corresponding to reactions (1). Unfortunately, identification of disintegrations corresponding to reactions (1) is in general difficult. However, in the special case of π^--meson capture by the Be_4^9 nucleus, the reaction

$$\begin{array}{l} Be^9+\pi^-\rightarrow Li^8+n_0^1 \\ \qquad\qquad\quad {\scriptstyle\beta^-}\searrow \\ \qquad\qquad\qquad Be^{8*}\rightarrow 2\alpha \end{array} \tag{3}$$

can be easily detected in emulsion by means of characteristic "lithium hammers." Twelve stars corresponding to reaction (3) were found in nuclear emulsions NIKFI type 1a and NIKFI type K loaded with BeF_2 and irradiated by slow π^- mesons in the meson beam from the synchrocyclotron of the Joint Institute of Nuclear Research. A typical example of such a star is shown in the figure. The range of Li^8 fragments was found to be equal to 34 μ in all cases, with a spread of ± 1 μ. The mean value of the Li^8 fragment energy amounts to 14.4 ± 0.3 Mev.* The corresponding neutron energy, calculated from momentum conservation law, is 108 ± 2 Mev (accounting for relativistic correc-

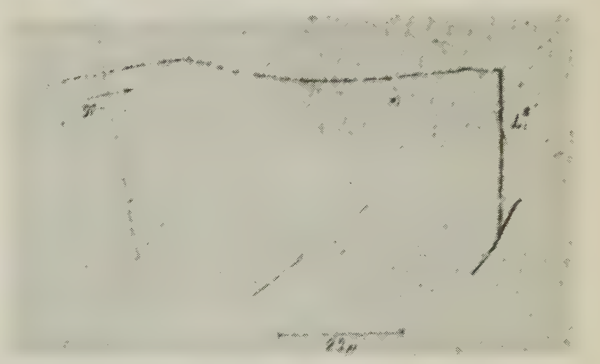

Microphotograph of a star corresponding to the reaction $Be^9+\pi^-\rightarrow Li^8+n_0^1$.

tions). For the total energy free in the reaction (accounting the loss of 18.2 Mev for the binding energy) we have, therefore, the value 140.6 Mev, which corresponds very well to the π^--meson rest energy (139.6 Mev). Consequently, in our case, Li^8 fragments are produced either in ground state or with an excitation energy less than 2 Mev. This follows also from the fact that, for excitation energies larger than ~2 Mev, Li^8 should disintegrate emitting a neutron. The yield of reaction (3), estimated under the assumption that the probability of π^- meson capture by any emulsion nucleus is proportional to the number of nuclei of a given type,[7] amounts to ~0.2% of the total number of captures by beryllium.

The character of the observed disintegrations is clearly in disagreement with the assumption that the rest energy of the π^- meson is distributed, in the primary act, among a group consisting of a small number of nucleons. If such a group consisted even of 4 nucleons, the excitation energy of Li^8 should have amounted to not less than ~30 Mev. Consequently, the fast neutron obtains its energy as the result of an interaction in which take part all nucleons of the residual Li^8 nucleus.

The existence of disintegrations corresponding to reaction (3) indicates that collective interactions of nucleons in the nucleus can play an important role in the process of slow π^--meson absorption. A study of a wider class of stars confirms this conclusion.

The author thanks the supervisor of the work, Prof. V. I. Veksler, for constant interest and valuable discussion, to V. G. Larionova for help in planning the experiments, as well as to S. M. Kornechenko and V. J. Zinov for help in work with the meson beam.

---

*Energy of the Li^8 fragments was determined from an experimental range-energy relation obtained by V. N. Maikov in a study of photonuclear reactions, Приборы и техника эксперимента (Instrum. & Instrum. Engg.) (in press).

---

[1] D. H. Perkins, Phil. Mag. **40**, 601 (1949).

[2] Menon, Muirhead, and Rochat, Phil. Mag. **41**, 583 (1950).

[3] W. B. Cheston and L. J. B. Goldfarb, Phys. Rev. **78**, 683 (1950).

[4] F. L. Adelman, Phys. Rev. **85**, 249 (1952).

[5] G. Vanderhaeghe and M. Demeur, Nuovo cimento Suppl. **4**, 931 (1956).

[6] P. Ammiraju and L. M. Lederman, Nuovo cimento **4**, 283 (1956).

[7] Sens, Swanson, Telegdi, and Yovanovitch, Nuovo cimento **7**, 536 (1958).

Translated by H. Kasha
108

ENERGY DEPENDENCE OF THE ASYMMETRY COEFFICIENT IN $\pi^+ \rightarrow \mu^+ \rightarrow e^+$ DECAYS FOR THE LOW ENERGY PART OF THE POSITRON SPECTRUM

V. V. BARMIN, V. P. KANAVETS, B. V. MOROZOV and I. I. PERSHIN

Submitted to JETP editor May 21, 1958

J. Exptl. Theoret. Phys. (U.S.S.R.) **35**, 542-544 (August, 1958)

WE have found earlier[1] that the asymmetry coefficient a in $\pi^+ \rightarrow \mu^+ \rightarrow e^+$ decays, taken over the whole positron spectrum in propane filling a bubble chamber, is -0.19 ± 0.03.

Recently we studied the asymmetry coefficient a′ for various parts of the positron energy spectrum. Positron energies were measured by multiple scattering.

The distribution function for positron decays, according to the four-component theory taking account of nonconservation of parity, has the form[2]

$$dN(\varepsilon, \theta) = A\left\{3(1-\varepsilon) + 2\rho\left(\frac{4}{3}\varepsilon - 1\right) - \xi\cos\theta\left[(1-\varepsilon) + 2\delta\left(\frac{4}{3}\varepsilon - 1\right)\right]\right\}\varepsilon^2\, d\varepsilon\, d\Omega,$$

where $\epsilon = E/E_{max}$ is the positron energy as a fraction of the maximum energy; ρ, ξ and δ are parameters of the theory which depend on the coupling constant. In the two-component theory $\rho = 0.75$; $-1 < \xi < +1$; $\delta = 0.75$.[3]

The existing experimental data mainly concern the determination of the constant ρ: $\rho = 0.68 \pm 0.02$;[4] $\xi = 0.8 \pm 0.15$.[5] Data on the determination of the parameter δ are few up to the present.[6]

The difference in the values of the quantity a'_{II}, calculated from the two-component theory (i.e., where $\delta = 0.75$) and the quantity a'_{IV}, calculated from the four-component theory (where $\delta > 0.75$) relative to the value a'_{II} (i.e., the quantity $|a'_{II} - a'_{IV}|/a'_{II}$) is much smaller in the high-energy part of the spectrum than in the low-energy part.

Energy interval in units $\varepsilon = E/E_{max}$	Number of positrons	Experimental value* $a'_{0-\varepsilon}$ calculated according to		Expected value of $a'_{0-\varepsilon}$ from the two-component theory according to data for the "corrected" spectra with $a = -0.19$.
		"Forward-backward" ratio	Mean cosine	
0—0.2	62	+0.35±0.27	+0.34±0.25	+0.095
0—0.3	183	+0.29±0.16	+0.25±0.15	+0.08
0—0.4	312	+0.18±0.12	+0.14±0.11	+0.065

*$a'_{0-\varepsilon}$ is the asymmetry coefficient for positions in the interval of energy from 0 to ε.

Because of this, and also because of the dependence of the parameter δ on the interference terms, experiments studying the quantity* $a'_{1.e.}$ afford especially sensitive tests of various variants of the theories of $\mu \rightarrow e$ decays.

Experimental data on the determination of the quantity $a'_{1.e.}$ are given in a few experimental works (see references 7 and 8).

In order to determine the quantity $a'_{1.e.}$, we used the low-energy positron tracks from 10,000 $\pi^+ \rightarrow \mu^+ \rightarrow e^+$ decays considered in reference 1.

In measuring positron energies by multiple scattering, the measurements are not affected by positron annihilation in flight (which might make the determination of $a'_{1.e.}$ incorrect because of a misleading relative transfer of part of the positrons from the region of high energies into the region of low ones). Effects from fluctuations in the energy loss by bremsstrahlung are unimportant in this method. The influence of the mean square error, which is less than 30%, in measuring energies by second differences, affects the quantity $a'_{1.e.}$ significantly less than radiative corrections[2] for bremsstrahlung.

Values of the asymmetry coefficient $a'_{1.e.}$ are given in the table for energy intervals $0 - 0.2\,\epsilon$; $0 - 0.3\,\epsilon$; $0 - 0.4\,\epsilon$.

In the measurements we used positron tracks tentatively chosen by visual estimate of their energies from multiple-scattering measurements. For the positron tracks found by energy measurements to be outside of the interval from 0 to 20 Mev, the coefficient $a'_{0-\epsilon}$ was observed to decrease with increasing energy. For $\epsilon = 0.7\,E/E_{max}$ the quantity $a'_{0-\epsilon}$ was approximately zero.

The angular distribution for the positrons included in the table fits well $1 + a \cos \varphi$ law (see figure).

The error in the values of $a'_{1.e.}$ was determined from the 'forward-backward' ratio according to the formula $2.2/\sqrt{N}$, or the mean cosine according to the formula $1.98/\sqrt{N}$.

The expected value of $a'_{1.e.}$ in the two-component theory was calculated from the theoretical spectrum, 'corrected' for the effects of errors in the measured energies,[9] radiative corrections,[2] and effects of bremsstrahlung.

The measured values $a'_{1.e.}$ in the energy region up to 20 Mev indicate that the sign of the coefficient $a'_{1.e.}$ is positive. From our data the probability of a negative sign for $a'_{1.e.}$ in the energy interval from 0 to 15 Mev is less than 5%.

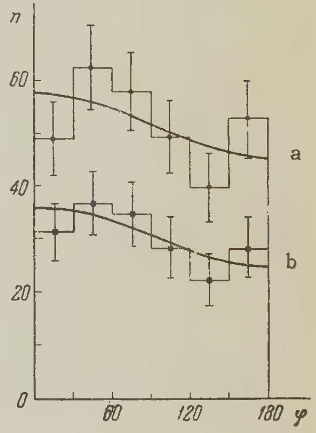

a – positrons of energy up to 0.4 ε. b – positrons of energy up to 0.3 ε.

Vaisenberg et al.[10] have found from measurements in photoemulsions that $a'_{0-0.3\epsilon}$ is equal to 0.14 ± 0.10 (according to the two-component theory the value of $a'_{0-0.3\epsilon}$ for this case is equal to 0.04). From our experiments, using the same method for calculating $a'_{1.e.}$, its value for the energy 0 to $0.3\,\epsilon$ interval is equal to 0.25 ± 0.15 (according to the two-component theory $a'_{0-0.3} = 0.08$). These experimental data, viewed as a whole, do not contradict the two-component theory, but agree better with the four-component theory if $\rho \approx 0.68$ and $\delta > 0.8$ are used.

To obtain a reliable experimental value for $a'_{0-\epsilon}$, it would be necessary to increase the statistical accuracy of the result.

We should like to express our gratitude to Acad. A. I. Alikhanov for suggesting this subject and for discussion of results, to A. O. Vaisenberg for discussion of a series of problems, to Prof. V. P. Dzhelepov for making it possible to use the π^+-meson beam from the synchrocyclotron of the

Joint Institute for Nuclear Research, and to A. P. Birzgal for carrying out the calculations.

---

*$a'_{l.e.}$ is the asymmetry coefficient for the low-energy part of the decay positron spectrum.

---

[1] Barmin, Kanavets, Morozov and Pershin, J. Exptl. Theoret. Phys. (U.S.S.R.) **34**, 830 (1958), Soviet Phys. JETP **7**, 573 (1958).

[2] T. Kinoshita and A. Sirlin, Phys. Rev. **107**, 593 (1957).

[3] T. D. Lee and C. N. Yang, Phys. Rev. **105**, 1671 (1957); L. D. Landau, J. Exptl. Theoret. Phys. (U.S.S.R.) **32**, 407 (1957); Soviet Phys. JETP **5**, 337 (1957).

[4] K. M. Crowe, Bull. Amer. Phys. Soc., Ser. II, **2**, 206 (1957).

[5] M. F. Kaplon, Proc. Rochester Conference, 1957.

[6] Berley, Coffin, Garwin, Lederman, and Weinrich, Phys. Rev. **106**, 835 (1957).

[7] Pless et al., Phys. Rev. **108**, 159 (1957).

[8] A. O. Vaisenberg and V. A. Smirnitskii, J. Exptl. Theoret. Phys. (U.S.S.R.) **32**, 1340 (1957); Soviet Phys. JETP **5**, 1093 (1957); J. Exptl. Theoret. Phys. (U.S.S.R.) **33**, 621 (1957); Soviet Phys. JETP **6**, 477 (1958).

[9] Bonetti, Levi-Setti, Panetti, Rossi and Tomasini, Nuovo cimento **3**, 33 (1956).

[10] Vaisenberg, Smirnitskii, Kolganova, Minervina, Pesotskaia, and Rabin, J. Exptl. Theoret. Phys. (U.S.S.R.) **35**, 645 (1958).

Translated by G. E. Brown
109

RANGES OF Na^{24} *RECOIL NUCLEI AND THE MECHANISM OF CERTAIN PHOTONUCLEAR REACTIONS*

F. P. DENISOV and P. A. CERENKOV

P. N. Lebedev Physics Institute, Academy of Sciences, U.S.S.R.

Submitted to JETP editor May 21, 1958

J. Exptl. Theoret. Phys. (U.S.S.R.) **35**, 544-546 (August, 1958)

PHOTONUCLEAR reactions at high photon energies (~100 to 200 Mev) are usually described by means of the so called "quasi-deuteron" model, according to which the reaction is represented in the form of three successive processes: (1) absorption of a gamma quantum by a pair of nucleons of the nucleus,[1] (2) intranuclear nucleon cascade produced by these nucleons,[2] and (3) evaporation of particles from the excited nucleus that is formed after the cascade.[3]

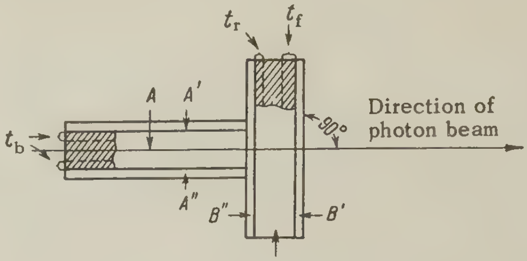

FIG. 1. Irradiation geometry. A and B – specimens; A', A'', B', and B'' – films to gather the recoil nuclei from the specimens; t_b – effective thickness for recoil nuclei from specimen A; t_f and t_r – effective thicknesses for recoil nuclei emerging from specimen B in the forward and reverse directions relative to the γ-quanta beam.

One of the most direct methods of verifying this model is to measure the ranges of the recoil nuclei.[4] In our experiments, we measured a quantity proportional to the range, namely the effective thickness t of the specimen for Na^{24} recoil nuclei produced by photonuclear reactions from aluminum, silicon, phosphorus, and sulphur. The value of t was determined from the expression $t = N/a_0$, where N is the number of recoil nuclei per square centimeter of a specimen whose thickness is greater than the maximum range of the recoil nuclei, while

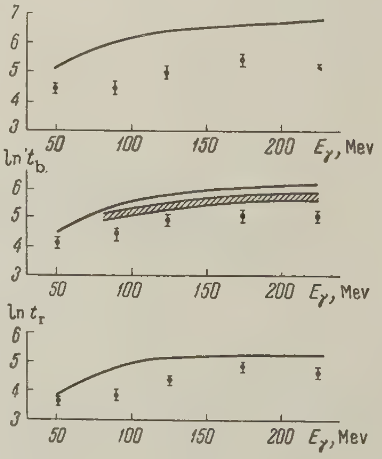

FIG. 2. Dependence of the effective thicknesses t_f, t_b, and t_r for the Na^{24} recoil nuclei, produced in the reaction Al^{27} (γ, 2pn), on the energy E_γ of the gamma quanta. ● – experimental values of the mean effective thickness in the photon-energy intervals (35 – 80, 80 – 100, 100 – 150, 150 – 200, and 200 – 260 Mev). Solid curve – calculated from the compound-nucleus theory. Cross-hatched curve – calculated by the "quasi-deuteron" model.

Average Effective Thicknesses for Na^{24} Recoil Nuclei at $E\gamma_{max}$ = 260 Mev.

Reaction	t_f (micrograms/cm²)		t_b (micrograms/cm²)			t_r (micrograms/cm²)	
	Experimental	Compound nucleus	Experimental	Compound nucleus	"Quasi-deuteron" model	Experimental	Compound nucleus
Al^{27} (γ, $2pn$)	125±3	515±50	102±3	271±30	180±30	72±3	122±15
Si^{28} (γ, $3pn$)	80±8	530±50	80±16	200±20	160±30	40±8	48±5
P^{31} (γ, $4p3n$)	80±8	680±70	50±16	250±30	160±30	20±8	44±5
S^{32} (γ, $5p3n$)	40±8	660±70	20±8	240±30	—	0±8	40±5

a_0 is the total number of recoil nuclei produced per unit mass of the specimen. To determine N, the investigated specimens were coated with triacetate films 20 microns thick. These films served to gather the Na^{24} recoil nuclei from the specimen. Stacks made up of the specimens and films were placed in the bremsstrahlung beam of the 260-Mev synchroton of the Physics Institute of the Academy of Sciences, both parallel and perpendicular to the beam (Fig. 1), and exposed for 10 to 15 hours. Ten to 15 hours after the end of the exposure, only the characteristic activity of Na^{24} was observed on the films and specimens. The ratio N/a_0 was calculated from the measured activities of Na^{24} by introducing corrections for the decay and for the self absorption. The experiments with aluminum were carried out at maximum bremsstrahlung energies ($E\gamma_{max}$) of 80, 100, 150, 200, and 260 Mev. The experiments with silicon, phosphorus, and sulphur were carried out at $E\gamma_{max}$ = 260 Mev.

The experimental results are shown in Fig. 2 and in the table, which lists also the values of t_f, t_b and t_r (see Fig. 1), calculated with the compound-nucleus model, and tentative values of t_b calculated with the "quasi-deuteron" model. As can be seen from Fig. 2 and from the table, the values of t calculated with the compound-nucleus model are several times greater than the experimental ones. This shows that a model that assumes the formation of a compound nucleus with subsequent evaporation of the nucleons cannot be used to explain the reactions investigated. The values t_b calculated by the "quasi-deuteron" model are also considerably greater than the experimental ones. Further experiments and refinement of the calculations should show whether these discrepancies can be eliminated by a suitable modification of the "quasi-deuteron" model or whether deep photofissions of this kind must be explained by introducing a substantially different mechanism of interaction, for example a mechanism that takes into account the interaction between the gamma quanta and the alpha particles or the more complicated fragments of the nuclei.

---

[1] J. S. Levinger, Phys. Rev. **84**, 43 (1951).

[2] R. Serber, Phys. Rev. **72**, 1114 (1947).

[3] K. J. LeCouteur, Proc. Phys. Soc. **A63**, 259 (1950).

[4] F. A. Si-Chang and I. Perlman, Phys. Rev. **87**, 723 (1952).

Translated by J. G. Adashko
110

ISOTOPIC INVARIANCE IN ANTI-HYPERON PROCESSES

S. G. MATINIAN and G. R. KHUTSISHVILI

Institute of Physics, Academy of Sciences, Georgian S.S.R.

Submitted to JETP editor May 20, 1958

J. Exptl. Theoret. Phys. (U.S.S.R.) **35**, 546-547 (August, 1958)

IN this note we consider formation and interaction processes of anti-hyperons with nucleons and light nuclei on the basis of isotopic invariance.

As was shown by Amati and Vitale,[1] the most convenient process for the identification and study of the anti-hyperons is not the nucleon-nucleon collision, but the reaction involving a beam of K particles:

$$K + N \to \tilde{Y} + N + N. \tag{1}$$

Using K^+ particles and protons in reaction (1), we get two channels for the charge states (with formation of $\tilde{\Sigma}$ anti-hyperons):

$$\begin{aligned} K^+ + p &\to \tilde{\Sigma}^0 + p + p, && \text{(a)} \\ &\to \tilde{\Sigma}^- + p + n. && \text{(b)} \end{aligned} \tag{1'}$$

Applying, in the usual way,[2] the hypothesis of isotopic invariance, we obtain for the cross sections of processes (a) and (b) the following expressions:

$$\sigma_a = {}^1/_2\,|A_1^1|^2, \quad \sigma_b = |A_0^1|^2 + {}^1/_2\,|A_1^1|^2, \tag{2}$$

where A_t^T is the amplitude for the transition into a final state with total isotopic spin T, while the isotopic spin of the two-nucleon system is equal to t (= 0, 1). From this we only get an unequality for the cross sections:

$$\sigma_b \geqslant \sigma_a. \tag{3}$$

In reference 1 the interaction of the $\widetilde{\Sigma}^+$ anti-hyperon with deuterium was discussed. The $\widetilde{\Sigma}^+$ anti-hyperon has negative charge, and is thus slowed down by ionization losses. After coming to rest, it is absorbed. The following reactions take place:

$$\begin{aligned} \widetilde{\Sigma}^+ + d &\to n + \pi^- + K^+, && \text{(a)} \\ &\to n + \pi^0 + K^0, && \text{(b)} \\ &\to p + \pi^- + K^0. && \text{(c)} \end{aligned} \tag{4}$$

We investigate these reactions in somewhat more detail than was done in reference 1. The amplitudes for the processes (a), (b), and (c) in Eq. (4) have, under the hypothesis of isotopic invariance, the following form:

$$\begin{gathered} F_a = \frac{1}{\sqrt{2}}\left(-A_0^1 + \frac{1}{\sqrt{2}}A_1^1\right) = -\frac{\sqrt{3}}{2}B^1_{3/2}, \\ F_b = -\frac{1}{\sqrt{2}}A_1^1 = \frac{1}{\sqrt{3}}\left(B^1_{1/2} + \frac{1}{\sqrt{2}}B^1_{3/2}\right), \\ F_c = \frac{1}{\sqrt{2}}\left(A_0^1 + \frac{1}{\sqrt{2}}A_1^1\right) = \frac{1}{\sqrt{3}}\left(-\sqrt{2}B^1_{1/2} + \frac{1}{2}B^1_{3/2}\right), \end{gathered} \tag{5}$$

where A_t^1 is the amplitude for the transition into a final state, with the isotopic spin of the system K meson — nucleon equal to t (= 0, 1); $B_{t'}^1$ has the same meaning for the system π meson — nucleon (t′ = ½, ³⁄₂).

If we express the amplitudes for the processes by the amplitudes A_t^1, characterizing the system K meson — nucleon in the final state, we obtain the inequality

$$\sigma_a + \sigma_c \geqslant \sigma_b. \tag{6}$$

The equality sign holds for the case when the interaction amplitude for the system K meson — nucleon in the state with isotopic spin t = 1 predominates over the amplitude for the same system with t = 0. We note that the experimental data point to a strong interaction in the system N – K for t = 1. In this limiting case σ(a) : σ(b) : σ(c) = 1 : 2 : 1, and the ratio K^+/K^0 = ⅓, i.e., we get the result of reference 1.

If we express the amplitudes F_i by the amplitudes $B_{t'}^1$, characterizing the system π meson – nucleon in the state with isotopic spin t′, we obtain the inequality

$$\sigma_b + \sigma_c \geqslant \sigma_a/3. \tag{7}$$

In the limiting case of a predomination of the interaction amplitude for the system π-N in the state with t′ = ³⁄₂ we get an equality, and σ(a) : σ(b) : σ(c) = 9 : 2 : 1, K^+/K^0 = 3 (cf. reference 1).

In the general case we must be content with the inequalities (6) and (7). Their violation would indicate the absence of isotopic invariance in anti-hyperon processes.

Specific inequalities between the cross sections can also be obtained from the obvious fact that $|F_a|$, $\sqrt{2}\,|F_b|$, and $|F_c|$ may be regarded as the lengths of the edges of a triangle. This leads to the following set of inequalities:

$$\begin{gathered} |\sqrt{\sigma_a} - \sqrt{\sigma_c}| \leqslant \sqrt{2\sigma_b} \leqslant \sqrt{\sigma_a} + \sqrt{\sigma_c}, \\ |\sqrt{2\sigma_b} - \sqrt{\sigma_c}| \leqslant \sqrt{\sigma_a} \leqslant \sqrt{2\sigma_b} + \sqrt{\sigma_c}, \\ |\sqrt{\sigma_a} - \sqrt{2\sigma_b}| \leqslant \sqrt{\sigma_c} \leqslant \sqrt{\sigma_a} + \sqrt{2\sigma_b}, \end{gathered} \tag{8}$$

The experimental verification of these relations is also of interest for the applicability of the hypothesis of isotopic invariance for interactions involving strange particles, and in particular, anti-hyperons.

We note that these considerations are immediately generalized for the case of light nuclei with isotopic spin zero (He^4, C^{12}, etc.).

---

[1] D. Amati and B. Vitale, J. Exptl. Theoret. Phys. (U.S.S.R.) **33**, 556 (1957); Soviet Phys. JETP **6**, 435 (1958).

[2] S. G. Matinian, J. Exptl. Theoret. Phys. (U.S.S.R.) **31**, 528 (1956); Soviet Phys. JETP **4**, 431 (1957).

Translated by R. Lipperheide
111

LOWER EXCITED STATES OF Th²³¹

Iu. I. FILIMONOV and B. V. PSHENICHNIKOV

Leningrad Physico-Technical Institute, Academy of Sciences, U.S.S.R.

Submitted to JETP editor May 26, 1958

J. Exptl. Theoret. Phys. (U.S.S.R.) **35**, 548-549 (August, 1958)

A considerable fraction of the Th^{231} produced in the alpha decay of U^{235} is in excited states. Up to recently it was assumed that the gamma transitions between the levels of Th^{231} occur at energies of 74, 110, 184, 200, 289, and 382 kev.[1] The multiplicity of the transitions remained unknown.

In the present work we investigated the γ-ray spectrum of Th^{231}, using a scintillation spectrometer with a NaI (Tl) crystal. The resolution of the spectrometer on the Cs^{137} was 7%. We counted the gamma quanta in coincidence with the alpha particles of the U^{235}. The spectrum obtained is shown in Fig. 1. The most intense line of the spectrum corresponds to 184-kev gamma quanta. The intensity of the 144-kev line is 25 to 30% of that of the 184-kev line. In the region of the spectrum from 110 to 70 kev, there are several unresolved lines: 92 kev — the characteristic thorium x-rays that accompany the internal conversion of the gamma quanta, and 95 kev — the characteristic uranium x-rays produced by slowing down the alpha and beta particles in the source. It is possible that lines corresponding to gamma transitions in Th^{231} are also present. The 40-kev line is connected with the gamma transition during the α decay of the U^{234} present in the specimen. It is also possible, however, that a transition of like energy occurs during the decay of U^{235}.

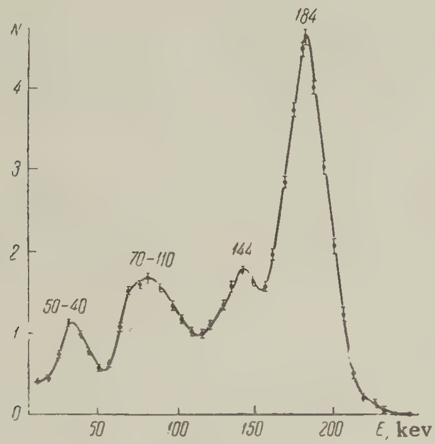

FIG. 1

It was established in control experiments with sources of various thickness and in investigations of the gamma spectrum of a Te^{123m} reference that no 144-kev gamma quanta can result from backward scattering of gamma rays with energies of 184 to 200 kev. We must assume that these quanta are emitted by Th^{231} during the transition from 184-kev to the 40-kev excited level. The latter may be the first excited level of the rotation band.

On the basis of the Nielson scheme, the spin of the ground state of Th^{231} must be assumed to be $^5/_2$. The second excited level of the rotation band should then have an approximate energy of 93 kev and a spin of $^9/_2$.

The intensity of the unresolved lines in the spectrum region from 70 to 110 kev is approximately 40% of the intensity of the 184-kev line. If we assume that this region contains only the characteristic x-radiation of thorium, the K-shell coefficients of internal conversion (i.c.c.) of the 184- and 144-kev gamma quanta cannot exceed unity. The presence of other gamma quanta, with energies from 70 to 110 kev, reduces still further the upper limits for the i.c.c. Such a limitation of the value of the i.c.c. makes it possible to exclude the possibility of magnetic gamma transitions, for even in M1 transitions with energies of 184 and 144 kev, the values of the i.c.c. are ~ 3 and 5 respectively.

By assuming the 40-kev excitation level to be rotational, we can classify the transitions with energies of 184 and 144 kev only as E1 or E1 + M2. The existence of an E1 + M2 radiation with 184 kev energy is confirmed by measuring the angular correlation between these quanta and the 4.4-Mev alpha particles for U^{235}. The angular correlation were measured with a pulsed ionization chamber and a scintillation spectrometer. The distribution function obtained is of the form

$$W(\theta) = 1 + (0.109 \pm 0.020) P_2(\cos\theta) - (0.055 \pm 0.018) P_4(\cos\theta).$$

The scheme proposed for the Th^{231} levels was reported at the Conference on Nuclear Spectroscopy[2] and is shown in Fig. 2.

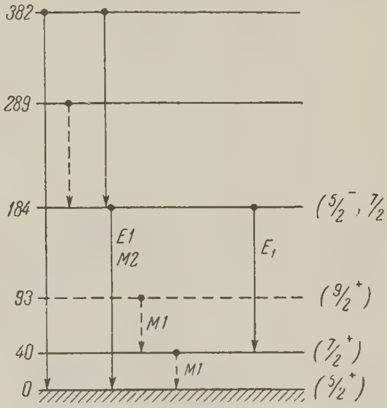

FIG. 2

The existence of rotational levels in Th^{231} was indicated independently by Pilger et al.[3]

The authors thank Professor L. I. Rusinov for constant attention to this work.

---

[1] S. A. Johansson, Ark. f. Fysik **10**, 97 (1956).

[2] Program and Topics of the Eighth Annual Conference on Nuclear Spectroscopy in Leningrad,

January 27 — February 3, 1958.

[3] Pilger, Stephens, Asaro, and Perlman, Bull. Phys. Soc. **2**, 394 (1957).

Translated by J. G. Adashko
112

THE SATURATION MAGNETIZATION OF NICKEL-COPPER ALLOYS AT LOW TEMPERATURES

E. I. KONDORSKII, V. E. RODE, and U. GOFMAN

Moscow State University

Submitted to JETP editor May 28, 1958

J. Exptl. Theoret. Phys. (U.S.S.R.) **35**, 549-550 (August, 1958)

THE aim of the present investigation was to check the $\frac{3}{2}$-law, $I = I_0(1 - CT^{3/2})$, for the saturation magnetization at low temperatures, and to determine the constant C in that law for nickel-copper alloys with copper content of up to 50%.

The measurement was carried out on a setup which made it possible to follow directly the change in the saturation magnetization of the sample while its temperature was changed. The temperature of the specimen was varied by pumping out vapors of boiling liquids (oxygen, nitrogen, hydrogen, and helium) in which the specimen was placed. The temperature was determined by the vapor pressure in the cryostat. The change in the magnetization was determined by a photoelectric flux meter. The sensitivity of the flux meter was equal to 20 μ sec-v for one division of the scale, which made it possible to measure a magnetization of the order of 10^{-3} gauss.

In the table we have given the values of the magnetization I_0 of nickel and nickel-copper alloys in a field H = 3500 Oe at different temperatures, the value of

$$n = \ln(\Delta I_1/\Delta I_2)/\ln(T_1/T_2) + 1,$$

where ΔI_1 and ΔI_2 are the change in magnetization found respectively at the temperatures T_1 and T_2 for the same lowering of the temperature (for a change of the temperature by the same small amount ΔT). In the table is also given the value of C evaluated by means of the Bloch equation for an observed value of ΔI/ΔT and the value $\Theta' = C^{-2/3}$. One sees easily that the difference $n - \frac{3}{2}$ lies within the limits of the errors, assumed in the determination of n. Hence it follows that, within the limits of the errors, the experiments observe the $\frac{3}{2}$ law for all alloys which were investigated.

Cu content (%) in the alloys	Magnetization, gauss				n	$C\cdot10^6$	Θ', °K	J/k	$2S^*$	J^*/k
	4.2° K	20°K	77°K	286°K						
0	512	512	510	496	1.6 ±0.2	9	2300	217	0.606	485
10	423	422	420	369	1.55±0.1	17	1500	144	0.502	475
20	348	347	342	272	1.43±0.2	32	990	94.5	0.412	440
30	255	253	246	124	1.53±0.2	67	610	58	0.302	445
44	124	121	97.5	—	1.56±0.2	320	215	20	0.147	470
50	82.5	77.5	35.5	—	1.48±0.2	780	118.5	11.5	0.098	495

From the value of C from the Bloch-Møller equation

$$C = (0.1174/2S\alpha)\left(\frac{k}{2SJ}\right)^{3/2},$$

in which S is the spin, α = 1, 2, 4 for simple, body-centered, and face-centered cubic lattices, respectively, one can evaluate the exchange integral J for pure metals. To evaluate the exchange integral of iron we take[1-3] 2S = 2; for nickel we take 2S = 1. However, for nickel and its alloys the average magnetic moment for one atom is not equal to an integral number of Bohr magnetons, and the above expression for C loses its meaning. We can, however, by considering J as a parameter characterizing the alloy, attempt to determine its value substituting for 2S the number 2S* of Bohr magnetons per atom of the alloy obtained from the experimental values for the magnetic saturation.

The results of these calculations are given in the table.

The exchange parameter J* evaluated in this way stays constant for all the copper-nickel alloys investigated within an accuracy of 10 to 15%.

---

[1] E. M. Lifshitz, J. Exptl. Theoret. Phys. (U.S.S.R.) **15**, 97 (1945), J. Phys. (U.S.S.R.) **8**, 337 (1944).

[2] E. I. Kondorskii and L. N. Fedotov, Izv. Akad. Nauk SSSR, Ser. Fiz. **16**, 432 (1952).

[3] C. Kittel, Revs. Modern Phys. **21**, 541 (1949).

Translated by D. ter Haar
113

PARAMAGNETIC RESONANCE OF THE FREE RADICALS OBTAINED BY FREEZING A PLASMA OF H_2S

S. D. KAITMAZOV and A. M. PROKHOROV

P. N. Lebedev Physical Institute, Academy of Science, U.S.S.R.

Submitted to JETP editor May 31, 1958

J. Exptl. Theoret. Phys. (U.S.S.R.) **35**, 551 (August, 1958)

HYDROGEN sulfide, generated by the usual method and dried over calcium chloride under a pressure of 0.3 mm Hg, was passed into a quartz tube in which a high frequency electrodeless discharge was excited. The power in the discharge was 120 w and the frequency was 40 Mcs. The discharge tube was joined to a quartz trap cooled by liquid nitrogen. The dissociation products of the H_2S were frozen out on the inner surface of the trap. The electron paramagnetic resonance spectrum was observed for the material condensed below the nitrogen level. The substance had a dark green color and a snow-like structure.

Observations were carried out at 1300 and 9400 Mcs. For observation at 1300 Mcs, the frozen material was placed in a previously cooled through-type quarter-wave coaxial resonator connected to a vacuum pump. The absorption spectrum was observed on the screen of an oscillograph. Observations were made at 77°K. The line observed was 16 ± 1 gauss wide at half intensity and had a nearly Gaussian shape.

The dependence of the absorption line on preliminary warming of the specimen was qualitatively investigated. It was found that keeping the specimen for an hour at 120 to 130°K is not accompanied by an essential change in the intensity and shape of the line. Keeping the specimen at 170°K for an hour causes a several-fold drop in intensity and a narrowing of the line to 12 gauss. A very weak line continued to be observed after 30 min at dry-ice temperature. Let us note that storing the specimen at 77°K for two months did not give rise to a noticeable change of intensity of the line.

Observations at 9400 Mcs were carried out on a superheterodyne spectroscope[1] in a cylindrical resonator in an H_{011} mode. The shape of the line differed radically from Gaussian. The line breadth was 85 ± 5 gauss, and the spectroscopic splitting factor $g \approx 2.03$. On warming the specimen, the peak of the line deformed asymmetrically. The change of shape of the line on warming indicates that the condensed material contains two radicals with different stability to warming.

A comparison of the line breadths at 1300 and 9400 Mcs, as well as the asymmetry of the line at 9400 Mcs, are evidence of a strong anisotropy of broadening $(g_{||} > g_{\perp})$.

The authors express their thanks to G. Ia. Vzenkova for her part in the work.

---

[1] A. A. Manenkov and A. M. Prokhorov, Радиотехника и электроника (Radio Engg. and Electronics) **1**, 469 (1956).

Translated by R. Eisner
114

ON THE PROBLEM OF ANGULAR CORRELATION OF SECONDARY PARTICLES PRODUCED IN HIGH-ENERGY NUCLEAR COLLISIONS

I. M. GRAMENITSKII, M. Ia. DANYSH, V. B. LIUBIMOV, M. I. PODGORETSKII, and D. TUVDENDORZH

Joint Institute for Nuclear Research

Submitted to JETP editor May 31, 1958

J. Exptl. Theoret. Phys. (U.S.S.R.) **35**, 552-553 (August, 1958)

WE report here the results of a study of the correlation between the emission angles of secondary relativistic particles produced in interactions between ~ 9-Bev protons and emulsion nuclei. The coefficient of correlation between the number of particles emitted within various solid angles was measured for that purpose.

Consider two non-overlapping solid angles Ω_1 and Ω_2, and two random variables n_1 and n_2, equal to the number of secondary relativistic particles in a given star emitted within Ω_1 and Ω_2 respectively. We denote by p_1 and p_2 the emission probabilities of secondary particles within the angles Ω_1 and Ω_2, by $\bar{n}$ the mean number of particles in stars, and by D_n the dispersion of the number of particles. If we assume that the directions of emission of secondary particles are statistically independent, we obtain for the correlation coefficient $R = (\overline{n_1 n_2} - \overline{n_1}\overline{n_2})$ the relation $R = p_1 p_2 (D_n - \bar{n})$.

450 stars, found in scanning of an emulsion chamber consisting of layers of the NIKFI-R emulsion 400 μ thick, were used for the determination of R. The chamber was irradiated by the internal proton beam of the Joint Institute for Nuclear Research synchrophasotron. Scanning was carried out along the tracks produced by primary protons.

The measured values of D_n and $\bar{n}$ were found to be 3.64 ± 0.15 and 3.23 ± 0.09 respectively. The value of $Q = R - p_1 p_2 (D_n - n)$ was then measured for different angles Ω_1 and Ω_2.* The results are given below. The choice of the angles Ω_1 and Ω_2 is illustrated in the figure.

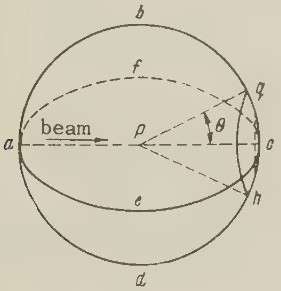

P – point of interaction; afcea – emulsion plane; I – angle between the planes afcPa and abcPa, II – angle between the planes abcPa and aPcea, III – angle between the planes aPcea and aPcfa, IV – angle between the planes aPcda and aPcfa, V – solid angle qPh ($\theta = 27°$), VI – solid angle (4π – qPh).

Ω_1	I + II or I + III	I + IV	V
Ω_2	III + IV or II + IV	II + III	VI
p_1	0.5	0.5	0.5
p_2	0.5	0.5	0.5
Q	0.10±0.03	—0.02±0.06	—0.17±0.06

The results indicate that the directions of emission of secondary particles are not entirely independent statistically.

In addition, we studied the problem of narrow particle pairs, the presence of which would indicate either the existence of intermediate rapidly-decaying particles[2] or a strong attraction between some secondary particles.[3] We selected particles pairs in stars with a difference in the angle of emission less than $\Delta = 3.5 \times 10^{-2}$. Six such pairs were observed in the analysis of 375 splittings, not counting, naturally, pairs due to π^0 decay according to the scheme $\pi^0 \rightarrow e^+ + e^- + \gamma$. The number of chance pairs, calculated under the assumption of statistical independence of the directions of emission of secondary particles, was found to be 5.9, which is in a good agreement with the observed value.

The study of correlations of the emission angles of secondary particles may prove useful as a check of the statistical theory of multiple-particle production.[4]

For this purpose it would be advantageous to investigate elementary collisions of nucleons and π mesons with nucleons. It is also necessary to account for possible angular correlations connected with conservation laws.

The authors thank E. V. Esin, T. V. Pokidov, L. I. Fedorov, and M. I. Filipov who took part in carrying out the measurements, and to D. S. Chernavskii for a discussion of the results.

---

*The dispersion D_m of the number of particles m in different fixed solid angles Ω was determined at the same time. It was found that in all cases $D_m \approx m$, i.e., $\alpha = D_m/\bar{m} \approx 1$. This result may be used in determination of the interaction energy from the angular distribution of secondary particles (cf., e.g., reference 1).

---

[1] A. I. Nikishov and I. L. Rozental', J. Exptl. Theoret. Phys. (U.S.S.R.) **35**, 165 (1958), Soviet Phys. JETP **8**, 115 (1959).

[2] Danysz, Lock, and Yekutieli, Nature **169**, 365 (1952).

[3] K. A. Brueckner and K. M. Watson, Phys. Rev. **87**, 621 (1952).

[4] E. Fermi, Usp. Fiz. Nauk **46**, 71 (1952).

Translated by H. Kasha
115

TRANSITION EFFECT FOR ELECTRONS IN WALLS OF AN IONIZATION CHAMBER

V. A. DMITRIEV

Moscow State University

Submitted to JETP editor April 25, 1958

J. Exptl. Theoret. Phys. (U.S.S.R.) 35, 553-554 (August, 1958)

IONIZATION chambers have been used recently in a number of experiments[1] on the determination of the energy of nuclear active particles. A lead absorber is placed directly above the chamber, in which the electron-photon cascade, initiated by π^0 mesons produced in nuclear interactions, develops.

The energy carried away by π^0 mesons is determined from the number of electrons in the chamber. The transition effect in the chamber walls changes the picture. The transition effect, however, has not been accounted for in any of the experiments, although the thickness of the walls vary considerably.

We calculated the change of the number of electrons in the transition of the cascade from lead into the iron wall of the chamber. The calculations were carried out according to formulae given in Ch. VI of the book of Belenkii.[2] The calculations given there, however, do not take into account the scattering of low energy electrons which influences considerably the effective range of such electrons. We accounted for the variation of the range of low energy electrons due to their scattering according to Chap. VII, § 27 of the book. An equilibrium electron spectrum and a photon spectrum accounting for the energy dependence of the total photon absorption coefficient were used. The calculation is applicable to a thickness of lead equal to or greater than t_{max} since the electron spectrum in lead at cascade maximum is close to equilibrium and slowly varies with depth[3] (t_{max} is the depth of cascade maximum). The result of the calculation for the transition effect lead-iron is shown in the figure. The sharp decrease in the number of electrons for a small thickness of iron is due to ionization stopping of electrons and can be explained by the soft energy spectrum in lead. The difference in the transition effect due to variation of the chamber wall thickness from 1 to 3 mm amounts to 8% only.

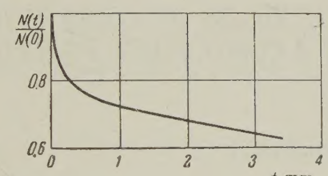

The author would like to express his gratitude to J. B. Khristiansen for a helpful discussion of the results.

---

[1] H. Carmichael and I. F. Steljes, Phys. Rev. 99, 1542 (1955); Grigorov, Shestoperov, et al., J. Exptl. Theoret. Phys. (U.S.S.R.) 33, 1099 (1957), Soviet Phys. JETP 6, 848 (1958); Zatsepin, Murzina, et al., J. Exptl. Theoret. Phys. (U.S.S.R.) 34, 298 (1958), Soviet Phys. JETP 7, 207 (1958).

[2] S. Z. Belen'kii, Лавинные процессы в космических лучах (Cascade Processes in Cosmic Rays), M — L, 1948.

[3] I. P. Ivanenko, J. Exptl. Theoret. Phys. (U.S.S.R.) 32, 491 (1957), Soviet Phys. JETP 5, 413 (1957).

Translated by H. Kasha
116

ANISOTROPY OF THE ELECTRICAL RESISTANCE OF A GOLD MONOCRYSTAL IN A MAGNETIC FIELD AT 4.2°K

N. E. ALEKSEEVSKII and Iu. P. GAIDUKOV

Institute for Physical Problems, Academy of Sciences, U.S.S.R.

Submitted to JETP editor June 14, 1958

J. Exptl. Theoret. Phys. (U.S.S.R.) 35, 554-555 (August, 1958)

THE results of numerous experiments (cf., for example, references 1 and 2) concerned with the investigation of the galvanomagnetic properties of monovalent metals are in disagreement with theory. In view of this, it appeared of interest to investigate the character of the electrical resistance of these metals in a magnetic field for various crystalline orientations.

A gold monocrystal is most suitable for this purpose. The monocrystal was prepared from gold of 99.9999% purity. It was in the form of a cylinder 30 mm in height and 0.3 mm in diameter. The resistance of the sample varied by a factor of 1650 between room temperature and 4.2°K. The fourth-order axis of the crystal was oriented approximately along the axis of the sample. To avoid the secondary effects commonly observed with sufficiently pure metals in a magnetic field, the gold crystal was mounted with the results of reference 3 taken into consideration.

A polar diagram was taken for this crystal at 4.2°K, in a magnetic field $H = 23$ kilooersteds, which was rotated in a plane perpendicular to the axis of the sample.

The dependence of $\Delta r_H/r_0 = (r_H - r_0)/r_0$ (where r_H and r_0 are the resistances in the presence and the absence of the magnetic field) upon the magnetic field was determined for the directions of the greatest of the maxima and the smallest of the minima of the polar diagram. The results of these measurements are illustrated in Figs. 1 and 2 (the region represented in Fig. 2 is indicated by the rectangle in Fig. 1). The mag-

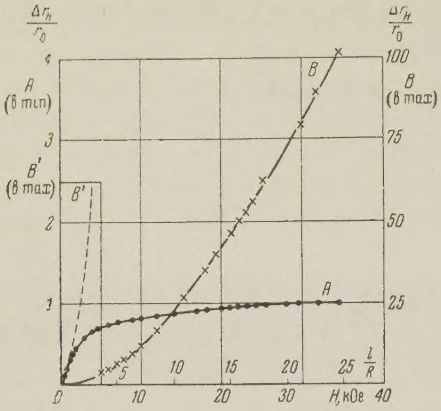

FIG. 1

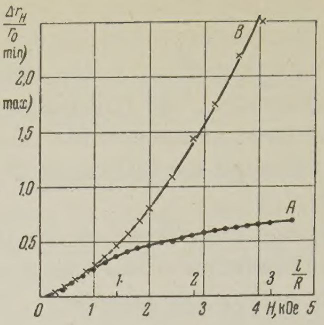

FIG. 2

nitude of the ratio of the mean free path l to the radius of curvature R of the trajectory of the conduction electrons in the magnetic field ($l/R = H/\rho nec$, where e and n are the charge and density of the conduction electrons, ρ is the resistivity, and c is the velocity of light) is given along the x axis in addition to the magnetic field intensity.

From the dependences shown in the figures it is evident that while in the direction of the maximum the resistance increases indefinitely ($\Delta r_H/r_0 \sim H^{1.8}$), the resistance in the direction of the minimum becomes completely saturated,* with $\Delta r_H/r_0 \approx 1$ for fields $H \gg H_0$ (H_0 is determined from the equality $l/R = 1$, and is in the present case equal to 1.4 koe). Analogous behavior is observed for all of the maxima and minima of the polar diagram.

It should be noted that for monocrystals of Pb[4] and Cu[5] a weak tendency towards saturation has been observed in the direction of the minimum.

On the basis of the results obtained it may be suggested that the linear increase in resistance in a magnetic field found by Kapitza,[6] observable in polycrystalline samples,[1,2] is the result of an averaging over angle of the various dependences† for $\Delta r_H/r_0$.

We assume that the considerable anisotropy of the resistance in a magnetic field is associated with the existence of an open Fermi energy surface for gold.[7]

We regard it as a pleasant duty to express our gratitude to Academician P. L. Kapitza for his consideration of the results obtained.

---

*The copper monocrystal with which preliminary measurements were carried out behaves in a similar fashion.

†We have averaged the experimental curves of $\Delta r_H/r_0$ obtained for various angles with the gold monocrystal. The averaged dependence of $\Delta r_H/r_0$ upon H thus obtained has indeed a linear character.

[1] R. G. Chambers, Proc. Roy. Soc. (London) **238**, 344 (1957).

[2] E. Justi, Z. Physik **41**, 486 (1940).

[3] Alekseevskii, Brandt, and Kostina, J. Exptl. Theoret. Phys. (U.S.S.R.) **34**, 1339 (1958), Soviet Phys. JETP **7**, 924 (1958).

[4] E. Justi and H. Scheffers, Z. Physik **39**, 591 (1938).

[5] E. Gruneisen and H. Adenstedt, Ann. Physik **31**, 714 (1938).

[6] P. L. Kapitza, Proc. Roy. Soc. (London) **123**, 292 (1929).

[7] Lifshitz, Azbel', and Kaganov, J. Exptl. Theoret. Phys. (U.S.S.R.) **31**, 63 (1956), Soviet Phys. JETP **4**, 41 (1957).

Translated by S. D. Elliott
117

OPTICAL METHODS OF OBSERVING THE IONIZATION ALONG FAST PARTICLE TRACKS

V. V. VLADIMIRSKII

Submitted to JETP editor June 9, 1958

J. Exptl. Theoret. Phys. (U.S.S.R.) **35**, 556-557 (August, 1958)

THE following processes accompany the passage of ionizing particles through a gas: ionization, excitation of atoms and molecules, and dissociation of molecules. Two of the processes are used for particle detection: ionization (ionization chambers, gas counters) and excitation (scintillation detectors). For observation of the tracks, the method of vapor condensation on ions is used in cloud and diffusion chambers. The amount of light from excited atoms in the gas is too small for a direct observation of particle tracks. So far, a similar method has been successful only in solid luminescence chambers.

It can be shown that when atoms and ions produced along the tracks are illuminated by resonance light, the number of scattered photons is much larger than the number of photons that can be recorded in a direct observation of scintillations in the gas. This opens a possibility of direct observation of tracts without vapor condensation on ions. In principle, it is possible to record optically both the ions and the neutral atoms originating in the dissociation of molecules along the particle tracks. In observation of neutral atoms it is easier to obtain a suitable intensive light source, but difficulties arise due to quenching of the resonance fluorescence by the gas molecules. Besides, for neutral atoms it is difficult to devise a method of cleaning the chamber of old tracks and the background due to thermal and photodissociation of molecules. Unnecessary ions can be removed from the working volume by means of an electric field. In connection with this, a method utilizing ions is preferable.

We shall estimate the intensity of light scattered by an ion. The scattering cross-section[2,5] at resonance line maximum for a dipole transition is

$$\sigma_0 = 2\pi\lambda^2 (2J_r + 1)/(2J_0 + 1),$$

where J_0 and J_r are the moments of the initial and resonance states respectively. The integral cross section is given by the expression

$$\int \sigma d\omega = (\pi^2\lambda^2/\tau)(2J_r + 1)/(2J_0 + 1),$$

where τ is half-life of the excited state which is connected with the oscillator force f by the relation

$$(2J_r + 1)/\tau(2J_0 + 1) = 2r_0 cf/\lambda^2.$$

Most of the suitable transition are formed by dublets ${}^2S_{1/2} \rightarrow {}^2P_{3/2}$, for which the sum of statistical factors is 3, and τ is in the range 10^{-8} to 10^{-9} [5] The maximum flux of light quanta of both polarization senses from a light source per unit solid angle is

$$\frac{2\omega^2 d\omega}{(2\pi)^3 c^2} (e^{h\omega/kT} - 1)^{-1},$$

where kT can attain the value of 1 ev in intensive discharges. Assuming for simplicity that the scattering is isotropic, and that the line width of the source is greater than that of the scattering medium, and taking the statistical factor equal to 3, we obtain the total number of scattered photons

$$3 \frac{\Omega_1\Omega_2}{16\pi^2} \frac{t}{\tau} (e^{h\omega/kT} - 1)^{-1}, \qquad (1)$$

where t is the time of observation and Ω_1 and Ω_2 are the solid angle of illumination and observation respectively.

The time of observation is limited by the diffusion of ions and can be chosen from 0.01 to 0.1 sec. For $t = 0.03$ sec, $\Omega_1 = 2$, $\Omega_2 = 0.1$, $\exp(-h\omega/kT) = 0.05$, and $\tau = 3 \times 10^{-9}$, Eq. (1) yields the number of photons from a single scattering ion, $\sim 2 \times 10^3$. Such an amount of light can be detected by means of a photoelectric device. Direct photographic recording is, probably, possible for thick tracks of heavily-ionizing particles.

Singly-charged ions of Mg, Ca, Sr. Ba, Cd, Zn, and Pb have suitable lines in the visible part of the spectrum and in the near ultraviolet.[3] Mercury would be advantageous in view of its high vapor tension, but the resonance lines Hg II lie in far ultraviolet. It is probable that a combination of one of the above mentioned metals with a noble gas, say A + Cd, would be more suitable. Since the ionization potential of argon is greater than the sum of the energies of ionization and excitation of the resonance level of Cd, one would expect that argon ions will be neutralized irreversibly in collisions $A^+ + Cd \rightarrow A + Cd^+$, and that a number of Cd ions sufficient for recording will be obtained at a relatively low pressure of cadmium vapor. Noble gases practically do not quench resonance fluorescence and the pressure can be therefore sufficiently high.

Ions of Ca, Sr, and Ba have metastable[4] states and can be used for observing the Raman scattering if the difficulties due to the general background of scattered light in observation of unshifted lines turn out to be too great.

It is difficult to say at present if the proposed method would be advantageous compared with conventional methods, but the possibility of its realization is beyond any serious doubt.

The author takes the advantage to express his thanks to I. S. Abramson for valuable advice.

---

[1] Zavoiskii, Butelov, Plakhov, and Smolkin, Атомная энергия (Atomic Energy) 1, No. 4, 34 (1956).

[2] G. Placzek, Rayleigh Scattering and the Raman Effect (Russ. Transl.) Kharkov-Kiev 1935, p. 49.

[3] Zaidel', Prokof'ev, and Raiskii, Таблицы спектральных линий (Tables of Spectral Lines) M — L, 1952.

[4] W. Grotrian, Graphische Darstellung der Spektren von Atomen und Ionen mit ein, zwei und

drei Valenzelektronen, vol. II, Berlin, 1928.

[5] A. Mitchell and M. Zemansky, Resonance Radiation and Excited Atoms, Cambridge Univ. Press, 1934 (Russian Transl. M.-L, 1937).

Translated by H. Kasha
118

A METHOD FOR THE OBSERVATION OF HELIUM II FILMS

A. I. SHAL' NIKOV

Institute for Physics Problems, Academy of Sciences, U.S.S.R.

Submitted to JETP editor July 26, 1958

J. Exptl. Theoret. Phys. (U.S.S.R.) 35, 558 (August, 1958)

FOR the observation of helium II films and the investigation of their behavior, a simple method has been employed which makes use of the absorption within the film of photoelectrons ejected from the surface upon which the film is formed. With the aid of this method it is readily possible to follow the formation of the film in various regions of temperature and pressure. The magnitude of the photoelectric current, characterizing the state of the film, was measured with the aid of an inverse-feedback electrometer amplifier connected to the output of the apparatus described, making it possible in some cases to follow as well the kinetics of the processes involved.

I am deeply grateful to D. I. Vasil'ev for aid in the performance of these experiments.

Translated by S. D. Elliott
119